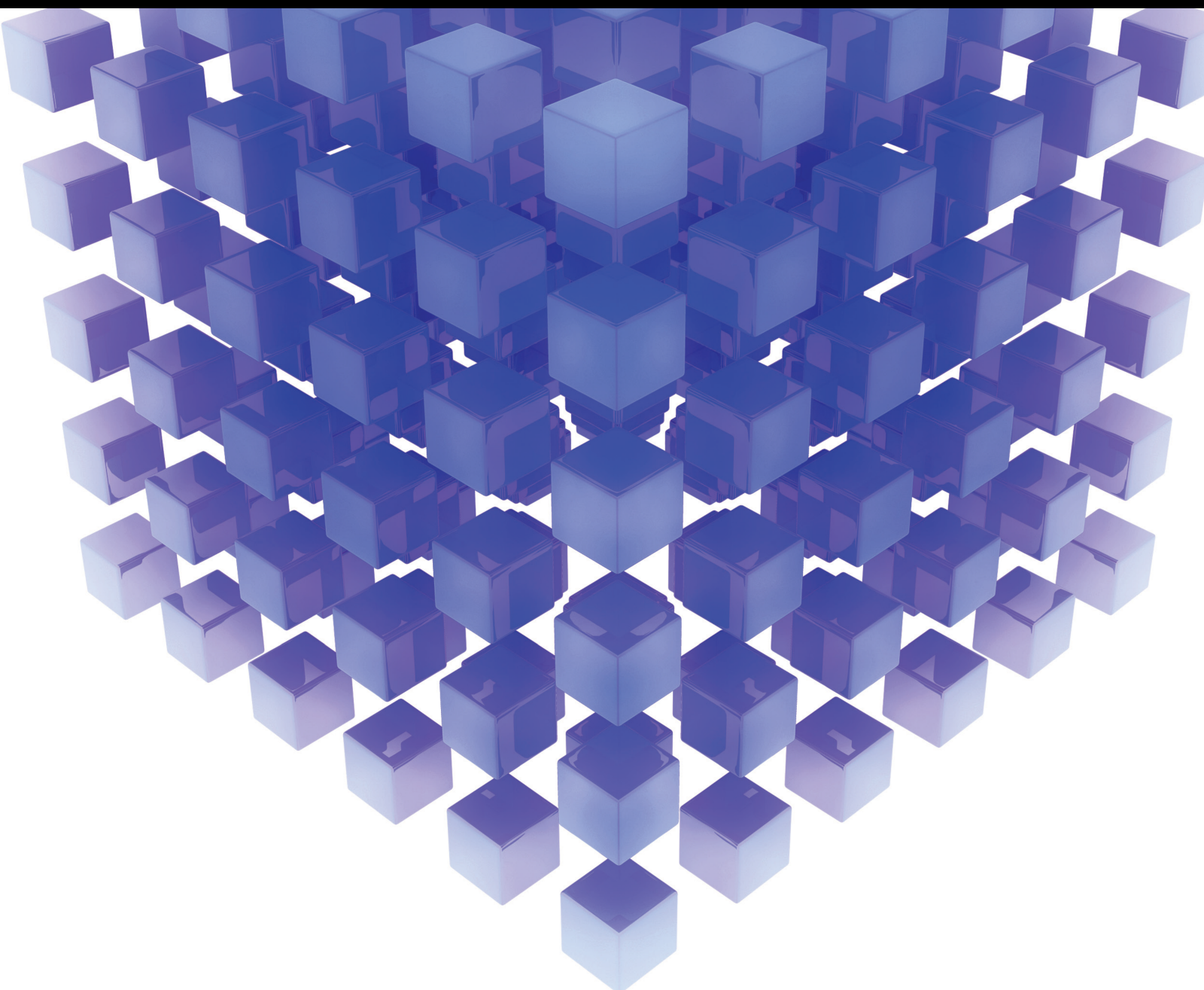


# Graph Invariants and Their Applications

Lead Guest Editor: Ali Ahmad

Guest Editors: Andrea Semaničová-Feňovčíková, Roslan Hasni, and Sakander Hayat



---

# **Graph Invariants and Their Applications**

Mathematical Problems in Engineering

---

## **Graph Invariants and Their Applications**

Lead Guest Editor: Ali Ahmad

Guest Editors: Andrea Semaničová-Feňovčíková,  
Roslan Hasni, and Sakander Hayat




---

Copyright © 2021 Hindawi Limited. All rights reserved.

This is a special issue published in “Mathematical Problems in Engineering.” All articles are open access articles distributed under the Creative Commons Attribution License, which permits unrestricted use, distribution, and reproduction in any medium, provided the original work is properly cited.

# Chief Editor

Guangming Xie , China

## Academic Editors

Kumaravel A , India  
Waqas Abbasi, Pakistan  
Mohamed Abd El Aziz , Egypt  
Mahmoud Abdel-Aty , Egypt  
Mohammed S. Abdo, Yemen  
Mohammad Yaghoub Abdollahzadeh  
Jamalabadi , Republic of Korea  
Rahib Abiyev , Turkey  
Leonardo Acho , Spain  
Daniela Addessi , Italy  
Arooj Adeel , Pakistan  
Waleed Adel , Egypt  
Ramesh Agarwal , USA  
Francesco Aggogeri , Italy  
Ricardo Aguilar-Lopez , Mexico  
Afaq Ahmad , Pakistan  
Naveed Ahmed , Pakistan  
Elias Aifantis , USA  
Akif Akgul , Turkey  
Tareq Al-shami , Yemen  
Guido Ala, Italy  
Andrea Alaimo , Italy  
Reza Alam, USA  
Osamah Albahri , Malaysia  
Nicholas Alexander , United Kingdom  
Salvatore Alfonzetti, Italy  
Ghous Ali , Pakistan  
Nouman Ali , Pakistan  
Mohammad D. Aliyu , Canada  
Juan A. Almendral , Spain  
A.K. Alomari, Jordan  
José Domingo Álvarez , Spain  
Cláudio Alves , Portugal  
Juan P. Amezcua-Sanchez, Mexico  
Mukherjee Amitava, India  
Lionel Amodeo, France  
Sebastian Anita, Romania  
Costanza Arico , Italy  
Sabri Arik, Turkey  
Fausto Arpino , Italy  
Rashad Asharabi , Saudi Arabia  
Farhad Aslani , Australia  
Mohsen Asle Zaem , USA

Andrea Avanzini , Italy  
Richard I. Avery , USA  
Viktor Avrutin , Germany  
Mohammed A. Awadallah , Malaysia  
Francesco Aymerich , Italy  
Sajad Azizi , Belgium  
Michele Bacciocchi , Italy  
Seungik Baek , USA  
Khaled Bahlali, France  
M.V.A Raju Bahubalendruni, India  
Pedro Balaguer , Spain  
P. Balasubramaniam, India  
Stefan Balint , Romania  
Ines Tejado Balsera , Spain  
Alfonso Banos , Spain  
Jerzy Baranowski , Poland  
Tudor Barbu , Romania  
Andrzej Bartoszewicz , Poland  
Sergio Baselga , Spain  
S. Caglar Baslamisli , Turkey  
David Bassir , France  
Chiara Bedon , Italy  
Azeddine Beghdadi, France  
Andriette Bekker , South Africa  
Francisco Beltran-Carbajal , Mexico  
Abdellatif Ben Makhlof , Saudi Arabia  
Denis Benasciutti , Italy  
Ivano Benedetti , Italy  
Rosa M. Benito , Spain  
Elena Benvenuti , Italy  
Giovanni Berselli, Italy  
Michele Betti , Italy  
Pietro Bia , Italy  
Carlo Bianca , France  
Simone Bianco , Italy  
Vincenzo Bianco, Italy  
Vittorio Bianco, Italy  
David Bigaud , France  
Sardar Muhammad Bilal , Pakistan  
Antonio Bilotta , Italy  
Sylvio R. Bistafa, Brazil  
Chiara Boccaletti , Italy  
Rodolfo Bontempo , Italy  
Alberto Borboni , Italy  
Marco Bortolini, Italy

Paolo Boscariol, Italy  
Daniela Boso , Italy  
Guillermo Botella-Juan, Spain  
Abdesselem Boulkroune , Algeria  
Boulaïd Boulkroune, Belgium  
Fabio Bovenga , Italy  
Francesco Braghin , Italy  
Ricardo Branco, Portugal  
Julien Bruchon , France  
Matteo Bruggi , Italy  
Michele Brun , Italy  
Maria Elena Bruni, Italy  
Maria Angela Butturi , Italy  
Bartłomiej Błachowski , Poland  
Dhanamjayulu C , India  
Raquel Caballero-Águila , Spain  
Filippo Cacace , Italy  
Salvatore Caddemi , Italy  
Zuowei Cai , China  
Roberto Caldelli , Italy  
Francesco Cannizzaro , Italy  
Maosen Cao , China  
Ana Carpio, Spain  
Rodrigo Carvajal , Chile  
Caterina Casavola, Italy  
Sara Casciati, Italy  
Federica Caselli , Italy  
Carmen Castillo , Spain  
Inmaculada T. Castro , Spain  
Miguel Castro , Portugal  
Giuseppe Catalanotti , United Kingdom  
Alberto Cavallo , Italy  
Gabriele Cazzulani , Italy  
Fatih Vehbi Celebi, Turkey  
Miguel Cerrolaza , Venezuela  
Gregory Chagnon , France  
Ching-Ter Chang , Taiwan  
Kuei-Lun Chang , Taiwan  
Qing Chang , USA  
Xiaoheng Chang , China  
Prasenjit Chatterjee , Lithuania  
Kacem Chehdi, France  
Peter N. Cheimets, USA  
Chih-Chiang Chen , Taiwan  
He Chen , China

Kebing Chen , China  
Mengxin Chen , China  
Shyi-Ming Chen , Taiwan  
Xizhong Chen , Ireland  
Xue-Bo Chen , China  
Zhiwen Chen , China  
Qiang Cheng, USA  
Zeyang Cheng, China  
Luca Chiapponi , Italy  
Francisco Chicano , Spain  
Tirivanhu Chinyoka , South Africa  
Adrian Chmielewski , Poland  
Seongim Choi , USA  
Gautam Choubey , India  
Hung-Yuan Chung , Taiwan  
Yusheng Ci, China  
Simone Cinquemani , Italy  
Roberto G. Citarella , Italy  
Joaquim Ciurana , Spain  
John D. Clayton , USA  
Piero Colajanni , Italy  
Giuseppina Colicchio, Italy  
Vassilios Constantoudis , Greece  
Enrico Conte, Italy  
Alessandro Contento , USA  
Mario Cools , Belgium  
Gino Cortellessa, Italy  
Carlo Cosentino , Italy  
Paolo Crippa , Italy  
Erik Cuevas , Mexico  
Guozeng Cui , China  
Mehmet Cunkas , Turkey  
Giuseppe D'Aniello , Italy  
Peter Dabnichki, Australia  
Weizhong Dai , USA  
Zhifeng Dai , China  
Purushothaman Damodaran , USA  
Sergey Dashkovskiy, Germany  
Adiel T. De Almeida-Filho , Brazil  
Fabio De Angelis , Italy  
Samuele De Bartolo , Italy  
Stefano De Miranda , Italy  
Filippo De Monte , Italy



































José António Fonseca De Oliveira  
Correia , Portugal  
Jose Renato De Sousa , Brazil  
Michael Defoort, France  
Alessandro Della Corte, Italy  
Laurent Dewasme , Belgium  
Sanku Dey , India  
Gianpaolo Di Bona , Italy  
Roberta Di Pace , Italy  
Francesca Di Puccio , Italy  
Ramón I. Diego , Spain  
Yannis Dimakopoulos , Greece  
Hasan Dinçer , Turkey  
José M. Domínguez , Spain  
Georgios Dounias, Greece  
Bo Du , China  
Emil Dumic, Croatia  
Madalina Dumitriu , United Kingdom  
Premraj Durairaj , India  
Saeed Eftekhari Azam, USA  
Said El Kafhali , Morocco  
Antonio Elipse , Spain  
R. Emre Erkmen, Canada  
John Escobar , Colombia  
Leandro F. F. Miguel , Brazil  
FRANCESCO FOTI , Italy  
Andrea L. Facci , Italy  
Shahla Faisal , Pakistan  
Giovanni Falsone , Italy  
Hua Fan, China  
Jianguang Fang, Australia  
Nicholas Fantuzzi , Italy  
Muhammad Shahid Farid , Pakistan  
Hamed Faruqi, Iran  
Yann Favennec, France  
Fiorenzo A. Fazzolari , United Kingdom  
Giuseppe Fedele , Italy  
Roberto Fedele , Italy  
Baowei Feng , China  
Mohammad Ferdows , Bangladesh  
Arturo J. Fernández , Spain  
Jesus M. Fernandez Oro, Spain  
Francesco Ferrise, Italy  
Eric Feulvarch , France  
Thierry Floquet, France

Eric Florentin , France  
Gerardo Flores, Mexico  
Antonio Forcina , Italy  
Alessandro Formisano, Italy  
Francesco Franco , Italy  
Elisa Francomano , Italy  
Juan Frausto-Solis, Mexico  
Shujun Fu , China  
Juan C. G. Prada , Spain  
HECTOR GOMEZ , Chile  
Matteo Gaeta , Italy  
Mauro Gaggero , Italy  
Zoran Gajic , USA  
Jaime Gallardo-Alvarado , Mexico  
Mosè Gallo , Italy  
Akemi Gálvez , Spain  
Maria L. Gandarias , Spain  
Hao Gao , Hong Kong  
Xingbao Gao , China  
Yan Gao , China  
Zhiwei Gao , United Kingdom  
Giovanni Garcea , Italy  
José García , Chile  
Harish Garg , India  
Alessandro Gasparetto , Italy  
Stylianos Georgantzinou, Greece  
Fotios Georgiades , India  
Parviz Ghadimi , Iran  
Ştefan Cristian Gherghina , Romania  
Georgios I. Giannopoulos , Greece  
Agathoklis Giaralis , United Kingdom  
Anna M. Gil-Lafuente , Spain  
Ivan Giorgio , Italy  
Gaetano Giunta , Luxembourg  
Jefferson L.M.A. Gomes , United Kingdom  
Emilio Gómez-Déniz , Spain  
Antonio M. Gonçalves de Lima , Brazil  
Qunxi Gong , China  
Chris Goodrich, USA  
Rama S. R. Gorla, USA  
Veena Goswami , India  
Xunjie Gou , Spain  
Jakub Grabski , Poland

Antoine Grall , France  
George A. Gravvanis , Greece  
Fabrizio Greco , Italy  
David Greiner , Spain  
Jason Gu , Canada  
Federico Guarracino , Italy  
Michele Guida , Italy  
Muhammet Gul , Turkey  
Dong-Sheng Guo , China  
Hu Guo , China  
Zhaoxia Guo, China  
Yusuf Gurefe, Turkey  
Salim HEDDAM , Algeria  
ABID HUSSANAN, China  
Quang Phuc Ha, Australia  
Li Haitao , China  
Petr Hájek , Czech Republic  
Mohamed Hamdy , Egypt  
Muhammad Hamid , United Kingdom  
Renke Han , United Kingdom  
Weimin Han , USA  
Xingsi Han, China  
Zhen-Lai Han , China  
Thomas Hanne , Switzerland  
Xinan Hao , China  
Mohammad A. Hariri-Ardebili , USA  
Khalid Hattaf , Morocco  
Defeng He , China  
Xiao-Qiao He, China  
Yanchao He, China  
Yu-Ling He , China  
Ramdane Hedjar , Saudi Arabia  
Jude Hemanth , India  
Reza Hemmati, Iran  
Nicolae Herisanu , Romania  
Alfredo G. Hernández-Díaz , Spain  
M.I. Herreros , Spain  
Eckhard Hitzer , Japan  
Paul Honeine , France  
Jaromir Horacek , Czech Republic  
Lei Hou , China  
Yingkun Hou , China  
Yu-Chen Hu , Taiwan  
Yunfeng Hu, China  
Can Huang , China  
Gordon Huang , Canada  
Linsheng Huo , China  
Sajid Hussain, Canada  
Asier Ibeas , Spain  
Orest V. Iftime , The Netherlands  
Przemyslaw Ignaciuk , Poland  
Giacomo Innocenti , Italy  
Emilio Insfran Pelozo , Spain  
Azeem Irshad, Pakistan  
Alessio Ishizaka, France  
Benjamin Ivorra , Spain  
Breno Jacob , Brazil  
Reema Jain , India  
Tushar Jain , India  
Amin Jajarmi , Iran  
Chiranjibe Jana , India  
Łukasz Jankowski , Poland  
Samuel N. Jator , USA  
Juan Carlos Jáuregui-Correa , Mexico  
Kandasamy Jayakrishna, India  
Reza Jazar, Australia  
Khalide Jbilou, France  
Isabel S. Jesus , Portugal  
Chao Ji , China  
Qing-Chao Jiang , China  
Peng-fei Jiao , China  
Ricardo Fabricio Escobar Jiménez , Mexico  
Emilio Jiménez Macías , Spain  
Maolin Jin, Republic of Korea  
Zhuo Jin, Australia  
Ramash Kumar K , India  
BHABEN KALITA , USA  
MOHAMMAD REZA KHEDMATI , Iran  
Viacheslav Kalashnikov , Mexico  
Mathiyalagan Kalidass , India  
Tamas Kalmar-Nagy , Hungary  
Rajesh Kaluri , India  
Jyotheeswara Reddy Kalvakurthi, India  
Zhao Kang , China  
Ramani Kannan , Malaysia  
Tomasz Kapitaniak , Poland  
Julius Kaplunov, United Kingdom  
Konstantinos Karamanos, Belgium  
Michal Kawulok, Poland



Irfan Kaymaz , Turkey  
Vahid Kayvanfar , Qatar  
Krzysztof Kecik , Poland  
Mohamed Khader , Egypt  
Chaudry M. Khalique , South Africa  
Mukhtaj Khan , Pakistan  
Shahid Khan , Pakistan  
Nam-Il Kim, Republic of Korea  
Philipp V. Kiryukhantsev-Korneev ,  
Russia  
P.V.V Kishore , India  
Jan Koci , Czech Republic  
Ioannis Kostavelis , Greece  
Sotiris B. Kotsiantis , Greece  
Frederic Kratz , France  
Vamsi Krishna , India  
Edyta Kucharska, Poland  
Krzysztof S. Kulpa , Poland  
Kamal Kumar, India  
Prof. Ashwani Kumar , India  
Michal Kunicki , Poland  
Cedrick A. K. Kwuimy , USA  
Kyandoghere Kyamakya, Austria  
Ivan Kyrchei , Ukraine  
Márcio J. Lacerda , Brazil  
Eduardo Lalla , The Netherlands  
Giovanni Lancioni , Italy  
Jaroslaw Latalski , Poland  
Hervé Laurent , France  
Agostino Lauria , Italy  
Aimé Lay-Ekuakille , Italy  
Nicolas J. Leconte , France  
Kun-Chou Lee , Taiwan  
Dimitri Lefebvre , France  
Eric Lefevre , France  
Marek Lefik, Poland  
Yaguo Lei , China  
Kauko Leiviskä , Finland  
Ervin Lenzi , Brazil  
ChenFeng Li , China  
Jian Li , USA  
Jun Li , China  
Yueyang Li , China  
Zhao Li , China































Zhen Li , China  
En-Qiang Lin, USA  
Jian Lin , China  
Qibin Lin, China  
Yao-Jin Lin, China  
Zhiyun Lin , China  
Bin Liu , China  
Bo Liu , China  
Heng Liu , China  
Jianxu Liu , Thailand  
Lei Liu , China  
Sixin Liu , China  
Wanquan Liu , China  
Yu Liu , China  
Yuanchang Liu , United Kingdom  
Bonifacio Llamazares , Spain  
Alessandro Lo Schiavo , Italy  
Jean Jacques Loiseau , France  
Francesco Lolli , Italy  
Paolo Lonetti , Italy  
António M. Lopes , Portugal  
Sebastian López, Spain  
Luis M. López-Ochoa , Spain  
Vassilios C. Loukopoulos, Greece  
Gabriele Maria Lozito , Italy  
Zhiguo Luo , China  
Gabriel Luque , Spain  
Valentin Lychagin, Norway  
YUE MEI, China  
Junwei Ma , China  
Xuanlong Ma , China  
Antonio Madeo , Italy  
Alessandro Magnani , Belgium  
Toqeer Mahmood , Pakistan  
Fazal M. Mahomed , South Africa  
Arunava Majumder , India  
Sarfraz Nawaz Malik, Pakistan  
Paolo Manfredi , Italy  
Adnan Maqsood , Pakistan  
Muazzam Maqsood, Pakistan  
Giuseppe Carlo Marano , Italy  
Damijan Markovic, France  
Filipe J. Marques , Portugal  
Luca Martinelli , Italy  
Denizar Cruz Martins, Brazil

Francisco J. Martos , Spain  
Elio Masciari , Italy  
Paolo Massioni , France  
Alessandro Mauro , Italy  
Jonathan Mayo-Maldonado , Mexico  
Pier Luigi Mazzeo , Italy  
Laura Mazzola, Italy  
Driss Mehdi , France  
Zahid Mehmood , Pakistan  
Roderick Melnik , Canada  
Xiangyu Meng , USA  
Jose Merodio , Spain  
Alessio Merola , Italy  
Mahmoud Mesbah , Iran  
Luciano Mescia , Italy  
Laurent Mevel , France  
Constantine Michailides , Cyprus  
Mariusz Michta , Poland  
Prankul Middha, Norway  
Aki Mikkola , Finland  
Giovanni Minafò , Italy  
Edmondo Minisci , United Kingdom  
Hiroyuki Mino , Japan  
Dimitrios Mitsotakis , New Zealand  
Ardashir Mohammadzadeh , Iran  
Francisco J. Montáns , Spain  
Francesco Montefusco , Italy  
Gisele Mophou , France  
Rafael Morales , Spain  
Marco Morandini , Italy  
Javier Moreno-Valenzuela , Mexico  
Simone Morganti , Italy  
Caroline Mota , Brazil  
Aziz Moukrim , France  
Shen Mouquan , China  
Dimitris Mourtzis , Greece  
Emiliano Mucchi , Italy  
Taseer Muhammad, Saudi Arabia  
Ghulam Muhiuddin, Saudi Arabia  
Amitava Mukherjee , India  
Josefa Mula , Spain  
Jose J. Muñoz , Spain  
Giuseppe Muscolino, Italy  
Marco Mussetta , Italy

Hariharan Muthusamy, India  
Alessandro Naddeo , Italy  
Raj Nandkeolyar, India  
Keivan Navaie , United Kingdom  
Soumya Nayak, India  
Adrian Neagu , USA  
Erivelton Geraldo Nepomuceno , Brazil  
AMA Neves, Portugal  
Ha Quang Thinh Ngo , Vietnam  
Nhon Nguyen-Thanh, Singapore  
Papakostas Nikolaos , Ireland  
Jelena Nikolic , Serbia  
Tatsushi Nishi, Japan  
Shanzhou Niu , China  
Ben T. Nohara , Japan  
Mohammed Nouari , France  
Mustapha Nourelfath, Canada  
Kazem Nouri , Iran  
Ciro Núñez-Gutiérrez , Mexico  
Włodzimierz Ogryczak, Poland  
Roger Ohayon, France  
Krzysztof Okarma , Poland  
Mitsuhiro Okayasu, Japan  
Murat Olgun , Turkey  
Diego Oliva, Mexico  
Alberto Olivares , Spain  
Enrique Onieva , Spain  
Calogero Orlando , Italy  
Susana Ortega-Cisneros , Mexico  
Sergio Ortobelli, Italy  
Naohisa Otsuka , Japan  
Sid Ahmed Ould Ahmed Mahmoud , Saudi Arabia  
Taoreed Owolabi , Nigeria  
EUGENIA PETROPOULOU , Greece  
Arturo Pagano, Italy  
Madhumangal Pal, India  
Pasquale Palumbo , Italy  
Dragan Pamučar, Serbia  
Weifeng Pan , China  
Chandan Pandey, India  
Rui Pang, United Kingdom  
Jürgen Pannek , Germany  
Elena Panteley, France  
Achille Paolone, Italy

George A. Papakostas , Greece  
Xosé M. Pardo , Spain  
You-Jin Park, Taiwan  
Manuel Pastor, Spain  
Pubudu N. Pathirana , Australia  
Surajit Kumar Paul , India  
Luis Payá , Spain  
Igor Pažanin , Croatia  
Libor Pekař , Czech Republic  
Francesco Pellicano , Italy  
Marcello Pellicciari , Italy  
Jian Peng , China  
Mingshu Peng, China  
Xiang Peng , China  
Xindong Peng, China  
Yuxing Peng, China  
Marzio Pennisi , Italy  
Maria Patrizia Pera , Italy  
Matjaz Perc , Slovenia  
A. M. Bastos Pereira , Portugal  
Wesley Peres, Brazil  
F. Javier Pérez-Pinal , Mexico  
Michele Perrella, Italy  
Francesco Pesavento , Italy  
Francesco Petrini , Italy  
Hoang Vu Phan, Republic of Korea  
Lukasz Pieczonka , Poland  
Dario Piga , Switzerland  
Marco Pizzarelli , Italy  
Javier Plaza , Spain  
Goutam Pohit , India  
Dragan Poljak , Croatia  
Jorge Pomares , Spain  
Hiram Ponce , Mexico  
Sébastien Poncet , Canada  
Volodymyr Ponomaryov , Mexico  
Jean-Christophe Ponsart , France  
Mauro Pontani , Italy  
Sivakumar Poruran, India  
Francesc Pozo , Spain  
Aditya Rio Prabowo , Indonesia  
Anchasa Pramuanjaroenkij , Thailand  
Leonardo Primavera , Italy  
B Rajanarayan Prusty, India

Krzysztof Puszynski , Poland  
Chuan Qin , China  
Dongdong Qin, China  
Jianlong Qiu , China  
Giuseppe Quaranta , Italy  
DR. RITU RAJ , India  
Vitomir Racic , Italy  
Carlo Rainieri , Italy  
Kumbakonam Ramamani Rajagopal, USA  
Ali Ramazani , USA  
Angel Manuel Ramos , Spain  
Higinio Ramos , Spain  
Muhammad Afzal Rana , Pakistan  
Muhammad Rashid, Saudi Arabia  
Manoj Rastogi, India  
Alessandro Rasulo , Italy  
S.S. Ravindran , USA  
Abdolrahman Razani , Iran  
Alessandro Reali , Italy  
Jose A. Reinoso , Spain  
Oscar Reinoso , Spain  
Haijun Ren , China  
Carlo Renno , Italy  
Fabrizio Renno , Italy  
Shahram Rezapour , Iran  
Ricardo Rianza , Spain  
Francesco Riganti-Fulginei , Italy  
Gerasimos Rigatos , Greece  
Francesco Ripamonti , Italy  
Jorge Rivera , Mexico  
Eugenio Roanes-Lozano , Spain  
Ana Maria A. C. Rocha , Portugal  
Luigi Rodino , Italy  
Francisco Rodríguez , Spain  
Rosana Rodríguez López, Spain  
Francisco Rossomando , Argentina  
Jose de Jesus Rubio , Mexico  
Weiguo Rui , China  
Rubén Ruiz , Spain  
Ivan D. Rukhlenko , Australia  
Dr. Eswaramoorthi S. , India  
Weichao SHI , United Kingdom  
Chaman Lal Sabharwal , USA  
Andrés Sáez , Spain

Bekir Sahin, Turkey  
Laxminarayan Sahoo , India  
John S. Sakellariou , Greece  
Michael Sakellariou , Greece  
Salvatore Salamone, USA  
Jose Vicente Salcedo , Spain  
Alejandro Salcido , Mexico  
Alejandro Salcido, Mexico  
Nunzio Salerno , Italy  
Rohit Salgotra , India  
Miguel A. Salido , Spain  
Sinan Salih , Iraq  
Alessandro Salvini , Italy  
Abdus Samad , India  
Sovan Samanta, India  
Nikolaos Samaras , Greece  
Ramon Sancibrian , Spain  
Giuseppe Sanfilippo , Italy  
Omar-Jacobo Santos, Mexico  
J Santos-Reyes , Mexico  
José A. Sanz-Herrera , Spain  
Musavarah Sarwar, Pakistan  
Shahzad Sarwar, Saudi Arabia  
Marcelo A. Savi , Brazil  
Andrey V. Savkin, Australia  
Tadeusz Sawik , Poland  
Roberta Sburlati, Italy  
Gustavo Scaglia , Argentina  
Thomas Schuster , Germany  
Hamid M. Sedighi , Iran  
Mijanur Rahaman Seikh, India  
Tapan Senapati , China  
Lotfi Senhadji , France  
Junwon Seo, USA  
Michele Serpilli, Italy  
Silvestar Šesnić , Croatia  
Gerardo Severino, Italy  
Ruben Sevilla , United Kingdom  
Stefano Sfarra , Italy  
Dr. Ismail Shah , Pakistan  
Leonid Shaikhet , Israel  
Vimal Shanmuganathan , India  
Prayas Sharma, India  
Bo Shen , Germany  
Hang Shen, China

Xin Pu Shen, China  
Dimitri O. Shepelsky, Ukraine  
Jian Shi , China  
Amin Shokrollahi, Australia  
Suzanne M. Shontz , USA  
Babak Shotorban , USA  
Zhan Shu , Canada  
Angelo Sifaleras , Greece  
Nuno Simões , Portugal  
Mehakpreet Singh , Ireland  
Piyush Pratap Singh , India  
Rajiv Singh, India  
Seralathan Sivamani , India  
S. Sivasankaran , Malaysia  
Christos H. Skiadas, Greece  
Konstantina Skouri , Greece  
Neale R. Smith , Mexico  
Bogdan Smolka, Poland  
Delfim Soares Jr. , Brazil  
Alba Sofi , Italy  
Francesco Soldovieri , Italy  
Raffaele Solimene , Italy  
Yang Song , Norway  
Jussi Sopanen , Finland  
Marco Spadini , Italy  
Paolo Spagnolo , Italy  
Ruben Specogna , Italy  
Vasilios Spitas , Greece  
Ivanka Stamova , USA  
Rafał Stanisławski , Poland  
Miladin Stefanović , Serbia  
Salvatore Strano , Italy  
Yakov Strelniker, Israel  
Kangkang Sun , China  
Qiuqin Sun , China  
Shuaishuai Sun, Australia  
Yanchao Sun , China  
Zong-Yao Sun , China  
Kumarasamy Suresh , India  
Sergey A. Suslov , Australia  
D.L. Suthar, Ethiopia  
D.L. Suthar , Ethiopia  
Andrzej Swierniak, Poland  
Andras Szekrenyes , Hungary  
Kumar K. Tamma, USA

Yong (Aaron) Tan, United Kingdom  
Marco Antonio Taneco-Hernández , Mexico  
Lu Tang , China  
Tianyou Tao, China  
Hafez Tari , USA  
Alessandro Tasora , Italy  
Sergio Teggi , Italy  
Adriana del Carmen Téllez-Anguiano , Mexico  
Ana C. Teodoro , Portugal  
Efstathios E. Theotokoglou , Greece  
Jing-Feng Tian, China  
Alexander Timokha , Norway  
Stefania Tomasiello , Italy  
Gisella Tomasini , Italy  
Isabella Torcicollo , Italy  
Francesco Tornabene , Italy  
Mariano Torrisi , Italy  
Thang nguyen Trung, Vietnam  
George Tsiatas , Greece  
Le Anh Tuan , Vietnam  
Nerio Tullini , Italy  
Emilio Turco , Italy  
Ilhan Tuzcu , USA  
Efstratios Tzirtzilakis , Greece  
FRANCISCO UREÑA , Spain  
Filippo Ubertini , Italy  
Mohammad Uddin , Australia  
Mohammad Safi Ullah , Bangladesh  
Serdar Ulubeyli , Turkey  
Mati Ur Rahman , Pakistan  
Panayiotis Vafeas , Greece  
Giuseppe Vairo , Italy  
Jesus Valdez-Resendiz , Mexico  
Eusebio Valero, Spain  
Stefano Valvano , Italy  
Carlos-Renato Vázquez , Mexico  
Martin Velasco Villa , Mexico  
Franck J. Vernerey, USA  
Georgios Veronis , USA  
Vincenzo Vespri , Italy  
Renato Vidoni , Italy  
Venkatesh Vijayaraghavan, Australia

Anna Vila, Spain  
Francisco R. Villatoro , Spain  
Francesca Vipiana , Italy  
Stanislav Vitek , Czech Republic  
Jan Vorel , Czech Republic  
Michael Vynnycky , Sweden  
Mohammad W. Alomari, Jordan  
Roman Wan-Wendner , Austria  
Bingchang Wang, China  
C. H. Wang , Taiwan  
Dagang Wang, China  
Guoqiang Wang , China  
Huaiyu Wang, China  
Hui Wang , China  
J.G. Wang, China  
Ji Wang , China  
Kang-Jia Wang , China  
Lei Wang , China  
Qiang Wang, China  
Qingling Wang , China  
Weiwei Wang , China  
Xinyu Wang , China  
Yong Wang , China  
Yung-Chung Wang , Taiwan  
Zhenbo Wang , USA  
Zhibo Wang, China  
Waldemar T. Wójcik, Poland  
Chi Wu , Australia  
Qihong Wu, China  
Yuqiang Wu, China  
Zhibin Wu , China  
Zhizheng Wu , China  
Michalis Xenos , Greece  
Hao Xiao , China  
Xiao Ping Xie , China  
Qingzheng Xu , China  
Binghan Xue , China  
Yi Xue , China  
Joseph J. Yame , France  
Chuanliang Yan , China  
Xinggang Yan , United Kingdom  
Hongtai Yang , China  
Jixiang Yang , China  
Mijia Yang, USA  
Ray-Yeng Yang, Taiwan

Zaoli Yang , China  
Jun Ye , China  
Min Ye , China  
Luis J. Yebra , Spain  
Peng-Yeng Yin , Taiwan  
Muhammad Haroon Yousaf , Pakistan  
Yuan Yuan, United Kingdom  
Qin Yuming, China  
Elena Zaitseva , Slovakia  
Arkadiusz Zak , Poland  
Mohammad Zakwan , India  
Ernesto Zambrano-Serrano , Mexico  
Francesco Zammori , Italy  
Jessica Zangari , Italy  
Rafal Zdunek , Poland  
Ibrahim Zeid, USA  
Nianyin Zeng , China  
Junyong Zhai , China  
Hao Zhang , China  
Haopeng Zhang , USA  
Jian Zhang , China  
Kai Zhang, China  
Lingfan Zhang , China  
Mingjie Zhang , Norway  
Qian Zhang , China  
Tianwei Zhang , China  
Tongqian Zhang , China  
Wenyu Zhang , China  
Xianming Zhang , Australia  
Xuping Zhang , Denmark  
Yinyan Zhang, China  
Yifan Zhao , United Kingdom  
Debao Zhou, USA  
Heng Zhou , China  
Jian G. Zhou , United Kingdom  
Junyong Zhou , China  
Xueqian Zhou , United Kingdom  
Zhe Zhou , China  
Wu-Le Zhu, China  
Gaetano Zizzo , Italy  
Mingcheng Zuo, China





# Contents

## **On the Fractional Metric Dimension of Convex Polytopes**

M. K. Aslam, Muhammad Javaid , Q. Zhu, and Abdul Raheem 

Review Article (13 pages), Article ID 3925925, Volume 2021 (2021)




## **On Hamilton-Connectivity and Detour Index of Certain Families of Convex Polytopes**

Sakander Hayat , Muhammad Yasir Hayat Malik , Ali Ahmad , Suliman Khan , Faisal

Yousafzai , and Roslan Hasni 

Research Article (18 pages), Article ID 5553216, Volume 2021 (2021)

## **Computing Bounds for Second Zagreb Coindex of Sum Graphs**

Muhammad Javaid , Muhammad Ibraheem , Uzma Ahmad , and Q. Zhu



Research Article (19 pages), Article ID 4671105, Volume 2021 (2021)

## **Estimates for the Norm of Generalized Maximal Operator on Strong Product of Graphs**

Zaryab Hussain , Ghulam Murtaza , Toqeer Mahmood , and Jia-Bao Liu 



Research Article (9 pages), Article ID 9338269, Volume 2021 (2021)

## **Improving Neural Machine Translation with AMR Semantic Graphs**

Long H. B. Nguyen , Viet H. Pham, and Dien Dinh 


Research Article (12 pages), Article ID 9939389, Volume 2021 (2021)

## **Some Bounds on Bond Incident Degree Indices with Some Parameters**

Muhammad Rizwan, Akhlaq Ahmad Bhatti, Muhammad Javaid , and Fahd Jarad 

Research Article (10 pages), Article ID 8417486, Volume 2021 (2021)

## **On Computation and Analysis of Entropy Measures for Crystal Structures**

Muhammad Kamran Siddiqui, Shazia Manzoor, Sarfraz Ahmad, and Mohammed K. A. Kaabar 




Research Article (16 pages), Article ID 9936949, Volume 2021 (2021)

## **Hypergraphical Metric Spaces and Fixed Point Theorems**

Xiaodong Li , Farhan Khan, Gohar Ali , Lubna Gul, and Muhammad Sarwar 



Research Article (7 pages), Article ID 9961734, Volume 2021 (2021)

## **Extremal Values of Randić Index among Some Classes of Graphs**

Ali Ghalavand , Ali Reza Ashrafi , and Marzieh Pourbabaee 


Research Article (11 pages), Article ID 7758172, Volume 2021 (2021)

## **Sharp Bounds for the Inverse Sum Indeg Index of Graph Operations**

Anam Rani, Muhammad Imran , and Usman Ali 



Research Article (11 pages), Article ID 5561033, Volume 2021 (2021)

## **On the Spectrum of Laplacian Matrix**

Akbar Jahanbani , Seyed Mahmoud Sheikholeslami , and Rana Khoelilar



Research Article (4 pages), Article ID 8096874, Volume 2021 (2021)

### **Distance-Based Topological Polynomials Associated with Zero-Divisor Graphs**

Ali Ahmad  and S. C. López 


Research Article (8 pages), Article ID 4959559, Volume 2021 (2021)

### **New Results on Zagreb Energy of Graphs**

Seyed Mahmoud Sheikholeslami , Akbar Jahanbani , and Rana Khoeilar



Research Article (6 pages), Article ID 9969845, Volume 2021 (2021)

### **Grid Partition Variable Step Alpha Shapes Algorithm**

Zhenxiu Liao , Jun Liu, Guodong Shi, and Junxia Meng





Research Article (8 pages), Article ID 9919003, Volume 2021 (2021)




### **The Behavior of Weighted Graph's Orbit and Its Energy**

Ali A. Shukur , Akbar Jahanbani , and Haider Shelash

Research Article (6 pages), Article ID 9933072, Volume 2021 (2021)



### **Study of Carbon Nanocones $CNC_k(n)$ via Connection Zagreb Indices**

Muhammad Asif , Muhammad Hussain , Hamad Almohamedh , Khalid M Alhamed , Rana

Alabdan , Abdulrazaq A. Almutairi , and Sultan Almotairi 



Research Article (13 pages), Article ID 5539904, Volume 2021 (2021)

### **Cayley Graphs over LA-Groups and LA-Polygroups**

Nabilah Abughazalah , Naveed Yaqoob , and Asif Bashir

Research Article (9 pages), Article ID 4226232, Volume 2021 (2021)



### **The Role of Motivation and Desire in Explaining Students' VR Games Addiction: A Cognitive-Behavioral Perspective**

Xuesong Zhai , Fahad Asmi , Jing Yuan, Muhammad Azfar Anwar, Nabia Luqman Siddiquei, Intikhab

Ahmad , and Rongting Zhou 

Research Article (10 pages), Article ID 5526046, Volume 2021 (2021)

### **Improved Lower Bound of LFMD with Applications of Prism-Related Networks**

Muhammad Javaid , Hassan Zafar, Q. Zhu, and Abdulaziz Mohammed Alanazi 



Research Article (9 pages), Article ID 9950310, Volume 2021 (2021)

### **Multihop Neighbor Information Fusion Graph Convolutional Network for Text Classification**

Fangyuan Lei , Xun Liu , Zhengming Li , Qingyun Dai , and Senhong Wang 

Research Article (9 pages), Article ID 6665588, Volume 2021 (2021)

### **Computing Exact Values for Gutman Indices of Sum Graphs under Cartesian Product**







Abdulaziz Mohammed Alanazi , Faiz Farid, Muhammad Javaid , and Augustine Munagi

Research Article (20 pages), Article ID 5569997, Volume 2021 (2021)





# Contents

## **Dominating Topological Analysis and Comparison of the Cellular Neural Network**

Farukh Ejaz , Muhammad Hussain , Hamad Almohamedh , Khalid M. Alhamed , Rana Alabdan , and Sultan Almotairi 



Research Article (9 pages), Article ID 6613433, Volume 2021 (2021)

## **On Cyclic-Vertex Connectivity of $(n, k)$ -Star Graphs**

Yalan Li , Shumin Zhang , and Chengfu Ye


Research Article (4 pages), Article ID 5570761, Volume 2021 (2021)

## **On the Edge Metric Dimension of Different Families of Möbius Networks**

Bo Deng, Muhammad Faisal Nadeem , and Muhammad Azeem 

Research Article (9 pages), Article ID 6623208, Volume 2021 (2021)

## **Computing Edge Weights of Symmetric Classes of Networks**

Hafiz Usman Afzal, Muhammad Javaid , Abdulaziz Mohammed Alanazi, and Maryam Gharamah Alshehri




Research Article (22 pages), Article ID 5562544, Volume 2021 (2021)

## **Near-Coincidence Point Results in Norm Interval Spaces via Simulation Functions**

Misbah Ullah, Muhammad Sarwar , Hassen Aydi , and Yaé Ulrich Gaba 



Research Article (8 pages), Article ID 6640593, Volume 2021 (2021)

## **Graphs Associated with the Ideals of a Numerical Semigroup Having Metric Dimension 2**

Ying Wang, Muhammad Ahsan Binyamin , Wajid Ali, Adnan Aslam , and Yongsheng Rao 

Research Article (6 pages), Article ID 6697980, Volume 2021 (2021)

## **Connectivity and Wiener Index of Fuzzy Incidence Graphs**

Juanyan Fang, Irfan Nazeer, Tabasam Rashid , and Jia-Bao Liu 

Research Article (7 pages), Article ID 6682966, Volume 2021 (2021)

## Review Article

# On the Fractional Metric Dimension of Convex Polytopes

M. K. Aslam,<sup>1</sup> Muhammad Javaid <sup>1</sup>, Q. Zhu,<sup>2,3</sup> and Abdul Raheem <sup>4</sup>

<sup>1</sup>Department of Mathematics, School of Science, University of Management and Technology, Lahore, Pakistan

<sup>2</sup>School of Mathematics and Statistics, Hunan Normal University, Changsha 4100081, Hunan, China

<sup>3</sup>Department of Mathematics, School of Information Science and Engineering, Chengdu University, Chengdu 610106, China

<sup>4</sup>Department of Mathematics, National University of Singapore 119077, Singapore

Correspondence should be addressed to Abdul Raheem; rahimciit7@gmail.com

Received 23 April 2021; Revised 25 May 2021; Accepted 9 August 2021; Published 23 September 2021

Academic Editor: Ines Tejado Balsera

Copyright © 2021 M. K. Aslam et al. This is an open access article distributed under the Creative Commons Attribution License, which permits unrestricted use, distribution, and reproduction in any medium, provided the original work is properly cited.

In order to identify the basic structural properties of a network such as connectedness, centrality, modularity, accessibility, clustering, vulnerability, and robustness, we need distance-based parameters. A number of tools like these help computer and chemical scientists to resolve the issues of informational and chemical structures. In this way, the related branches of aforementioned sciences are also benefited with these tools as well. In this paper, we are going to study a symmetric class of networks called convex polytopes for the upper and lower bounds of fractional metric dimension (FMD), where FMD is a latest developed mathematical technique depending on the graph-theoretic parameter of distance. Apart from that, we also have improved the lower bound of FMD from unity for all the arbitrary connected networks in its general form.

## 1. Introduction

A network  $\aleph = (V(\aleph), E(\aleph))$  is a mathematical structure consisting of two set of vertices  $V(\aleph)$  and set of edges  $E(\aleph) \subseteq V(\aleph) \times V(\aleph)$ , where  $|V(\aleph)| = v$  and  $|E(\aleph)| = e$  are called order and size of  $\aleph$ , respectively. In  $\aleph$ , the length of the shortest path between any two vertices  $a, b \in V(\aleph)$  is called distance which is usually denoted by  $d(a, b)$ . For more information regarding graph-theoretic terminologies, we refer to [1–3].

With every passing day, technological boom is reshaping our lives in such a way that the replacement of manpower is being done by robots, devices, and machineries. At the same instance, we cannot compromise on the constraints of employing minimum number of these and their operational cost. In order to overcome these constraints with ease, we have to get the aid of distance-based parameters such as metric dimension (MD). Consider  $\mathbb{M} = \{m_1, m_2, \dots, m_k\} \subseteq V(\aleph)$ ; then,  $\mathbb{M}$  becomes an ordered set of vertices bearing some ordering imposed by us. For any  $b \in V(\aleph)$ , the distance of  $b$  from all the elements of  $\mathbb{M}$  in  $k$ -tuple metric form is given by  $r(b|\mathbb{M}) = (d(b, m_1), d(b, m_2), d(b, m_3), \dots, d(b, m_k))$ . The set  $\mathbb{M}$  becomes a resolving set if,

for any pair of distinct vertices  $a, b \in V(\aleph) - \mathbb{M}$ , we have  $r(a|\mathbb{M}) \neq r(b|\mathbb{M})$ . The resolving set bearing minimum number of vertices in  $\aleph$  forms the metric basis of  $\aleph$ , and its cardinality represents the MD of  $\aleph$  denoted by  $\lambda(\aleph)$  [4, 5].

Slater gave the terminology of resolving sets by proclaiming them as the locating set for any connected network [6, 7]. After studying these terminologies by themselves, Harary and Melter gave them the name of MD of a network. Afterwards, a large number of researchers computed the MD of different families of networks. The families of networks having constant and bounded MD have been the topic of [8]. Chartrand et al., on the contrary, proved the MD of path and cycle [4]. In the same manner,  $\mathbb{P}(n, 2)$ ,  $\mathbb{A}_m$ , and  $\mathbb{C}_m^2$  have been proved to be the networks with constant MD in [8]. Moreover, in [9], the MD of generalized Petersen network is proved to be bounded.

Chartrand et al. utilized MD to present the solution of integer programming problem (IPP) [4]. Later on, for the sake of acquiring a higher accuracy solution of an IPP, Currie and Oellermann [10] founded the concept of fractional metric dimension (FMD). Fehr et al. employed FMD to get the optimal solution of a certain linear programming relaxation problem [11]. Arumugam and Mathew brought

some undiscovered features of FMD to light [12]. Afterwards, a large number of results appeared related to the FMD of several networks that are formed as an aftermath of graph products, namely, Cartesian, hierarchial, corona, lexicographic, and comb products, see [12], [13–15], and [16]. Similarly, Liu et al. computed the FMD of generalized Jahangir network [17]. In a recent time, Raza et al. evaluated the FMD of metal organic networks [18].

Aisyah et al. pioneered the terminology of local fractional metric dimension (LFMD) and calculated for the corona product of two networks [19]. In the same manner, Liu et al. calculated the LFMD of rotationally symmetric and planar networks [20]. More recently, Javaid et al. evaluated the sharp extremal values of LFMD of connected networks [21]. In this paper, firstly, we improved the lower bound of FMD from unity, and secondly, the FMD of a family of network bearing rotational symmetry called convex polytopes is computed in the form of bounds. The flux of this paper is in the following sequence. Section 1 is introduction. Section 2 is related to the MD's role in Robotics and Chemistry. Section 3 is of preliminaries. In Section 4, the theoretical development of improved lower bound of FMD of a connected network is done. Section 5 contains the main results regarding the FMD of convex polytopes. Section 6 winds up the paper with a hand full of concluding remarks.

## 2. Applications

The increasing demand of networking is nurturing the development in distance-based dimensions. All such tools help in the allocation of an interpolator to a suitable region for employing it effectively [6, 22]. In the same way, allocating the robots in some production units and in public health facilities have been discussed in [23]. Moreover, for various techniques for the rectification of example and picture handling and information handling, we refer to [24]. Similarly, a chemical compound in the graph-theoretic form is regarded as a molecular graph having nodes as atoms and links between them as bonds [4]. With the aid of picturesque form of a compound and distance-based parameters, chemists are now able to not only remove discrepancies in some chemical structure but also are able to find the sites showing similar properties in them. All these techniques are the topic of [5, 6, 24, 25]. More recently, the same tools are found helpful in solving resolvability problems in nanotechnology and polymer-based industries [26, 27].

## 3. Preliminaries

In a network  $\aleph = (V(\aleph), E(\aleph))$ , for  $\{a, b\} \subseteq V(\aleph)$ , a vertex  $c$  resolves  $\{a, b\}$  in  $\aleph$  if  $d(a, c) \neq d(b, c)$ . For any pair of vertices  $a, b \in V(\aleph)$ , the resolving neighbourhood set (RNs) of  $\{a, b\}$  is given by  $R\{a, b\} = \{c \in V(\aleph) | d(a, c) \neq d(b, c)\}$ .

Suppose that, in a connected network,  $\aleph = (V(\aleph), E(\aleph))$ , bearing  $\nu$  as its order. A function  $\psi: V(\aleph) \rightarrow [0, 1]$  is called the upper resolving function

(URF) of  $\aleph$  if  $\psi(R\{a, b\}) \geq 1, \forall R\{a, b\}$  in  $\aleph$ , where  $\psi(R\{a, b\}) = \sum_{c \in R\{a, b\}} \psi(c)$ .

A URF  $\psi$  is called the minimal upper resolving function (MURF) if  $\exists$  is another URF  $\eta$  such that  $\eta \leq \psi$  and  $\eta(c) \neq \psi(c)$  for at least one  $c \in V(\aleph)$ . Similarly, a function defined as  $\kappa: V(\aleph) \rightarrow [0, 1]$  is called lower resolving function (LRF) if  $\kappa(R\{a, b\}) \leq 1, \forall R\{a, b\}$  in  $\aleph$ . An LRF  $\kappa$  is called the maximal lower resolving function (MLRF) if  $\exists$  is another LRF  $\mu$  such that  $\mu \geq \kappa$  and  $\mu(c) \neq \kappa(c)$  for at least one  $c \in V(\aleph)$ . The FMD of a connected network is defined as  $\dim_f(\aleph) = \chi$ , where  $\chi = \min\{|\psi|: \psi$  is the upper minimal resolving function} or  $\chi = \max\{|\kappa|: \kappa$  is the lower maximal resolving function}.

**3.1. Convex Polytopes.** The network  $\aleph \cong \mathbb{B}_m$  of convex polytope type I bearing  $3m$  3-sided faces,  $m$  4-sided faces,  $n$  5-sided faces, and a pair of  $n$ -sided faces is obtained by the combination of the network of convex polytope  $\mathbb{Q}_n$  and prism network  $\mathbb{D}_n$  [28]. The sets  $V(\mathbb{B}_m)$  and  $E(\mathbb{B}_m)$  are  $V(\mathbb{B}_m) = \{v_r, w_r, x_r, y_r, z_r | 1 \leq r \leq m\}$  and  $E(\mathbb{B}_m) = \{v_r, v_{r+1}, w_r, w_{r+1}, x_r, x_{r+1}, y_r, y_{r+1}, z_r, z_{r+1} | 1 \leq r \leq m\} \cup \{v_r, w_r, w_r, x_r, w_{r+1}, x_r, x_r, y_r, y_r, z_r | 1 \leq r \leq m\}$ , respectively. In the same manner, the cycles induced by  $\{v_r | 1 \leq r \leq m\}$ ,  $\{w_r | 1 \leq r \leq m\}$ ,  $\{x_r | 1 \leq r \leq m\}$ ,  $\{y_r | 1 \leq r \leq m\}$ , and  $\{z_r | 1 \leq r \leq m\}$  are called by inner, interior, exterior, and outer cycle, respectively. Figure 1 illustrates  $\mathbb{B}_m$ .

The network of convex polytope type II  $\aleph \cong \mathbb{C}_m$  is created out of the network of  $\mathbb{B}_m$  by adding new edges  $y_{r+1}z_r$ . It comprises of  $3m$  3-sided faces,  $m$  4-sided faces,  $m$  5-sided faces, and a pair of  $m$ -sided faces. Similarly, the cycles induced by  $\{v_r | 1 \leq r \leq m\}$ ,  $\{w_r | 1 \leq r \leq m\}$ ,  $\{x_r | 1 \leq r \leq m\}$ ,  $\{y_r | 1 \leq r \leq m\}$ , and  $\{z_r | 1 \leq r \leq m\}$  are called by inner, interior, exterior, and outer cycle, respectively. Figure 2 illustrates  $\mathbb{C}_m$ .

The sets  $V(\mathbb{C}_m)$  and  $E(\mathbb{C}_m)$  are given by  $V(\mathbb{C}_m) = \{v_r, w_r, x_r, y_r, z_r | 1 \leq r \leq m\}$  and  $E(\mathbb{C}_m) = \{v_r, v_{r+1}, w_r, w_{r+1}, x_r, x_{r+1}, y_r, y_{r+1}, z_r, z_{r+1} | 1 \leq r \leq m\} \cup \{v_r, w_r, w_r, x_r, w_{r+1}, x_r, x_r, y_{r+1}, z_r | 1 \leq r \leq m\}$ , respectively.

## 4. Lower Bound of FMD of Connected Network

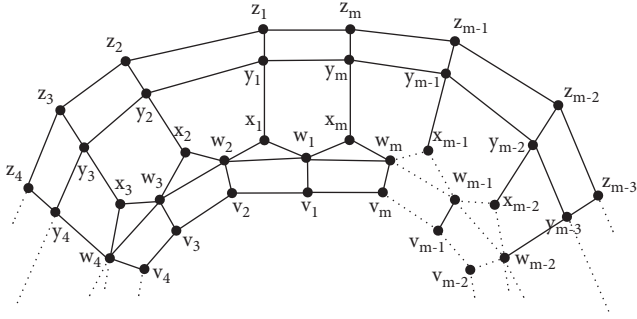
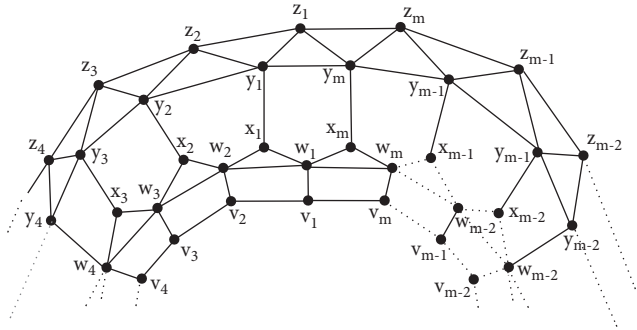
In this section, we develop criteria for the improved lower bound of FMD of connected network. Before going further, we give the following proposition.

**Proposition 1.** Suppose that  $\aleph$  is a connected network and  $R = R\{a, b\}$  is the resolving neighbourhood set for any  $\{a, b\} \subseteq V(\aleph)$ . For  $\kappa = \max\{|R|\}$ , if  $Y = \cup\{R: |R| = \kappa\} \subseteq V(\aleph)$ , then  $|R \cap Y| \leq \kappa$  for each resolving neighbourhood set of  $\aleph$ .

**Lemma 1.** Let  $\aleph$  be a connected network and  $R$  be the resolving neighbourhood set. Then,

$$\frac{|V(\aleph)|}{\kappa} \leq \dim_f(\aleph), \quad (1)$$

where  $\kappa = \max\{|R|\}$  and  $2 \leq \kappa \leq |V(\aleph)|$ .


 FIGURE 1: Type I convex polytope  $\mathbb{B}_m$ .

 FIGURE 2: Type II convex polytope  $\mathbb{C}_m$ .

*Proof.* Here, we define a mapping  $\eta: V(\aleph) \rightarrow [0, 1]$  such that  $\eta(b) = (1/\kappa)$  for  $b \in V(\aleph)$ . By Proposition 1, for  $\{a, b\} \subset V(\aleph)$ , we have

$$\eta(R) = \sum_{x \in R} \eta(x) = \sum_{x \in R \cap V(\aleph)} \frac{1}{\kappa} = |R \cap V(\aleph)| \frac{1}{\kappa} \leq 1. \quad (2)$$

This shows the fact that  $\eta$  is a lower resolving function (LRF). In order to show that  $\eta$  is maximal LRF, suppose that there exists another LRF  $\phi$  such that  $\phi(x) \geq \eta(x)$ , where  $\phi(x) \neq \eta(x)$  for at least one  $x \in V(\aleph)$ . For all  $x \in R$  such that  $|R| = \kappa$ , we have

$$\phi(R) = \sum_{x \in R} \phi(x) > \sum_{x \in R} \eta(x) = 1. \quad (3)$$

Hence,  $\phi(R) > 1$ . This shows that  $\phi$  is not LRF, and consequently,  $\eta$  is maximal LRF. Let  $\bar{\eta}$  be another maximal LRF of  $\aleph$ . Then,

$$|\bar{\eta}| = \sum_{x \in V(\aleph)} \eta(x). \quad (4)$$

Now, we assume the following three cases: (a)  $\bar{\eta}(x) > (1/\kappa), \forall x \in V(\aleph)$ , (b)  $\bar{\eta}(x) \leq (1/\kappa), \forall x \in V(\aleph)$ , and (c)  $\bar{\eta}(x) > (1/\kappa)$  for some  $x \in V(\aleph)$ .

Case (a): if  $\bar{\eta}(x) > (1/\kappa), \forall x \in V(\aleph)$ . For  $R \subseteq Y$  such that  $|R| = \kappa$ , we have  $\bar{\eta}(R) > 1$ . This shows that  $\bar{\eta}$  is not LRF. Hence, this case does not hold.

Case (b): suppose that  $\bar{\eta}(x) \leq (1/\kappa), \forall x \in V(\aleph)$ . Then,

$$|\bar{\eta}| = \sum_{x \in V(\aleph)} \bar{\eta}(x) \leq \frac{|V(\aleph)|}{\kappa} = |\eta|. \quad (5)$$

Consequently,

$$\dim_f(\aleph) = \frac{|V(\aleph)|}{\kappa}. \quad (6)$$

Case (c): if  $\bar{\eta}(x) > (1/\kappa)$  for some  $x \in V(\aleph)$ , suppose that  $S = \{t \in V(\aleph) | \bar{\eta}(t) > (1/\kappa)\}$  and  $Y = \cup \{R: |R| = \kappa\}$ . We observe that  $S \cap Y = \Phi$ ; otherwise, for  $\kappa = |R|$ ,  $\bar{\eta}(x) > 1$  which implies that  $\bar{\eta}$  is not a LRF. Consider

$$|\bar{\eta}| = \sum_{x \in V(\aleph)} \bar{\eta}(x) = \sum_{x \in Y} \bar{\eta}(x) + \sum_{x \in V(\aleph) - Y} \bar{\eta}(x). \quad (7)$$

As  $\sum_{x \in V(\aleph) - Y} \bar{\eta}(x) \geq \sum_{x \in V(\aleph) - Y} \eta(x)$ , hence,

$$\begin{aligned} |\bar{\eta}| &= \sum_{x \in V(\aleph)} \bar{\eta}(x) = \sum_{x \in Y} \bar{\eta}(x) + \sum_{x \in V(\aleph) - Y} \bar{\eta}(x) \geq \sum_{x \in Y} \eta(x) \\ &+ \sum_{x \in V(\aleph) - Y} \eta(x) = \frac{|V(\aleph)|}{\kappa} = |\eta|. \end{aligned} \quad (8)$$

Consequently,

$$\dim_f(\aleph) = |\bar{\eta}| \geq |\eta| = \frac{|V(\aleph)|}{\kappa}. \quad (9)$$

Therefore, from all the above case, we have

$$\frac{|V(\aleph)|}{\kappa} \leq \dim_f(\aleph). \quad (10)$$

This completes the proof.  $\square$

## 5. Main Results

In this part of paper, we discuss the main results of our findings regarding the networks under consideration. Lemmas 2 and 3 concern with RNs of  $\mathbb{B}_m$  and  $\mathbb{C}_m$ , respectively. Similarly, Theorems 1 and 2 give the upper and lower bounds of FMD of the aforementioned networks.

**Lemma 2.** Let  $\aleph \cong \mathbb{B}_m$  be a type I convex polytope, with  $m \geq 6$  and  $m \equiv 0 \pmod{2}$ . For  $1 \leq l, r \leq m$ ,  $p \geq 3$ , and  $s \geq 2$ ,  $s \equiv 0 \pmod{2}$  and  $p \equiv 1 \pmod{2}$ ; then,

- $|R_l| = |R\{w_l, x_l\}| = |R_r| = |R\{w_r, x_{r-1}\}| = (7m/2) + 1$ ,  $|\cup_{l=1}^m R_l| = 5m$ ,  $|\cup_{r=1}^m R_r| = 5m$ , and  $|\cup_{r=1}^m R_r \cup (\cup_{r=1}^m R_r)| = 5m$
- $|R_r| < |R'_1| = |R\{v_r, x_r\}| = |R'_2| = |R\{v_r, x_{r-1}\}|$  and  $|R'_u \cap \cup_{r=1}^m R_r| \geq |R_r|$
- $|R_r| < |R'_3| = |R\{v_r, v_{r+1}\}| = |R'_4| = |R\{v_r, v_{r+p}\}| = |R'_5| = |R\{w_r, w_{r+1}\}| = |R'_6| = |R\{w_r, w_{r+p}\}| = |R'_7| = |R\{x_r, x_{r+s}\}| = |R'_8| = |R\{y_r, y_{r+s}\}| = |R'_9| = |R\{z_r, z_{r+s}\}| = 5m - 6$  and  $|R'_u \cap \cup_{r=1}^m R_r| \geq |R_r|$  with  $v_{m+1} = v_1$
- $|R_r| < |R'_{10}| = |R\{v_r, v_{r+s}\}| = |R'_{11}| = |R\{w_r, w_{r+s}\}| = |R'_{12}| = |R\{x_r, x_{r+1}\}| = |R'_{13}| = |R\{x_r, x_{r+p}\}| = |R'_{14}| = |R\{y_r, y_{r+1}\}| = |R'_{15}| = |R\{y_r, y_{r+p}\}| = |R'_{16}| = |R\{z_r, z_{r+1}\}| = |R'_{17}| = |R\{z_r, z_{r+p}\}| = |R'_{18}| = |R\{v_r,$

- $w_{r+p}\} = |R'_{19}| = |R\{y_r, z_{r+p}\}| = 5m - 4$ , where  $p \geq 3$  and  $|R'_u \cap \cup_{r=1}^m R_r| \geq |R_r|$
- (e)  $|R_t| < |R_{20}| = |R\{w_r, x_{r+p}\}| = |R_{21}| = |R\{w_r, x_{r+s}\}| = |R'_{22}| = |R\{v_r, z_{r+p}\}| = |R'_{23}| = |R\{v_r, y_{r+s}\}| = 5m - 3$ , where  $|R'_u \cap \cup_{r=1}^m R_r| \geq |R_r|$
- (f)  $|R_t| < |R'_{24}| = |R\{v_r, z_{r+s}\}| = |R'_{25}| = |R\{w_r, z_{r+p}\}| = |R'_{26}| = |R\{w_r, z_{r+s}\}| = |R'_{27}| = |R\{v_r, y_{r+p}\}| = |R'_{28}| = |R\{x_r, y_r\}| = |R'_{29}| = |R\{y_r, z_r\}|5m - 2$  and  $|R'_u \cap \cup_{r=1}^m R_r| \geq |R_r|$
- (g)  $|R_t| < |R'_{30}| = |R\{x_r, z_r\}|$  and  $|R'_u \cap \cup_{r=1}^m R_r| \geq |R_r|$
- (h)  $|R_t| < |R'_{24}| = |R\{v_r, z_{r+s}\}| = |R'_{25}| = |R\{w_r, z_{r+p}\}| = |R'_{26}| = |R\{w_r, z_{r+s}\}| = |R'_{27}| = |R\{v_r, y_{r+p}\}| = |R'_{28}| = |R\{x_r, y_r\}| = |R'_{29}| = |R\{y_r, z_r\}|5m - 2$  and  $|R'_u \cap \cup_{r=1}^m R_r| \geq |R_r|$
- (i)  $|R_t| < |R'_{39}| = |R\{v_r, w_r\}| = 5m$  and  $|R'_u \cap \cup_{r=1}^m R_r| \geq |R_r|$

*Proof*

- (a) The RNs of  $w_l, x_l$  and  $w_r, x_{r-1}$  are  $R\{w_l, x_l\} = V(\mathbb{B}_m) - \{v_h|h \equiv l+1, l+2, \dots, l+(m/2) \pmod{m}\} \cup \{w_h|h \equiv l+1, l+2, \dots, l+(m/2) \pmod{m}\} \cup \{x_h|h \equiv l+1, l+2, \dots, l+(m/2)-1 \pmod{m}\}$  and  $R\{w_r, x_{r-1}\} = V(\mathbb{B}_m) - \{v_h|h \equiv r-1, r-2, \dots, r-(m/2) \pmod{m}\} \cup \{w_h|h \equiv r-1, r-2, \dots, r-(m/2) \pmod{m}\} \cup \{x_h|h \equiv r-2, r-3, \dots, r-(m/2)+1 \pmod{m}\}$ . We note that  $\cup_{l=1}^m R_l = V(\mathbb{B}_m)$ ,  $\cup_{r=1}^m R_r = V(\mathbb{B}_m)$  and  $|\cup_{l=1}^m R_l| = |\cup_{r=1}^m R_r| = 5m$ , and  $|\cup_{l=1}^m R_l \cup \cup_{r=1}^m R_r| = 5m$ .
- (b) The RNs of  $\{v_r, x_r\}$  and  $\{v_r, x_{r-1}\}$  are  $\hat{R}_1 = R\{v_r, x_r\} = V(\mathbb{G}) - \{w_h|h \equiv r, r-1, \dots, r-(m/2)+1 \pmod{m}\} \cup \{x_h|h \equiv r, r-1, \dots, r-(m/2) \pmod{m}\}$  and  $\hat{R}_2 = R\{v_r, x_{r-1}\} = V(\mathbb{G}) - \{w_h|h \equiv r+1, r+2, \dots, r+(m/2) \pmod{m}\} \cup \{x_h|h \equiv r+1, r+2, \dots, r+(m/2) \pmod{m}\}$ , respectively. It is clear from the above that  $|R_r| < |\hat{R}_u|$  and  $|\hat{R}_u \cap \cup_{r=1}^m R_r| \geq |R_r|$ .
- (c) The RNs of  $\{v_r, v_{r+1}\}, \{v_r, v_{r+p}\}, \{w_r, w_{r+1}\}, \{w_r, w_{r+p}\}, \{x_r, x_{r+s}\}, \{x_r, x_{r+s}\}, \{y_r, y_{r+s}\},$  and  $\{z_r, z_{r+s}\}$  are  $R'_3 = R\{v_r, v_{r+1}\} = V(\mathbb{B}_m) - \{x_h|h \equiv r, r+(m/2) \pmod{m}\} \cup \{y_h|h \equiv r, r+(m/2) \pmod{m}\} \cup \{z_h|h \equiv r, r+(m/2) \pmod{m}\} = R'_5 = R\{w_r, w_{r+p}\}, R'_4 = R\{v_r, v_{r+p}\} = V(\mathbb{B}_m) - \{x_h|h \equiv r+((p-1)/2), r+((p+m-1)/2) \pmod{m}\} \cup \{y_h|h \equiv r+((p-1)/2), r+((p+m-1)/2) \pmod{m}\} \cup \{z_h|h \equiv r+((p-1)/2), r+((p+m-1)/2) \pmod{m}\} = R'_6 = R\{w_r, w_{r+p}\}, R'_7 = R\{x_r, x_{r+s}\} = V(\mathbb{B}_m) - \{x_h|h \equiv r+(s/2), r+((m+s)/2) \pmod{m}\} \cup \{y_h|h \equiv r+(s/2), r+((m+s)/2) \pmod{m}\} \cup \{z_h|h \equiv r+(s/2), r+((m+s)/2) \pmod{m}\} = R'_8 = R\{y_r, y_{r+s}\} = R'_9 = R\{z_r, z_{r+s}\},$

respectively. Clearly,  $|R'_u| = 5m - 6$ . Since  $|R_r| = (7m/2) + 1 < |R'_u|$ , then  $|R'_u \cap \cup_{r=1}^m R_r| = 5m - 6 \geq |R_r|$ .

- (d) The RN's of  $\{v_r, v_{r+s}\}, \{w_r, w_{r+s}\}, \{x_r, x_{r+1}\}, \{x_r, x_{r+p}\}, \{y_r, y_{r+1}\}, \{y_r, y_{r+p}\}, \{z_r, z_{r+1}\}, \{z_r, z_{r+p}\}, \{v_r, w_{r+p}\},$  and  $\{y_r, z_{r+p}\}$  are given by  $\hat{R}_{10} = R\{v_r, v_{r+s}\} = V(\mathbb{B}_m) - \{v_h|h \equiv r+(s/2), r+((s+m)/2) \pmod{m}\} \cup \{w_h|h \equiv r+(s/2), r+((s+m)/2) \pmod{m}\} = \hat{R}_{11} = R\{w_r, w_{r+s}\} = \hat{R}_{13} = R\{x_r, x_{r+p}\} = \hat{R}_{15} = R\{y_r, y_{r+p}\} = \hat{R}_{17} = R\{z_r, z_{r+p}\}, \hat{R}_{18} = R\{v_r, w_{r+p}\} = V(\mathbb{B}_m) - \{v_h|h \equiv r+((p+1)/2), r+((p+m+1)/2) \pmod{m}\} \cup \{w_h|h \equiv r+((p-1)/2), r-((p-1)/2) \pmod{m}\} \cup \{x_h|h \equiv r+((p+1)/2), r+((p+m+1)/2) \pmod{m}\} \cup \{y_h|h \equiv r+((p+1)/2), r+((p+m+1)/2) \pmod{m}\}$  where  $\hat{R}_{12} = R\{x_r, x_{r+1}\} = \hat{R}_{14} = R\{y_r, y_{r+1}\} = \hat{R}_{16} = R\{z_r, z_{r+1}\} = R\{v_r, v_{r+s}\}$ . We can see that  $|\hat{R}_u| = 5m - 4 > |R_t|$  and  $|\hat{R}_u \cap \cup_{t=1}^2 R_t| \geq |R_t|$ .
- (e) The RNs of  $\{w_r, x_{r+p}\}, \{w_r, x_{r+s}\}, \{v_r, z_{r+p}\},$  and  $\{v_r, y_{r+s}\}$  are  $\hat{R}_{20} = R\{w_r, x_{r+p}\} = V(\mathbb{G}) - \{v_h|h \equiv r+((p+1)/2) \pmod{m}\} \cup \{w_h|h \equiv r+((p+1)/2) \pmod{m}\} \cup \{x_h|h \equiv r+((p+m+1)/2) \pmod{m}\} = \hat{R}_{21} = R\{w_r, x_{r+s}\} = V(\mathbb{G}) - \{v_h|h \equiv r+((m+s)/2) \pmod{m}\} \cup \{w_h|h \equiv r+((m+s)/2) \pmod{m}\} \cup \{x_h|h \equiv r+(s/2) \pmod{m}\} \cup \{y_h|h \equiv r+(s-2)/2) \pmod{m}\} \cup \{z_h|h \equiv r+((s-2)/2) \pmod{m}\}$ , and  $\hat{R}_{23} = R\{v_r, z_{r+p}\} = V(\mathbb{B}_m) - \{w_h|h \equiv r+((p+1)/2) \pmod{m}\}$ , and  $\hat{R}_{28} = R\{x_r, y_r\} = V(\mathbb{B}_m) - \{v_h|h \equiv r-1, r+1 \pmod{m}\} = \hat{R}_{29} = R\{y_r, z_r\}$ , respectively. We can see that  $|\hat{R}_u| = 5m - 3 > |R_t|$  and  $|\hat{R}_u \cap \cup_{t=1}^2 R_t| \geq |R_t|$ .
- (g) The resolving neighbourhood of  $\{x_r, z_r\}$  is  $\hat{R}_{30} = R\{x_r, z_r\} = V(\mathbb{B}_m) - \{y_h|1 \leq h \leq 6\}$ . We can see that  $|\hat{R}_u| = 4m > |R_t|$  and  $|\hat{R}_u \cap \cup_{t=1}^m R_t| > |R_t|$ .
- (h) The resolving neighbourhoods of  $\{v_r, w_{r+1}\}$  and  $\{v_r, z_{r+1}\}$  are  $\hat{R}_{31} = R\{v_r, w_{r+1}\} = V(\mathbb{B}_m) - \{v_h|h \equiv r+1, r+2, \dots, r+(m/2) \pmod{m}\}$ ,  $\hat{R}_{32} = R\{v_r, z_{r+1}\} = V(\mathbb{B}_m) - \{z_h|h \equiv r+1, r+2, \dots, r+(m/2) \pmod{m}\}$ ,  $\hat{R}_{33} = R\{v_r, x_{r+1}\} = V(\mathbb{B}_m) - \{z_h|h \equiv r+2, r+3, \dots, r+(m/2) \pmod{m}\} \cup \{x_h|h \equiv r \pmod{m}\}$ ,  $\hat{R}_{34} = R\{w_r, z_{r+1}\} = V(\mathbb{B}_m) - \{w_h|h \equiv r+2, r+3, \dots, r+(m/2) \pmod{m}\} \cup \{y_h|h \equiv r \pmod{m}\}$ ,  $\hat{R}_{35} = R\{v_r, w_{r-1}\} = V(\mathbb{B}_m) - \{v_h|h \equiv r-1, r-2, \dots, r-(m/2) \pmod{m}\}$ ,  $\hat{R}_{36} = R\{v_r, z_{r-1}\} = V(\mathbb{B}_m) - \{z_h|h \equiv r-1, r-2, \dots, r-(m/2) \pmod{m}\}$ ,  $\hat{R}_{37} = R\{v_r, x_{r-1}\} = V(\mathbb{B}_m) - \{z_h|h \equiv r-2, r-3, \dots, r-(m/2) \pmod{m}\} \cup \{x_h|h \equiv r-1 \pmod{m}\}$ , and  $\hat{R}_{38} = R\{w_r, z_{r-1}\} = V(\mathbb{B}_m) - \{w_h|h \equiv r-2, r-3, \dots, r-(m/2) \pmod{m}\} \cup \{y_h|h \equiv r-1 \pmod{m}\}$ ,

respectively. We can see that  $|\dot{R}_u| = (9m/2) > |R_t|$  and  $|\dot{R}_u \cap \cup_{t=1}^m R_t| > |R_t|$ .

- (i) The RN of  $\{v_r, w_r\}$  is  $\dot{R}_{39} = R\{v_r, w_r\} = V(\mathbb{B}_m)$ . Clearly,  $R\{w_r, x_r\} = (3m/2) + 1 < |R\{v_r, w_r\}|$  and  $|R\{v_r, w_r\} \cap \cup_{r=1}^m R_r| = 3n \geq |R_r|$ .  $\square$

**Theorem 1.** *If  $\mathbb{N} \cong \mathbb{B}_m$  with  $m \geq 6$  and  $m \equiv 0 \pmod{2}$ , then  $\dim_f(\mathbb{B}_m) < (10m/(7m+2))$ .*

*Proof*

Case I  $m = 6$ .

The RNs are given as follows.

In the same way, from Lemma 2, we can see that  $R\{x_r, x_{r+s}\} = R\{y_r, y_{r+s}\} = R\{z_r, z_{r+s}\} = R\{v_r, v_{r+p-1}\}$ .

Similarly, from Lemma 2, we can see that  $R\{v_r, v_{r+s}\} = R\{y_r, y_{r+s}\} = R\{z_r, z_{r+p}\}$ .

Tables 1 and 2 represent the RNs having cardinality of 24, whereas Tables 3–6 show the RNs with cardinalities of 26, 27, 28, and 30, respectively. On the contrary, Table 7 bears RNs with minimum cardinality of 22. Also, it is observed that  $\cup_{r=1}^{12} R_r = V(\mathbb{B}_6)$ ; this implies  $|\cup_{r=1}^{12} R_r| = 30$  and  $|\dot{R}_r \cap \cup_{r=1}^6 R_r| \geq |R_r|$ .

Now, we define a function  $\mu: V(\mathbb{B}_6) \rightarrow [0, 1]$  such that  $\mu(v_r) = \mu(w_r) = \mu(x_r) = \mu(y_r) = \mu(z_r) = (1/22)$ . As  $R_r$  for  $1 \leq t \leq 12$  of  $\mathbb{B}_6$  are pairwise overlapping, hence,  $\exists$  is another minimal resolving function  $\bar{\mu}$  of  $\mathbb{B}_6$  such that  $|\bar{\mu}| < |\mu|$ . As a result,  $\dim_f(\mathbb{B}_6) < \sum_{r=1}^{18} (1/10) < (30/22)$ .

Similarly, Table 7 shows the RNs with maximum cardinality of  $30 = \kappa$ ; hence, by Lemma 1,  $(|V(\mathbb{B}_6)|/\kappa) = (30/30) = 1 < \dim_f(\mathbb{B}_6)$ .

Therefore,

$$1 < \dim_f(\mathbb{B}_6) < \frac{30}{22}. \tag{11}$$

Case II  $m \geq 8$ .

We have seen from Lemma 2 that the RNs with minimum cardinality of  $(7m/2) + 1$  are  $R\{w_t, x_t\}$  and  $R\{w_r, x_{r-1}\}$  and  $\cup_{t=1}^m R_t = V(\mathbb{B}_m)$ . Let  $\lambda = (7m/2) + 1$  and  $\delta = |\cup_{t=1}^m R_t| = 5m$ . Now, we define a mapping  $\mu: V(\mathbb{B}_m) \rightarrow [0, 1]$  such that

$$\mu(a) = \begin{cases} \frac{1}{\lambda}, & \text{for } a \in \cup_{t=1}^m R_t, \\ 0, & \text{for } a \in V(\mathbb{B}) - \cup_{t=1}^m R_t. \end{cases} \tag{12}$$

We can see that  $\mu$  is a RF for  $\mathbb{B}_m$  with  $m \geq 3$  because  $\mu(R\{u, v\}) \geq 1, \forall u, v \in V(\mathbb{B}_m)$ . On the contrary, assume that there is another resolving function  $\rho$ , such that  $\rho(u) \leq \mu(u)$ , for at least one  $u \in V(\mathbb{B}_m), \rho(u) \neq \mu(u)$ . As a

consequence,  $\rho(R\{u, v\}) < 1$ , where  $R\{u, v\}$  is a RN of  $\mathbb{B}_m$  with minimum cardinality  $\lambda$ . This implies that  $\rho$  is not a resolving function which is contradiction. Therefore,  $\mu$  is a minimal resolving function that attains minimum  $|\mu|$  for  $\mathbb{B}_m$ . Since all  $R_r$  are having pairwise nonempty intersection, so there is another minimal resolving function of  $\bar{\mu}$  of  $\mathbb{B}_m$  such that  $|\bar{\mu}| \leq |\mu|$ . Hence, assigning  $(1/\lambda)$  to the vertices of  $\mathbb{B}_m$  in  $\cup_{t=1}^{2m} R_t$  and calculating the summation of all the weights, we obtain

$$\dim_f(\mathbb{B}_m) = \sum_{t=1}^{\delta} \frac{1}{\lambda} \leq \frac{5m}{(7m/2) + 1} = \frac{10m}{7m+2}. \tag{13}$$

Also, the RN with maximum cardinality of  $5m$  is  $R\{v_r, w_r\}$ . Let  $|V(\mathbb{B}_m)| = \omega$  and  $|R\{v_r, w_r\}| = \kappa$ ; thus, from Lemma 2, we have  $(|V(\mathbb{B}_m)|/\kappa) = (\omega/\kappa) = (5m/5m) = 1 < \dim_f(\mathbb{B}_m)$ .

Therefore, we conclude the following:

$$1 < \dim_f(\mathbb{B}_m) < \frac{10m}{7m+2}. \tag{14} \quad \square$$

**Lemma 3.** *Let  $\mathbb{N} \cong \mathbb{C}_m$  be a type II convex polytope, where  $m \geq 6$  and  $m \equiv 0 \pmod{2}$ . For  $1 \leq l, r \leq m, p \geq 3, s \geq 2, s \equiv 0 \pmod{2}$ , and  $p \equiv 1 \pmod{2}$ , then*

- (a)  $|R_l| = |R\{y_l, z_l\}| = |R_r| = |R\{y_r, z_{r-1}\}| = 3(m+1), |\cup_{l=1}^m R_l| = 5m, |\cup_{r=1}^m R_r| = 5m, \text{ and } |(\cup_{r=1}^m R_r) \cap (\cup_{l=1}^m R_l)| = 5m$
- (b)  $|R_r| < |\dot{R}_1| = |R\{w_r, x_r\}| = |\dot{R}_2| = |R\{w_r, x_{r-1}\}| = (7m/2) + 1 \text{ and } |\cup_{r=1}^m R_r| = 5m$
- (c)  $|R_r| < |R'_3| = |R\{v_r, v_{r+1}\}| = |R'_4| = |R\{v_r, v_{r+p}\}| = |R'_5| = |R\{w_r, w_{r+1}\}| = |R'_6| = |R\{w_r, w_{r+p}\}| = |R'_7| = |R\{x_r, x_{r+s}\}| = |R'_8| = |R\{x_r, x_{r+1}\}| = |R'_9| = |R\{x_r, x_{r+p}\}| = |R'_{10}| = |R\{y_r, y_{r+1}\}| = |R'_{11}| = |R\{y_r, y_{r+p}\}| = |R'_{12}| = |R\{z_r, z_{r+s}\}| = |R'_{13}| = |R\{v_r, w_{r+p}\}| = 5m - 6 \text{ and } |R'_u \cap \cup_{r=1}^m R_r| \geq |R_r|$
- (d)  $|R_r| < |R'_{14}| = |R\{z_r, z_{r+p}\}| = |R'_{15}| = |R\{v_r, z_{r+s}\}| = |R'_{16}| = |R\{w_r, x_{r+p}\}| = |R'_{17}| = |R\{w_r, y_{r+s}\}| = |R'_{18}| = |R\{x_r, y_{r+s}\}| = |R'_{19}| = |R\{x_r, z_{r+s}\}| = 5m - 4 \text{ and } |R'_u \cap \cup_{r=1}^m R_r| \geq |R_r|, \text{ where } p \geq 3$
- (e)  $|R_r| < |R'_{20}| = |R\{v_r, x_{r+p}\}| = |R'_{21}| = |R\{v_r, x_{r+s}\}| = |R'_{22}| = |R\{v_r, y_{r+s}\}| = |R'_{23}| = |R\{w_r, y_{r+p}\}| = |R'_{24}| = |R\{w_r, z_{r+s}\}| = |R'_{25}| = |R\{y_r, z_{r+s}\}| = |R'_{26}| = |R\{x_r, z_{r+p}\}| = 5m - 3 \text{ and } |R'_u \cap \cup_{r=1}^m R_r| \geq |R_r| \text{ with } v_{m+1} = v_1, \text{ where } p \geq 3$
- (f)  $|R_r| < |\dot{R}_{27}| = |R\{w_r, y_r\}| = |\dot{R}_{28}| = |R\{w_r, z_r\}| = |\dot{R}_{29}| = |R\{v_r, y_{r+p}\}| = |\dot{R}_{30}| = |R\{x_r, y_{r+p}\}| = 5m - 2 \text{ and } |\dot{R}_u \cap \cup_{r=1}^m R_r| \geq |R_r|, \text{ where } p \geq 3$
- (g)  $|R_r| < |\dot{R}_{31}| = |R\{y_r, z_{r+p}\}| = |\dot{R}_{32}| = |R\{y_r, z_{r+p}\}| = 5(n-1) \text{ and } |\dot{R}_u \cap \cup_{r=1}^m R_r| \geq |R_r|, \text{ where } p \geq 3$

TABLE 1: The representation of  $R_u'$  for  $1 \leq u \leq 41$ .

RNs	Elements	Equality
$R\{v_1, v_2\}$	$V(\mathbb{B}_6) - \{x_1, x_4\} \cup \{y_1, y_4\} \cup \{z_1, z_4\}$	$R\{v_4, v_5\}, R\{w_1, w_2\}, R\{w_3, w_6\},$ $R\{v_3, v_6\}, R\{w_4, w_7\}, R\{x_4, x_7\}, R\{x_3, x_5\}$ $R\{v_5, v_6\}, R\{w_2, w_3\}, R\{w_5, w_6\},$ $R\{v_1, v_4\}, R\{w_1, w_4\}, R\{v_5, v_8\},$ $R\{w_5, w_8\}, R\{x_1, x_3\}, R\{w_5, w_8\}, R\{x_1, x_3\},$ $R\{x_4, x_6\}$
$R\{v_2, v_3\}$	$V(\mathbb{B}_6) - \{x_2, x_5\} \cup \{y_2, y_5\} \cup \{z_2, z_5\}$	$R\{v_1, v_6\}, R\{w_1, w_6\}, R\{w_1, w_8\},$ $R\{v_2, v_5\}, R\{w_2, w_5\}, R\{v_1, v_6\},$ $R\{w_1, w_6\}, R\{x_2, x_4\}, R\{x_1, x_5\}$
$R\{v_3, v_4\}$	$V(\mathbb{B}_6) - \{x_3, x_6\} \cup \{y_3, y_6\} \cup \{z_3, z_6\}$	
$R\{v_1, x_1\}$	$V(\mathbb{B}_6) - \{w_1, w_5, w_6\} \cup \{x_4, x_5, x_6\}$	
$R\{v_2, x_2\}$	$V(\mathbb{B}_6) - \{w_1, w_2, w_6\} \cup \{x_1, x_5, x_6\}$	
$R\{v_3, x_3\}$	$V(\mathbb{B}_6) - \{w_1, w_2, w_3\} \cup \{x_1, x_2, x_6\}$	
$R\{v_4, x_4\}$	$V(\mathbb{B}_6) - \{w_2, w_3, w_4\} \cup \{x_1, x_2, x_3\}$	
$R\{v_5, x_5\}$	$V(\mathbb{B}_6) - \{w_3, w_4, w_5\} \cup \{x_2, x_3, x_4\}$	
$R\{v_6, x_6\}$	$V(\mathbb{B}_6) - \{w_4, w_5, w_6\} \cup \{x_3, x_4, x_5\}$	
$R\{v_2, x_1\}$	$V(\mathbb{B}_6) - \{w_2, w_3, w_4\} \cup \{x_2, x_3, x_4\}$	
$R\{v_3, x_2\}$	$V(\mathbb{B}_6) - \{w_3, w_4, w_5\} \cup \{x_3, x_4, x_5\}$	
$R\{v_4, x_3\}$	$V(\mathbb{B}_6) - \{w_4, w_5, w_6\} \cup \{x_4, x_5, x_6\}$	
$R\{v_5, x_4\}$	$V(\mathbb{B}_6) - \{w_1, w_5, w_6\} \cup \{x_1, x_5, x_6\}$	
$R\{v_6, x_5\}$	$V(\mathbb{B}_6) - \{w_1, w_2, w_6\} \cup \{x_1, x_2, x_6\}$	

TABLE 2: The representation of  $R_u'$  for  $42 \leq u \leq 47$ .

RNs	Elements
$R\{x_1, z_1\}$	$R\{x_2, z_2\}$
$R\{x_3, z_3\}$	$R\{x_4, z_4\}$
$R\{x_5, z_5\}$	$R\{x_5, z_5\}$

$V(\mathbb{B}_6) - \{y_h | 1 \leq h \leq 6\}$

TABLE 3: The representation of  $R_u'$  for  $48 \leq u \leq 81$ .

RNs	Elements	Equality
$R\{v_1, v_3\}$	$V(\mathbb{B}_6) - \{v_2, v_5\} \cup \{w_2, w_5\}$	$R\{v_5, v_7\}, R\{w_1, w_3\}, R\{w_5, w_7\},$ $R\{v_4, v_8\}, R\{w_4, w_8\}, R\{x_1, x_2\},$ $R\{x_4, x_5\}, R\{x_5, x_8\}$
$R\{v_2, v_4\}$	$V(\mathbb{B}_6) - \{v_3, v_6\} \cup \{w_3, w_6\}$	$R\{v_6, v_8\}, R\{w_2, w_4\}, R\{w_6, w_8\},$ $R\{v_1, v_5\}, R\{w_1, w_5\}, R\{x_2, x_3\},$ $R\{x_5, x_6\}, R\{x_1, x_4\}, R\{x_1, x_6\}$
$R\{v_3, v_5\}$	$V(\mathbb{B}_6) - \{v_4, v_7\} \cup \{w_4, w_7\}$	$R\{v_1, v_7\}, R\{w_3, w_5\}, R\{w_1, w_7\},$ $R\{w_2, w_6\}, R\{x_3, x_4\}, R\{x_6, x_7\},$ $R\{x_2, x_5\}, R\{x_2, x_7\}, R\{v_2, v_6\}$
$R\{y_1, z_4\}$	$V(\mathbb{B}_6) - \{x_3, x_6\} \cup \{y_3, y_6\}$	
$R\{y_2, z_5\}$	$V(\mathbb{B}_6) - \{x_1, x_4\} \cup \{y_1, y_4\}$	
$R\{y_3, z_6\}$	$V(\mathbb{B}_6) - \{x_2, x_5\} \cup \{y_2, y_5\}$	
$R\{v_1, w_4\}$	$V(\mathbb{B}_6) - \{v_3, v_6\} \cup \{w_2, w_6\}$	
$R\{v_2, w_5\}$	$V(\mathbb{B}_6) - \{v_1, v_4\} \cup \{w_1, y_2\}$	
$R\{v_3, w_6\}$	$V(\mathbb{B}_6) - \{v_2, v_5\} \cup \{w_2, w_4\}$	

TABLE 4: The representation of  $R_u$  for  $82 \leq u \leq 136$ .

RNs	Elements	Equality
$R\{v_1, y_3\}$	$V(\mathbb{B}_6) - \{w_1\} \cup \{y_1\} \cup \{z_3\}$	$R\{v_4, y_6\}$
$R\{v_2, y_4\}$	$V(\mathbb{B}_6) - \{w_2\} \cup \{y_2\} \cup \{z_4\}$	$R\{v_1, y_5\}$
$R\{v_3, y_5\}$	$V(\mathbb{B}_6) - \{w_3\} \cup \{y_3\} \cup \{z_5\}$	$R\{v_2, y_6\}$
$R\{v_1, z_4\}$	$V(\mathbb{B}_6) - \{w_5\} \cup \{x_5\} \cup \{y_6\}$	
$R\{v_2, z_5\}$	$V(\mathbb{B}_6) - \{w_6\} \cup \{y_6\} \cup \{y_1\}$	
$R\{v_3, z_6\}$	$V(\mathbb{B}_6) - \{w_1\} \cup \{y_1\} \cup \{y_2\}$	
$R\{v_1, w_2\}$	$V(\mathbb{B}_6) - \{v_2, v_3, v_4\}$	$R\{v_5, w_4\}$
$R\{v_2, w_3\}$	$V(\mathbb{B}_6) - \{v_3, v_4, v_5\}$	$R\{v_6, w_5\}$
$R\{v_3, w_4\}$	$V(\mathbb{B}_6) - \{v_4, v_5, v_6\}$	
$R\{v_4, w_5\}$	$V(\mathbb{B}_6) - \{v_1, v_5, v_6\}$	$R\{v_2, w_1\}$
$R\{v_5, w_6\}$	$V(\mathbb{B}_6) - \{v_1, v_2, v_6\}$	$R\{v_3, w_2\}$
$R\{v_1, w_6\}$	$V(\mathbb{B}_6) - \{z_1, v_2, v_3\}$	$R\{v_4, w_3\}$
$R\{v_1, z_2\}$	$V(\mathbb{B}_6) - \{z_2, z_3, z_4\}$	$R\{v_5, z_4\}$
$R\{v_2, z_3\}$	$V(\mathbb{B}_6) - \{z_3, z_4, z_5\}$	$R\{v_6, z_5\}$
$R\{v_3, z_4\}$	$V(\mathbb{B}_6) - \{z_4, z_5, z_6\}$	
$R\{v_4, z_5\}$	$V(\mathbb{B}_6) - \{z_1, z_5, z_6\}$	$R\{v_2, z_1\}$
$R\{v_5, z_6\}$	$V(\mathbb{B}_6) - \{z_1, z_2, z_6\}$	$R\{v_3, z_2\}$
$R\{v_1, z_6\}$	$V(\mathbb{B}_6) - \{z_1, z_2, z_3\}$	$R\{v_4, z_3\}$
$R\{v_1, x_2\}$	$V(\mathbb{B}_6) - \{z_3, z_4\} \cup \{x_1\}$	
$R\{v_2, x_3\}$	$V(\mathbb{B}_6) - \{z_4, z_5\} \cup \{x_2\}$	
$R\{v_3, x_4\}$	$V(\mathbb{B}_6) - \{z_5, z_6\} \cup \{x_3\}$	
$R\{v_4, x_5\}$	$V(\mathbb{B}_6) - \{z_1, z_6\} \cup \{x_4\}$	
$R\{v_5, x_6\}$	$V(\mathbb{B}_6) - \{z_1, z_2\} \cup \{x_5\}$	
$R\{v_1, x_6\}$	$V(\mathbb{B}_6) - \{z_2, z_3\} \cup \{x_6\}$	
$R\{v_2, x_1\}$	$V(\mathbb{B}_6) - \{z_5, z_6\} \cup \{x_1\}$	
$R\{v_3, x_2\}$	$V(\mathbb{B}_6) - \{z_1, z_6\} \cup \{x_2\}$	
$R\{v_4, x_3\}$	$V(\mathbb{B}_6) - \{z_1, z_2\} \cup \{x_3\}$	
$R\{v_5, x_4\}$	$V(\mathbb{B}_6) - \{z_2, z_3\} \cup \{x_4\}$	
$R\{v_6, x_5\}$	$V(\mathbb{B}_6) - \{z_3, z_4\} \cup \{x_5\}$	
$R\{w_1, z_2\}$	$V(\mathbb{B}_6) - \{z_3, z_4\} \cup \{y_1\}$	
$R\{w_2, z_3\}$	$V(\mathbb{B}_6) - \{w_4, z_5\} \cup \{y_2\}$	
$R\{w_3, z_4\}$	$V(\mathbb{B}_6) - \{w_5, w_6\} \cup \{y_3\}$	
$R\{w_4, z_5\}$	$V(\mathbb{B}_6) - \{w_1, w_6\} \cup \{y_4\}$	
$R\{w_5, z_6\}$	$V(\mathbb{B}_6) - \{w_1, w_2\} \cup \{y_5\}$	
$R\{w_1, z_6\}$	$V(\mathbb{B}_6) - \{w_2, w_3\} \cup \{y_6\}$	
$R\{w_2, z_1\}$	$V(\mathbb{B}_6) - \{w_5, w_6\} \cup \{y_1\}$	
$R\{w_3, z_2\}$	$V(\mathbb{B}_6) - \{w_1, w_6\} \cup \{y_2\}$	
$R\{w_4, z_3\}$	$V(\mathbb{B}_6) - \{w_1, w_2\} \cup \{y_3\}$	
$R\{w_5, z_4\}$	$V(\mathbb{B}_6) - \{w_2, w_3\} \cup \{y_4\}$	
$R\{w_6, z_5\}$	$V(\mathbb{B}_6) - \{w_3, w_4\} \cup \{y_5\}$	
$R\{w_1, z_6\}$	$V(\mathbb{B}_6) - \{w_4, w_5\} \cup \{y_6\}$	

TABLE 5: The representation of  $R_u$  for  $137 \leq u \leq 174$ .

RNs	Elements	Equality
$R\{v_1, z_3\}$	$V(\mathbb{B}_6) - \{w_3\} \cup \{y_1\}$	$R\{v_4, y_6\}$
$R\{v_2, z_4\}$	$V(\mathbb{B}_6) - \{w_4\} \cup \{y_2\}$	$R\{v_1, y_5\}$
$R\{v_3, z_5\}$	$V(\mathbb{B}_6) - \{w_5\} \cup \{y_3\}$	
$R\{v_4, z_6\}$	$V(\mathbb{B}_6) - \{w_6\} \cup \{y_4\}$	
$R\{v_1, z_5\}$	$V(\mathbb{B}_6) - \{w_2\} \cup \{y_5\}$	
$R\{v_2, z_6\}$	$V(\mathbb{B}_6) - \{w_1\} \cup \{y_6\}$	
$R\{w_1, z_4\}$	$V(\mathbb{B}_6) - \{x_3\} \cup \{y_2\}$	
$R\{w_2, z_5\}$	$V(\mathbb{B}_6) - \{x_4\} \cup \{y_3\}$	
$R\{w_3, z_6\}$	$V(\mathbb{B}_6) - \{x_5\} \cup \{y_4\}$	
$R\{w_1, z_3\}$	$V(\mathbb{B}_6) - \{x_4\} \cup \{y_5\}$	
$R\{w_2, z_4\}$	$V(\mathbb{B}_6) - \{x_4\} \cup \{y_6\}$	
$R\{w_3, z_5\}$	$V(\mathbb{B}_6) - \{x_5\} \cup \{y_1\}$	
$R\{w_4, z_6\}$	$V(\mathbb{B}_6) - \{x_6\} \cup \{y_2\}$	
$R\{w_1, z_5\}$	$V(\mathbb{B}_6) - \{x_1\} \cup \{y_3\}$	
$R\{w_2, z_6\}$	$V(\mathbb{B}_6) - \{x_2\} \cup \{y_4\}$	
$R\{v_1, y_4\}$	$V(\mathbb{B}_6) - \{w_3\} \cup \{y_1\}$	
$R\{v_2, y_5\}$	$V(\mathbb{B}_6) - \{w_4\} \cup \{y_2\}$	
$R\{v_3, y_6\}$	$R\{v_1, y_4\}$	
$R\{v_1, y_3\}$	$V(\mathbb{B}_6) - \{v_4\} \cup \{w_5\}$	
$R\{v_2, y_4\}$	$V(\mathbb{B}_6) - \{v_5\} \cup \{w_6\}$	
$R\{v_3, y_5\}$	$V(\mathbb{B}_6) - \{v_6\} \cup \{w_1\}$	
$R\{v_4, y_6\}$	$V(\mathbb{B}_6) - \{v_1\} \cup \{w_2\}$	
$R\{v_1, y_5\}$	$V(\mathbb{B}_6) - \{v_2\} \cup \{w_3\}$	
$R\{v_2, y_6\}$	$V(\mathbb{B}_6) - \{v_3\} \cup \{w_4\}$	
$R\{x_1, y_1\}$	$V(\mathbb{B}_6) - \{v_2, v_6\}$	$R\{y_1, z_1\}$
$R\{x_2, y_2\}$	$V(\mathbb{B}_6) - \{v_1, v_3\}$	$R\{y_2, z_2\}$
$R\{x_3, y_3\}$	$V(\mathbb{B}_6) - \{v_2, v_4\}$	$R\{y_3, z_3\}$
$R\{x_4, y_4\}$	$V(\mathbb{B}_6) - \{v_3, v_5\}$	$R\{y_4, z_4\}$
$R\{x_5, y_5\}$	$V(\mathbb{B}_6) - \{v_4, v_6\}$	$R\{y_5, z_5\}$
$R\{x_6, y_6\}$	$V(\mathbb{B}_6) - \{v_1, v_5\}$	$R\{y_6, z_6\}$

TABLE 6: The representation of  $R_u$  for  $175 \leq u \leq 180$ .

RNs	Elements
$R\{v_1, w_1\}$	$R\{v_2, w_2\}$
$R\{v_3, w_3\}$	$R\{v_4, w_4\}$
$R\{v_5, w_5\}$	$R\{v_5, w_5\}$

$V(\mathbb{B}_6)$

TABLE 7: The representation of  $R_r$  for  $1 \leq r \leq 12$ .

RNs	Elements
$R_1 = R\{w_1, x_1\}$	$V(\mathbb{B}_6) - \{v_2, v_3, v_4\} \cup \{w_2, w_3, w_4\} \cup \{x_2, x_3\}$
$R_2 = R\{w_2, x_2\}$	$V(\mathbb{B}_6) - \{v_3, v_4, v_5\} \cup \{w_3, w_4, w_5\} \cup \{x_3, x_4\}$
$R_3 = R\{w_3, x_3\}$	$V(\mathbb{B}_6) - \{v_4, v_5, v_6\} \cup \{w_4, w_5, w_6\} \cup \{x_4, x_5\}$
$R_4 = R\{w_4, x_4\}$	$V(\mathbb{B}_6) - \{v_1, v_5, v_6\} \cup \{w_1, w_5, w_6\} \cup \{x_5, x_6\}$
$R_5 = R\{w_5, x_5\}$	$V(\mathbb{B}_6) - \{v_1, v_2, v_6\} \cup \{w_1, w_2, w_6\} \cup \{x_1, x_6\}$
$R_6 = R\{w_6, x_6\}$	$V(\mathbb{B}_6) - \{v_1, v_2, v_3\} \cup \{w_1, w_2, w_3\} \cup \{x_1, x_2\}$
$R_7 = R\{w_2, x_1\}$	$V(\mathbb{B}_6) - \{v_1, v_5, v_6\} \cup \{w_1, w_5, w_6\} \cup \{x_5, x_6\}$
$R_8 = R\{w_3, x_2\}$	$V(\mathbb{B}_6) - \{v_1, v_2, v_6\} \cup \{w_1, w_2, w_6\} \cup \{x_1, x_6\}$
$R_9 = R\{w_4, x_3\}$	$V(\mathbb{B}_6) - \{v_1, v_2, v_3\} \cup \{w_1, w_2, w_3\} \cup \{x_1, x_2\}$
$R_{10} = R\{w_5, x_4\}$	$V(\mathbb{B}_6) - \{v_2, v_3, v_4\} \cup \{w_2, w_3, w_4\} \cup \{x_2, x_3\}$
$R_{11} = R\{w_6, x_5\}$	$V(\mathbb{B}_6) - \{v_3, v_4, v_5\} \cup \{w_3, w_4, w_5\} \cup \{x_3, x_4\}$
$R_{12} = R\{w_1, x_6\}$	$V(\mathbb{B}_6) - \{v_4, v_5, v_6\} \cup \{w_4, w_5, w_6\} \cup \{x_4, x_5\}$

- (h)  $|R_r| < |\dot{R}_{33}| = |R\{v_r, x_r\}| = |\dot{R}_{34}| = |R\{v_r, x_{r-1}\}| = 4m + 1$  and  $|\dot{R}_u \cap \cup_{r=1}^m R_r| \geq |R_r|$ , where  $p \geq 3$
- (i)  $|R_r| < |\dot{R}_{35}| = |R\{x_r, y_{r+1}\}| = 4m + 2$  and  $|\dot{R}_u \cap \cup_{r=1}^m R_r| \geq |R_r|$
- (j)  $|R_r| < |\dot{R}_{36}| = |R\{x_r, z_{r+1}\}| = 4m$  and  $|\dot{R}_u \cap \cup_{r=1}^m R_r| \geq |R_r|$
- (k)  $|R_r| < |\dot{R}_{37}| = |R\{v_r, w_{r+1}\}| = |\dot{R}_{38}| = |R\{v_r, y_r\}| = (9m/2)$  and  $|\dot{R}_u \cap \cup_{r=1}^m R_r| \geq |R_r|$
- (l)  $|R_r| < |\dot{R}_{39}| = |R\{v_r, x_{r+1}\}| = (9m/2) - 1$  and  $|\dot{R}_u \cap \cup_{r=1}^m R_r| \geq |R_r|$
- (m)  $|R_r| < |\dot{R}_{40}| = |R\{v_r, z_r\}| = |\dot{R}_{41}| = |R\{x_r, z_r\}| = (9m/2) + 1$  and  $|\dot{R}_u \cap \cup_{r=1}^m R_r| \geq |R_r|$
- (n)  $|R_r| < |\dot{R}_{42}| = |R\{v_r, w_r\}| = |\dot{R}_{43}| = |R\{x_r, y_r\}| = 5m$  and  $|\dot{R}_u \cap \cup_{r=1}^m R_r| \geq |R_r|$



TABLE 8: The representation of  $R_u$  for  $1 \leq u \leq 12$ .

RNs	Elements
$R\{w_1, x_1\}$	$V(C_6) - \{v_2, v_3, v_4\} \cup \{w_2, w_3, w_4\} \cup \{x_2, x_3\}$
$R\{w_2, x_2\}$	$V(C_6) - \{v_3, v_4, v_5\} \cup \{w_3, w_4, w_5\} \cup \{x_3, x_4\}$
$R\{w_3, x_3\}$	$V(C_6) - \{v_4, v_5, v_6\} \cup \{w_4, w_5, w_6\} \cup \{x_4, x_5\}$
$R\{w_4, x_4\}$	$V(C_6) - \{v_1, v_5, v_6\} \cup \{w_1, w_5, w_6\} \cup \{x_5, x_6\}$
$R\{w_5, x_5\}$	$V(C_6) - \{v_1, v_2, v_6\} \cup \{w_1, w_2, w_6\} \cup \{x_1, x_6\}$
$R\{w_6, x_6\}$	$V(C_6) - \{v_1, v_2, v_3\} \cup \{w_1, w_2, w_3\} \cup \{x_1, x_2\}$
$R\{w_2, x_1\}$	$V(C_6) - \{v_1, v_5, v_6\} \cup \{w_1, w_5, w_6\} \cup \{x_5, x_6\}$
$R\{w_3, x_2\}$	$V(C_6) - \{v_1, v_2, v_6\} \cup \{w_1, w_2, w_6\} \cup \{x_1, x_6\}$
$R\{w_4, x_3\}$	$V(C_6) - \{v_1, v_2, v_3\} \cup \{w_1, w_2, w_3\} \cup \{x_1, x_2\}$
$R\{w_5, x_4\}$	$V(C_6) - \{v_2, v_3, v_4\} \cup \{w_2, w_3, w_4\} \cup \{x_2, x_3\}$
$R\{w_6, x_5\}$	$V(C_6) - \{v_3, v_4, v_5\} \cup \{w_3, w_4, w_5\} \cup \{x_3, x_4\}$
$R\{w_1, x_6\}$	$V(C_6) - \{v_4, v_5, v_6\} \cup \{w_4, w_5, w_6\} \cup \{x_4, x_5\}$

*Proof*

- (a) The RNs of  $\{y_l, z_l\}$  and  $\{y_r, z_{r-1}\}$  are  $R\{y_l, z_l\} = V(C_m) - \{v_h|h \equiv l+2, l+3, \dots, l+(m/2) \pmod{m}\} \cup \{w_h|h \equiv l+2, l+3, \dots, l+(m/2) \pmod{m}\} \cup \{y_h|h \equiv l-1, l-2, \dots, l-(m/2)+1 \pmod{m}\} \cup \{z_h|h \equiv l-1, l-2, \dots, l-(m/2) \pmod{m}\}$  and  $R\{y_r, z_{r-1}\} = V(C_m) - \{v_h|h \equiv r-2, r-3, \dots, r-(m/2) \pmod{m}\} \cup \{w_h|h \equiv r-2, r-3, \dots, r-(m/2) \pmod{m}\} \cup \{y_h|h \equiv r+1, r+2, \dots, r+(m/2)-1 \pmod{m}\} \cup \{z_h|h \equiv r+1, r+2, \dots, r+(m/2) \pmod{m}\}$ , respectively. We note that  $|R_r| = |R_l| = 3(m+1)$ ,  $\cup_{l=1}^m R_l = V(C_m)$ ,  $\cup_{r=1}^m R_r = V(C_m)$  and  $|\cup_{l=1}^m R_l \cup \cup_{r=1}^m R_r| = 5m$ . Also,  $|\cup_{l=1}^m R_l| = |\cup_{r=1}^m R_r| = 5m$ .
- (b) The RNs of  $\{w_r, x_r\}$  and  $\{w_r, x_{r-1}\}$  are  $\hat{R}_1 = R\{w_r, x_r\} = V(C_m) - \{v_h|h \equiv r+1, r+2, \dots, r+(m/2) \pmod{m}\} \cup \{w_h|h \equiv r+1, r+2, \dots, r+(m/2) \pmod{m}\} \cup \{x_h|h \equiv r+1, r+2, \dots, r+(m/2)-1 \pmod{m}\}$ ,  $\hat{R}_2 = R\{w_r, x_{r-1}\} = V(C_m) - \{v_h|h \equiv r-1, r-2, \dots, r-(m/2) \pmod{m}\} \cup \{w_h|h \equiv r-1, r-2, \dots, r-(m/2) \pmod{m}\} \cup \{x_h|h \equiv r-2, r-3, \dots, r-(m/2)+1 \pmod{m}\}$ , and  $R\{y_r, z_r\} = V(C_m) - \{x_h|h \equiv r-1, r-2, \dots, r-(m/2)+1 \pmod{m}\}$ , respectively. Clearly,  $|\hat{R}_u| = (7m/2) + 1$ . Since  $|R_r| = (7m/2) + 1 < |\hat{R}_u|$ , then  $|\hat{R}_u \cap \cup_{r=1}^m R_r| \geq |R_r|$ ,  $|R_r| < |\hat{R}_3| = |R\{v_r, v_{r+1}\}| = |\hat{R}_4| = |R\{v_r, v_{r+p}\}| = |\hat{R}_5| = |R\{w_r, w_{r+p}\}| = |\hat{R}_6| = |R\{w_r, w_{r+p}\}| = |\hat{R}_7| = |R\{x_r, x_{r+s}\}| = |\hat{R}_8| = |R\{x_r, x_{r+p}\}| = |\hat{R}_9| = |R\{x_r, x_{r+p}\}| = |\hat{R}_{10}| = |R\{y_r, y_{r+1}\}| = |\hat{R}_{11}| = |R\{y_r, y_{r+p}\}| = |\hat{R}_{12}| = |R\{z_r, z_{r+s}\}| = |\hat{R}_{13}| = |R\{v_r, w_{r+p}\}| = |\hat{R}_{14}| = |R\{v_r, w_{r+s}\}| = |\hat{R}_{15}| = |R\{w_r, z_{r+p}\}| = 5m-6$
- (c) The RNs of  $\{v_r, v_{r+1}\}, \{v_r, v_{r+p}\}, \{w_r, w_{r+1}\}, \{w_r, w_{r+p}\}, \{x_r, x_{r+s}\}, \{x_r, x_{r+1}\}, \{x_r, x_{r+p}\}, \{y_r, y_{r+1}\}, \{y_r, y_{r+p}\}, \{z_r, z_{r+s}\}$  and  $\{v_r, w_{r+p}\}$  are  $\hat{R}_3 = R\{v_r, v_{r+1}\} = V(C_m) - \{x_h|h \equiv r + ((p-1)/2), r + ((p+m-1)/2) \pmod{m}\} \cup \{y_h|h \equiv r + ((p-1)/2), r + ((p+m-1)/2) \pmod{m}\} \cup \{z_h|h \equiv r + ((p-1)/2), r - ((p-1)/2) \pmod{m}\} = \hat{R}_5 = R\{w_r, w_{r+1}\}$ ,  $\hat{R}_4 = R\{v_r, v_{r+p}\} =$

- $V(C_m) - \{x_h|h \equiv r + ((p-1)/2), r + ((p+m-1)/2) \pmod{m}\} \cup \{y_h|h \equiv r + ((p-1)/2), r + ((p+m-1)/2) \pmod{m}\} \cup \{z_h|h \equiv r + ((p-1)/2), r - ((p-1)/2) \pmod{m}\} = \hat{R}_6 = R\{w_r, w_{r+p}\}$ ,  $\hat{R}_7 = R\{v_r, v_{r+s}\} = V(C_m) - \{v_h|r + (s/2), r + ((s+m)/2) \pmod{m}\} \cup \{w_h|r + (s/2), r + ((s+m)/2) \pmod{m}\} \cup \{z_h|r + ((s-2)/2), r + ((s+m-2)/2) \pmod{m}\} = \hat{R}_8 = R\{w_r, w_{r+s}\} = \hat{R}_9 = R\{x_r, x_{r+p}\} = \hat{R}_{11} = R\{y_r, y_{r+p}\}$ ,  $\hat{R}_{12} = R\{z_r, z_{r+s}\} = V(C_m) - \{v_h|h \equiv r + ((s+2)/2), r + ((s+m+2)/2) \pmod{m}\} \cup \{w_h|h \equiv r + ((s+2)/2), r + ((s+m+2)/2) \pmod{m}\} \cup \{z_h|r + (s/2), r + ((s+m)/2) \pmod{m}\} = \hat{R}_{13} = R\{v_r, w_{r+p}\} = V(C_m) - \{v_h|h \equiv r + ((p+1)/2), r + ((p+m-1)/2) \pmod{m}\} \cup \{w_h|h \equiv r + ((p-1)/2), r - ((p-1)/2) \pmod{m}\} \cup \{z_h|h \equiv r + ((p-3)/2), r + ((p+m-1)/2) \pmod{m}\}$ , and  $\hat{R}_8 = R\{x_r, x_{r+1}\} = R\{v_r, v_{r+2}\} = \hat{R}_{10} = R\{y_r, y_{r+1}\}$ . Clearly,  $|\hat{R}_u| = 5m-6$ . Since  $|R_r| = (7m/2) + 1 < |\hat{R}_u|$ , then  $|\hat{R}_u \cap \cup_{r=1}^m R_r| = 5m-6 \geq |R_r|$ .
- (d) The RN's of  $\{z_r, z_{r+p}\}, \{v_r, z_{r+s}\}, \{w_r, x_{r+p}\}, \{w_r, y_{r+s}\}, \{x_r, y_{r+s}\}$  and  $\{x_r, z_{r+s}\}$  are  $\hat{R}_{14} = R\{z_r, z_{r+p}\} = V(C_m) - \{x_h|h \equiv r + ((p+1)/2), r + ((p+1+m)/2) \pmod{m}\} \cup \{y_h|h \equiv r + ((p+1)/2), r + ((p+1+m)/2) \pmod{m}\}$ ,  $\hat{R}_{15} = R\{v_r, z_{r+s}\} = V(C_m) - \{x_h|h \equiv r + (s/2), r + ((s+m)/2) \pmod{m}\} \cup \{w_h|h \equiv r + ((s+2)/2), r + ((s+m)/2) \pmod{m}\} = \hat{R}_{16} = R\{w_r, x_{r+p}\} = V(C_m) - \{w_h|h \equiv r + ((p+1)/2) \pmod{m}\} \cup \{v_h|h \equiv r + ((p+1)/2) \pmod{m}\} \cup \{y_h|h \equiv r + ((p-1)/2) \pmod{m}\} \cup \{x_h|h \equiv r + ((p+m-1)/2) \pmod{m}\}$ ,  $\hat{R}_{17} = R\{w_r, y_{r+s}\} = V(C_m) - \{x_h|h \equiv r + (s/2) \pmod{m}\} \cup \{v_h|h \equiv r + ((s+2)/2) \pmod{m}\} \cup \{z_h|h \equiv r - (s/2), r - ((s+2)/2) \pmod{m}\}$ ,  $\hat{R}_{18} = R\{x_r, y_{r+s}\} = V(C_m) - \{v_h|h \equiv r + ((s+2)/2), r + ((m+s)/2) \pmod{m}\} \cup \{w_h|h \equiv r + ((s+2)/2), r + ((m+s)/2) \pmod{m}\} = \hat{R}_{19} = R\{x_r, z_{r+s}\} = V(C_m) - \{v_h|h \equiv r + ((s+4)/2), r + ((m+s)/2) \pmod{m}\} \cup \{w_h|h \equiv r + ((s+4)/2), r + ((m+s)/2) \pmod{m}\}$ , respectively. We can see that, for  $9 \leq u \leq 14$ ,  $|\hat{R}_u| = 5m-4 > |R_r|$  and  $|\hat{R}_u \cap \cup_{t=1}^m R_t| \geq |R_t|$ .
- (e) The RNs of  $\{v_r, x_{r+p}\}, \{v_r, x_{r+s}\}, \{v_r, y_{r+s}\}, \{w_r, y_{r+p}\}, \{w_r, z_{r+s}\}, \{y_r, z_{r+s}\}$ , and  $\{x_r, z_{r+p}\}$  are  $\hat{R}_{20} = R\{v_r, x_{r+p}\} = V(C_m) - \{v_h|h \equiv r + ((m+p-1)/2) \pmod{m}\} \cup \{w_h|h \equiv r + ((m+p+1)/2) \pmod{m}\} \cup \{x_h|h \equiv r + ((p-1)/2) \pmod{m}\} = \hat{R}_{21} = R\{v_r, x_{r+s}\} = V(C_m) - \{v_h|h \equiv r + ((s+2)/2) \pmod{m}\} \cup \{w_h|h \equiv r + (s/2) \pmod{m}\} \cup \{x_h|h \equiv r + ((m+s)/2) \pmod{m}\}$ ,  $\hat{R}_{22} = R\{v_r, y_{r+s}\} = V(C_m) - \{v_h|h \equiv r + ((s+m-2)/2) \pmod{m}\} \cup \{x_h|h \equiv r + ((s+m)/2) \pmod{m}\} \cup \{y_h|h \equiv r + ((s-2)/2) \pmod{m}\}$

TABLE 9: The representation of  $\hat{R}_u$  for  $13 \leq u \leq 67$ .

RNs	Elements	Equality
$R\{v_1, v_2\}$	$V(C_6) - \{x_1, x_4\} \cup \{y_1, y_4\} \cup \{z_1, z_6\}$	$R\{v_1, v_2\}, R\{w_1, w_2\}, R\{w_1, w_2\},$
$R\{v_2, v_3\}$	$V(C_6) - \{x_2, x_5\} \cup \{y_2, y_5\} \cup \{z_1, z_2\}$	$\{v_1, v_4\}, R\{w_2, w_3\}, R\{w_1, w_4\},$
$R\{v_3, v_4\}$	$V(C_6) - \{x_3, x_6\} \cup \{y_3, y_6\} \cup \{z_2, z_3\}$	$R\{v_2, v_5\}, R\{w_3, w_4\}, R\{w_2, w_5\},$
$R\{v_4, v_5\}$	$V(C_6) - \{x_1, x_4\} \cup \{y_1, y_4\} \cup \{z_3, z_4\}$	$R\{v_4, v_7\}, R\{w_4, w_7\}$
$R\{v_5, v_6\}$	$V(C_6) - \{x_2, x_5\} \cup \{y_2, y_5\} \cup \{z_4, z_5\}$	$R\{v_3, v_6\}, R\{w_4, w_5\}, R\{w_3, w_6\},$
$R\{v_1, v_6\}$	$V(C_6) - \{x_3, x_6\} \cup \{y_3, y_6\} \cup \{z_5, z_6\}$	$R\{w_5, w_6\},$
$R\{v_1, v_3\}$	$V(C_6) - \{v_2, v_5\} \cup \{w_2, w_5\} \cup \{z_1, z_4\}$	$R\{w_1, w_6\}, R\{v_1, v_4\},$
$R\{v_2, v_4\}$	$V(C_6) - \{v_3, v_6\} \cup \{w_3, w_6\} \cup \{z_2, z_5\}$	$R\{w_1, w_6\}, R\{v_4, v_6\}, R\{y_1, y_2\}$
$R\{v_3, v_5\}$	$V(C_6) - \{v_1, v_4\} \cup \{w_1, w_4\} \cup \{z_3, z_6\}$	$R\{y_4, y_5\}, R\{y_3, y_6\}, R\{z_2, z_6\}, R\{z_4, z_6\}$
$R\{v_1, w_4\}$	$V(C_6) - \{v_1, v_4\} \cup \{w_1, w_4\} \cup \{z_3, z_6\}$	$R\{w_1, w_6\}, R\{v_1, v_5\}, R\{y_2, y_3\}$
$R\{v_1, w_4\}$	$V(C_6) - \{v_3, v_5\} \cup \{w_2, w_6\} \cup \{z_1, z_5\}$	$R\{y_5, y_6\}, R\{y_1, y_4\}, R\{z_1, z_3\}$
$R\{v_2, w_5\}$	$V(C_6) - \{v_2, v_6\} \cup \{w_1, w_3\} \cup \{z_2, z_6\}$	$R\{w_1, w_6\}, R\{v_2, v_6\}, R\{y_3, y_4\}$
$R\{v_3, w_6\}$	$V(C_6) - \{v_1, v_5\} \cup \{w_2, w_4\} \cup \{z_1, z_3\}$	$R\{y_1, y_6\}, R\{y_2, y_5\}, R\{z_2, z_4\}$
$R\{v_1, x_1\}$	$V(C_6) - \{w_1, w_5, w_6\} \cup \{x_4, x_5, x_6\}$	$R\{w_1, w_6\}, R\{v_2, v_6\}, R\{y_3, y_4\}$
$R\{v_2, x_2\}$	$V(C_6) - \{w_1, w_2, w_6\} \cup \{x_1, x_5, x_6\}$	$R\{y_1, y_6\}, R\{y_2, y_5\}, R\{z_2, z_4\}$
$R\{v_3, x_3\}$	$V(C_6) - \{w_1, w_2, w_3\} \cup \{x_1, x_2, x_6\}$	$R\{y_1, y_6\}, R\{y_2, y_5\}, R\{z_2, z_4\}$
$R\{v_4, x_4\}$	$V(C_6) - \{w_2, w_3, w_4\} \cup \{x_1, x_2, x_3\}$	$R\{y_1, y_6\}, R\{y_2, y_5\}, R\{z_2, z_4\}$
$R\{v_5, x_5\}$	$V(C_6) - \{w_3, w_4, w_5\} \cup \{x_2, x_3, x_4\}$	$R\{y_1, y_6\}, R\{y_2, y_5\}, R\{z_2, z_4\}$
$R\{v_6, x_6\}$	$V(C_6) - \{w_4, w_5, w_6\} \cup \{x_3, x_4, x_5\}$	$R\{y_1, y_6\}, R\{y_2, y_5\}, R\{z_2, z_4\}$
$R\{v_2, x_1\}$	$V(C_6) - \{w_2, w_3, w_4\} \cup \{x_3, x_4, x_5\}$	$R\{y_1, y_6\}, R\{y_2, y_5\}, R\{z_2, z_4\}$
$R\{v_3, x_2\}$	$V(C_6) - \{w_3, w_4, w_4\} \cup \{x_4, x_5, x_6\}$	$R\{y_1, y_6\}, R\{y_2, y_5\}, R\{z_2, z_4\}$
$R\{v_4, x_3\}$	$V(C_6) - \{w_4, w_5, w_6\} \cup \{x_1, x_5, x_6\}$	$R\{y_1, y_6\}, R\{y_2, y_5\}, R\{z_2, z_4\}$
$R\{v_5, x_4\}$	$V(C_6) - \{w_1, w_5, w_6\} \cup \{x_1, x_2, x_6\}$	$R\{y_1, y_6\}, R\{y_2, y_5\}, R\{z_2, z_4\}$
$R\{v_6, x_5\}$	$V(C_6) - \{w_1, w_2, w_6\} \cup \{x_1, x_2, x_3\}$	$R\{y_1, y_6\}, R\{y_2, y_5\}, R\{z_2, z_4\}$
$R\{v_1, x_6\}$	$V(C_6) - \{w_1, w_2, w_3\} \cup \{x_2, x_3, x_4\}$	$R\{y_1, y_6\}, R\{y_2, y_5\}, R\{z_2, z_4\}$

TABLE 10: The representation of  $\hat{R}_u$  for  $68 \leq u \leq 79$ .

RNs	Elements
$R\{y_1, z_4\}$	$V(C_6) - \{v_3, v_6\} \cup \{w_3, w_6\} \cup \{z_2\}$
$R\{y_2, z_5\}$	$V(C_6) - \{v_1, v_4\} \cup \{w_1, w_4\} \cup \{z_3\}$
$R\{y_3, z_6\}$	$V(C_6) - \{v_2, v_5\} \cup \{w_2, w_5\} \cup \{z_4\}$
$R\{w_1, z_4\}$	$V(C_6) - \{x_3, x_6\} \cup \{y_2, y_6\} \cup \{w_4\}$
$R\{w_2, z_5\}$	$V(C_6) - \{x_1, x_4\} \cup \{y_1, y_3\} \cup \{w_5\}$
$R\{w_3, z_6\}$	$V(C_6) - \{x_2, x_5\} \cup \{y_1, y_2\} \cup \{w_6\}$
$R\{v_1, x_2\}$	$V(C_6) - \{v_2, v_3, v_4\} \cup \{x_1\} \cup \{w_5\}$
$R\{v_2, x_3\}$	$V(C_6) - \{v_3, v_4, v_5\} \cup \{x_2\} \cup \{w_6\}$
$R\{v_3, x_4\}$	$V(C_6) - \{v_4, v_5, v_6\} \cup \{x_3\} \cup \{w_1\}$
$R\{v_4, x_5\}$	$V(C_6) - \{v_1, v_5, v_6\} \cup \{x_4\} \cup \{w_2\}$
$R\{v_5, x_6\}$	$V(C_6) - \{v_1, v_2, v_3\} \cup \{x_5\} \cup \{w_3\}$
$R\{v_1, x_6\}$	$V(C_6) - \{v_2, v_3, v_4\} \cup \{x_6\} \cup \{w_4\}$

$(\text{modn})\}, \hat{R}_{23} = R\{w_r, y_{r+p}\} = V(C_m) - \{w_h|h \equiv r + ((p+1)/2) (\text{modn})\} \cup \{y_h|h \equiv r - ((p-1)/2) (\text{modn})\} \cup \{z_h|h \equiv r + ((p-3)/2) (\text{modn})\}$ ,  $\hat{R}_{24} = R\{w_r, z_{r+s}\} = V(C_m) - \{v_h|h \equiv r + s + 1 (\text{modn})\} \cup \{w_h|h \equiv r + s + 1 (\text{modn})\} \cup \{z_n\}$ ,  $\hat{R}_{25} = R\{y_r, z_{r+s}\} = V(C_m) - \{v_h|h \equiv r + ((s+2)/2) (\text{modn})\} \cup \{w_h|h \equiv r + ((s+2)/2) (\text{modn})\} \cup \{x_h|h \equiv r + (s/2) (\text{modn})\}$  and  $\hat{R}_{26} = R\{x_r, z_{r+p}\} = V(C_m) - \{v_h|h \equiv r + p (\text{modn})\} \cup \{w_h|h \equiv r + p (\text{modn})\} \cup \{x_h|h \equiv r + p - 1 (\text{modn})\}$ , respectively. We can see that, for

$17 \leq u \leq 23$ ,  $|\hat{R}_u| = 5m - 3 > |R_t|$  and  $|\hat{R}_u \cap \cup_{t=1}^m R_t| \geq |R_t|$ .

- (f) The RNs of  $\{w_r, y_r\}, \{v_r, y_{r+p}\}, \{w_r, z_r\}$  and  $\{x_r, y_{r+p}\}$  are  $\hat{R}_{27} = R\{w_r, y_r\} = V(C) - \{x_h|h \equiv r (\text{modm})\} \cup \{y_h|h \equiv r - 1 (\text{modm})\}$ ,  $\hat{R}_{28} = R\{w_r, z_r\} = V(C) - \{x_h|h \equiv r + 1, r + 2 (\text{modm})\}$ ,  $\hat{R}_{29} = R\{v_r, y_{r+p}\} = V(C) - \{w_h|h \equiv r + ((p+1)/2) (\text{modm})\} \cup \{x_h|h \equiv r + ((p-1)/2) (\text{modm})\}$  and  $\hat{R}_{30} = R\{x_r, y_{r+p}\} = V(C) - \{x_h|h \equiv r + ((p+1)/2), r - ((p+1)/2) (\text{modm})\}$ , respectively. Clearly,  $|\hat{R}_u| = 5m - 2$  for  $27 \leq u \leq 30$  and  $|\hat{R}_u \cap \cup_{r=1}^m R_r| \geq |R_r|$ .
- (g) The RNs of  $\{w_r, z_{r+p}\}$  and  $\{y_r, z_{r+p}\}$  is  $\hat{R}_{31} = V(C_m) - \{v_h|r \equiv r + ((p+3)/2), r + ((p+m+1)/2) (\text{modm})\} \cup \{w_h|r \equiv r + ((p+3)/2), r + ((p+m+1)/2) (\text{modm})\} \cup \{z_h|r \equiv r + ((p-1)/2) (\text{modm})\}$  and  $\hat{R}_{32} = R\{w_r, z_{r+p}\} = V(C_m) - \{x_h|h \equiv r + ((p+1)/2), r + ((p+m+1)/2) (\text{modm})\} \cup \{y_h|h \equiv r + ((p-1)/2), r - ((p-1)/2) (\text{modm})\} \cup \{w_h|h \equiv r + ((p+3)/2) (\text{modm})\}$ , respectively. Clearly,  $|\hat{R}_{29}| > |R_t|$  and  $|\hat{R}_u \cap \cup_{r=1}^m R_r| \geq |R_r|$ .
- (h) The RNs of  $\{v_r, x_r\}$  and  $\{v_r, x_{r-1}\}$  are  $\hat{R}_{33} = R\{v_r, x_r\} = V(C_m) - \{w_h|h \equiv r, r - 1, r - 2, \dots, r - (n/2) +$

TABLE 11: The representation of  $R_u$  for  $80 \leq u \leq 127$ .

RNs	Elements	Equality
$R\{z_1, z_2\}$	$V(C_6) - \{x_2, x_5\} \cup \{y_2, y_5\}$	$R\{z_4, z_5\}, R\{z_3, z_6\}$
$R\{z_2, z_3\}$	$V(C_6) - \{x_3, x_6\} \cup \{y_3, y_6\}$	$R\{z_5, z_6\}, R\{z_1, z_4\}$
$R\{z_3, z_4\}$	$V(C_6) - \{x_1, x_4\} \cup \{y_3, y_6\}$	$R\{z_1, z_6\}, R\{z_2, z_5\}$
$R\{v_1, z_3\}$	$V(C_6) - \{x_2, x_5\} \cup \{w_3, w_5\}$	$R\{w_4, z_6\}$
$R\{v_2, z_4\}$	$V(C_6) - \{x_3, x_6\} \cup \{w_4, w_6\}$	$R\{w_1, z_5\}$
$R\{v_3, z_5\}$	$V(C_6) - \{x_1, x_4\} \cup \{w_1, w_5\}$	$R\{w_2, z_6\}$
$R\{w_1, x_4\}$	$V(C_6) - \{w_3\} \cup \{v_3\} \cup \{y_2\} \cup \{x_5\}$	
$R\{w_2, x_5\}$	$V(C_6) - \{w_4\} \cup \{v_4\} \cup \{y_3\} \cup \{x_6\}$	
$R\{w_3, x_6\}$	$V(C_6) - \{w_5\} \cup \{v_5\} \cup \{y_4\} \cup \{x_1\}$	
$R\{w_1, x_3\}$	$V(C_6) - \{x_2\} \cup \{v_3\} \cup \{z_5, z_6\}$	
$R\{w_2, x_4\}$	$V(C_6) - \{x_3\} \cup \{v_4\} \cup \{z_1, z_6\}$	
$R\{w_3, x_5\}$	$V(C_6) - \{x_4\} \cup \{v_5\} \cup \{z_1, z_2\}$	
$R\{w_4, x_6\}$	$V(C_6) - \{x_5\} \cup \{v_6\} \cup \{z_2, z_3\}$	
$R\{w_1, x_5\}$	$V(C_6) - \{x_6\} \cup \{v_1\} \cup \{z_3, z_4\}$	
$R\{w_2, x_6\}$	$V(C_6) - \{x_1\} \cup \{v_2\} \cup \{z_4, z_5\}$	
$R\{x_1, y_3\}$	$V(C_6) - \{v_3, v_5\} \cup \{w_3, w_5\}$	
$R\{x_2, y_4\}$	$V(C_6) - \{v_4, v_6\} \cup \{w_4, w_6\}$	
$R\{x_3, y_5\}$	$V(C_6) - \{v_1, v_5\} \cup \{w_1, w_5\}$	
$R\{x_4, y_6\}$	$V(C_6) - \{v_2, v_6\} \cup \{w_2, w_6\}$	
$R\{x_1, y_5\}$	$V(C_6) - \{v_1, v_3\} \cup \{w_1, w_3\}$	
$R\{x_2, y_6\}$	$V(C_6) - \{v_2, v_4\} \cup \{w_2, w_4\}$	
$R\{x_1, z_3\}$	$V(C_6) - \{v_4, v_5\} \cup \{w_4, w_5\}$	
$R\{x_2, z_4\}$	$V(C_6) - \{v_5, v_6\} \cup \{w_6, w_6\}$	
$R\{x_3, z_5\}$	$V(C_6) - \{v_1, v_6\} \cup \{w_1, w_6\}$	
$R\{x_4, z_6\}$	$V(C_6) - \{v_1, v_2\} \cup \{w_1, w_2\}$	
$R\{x_1, z_5\}$	$V(C_6) - \{v_2, v_3\} \cup \{w_2, w_3\}$	
$R\{x_2, z_6\}$	$V(C_6) - \{v_3, v_4\} \cup \{w_3, w_4\}$	
$R\{x_1, y_2\}$	$V(C_6) - \{y_5, y_6\} \cup \{z_5, z_6\}$	
$R\{x_2, y_3\}$	$V(C_6) - \{y_1, y_6\} \cup \{z_1, z_6\}$	
$R\{x_3, y_4\}$	$V(C_6) - \{y_1, y_2\} \cup \{z_1, z_2\}$	
$R\{x_4, y_5\}$	$V(C_6) - \{y_2, y_3\} \cup \{z_2, z_3\}$	
$R\{x_5, y_6\}$	$V(C_6) - \{y_3, y_4\} \cup \{z_3, z_4\}$	
$R\{x_1, y_6\}$	$V(C_6) - \{y_4, y_5\} \cup \{z_4, z_5\}$	
$R\{v_1, z_1\}$	$V(C_6) - \{w_3, w_4\} \cup \{x_1, x_4\}$	
$R\{v_2, z_2\}$	$V(C_6) - \{w_4, w_5\} \cup \{x_2, x_5\}$	
$R\{v_3, z_3\}$	$V(C_6) - \{w_5, w_6\} \cup \{x_3, x_6\}$	
$R\{v_4, z_4\}$	$V(C_6) - \{w_1, w_6\} \cup \{x_1, x_4\}$	
$R\{v_5, z_5\}$	$V(C_6) - \{w_1, w_2\} \cup \{x_2, x_5\}$	
$R\{v_6, z_6\}$	$V(C_6) - \{w_2, w_3\} \cup \{x_3, x_6\}$	

TABLE 12: The representation of  $R_u$  for  $128 \leq u \leq 163$ .

RNs	Elements
$R\{v_1, x_4\}$	$V(C_6) - \{v_5\} \cup \{x_2\} \cup \{w_6\}$
$R\{v_2, x_5\}$	$V(C_6) - \{v_6\} \cup \{x_3\} \cup \{w_1\}$
$R\{v_1, w_3\}$	$V(C_6) - \{v_3\} \cup \{x_5\} \cup \{w_2\}$
$R\{v_2, w_4\}$	$V(C_6) - \{v_4\} \cup \{x_6\} \cup \{w_3\}$
$R\{v_3, w_5\}$	$V(C_6) - \{v_5\} \cup \{x_1\} \cup \{w_4\}$
$R\{v_4, w_6\}$	$V(C_6) - \{v_6\} \cup \{x_2\} \cup \{w_5\}$
$R\{v_1, w_5\}$	$V(C_6) - \{v_1\} \cup \{x_3\} \cup \{w_6\}$
$R\{v_2, w_6\}$	$V(C_6) - \{v_2\} \cup \{x_4\} \cup \{w_1\}$
$R\{v_1, y_3\}$	$V(C_6) - \{v_4\} \cup \{w_5\} \cup \{y_1\}$
$R\{v_2, y_4\}$	$V(C_6) - \{v_5\} \cup \{w_6\} \cup \{y_2\}$
$R\{v_3, y_5\}$	$V(C_6) - \{v_6\} \cup \{w_1\} \cup \{y_3\}$
$R\{v_4, y_6\}$	$(C_6) - \{v_1\} \cup \{w_2\} \cup \{y_4\}$
$R\{v_1, y_5\}$	$V(C_6) - \{v_2\} \cup \{w_3\} \cup \{y_5\}$
$R\{v_2, y_6\}$	$V(C_6) - \{v_3\} \cup \{w_4\} \cup \{y_6\}$
$R\{x_1, z_4\}$	$V(C_6) - \{v_4\} \cup \{w_4\} \cup \{x_3\}$
$R\{x_2, z_5\}$	$V(C_6) - \{v_5\} \cup \{w_5\} \cup \{x_4\}$

TABLE 12: Continued.

RNs	Elements
$R\{x_3, z_6\}$	$V(C_6) - \{v_6\} \cup \{w_6\} \cup \{x_5\}$
$R\{x_1, z_4\}$	$V(C_6) - \{v_1\} \cup \{w_1\} \cup \{x_6\}$
$R\{v_1, w_2\}$	$V(C_6) - \{v_2, v_3, v_4\}$
$R\{v_2, w_3\}$	$V(C_6) - \{v_3, v_4, v_5\}$
$R\{v_3, w_4\}$	$V(C_6) - \{v_4, v_5, v_6\}$
$R\{v_4, w_5\}$	$V(C_6) - \{v_1, v_5, v_6\}$
$R\{v_5, w_6\}$	$V(C_6) - \{v_1, v_2, v_3\}$
$R\{v_1, w_6\}$	$V(C_6) - \{v_2, v_3, v_4\}$
$R\{v_1, y_1\}$	$V(C_6) - \{w_2, w_3, w_4\}$
$R\{v_2, y_2\}$	$V(C_6) - \{w_3, w_4, w_5\}$
$R\{v_3, y_3\}$	$V(C_6) - \{w_4, w_5, w_6\}$
$R\{v_4, y_4\}$	$V(C_6) - \{w_1, w_5, w_6\}$
$R\{v_5, y_5\}$	$V(C_6) - \{w_1, w_2, w_3\}$
$R\{v_6, y_6\}$	$V(C_6) - \{w_2, w_3, w_4\}$
$R\{x_1, z_1\}$	$V(C_6) - \{x_3, x_4\} \cup \{y_1\}$
$R\{x_2, z_2\}$	$V(C_6) - \{x_4, x_5\} \cup \{y_2\}$
$R\{x_3, z_3\}$	$V(C_6) - \{x_5, x_6\} \cup \{y_3\}$
$R\{x_4, z_4\}$	$V(C_6) - \{x_1, x_6\} \cup \{y_4\}$
$R\{x_5, z_5\}$	$V(C_6) - \{x_1, x_2\} \cup \{y_5\}$
$R\{x_6, z_6\}$	$V(C_6) - \{x_2, x_3\} \cup \{y_6\}$

TABLE 13: The representation of  $R_u$  for  $164 \leq u \leq 186$ .

RNs	Elements
$R\{w_1, y_1\}$	$V(C_m) - \{x_1\} \cup \{y_6\}$
$R\{w_2, y_2\}$	$V(C_m) - \{x_2\} \cup \{y_1\}$
$R\{w_3, y_3\}$	$V(C_m) - \{x_3\} \cup \{y_2\}$
$R\{w_4, y_4\}$	$V(C_m) - \{x_4\} \cup \{y_3\}$
$R\{w_5, y_5\}$	$V(C_m) - \{x_5\} \cup \{y_4\}$
$R\{w_6, y_6\}$	$V(C_m) - \{x_6\} \cup \{y_5\}$
$R\{v_1, y_4\}$	$V(C_m) - \{x_2\} \cup \{w_3\}$
$R\{v_2, y_5\}$	$V(C_m) - \{x_3\} \cup \{w_4\}$
$R\{v_3, y_6\}$	$V(C_m) - \{x_4\} \cup \{w_5\}$
$R\{w_1, z_1\}$	$V(C_m) - \{x_2, x_3\}$
$R\{w_2, z_2\}$	$V(C_m) - \{x_3, x_4\}$
$R\{w_3, z_3\}$	$V(C_m) - \{x_4, x_5\}$
$R\{w_4, z_4\}$	$V(C_m) - \{x_5, x_6\}$
$R\{w_5, z_5\}$	$V(C_m) - \{x_1, x_6\}$
$R\{w_6, z_6\}$	$V(C_m) - \{x_1, x_2\}$
$R\{x_1, y_4\}$	$V(C_m) - \{x_3, x_5\}$
$R\{x_2, y_5\}$	$V(C_m) - \{x_4, x_6\}$
$R\{x_3, y_6\}$	$V(C_m) - \{x_1, x_5\}$
$R\{x_1, z_2\}$	$V(C_6) - \{v_4\} \cup \{w_4\}$
$R\{x_2, z_3\}$	$V(C_5) - \{v_5\} \cup \{w_5\}$
$R\{x_3, z_4\}$	$V(C_6) - \{v_6\} \cup \{w_6\}$
$R\{x_4, z_5\}$	$V(C_6) - \{v_1\} \cup \{w_1\}$
$R\{x_5, z_6\}$	$V(C_6) - \{v_2\} \cup \{w_2\}$
$R\{x_1, z_6\}$	$V(C_6) - \{v_3\} \cup \{w_3\}$

TABLE 14: The representation of  $R_u$  for  $187 \leq u \leq 198$ .

RNs	Elements
$R\{v_1, w_1\}$	$R\{v_2, w_2\}$
$R\{v_3, w_3\}$	$R\{v_4, w_4\}$
$R\{v_5, w_5\}$	$R\{v_5, w_5\}$
$R\{x_1, y_1\}$	$R\{x_2, y_2\}$
$R\{x_3, y_3\}$	$R\{x_4, y_4\}$
$R\{x_5, y_5\}$	$R\{x_5, y_5\}$

$V(C_6)$

TABLE 15: The representation of  $R_r$  for  $1 \leq r \leq 12$ .

RNs	Elements
$R_1 = R\{y_1, z_1\}$	$V(C_6) - \{v_3, v_4\} \cup \{w_3, w_4\} \cup \{y_5, y_6\} \cup \{z_4, z_5, z_6\}$
$R_2 = R\{y_2, z_2\}$	$V(C_6) - \{v_4, v_5\} \cup \{w_4, w_5\} \cup \{y_1, y_6\} \cup \{z_1, z_5, z_6\}$
$R_3 = R\{y_3, z_3\}$	$V(C_6) - \{v_5, v_6\} \cup \{w_5, w_6\} \cup \{y_1, y_2\} \cup \{z_1, z_2, z_6\}$
$R_4 = R\{y_4, z_4\}$	$V(C_6) - \{v_1, v_6\} \cup \{w_1, w_6\} \cup \{y_2, y_3\} \cup \{z_1, z_2, z_3\}$
$R_5 = R\{y_5, z_5\}$	$V(C_6) - \{v_1, v_2\} \cup \{w_1, w_2\} \cup \{y_3, y_4\} \cup \{z_2, z_3, z_4\}$
$R_6 = R\{y_6, z_6\}$	$V(C_6) - \{v_2, v_3\} \cup \{w_2, w_3\} \cup \{y_4, y_5\} \cup \{z_3, z_4, z_5\}$
$R_7 = R\{y_2, z_1\}$	$V(C_6) - \{v_5, v_6\} \cup \{w_5, w_6\} \cup \{y_3, y_4\} \cup \{z_3, z_4, z_5\}$
$R_8 = R\{y_3, z_2\}$	$V(C_6) - \{v_1, v_6\} \cup \{w_1, w_6\} \cup \{y_4, y_5\} \cup \{z_4, z_5, z_6\}$
$R_9 = R\{y_4, z_3\}$	$V(C_6) - \{v_1, v_2\} \cup \{w_1, w_2\} \cup \{y_5, y_6\} \cup \{z_1, z_5, z_6\}$
$R_{11} = R\{y_6, z_5\}$	$V(C_6) - \{v_3, v_4\} \cup \{w_3, w_4\} \cup \{y_1, y_2\} \cup \{z_1, z_2, z_3\}$
$R_{12} = R\{y_1, z_6\}$	$V(C_6) - \{v_4, v_5\} \cup \{w_4, w_5\} \cup \{y_2, y_3\} \cup \{z_2, z_3, z_4\}$

TABLE 16: FMD of convex polytopes for  $m \geq 6$ .

Network	Lower bound of $\dim_f$	Upper bound of $\dim_f$	Comment
$\mathbb{B}_m$	1	$(10m/(7m+2))$	Bounded
$C_m$	1	$(5m/(3(m+1)))$	Bounded

$1 \pmod{m}\} \cup \{x_h | h \equiv r-1, r-2, \dots, r - (n/2) \pmod{m}\}$  and  $\dot{R}_{34} = R\{v_r, x_{r-1}\} = V(C_m) - \{w_h | h \equiv r, r+1, r+2, \dots, r + (n/2) - 1 \pmod{m}\} \cup \{x_h | h \equiv r+1, r+2, \dots, r + (n/2) \pmod{m}\}$ , respectively. Clearly,  $|\dot{R}_u| = 4m > |R_r|$  and  $|\dot{R}_u \cap \cup_{r=1}^m R_r| \geq |R_r|$ .

(i) The RN of  $\{x_r, y_{r+1}\}$  is  $\dot{R}_{35} = R\{x_r, y_{r+1}\} = V(C_m) - \{y_h | h \equiv r-1, r-2, \dots, r - (m/2) + 1 \pmod{m}\} \cup$

$\{z_h | h \equiv r-1, r-2, \dots, r - (m/2) + 1 \pmod{m}\}$ . Clearly,  $|\dot{R}_{35}| = 4m + 2 > |R_r|$  and  $|\dot{R}_u \cap \cup_{r=1}^m R_r| \geq |R_r|$ .

TABLE 17: Upper bounds of FMD as they tend to  $\infty$ , where  $m \geq 6 \wedge m \equiv 0 \pmod{2}$ .

Network	Values of FMD as they tend to $\infty$	
$\mathbb{B}_m$	$\lim_{m \rightarrow \infty} (10m/(7m+2))$	(10/7)
$\mathbb{C}_m$	$\lim_{m \rightarrow \infty} (5m/(3(m+1)))$	(5/3)

- (j) The RN of  $\{x_r, z_{r+1}\}$  is  $\dot{R}_{36} = R\{x_r, z_{r+1}\} = V(\mathbb{C}_m) - \{v_h | h \equiv r+3, r+4, \dots, r+(m/2) \pmod{m}\} \cup \{w_h | h \equiv r+3, r+4, \dots, r+(m/2) \pmod{m}\}$  as we can see that  $|\dot{R}_{36}| > |R_t|$  and  $|\dot{R}_u \cap \cup_{r=1}^m R_r| \geq |R_r|$ .
- (k) The RNs of  $\{v_r, w_{r+1}\}$  and  $\{v_r, y_r\}$  are  $\dot{R}_{37} = R\{v_r, w_{r+1}\} = V(\mathbb{C}_m) - \{v_h | h \equiv r+1, r+2, \dots, r+(m/2) \pmod{m}\}$  and  $\dot{R}_{38} = R\{v_r, y_r\} = V(\mathbb{C}_m) - \{w_h | h \equiv r+1, r+2, \dots, r+(m/2) \pmod{m}\}$ , as we can see that  $|R_u| = (9m/2) > |R_t|$  and  $|\dot{R}_u \cap \cup_{r=1}^m R_r| \geq |R_r|$ .
- (l) The RN of  $\{v_r, x_{r+1}\}$  is  $\dot{R}_{39} = R\{v_r, x_{r+1}\} = V(\mathbb{C}_m) - \{v_h | h \equiv r+1, r+2, \dots, r+(n/2) \pmod{m}\} \cup \{x_h | h \equiv r \pmod{m}\} \cup \{w_h | h \equiv r+(m+2)/2 \pmod{m}\}$ . Clearly,  $|\dot{R}_{39}| = (9m/2) - 1 > |R_t|$  and  $|\dot{R}_u \cap \cup_{r=1}^m R_r| \geq |R_r|$ .
- (m) The RNs of  $\{v_r, z_r\}$  and  $\{x_r, z_r\}$  are  $\dot{R}_{40} = R\{v_r, z_r\} = V(\mathbb{C}_m) - \{x_h | h \equiv r, r+(n/2) \pmod{m}\} \cup \{w_h | h \equiv r+2, r+3, \dots, r+(n/2) \pmod{m}\}$  and  $\dot{R}_{41} = R\{x_r, z_r\} = V(\mathbb{C}_m) - \{x_h | h \equiv r+2, r+3, \dots, r+(n/2) \pmod{m}\} \cup \{y_r\}$ , respectively. Clearly,  $|R_u| = (9m/2) + 1 > |R_t|$  and  $|\dot{R}_u \cap \cup_{r=1}^m R_r| \geq |R_r|$ .
- (n) The RNs of  $\{v_r, w_r\}$  and  $\{x_r, y_r\}$  are  $\dot{R}_{42} = R\{v_r, w_r\} = \dot{R}_{43} = R\{x_r, y_r\} = V(\mathbb{C}_m)$ , as both are equal to  $V(\mathbb{C}_m)$ ; therefore,  $|\dot{R}_u \cap \cup_{r=1}^m R_r| \geq |R_r|$ .  $\square$

**Theorem 2.** If  $\mathbb{N} \cong \mathbb{C}_m$  with  $m \geq 6$  and  $m \equiv 0 \pmod{2}$ , then  $\dim_f(\mathbb{C}_m) < (5m/(3(m+1)))$ .

*Proof*

Case I  $m = 6$ .

The RNs are given as follows.

From Lemma 3, we see that  $R\{y_r, y_{r+p}\} = R\{x_r, x_{r+p}\}$ .

In Tables 8–14, the RNs have cardinalities of 22, 24, 25, 26, 27, 28, and 30, respectively. On the contrary, Table 15 represents RNs with minimum cardinality of 21. We can see that  $\cup_{r=1}^{12} R_r = V(\mathbb{C}_6)$  this implies  $|\cup_{r=1}^{12} R_r| = 30$  and  $|\dot{R}_r \cap \cup_{r=1}^{12} R_r| \geq |R_r|$ , where  $1 \leq u \leq 198$ .

Now, we define a function  $\mu: V(\mathbb{B}_6) \rightarrow [0, 1]$  such that  $\mu(v_r) = \mu(w_r) = \mu(x_r) = \mu(y_r) = \mu(z_r) = (1/22)$ , as  $R_r$  for  $1 \leq r \leq 12$  of  $\mathbb{C}_6$  are pairwise overlapping; hence,  $\exists$  is another minimal resolving function  $\bar{\mu}$  of  $\mathbb{C}_6$  such that  $|\bar{\mu}| < |\mu|$ . As a result,  $\dim_f(\mathbb{C}_6) < \sum_{r=1}^{12} (1/10) < (30/21)$ .

On the contrary, Table 4 shows the RNs with maximum cardinality of  $30 = \kappa$ ; hence, by Lemma 1,  $(|V(\mathbb{C}_6)|/\kappa) = (30/30) = 1 < \dim_f(\mathbb{C}_6)$ . Therefore,

$$1 < \dim_f(\mathbb{C}_6) < \frac{30}{21}. \quad (15)$$

Case II  $m \geq 6$ .

We have seen from Lemma 3 that the RNs with minimum cardinality of  $3(m+1)$  are  $R\{y_r, z_r\}$  and  $R\{y_r, z_{r-1}\}$  and  $\cup_{r=1}^m R_t = V(\mathbb{C}_m)$ . Let  $\lambda = 3(m+1)$  and  $\delta = |\cup_{t=1}^m R_t| = 5m$ . Now, we define a mapping  $\mu: V(\mathbb{C}_m) \rightarrow [0, 1]$  such that

$$\mu(a) = \begin{cases} \frac{1}{\lambda}, & \text{for } a \in \cup_{t=1}^m R_t, \\ 0, & \text{for } a \in V(\mathbb{C}) - \cup_{t=1}^m R_t. \end{cases} \quad (16)$$

We can see that  $\mu$  is a RF for  $\mathbb{C}_m$  with  $m \geq 3$  because  $\mu(R\{u, v\}) \geq 1, \forall u, v \in V(\mathbb{C}_m)$ . On the contrary, assume that there is another resolving function  $\rho$ , such that  $\rho(u) \leq \mu(u)$ , for at least one  $u \in V(\mathbb{C}_m), \rho(u) \neq \mu(u)$ . As a consequence,  $\rho(R\{u, v\}) < 1$ , where  $R\{u, v\}$  is a RN of  $\mathbb{C}_m$  with minimum cardinality  $\lambda$ . This implies that  $\rho$  is not a resolving function which is contradiction. Therefore,  $\mu$  is a minimal resolving function that attains minimum  $|\mu|$  for  $\mathbb{C}_m$ . Since all  $R_r$  are having pairwise nonempty intersection, so there is another minimal resolving function of  $\bar{\mu}$  of  $\mathbb{C}_m$  such that  $|\bar{\mu}| \leq |\mu|$ . Hence, assigning  $(1/\lambda)$  to the vertices of  $\mathbb{C}_m$  in  $\cup_{r=1}^m R_r$  and calculating the summation of all the weights, we obtain

$$\dim_f(\mathbb{C}_m) = \sum_{r=1}^{\delta} \frac{1}{\lambda} \leq \frac{5m}{(7m/2) + 1} = \frac{10m}{7m+2}. \quad (17)$$

Also, the RNs with maximum cardinality of  $5m$  are  $R\{v_r, w_r\}$  and  $R\{x_r, y_r\}$ . Let  $|V(\mathbb{C}_m)| = \omega$  and  $|R\{v_r, w_r\}| = |R\{x_r, y_r\}| = \kappa$ ; thus, from Lemma 1, we have  $(|V(\mathbb{C}_m)|/\kappa) = (\omega/\kappa) = (5m/5m) = 1 < \dim_f(\mathbb{C}_m)$ .

Therefore, we conclude the following:

$$1 < \dim_f(\mathbb{C}_m) < \frac{5m}{3(m+1)}. \quad (18)$$

□

## 6. Conclusion

In this paper,

- (i) We have found the improved lower bound of FMD of connected networks
- (ii) Apart from that, we have calculated the lower and upper bounds of FMD of symmetric networks called by convex polytopes' Type I and Type II  $\mathbb{B}_m$  and  $\mathbb{C}_m$
- (iii) Table 16 shows the summary of main results and Table 17 gives the values of FMDs as they tend to  $\infty$

**6.1. Open Problem.** To characterize the networks with lower bound of FMD greater than 1 is still an open problem.

## Data Availability

The data used to support the findings of the study are included within the article. However, more details of the data can be obtained from the corresponding author upon request.

## Conflicts of Interest

The authors have no conflicts of interest.

## References

- [1] G. Chartrand and L. Lesniak, *Graphs & Digraphs*, Chapman & Hall, CRC, Boca Raton, FL, USA, 4th edition, 2005.
- [2] J. L. Gross and J. Yellen, *Graph Theory and its Applications*, Chapman and Hall/CRC, Boca Raton, FL, USA, 2nd edition, 2005.
- [3] D. B. West, *Introduction to Graph Theory*, Prentice-Hall, Hoboken, NJ, USA, 2001.
- [4] G. Chartrand, L. Eroh, M. A. Johnson, and O. R. Oellermann, "Resolvability in graphs and the metric dimension of a graph," *Discrete Applied Mathematics*, vol. 105, no. 1-3, pp. 99–113, 2000.
- [5] P. S. Buczkowski, G. Chartrand, C. Poisson, and P. Zhang, "On k-dimensional graphs and their bases," *Periodica Mathematica Hungarica*, vol. 46, no. 1, pp. 9–15, 2003.
- [6] P. J. Slater, "Abstracts," *Stroke*, vol. 6, no. 5, pp. 549–559, 1975.
- [7] P. J. Slater, "Domination and location in acyclic graphs," *Networks*, vol. 17, no. 1, pp. 55–64, 1987.
- [8] I. Javaid, M. T. Rahim, and K. Ali, "Families of regular graphs with constant metric dimension," *Utilitas Mathematica*, vol. 75, pp. 21–33, 2008.
- [9] M. Imran, A. Q. Baig, M. K. Shafiq, and I. Tomescu, "On metric dimension of generalized Petersen graphs  $P(n, 3)$ ," *Ars Combinatoria*, vol. 117, pp. 113–130, 2014.
- [10] J. Currie and O. R. Oellermann, "The metric dimension and metric independence of a graph," *Journal of Combinatorial Mathematics and Combinatorial Computing*, vol. 39, pp. 157–167, 2001.
- [11] M. Fehr, S. Gosselin, and O. R. Oellermann, "The metric dimension of Cayley digraphs," *Discrete Mathematics*, vol. 306, no. 1, pp. 31–41, 2006.
- [12] S. Arumugam and V. Mathew, "The fractional metric dimension of graphs," *Discrete Mathematics*, vol. 312, no. 9, pp. 1584–1590, 2012.
- [13] M. Feng, B. Lv, and K. Wang, "On the fractional metric dimension of graphs," *Discrete Applied Mathematics*, vol. 170, no. 19, pp. 55–63, 2014.
- [14] M. Feng and K. Wang, "On the metric dimension and fractional metric dimension for hierarchical product of graphs," *Applicable Analysis and Discrete Mathematics*, vol. 7, no. 2, pp. 302–313, 2013.
- [15] M. Feng and K. Wang, "On the fractional metric dimension of corona product graphs and lexicographic product graphs," <https://arxiv.org/abs/1206.1906>.
- [16] S. W. Saputro, A. Semanicova Fenovcikova, M. Baca, and M. Lascsakova, "On fractional metric dimension of comb product graphs," *Stat., Optim. Inf. Comput.* vol. 6, pp. 150–158, 2018.
- [17] B. Jia, A. Kashif, T. Rasheed, and M. Javaid, "Fractional metric dimension of generalized Jahangir graph," *Mathematics*, vol. 4, pp. 371–376, 2019.
- [18] M. Raza, M. Javaid, and N. Saleem, "Fractional metric dimension of metal-organic frameworks," *Main Group Metal Chemistry*, vol. 44, no. 1, pp. 92–102, 2021.
- [19] S. Aisyah, M. I. Utoyo, and L. Susilowati, "On the local fractional metric dimension of corona product graphs," *IOP Conference Series: Earth and Environmental Science, Hungarica*, vol. 243, 2019.
- [20] J.-B. Liu, M. K. Aslam, and M. Javaid, "Local fractional metric dimensions of rotationally symmetric and planar networks," *IEEE Access*, vol. 8, no. 1, pp. 82404–82420, 2020.
- [21] M. Javaid, M. Raza, P. Kumam, and J.-B. Liu, "Sharp bounds of local fractional metric dimensions of connected networks," *IEEE Access*, vol. 8, no. 2, pp. 172329–172342, 2020.
- [22] F. Harary and R. A. Melter, "On the metric dimension of a graph," *Ars Combinatoria*, vol. 2, pp. 191–195, 1976.
- [23] S. Khuller, B. Raghavachari, and A. Rosenfeld, "Landmarks in graphs," *Discrete Applied Mathematics*, vol. 70, no. 3, pp. 217–229, 1996.
- [24] R. A. Melter and I. Tomescu, "Metric bases in digital geometry," *Computer Vision, Graphics, and Image Processing*, vol. 25, no. 1, pp. 113–121, 1984.
- [25] P. J. Slater, "Dominating and reference sets in graphs," *Journal of Mathematical and Physical Sciences*, vol. 22, pp. 445–455, 1998.
- [26] A. Shabbir and M. Azeem, "On the partition dimension of tri-hexagonal  $\alpha$ -boron nanotube $\alpha$ ," *IEEE Access*, vol. 9, no. 1, pp. 55644–55653, 2021.
- [27] M. F. Nadeem, M. Hassan, M. Azeem et al., "Application of resolvability technique to investigate the different polyphenyl structures for polymer industry," *Journal of Chemistry*, vol. 2021, Article ID 6633227, 8 pages, 2021.
- [28] M. Bača, "On magic labellings of convex polytopes," *Annals of Discrete Mathematics*, vol. 51, pp. 13–16, 1992.

## Research Article

# On Hamilton-Connectivity and Detour Index of Certain Families of Convex Polytopes

Sakander Hayat <sup>1</sup>, Muhammad Yasir Hayat Malik <sup>2</sup>, Ali Ahmad <sup>3</sup>, Suliman Khan <sup>1</sup>,  
Faisal Yousafzai <sup>4</sup> and Roslan Hasni <sup>5</sup>

<sup>1</sup>Faculty of Engineering Sciences, GIK Institute of Engineering Sciences and Technology, Topi, Khyber Pakhtunkhwa 23460, Pakistan

<sup>2</sup>Department of Mathematics, Government College University, Faisalabad 38000, Pakistan

<sup>3</sup>College of Computer Science and Information Technology, Jazan University, Jazan 45142, Saudi Arabia

<sup>4</sup>Military College of Engineering, National University of Sciences and Technology (NUST), Islamabad 44000, Pakistan

<sup>5</sup>School of Informatics and Applied Mathematics, University Malaysia Terengganu, Kuala Terengganu, Terengganu 21030, Malaysia

Correspondence should be addressed to Sakander Hayat; sakander1566@gmail.com

Received 11 February 2021; Revised 21 June 2021; Accepted 8 July 2021; Published 19 July 2021

Academic Editor: Abdul Qadeer Khan

Copyright © 2021 Sakander Hayat et al. This is an open access article distributed under the Creative Commons Attribution License, which permits unrestricted use, distribution, and reproduction in any medium, provided the original work is properly cited.

A convex polytope is the convex hull of a finite set of points in the Euclidean space  $\mathbb{R}^n$ . By preserving the adjacency-incidence relation between vertices of a polytope, its structural graph is constructed. A graph is called Hamilton-connected if there exists at least one Hamiltonian path between any of its two vertices. The detour index is defined to be the sum of the lengths of longest distances, i.e., detours between vertices in a graph. Hamiltonian and Hamilton-connected graphs have diverse applications in computer science and electrical engineering, whereas the detour index has important applications in chemistry. Checking whether a graph is Hamilton-connected and computing the detour index of an arbitrary graph are both NP-complete problems. In this paper, we study these problems simultaneously for certain families of convex polytopes. We construct two infinite families of Hamilton-connected convex polytopes. Hamilton-connectivity is shown by constructing Hamiltonian paths between any pair of vertices. We then use the Hamilton-connectivity to compute the detour index of these families. A family of non-Hamilton-connected convex polytopes has also been constructed to show that not all convex polytope families are Hamilton-connected.

## 1. Introduction and Preliminaries

All graphs in this paper are simple, loopless, finite, and connected.

A graph  $G$  is an ordered pair  $G = (V(G), E(G))$  with  $V(G)$  as its vertex set (i.e., set of points called vertices) and  $E(G) \subseteq \binom{V(G)}{2}$  as its edge set (i.e., set of lines connecting points called edges). The number of vertices, say  $n: = |V(G)|$ , is called the order of  $G$  and the number of edges, say  $m: = |E(G)|$ , is called the size of  $G$ . For two vertices  $x, y \in V(G)$ , we write  $x \sim y$  if both  $x$  and  $y$  are adjacent, i.e., they are connected by an edge. For  $U \subseteq V(G)$

and  $x, y \in V(G)$ , if  $U = \{u_i: 1 \leq i \leq p\}$ , then  $x \circ \{u_i: 1 \leq i \leq p\} \circ y$  means that  $x \sim u_1$  and  $u_p \sim y$  and adjacency in the rest of  $u_i$ 's ( $2 \leq i \leq p$ ) stays the same. For a positive integer  $\nu \in \mathbb{Z}^+$ , we write  $\nu|2$  (resp.  $\nu \nmid 2$ ) if  $\nu$  is even (resp. odd).

A Hamiltonian cycle  $C_H(x)$  in a connected graph  $G$  starting and finishing at the vertex  $x$  is a cycle traversing all the vertices of  $G$ . Similarly, a Hamiltonian path  $P_H(x, y)$  between vertices  $x$  and  $y$  is the one covering the entire graph without missing any vertex. A graph comprising a Hamiltonian path (resp. Hamiltonian cycle) is called traceable (resp. Hamiltonian). Every Hamiltonian graph, by definition, is traceable, whereas the converse is not true in general.

For instance, the so-called Petersen graph does not contain any Hamiltonian cycle and, thus, is not Hamiltonian. However, you can easily find a Hamiltonian path between two of its vertices, which makes it traceable but not Hamiltonian. Graphs comprising Hamiltonian paths between every pair of its vertices are called Hamilton-connected. They were introduced and studied in 1963 by Ore [1]. Trivalent Hamiltonian graphs and their canonical representation were studied by Frucht [2]. Hamilton-connectivity and Hamiltonianity possess some extensive available literature. See, for example, [3–7].

By preserving the vertex-edge incidence relation in convex polytopes, their graphs are constructed. Bača [8–10] was among the first researchers to consider these families of geometric graphs. In [10] (resp. [9]), Bača studied the problem of magic (resp. graceful and antigraceful) labeling of convex polytopes, whereas in [8], the problem of face antimagic labeling of convex polytopes was studied. Miller et al. [11] studied the vertex-magic total labeling of convex polytopes. Imran et al. [12–15] computed the minimum metric dimension of various infinite families of convex polytopes. In particular, they showed that these infinite families of convex polytopes have constant metric dimension. Malik and Sarwar [16] also constructed two infinite families of convex polytopes having constant metric dimension. Other closely related infinite families of graphs with constant metric dimension are studied in [17]. Kratica et al. [18] studied the strong metric dimension of certain infinite families of convex polytopes by constructing their doubly resolving sets. The fault-tolerant metric dimension (resp. mixed metric dimension) of convex polytopes was studied by Raza et al. [19] (resp. Raza et al. [20]). The binary locating-dominating number of convex polytopes is studied by Simić et al. [21] and Raza et al. [22]. The open-locating-dominating number of certain convex polytopes has recently been studied by Savić et al. [23]. Hayat et al. [24] studied Hamilton-connectivity and detour index in convex polytopes.

For a graph  $G$ , let  $\ell(x, y)$  be the length of the longest path (i.e., detour) between vertices  $x$  and  $y$  of  $G$ . The detour index [25] is defined to be the sum of the lengths of the detour between unordered pairs of vertices in  $G$ . The detour index of a graph  $G$  is usually denoted by  $\omega(G)$ .

$$\omega(G) = \sum_{\{x,y\} \subset V(G)} \ell(x, y). \quad (1)$$

In chemistry, the detour index has diverse applications. Lukovits [26] put forward its QSAR/QSPR applications. Trinajstić et al. [27] presented some more of its chemical applications and compared its predictive potential in correlating the normal boiling points of benzenoid hydrocarbons with the performance of Wiener index. Rucker and Rucker [28] presented more of its rigorous applications for correlating the boiling points of acyclic and cyclic alkanes. The calculation of the detour index for a given graph has been shown an NP-complete problem in [29].

Mahmiani et al. [30] proposed the edge versions of the detour index and studied their mathematical properties.

Zhou and Cai [31] proved some upper and lower bounds on the detour index of graphs. Qi and Zhou [32] studied minimum unicyclic graphs with respect to the detour index. Du [33] studied the minimum detour index of bicyclic graphs. Fang et al. [34] characterized the minimum detour index of some families of tricyclic graphs. Karbasioun et al. [35] studied the applications of the detour index in infinite families of nanostar dendrimers. Wu and Deng [36] computed the detour index for a chain of C20 fullerenes. Kaladevi and Abinayaa [37] studied spectral properties of the detour index in relation with the Laplacian energy of graphs. Recently, Abdullah and Omar [38] introduced the restricted edge version of the detour index and studied it for some families of graphs. Tang et al. [39] studied Zagreb connection indices of some operation of graphs.

Let  $S_\nu$  denote the  $\nu$ -dimensional star graph on  $\nu + 1$  vertices. We end this section with an important and well-known result bounding the detour index in terms of its order.

**Theorem 1 [40].** *Let  $G$  be an  $\nu$ -vertex graph with  $\nu \geq 3$  and  $\omega(G)$  be its detour index. Then,*

$$(\nu - 1)^2 \leq \omega(G) \leq \frac{\nu(\nu - 1)^2}{2}, \quad (2)$$

*with left equality if and only if  $G \cong S_\nu$ , and right inequality holds if and only if  $G$  is Hamilton-connected.*

## 2. A Family of Non-Hamilton-Connected Convex Polytopes

Bača [10] introduced the graph of convex polytope  $D_\nu$  for  $\nu \geq 4$ . It is a family of convex polytopes comprising  $2\nu$  pentagonal faces. See Figure 1 for the  $\nu$ -dimensional family of convex polytopes  $D_\nu$ .

Mathematically, the vertex set of  $D_\nu$  consists of four layers of vertices, i.e.,  $w_p, x_p, y_p$ , and  $z_p$ . That is to say that  $V(D_\nu) = \{w_p, x_p, y_p, z_p : 1 \leq p \leq \nu\}$ . Accordingly, the edge set of  $D_\nu$  is as follows:

$$E(D_\nu) = \{w_p w_{p+1}, z_p z_{p+1}, w_p x_p, x_p y_p, x_{p+1} y_p, y_p z_p : 1 \leq p \leq \nu\}. \quad (3)$$

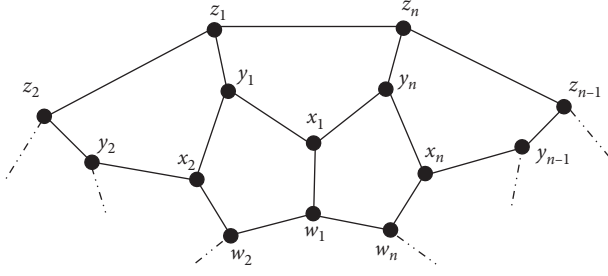
The subscripts are to be considered modulo  $\nu$ . The layer of vertices comprising  $w_p$  is called the inner layer, whereas the layer comprising  $z_p$  is called the outer layer of  $D_\nu$ . The vertices  $x_p$  and  $y_p$ ,  $1 \leq p \leq \nu$  form the middle layers.

The following result shows that the infinite family  $D_\nu$  of convex polytopes is not Hamilton-connected.

**Proposition 1.** *The  $\nu$ -dimensional convex polytope  $D_\nu$ , with  $\nu \geq 4$ , is non-Hamilton-connected.*

*Proof.* It is enough to show that there exist two vertices in the  $\nu$ -dimensional convex polytope  $D_\nu$  such that no Hamiltonian path exists between them.




 FIGURE 1: The graph of convex polytope  $D_\nu$ .

It is easy to see that, between every pair of vertices at distance two on the outer layer, i.e., between  $z_p$  and  $z_{p+2}$  ( $1 \leq p \leq \nu - 1$ ), there exists no Hamiltonian path because of the two pentagonal layers of faces. This shows that the  $\nu$ -dimensional convex polytope  $D_\nu$  is non-Hamilton-connected.  $\square$

### 3. Hamilton-Connectivity and the Detour Index of $H_\nu$

In this section, we show that the graph of  $\nu$ -dimensional convex polytope  $H_\nu$  is Hamilton-connected. Then, we use its Hamilton-connectivity to find a formula for its detour index. This family of convex polytopes was introduced by Imran and Siddiqui [14].

Mathematically, the vertex set of  $H_\nu$  consists of four layers of vertices, i.e.,  $v_p, w_p, x_p, y_p$ , and  $z_p$ . That is to say

that  $V(H_\nu) = \{v_p, w_p, x_p, y_p, z_p : 1 \leq p \leq \nu\}$ . Accordingly, the edge set of  $H_\nu$  is as follows:

$$E(H_\nu) = \{v_p v_{p+1}, v_p w_p, w_p v_{p+1}, w_p w_{p+1}, w_p x_p, x_p x_{p+1}, x_p y_p, y_p x_{p+1}, y_p y_{p+1}, y_p z_p, z_p z_{p+1} : 1 \leq p \leq \nu\}. \quad (4)$$

The subscripts are to be considered modulo  $\nu$ . See Figure 2 to view the  $\nu$ -dimensional convex polytope graph  $H_\nu$ .

The following is the main result of this section.

**Theorem 2.** *The graph of  $\nu$ -dimensional convex polytope  $H_\nu$ , with  $\nu \geq 5$ , is Hamilton-connected.*

*Proof.* We prove this result by definition. For this, we have to show that there exist Hamiltonian paths between any pair of vertices of  $H_\nu$ .

Let  $P_H(u, v)$  be a Hamiltonian path between vertices  $u$  and  $v$  in  $H_\nu$ . Let  $V(H_\nu) = Z \cup Y \cup X \cup W \cup V$  such that  $Z = \{z_1, z_2, \dots, z_\nu\}$ ,  $Y = \{y_1, y_2, \dots, y_\nu\}$ ,  $X = \{x_1, x_2, \dots, x_\nu\}$ ,  $W = \{w_1, w_2, \dots, w_\nu\}$ , and  $V = \{v_1, v_2, \dots, v_\nu\}$  (see Figure 2).

**Case 1:**  $u' = z_1$  and  $v' = z_p, 2 \leq p \leq \nu$

Subcase 1.1:  $2 \leq p \leq \nu - 2$ :

$$P_H(u', v'): u' = z_1 \circ \{z_{\nu-q} : 0 \leq q \leq \nu - p - 1\} \circ \{y_{p-q+1} : 0 \leq q \leq p - 2\} \circ \{x_q : 3 \leq q \leq p + 1\} \circ \{x_q y_q : p + 2 \leq q \leq \nu\} \circ y_1 x_1 w_1 \circ \{v_q : 1 \leq q \leq \nu\} \circ \{w_{\nu-q} : 0 \leq q \leq \nu - 2\} \circ x_2 y_2 \circ \{z_q : 2 \leq q \leq p\} = v'. \quad (5)$$

Subcase 1.2:  $p = \nu - 1$ :

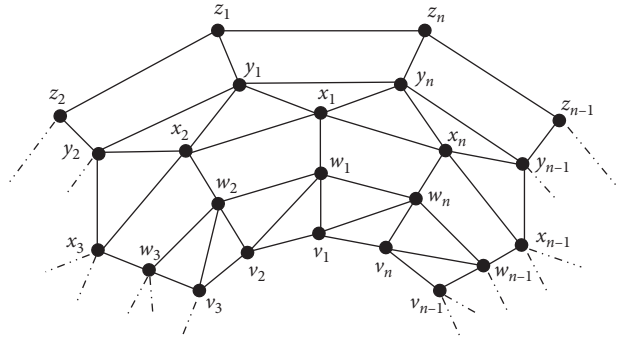
$$P_H(u', v'): u' = z_1 z_\nu y_\nu y_1 x_1 w_1 \circ \{y_q : 1 \leq q \leq \nu\} \circ \{w_{\nu-q} : 0 \leq q \leq \nu - 2\} \circ \{x_q : 2 \leq q \leq \nu\} \circ \{y_{\nu-q} : 1 \leq q \leq \nu - 2\} \circ \{z_q : 2 \leq q \leq \nu - 1\} = v'. \quad (6)$$

Subcase 1.3:  $p = \nu$ :

$$P_H(u', v'): u' = z_1 y_1 x_1 w_1 \circ \{v_q : 1 \leq q \leq \nu\} \circ \{w_{\nu-q} : 0 \leq q \leq \nu - 2\} \circ \{x_q : 2 \leq q \leq \nu\} \circ \{y_{\nu-q} : 0 \leq q \leq \nu - 2\} \circ \{z_q : 2 \leq q \leq \nu\} = v'. \quad (7)$$

**Case 2:**  $u' = z_1$  and  $v' = y_p, 1 \leq p \leq \nu$

Subcase 2.1:  $1 \leq p \leq \nu - 1$ :

FIGURE 2: The  $v$ -dimensional convex polytope  $H_v$ .

$$P_H(u', v'): u' = \{z_q: 1 \leq q \leq v\} \circ \{y_{v-q}: 0 \leq q \leq v-p-1\} \circ \{x_q: p+1 \leq q \leq v\} \circ \{w_{v-q}: 0 \leq q \leq v-2\} \circ \{v_q: 2 \leq q \leq v\} \circ v_1 w_1 \circ \{x_q y_q: 1 \leq q \leq p\} = v'. \quad (8)$$

Subcase 2.2:  $p = v$ :

$$P_H(u', v'): u' = z_1 \circ \{z_{v-q}: 0 \leq q \leq v-2\} \circ \{y_q: 2 \leq q \leq v-1\} \circ \{x_{v-q}: 0 \leq q \leq v-2\} \circ \{w_q: 2 \leq q \leq v\} \circ \{v_{v-q}: 0 \leq q \leq v-1\} \circ w_1 x_1 y_1 v_v = v'. \quad (9)$$

Case 3:  $u' = z_1$  and  $v' = x_p, 1 \leq p \leq v$

Subcase 3.1:  $1 \leq p \leq v-1$ :

$$P_H(u', v'): u' = \{z_q: 1 \leq q \leq v\} \circ \{y_{v-q}: 0 \leq q \leq v-p\} \circ \{x_q: p+1 \leq q \leq v\} \circ \{w_{v-q}: 0 \leq q \leq v-2\} \circ \{v_q: 2 \leq q \leq v\} \circ v_1 w_1 \circ \{x_q y_q: 1 \leq q \leq p-1\} \circ x_p = v'. \quad (10)$$

Subcase 3.2:  $p = v$ :

$$P_H(u', v'): u' = \{z_q: 1 \leq q \leq v\} \circ \{y_{v-q}: 0 \leq q \leq v-1\} \circ \{x_q: 1 \leq q \leq v-1\} \circ \{w_{v-q}: 1 \leq q \leq v-1\} \circ \{v_q: 1 \leq q \leq v\} \circ w_v x_v = v'. \quad (11)$$

Case 4:  $u' = z_1$  and  $v' = w_p, 1 \leq p \leq v$

Subcase 4.1:  $1 \leq p \leq v-1$ :

$$P_H(u', v'): u' = \{z_q: 1 \leq q \leq v\} \circ \{y_{v-q}: 0 \leq q \leq v-1\} \circ \{x_q: 1 \leq q \leq v\} \circ \{w_{v-q}: 0 \leq q \leq v-p-1\} \circ \{v_q: p+1 \leq q \leq v\} \circ \{v_q w_q: 1 \leq q \leq p\} = v'. \quad (12)$$

Subcase 4.2:  $p = v$ :

$$P_H(u', v'): u' = \{z_q: 1 \leq q \leq \nu\} \circ \{y_{\nu-q}: 0 \leq q \leq \nu - 1\} \circ x_1 \circ \{x_{\nu-q}: 0 \leq q \leq \nu - 2\} \circ \{w_q: 2 \leq q \leq \nu - 1\} \circ \{v_{\nu-q}: 0 \leq q \leq \nu - 1\} \circ v_1 w_\nu = v'. \quad (13)$$

**Case 5:**  $u' = z_1$  and  $v' = v_p, 1 \leq p \leq \nu$

$$P_H(u', v'): u' = \{z_q: 1 \leq q \leq \nu\} \circ \{y_{\nu-q}: 0 \leq q \leq \nu - 1\} \circ \{x_q: 1 \leq q \leq \nu\} \circ \{w_{\nu-q}: 0 \leq q \leq \nu - p\} \circ \{v_q: p + 1 \leq q \leq \nu\} \circ \{v_q w_q: 1 \leq q \leq p - 1\} \circ v_p = v'. \quad (14)$$

**Case 6:**  $u' = y_1$  and  $v' = z_p, 1 \leq p \leq \nu$

Subcase 6.1:  $1 \leq p \leq \nu - 1$ :

$$P_H(u', v'): u' = y_1 x_1 w_1 \circ \{v_q: 1 \leq q \leq \nu\} \circ \{w_{\nu-q}: 0 \leq q \leq \nu - 2\} \circ \{x_q y_q: 2 \leq q \leq p\} \circ \{x_q: p + 1 \leq q \leq \nu\} \circ \{y_{\nu-q}: 0 \leq q \leq \nu - p - 1\} \circ \{z_q: p + 1 \leq q \leq \nu\} \circ \{z_q: 1 \leq q \leq p\} = v'. \quad (15)$$

Subcase 6.2:  $p = \nu$ :

$$P_H(u', v'): u' = y_1 \circ \{z_q: 1 \leq q \leq \nu - 1\} \circ \{y_{\nu-q}: 1 \leq q \leq \nu - 2\} \circ \{x_q: 2 \leq q \leq \nu\} \circ \{w_{\nu-q}: 0 \leq q \leq \nu - 2\} \circ \{v_q: 2 \leq q \leq \nu\} \circ v_1 w_1 x_1 y_\nu z_\nu = v'. \quad (16)$$

**Case 7:**  $u' = y_1$  and  $v' = y_p, 2 \leq p \leq \nu$

Subcase 8.1:  $2 \leq p \leq \nu - 1$ :

$$P_H(u', v'): u' = y_1 \circ \{z_q: 1 \leq q \leq \nu\} \circ \{y_{\nu-q}: 0 \leq q \leq \nu - p - 1\} \circ \{x_q: p + 1 \leq q \leq \nu\} \circ \{w_{\nu-q}: 0 \leq q \leq \nu - 2\} \circ \{v_q: 2 \leq q \leq \nu\} \circ v_1 w_1 x_1 \circ \{x_q y_q: 2 \leq q \leq p\} = v'. \quad (17)$$

Subcase 8.2:  $p = \nu$ :

$$P_H(u', v'): u' = y_1 z_1 \circ \{z_{\nu-q}: 0 \leq q \leq \nu - 2\} \circ \{y_q: 2 \leq q \leq \nu - 1\} \circ \{x_{\nu-q}: 1 \leq q \leq \nu - 1\} \circ \{w_q: 1 \leq q \leq \nu - 1\} \circ \{v_{\nu-q}: 1 \leq q \leq \nu - 1\} \circ v_\nu w_\nu x_\nu y_\nu = v'. \quad (18)$$

**Case 8:**  $u' = y_1$  and  $v' = x_p, 1 \leq p \leq \nu$

Subcase 8.1:  $p = 1$ :

$$P_H(u', v'): u' = y_1 z_1 \circ \{z_{\nu-q}: 0 \leq q \leq \nu - 2\} \circ \{y_q: 2 \leq q \leq \nu\} \circ \{x_{\nu-q}: 0 \leq q \leq \nu - 2\} \circ \{w_q: 2 \leq q \leq \nu\} \circ \{v_{\nu-q}: 0 \leq q \leq \nu - 2\} \circ v_1 w_1 x_1 = v'. \quad (19)$$

Subcase 8.2:  $2 \leq p \leq \nu - 1$ :

$$P_H(u', v'): u' = y_1 \circ \{z_q: 1 \leq q \leq \nu\} \circ \{y_{\nu-q}: 0 \leq q \leq \nu - p\} \circ \{x_q: p + 1 \leq q \leq \nu\} \circ \{w_{\nu-q}: 0 \leq q \leq \nu - 2\} \circ \{v_q: 2 \leq q \leq \nu\} \circ v_1 w_1 x_1 \circ \{x_q y_q: 2 \leq q \leq p - 1\} \circ x_p = v'. \quad (20)$$

Subcase 8.3:  $p = \nu$ :

$$P_H(u', v'): u' = y_1 z_1 \circ \{z_{\nu-q}: 0 \leq q \leq \nu - 2\} \circ \{y_q: 2 \leq q \leq \nu\} \circ \{x_q: 1 \leq q \leq \nu - 1\} \circ \{w_{\nu-q}: 1 \leq q \leq \nu - 1\} \circ \{v_q: 1 \leq q \leq \nu\} \circ w_\nu x_\nu = v'. \quad (21)$$

Case 9:  $u' = y_1$  and  $v' = w_p, 1 \leq p \leq \nu$

Subcase 9.1:  $1 \leq p \leq \nu - 1$ :

$$P_H(u', v'): u' = y_1 z_1 \circ \{z_{\nu-q}: 0 \leq q \leq \nu - 2\} \circ \{y_q: 2 \leq q \leq \nu\} \circ \{x_q: 1 \leq q \leq \nu\} \circ \{w_{\nu-q}: 0 \leq q \leq \nu - p - 1\} \circ \{v_q: p + 1 \leq q \leq \nu\} \circ \{v_q w_q: 1 \leq q \leq p\} = v'. \quad (22)$$

Subcase 9.2:  $p = \nu$ :

$$P_H(u', v'): u' = y_1 z_1 \circ \{z_{\nu-q}: 0 \leq q \leq \nu - 2\} \circ \{y_q: 2 \leq q \leq \nu\} \circ \{x_{\nu-q}: 0 \leq q \leq \nu - 1\} \circ \{w_q: 1 \leq q \leq \nu - 1\} \circ \{v_{\nu-q}: 1 \leq q \leq \nu - 1\} \circ v_\nu w_\nu = v'. \quad (23)$$

Case 10:  $u' = y_1$  and  $v' = v_p, 1 \leq p \leq \nu$

Subcase 10.1:  $1 \leq p \leq \nu - 1$ :

$$P_H(u', v'): u' = y_1 z_1 \circ \{z_{\nu-q}: 0 \leq q \leq \nu - 2\} \circ \{y_q: 2 \leq q \leq \nu\} \circ \{x_q: 1 \leq q \leq \nu\} \circ \{w_{\nu-q}: 0 \leq q \leq \nu - p\} \circ \{v_q: p + 1 \leq q \leq \nu\} \circ v_1 \circ \{w_q v_{q+1}: 1 \leq q \leq p - 1\} = v'. \quad (24)$$

Subcase 10.2:  $p = \nu$ :

$$P_H(u', v'): u' = y_1 z_1 \circ \{z_{\nu-q}: 0 \leq q \leq \nu - 2\} \circ \{y_q: 2 \leq q \leq \nu\} \circ \{x_q: 1 \leq q \leq \nu\} \circ \{w_{\nu-q}: 0 \leq q \leq \nu - 1\} \circ \{v_q: 1 \leq q \leq \nu\} = v'. \quad (25)$$

Case 11:  $u' = x_1$  and  $v' = z_p, 1 \leq p \leq \nu$

Subcase 11.1:  $1 \leq p \leq \nu - 1$ :

$$P_H(u', v'): u' = x_1 w_1 v_1 \circ \{v_{\nu-q}: 0 \leq q \leq \nu - 2\} \circ \{w_q: 2 \leq q \leq \nu\} \circ \{x_{\nu-q}: 0 \leq q \leq \nu - p - 1\} \circ \{y_{p-q} x_{p-q}: 0 \leq q \leq p - 2\} \circ y_1 \circ \{y_{\nu-q}: 0 \leq q \leq \nu - p - 1\} \circ \{z_q: p + 1 \leq q \leq \nu\} \circ \{z_q: 1 \leq q \leq p\} = v'. \quad (26)$$

Subcase 11.2:  $p = \nu$ :

$$P_H(u', v'): u' = \{x_q: 1 \leq q \leq \nu - 1\} \circ \{w_{\nu-q}: 1 \leq q \leq \nu - 1\} \circ \{v_q: 1 \leq q \leq \nu\} \circ w_\nu x_\nu \circ \{y_{\nu-q}: 0 \leq q \leq \nu - 1\} \circ \{z_q: 1 \leq q \leq \nu\} = v'. \quad (27)$$

**Case 12:**  $u' = x_1$  and  $v' = y_p, 2 \leq p \leq \nu$

Subcase 12.1:  $1 \leq p \leq \nu - 1$ :

$$P_H(u', v'): u' = x_1 w_1 v_1 \circ \{v_q w_q: 1 \leq q \leq \nu\} \circ \{x_{\nu-q}: 0 \leq q \leq \nu - p - 1\} \circ \{y_q: p + 1 \leq q \leq \nu\} \circ \{z_{\nu-q}: 0 \leq q \leq \nu - 1\} \circ y_1 \circ \{x_q v_q: 2 \leq q \leq p\} = v'. \quad (28)$$

Subcase 12.2:  $p = \nu$ :

$$P_H(u', v'): u' = x_1 w_1 v_1 \circ \{v_q w_q: 2 \leq q \leq \nu\} \circ \{x_{\nu-q}: 0 \leq q \leq \nu - 2\} \circ \{y_q: 1 \leq q \leq \nu - 1\} \circ \{z_{\nu-q}: 1 \leq q \leq \nu - 1\} \circ z_\nu y_\nu = v'. \quad (29)$$

**Case 13:**  $u' = x_1$  and  $v' = x_p, 2 \leq p \leq \nu$

Subcase 13.1:  $2 \leq p \leq \nu - 1$ :

$$P_H(u', v'): u' = x_1 y_1 \circ \{z_q: 1 \leq q \leq \nu\} \circ \{y_{\nu-q}: 0 \leq q \leq \nu - p\} \circ \{y_{p-q} x_{p-q}: 1 \leq q \leq p - 1\} \circ \{x_{\nu-q}: 0 \leq q \leq \nu - p - 1\} \circ \{w_q: p + 1 \leq q \leq \nu\} \circ \{v_{\nu-q}: 0 \leq q \leq \nu - 1\} \circ \{w_q: 1 \leq q \leq p\} \circ x_p = v'. \quad (30)$$

Subcase 13.2:  $p = \nu$ :

$$P_H(u', v'): u' = x_1 y_1 \circ \{z_q: 1 \leq q \leq \nu\} \circ \{y_{\nu-q}: 0 \leq q \leq \nu - 2\} \circ \{x_q: 2 \leq q \leq \nu - 1\} \circ \{w_{\nu-q}: 1 \leq q \leq \nu - 1\} \circ \{w_q: 1 \leq q \leq \nu\} \circ w_\nu x_\nu = v'. \quad (31)$$

**Case 14:**  $u' = x_1$  and  $v' = w_p, 1 \leq p \leq \nu$

Subcase 14.1:  $1 \leq p \leq \nu - 1$ :

$$P_H(u', v'): u' = x_1 y_1 \circ \{z_q: 1 \leq q \leq \nu\} \circ \{y_{\nu-q}: 0 \leq q \leq \nu - 2\} \circ \{x_q: 2 \leq q \leq \nu\} \circ \{w_{\nu-q}: 0 \leq q \leq \nu - p - 1\} \circ \{v_q: p + 1 \leq q \leq \nu\} \circ \{v_q w_q: 1 \leq q \leq p\} = v'. \quad (32)$$

Subcase 14.2:  $p = \nu$ :

$$P_H(u', v'): u' = x_1 y_1 z_1 \circ \{z_{\nu-q}: 0 \leq q \leq \nu - 2\} \circ \{y_q: 2 \leq q \leq \nu\} \circ \{x_{\nu-q}: 0 \leq q \leq \nu - 2\} \circ \{w_q: 2 \leq q \leq \nu - 1\} \circ \{v_{\nu-q}: 0 \leq q \leq \nu - 1\} \circ w_1 w_\nu = v'. \quad (33)$$

**Case 15:**  $u' = x_1$  and  $v' = v_p, 1 \leq p \leq \nu$

Subcase 15.1:  $1 \leq p \leq \nu - 1$ :

$$P_H(u', v'): u' = x_1 y_1 \circ \{z_q: 1 \leq q \leq \nu\} \circ \{y_{\nu-q}: 0 \leq q \leq \nu - 2\} \circ \{x_q: 2 \leq q \leq \nu\} \circ \{w_{\nu-q}: 0 \leq q \leq \nu - p\} \circ \{v_q: p + 1 \leq q \leq \nu\} \circ \{v_q w_q: 1 \leq q \leq p - 1\} \circ v_p = v'. \quad (34)$$

Subcase 15.2:  $p = \nu$ :

$$P_H(u', v'): u' = x_1 y_1 \circ \{z_q: 1 \leq q \leq \nu\} \circ \{y_{\nu-q}: 0 \leq q \leq \nu - 2\} \circ \{x_q: 2 \leq q \leq \nu\} \circ \{w_{\nu-q}: 0 \leq q \leq \nu - 1\} \circ \{v_q: 1 \leq q \leq \nu\} = v'. \quad (35)$$

**Case 16:**  $u' = w_1$  and  $v' = z_p, 1 \leq p \leq \nu$

Subcase 16.1:  $1 \leq p \leq \nu - 1$ :

$$P_H(u', v'): u' = w_1 v_1 \circ \{v_{\nu-q}: 0 \leq q \leq \nu - 2\} \circ \{w_q: 2 \leq q \leq \nu\} \circ \{x_{\nu-q}: 0 \leq q \leq \nu - p\} \circ \{y_q: p \leq q \leq \nu\} \circ \{x_q y_q: 1 \leq q \leq p - 1\} \circ \{z_{p-q}: 1 \leq q \leq p - 1\} \circ \{z_{\nu-q}: 0 \leq q \leq \nu - p\} = v'. \quad (36)$$

Subcase 16.2:  $p = \nu$ :

$$P_H(u', v'): u' = w_1 \circ \{v_q: 1 \leq q \leq \nu\} \circ \{w_{\nu-q}: 0 \leq q \leq \nu - 2\} \circ \{x_q: 2 \leq q \leq \nu\} \circ x_1 \circ \{y_{\nu-q}: 0 \leq q \leq \nu - 1\} \circ \{z_q: 1 \leq q \leq \nu\} = v'. \quad (37)$$

**Case 17:**  $u' = w_1$  and  $v' = y_p, 1 \leq p \leq \nu$

Subcase 17.1:  $1 \leq p \leq \nu - 1$ :

$$P_H(u', v'): u' = w_1 v_1 \circ \{v_{\nu-q}: 0 \leq q \leq \nu - 2\} \circ \{w_q: 2 \leq q \leq \nu\} \circ \{x_{\nu-q}: 0 \leq q \leq \nu - p\} \circ \{y_{p-q} x_{p-q}: 1 \leq q \leq p - 1\} \circ \{y_{\nu-q}: 0 \leq q \leq \nu - p - 1\} \circ \{z_q: p + 1 \leq q \leq \nu\} \circ \{z_q: 1 \leq q \leq p\} \circ y_p = v'. \quad (38)$$

Subcase 17.2:  $p = \nu$ :

$$P_H(u', v'): u' = w_1 v_1 \circ \{v_{\nu-q}: 0 \leq q \leq \nu - 2\} \circ \{w_q: 2 \leq q \leq \nu\} \circ \{x_{\nu-q}: 0 \leq q \leq \nu - 1\} \circ \{y_{\nu-q}: 0 \leq q \leq \nu - 1\} \circ \{z_q: 1 \leq q \leq \nu\} = v'. \quad (39)$$

**Case 18:**  $u' = w_1$  and  $v' = x_p, 1 \leq p \leq \nu$

Subcase 18.1:  $1 \leq p \leq \nu - 1$ :

$$P_H(u', v'): u' = w_1 v_1 \circ \{v_{\nu-q}: 0 \leq q \leq \nu - 2\} \circ \{w_q: 2 \leq q \leq \nu\} \circ \{x_{\nu-q}: 0 \leq q \leq \nu - p - 1\} \circ \{y_q: p + 1 \leq q \leq \nu - 1\} \circ \{z_{\nu-q}: 1 \leq q \leq \nu - 1\} \circ z_\nu y_\nu \circ \{x_q y_q: 1 \leq q \leq p - 1\} \circ x_p = v'. \quad (40)$$

Subcase 18.2:  $p = \nu$ :

$$P_H(u', v'): u' = w_1 \circ \{v_q: 1 \leq q \leq \nu\} \circ \{w_{\nu-q}: 0 \leq q \leq \nu - 2\} \circ \{x_q: 2 \leq q \leq \nu - 1\} \circ \{y_{\nu-q}: 1 \leq q \leq \nu - 1\} \circ \{z_q: 1 \leq q \leq \nu\} \circ y_\nu x_1 x_\nu = v'. \quad (41)$$

**Case 19:**  $u' = w_1$  and  $v' = w_p, 2 \leq p \leq \nu$

Subcase 19.1:  $2 \leq p \leq \nu - 1$ :

$$P_H(u', v'): u' = w_1 x_1 y_1 \circ \{z_q: 1 \leq q \leq \nu\} \circ \{y_{\nu-q}: 0 \leq q \leq \nu - 2\} \circ \{x_q: 2 \leq q \leq \nu\} \circ \{w_{\nu-q}: 0 \leq q \leq \nu - p - 1\} \circ \{v_q: p + 1 \leq q \leq \nu\} \circ \{v_q w_q: 1 \leq q \leq p\} = v'. \quad (42)$$

Subcase 19.2:  $p = \nu$ :

$$P_H(u', v'): u' = w_1 x_1 y_1 z_1 \circ \{z_{\nu-q}: 0 \leq q \leq \nu - 2\} \circ \{y_q: 2 \leq q \leq \nu\} \circ \{x_{\nu-q}: 0 \leq q \leq \nu - 2\} \circ \{w_q: 2 \leq q \leq \nu - 1\} \circ \{v_{\nu-q}: 0 \leq q \leq \nu - 1\} \circ v_\nu w_\nu = v'. \quad (43)$$

**Case 20:**  $u' = w_1$  and  $v' = v_p, 1 \leq p \leq \nu$

Subcase 20.1:  $p = 1$ :

$$P_H(u', v'): u' = w_1 x_1 y_1 \circ \{z_q: 1 \leq q \leq \nu\} \circ \{y_{\nu-q}: 0 \leq q \leq \nu - 2\} \circ \{x_q: 2 \leq q \leq \nu\} \circ \{w_{\nu-q}: 0 \leq q \leq \nu - 2\} \circ \{v_q: 2 \leq q \leq \nu\} \circ v_1 = v'. \quad (44)$$

Subcase 20.2:  $2 \leq p \leq \nu - 1$ :

$$P_H(u', v'): u' = w_1 x_1 y_1 \circ \{z_q: 1 \leq q \leq \nu\} \circ \{y_{\nu-q}: 0 \leq q \leq \nu - 2\} \circ \{x_q: 2 \leq q \leq \nu\} \circ \{w_{\nu-q}: 0 \leq q \leq \nu - p\} \circ \{v_q: p + 1 \leq q \leq \nu\} \circ \{v_q w_q: 1 \leq q \leq p - 1\} \circ v_p = v'. \quad (45)$$

Subcase 20.3:  $p = \nu$ :

$$P_H(u', v'): u' = w_1 \circ \{v_q: 1 \leq q \leq \nu - 1\} \circ \{w_{\nu-q}: 0 \leq q \leq \nu - 2\} \circ \{x_q: 2 \leq q \leq \nu - 1\} \circ \{y_{\nu-q}: 1 \leq q \leq \nu - 1\} \circ \{z_q: 1 \leq q \leq \nu\} \circ y_\nu x_1 x_\nu w_\nu v_\nu = v'. \quad (46)$$

**Case 21:**  $u' = v_1$  and  $v' = z_p, 1 \leq p \leq \nu$

Subcase 21.1:  $p = 1$ :

$$P_H(u', v'): u' = \{v_q: 1 \leq q \leq \nu\} \circ \{w_{\nu-q}: 0 \leq q \leq \nu - 1\} \circ x_1 \circ \{x_{\nu-q}: 0 \leq q \leq \nu - 2\} \circ \{w_q: 1 \leq q \leq \nu\} \circ \{z_{\nu-q}: 0 \leq q \leq \nu - 1\} = v'. \quad (47)$$

Subcase 21.2:  $2 \leq p \leq \nu - 1$ :

$$P_H(u', v'): u' = \{v_q: 1 \leq q \leq \nu\} \circ \{w_{\nu-q}: 0 \leq q \leq \nu - 1\} \circ \{x_q y_q: 1 \leq q \leq p - 2\} \circ \{x_q: p - 1 \leq q \leq \nu\} \circ \{y_{\nu-q}: 0 \leq q \leq \nu - p + 1\} \circ \{z_{p-q}: 1 \leq q \leq p - 1\} \circ \{z_{\nu-q}: 0 \leq q \leq \nu - p\} = v'. \quad (48)$$

Subcase 21.3:  $p = \nu$ :

$$P_H(u', v'): u' = \{v_q: 1 \leq q \leq \nu\} \circ \{w_{\nu-q}: 0 \leq q \leq \nu - 1\} \circ \{x_q: 1 \leq q \leq \nu\} \circ \{y_{\nu-q}: 0 \leq q \leq \nu - 1\} \circ \{z_q: 1 \leq q \leq \nu\} = v'. \quad (49)$$

**Case 22:**  $u' = v_1$  and  $v' = y_p, 1 \leq p \leq \nu$

Subcase 22.1:  $1 \leq p \leq \nu - 1$ :

$$P_H(u', v'): u' = \{v_q: 1 \leq q \leq \nu\} \circ \{w_{\nu-q}: 0 \leq q \leq \nu - 1\} \circ \{x_q y_q: 1 \leq q \leq p - 1\} \circ \{x_q: p \leq q \leq \nu\} \circ \{y_{\nu-q}: 0 \leq q \leq \nu - p - 1\} \circ \{z_q: p + 1 \leq q \leq \nu\} \circ \{z_q: 1 \leq q \leq p\} = v'. \quad (50)$$

Subcase 22.2:  $p = \nu$ :

$$P_H(u', v'): u' = \{v_q: 1 \leq q \leq \nu\} \circ \{w_{\nu-q}: 0 \leq q \leq \nu - 1\} \circ \{x_{\nu-q}: 0 \leq q \leq \nu - 1\} \circ \{y_q: 1 \leq q \leq \nu - 1\} \circ \{z_{\nu-q}: 1 \leq q \leq \nu - 1\} \circ z_\nu y_\nu = v'. \quad (51)$$

**Case 23:**  $u' = v_1$  and  $v' = x_p, 1 \leq p \leq \nu$

Subcase 23.1:  $1 \leq p \leq \nu - 1$ :

$$P_H(u', v'): u' = v_1 \circ \{v_{\nu-q}: 0 \leq q \leq \nu - 2\} \circ \{w_q: 1 \leq q \leq \nu\} \circ \{x_{\nu-q}: 0 \leq q \leq \nu - p - 1\} \circ \{y_q: p \leq q \leq \nu - 1\} \circ \{z_{\nu-q}: 1 \leq q \leq \nu - 1\} \circ z_\nu y_\nu \circ \{x_q y_q: 1 \leq q \leq p - 1\} \circ x_p = v'. \quad (52)$$

Subcase 23.2:  $p = \nu$ :

$$P_H(u', v'): u' = \{v_q: 1 \leq q \leq \nu\} \circ \{w_{\nu-q}: 0 \leq q \leq \nu - 1\} \circ \{x_q: 1 \leq q \leq \nu - 1\} \circ \{y_{\nu-q}: 1 \leq q \leq \nu - 1\} \circ \{z_q: 1 \leq q \leq \nu\} \circ y_\nu x_\nu = v'. \quad (53)$$

**Case 24:**  $u' = v_1$  and  $v' = w_p, 1 \leq p \leq \nu$

Subcase 24.1:  $1 \leq p \leq \nu - 1$ :

$$P_H(u', v'): u' = \{v_q w_q: 1 \leq q \leq p - 1\} \circ \{v_q: p \leq q \leq \nu\} \circ \{w_{\nu-q}: 0 \leq q \leq \nu - p - 1\} \circ \{x_q: p + 1 \leq q \leq \nu\} \circ \{y_{\nu-q}: 0 \leq q \leq \nu - 2\} \circ \{z_q: 2 \leq q \leq \nu\} \circ z_1 y_1 \circ \{x_q: 1 \leq q \leq p\} \circ w_p = v'. \quad (54)$$

Subcase 24.2:  $p = \nu$ :



$$P_H(u', v'): u' = v_1 \circ \{v_{\nu-q}: 0 \leq q \leq \nu - 2\} \circ \{w_q: 1 \leq q \leq \nu - 1\} \circ \{x_{\nu-q}: 0 \leq q \leq \nu - 1\} \circ \{y_q: 1 \leq q \leq \nu - 1\} \circ \{z_{\nu-q}: 1 \leq q \leq \nu - 1\} \circ z_\nu y_\nu x_\nu w_\nu = v'. \quad (55)$$

Case 25:  $u' = v_1$  and  $v' = v_p, 2 \leq p \leq \nu$

Subcase 25.1:  $2 \leq p \leq \nu - 1$ :

$$P_H(u', v'): u' = v_1 w_1 x_1 y_1 \circ \{z_q: 1 \leq q \leq \nu\} \circ \{y_{\nu-q}: 0 \leq q \leq \nu - 2\} \circ \{x_q: 2 \leq q \leq \nu\} \circ \{w_{\nu-q} v_{\nu-q}: 0 \leq q \leq \nu - p - 1\} \circ \{w_{p-q}: 0 \leq q \leq p - 2\} \circ \{v_q: 2 \leq q \leq p\} = v'. \quad (56)$$

Subcase 25.2:  $p = \nu$ :

$$P_H(u', v'): u' = v_1 w_1 x_1 y_1 \circ \{z_q: 1 \leq q \leq \nu\} \circ \{y_{\nu-q}: 0 \leq q \leq \nu - 2\} \circ \{x_q: 2 \leq q \leq \nu\} \circ \{w_{\nu-q}: 0 \leq q \leq \nu - 2\} \circ \{v_q: 2 \leq q \leq \nu\} = v'. \quad (57)$$

The existence of the Hamiltonian path between every pair of vertices of the  $H_\nu$  completes the proof.

Using Theorems 1 and 2, the following proposition computes the detour index of  $H_\nu$ .  $\square$

**Corollary 1.** *Let  $G = H_\nu$ , where  $\nu \geq 4$ . Then, the detour index of  $G$  is*

$$\omega(G) = \frac{5\nu(5\nu - 1)^2}{2}. \quad (58)$$

*Proof.* The number of vertices in the graph  $G$  is  $5\nu$ . Replacing  $5\nu$  with  $n$  in Theorem 1 gives the proposition.  $\square$

#### 4. Hamilton-Connectivity and the Detour Index of $G_\nu$

In this section, we show that the graph  $G_\nu$  is Hamilton-connected. Afterwards, we use the Hamilton-connectivity to find the analytical exact expression of the detour index of the graph  $G_\nu$ .

The vertex set of  $G_\nu$  consists of four layers of vertices, i.e.,  $w_p, x_p, y_p$ , and  $z_p$ . That is to say that  $V(G_\nu) = \{w_p, x_p, y_p, z_p: 1 \leq p \leq \nu\}$ . Accordingly, the edge set of  $G_\nu$  is as follows:

$$E(G_\nu) = \{w_p w_{p+1}, x_p x_{p+1}, y_p y_{p+1}, z_p z_{p+1}, w_p x_p, x_p y_p, y_p x_{p+1}, y_p z_p: 1 \leq p \leq \nu - 1\}. \quad (59)$$

The subscripts are to be considered modulo  $\nu$ . Figure 3 presents the  $\nu$ -dimensional convex polytope  $G_\nu$ , with proper labeling of vertices which will be used to show its Hamilton-connectivity.

The following is the main result of this section.

**Theorem 3.** *The graph  $\nu$ -dimensional convex polytope  $G_\nu$ , with  $\nu \geq 5$ , is Hamilton-connected.*

*Proof.* We prove this result by definition. For this, we have to show that there exist Hamiltonian paths between any pair of vertices of  $G_\nu$ .

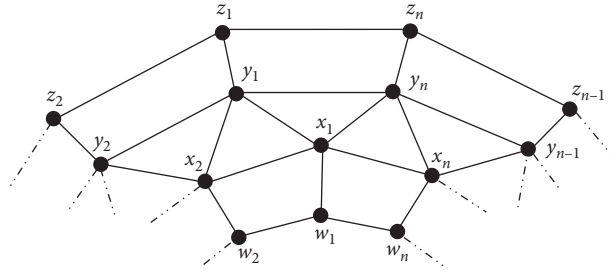
Let  $P_H(u, v)$  be a Hamiltonian path between vertices  $u$  and  $v$  in  $G_\nu$ . Let  $G_\nu = Z \cup Y \cup X \cup W$  such that  $Z = \{z_1, z_2, \dots, z_\nu\}$ ,  $Y = \{y_1, y_2, \dots, y_\nu\}$ ,  $X = \{x_1, x_2, \dots, x_\nu\}$ , and  $W = \{w_1, w_2, \dots, w_\nu\}$  (see Figure 3).

**Case 1:**  $u = z_1$  and  $v = z_p, 2 \leq p \leq \nu$

Subcase 1.1:  $2 \leq p \leq \nu - 2$ :

$$P_H(u, v): u = z_1 \circ \{z_{\nu-q}: 0 \leq q \leq \nu - p - 1\} \circ \{y_{p-q+1}: 0 \leq q \leq p - 2\} \circ \{x_q: 3 \leq q \leq p + 1\} \circ \{x_q y_q: p + 2 \leq q \leq \nu\} \circ y_1 x_1 w_1 \circ \{w_{\nu-q}: 0 \leq q \leq \nu - 2\} \circ x_2 y_2 \circ \{z_q: 2 \leq q \leq p\} = v. \quad (60)$$

Subcase 1.2:  $p = \nu - 1$ :

FIGURE 3: The  $\nu$ -dimensional convex polytope  $G_\nu$ .

$$P_H(u, v): u = z_1 z_\nu \circ \{y_{\nu-q}; 0 \leq q \leq \nu - 3\} \circ \{x_q; 3 \leq q \leq \nu\} \circ \{w_{\nu-q}; 0 \leq q \leq \nu - 1\} \circ x_1 y_1 x_2 y_2 \circ \{z_q; 2 \leq q \leq \nu - 1\} = v. \quad (61)$$

Subcase 1.3:  $p = \nu$ :

$$P_H(u, v): u = z_1 y_1 x_1 w_1 \circ \{w_{\nu-q}; 0 \leq q \leq \nu - 2\} \circ \{x_q; 2 \leq q \leq \nu\} \circ \{y_{\nu-q}; 0 \leq q \leq \nu - 2\} \circ \{z_q; 2 \leq q \leq \nu\} = v. \quad (62)$$

Case 2:  $u = z_1$  and  $v = y_p, 1 \leq p \leq \nu$ Subcase 2.1:  $1 \leq p \leq \nu - 1$ :

$$P_H(u, v): u = \{z_q; 1 \leq q \leq \nu\} \circ \{y_{\nu-q}; 0 \leq q \leq \nu - p - 1\} \circ \{x_q; p + 1 \leq q \leq \nu\} \circ \{w_{\nu-q}; 0 \leq q \leq \nu - 1\} \circ \{x_q y_q; 1 \leq q \leq p\} = v. \quad (63)$$

Subcase 2.2:  $p = \nu$ :

$$P_H(u, v): u = z_1 \circ \{z_{\nu-q}; 0 \leq q \leq \nu - 2\} \circ \{y_q; 2 \leq q \leq \nu - 1\} \circ \{x_{\nu-q}; 1 \leq q \leq \nu - 2\} \circ y_1 x_1 \circ \{w_q; 1 \leq q \leq \nu\} \circ x_\nu y_\nu = v. \quad (64)$$

Case 3:  $u = z_1$  and  $v = x_p, 1 \leq p \leq \nu$ Subcase 3.1:  $1 \leq p \leq \nu - 1$ :

$$P_H(u, v): u = z_1 \circ \{z_q; 2 \leq q \leq \nu\} \circ \{y_{\nu-q}; 0 \leq q \leq \nu - p\} \circ \{x_q; p + 1 \leq q \leq \nu\} \circ \{w_{\nu-q}; 0 \leq q \leq \nu - 1\} \circ \{x_q y_q; 2 \leq q \leq p - 1\} \circ x_p = v. \quad (65)$$

Subcase 3.2:  $p = \nu$ :

$$P_H(u, v): u = \{z_q; 1 \leq q \leq \nu\} \circ \{y_{\nu-q}; 0 \leq q \leq \nu - 1\} \circ \{x_q; 1 \leq q \leq \nu - 1\} \circ \{w_{\nu-q}; 1 \leq q \leq \nu - 1\} \circ w_\nu x_\nu = v. \quad (66)$$

**Case 4:**  $u = z_1$  and  $v = w_p, 1 \leq p \leq \nu$

Subcase 4.2:  $2 \leq p \leq \nu$ :

Subcase 4.1:  $p = 1$ :

$$\begin{aligned} P_H(u, v): u &= \{z_q: 1 \leq q \leq \nu\} \circ \{y_{\nu-q}: 0 \leq q \leq \nu - 1\} \\ &\circ \{x_q: 1 \leq q \leq \nu\} \circ \\ &\{w_{\nu-q}: 0 \leq q \leq \nu - 1\} = v. \end{aligned} \quad (67)$$

---


$$\begin{aligned} P_H(u, v): u &= \{z_q: 1 \leq q \leq \nu\} \circ \{y_{\nu-q}: 0 \leq q \leq \nu - p + 1\} \circ \{x_q: p \leq q \leq \nu\} \circ \\ &\{x_q y_q: 1 \leq q \leq p - 2\} \circ x_{p-1} \circ \{w_{p-q}: 1 \leq q \leq p - 1\} \circ \{w_{\nu-q}: 0 \leq q \leq \nu - p\} = v. \end{aligned} \quad (68)$$


---

**Case 5:**  $u = y_1$  and  $v = z_p, 1 \leq p \leq \nu$

Subcase 5.1:  $1 \leq p \leq \nu - 1$ :

---


$$\begin{aligned} P_H(u, v): u &= y_1 x_1 w_1 \circ \{w_{\nu-q}: 0 \leq q \leq \nu - 2\} \circ \{x_q y_q: 2 \leq q \leq p\} \circ \{x_q: p + 1 \leq q \leq \nu\} \circ \\ &\{y_{\nu-q}: 0 \leq q \leq \nu - p - 1\} \circ \{z_q: p + 1 \leq q \leq \nu\} \circ \{z_q: 1 \leq q \leq p\} = v. \end{aligned} \quad (69)$$


---

Subcase 5.2:  $p = \nu$ :

---


$$\begin{aligned} P_H(u, v): u &= y_1 \circ \{z_q: 1 \leq q \leq \nu - 1\} \circ \{y_{\nu-q}: 1 \leq q \leq \nu - 2\} \circ \{x_q: 2 \leq q \leq \nu - 1\} \circ \\ &\{w_{\nu-q}: 1 \leq q \leq \nu - 1\} \circ w_{\nu} x_{\nu} x_1 y_{\nu} z_{\nu} = v. \end{aligned} \quad (70)$$


---

**Case 6:**  $u = y_1$  and  $v = y_p, 2 \leq p \leq \nu$

Subcase 6.1:  $2 \leq p \leq \nu - 1$ :

---


$$\begin{aligned} P_H(u, v): u &= y_1 \circ \{z_q: 1 \leq q \leq \nu\} \circ \{y_{\nu-q}: 0 \leq q \leq \nu - p - 1\} \circ \{x_q: p + 1 \leq q \leq \nu\} \circ \\ &\{w_{\nu-q}: 0 \leq q \leq \nu - 1\} \circ x_1 \circ \{x_q y_q: 2 \leq q \leq p\} = v. \end{aligned} \quad (71)$$


---

Subcase 6.2:  $p = \nu$ :

---


$$\begin{aligned} P_H(u, v): u &= y_1 z_1 \circ \{z_{\nu-q}: 0 \leq q \leq \nu - 2\} \circ \{y_q: 2 \leq q \leq \nu - 1\} \circ \{x_{\nu-q}: 1 \leq q \leq \nu - 1\} \circ \\ &\{w_q: 1 \leq q \leq \nu\} \circ x_{\nu} y_{\nu} = v. \end{aligned} \quad (72)$$


---

**Case 7:**  $u = y_1$  and  $v = x_p, 1 \leq p \leq \nu$

Subcase 7.1:  $p = 1$ :

---


$$\begin{aligned} P_H(u, v): u &= y_1 \circ \{z_q: 1 \leq q \leq \nu\} \circ \{y_{\nu-q}: 0 \leq q \leq \nu - 2\} \circ \{x_q: 2 \leq q \leq \nu\} \circ \\ &\{w_{\nu-q}: 0 \leq q \leq \nu - 1\} \circ x_1 = v. \end{aligned} \quad (73)$$

Subcase 7.2:  $2 \leq p \leq \nu - 1$ :

$$P_H(u, \nu): u = y_1 \circ \{z_q: 1 \leq q \leq \nu\} \circ \{y_{\nu-q}: 0 \leq q \leq \nu - p\} \circ \{x_q: p + 1 \leq q \leq \nu\} \circ \{w_{\nu-q}: 0 \leq q \leq \nu - 1\} \circ x_1 \circ \{x_q y_q: 2 \leq q \leq p - 1\} \circ x_p = \nu. \quad (74)$$

Subcase 7.3:  $p = \nu$ :

$$P_H(u, \nu): u = y_1 z_1 \circ \{z_{\nu-q}: 0 \leq q \leq \nu - 2\} \circ \{y_q: 2 \leq q \leq \nu\} \circ \{x_q: 1 \leq q \leq \nu - 1\} \circ \{w_{\nu-q}: 1 \leq q \leq \nu - 1\} \circ w_\nu x_\nu = \nu. \quad (75)$$

**Case 8:**  $u = y_1$  and  $\nu = w_p, 1 \leq p \leq \nu$

Subcase 8.1:  $p = 1$ :

$$P_H(u, \nu): u = y_1 z_1 \circ \{z_{\nu-q}: 0 \leq q \leq \nu - 2\} \circ \{y_q: 2 \leq q \leq \nu\} \circ \{x_q: 1 \leq q \leq \nu\} \circ \{w_{\nu-q}: 0 \leq q \leq \nu - 1\} = \nu. \quad (76)$$

Subcase 8.2:  $2 \leq p \leq \nu - 1$ :

$$P_H(u, \nu): u = y_1 x_1 \circ \{x_q y_q: 2 \leq q \leq p\} \circ \{z_{p-q}: 0 \leq q \leq p - 1\} \circ \{z_{\nu-q}: 0 \leq q \leq \nu - p - 1\} \circ \{y_q: p + 1 \leq q \leq \nu\} \circ \{x_{\nu-q}: 0 \leq q \leq \nu - p - 1\} \circ \{w_q: p + 1 \leq q \leq \nu\} \circ \{w_q: 1 \leq q \leq p\} = \nu. \quad (77)$$

Subcase 8.3:  $p = \nu$ :

$$P_H(u, \nu): u = y_1 \circ \{z_q: 1 \leq q \leq \nu\} \circ \{y_{\nu-q}: 0 \leq q \leq \nu - 2\} \circ \{x_q: 2 \leq q \leq \nu\} \circ x_1 \circ \{w_q: 1 \leq q \leq \nu\} = \nu. \quad (78)$$

**Case 9:**  $u = x_1$  and  $\nu = z_p, 1 \leq p \leq \nu$

Subcase 9.1:  $1 \leq p \leq \nu - 1$ :

$$P_H(u, \nu): u = x_1 \circ \{w_q: 1 \leq q \leq \nu\} \circ \{x_{\nu-q}: 0 \leq q \leq \nu - p - 1\} \circ \{y_{p-q} x_{p-q}: 0 \leq q \leq p - 2\} \circ y_1 \circ \{y_{\nu-q}: 0 \leq q \leq \nu - p - 1\} \circ \{z_q: p + 1 \leq q \leq \nu\} \circ \{z_q: 1 \leq q \leq p\} = \nu. \quad (79)$$

Subcase 9.2:  $p = \nu$ :

$$P_H(u, \nu): u = x_1 \circ \{w_q: 1 \leq q \leq \nu\} \circ \{x_{\nu-q}: 0 \leq q \leq \nu - 2\} \circ \{y_q: 2 \leq q \leq \nu\} \circ y_1 \circ \{z_q: 1 \leq q \leq \nu\} = \nu. \quad (80)$$

**Case 10:**  $u = x_1$  and  $\nu = y_p, 1 \leq p \leq \nu$

Subcase 10.1:  $1 \leq p \leq \nu - 1$ :

$$P_H(u, v): u = x_1 \circ \{w_q: 1 \leq q \leq \nu\} \circ \{x_{\nu-q}: 0 \leq q \leq \nu - p - 1\} \circ \{y_q: p + 1 \leq q \leq \nu\} \circ \{z_{\nu-q}: 0 \leq q \leq \nu - 1\} \circ y_1 \circ \{x_q y_q: 2 \leq q \leq p\} = v. \quad (81)$$

Subcase 10.2:  $p = \nu$ :

$$P_H(u, v): u = x_1 \circ \{w_q: 1 \leq q \leq \nu\} \circ \{x_{\nu-q}: 0 \leq q \leq \nu - 2\} \circ \{y_q: 1 \leq q \leq \nu - 1\} \circ \{z_{\nu-q}: 1 \leq q \leq \nu - 1\} \circ z_\nu y_\nu = v. \quad (82)$$

**Case 11:**  $u = x_1$  and  $v = x_p, 2 \leq p \leq \nu$

Subcase 11.1:  $2 \leq p \leq \nu - 1$ :

$$P_H(u, v): u = x_1 \circ \{w_q: 1 \leq q \leq \nu\} \circ \{x_{\nu-q}: 0 \leq q \leq \nu - p - 1\} \circ \{y_q: p \leq q \leq \nu\} \circ \{z_{\nu-q}: 0 \leq q \leq \nu - 1\} \circ \{y_{q-1} x_q: 2 \leq q \leq p\} = v. \quad (83)$$

Subcase 11.2:  $p = \nu$ :

$$P_H(u, v): u = x_1 w_1 \circ \{w_{\nu-q}: 0 \leq q \leq \nu - 2\} \circ \{x_q: 2 \leq q \leq \nu - 1\} \circ \{y_{\nu-q}: 1 \leq q \leq \nu - 1\} \circ \{z_q: 1 \leq q \leq \nu\} \circ y_\nu x_\nu = v. \quad (84)$$

**Case 12:**  $u = x_1$  and  $v = w_p, 1 \leq p \leq \nu$

Subcase 12.2:  $2 \leq p \leq \nu - 1$ :

Subcase 12.1:  $p = 1$ :

$$P_H(u, v): u = x_1 y_1 \circ \{z_q: 1 \leq q \leq \nu\} \circ \{y_{\nu-q}: 0 \leq q \leq \nu - 2\} \circ \{x_q: 2 \leq q \leq \nu\} \circ \{w_{\nu-q}: 0 \leq q \leq \nu - 1\} = v. \quad (85)$$

$$P_H(u, v): u = x_1 \circ \{y_{q-1} x_q: 2 \leq q \leq p - 1\} \circ \{w_{p-q}: 1 \leq q \leq p - 1\} \circ \{w_{\nu-q}: 0 \leq q \leq \nu - p - 1\} \circ \{x_q: p + 1 \leq q \leq \nu\} \circ \{y_{\nu-q}: 0 \leq q \leq \nu - p\} \circ \{z_q: p \leq q \leq \nu\} \circ \{z_q: 1 \leq q \leq p - 1\} \circ y_{p-1} x_p w_p = v. \quad (86)$$

Subcase 12.3:  $p = \nu$ :

$$P_H(u, v): u = x_1 \circ \{w_q: 1 \leq q \leq \nu - 1\} \circ \{x_{\nu-q}: 1 \leq q \leq \nu - 2\} \circ \{y_q: 1 \leq q \leq \nu - 1\} \circ \{z_{\nu-q}: 1 \leq q \leq \nu - 1\} \circ z_\nu y_\nu x_\nu w_\nu = v. \quad (87)$$

**Case 13:**  $u = w_1$  and  $v = z_p, 1 \leq p \leq \nu$

Subcase 13.1:  $1 \leq p \leq \nu - 1$ :

$$P_H(u, v): u = \{w_q: 1 \leq q \leq v\} \circ \{x_{v-q}: 0 \leq q \leq v - p - 1\} \circ \{y_{p-q}x_{p-q}: 0 \leq q \leq p - 1\} \circ \{y_{v-q}: 0 \leq q \leq v - p - 1\} \circ \{z_q: p + 1 \leq q \leq v\} \circ \{z_q: 1 \leq q \leq p\} = v. \quad (88)$$

Subcase 13.2:  $p = v$ :

$$P_H(u, v): u = \{w_q: 1 \leq q \leq v\} \circ \{x_{v-q}: 0 \leq q \leq v - 1\} \circ \{y_{v-q}: 0 \leq q \leq v - 1\} \circ \{z_q: 1 \leq q \leq v\} = v. \quad (89)$$

**Case 14:**  $u = w_1$  and  $v = y_p, 1 \leq p \leq v$

Subcase 14.1:  $1 \leq p \leq v - 1$ :

$$P_H(u, v): u = \{w_q: 1 \leq q \leq v\} \circ \{x_{v-q}: 0 \leq q \leq v - p\} \circ \{y_{p-q}x_{p-q}: 1 \leq q \leq p - 1\} \circ \{y_{v-q}: 0 \leq q \leq v - p - 1\} \circ \{z_q: p + 1 \leq q \leq v\} \circ \{z_q: 1 \leq q \leq p\} \circ y_p = v. \quad (90)$$

Subcase 14.2:  $p = v$ :

$$P_H(u, v): u = \{w_q: 1 \leq q \leq v\} \circ \{x_{v-q}: 0 \leq q \leq v - 1\} \circ \{y_q: 1 \leq q \leq v - 1\} \circ \{z_{v-q}: 1 \leq q \leq v - 1\} \circ z_v y_v = v. \quad (91)$$

Subcase 15.1:  $p = 1$ :

$$P_H(u, v): u = \{w_q: 1 \leq q \leq v\} \circ \{x_{v-q}: 0 \leq q \leq v - 2\} \circ \{y_q: 2 \leq q \leq v\} \circ \{z_{v-q}: 0 \leq q \leq v - 1\} \circ y_1 x_1 = v. \quad (92)$$

**Case 15:**  $u = w_1$  and  $v = x_p, 1 \leq p \leq v$

Subcase 15.2:  $2 \leq p \leq v - 1$ :

$$P_H(u, v): u = \{w_q: 1 \leq q \leq v\} \circ \{x_{v-q}: 0 \leq q \leq v - p - 1\} \circ \{y_q: p \leq q \leq v\} \circ \{z_{v-q}: 0 \leq q \leq v - 1\} \circ y_1 x_1 \circ \{x_q y_q: 2 \leq q \leq p - 1\} \circ x_p = v. \quad (93)$$

Subcase 15.3:  $p = v$ :

$$P_H(u, v): u = w_1 \circ \{w_{v-q}: 0 \leq q \leq v - 2\} \circ \{x_q: 2 \leq q \leq v - 1\} \circ \{y_{v-q}: 1 \leq q \leq v - 1\} \circ \{z_q: 1 \leq q \leq v\} \circ y_v x_1 x_v = v. \quad (94)$$

**Case 16:**  $u = w_1$  and  $v = w_p, 2 \leq p \leq v$

Subcase 16.1:  $2 \leq p \leq v - 1$ :

$$P_H(u, v): u = w_1 \circ \{w_{v-q}: 0 \leq q \leq v - p - 1\} \circ \{x_q y_q: p + 1 \leq q \leq v\} \circ x_1 y_1 z_1 \circ \{z_{v-q}: 0 \leq q \leq v - 2\} \circ \{y_q: 2 \leq q \leq p\} \circ \{x_{p-q}: 0 \leq q \leq p - 2\} \circ \{w_q: 2 \leq q \leq p\} = v. \quad (95)$$

Subcase 16.2:  $p = v$ :

$$\begin{aligned}
 P_H(u, \nu): u = & \{w_q: 1 \leq q \leq \nu - 1\} \circ \{x_{\nu-q}: 1 \leq q \leq \nu - 1\} \\
 & \circ \{y_q: 1 \leq q \leq \nu - 1\} \circ \\
 & \{z_{\nu-q}: 1 \leq q \leq \nu - 1\} \circ z_\nu y_\nu x_\nu w_\nu = \nu.
 \end{aligned}
 \tag{96}$$

The existence of the Hamiltonian path between every pair of vertices of the  $G_\nu$  completes the proof.

Using Theorems 1 and 3, the following proposition computes the detour index of  $G_\nu$ .  $\square$

**Corollary 2.** *Let  $G = G_\nu$ , where  $\nu \geq 4$ . Then, the detour index of  $G$  is*

$$\omega(G) = \frac{4\nu(4\nu - 1)^2}{2}. \tag{97}$$

*Proof.* The number of vertices in the graph  $G$  is  $4\nu$ . Replacing  $4\nu$  with  $n$  in Theorem 1 gives the proposition.  $\square$

### 5. Conclusions and Future Work

Computing the detour index of a graph is NP-complete and checking if a graph is Hamilton-connected is also NP-complete. In this paper, we construct three infinite families of Hamilton-connected convex polytope networks. Furthermore, we construct an infinite family of non-Hamilton-connected convex polytope networks. The later construction shows that not all convex polytope networks are Hamilton-connected. More importantly, we compute exact analytical expressions for the detour index of the families of Hamilton-connected convex polytope networks.

In view of the work by Alspach and Liu [41], we propose the following conjectures [41]:

**Conjecture 1.**

- (i) *The generalized Petersen graph  $GP(\nu, 4)$   $\nu \geq 9$  is nonbipartite Hamilton-connected*
- (ii) *The generalized Petersen graph  $GP(\nu, 5)$   $\nu \geq 11$  is nonbipartite Hamilton-connected if  $\nu|2$  and bipartite Hamilton-laceable if  $\nu \nmid 2$*

### Data Availability

There are no data associated with the manuscript.

### Conflicts of Interest

The authors declare that there are no conflicts of interest.

### References

[1] O. Ore, "Hamilton-connected graphs," *Journal of Pure and Applied Algebra*, vol. 42, pp. 21–27, 1963.  
 [2] R. Frucht, "A canonical representation of trivalent Hamiltonian graphs," *Journal of Graph Theory*, vol. 1, pp. 45–60, 1976.

[3] V. S. Gordon, Y. L. Orlovich, and F. Werner, "Hamiltonian properties of triangular grid graphs," *Discrete Mathematics*, vol. 308, no. 24, pp. 6166–6188, 2008.  
 [4] S. Qiang, Z. Qain, and A. Yahui, "The Hamiltonicity of generalized honeycomb torus networks," *Information Processing Letters*, vol. 115, no. 2, pp. 104–111, 2005.  
 [5] I. A. Stewart, "Sufficient conditions for Hamiltonicity in multiswapped networks," *Journal of Parallel and Distributed Computing*, vol. 101, pp. 17–26, 2017.  
 [6] B. Wei, "Hamiltonian paths and Hamiltonian connectivity in graphs," *Discrete Mathematics*, vol. 121, no. 1–3, pp. 223–228, 1993.  
 [7] X. Yang, D. J. Evans, H. Lai, and G. M. Megson, "Generalized honeycomb torus is Hamiltonian," *Information Processing Letters*, vol. 92, no. 1, pp. 31–37, 2004.  
 [8] M. Bača, "Face anti-magic labelings of convex polytopes," *Utilitas Mathematica*, vol. 55, pp. 221–226, 1999.  
 [9] M. Baca, "Labelings of two classes of convex polytopes," *Utilitas Mathematica*, vol. 34, pp. 24–31, 1988.  
 [10] M. Bača, "On magic labellings of convex polytopes," *Annals of Discrete Mathematics*, vol. 51, pp. 13–16, 1992.  
 [11] M. Miller, M. Baca, and J. A. MacDougall, "Vertex-magic total labeling of generalized Petersen graphs and convex polytopes," *Journal of Combinatorial Mathematics and Combinatorial Computing*, vol. 59, pp. 89–99, 2006.  
 [12] M. Imran, A. Q. Baig, and A. Ahmad, "Families of plane graphs with constant metric dimension," *Utilitas Mathematica*, vol. 88, pp. 43–57, 2012.  
 [13] M. Imran, S. A. U. H. Bokhary, and A. Q. Baig, "On the metric dimension of rotationally-symmetric convex polytopes," *Journal of Algebra Combinatorics Discrete Structures and Applications*, vol. 3, pp. 45–59, 2015.  
 [14] M. Imran and H. M. A. Siddiqui, "Computing the metric dimension of convex polytopes generated by wheel related graphs," *Acta Mathematica Hungarica*, vol. 149, no. 1, pp. 10–30, 2016.  
 [15] M. Imran, S. A. Ul Haq Bokhary, and A. Q. Baig, "On families of convex polytopes with constant metric dimension," *Computers & Mathematics with Applications*, vol. 60, no. 9, pp. 2629–2638, 2010.  
 [16] M. A. Malik and M. Sarwar, "On the metric dimension of two families of convex polytopes," *Afrika Matematika*, vol. 27, no. 1–2, pp. 229–238, 2016.  
 [17] M. Imran, S. A. U. H. Bokhary, A. Ahmad, and A. Semaničová-Feňovčíková, "On classes of regular graphs with constant metric dimension," *Acta Mathematica Scientia*, vol. 33, no. 1, pp. 187–206, 2013.  
 [18] J. Kratica, V. Kovačević-Vučjić, M. Čangalović, and M. Stojanović, "Minimal doubly resolving sets and the strong metric dimension of some convex polytopes," *Applied Mathematics and Computation*, vol. 218, no. 19, pp. 9790–9801, 2012.  
 [19] H. Raza, S. Hayat, and X.-F. Pan, "On the fault-tolerant metric dimension of convex polytopes," *Applied Mathematics and Computation*, vol. 339, pp. 172–185, 2018.  
 [20] H. Raza, J.-B. Liu, and S. Qu, "On mixed metric dimension of rotationally symmetric graphs," *IEEE Access*, vol. 8, pp. 11560–11569, 2020.  
 [21] A. Simić, M. Bogdanović, and J. Milošević, "The binary locating-dominating number of some convex polytopes," *Ars Mathematica Contemporanea*, vol. 13, pp. 367–377, 2017.  
 [22] H. Raza, S. Hayat, and X.-F. Pan, "Binary locating-dominating sets in rotationally-symmetric convex polytopes," *Symmetry*, vol. 10, no. 12, pp. 727–745, 2018.

- [23] A. L. J. Savić, Z. L. J. Maksimović, and M. S. Bogdanović, "The open-locating-dominating number of some convex polytopes," *Filomat*, vol. 32, no. 2, pp. 635–642, 2018.
- [24] S. Hayat, A. Khan, S. Khan, and J.-B. Liu, "Hamilton connectivity of convex polytopes with applications to their detour index," *Complexity*, vol. 2021, Article ID 6684784, , 2021.
- [25] I. Lukovits, "The detour index," *Croatica Chemica Acta*, vol. 69, pp. 873–882, 1996.
- [26] I. Lukovits, "Indicators for atoms included in cycles," *Journal of Chemical Information and Computer Sciences*, vol. 36, no. 1, pp. 65–68, 1996.
- [27] N. Trinajstić, S. Nikolić, B. Lučić, D. Amić, and Z. Mihalić, "The detour matrix in chemistry," *Journal for Chemical Information and Computer Scientists*, vol. 37, pp. 631–638, 1997.
- [28] G. Rücker and C. Rücker, "Symmetry-aided computation of the detour matrix and the detour index," *Journal of Chemical Information and Computer Sciences*, vol. 38, no. 4, pp. 710–714, 1998.
- [29] F. Harary, *Graph Theory*, p. 203, Addison-Wesley, Reading, MA, USA, 1969.
- [30] A. Mahmiani, O. Khormali, and A. Iranmanesh, "The edge versions of detour index," *MATCH Communications in Mathematical and in Computer Chemistry*, vol. 62, no. 2, pp. 419–431, 2009.
- [31] B. Zhou and X. Cai, "Index," *Contesting Aging and Loss*, vol. 63, pp. 199–210, 2010.
- [32] X. Qi and B. Zhou, "Detour index of a class of unicyclic graphs," *Filomat*, vol. 24, no. 1, pp. 29–40, 2010.
- [33] C. Du, "Minimum detour index of bicyclic graphs," *MATCH Communications in Mathematical and in Computer Chemistry*, vol. 68, no. 1, pp. 357–370, 2012.
- [34] W. Fang, Z. Q. Cai, and X. X. Li, "Minimum detour index of tricyclic graphs," *Journal of Chemistry*, vol. 2019, Article ID 6031568, 8 pages, 2019.
- [35] A. Karbasioun, A. R. Ashrafi, and M. V. Diudea, "Distance and detour matrices of an infinite class of dendrimer nano-stars," *MATCH Communications in Mathematical and in Computer Chemistry*, vol. 63, no. 1, pp. 239–246, 2010.
- [36] R. Wu and H. Deng, "Graphene quantum dots," *Carbon Nanomaterials Sourcebook*, vol. 8, no. 2, pp. 45–82, 2016.
- [37] V. Kaladevi and A. Abinayaa, "On detour distance Laplacian energy," *Journal of Informatics and Mathematical Sciences*, vol. 9, no. 3, pp. 721–732, 2017.
- [38] H. O. Abdullah and Z. I. Omar, "Edge restricted detour index of some graphs," *Journal of Discrete Mathematical Sciences and Cryptography*, vol. 23, no. 4, pp. 861–877, 2020.
- [39] J.-H. Tang, U. Ali, M. Javaid, and K. Shabbir, "Zagreb connection indices of subdivision and semi-total point operations on graphs," *Journal of Chemistry*, vol. 2019, Article ID 9846913, 14 pages, 2019.
- [40] A. A. Dobrynin, R. Entringer, and I. Gutman, "Wiener index of trees: theory and applications," *Acta Applicandae Mathematicae*, vol. 66, no. 3, pp. 211–249, 2001.
- [41] B. Alspach and J. Liu, "On the Hamilton connectivity of generalized Petersen graphs," *Discrete Mathematics*, vol. 309, no. 17, pp. 5461–5473, 2009.



## Research Article

# Computing Bounds for Second Zagreb Coindex of Sum Graphs

Muhammad Javaid <sup>1</sup>, Muhammad Ibraheem <sup>1</sup>, Uzma Ahmad <sup>2</sup>, and Q. Zhu<sup>3,4</sup>

<sup>1</sup>Department of Mathematics, School of Science, University of Management and Technology, Lahore 54770, Pakistan

<sup>2</sup>Department of Mathematics, University of the Punjab, Lahore, Pakistan

<sup>3</sup>School of Mathematics and Statistics, Hunan Normal University, Changsha, Hunan 4100081, China

<sup>4</sup>Department of Mathematics, School of Information Science and Engineering, Chengdu University, Chengdu 610106, China

Correspondence should be addressed to Muhammad Javaid; [javidmath@gmail.com](mailto:javidmath@gmail.com)

Received 23 April 2021; Accepted 1 June 2021; Published 16 July 2021

Academic Editor: Stylianos Georgantzinos

Copyright © 2021 Muhammad Javaid et al. This is an open access article distributed under the Creative Commons Attribution License, which permits unrestricted use, distribution, and reproduction in any medium, provided the original work is properly cited.

Topological indices or coindices are one of the graph-theoretic tools which are widely used to study the different structural and chemical properties of the under study networks or graphs in the subject of computer science and chemistry, respectively. For these investigations, the operations of graphs always played an important role for the study of the complex networks under the various topological indices or coindices. In this paper, we determine bounds for the second Zagreb coindex of a well-known family of graphs called  $F$ -sum ( $S$ -sum,  $R$ -sum,  $Q$ -sum, and  $T$ -sum) graphs in the form of Zagreb indices and coindices of their factor graphs, where these graphs are obtained by using four subdivision-related operations and Cartesian product of graphs. At the end, we illustrate the obtained results by providing the exact and bonded values of some specific  $F$ -sum graphs.

## 1. Introduction

A topological index (TI) is a function from the set of graphs to the set of real numbers that assigns the different numerical values to the different graphs unless the graphs are isomorphic. Moreover, TIs are essential tools to discuss various physical and chemical properties of the graphs such as volume, density, connectivity, boiling point, freezing point, and heat of formation and evaporation [1, 2]. TIs are also used to study the quantitative structure property relationships (QSPRs), quantitative structure activity relationships (QSARs), and clinical practices of various medications in the subject of cheminformatics and pharmaceutical industries, respectively (see [3–5]). Mainly TIs have three types such as degree, distance, and polynomial based but the degree-based TIs are more studied than others (see the most recent review [6]).

Firstly, an American Chemist Harry Wiener (1947) used a distance-based TI to calculate the boiling point of paraffin (see [7]). First and second Zagreb indices are introduced by Gutman and Trinajstić in 1972; these indices are used to

calculate total  $\pi$ -electron energy of alternant hydrocarbons [8]. Kinkar and Gutman calculated different relations between the second Zagreb index of a graph and its complement (see [9]). Yan et al. computed sharp bounds for the second Zagreb index of different unicyclic graphs [10]. Carlos et al. calculated the second Zagreb index of the graphs with minimum and maximum vertex degrees. They also investigated trees with the maximum value of the second Zagreb index among all trees with maximum vertex degree [11].

Recently, Zagreb coindices are introduced by Ashrafi et al., and they studied them for the derived graphs obtained by the operations of joining, union, disjunction, Cartesian product, and corona product (see [12, 13]). Kinkar et al. calculated the first Zagreb index and multiplicative Zagreb coindices of tree (see [14]). Gutman obtained coindices of graphs and their complements (see [15]). Nilanjan et al. calculated  $F$ -coindex of some graph operations (see [16]). Javaid et al. calculated the first Zagreb connection index and coindex of some derived graphs [17]. Ramane et al. calculated coindices for the transmission and reciprocal

transmission-based graphs (see [18]). Mansour and Song computed  $a$  and  $(a, b)$ -analogs of Zagreb indices and coindices of graphs [19]. For further studies of Zagreb indices, see [20].

There are various operations on graphs such as union, intersection, complement, product, and subdivision. These operations on graphs are useful to obtain the new graphs from the old ones. Yan et al. listed five new graphs  $L(G)$ ,  $S(G)$ ,  $Q(G)$ ,  $R(G)$ , and  $T(G)$  with the help of five operations  $L$ ,  $S$ ,  $Q$ ,  $R$ , and  $T$  on a graph  $G$ , respectively, and studied the behavior of Wiener index of these graphs (see [4]). Eliasi and Taeri computed the Wiener indices of the  $F$ -sum graphs obtained by the Cartesian product of  $F(G_1)$  and  $G_2$ , where  $F \in \{S, R, Q, T\}$  [21]. Later on, many researchers worked on these  $F$ -sum graphs such as Deng et al. [22] computed first and second Zagreb indices, Akhtar and Imran calculated the forgotten index [23], Liu et al. computed first general Zagreb index [24], Ahmad et al. calculated sharp bounds of general sum-connectivity index [11], and Alanazi et al. calculated Gutman indices [25].

In this paper, we compute the bounds for the second Zagreb coindex of  $F$ -sum graphs in the form of Zagreb indices and coindices of their factor graphs. At the end, the obtained results are additionally illustrated with the assistance of examples of the exact and bonded values for some specific  $F$ -sum graphs. The rest of the paper is settled as follows: Section 2 contains the basic definitions and notions, Section 3 covers the main results, and Section 4 presents conclusion with specific examples related to the derived results.

## 2. Preliminaries

A graph denoted by  $G = (V(G), E(G))$  is formed by set of vertices  $V(G)$  and edges  $E(G)$ , where edge set is subset of the Cartesian product of set of vertices, i.e.,  $E(G) \subseteq V(G) \times V(G)$ . In a simple connected graph  $G = (V(G), E(G))$ , total number of vertices is called its order (denoted by  $|V(G)|$ ) and total number of edges is called its size (presented by  $|E(G)|$ ). The degree of a vertex  $u \in V(G)$  is number of its neighborhood vertices that is denoted by  $d(u)$ . The complement of  $G$  is denoted by  $\bar{G}$  and defined as  $V(\bar{G}) = V(G)$ , and any two vertices (say  $u$  and  $v$ ) imply that  $uv \in \bar{G}$  iff  $uv \notin G$ . Gutman and Trinajsti in 1972 [8] introduced the first and second Zagreb indices (denoted by  $M_1$  and  $M_2$ ) as follows:

$$\begin{aligned} M_1(G) &= \sum_{p_1 p_2 \in E(G)} [d_G(p_1) + d_G(p_2)], \\ M_2(G) &= \sum_{p_1 p_2 \in E(G)} [d_G(p_1)d_G(p_2)]. \end{aligned} \quad (1)$$

The second Zagreb coindex  $\bar{M}_2(G)$  is defined in [13] as follows:

$$\bar{M}_2(G) = \sum_{p_1 p_2 \notin E(G)} [d_G(p_1)d_G(p_2)]. \quad (2)$$

It is important to note that the above defined coindex uses degrees of  $G$  but run over  $E(\bar{G})$ .

Let  $G$  be a graph, then

- (i)  $S(G)$  is a graph obtained by inserting one vertex in every edge of  $G$
- (ii)  $R(G)$  is a graph obtained from  $S(G)$  by joining the adjacent vertices of  $G$
- (iii)  $Q(G)$  is a graph formed from  $S(G)$  by joining the pairs of new vertices which are on the adjacent edges (the edges with one common vertex) of  $G$
- (iv)  $T(G)$  is obtained by performing both operations of  $R(G)$  and  $Q(G)$  on  $S(G)$ , respectively

Let  $G_1$  and  $G_2$  be two simple connected graphs, then their  $F$ -sum graphs are denoted by  $G_{1+F}G_2$  having vertex set  $|V(G_{1+F}G_2)| = V(G_1) \cup E(G_1) \times V(G_2)$  and  $(u_1, u_2)(v_1, v_2) \in E(G_{1+F}G_2)$  iff

- (i)  $u_1 = v_1 \in V(G_1)$  and  $u_2 \sim v_2 \in G_2$
- (ii)  $u_2 = v_2 \in V(G_2)$  and  $u_1 \sim v_1 \in F(G_1)$ , where  $F \in \{S, R, Q, T\}$

For details, see Figures 1–3.

## 3. Main Results

In this section, main results of the second Zagreb coindex for the  $F$ -sum graphs are discussed.

**Theorem 1.** Let  $G_1$  and  $G_2$  be two simple connected graphs, then second Zagreb coindex of  $G_{1+S}G_2$  is given as follows:

$$\alpha_1 \leq \bar{M}_2(G_{1+S}G_2) \leq \alpha_2, \quad (3)$$

where

$$\begin{aligned} \alpha_1 &= 2n_2e_1^2((n_1 - 2) + n_1(n_2 - 1)) + 2(n_2^2e_1^2 - n_2e_1) + 4e_2e_1[(n_1 - 2) + n_1(n_2 - 1)] + 2(e_2 + \bar{e}_2)M_1(G_1) + 2e_2\bar{M}_1(G_1) \\ &\quad + (n_2 + 2(e_2 + \bar{e}_2))M_2(G_1)\bar{M}_2(G_1) + (e_1 + \bar{e}_1)M_1(G_2) + 2e_1\bar{M}_1(G_2) + 2(e_1 + \bar{e}_1)M_2(G_2) \\ &\quad + (n_1 + 2(e_1 + \bar{e}_1))\bar{M}_2(G_2) + (M_1(G_2) + \bar{M}_1(G_2))(M_1(G_1) + \bar{M}_1(G_1)), \\ \alpha_2 &= 4n_2e_1E(S(G_1))(n_2 - 1 + n_2(n_1 - 2)) + 2(n_2^2e_1^2 - n_2e_1) + 4e_2e_1[(n_1 - 2) + n_1(n_2 - 1)] + 2(e_2 + \bar{e}_2)M_1(G_1) \\ &\quad + 2e_2\bar{M}_1(G_1) + (n_2 + 2(e_2 + \bar{e}_2))M_2(G_1)\bar{M}_2(G_1) + (e_1 + \bar{e}_1)M_1(G_2) + 2e_1\bar{M}_1(G_2) + 2(e_1 + \bar{e}_1)M_2(G_2) \\ &\quad + (n_1 + 2(e_1 + \bar{e}_1))\bar{M}_2(G_2) + (M_1(G_2) + \bar{M}_1(G_2))(M_1(G_1) + \bar{M}_1(G_1)). \end{aligned} \quad (4)$$

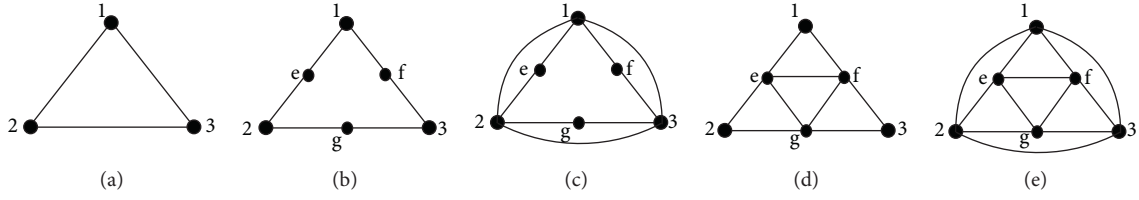


FIGURE 1: (a)  $G \cong C_3$ ; (b)  $S(G) \cong S(C_3)$ ; (c)  $Q(G) \cong Q(C_3)$ ; (d)  $R(G) \cong R(C_3)$ ; (e)  $T(G) \cong T(C_3)$ .

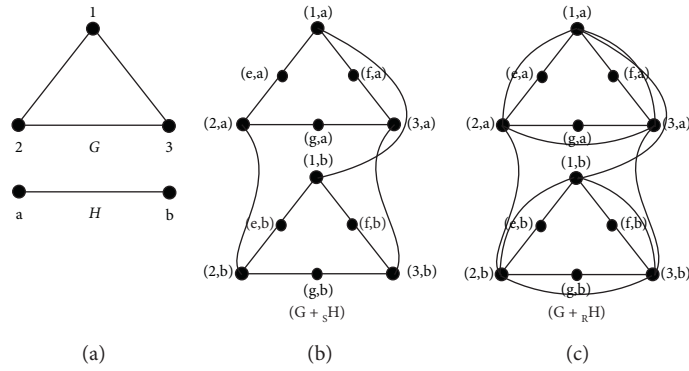


FIGURE 2:  $G \cong C_3$ ;  $H \cong P_2$ ;  $C_{3+S}P_2$ ;  $C_{3+R}P_2$ .

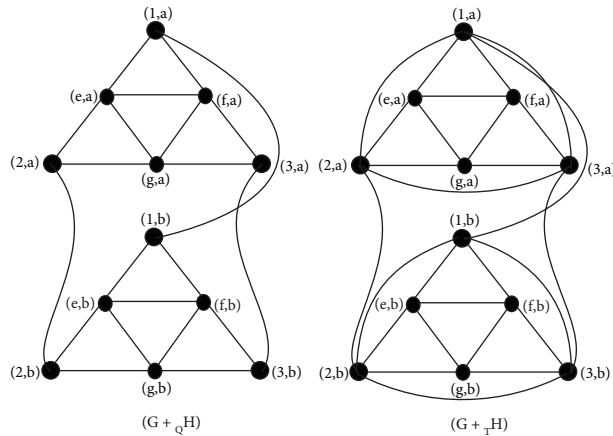


FIGURE 3:  $C_{3+Q}P_2$  and  $C_{3+T}P_2$ .

*Proof.* Using equation (2), we have

$$\overline{M}_2(G_{1+S}G_2) = \sum_{(p_1, p_2) (q_1, q_2) \notin E(G_{1+S}G_2)} [d(p_1, q_1)d(p_2, q_2)], \tag{5}$$

$$\overline{M}_2(G_{1+S}G_2) = \sum_{(p_1, p_2) (q_1, q_2) \in E(G_{1+S}G_2)} [d(p_1, q_1)d(p_2, q_2)] = \sum A + \sum B + \sum C,$$

$$\begin{aligned} \sum A &= \sum_{p_1, p_2 \in V(S(G_1)-V(G_1))} \sum_{q_1, q_2 \in V(G_2)} [d(p_1, q_1)(p_2, q_2)] \\ &= \sum_{p_1, p_2 \in V(S(G_1)-V(G_1))} \sum_{q_1, q_2 \in V(G_2)} [d_{S(G_1)}(p_1)d_{S(G_1)}(p_2)] = \sum_{p_1, p_2 \in V(S(G_1)-V(G_1))} \sum_{q_1, q_2 \in V(G_2)} (2 \times 2), \\ \sum A &= 2(n_2^2 e_1^2 - n_2 e_1), \end{aligned} \tag{6}$$

$$\begin{aligned}
\sum B &= \sum B_1 + \sum B_2 + \sum B_3 + \sum B_4 + \sum B_5 + \sum B_6, \\
\sum B_1 &= \sum_{p \in V_{G_1}} \sum_{q_1, q_2 \notin E_{G_2}} [d(t, q_1)d(t, q_2)] \\
&= \sum_{p \in V_{G_1}} \sum_{q_1, q_2 \notin E_{G_2}} [(d_{G_1}(p) + d_{G_2}(q_1)d_{G_1}(p) + d_{G_2}(q_2))] \\
&= \sum_{p \in V_{G_1}} \sum_{q_1, q_2 \notin E_{G_2}} [d_{G_1}(p)d_{G_1}(p) + d_{G_1}(p)d_{G_2}(q_2) + d_{G_1}(p)d_{G_2}(q_1) + d_{G_2}(q_1)d_{G_2}(q_2)] \\
&= M_1(G_1)\bar{e}_2 + 2e_1\bar{M}_1(G_2) + n_1\bar{M}_2(G_2), \\
\sum B_2 &= \sum_{p_1, p_2 \in V_{G_1}} \sum_{q \in V_{G_2}} [d(p_1, q)d(p_2, q)] \\
&= \sum_{q \in V_{G_2}} \sum_{p_1, p_2 \in E_{G_1}} [d(p_1, q)d(p_2, q)] + \sum_{q \in V_{G_2}} \sum_{p_1, p_2 \notin E_{G_1}} [d(p_1, q)d(p_2, q)] \\
&= \sum_{q \in V_{G_2}} \sum_{p_1, p_2 \in E_{G_1}} [(d_{G_1}(p_1) + d_{G_2}(q))(d_{G_1}(p_2) + d_{G_2}(q))] + \sum_{q \in V_{G_2}} \sum_{p_1, p_2 \notin E_{G_1}} [(d_{G_1}(p_1) + d_{G_2}(q))(d_{G_1}(p_2) + d_{G_2}(q))] \\
&= \sum_{q \in V_{G_2}} \sum_{p_1, p_2 \in E_{G_1}} [d_{G_1}(p_1)d_{G_1}(p_2) + d_{G_1}(p_1)d_{G_2}(q) + d_{G_1}(p_2)d_{G_2}(q) + d_{G_2}(q)^2] \\
&\quad + \sum_{q \in V_{G_2}} \sum_{p_1, p_2 \notin E_{G_1}} [d_{G_1}(p_1)d_{G_1}(p_2) + d_{G_1}(p_1)d_{G_2}(q) + d_{G_1}(p_2)d_{G_2}(q) + d_{G_2}(q)^2] \\
&= n_2M_2(G_1) + 2e_2M_1(G_1) + e_1M_1(G_2) + n_2\bar{M}_2(G_1) + 2e_2\bar{M}_1(G_1) + \bar{e}_1M_1(G_2), \\
\sum B_3 &= \sum_{p_1, p_2 \in E_{G_1}} \sum_{q_1, q_2 \in E_{G_2}} [d(p_1, q_1)d(p_2, q_2)] \\
&= \sum_{p_1, p_2 \in E_{G_1}} \sum_{q_1, q_2 \in E_{G_2}} [(d_{G_1}(p_1) + d_{G_2}(q_1))(d_{G_1}(p_2) + d_{G_2}(q_2))] \\
&= \sum_{p_1, p_2 \in E_{G_1}} \sum_{q_1, q_2 \in E_{G_2}} [d_{G_1}(p_1)d_{G_1}(p_2) + d_{G_1}(p_1)d_{G_2}(q_2) + d_{G_1}(p_2)d_{G_2}(q_1) + d_{G_2}(q_1)d_{G_2}(q_2)] \\
&= 2e_2M_2(G_1) + M_1(G_1)M_1(G_2) + 2e_1M_2(G_2), \\
\sum B_4 &= \sum_{p_1, p_2 \notin E_{G_1}} \sum_{q_1, q_2 \in E_{G_2}} [d(p_1, q_1)d(p_2, q_2)] \\
&= \sum_{p_1, p_2 \notin E_{G_1}} \sum_{q_1, q_2 \in E_{G_2}} [(d_{G_1}(p_1) + d_{G_2}(q_1))(d_{G_1}(p_2) + d_{G_2}(q_2))] \\
&= \sum_{p_1, p_2 \notin E_{G_1}} \sum_{q_1, q_2 \in E_{G_2}} [d_{G_1}(p_1)d_{G_1}(p_2) + d_{G_1}(p_1)d_{G_2}(q_2) + d_{G_1}(p_2)d_{G_2}(q_1) + d_{G_2}(q_1)d_{G_2}(q_2)] \\
&= 2e_2\bar{M}_2(G_1) + \bar{M}_1(G_1)M_1(G_2) + 2\bar{e}_1M_2(G_2), \\
\sum B_5 &= \sum_{p_1, p_2 \notin E_{G_1}} \sum_{q_1, q_2 \notin E_{G_2}} [d(p_1, q_1)d(p_2, q_2)] \\
&= \sum_{p_1, p_2 \notin E_{G_1}} \sum_{q_1, q_2 \notin E_{G_2}} [(d_{G_1}(p_1) + d_{G_2}(q_1))(d_{G_1}(p_2) + d_{G_2}(q_2))] \\
&= \sum_{p_1, p_2 \notin E_{G_1}} \sum_{q_1, q_2 \notin E_{G_2}} [d_{G_1}(p_1)d_{G_1}(p_2) + d_{G_1}(p_1)d_{G_2}(q_2) + d_{G_1}(p_2)d_{G_2}(q_1) + d_{G_2}(q_1)d_{G_2}(q_2)] \\
&= 2\bar{e}_2\bar{M}_2(G_1) + \bar{M}_1(G_1)\bar{M}_1(G_2) + 2\bar{e}_1\bar{M}_2(G_2), \\
\sum B_6 &= \sum_{p_1, p_2 \in E_{G_1}} \sum_{q_1, q_2 \notin E_{G_2}} [d(p_1, q_1)d(p_2, q_2)] \\
&= \sum_{p_1, p_2 \in E_{G_1}} \sum_{q_1, q_2 \notin E_{G_2}} [(d_{G_1}(p_1) + d_{G_2}(q_1))(d_{G_1}(p_2) + d_{G_2}(q_2))] \\
&= \sum_{p_1, p_2 \in E_{G_1}} \sum_{q_1, q_2 \notin E_{G_2}} [d_{G_1}(p_1)d_{G_1}(p_2) + d_{G_1}(p_1)d_{G_2}(q_2) + d_{G_1}(p_2)d_{G_2}(q_1) + d_{G_2}(q_1)d_{G_2}(q_2)]
\end{aligned} \tag{7}$$

$$\begin{aligned}
 &= 2\bar{e}_2 M_2(G_1) + M_1(G_1)\bar{M}_1(G_2) + 2e_1\bar{M}_2(G_2), \\
 \sum B &= 2[(e_2 + \bar{e}_2)M_1(G_1) + e_2\bar{M}_1(G_1)] + (n_2 + 2(e_2 + \bar{e}_2))M_2(G_1)\bar{M}_2(G_1) + (e_1 + \bar{e}_1)M_1(G_2) \\
 &\quad + 2[e_1\bar{M}_1(G_2) + (e_1 + \bar{e}_1)M_2(G_2)] + (n_1 + 2(e_1 + \bar{e}_1))\bar{M}_2(G_2) + (M_1(G_2) + \bar{M}_1(G_2))(M_1(G_1) + \bar{M}_1(G_1)), \\
 \sum C &= \sum C_1 + \sum C_2 + \sum C_3, \\
 \sum C_1 &= \sum_{\substack{p_1 p_2 \notin E(S(G_1)) \\ p_1 \in V(G_1) \\ p_2 \in V(S(G_1)-V(G_1))}} \sum_{q \in V_{G_2}} [d(p_1, q)d(p_2, q)] = \sum_{\substack{p_1 p_2 \notin E(S(G_1)) \\ p_1 \in V(G_1) \\ p_2 \in V(S(G_1)-V(G_1))}} \sum_{q \in V_{G_2}} [(d_{G_1}(p_1) + d_{G_2}(q))(d_{G_1}(p_2))] \\
 &= \sum_{\substack{p_1 p_2 \notin E(S(G_1)) \\ p_1 \in V(G_1) \\ p_2 \in V(S(G_1)-V(G_1))}} \sum_{q \in V_{G_2}} [(d_{G_1}(p_1) + d_{G_2}(q))2] + \sum_{\substack{p_1 p_2 \notin E(S(G_1)) \\ p_1 \in V(G_1) \\ p_2 \in V(S(G_1)-V(G_1))}} \sum_{q \in V_{G_2}} [2(d_{G_1}(p_1) + 2d_{G_2}(q))] \\
 &= 2n_2 \sum_{\substack{p_1 p_2 \notin E(S(G_1)) \\ p_1 \in V(G_1) \\ p_2 \in V(S(G_1)-V(G_1))}} d(p_1) + 4e_2 e_1 (n_1 - 2).
 \end{aligned} \tag{8}$$

Note that

$$\begin{aligned}
 e_1 &\leq \sum_{\substack{p_1 p_2 \notin E(S(G_1)) \\ p_1 \in V(G_1) \\ p_2 \in V(S(G_1)-V(G_1))}} [d(p_1)] \leq 2e_1 (n_1 - 2)E(S(G_1)), \\
 2n_2 e_1 + 4e_2 e_1 (n_1 - 2) &\leq \sum C_1 \leq 4n_2 e_1 (n_1 - 2)E(S(G_1)) + 4e_2 e_1 (n_1 - 2), \\
 \sum C_2 &= \sum_{\substack{p_1 p_2 \notin E(S(G_1)) \\ p_1 \in V(G_1) \\ p_2 \in V(S(G_1)-V(G_1))}} \sum_{q_1, q_2 \in V_{G_2}} [d(p_1, q_1)d(p_2, q_2)] = \sum_{\substack{p_1 p_2 \notin E(S(G_1)) \\ p_1 \in V(G_1) \\ p_2 \in V(S(G_1)-V(G_1))}} \sum_{q_1, q_2 \in V_{G_2}} [(d_{G_1}(p_1) + d(q_1))(d_{S(G_1)}(p_2))] \\
 &= \sum_{\substack{p_1 p_2 \notin E(S(G_1)) \\ p_1 \in V(G_1) \\ p_2 \in V(S(G_1)-V(G_1))}} \sum_{q_1, q_2 \in V_{G_2}} [(d_{G_1}(p_1) + d(q_1))2] = \sum_{\substack{p_1 p_2 \notin E(S(G_1)) \\ p_1 \in V(G_1) \\ p_2 \in V(S(G_1)-V(G_1))}} \sum_{q_1, q_2 \in V_{G_2}} [2d_{G_1}(p_1) + 2d(q_1)] \\
 &= 2n_2 (n_2 - 1) \sum_{\substack{p_1 p_2 \notin E(S(G_1)) \\ p_1 \in V(G_1) \\ p_2 \in V(S(G_1)-V(G_1))}} [d_{G_1}(p_1)] + 2(2e_2)e_1 (n_1 - 2)(n_2 - 1).
 \end{aligned} \tag{9}$$

Note that

$$\begin{aligned}
 e_1 &\leq \sum_{\substack{p_1 p_2 \notin E(S(G_1)) \\ p_1 \in V(G_1) \\ p_2 \in V(S(G_1)-V(G_1))}} d(p_1) \leq 2e_1(n_1 - 2)E(S(G_1)), \\
 2n_2(n_2 - 1)e_1 + 4e_2e_1(n_1 - 2)(n_2 - 1) &\leq \sum C_2 \leq 4n_2(n_2 - 1)e_1(n_1 - 2)E(S(G_1)) + 4e_2e_1(n_1 - 2)(n_2 - 1), \\
 \sum C_3 &= \sum_{\substack{p_1 p_2 \notin E(S(G_1)) \\ p_1 \in V(G_1) \\ p_2 \in V(S(G_1)-V(G_1))}} \sum_{q_1, q_2 \in V_{G_2}} [d(p_1, q_1) + d(p_2, q_2)] \\
 &= \sum_{\substack{p_1 p_2 \notin E(S(G_1)) \\ p_1 \in V(G_1) \\ p_2 \in V(S(G_1)-V(G_1))}} \sum_{q_1, q_2 \in V_{G_2}} [(d_{G_1}(p_1) + d(q_1))d_{S(G_1)}(p_2)] \\
 &= \sum_{\substack{p_1 p_2 \notin E(S(G_1)) \\ p_1 \in V(G_1) \\ p_2 \in V(S(G_1)-V(G_1))}} \sum_{q_1, q_2 \in V_{G_2}} [(d_{G_1}(p_1) + d(q_1))^2] \\
 &= \sum_{\substack{p_1 p_2 \notin E(S(G_1)) \\ p_1 \in V(G_1) \\ p_2 \in V(S(G_1)-V(G_1))}} \sum_{q_1, q_2 \in V_{G_2}} [2d_{G_1}(p_1) + 2d(q_1)] \\
 &= 2n_2(n_2 - 1) \sum_{\substack{p_1 p_2 \notin E(S(G_1)) \\ p_1 \in V(G_1) \\ p_2 \in V(S(G_1)-V(G_1))}} [d(p_1)] + 2(2e_2)(n_2 - 1)2e_1.
 \end{aligned} \tag{10}$$

Note that

$$\begin{aligned}
 2e_1 &\leq \sum_{\substack{p_1 p_2 \notin E(S(G_1)) \\ p_1 \in V(G_1) \\ p_2 \in V(S(G_1)-V(G_1))}} d(p_1) \leq 2e_1E(S(G_1)), \\
 4e_1n_2(n_2 - 1) + 8e_1e_2(n_2 - 1) &\leq \sum C_3 \leq 4e_1n_2(n_2 - 1)E(S(G_1)) + 8e_1e_2(n_2 - 1).
 \end{aligned} \tag{11}$$

Consequently,

$$\begin{aligned}
 &2n_2e_1 + 4e_2e_1(n_1 - 2) + 2n_2(n_2 - 1)e_1 + 4e_2e_1(n_1 - 2)(n_2 - 1) + 4e_1n_2(n_2 - 1) + 8e_1e_2(n_2 - 1) \\
 &\leq \sum C \leq 4n_2e_1(n_1 - 2)E(S(G_1)) + 4e_2e_1(n_1 - 2) + 4n_2(n_2 - 1)e_1(n_1 - 2)E(S(G_1)) \\
 &\quad + 4e_2e_1(n_1 - 2)(n_2 - 1) + 4e_1n_2(n_2 - 1)E(S(G_1)) + 8e_1e_2(n_2 - 1).
 \end{aligned} \tag{12}$$

We obtained the required result by putting the values of  $\sum A + \sum B + \sum C$  in equation (5).  $\square$

**Theorem 2.** Let  $G_1$  and  $G_2$  be two simple connected graphs, then second Zagreb coindex of  $G_{1+R}G_2$  is given as follows:

$$\alpha_1 \leq \overline{M}_2(G_{1+R}G_2) \leq \alpha_2, \quad (13) \quad \text{where}$$

$$\begin{aligned} \alpha_1 &= 4n_2e_1(3n_2 - 2) + 2(n_2^2e_1^2 - n_2e_1) + 4e_2e_1[n_2(n_1 - 2) + 2(n_2 - 1)] + 4\overline{e}_2M_1(G_1) + 4e_2\overline{M}_1(G_1) + \\ &8(e_2 + \overline{e}_2)M_2(G_1) + 4n_2 + 2(e_2 + \overline{e}_2)\overline{M}_2(G_1) + \overline{e}_1M_1(G_2) + 4e_1\overline{M}_1(G_2) + 2(e_1 + \overline{e}_1)M_2(G_2) \\ &+ (n_1 + 2(e_1 + \overline{e}_1))\overline{M}_2(G_2) + 2(M_1(G_2) + \overline{M}_1(G_2))(M_1(G_1) + \overline{M}_1(G_1)), \\ \alpha_2 &= 8n_2e_1E(R(G_1))(n_1 - 2 + (n_2 - 1)(n_1 - 1)) + 2(n_2^2e_1^2 - n_2e_1) + 4e_2e_1[n_2(n_1 - 2) + 2(n_2 - 1)] \\ &+ 4\overline{e}_2M_1(G_1) + 4e_2\overline{M}_1(G_1) + 8(e_2 + \overline{e}_2)M_2(G_1) + 4n_2 + 2(e_2 + \overline{e}_2)\overline{M}_2(G_1) + \overline{e}_1M_1(G_2) + 4e_1\overline{M}_1(G_2) \\ &+ 2(e_1 + \overline{e}_1)M_2(G_2) + (n_1 + 2(e_1 + \overline{e}_1))\overline{M}_2(G_2) + 2(M_1(G_2) + \overline{M}_1(G_2))(M_1(G_1) + \overline{M}_1(G_1)). \end{aligned} \quad (14)$$

*Proof.* Using equation (2), we have

Using equation (6), we directly have

$$\begin{aligned} \overline{M}_2(G_{1+R}G_2) &= \sum_{(p_1, p_2) \in (q_1, q_2) \notin E(G_{1+R}G_2)} [d(p_1, q_1)d(p_2, q_2)] \\ &= \sum A + \sum B + \sum C. \end{aligned} \quad (15)$$

$$\begin{aligned} \sum A &= 2(n_2^2e_1^2 - n_2e_1), \\ \sum B &= \sum B_1 + \sum B_2 + \sum B_3 + \sum B_4 + \sum B_5 + \sum B_6, \\ \sum B_1 &= \sum_{p \in V_{G_1}} \sum_{q_1, q_2 \notin E_{G_2}} [d(p, q_1)d(p, q_2)] = \sum_{p \in V_{G_1}} \sum_{q_1, q_2 \notin E_{G_2}} [(d_R(p) + d_{G_2}(q_1))d_R(p) + d_{G_2}(q_2)] \\ &= \sum_{p \in V_{G_1}} \sum_{q_1, q_2 \notin E_{G_2}} [d_R(p)d_R(p) + d_R(p)d_{G_2}(q_2) + d_R(p)d_{G_2}(q_1) + d_{G_2}(q_1)d_{G_2}(q_2)] \\ &= \sum_{p \in V_{G_1}} \sum_{q_1, q_2 \notin E_{G_2}} [4d_{G_1}(p)^2 + 2d_{G_1}(p)(d_{G_2}(q_2) + d_{G_2}(q_1)) + d_{G_2}(q_1)d_{G_2}(q_2)] \\ &= 4\overline{e}_2M_1(G_1) + 2(2e_1)\overline{M}_1(G_2) + n_1\overline{M}_2(G_2), \\ \sum B_2 &= \sum_{q \in V_{G_2}} \sum_{p_1, p_2 \in V_{G_1}} [d(p_1, q)d(p_2, q)] \\ &= \sum_{q \in V_{G_2}} \sum_{p_1, p_2 \in V_{G_1}} [d(p_1, q)d(p_2, q)] = \sum_{q \in V_{G_2}} \sum_{p_1, p_2 \in V_{G_1}} [(d_R(p_1) + d_{G_2}(q))(d_R(p_2) + d_{G_2}(q))] \\ &= \sum_{q \in V_{G_2}} \sum_{p_1, p_2 \in V_{G_1}} [(2d_{G_1}(p_1) + d_{G_2}(q))(2d_{G_1}(p_2) + d_{G_2}(q))] \\ &= \sum_{q \in V_{G_2}} \sum_{p_1, p_2 \in V_{G_1}} [4d_{G_1}(p_1)d_{G_1}(p_2) + 2d_{G_1}(p_1)d_{G_2}(q) + 2d_{G_1}(p_2)d_{G_2}(q) + d_{G_2}(q)^2] \\ &= 4n_2\overline{M}_2(G_1) + 2(2e_2)\overline{M}_1(G_1) + \overline{e}_1M_1(G_2), \\ \sum B_3 &= \sum_{p_1, p_2 \in E_{G_1}} \sum_{q_1, q_2 \in E_{G_2}} [d(p_1, q_1) + d(p_2, q_2)] \\ &= \sum_{p_1, p_2 \in E_{G_1}} \sum_{q_1, q_2 \in E_{G_2}} [(d_R(p)d_R(p) + d_R(p)d_{G_2}(q_2) + d_R(p)d_{G_2}(q_1) + d_{G_2}(q_1)d_{G_2}(q_2))] \\ &= \sum_{p_1, p_2 \in E_{G_1}} \sum_{q_1, q_2 \in E_{G_2}} [(d_R(p)d_R(p) + d_R(p)d_{G_2}(q_2) + d_R(p)d_{G_2}(q_1) + d_{G_2}(q_1)d_{G_2}(q_2))] \end{aligned}$$

$$\begin{aligned}
&= 2 \sum_{p_1, p_2 \in E_{G_1}} \sum_{q_1, q_2 \in E_{G_2}} [4d_{G_1}(p)^2 + 2d_{G_1}(p)(d_{G_2}(q_2) + d_{G_2}(q_1)) + d_{G_2}(q_1)d_{G_2}(q_2)] \\
&= 2[4e_2M_2(G_1) + e_1M_2(G_2)] + 2M_1(G_1)M_1(G_2), \\
\sum B_4 &= \sum_{p_1, p_2 \notin E_{G_1}} \sum_{q_1, q_2 \in E_{G_2}} [d(p_1, q_1)d(p_2, q_2)] \\
&= \sum_{p_1, p_2 \notin E_{G_1}} \sum_{q_1, q_2 \in E_{G_2}} [(d_R(p_1) + d_{G_2}(q_1))(d_R(p_2) + d_{G_2}(q_2))] \\
&= \sum_{p_1, p_2 \notin E_{G_1}} \sum_{q_1, q_2 \in E_{G_2}} [(2d_{G_1}(p_1) + d_{G_2}(q_1))(2d_{G_1}(p_2) + d_{G_2}(q_2))] \\
&= \sum_{p_1, p_2 \notin E_{G_1}} \sum_{q_1, q_2 \in E_{G_2}} [4d_{G_1}(p_1)d_{G_1}(p_2) + 2[d_{G_1}(p_1)d_{G_2}(q_2) + d_{G_1}(p_2)d_{G_2}(q_1)] + d_{G_2}(q_1)d_{G_2}(q_2)] \\
&= 2[4e_2\bar{M}_2(G_1) + \bar{e}_1M_2(G_2)] + 2\bar{M}_1(G_1)M_1(G_2), \tag{16}
\end{aligned}$$

$$\begin{aligned}
\sum B_5 &= \sum_{p_1, p_2 \notin E_{G_1}} \sum_{q_1, q_2 \notin E_{G_2}} [d(p_1, q_1)d(p_2, q_2)] \\
&= \sum_{p_1, p_2 \notin E_{G_1}} \sum_{q_1, q_2 \notin E_{G_2}} [(d_R(p_1) + d_{G_2}(q_1))(d_R(p_2) + d_{G_2}(q_2))] \\
&= \sum_{p_1, p_2 \notin E_{G_1}} \sum_{q_1, q_2 \notin E_{G_2}} [(2d_{G_1}(p_1) + d_{G_2}(q_1))(2d_{G_1}(p_2) + d_{G_2}(q_2))] \\
&= \sum_{p_1, p_2 \notin E_{G_1}} \sum_{q_1, q_2 \notin E_{G_2}} [4d_{G_1}(p_1)d_{G_1}(p_2) + 2[d_{G_1}(p_1)d_{G_2}(q_2) + d_{G_1}(p_2)d_{G_2}(q_1)] + d_{G_2}(q_1)d_{G_2}(q_2)] \\
&= 2[4\bar{e}_2\bar{M}_2(G_1) + \bar{e}_1\bar{M}_2(G_2)] + 2\bar{M}_1(G_1)\bar{M}_1(G_2), \\
\sum B_6 &= \sum_{p_1, p_2 \in E_{G_1}} \sum_{q_1, q_2 \notin E_{G_2}} [d(p_1, q_1)d(p_2, q_2)] \\
&= \sum_{p_1, p_2 \in E_{G_1}} \sum_{q_1, q_2 \notin E_{G_2}} [(d_R(p_1) + d_{G_2}(q_1))(d_R(p_2) + d_{G_2}(q_2))] \\
&= \sum_{p_1, p_2 \in E_{G_1}} \sum_{q_1, q_2 \notin E_{G_2}} [(2d_{G_1}(p_1) + d_{G_2}(q_1))(2d_{G_1}(p_2) + d_{G_2}(q_2))] \\
&= \sum_{p_1, p_2 \in E_{G_1}} \sum_{q_1, q_2 \notin E_{G_2}} [4d_{G_1}(p_1)d_{G_1}(p_2) + 2[d_{G_1}(p_1)d_{G_2}(q_2) + d_{G_1}(p_2)d_{G_2}(q_1)] + d_{G_2}(q_1)d_{G_2}(q_2)] \tag{17} \\
&= 2[4\bar{e}_2M_2(G_1) + e_1\bar{M}_2(G_2)] + 2M_1(G_1)\bar{M}_1(G_2),
\end{aligned}$$

$$\begin{aligned}
\sum B &= 4\bar{e}_2M_1(G_1) + 4e_2\bar{M}_1(G_1) + 8(e_2 + \bar{e}_2)M_2(G_1) + 4n_2 + 2(e_2 + \bar{e}_2)\bar{M}_2(G_1) + \bar{e}_1M_1(G_2) \\
&\quad + 4e_1\bar{M}_1(G_2) + 2(e_1 + \bar{e}_1)M_2(G_2) + (n_1 + +2(e_1 + \bar{e}_1)) \\
&\quad \bar{M}_2(G_2) + 2(M_1(G_2) + \bar{M}_1(G_2))(M_1(G_1) + \bar{M}_1(G_1)),
\end{aligned}$$

$$\sum C = \sum C_1 + \sum C_2 + \sum C_3,$$

$$\begin{aligned}
\sum C_1 &= \sum_{\substack{p_1, p_2 \notin E(R(G_1)) \\ p_1 \in V(G_1) \\ p_2 \in V(R(G_1)-V(G_1))}} \sum_{q \in V_{G_2}} dp_1, qd p_2, q = \sum_{\substack{p_1, p_2 \notin E(R(G_1)) \\ p_1 \in V(G_1) \\ p_2 \in V(R(G_1)-V(G_1))}} \sum_{q \in V_{G_2}} [(d_R(p_1) + d_{G_2}(q))(d_R(p_2))], \\
&\quad \cdot \sum C_1 \sum_{\substack{p_1, p_2 \notin E(R(G_1)) \\ p_1 \in V(G_1) \\ p_2 \in V(R(G_1)-V(G_1))}} \sum_{q \in V_{G_2}} [(2d_{G_1}(p_1) + d_{G_2}(q))2] \\
&= \sum_{\substack{p_1, p_2 \notin E(R(G_1)) \\ p_1 \in V(G_1) \\ p_2 \in V(S(G_1)-V(G_1))}} \sum_{q \in V_{G_2}} [4(d_{G_1}(p_1) + 2d_{G_2}(q))] = 4n_2 \sum_{\substack{p_1, p_2 \notin E(R(G_1)) \\ p_1 \in V(G_1) \\ p_2 \in V(S(G_1)-V(G_1))}} [d(p_1)] + 4e_2e_1(n_1 - 2).
\end{aligned}$$



Note that

so

$$e_1 \leq \sum_{\substack{p_1 p_2 \notin E(R(G_1)) \\ p_1 \in V(G_1) \\ p_2 \in V(S(G_1)-V(G_1))}} [d(p_1)] \leq 2e_1(n_1 - 2)E(S(G_1)), \quad (18)$$

$$\begin{aligned} 4n_2e_1 + 4e_2e_1(n_1 - 2) &\leq \sum C_1 \leq 8n_2e_1(n_1 - 2)E(R(G_1)) + 4e_2e_1(n_1 - 2), \\ \sum C_2 &= \sum_{\substack{p_1 p_2 \notin E(R(G_1)) \\ p_1 \in V(G_1) \\ p_2 \in V(R(G_1)-V(G_1))}} \sum_{q_1, q_2 \in V_{G_2}} [d(p_1, q_1)d(p_2, q_2)] \\ &= \sum_{\substack{p_1 p_2 \notin E(R(G_1)) \\ p_1 \in V(G_1) \\ p_2 \in V(R(G_1)-V(G_1))}} \sum_{q_1, q_2 \in V_{G_2}} [(d_R(p_1) + d(q_1))d_{R(G_1)}(p_2)] \\ &= \sum_{\substack{p_1 p_2 \notin E(R(G_1)) \\ p_1 \in V(G_1) \\ p_2 \in V(R(G_1)-V(G_1))}} \sum_{q_1, q_2 \in V_{G_2}} [(2d_{G_1}(p_1) + d(q_1))^2] \\ &= \sum_{\substack{p_1 p_2 \notin E(R(G_1)) \\ p_1 \in V(G_1) \\ p_2 \in V(R(G_1)-V(G_1))}} \sum_{q_1, q_2 \in V_{G_2}} [4d_{G_1}(p_1) + 2d(q_1)] \\ &= 4n_2(n_2 - 1) \sum_{\substack{p_1 p_2 \notin E(R(G_1)) \\ p_1 \in V(G_1) \\ p_2 \in V(R(G_1)-V(G_1))}} [d_{G_1}(p_1)] + 2(2e_2)e_1(n_1 - 2)(n_2 - 1). \end{aligned} \quad (19)$$

Note that

$$e_1 \leq \sum_{\substack{p_1 p_2 \notin E(R(G_1)) \\ p_1 \in V(G_1) \\ p_2 \in V(R(G_1)-V(G_1))}} d(p_1) \leq 2e_1(n_1 - 2)E(R(G_1)), \quad (20)$$

so

$$\begin{aligned}
 4n_2(n_2 - 1)e_1 + 4e_2e_1(n_1 - 2)(n_2 - 1) &\leq \sum C_2 \leq 8n_2(n_2 - 1)e_1(n_1 - 2)E(R(G_1)) + 4e_2e_1(n_1 - 2)(n_2 - 1), \\
 \sum C_3 &= \sum_{\substack{p_1 p_2 \notin E(R(G_1)) \\ p_1 \in V(G_1) \\ p_2 \in V(R(G_1) - V(G_1))}} \sum_{q_1, q_2 \in V_{G_2}} [d(p_1, q_1)(d(p_2, q_2))] \\
 &= \sum_{\substack{p_1 p_2 \notin E(R(G_1)) \\ p_1 \in V(G_1) \\ p_2 \in V(R(G_1) - V(G_1))}} \sum_{q_1, q_2 \in V_{G_2}} [(d_R(p_1) + d(q_1))(d_{R(G_1)}(p_2))] \\
 &= \sum_{\substack{p_1 p_2 \notin E(R(G_1)) \\ p_1 \in V(G_1) \\ p_2 \in V(R(G_1) - V(G_1))}} \sum_{q_1, q_2 \in V_{G_2}} [(2d_{G_1}(p_1) + d(q_1))2] \tag{21} \\
 &= \sum_{\substack{p_1 p_2 \notin E(R(G_1)) \\ p_1 \in V(G_1) \\ p_2 \in V(R(G_1) - V(G_1))}} \sum_{q_1, q_2 \in V_{G_2}} [4d_{G_1}(p_1) + 2d(q_1)] \\
 &= 4n_2(n_2 - 1) \sum_{\substack{p_1 p_2 \notin E(R(G_1)) \\ p_1 \in V(G_1) \\ p_2 \in V(R(G_1) - V(G_1))}} [d(p_1)] + 2(2e_2)(n_2 - 1)2e_1.
 \end{aligned}$$

Note that

$$2e_1 \leq \sum_{\substack{p_1 p_2 \notin E(R(G_1)) \\ p_1 \in V(G_1) \\ p_2 \in V(R(G_1) - V(G_1))}} d(p_1) \leq 2e_1 E(R(G_1)), \tag{22}$$

so

$$\begin{aligned}
 &8e_1n_2(n_2 - 1) + 8e_1e_2(n_2 - 1) \\
 &\leq \sum C_3 \leq 8e_1n_2(n_2 - 1)E(R(G_1)) + 8e_1e_2(n_2 - 1). \tag{23}
 \end{aligned}$$

Consequently,

$$\begin{aligned}
 &8e_1n_2(n_2 - 1) + 8e_1e_2(n_2 - 1) + 4n_2(n_2 - 1)e_1 + 4e_2e_1(n_1 - 2)(n_2 - 1) + 4n_2e_1 + 4e_2e_1(n_1 - 2) \\
 &\leq \sum C \\
 &\leq 8n_2e_1(n_1 - 2)E(R(G_1)) + 4e_2e_1(n_1 - 2) + 8n_2(n_2 - 1)e_1(n_1 - 2)E(R(G_1)) + 4e_2e_1(n_1 - 2)(n_2 - 1) \\
 &\quad + 8e_1n_2(n_2 - 1)E(R(G_1)) + 8e_1e_2(n_2 - 1). \tag{24}
 \end{aligned}$$

We obtained the required proof by putting the values of  $\sum A + \sum B + \sum C$  in equation (14).  $\square$

**Theorem 3.** Let  $G_1$  and  $G_2$  be two simple connected graphs, then second Zagreb coindex of  $G_{1+Q}G_2$  is given as follows:

$$\alpha_1 \leq \overline{M}_2(G_{1+Q}G_2) \leq \alpha_2, \quad (25) \quad \text{where}$$

$$\begin{aligned} \alpha_1 &= 4e_2[\overline{e}_1 + (n_2 - 1)(\overline{e}_1 + e_1)] + n_2^2\overline{M}_2(G_1) + n_2(n_2 - 1)M_2(G_1) + (n_2 - 1 + \overline{e}_2)(M_1(G_1) + 2M_2(G_1)) \\ &\quad + (2e_2 + \overline{e}_2)M_1(G_1) + 2e_2\overline{M}_1(G_1) + (n_2 + 2(e_2 + \overline{e}_2))M_2(G_1)\overline{M}_2(G_1) + (e_1 + \overline{e}_1)M_1(G_2) + 2e_1\overline{M}_1(G_2) \\ &\quad + 2(e_1 + \overline{e}_1)M_2(G_2) + (n_1 + 2(e_1 + \overline{e}_1))\overline{M}_2(G_2) + (M_1(G_2) + \overline{M}_1(G_2))(M_1(G_1) + \overline{M}_1(G_1)), \\ \alpha_2 &= 4e_2\left[\overline{e}_{Q(G_1)} + (n_2 - 1)(\overline{e}_{Q(G_1)} + e_{Q(G_1)})\right] + n_2^2\overline{M}_2(Q(G_1)) + n_2(n_2 - 1)M_2(Q(G_1)) \\ &\quad + (n_2 + 2(n_2 - 1 + \overline{e}_2))M_2(Q(G_1)) + (n_2 - 1 + \overline{e}_2)M_1(Q(G_1)) + 2(n_2 - 1 + \overline{e}_2)M_2(Q(G_1)) + (2e_2 + \overline{e}_2)M_1(G_1) \\ &\quad + 2e_2\overline{M}_1(G_1) + (n_2 + 2(e_2 + \overline{e}_2))M_2(G_1)\overline{M}_2(G_1) + (e_1 + \overline{e}_1)M_1(G_2) + 2e_1\overline{M}_1(G_2) + 2(e_1 + \overline{e}_1)M_2(G_2) \\ &\quad + (n_1 + 2(e_1 + \overline{e}_1))\overline{M}_2(G_2) + (M_1(G_2) + \overline{M}_1(G_2))(M_1(G_1) + \overline{M}_1(G_1)). \end{aligned} \quad (26)$$

*Proof.* Using equation (2), we have

$$\begin{aligned} \overline{M}_2(G_{1+Q}G_2) &= \sum_{(p_1, p_2)(x_1, x_2) \notin E(G_{1+Q}G_2)} [d(p_1, x_1)d(p_2, x_2)] = \sum A + \sum B + \sum C, \\ \sum A &= \sum A_1 + \sum A_2 + \sum A_3 + \sum A_4 + \sum A_5 + \sum A_6 + \sum A_7, \\ \sum A_1 &= \sum_{\substack{p_1, p_2 \notin E(Q(G_1)) \\ p_1, p_2 \in V(Q(G_1)-(G_1))}} \sum_{x \in V_{G_2}} [dp_1, xd p_2, x] = n_2 \sum_{\substack{p_1, p_2 \notin E(Q(G_1)) \\ p_1, p_2 \in V(Q(G_1)-(G_1))}} [d_{QG_1}p_1 d_{QG_1}p_2]. \end{aligned} \quad (27)$$

Note that

so

$$0 \leq \sum_{\substack{p_1, p_2 \notin E(Q(G_1)) \\ p_1, p_2 \in V(Q(G_1)-(G_1))}} [d_{Q(G_1)}(p_1)d_{Q(G_1)}(p_2)] \leq \overline{M}_2(Q(G_1)), \quad (28)$$

$$\begin{aligned} 0 &\leq \sum A_1 \leq n_2\overline{M}_2(Q(G_1)), \\ \sum A_2 &= \sum_{p \in V(Q(G_1)-(G_1))} \sum_{x_1, x_2 \in E_{G_2}} [d(p, x_1)d(p, x_2)] \\ &= \sum_{p \in V(Q(G_1)-(G_1))} \sum_{x_1, x_2 \in E_{G_2}} [d_{Q(G_1)}(p)d_{Q(G_1)}(p)] = (n_2 - 1) \sum_{p \in V(Q(G_1)-(G_1))} [d_{Q(G_1)}(p)^2]. \end{aligned} \quad (29)$$

Note that

$$M_1(G_1) \leq \sum_{p \in V(Q(G_1) - (G_1))} [d_{Q(G_1)}(p)^2] \leq M_1(Q(G_1)), \quad (30)$$


---

so

$$\begin{aligned} (n_2 - 1)M_1(G_1) &\leq \sum A_2 \leq (n_2 - 1)M_1(Q(G_1)), \\ \sum A_3 &= \sum_{p \in V(Q(G_1) - (G_1))} \sum_{x_1, x_2 \in E_{G_2}} [d(p, x_1)d(p, x_2)] \\ &= \sum_{p \in V(Q(G_1) - V(G_1))} \sum_{x_1, x_2 \in E_{G_2}} [d_{Q(G_1)}(p)d_{Q(G_1)}(p)] = \bar{e}_2 \sum_{t \in V(Q(G_1) - V(G_1))} [d_{Q(G_1)}(p)^2]. \end{aligned} \quad (31)$$


---

Note that

$$M_1(G_1) \leq \sum_{p \in V(Q(G_1) - V(G_1))} [d_{Q(G_1)}(p)^2] \leq M_1(Q(G_1)), \quad (32)$$


---

so

$$\begin{aligned} \bar{e}_2 M_1(G_1) &\leq \sum A_3 \leq \bar{e}_2 M_1(Q(G_1)), \\ \sum A_4 &= \sum_{\substack{p_1, p_2 \in E(Q(G_1)) \\ p_1, p_2 \in V(Q(G_1) - V(G_1))}} \sum_{x_1, x_2 \in E_{G_2}} [d(p_1, x_1)d(p_2, x_2)] \\ &= \sum_{\substack{p_1, p_2 \in E(Q(G_1)) \\ p_1, p_2 \in V(Q(G_1) - V(G_1))}} \sum_{x_1, x_2 \in E_{G_2}} [d_{p_1, x_1} d_{p_2, x_2}] = 2n_2 - 1 \sum_{\substack{p_1, p_2 \in E(Q(G_1)) \\ p_1, p_2 \in V(Q(G_1) - V(G_1))}} [d_{Q(G_1)} p_1 d_{Q(G_1)} p_2]. \end{aligned} \quad (33)$$


---

Note that

$$M_2(G_1) \leq \sum_{\substack{p_1, p_2 \in E(Q(G_1)) \\ p_1, p_2 \in V(Q(G_1) - V(G_1))}} [d_{Q(G_1)}(p_1) + d_{Q(G_1)}(p_2)] \leq M_2(Q(G_1)), \quad (34)$$

so

$$\begin{aligned}
2(n_2 - 1)M_2(G_1) &\leq \sum A_4 \leq 2(n_2 - 1)M_2(Q(G_1)), \\
\sum A_5 &= \sum_{\substack{p_1, p_2 \in E(Q(G_1)) \\ p_1, p_2 \in V(Q(G_1) - V(G_1))}} \sum_{x_1, x_2 \in E_{G_2}} [d(p_1, x_1)d(p_2, x_2)] \\
&= \sum_{\substack{p_1, p_2 \in E(Q(G_1)) \\ p_1, p_2 \in V(Q(G_1) - V(G_1))}} \sum_{x_1, x_2 \in E_{G_2}} [d(p_1, x_1)d(p_2, x_2)] = 2\bar{e}_2 \sum_{\substack{p_1, p_2 \in E(Q(G_1)) \\ p_1, p_2 \in V(Q(G_1) - V(G_1))}} [d_{Q(G_1)}(p_1)d_{Q(G_1)}(p_2)].
\end{aligned} \tag{35}$$

Note that

$$M_2(G_1) \leq \sum_{\substack{p_1, p_2 \in E(Q(G_1)) \\ p_1, p_2 \in V(Q(G_1) - V(G_1))}} [d_{Q(G_1)}(p_1) + d_{Q(G_1)}(p_2)] \leq M_2(Q(G_1)), \tag{36}$$

so

$$\begin{aligned}
2\bar{e}_2 M_2(G_1) &\leq \sum A_5 \leq 2\bar{e}_2 M_2(Q(G_1)), \\
\sum A_6 &= \sum_{\substack{p_1, p_2 \in E(Q(G_1)) \\ p_1, p_2 \in V(Q(G_1) - V(G_1))}} \sum_{x_1, x_2 \in E_{G_2}} [d(p_1, x_1)d(p_2, x_2)] \\
&= \sum_{\substack{p_1, p_2 \in E(Q(G_1)) \\ p_1, p_2 \in V(Q(G_1) - V(G_1))}} \sum_{x_1, x_2 \in E_{G_2}} [d(p_1, x_1)d(p_2, x_2)] = 2(n_2 - 1) \sum_{\substack{p_1, p_2 \in E(Q(G_1)) \\ p_1, p_2 \in V(Q(G_1) - V(G_1))}} [d_{Q(G_1)}(p_1)d_{Q(G_1)}(p_2)].
\end{aligned} \tag{37}$$

Note that

$$0 \leq \sum_{\substack{p_1, p_2 \in E(Q(G_1)) \\ p_1, p_2 \in V(Q(G_1) - V(G_1))}} [d_{Q(G_1)}(p_1)d_{Q(G_1)}(p_2)] \leq \bar{M}_2(Q(G_1)), \tag{38}$$

so

$$\begin{aligned}
0 &\leq \sum A_6 \leq 2(n_2 - 1)\bar{M}_2(Q(G_1)), \\
\sum A_7 &= \sum_{\substack{p_1, p_2 \notin E(Q(G_1)) \\ p_1, p_2 \notin V(Q(G_1) - V(G_1))}} \sum_{x_1, x_2 \in E_{G_2}} [d(p_1, x_1)d(p_2, x_2)] \\
&= \sum_{\substack{p_1, p_2 \notin E(Q(G_1)) \\ p_1, p_2 \notin V(Q(G_1) - V(G_1))}} \sum_{x_1, x_2 \in E_{G_2}} [d(p_1, x_1)d(p_2, x_2)] = 2\bar{e}_2 \sum_{\substack{p_1, p_2 \notin E(Q(G_1)) \\ p_1, p_2 \in V(Q(G_1) - V(G_1))}} [d_{Q(G_1)}(p_1)d_{Q(G_1)}(p_2)].
\end{aligned} \tag{39}$$

Note that

$$0 \leq \sum_{\substack{p_1 p_2 \notin E(Q(G_1)) \\ p_1, p_2 \in V(Q(G_1)-V(G_1))}} \left[ d_{Q(G_1)}(p_1) d_{Q(G_1)}(p_2) \right] \leq \overline{M}_2(Q(G_1)), \quad (40)$$

so

$$0 \leq \sum A_7 \leq 2\overline{e}_2 \overline{M}_2(Q(G_1)). \quad (41)$$

Consequently,

$$\begin{aligned} & 2\overline{e}_2 M_2(G_1) + 2(n_2 - 1)M_2(G_1) + (n_2 - 1)M_1(G_1) + \overline{e}_2 M_1(G_1) \\ & \leq \sum A \\ & \leq n_2 \overline{M}_2(Q(G_1)) + (n_2 - 1)M_1(Q(G_1)) + \overline{e}_2 M_1(Q(G_1)) + 2(n_2 - 1)M_2(Q(G_1)) + 2\overline{e}_2 M_2(Q(G_1)) \\ & \quad + 2(n_2 - 1)\overline{M}_2(Q(G_1)) + 2\overline{e}_2 \overline{M}_2(Q(G_1)). \end{aligned} \quad (42)$$

Using equation (7), we directly have

$$\begin{aligned} \sum B &= 2[(e_2 + \overline{e}_2)M_1(G_1) + e_2 \overline{M}_1(G_1)] + (n_2 + 2(e_2 + \overline{e}_2))M_2(G_1) \overline{M}_2(G_1) + (e_1 + \overline{e}_1)M_1(G_2) \\ & \quad + 2[e_1 \overline{M}_1(G_2) + (e_1 + \overline{e}_1)M_2(G_2)] + (n_1 + 2(e_1 + \overline{e}_1))\overline{M}_2(G_2) \\ & \quad + (M_1(G_2) + \overline{M}_1(G_2))(M_1(G_1) + \overline{M}_1(G_1)), \\ \sum C &= \sum C_1 + \sum C_2 + \sum C_3, \\ \sum C_1 &= \sum_{\substack{p_1 p_2 \notin E(Q(G_1)) \\ p_1 \in V(G_1) \\ p_2 \in V(Q(G_1)-V(G_1))}} \sum_{x \in V_{G_2}} d_{p_1, x} d_{p_2, x} = \sum_{\substack{p_1 p_2 \notin E(Q(G_1)) \\ p_1 \in V(G_1) \\ p_2 \in V(Q(G_1)-V(G_1))}} \sum_{x \in V_{G_2}} \left[ (d_{G_1}(p_1) + d(x)) d_{Q(G_1)}(p_2) \right] \\ &= n_2 \sum_{\substack{p_1 p_2 \notin E(Q(G_1)) \\ p_1 \in V(G_1) \\ p_2 \in V(Q(G_1)-V(G_1))}} \left[ d_{G_1}(p_1) d_{Q(G_1)}(p_2) + 2e_2 d_{Q(G_1)}(p_2) \right] \\ &= n_2 \sum_{\substack{p_1 p_2 \notin E(Q(G_1)) \\ p_1 \in V(G_1) \\ p_2 \in V(Q(G_1)-V(G_1))}} d_{G_1}(p_1) d_{Q(G_1)}(p_2) + d(x) \sum_{\substack{p_1 p_2 \notin E(Q(G_1)) \\ p_1 \in V(G_1) \\ p_2 \in V(Q(G_1)-V(G_1))}} d_{Q(G_1)}(p_2). \end{aligned} \quad (43)$$

Note that

$$\begin{aligned}
 \overline{M}_2(G_1) &\leq \sum_{\substack{p_1 p_2 \notin E(Q(G_1)) \\ p_1 \in V(G_1) \\ p_2 \in V(Q(G_1) - V(G_1))}} d_{Q(G_1)}(p_1) \leq \overline{M}_2 Q(G_1), \\
 2\overline{e}_1 &\leq \sum_{\substack{p_1 p_2 \notin E(Q(G_1)) \\ p_1 \in V(G_1) \\ p_2 \in V(Q(G_1) - V(G_1))}} d_{Q(G_1)}(p_2) \leq 2\overline{e}_{Q(G_1)}, \\
 n_2 \overline{M}_2(G_1) + 4e_2 \overline{e}_1 &\leq \sum C_1 \leq n_2 \overline{M}_2(Q(G_1)) + 4e_2 \overline{e}_{Q(G_1)}, \\
 \sum C_2 &= \sum_{\substack{p_1 p_2 \notin E(Q(G_1)) \\ p_1 \in V(G_1) \\ p_2 \in V(Q(G_1) - V(G_1))}} \sum_{x_1, x_2 \in V_{G_2}} [d(p_1, x_1) d(p_2, x_2)] \\
 &= \sum_{\substack{p_1 p_2 \notin E(Q(G_1)) \\ p_1 \in V(G_1) \\ p_2 \in V(Q(G_1) - V(G_1))}} \sum_{x_1, x_2 \in V_{G_2}} [(d_{G_1}(p_1) + d(x_1)) d_{Q(G_1)}(p_2)] \\
 &= \sum_{\substack{p_1 p_2 \notin E(Q(G_1)) \\ p_1 \in V(G_1) \\ p_2 \in V(Q(G_1) - V(G_1))}} \sum_{x_1, x_2 \in V_{G_2}} [d_{G_1}(p_1) d_{Q(G_1)}(p_2) + d(x_1) d_{Q(G_1)}(p_2)] \\
 &= \sum_{\substack{x_1, x_2 \in V_{G_2} \\ p_1 p_2 \notin E(Q(G_1)) \\ p_1 \in V(G_1) \\ p_2 \in V(Q(G_1) - V(G_1))}} d_{G_1}(p_1) d_{Q(G_1)}(p_2) + d(x_1) \sum_{\substack{p_1 p_2 \notin E(Q(G_1)) \\ p_1 \in V(G_1) \\ p_2 \in V(Q(G_1) - V(G_1))}} d_{Q(G_1)}(p_2).
 \end{aligned}
 \tag{44}$$

Note that

$$\begin{aligned}
\overline{M}_2(G_1) &\leq \sum_{\substack{p_1 p_2 \notin E(Q(G_1)) \\ p_1 \in V(G_1) \\ p_2 \in V(Q(G_1) - V(G_1))}} d_{Q(G_1)}(p_1) \leq \overline{M}_2 Q(G_1), \\
2\overline{e}_1 &\leq \sum_{\substack{p_1 p_2 \notin E(Q(G_1)) \\ p_1 \in V(G_1) \\ p_2 \in V(Q(G_1) - V(G_1))}} \sum d_{Q(G_1)}(p_2) \leq 2\overline{e}_{Q(G_1)}, \\
n_2(n_2 - 1)\overline{M}_2(G_1) + 4e_2(n_2 - 1)\overline{e}_1 &\leq \sum C_2 \leq n_2(n_2 - 1)\overline{M}_2(Q(G_1)) + 4e_2(n_2 - 1)\overline{e}_{Q(G_1)}, \\
\sum C_3 &= \sum_{\substack{p_1 p_2 \notin E(Q(G_1)) \\ p_1 \in V(G_1) \\ p_2 \in V(Q(G_1) - V(G_1))}} \sum_{x_1, x_2 \in V_{G_2}} [d(p_1, x_1)d(p_2, x_2)] \\
&= \sum_{\substack{p_1 p_2 \notin E(Q(G_1)) \\ p_1 \in V(G_1) \\ p_2 \in V(Q(G_1) - V(G_1))}} \sum_{x_1, x_2 \in V_{G_2}} \left[ (d_{G_1}(p_1) + d(x_1))d_{Q(G_1)}(p_2) \right] \\
&= \sum_{\substack{p_1 p_2 \notin E(Q(G_1)) \\ p_1 \in V(G_1) \\ p_2 \in V(Q(G_1) - V(G_1))}} \sum_{x_1, x_2 \in V_{G_2}} \left[ d_{G_1}(p_1)d_{Q(G_1)}(p_2) + d(x_1)d_{Q(G_1)}(p_2) \right] \\
&= \sum_{x_1, x_2 \in V_{G_2}} \sum_{\substack{p_1 p_2 \notin E(Q(G_1)) \\ p_1 \in V(G_1) \\ p_2 \in V(Q(G_1) - V(G_1))}} d_{G_1}(p_1)d_{Q(G_1)}(p_2) + d(x_1) \sum_{\substack{p_1 p_2 \notin E(Q(G_1)) \\ p_1 \in V(G_1) \\ p_2 \in V(Q(G_1) - V(G_1))}} d_{Q(G_1)}(p_2).
\end{aligned} \tag{45}$$



Note that

$$\begin{aligned}
 M_2(G_1) &\leq \sum_{\substack{p_1 p_2 \notin E(Q(G_1)) \\ p_1 \in V(G_1) \\ p_2 \in V(Q(G_1)-V(G_1))}} d_{Q(G_1)}(p_1) \leq M_2(Q(G_1)), \\
 2e_1 &\leq \sum_{\substack{p_1 p_2 \notin E(Q(G_1)) \\ p_1 \in V(G_1) \\ p_2 \in V(Q(G_1)-V(G_1))}} d_{Q(G_1)}(p_2) \leq 2e_{Q(G_1)},
 \end{aligned} \tag{46}$$

$$n_2(n_2 - 1)M_2(G_1) + 4e_2(n_2 - 1)e_1 \leq \sum C_3 \leq n_2(n_2 - 1)M_2(Q(G_1)) + 4e_2(n_2 - 1)e_{Q(G_1)}.$$

Consequently,

$$\begin{aligned}
 &n_2 \overline{M}_2(G_1) + 4e_2 \overline{e}_1 + n_2(n_2 - 1) \overline{M}_2(G_1) + 4e_2(n_2 - 1) \overline{e}_1 + n_2(n_2 - 1)M_2(G_1) + 4e_2(n_2 - 1)e_1 \\
 &\leq \sum C \\
 &\leq n_2 \overline{M}_2(Q(G_1)) + 4e_2 \overline{e}_{Q(G_1)} + n_2(n_2 - 1) \overline{M}_2(Q(G_1)) + 4e_2(n_2 - 1) \overline{e}_{Q(G_1)} + n_2(n_2 - 1)M_2(Q(G_1)) + 4e_2(n_2 - 1)e_{Q(G_1)}.
 \end{aligned} \tag{47}$$

$$\alpha_1 \leq \overline{M}_2(G_{1+T}G_2) \leq \alpha_2, \tag{48}$$

We obtained the required proof by putting the values of  $\sum A + \sum B + \sum C$  in equation (25).  $\square$  where

**Theorem 4.** Let  $G_1$  and  $G_2$  be two graphs, then second Zagreb coindex of  $G_{1+T}G_2$  is given as follows:

$$\begin{aligned}
 \alpha_1 &= 4e_2[\overline{e}_1 + (n_2 - 1)(\overline{e}_1 + e_1)] + 2n_2[\overline{M}_2(G_1) + (n_2 - 1)(\overline{M}_2(G_1) + M_2(G_1))] + (n_2 - 1 + \overline{e}_2)(M_1(G_1) + 2M_2(G_1)) \\
 &\quad + 4\overline{e}_2 M_1(G_1) + 4e_2 \overline{M}_1(G_1) + 8(e_2 + \overline{e}_2)M_2(G_1) + 4(n_2 + 2(e_2 + \overline{e}_2))\overline{M}_2(G_1) + \overline{e}_1 M_1(G_2) \\
 &\quad + 4e_1 \overline{M}_1(G_2) + 2(e_1 + \overline{e}_1)M_2(G_2) + (n_1 + 2(e_1 + \overline{e}_1))\overline{M}_2(G_2) + 2(M_1(G_2) + \overline{M}_1(G_2))(M_1(G_1) + \overline{M}_1(G_1)), \\
 \alpha_2 &= 4e_2[\overline{e}_{T(G_1)} + (n_2 - 1)(\overline{e}_{T(G_1)} + e_{T(G_1)})] + 2n_2(\overline{M}_2(T(G_1))) + (n_2 - 1)(M_2(T(G_1)) + \overline{M}_2(T(G_1))), \\
 \alpha_2 &= 4e_2[\overline{e}_{T(G_1)} + (n_2 - 1)(\overline{e}_{T(G_1)} + e_{T(G_1)})] + 2n_2(\overline{M}_2(T(G_1))) + (n_2 - 1)(M_2(T(G_1)) + \overline{M}_2(T(G_1))) \\
 &\quad + 8(e_2 + \overline{e}_2)M_2(G_1) + 4(n_2 + 2(e_2 + \overline{e}_2))\overline{M}_2(G_1) + \overline{e}_1 M_1(G_2) + 4e_1 \overline{M}_1(G_2) + 2(e_1 + \overline{e}_1)M_2(G_2) \\
 &\quad + (n_1 + 2(e_1 + \overline{e}_1))\overline{M}_2(G_2) + 2(M_1(G_2) + \overline{M}_1(G_2))(M_1(G_1) + \overline{M}_1(G_1)).
 \end{aligned} \tag{49}$$

*Proof.* Using equation (2), we have

$$\overline{M}_2(G_{1+T}G_2) = \sum_{(p_1, p_2) \in (q_1, q_2) \notin E(G_{1+T}G_2)} [d(p_1, q_1)d(p_2, q_2)] = \sum A + \sum B + \sum C. \tag{50}$$

Using equation (40), we directly have

$$\begin{aligned}
 & 2\bar{e}_2 M_2(G_1) + 2(n_2 - 1)M_2(G_1) + (n_2 - 1)M_1(G_1) + \bar{e}_2 M_1(G_1) \\
 & \leq \sum_{A \leq n_2} \bar{M}_2(T(G_1)) + (n_2 - 1)M_1(T(G_1)) \\
 & \quad + \bar{e}_2 M_1(T(G_1)) + 2(n_2 - 1)M_2(T(G_1)) + 2\bar{e}_2 M_2(T(G_1)) + 2(n_2 - 1)\bar{M}_2(T(G_1)) + 2\bar{e}_2 \bar{M}_2(T(G_1)).
 \end{aligned} \tag{51}$$

Using equation (15), we directly have

$$\begin{aligned}
 \sum B &= 4\bar{e}_2 M_1(G_1) + 4e_2 \bar{M}_1(G_1) + 8(e_2 + \bar{e}_2)M_2(G_1) + 4n_2 + 2(e_2 + \bar{e}_2)\bar{M}_2(G_1) \\
 & \quad + \bar{e}_1 M_1(G_2) + 4e_1 \bar{M}_1(G_2) \\
 & \quad + 2(e_1 + \bar{e}_1)M_2(G_2) + (n_1 + 2(e_1 + \bar{e}_1))\bar{M}_2(G_2) + 2(M_1(G_2) \\
 & \quad + \bar{M}_1(G_2))(M_1(G_1) + \bar{M}_1(G_1)), \\
 \sum C &= \sum C_1 + \sum C_2 + \sum C_3, \\
 \sum C_1 &= \sum_{\substack{t_1 t_2 \notin E(T(G_1)) \\ p_1 \in V(G_1) \\ p_2 \in V(T(G_1) - G_1)}} \sum_{q \in V_{G_2}} [d(p_1, q)d(p_2, q)] \\
 2n_2 \bar{M}_2(G_1) + 4e_2 \bar{e}_1 &\leq \sum C_1 \leq 2n_2 \bar{M}_2(T(G_1)) + 4e_2 \bar{e}_T(G_1), \\
 \sum C_2 &= \sum_{\substack{p_1 p_2 \notin E(T(G_1)) \\ p_1 \in V(G_1) \\ p_2 \in V(T(G_1) - V(G_1))}} \sum_{q_1, q_2 \in V_{G_2}} [d(p_1, q_1)d(p_2, q_2)] \\
 2n_2(n_2 - 1)\bar{M}_2(G_1) + 4e_2(n_2 - 1)\bar{e}_1 &\leq \sum C_2 \leq 2n_2(n_2 - 1)\bar{M}_2(T(G_1)) + 4e_2(n_2 - 1)\bar{e}_T(G_1), \\
 \sum C_3 &= \sum_{\substack{p_1 p_2 \in E(T(G_1)) \\ p_1 \in V(G_1) \\ p_2 \in V(T(G_1) - V(G_1))}} \sum_{q_1, q_2 \in V_{G_2}} [d(p_1, q_1)d(p_2, q_2)] \\
 2n_2(n_2 - 1)M_2(G_1) + 4e_2(n_2 - 1)e_1 &\leq \sum C_3 \leq 2n_2(n_2 - 1)M_2(T(G_1)) + 4e_2(n_2 - 1)e_T(G_1).
 \end{aligned} \tag{52}$$

Consequently,

$$\begin{aligned}
 & 2n_2 \bar{M}_2(G_1) + 4e_2 \bar{e}_1 + 2n_2(n_2 - 1)\bar{M}_2(G_1) + 4e_2(n_2 - 1)\bar{e}_1 + 2n_2(n_2 - 1)M_2(G_1) + 4e_2(n_2 - 1)e_1 \\
 & \leq \sum C \\
 & \leq 2n_2 \bar{M}_2(T(G_1)) + 4e_2 \bar{e}_T(G_1) + 2n_2(n_2 - 1)\bar{M}_2(T(G_1)) + 4e_2(n_2 - 1)\bar{e}_T(G_1) + 2n_2(n_2 - 1)M_2(T(G_1)) + 4e_2(n_2 - 1)e_T(G_1).
 \end{aligned} \tag{53}$$

TABLE 1: Exact and bounded values of certain  $F$ -sum graphs.

F-sum operation	Lower bounds	Exact values	Upper bounds
$\overline{M}_2(G_{1+S}G_2)$	152	160	312
$\overline{M}_2(G_{1+R}G_2)$	216	232	728
$\overline{M}_2(G_{1+Q}G_2)$	106	220	338
$\overline{M}_2(G_{1+T}G_2)$	150	300	642

We obtained required results by putting the values of  $\sum A + \sum B + \sum C$  in equation (48).  $\square$

#### 4. Conclusion

In this paper, we have computed second Zagreb coindex of  $F$ -sum graphs such as  $\overline{M}_2(G_{1+S}G_2)$ ,  $\overline{M}_2(G_{1+R}G_2)$ ,  $\overline{M}_2(G_{1+Q}G_2)$ , and  $\overline{M}_2(G_{1+T}G_2)$ . The obtained results are illustrated with the help of specific class graphs of  $F$ -sum graphs. Let  $G_1 \cong P_3$  and  $G_2 \cong P_2$ , then the lower and upper bounds of first Zagreb coindex for their  $F$ -sum graph are given in Table 1.

Now, we close our discussion that the problem is still open to compute the other generalized coindices (first general Zagreb and general Randic coindices) for the  $F$ -sum graphs.

#### Data Availability

The data used to support this study are included within the article. However, the reader may request the corresponding author for more details of the data.

#### Conflicts of Interest




The authors declare that they have no conflicts of interest.

#### References

- [1] G. Rucker and C. Rucker, "On topological indices, boiling points, and cycloalkanes," *Journal of Chemical Information and Computer Sciences*, vol. 39, no. 5, pp. 788–802, 1999.
- [2] A. R. Matamala and E. Estrada, "Generalised topological indices: optimisation methodology and physico-chemical interpretation," *Chemical Physics Letters*, vol. 410, no. 4–6, pp. 343–347, 2005.
- [3] H. Gonzalez-Diaz, S. Vilar, L. Santana, and E. Uriarte, "Medicinal chemistry and bioinformatics - current trends in drugs discovery with networks topological indices," *Current Topics in Medicinal Chemistry*, vol. 7, no. 10, pp. 1015–1029, 2007.
- [4] W. Yan, B.-Y. Yang, and Y.-N. Yeh, "The behavior of Wiener indices and polynomials of graphs under five graph decorations," *Applied Mathematics Letters*, vol. 20, no. 3, pp. 290–295, 2007.
- [5] M. V. Diudea, *QSPR/QSAR Studies by Molecular Descriptors*, Nova science Publishers, Hauppauge, NY, USA, 2001.
- [6] I. Gutman, "Degree-based topological indices," *Croatica Chemica Acta*, vol. 86, no. 4, pp. 351–361, 2013.
- [7] H. Wiener, "Structural determination of paraffin boiling points," *Journal of the American Chemical Society*, vol. 69, no. 1, pp. 17–20, 1947.
- [8] I. Gutman and N. Trinajstić, "Graph theory and molecular orbitals. Total  $\phi$ -electron energy of alternant hydrocarbons," *Chemical Physics Letters*, vol. 17, no. 4, pp. 535–538, 1972.
- [9] K. C. Das and I. Gutman, "Some properties of the second Zagreb index," *Communications in Mathematical and in Computer Chemistry*, vol. 52, no. 1, pp. 1–3, 2004.
- [10] Z. Yan, H. Liu, and H. Liu, "Sharp bounds for the second Zagreb index of unicyclic graphs," *Journal of Mathematical Chemistry*, vol. 42, no. 3, pp. 565–574, 2007.
- [11] M. Ahmad, M. Saeed, M. Javaid, and M. Hussain, "Exact formula and improved bounds for general sum-connectivity index of graph-operations," *IEEE Access*, vol. 7, pp. 167290–167299, 2019.
- [12] A. R. Ashrafi, T. Došlić, and A. Hamzeh, "The Zagreb coindices of graph operations," *Discrete Applied Mathematics*, vol. 158, no. 15, pp. 1571–1578, 2010.
- [13] A. R. Ashrafi, T. Došlić, and A. Hamzeh, "Extremal graphs with respect to the Zagreb coindices," *MATCH Communications in Mathematical and in Computer Chemistry*, vol. 65, no. 1, pp. 85–92, 2011.
- [14] K. C. Das, N. Akgunes, M. Togan, A. Yurttas, I. N. Cangul, and A. S. Cevik, "On the first Zagreb index and multiplicative Zagreb coindices of graphs," *Analele Universitatii "Ovidius" Constanta - Seria Matematica*, vol. 24, no. 1, pp. 153–176, 2016.
- [15] I. Gutman, "On coindices of graphs and their complements," *Applied Mathematics and Computation*, vol. 305, pp. 161–165, 2017.
- [16] N. De, S. M. A. Nayeem, and A. Pal, "The F-coindex of some graph operations," *Springer*, vol. 5, no. 1, pp. 1–13, 2016.
- [17] M. Javaid, U. Ali, and J. B. Liu, "Computing analysis for first Zagreb connection index and coindex of resultant graphs," *Mathematical Problems in Engineering*, vol. 2021, Article ID 6019517, 19 pages, 2021.
- [18] S. H. Ramane and Y. Saroja, "Talwar and ismail naci Cangul, "Transmission and reciprocal transmission based topological Co-indices of graphs," *European Journal of Pure and Applied Mathematics*, vol. 5, pp. 1057–1071, 2020.
- [19] T. Mansour and C. Song, "The  $a$  and  $(a, b)$  analogs of zagreb indices and coindices of graphs," *International Journal of Combinatorics*, vol. 2012, Article ID 909285, 10 pages, 2012.
- [20] C. M. Da Fonseca and D. Stevanovic, "Further properties of the second Zagreb index," *Communications in Mathematical and in Computer Chemistry*, vol. 72, pp. 655–668, 2014.
- [21] M. Eliasi and B. Taeri, "Four new sums of graphs and their Wiener indices," *Discrete Applied Mathematics*, vol. 157, no. 4, pp. 794–803, 2009.
- [22] H. Deng, D. Sarala, S. K. Ayyaswamy, and S. Balachandran, "The Zagreb indices of four operations on graphs," *Applied Mathematics and Computation*, vol. 275, pp. 422–431, 2016.
- [23] S. Akhter and M. Imran, "Computing the forgotten topological index of four operations on graphs," *AKCE International Journal of Graphs and Combinatorics*, vol. 14, no. 1, pp. 70–79, 2017.
- [24] J.-B. Liu, S. Javed, M. Javaid, and K. Shabbir, "Computing first general Zagreb index of operations on graphs," *IEEE Access*, vol. 7, pp. 47494–47502, 2019.
- [25] A. M. Alanazi, F. Farid, M. Javaid, and A. Munagi, "Computing exact values for gutman indices of sum graphs under cartesian product," *Mathematical Problems in Engineering*, vol. 2021, Article ID 5569997, 20 pages, 2021.

## Research Article

# Estimates for the Norm of Generalized Maximal Operator on Strong Product of Graphs

Zaryab Hussain <sup>1,2</sup>, Ghulam Murtaza <sup>3</sup>, Toqeer Mahmood <sup>4</sup> and Jia-Bao Liu <sup>5</sup>

<sup>1</sup>School of Mathematics and Statistics, Northwestern Polytechnical University, Xi'an, Shaanxi 710129, China

<sup>2</sup>Department of Mathematics, Government College University, Faisalabad 38000, Pakistan

<sup>3</sup>Department of Mathematics, School of Science, University of Management and Technology, Lahore 54000, Pakistan

<sup>4</sup>Department of Computer Science, National Textile University, Faisalabad 37610, Pakistan

<sup>5</sup>School of Mathematics and Physics, Anhui Jianzhu University, Hefei 230601, China

Correspondence should be addressed to Toqeer Mahmood; toqeer.mahmood@yahoo.com

Received 20 April 2021; Accepted 11 June 2021; Published 9 July 2021

Academic Editor: Sakander Hayat

Copyright © 2021 Zaryab Hussain et al. This is an open access article distributed under the Creative Commons Attribution License, which permits unrestricted use, distribution, and reproduction in any medium, provided the original work is properly cited.

Let  $G = G_1 \times G_2 \times \dots \times G_m$  be the strong product of simple, finite connected graphs, and let  $\phi: \mathbb{N} \rightarrow (0, \infty)$  be an increasing function. We consider the action of generalized maximal operator  $M_G^\phi$  on  $\ell^p$  spaces. We determine the exact value of  $\ell^p$ -quasi-norm of  $M_G^\phi$  for the case when  $G$  is strong product of complete graphs, where  $0 < p \leq 1$ . However, lower and upper bounds of  $\ell^p$ -norm have been determined when  $1 < p < \infty$ . Finally, we computed the lower and upper bounds of  $\|M_G^\phi\|_p$  when  $G$  is strong product of arbitrary graphs, where  $0 < p \leq 1$ .

## 1. Introduction

We review some of the standard facts on graphs and metric on the graphs. All the graphs considered in this paper are simple, finite, and connected. Let  $G(V(G), E(G))$  be a graph, where  $V(G)$  is the set of vertices and  $E(G)$  is the set of edges of  $G$ . The vertices which are at distance one from any vertex  $x \in V(G)$  are called neighbors of  $x$ . The set of neighbors of  $x \in V(G)$  is denoted by  $N_G(x)$ . The degree of any vertex  $x \in V(G)$  is the cardinality of the set  $N_G(x)$  and is denoted by  $d_G(x)$ . The distance between two vertices  $x$  and  $y$  denoted by  $d(x, y)$  is the length of the shortest path between  $x$  and  $y$ . For more details on graph theory, we refer the readers to [1–3]. The metric (graph metric)  $d_G: V(G) \times V(G) \rightarrow \mathbb{R}$  on graph  $G$  is defined as

$$d_G(x, y) = \text{distance between } x \text{ and } y, \quad (1)$$

where  $x, y \in V(G)$ . This metric space  $(G, d_G)$  is called geodesic metric space. For any function  $f: V(G) \rightarrow \mathbb{R}$ , the

Hardy–Littlewood maximal operator  $M_G^x: \ell^p \rightarrow \ell^p$  [4–7] is defined as

$$M_G^x f(q) = \sup_{r \geq 0} \frac{1}{|B(q, r)|} \sum_{w \in B(q, r)} |f(w)|, \quad (2)$$

where  $B(q, r) = \{s \in V(G): d_G(q, s) \leq r\}$  is the ball with center  $q \in V(G)$  and radius  $r$  on a graph  $G$ . It contains all the vertices of  $G$  which are at distance at most  $r$  from the vertex  $q$ . It is clear from the definition that if  $r = 0$ , then  $|B(q, r)| = 1$ , and if  $r \geq 1$ , then  $|B(q, r)| \geq 2$ . The values of metric function  $d_G$  are natural numbers and radius  $r \geq 0$ ; therefore, equation (2) can be written as

$$M_G^x f(q) = \max_{r \in \mathbb{N}} \frac{1}{|B(q, r)|} \sum_{w \in B(q, r)} |f(w)|. \quad (3)$$

The fractional maximal operator [8] on graphs is defined as

$$M_G^{1-(t/n)} f(q) = \max_{r \in \mathbb{N}} \frac{1}{|B(q,r)|^{1-(t/n)}} \sum_{w \in B(q,r)} |f(w)|, \quad (4)$$

where  $0 \leq t \leq n$ . If  $t = 0$ , then equation (4) reduces to equation (3). For  $0 < p < \infty$ , the  $\ell^p$  norm of the Hardy–Littlewood maximal operator is defined as

$$\|M_G^x\|_{\ell^p} := \sup_{f \neq 0} \frac{\|M_G^x f\|_{\ell^p}}{\|f\|_{\ell^p}}, \quad (5)$$

where  $\|f\|_{\ell^p} = (\sum_{s \in V(G)} |f(s)|^p)^{(1/p)}$ .

For every function  $f: V(G) \rightarrow \mathbb{R}$ , the generalized maximal operator  $M_G^\phi: \ell^p \rightarrow \ell^p$  [9, 10] is defined as

$$M_G^\phi f(q) = \max_{r \in \mathbb{N}} \frac{1}{\phi(|B(q,r)|)} \sum_{w \in B(q,r)} |f(w)|, \quad (6)$$

where  $\phi: \mathbb{N} \rightarrow (0, \infty)$  is an increasing function. Note that if we take  $\phi(x) = x$  in equation (6), then we get the classical Hardy–Littlewood maximal operator  $M_G^x$ , and if we take  $\phi(x) = x^{1-(t/n)}$  in equation (5), then we get equation (4).

Let  $K_n$  be complete graph on  $n$  vertices. For any vertex  $q \in V(K_n)$ , the ball  $B(q,r)$  with center  $q$  and radius  $r$  is defined as

$$B(q,r) = \begin{cases} \{q\}, & \text{for } r = 0, \\ V(K_n), & \text{for } r \geq 1. \end{cases} \quad (7)$$

Therefore, the generalized maximal operator on complete graph  $K_n$  takes the form

$$M_{K_n}^\phi f(q) = \max \left\{ \frac{1}{\phi(1)} |f(q)|, \frac{1}{\phi(n)} \sum_{v \in V(K_n)} |f(v)| \right\}. \quad (8)$$

For any vertex  $i \in V(G)$ , the Kronecker delta function is defined as

$$\delta_q(i) = \begin{cases} 1, & q = i, \\ 0, & q \neq i. \end{cases} \quad (9)$$

Soria and Tradacete [6] estimated the norm of maximal operator  $M_G^x$  in the following form.

---


$$M_G^\phi f(u_1, u_2, \dots, u_m) = \max_{r \in \mathbb{N}} \frac{\sum_{v_1 \in G_1} \sum_{v_2 \in G_2} \dots \sum_{v_m \in G_m} |f(v_1, v_2, \dots, v_m)|}{\phi(|B_{G_1}| \times |B_{G_2}| \times \dots \times |B_{G_m}|)}, \quad (13)$$


---

where  $B_{G_i} = B(u_i, r)$ ,  $i = 1, 2, \dots, m$ . The norm  $\|M_G^\phi\|_p$  of the generalized maximal operator is defined as

$$\|M_G^\phi\|_p = \sup_{f \neq 0} \frac{\|M_G^\phi f\|_p}{\|f\|_p}, \quad (14)$$

**Proposition 1** (see [6])

(i) If  $0 < p \leq 1$ , then

$$\|M_{K_n}\|_p = \left(1 + \frac{n-1}{n^p}\right)^{(1/p)}. \quad (10)$$

(ii) If  $1 < p < \infty$ , then

$$\left(1 + \frac{n-1}{n^p}\right)^{(1/p)} \leq \|M_{K_n}\|_p \leq \left(1 + \frac{n-1}{n}\right)^{(1/p)}. \quad (11)$$

For more details on this topic of research, see [4, 8, 10–13]. The main motivation of this paper is from [4–7, 10].

The paper is structured as follows. Section 2 contains the definitions which are helpful to prove the main results. Section 3 contains the main results; we find the exact value of  $\|M_{K_n}^\phi\|_p$  for the case  $0 < p \leq 1$  and give lower and upper bound when  $1 < p < \infty$ . An example is given to show that these bounds are not optimal. Finally, Section 4 concludes the study.

## 2. Preliminaries

Let  $G_1, G_2, \dots, G_m$  be  $m$  graphs; then, their strong product  $G = G_1 \times G_2 \times \dots \times G_m$  is a graph having vertex set,

$$V(G) = \{(u_1, u_2, \dots, u_m) : u_i \in G_i \forall i = 1, 2, \dots, m\}, \quad (12)$$

and the edge set, which is defined in the following manner; there will be an edge between  $(u_1, u_2, \dots, u_m)$  and  $(v_1, v_2, \dots, v_m)$  in  $G$  if

- (a)  $u_i = v_i$  and  $(u_j, v_j) \in E(G_j)$ ,  $j \neq i$
- (b)  $u_i \neq v_i$  and  $(u_i, v_i) \in E(G_i)$ ,  $\forall i$

*Example 1.* Let  $K_2$  be complete graph on two vertices. The strong product  $K = K_2 \times K_2 \times K_2$  of three  $K_2$  graphs is shown in Figure 1.

Let  $G$  be the strong product of  $m$  graphs. Then, for every function  $f: V(G) \rightarrow \mathbb{R}$ , we can consider the generalized maximal operator  $M_G^\phi: \ell^p \rightarrow \ell^p$  as

---

where  $\|f\|_p = (\sum_{v_1 \in G_1} \sum_{v_2 \in G_2} \dots \sum_{v_m \in G_m} |f(v_1, v_2, \dots, v_m)|^p)^{(1/p)}$ .

Let  $K = K_{n_1} \times K_{n_2} \times \dots \times K_{n_m}$  be the strong product of  $m$  complete graphs with  $n_1, n_2, \dots, n_m$  vertices, respectively; then,

$$B(u_1, r) \times B(u_2, r) \times \cdots \times B(u_m, r) = \begin{cases} \{(u_1, u_2, \dots, u_m)\}, & \text{for } r = 0, \\ V(K), & \text{for } r \geq 1. \end{cases} \quad (15)$$

For every function  $f: V(K) \rightarrow \mathbb{R}$ , the generalized maximal operator takes the form

$$M_K^\phi f(u_1, u_2, \dots, u_m) = \max \left\{ \begin{array}{l} \frac{1}{\phi(1)} |f(u_1, u_2, \dots, u_m)|, \\ \frac{1}{\phi(n_1 \times n_2 \times \cdots \times n_m)} \sum_{v_1 \in K_{n_1}} \sum_{v_2 \in K_{n_2}} \cdots \sum_{v_m \in K_{n_m}} |f(v_1, v_2, \dots, v_m)| \end{array} \right\}. \quad (16)$$

Note that the operator  $M_K^\phi$  is the smallest in the pointwise ordering among all  $M_{G=G_1 \times G_2 \times \cdots \times G_m}^\phi$ , where each  $G_i$  is a graph with  $n_i$  vertices for  $i = 1, 2, \dots, m$ . That is, for every nonnegative function  $f$  and every vertex  $(u_1, u_2, \dots, u_m) \in G$ , we have that

$$M_K^\phi f(u_1, u_2, \dots, u_m) \leq M_G^\phi f(u_1, u_2, \dots, u_m). \quad (17)$$

In particular, if  $0 < p < \infty$ , then

$$\|M_K^\phi\|_p^p \leq \|M_G^\phi\|_p^p. \quad (18)$$

For any vertex  $(u_1, u_2, \dots, u_m) \in V(K)$ , the  $m$  Dirac delta function is defined as

$$\Gamma_{(u_1, u_2, \dots, u_m)}(v_1, v_2, \dots, v_m) = \delta_{u_1}(v_1) \cdot \delta_{u_2}(v_2) \cdots \delta_{u_m}(v_m). \quad (19)$$

It is easy to check that

$$\Gamma_{(u_1, u_2, \dots, u_m)}(v_1, v_2, \dots, v_m) = \begin{cases} 0, & \text{for } u_j \neq v_j, \text{ for some } j, \\ 1, & \text{for } u_i = v_i, \forall i = 1, 2, \dots, m. \end{cases} \quad (20)$$

### 3. Main Results

This section details the steps to find the quasi-norm of  $M_K^\phi$ , for the case  $0 < p \leq 1$ , and to find bounds of  $\|M_K^\phi\|_p$ , for the case of  $1 < p < \infty$ . Also, we estimate the bounds of  $\|M_G^\phi\|_p$  for  $0 < p \leq 1$ . Moreover, some examples are presented to support the results.

**Lemma 1.** *Let  $G$  be the strong product of  $m$  graphs, and  $\Omega: \ell^p \rightarrow \ell^p$  be a sublinear operator, with  $0 < p \leq 1$ . Then,*

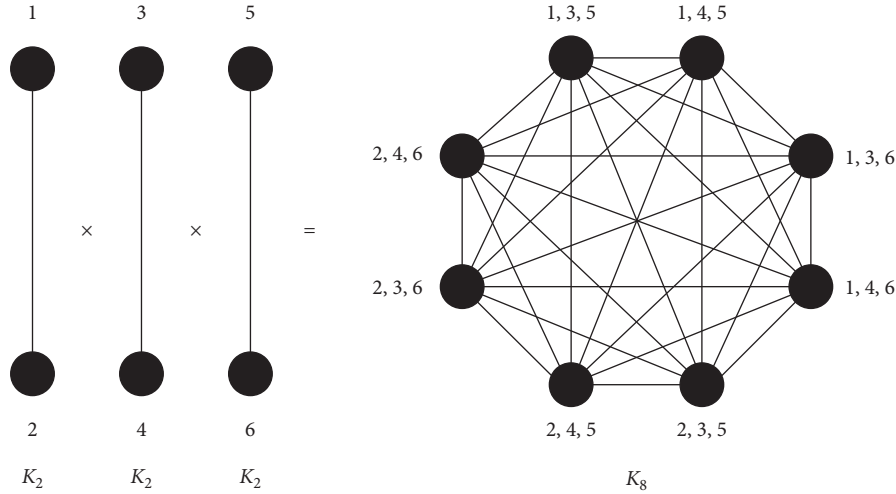
$$\|\Omega\|_p = \max_{(u_1, u_2, \dots, u_m) \in V(G)} \|\Omega\Gamma_{(u_1, u_2, \dots, u_m)}\|_p. \quad (21)$$

*Proof.* Since  $\|\Gamma_{(u_1, u_2, \dots, u_m)}\|_p = 1$ , therefore  $\|\Omega\|_p \geq \max_{(u_1, u_2, \dots, u_m) \in V(G)} \|\Omega\Gamma_{(u_1, u_2, \dots, u_m)}\|_p$ . To prove the other inequality, let  $h: V(G) \rightarrow \mathbb{R}$ , with  $\|h\|_p \leq 1$ , that is,

$$h = \sum_{u_1 \in G_1} \sum_{u_2 \in G_2} \cdots \sum_{u_m \in G_m} a(u_1, u_2, \dots, u_m) \Gamma_{(u_1, u_2, \dots, u_m)}, \quad (22)$$

with  $\sum_{u_1 \in G_1} \sum_{u_2 \in G_2} \cdots \sum_{u_m \in G_m} |a(u_1, u_2, \dots, u_m)|^p \leq 1$ . Using Hölder's inequality for  $0 < p \leq 1$ , it follows that

$$\begin{aligned} \|\Omega h\|_p^p &= \sum_{v_1 \in G_1} \sum_{v_2 \in G_2} \cdots \sum_{v_m \in G_m} |\Omega h(v_1, v_2, \dots, v_m)|^p \\ &= \sum_{v_1 \in G_1} \sum_{v_2 \in G_2} \cdots \sum_{v_m \in G_m} \left| \Omega \left( \sum_{u_1 \in G_1} \sum_{u_2 \in G_2} \cdots \sum_{u_m \in G_m} a(u_1, u_2, \dots, u_m) \Gamma_{(u_1, u_2, \dots, u_m)}(v_1, v_2, \dots, v_m) \right) \right|^p \\ &\leq \sum_{v_1 \in G_1} \sum_{v_2 \in G_2} \cdots \sum_{v_m \in G_m} \left| \sum_{u_1 \in G_1} \sum_{u_2 \in G_2} \cdots \sum_{u_m \in G_m} |a(u_1, u_2, \dots, u_m)| \Omega\Gamma_{(u_1, u_2, \dots, u_m)}(v_1, v_2, \dots, v_m) \right|^p \\ &\leq \sum_{v_1 \in G_1} \sum_{v_2 \in G_2} \cdots \sum_{v_m \in G_m} \sum_{u_1 \in G_1} \sum_{u_2 \in G_2} \cdots \sum_{u_m \in G_m} |a(u_1, u_2, \dots, u_m)| \Omega\Gamma_{(u_1, u_2, \dots, u_m)}(v_1, v_2, \dots, v_m)^p \\ &= \sum_{u_1 \in G_1} \sum_{u_2 \in G_2} \cdots \sum_{u_m \in G_m} |a(u_1, u_2, \dots, u_m)|^p \sum_{v_1 \in G_1} \sum_{v_2 \in G_2} \cdots \sum_{v_m \in G_m} |\Omega\Gamma_{(u_1, u_2, \dots, u_m)}(v_1, v_2, \dots, v_m)|^p \\ &= \sum_{u_1 \in G_1} \sum_{u_2 \in G_2} \cdots \sum_{u_m \in G_m} |a(u_1, u_2, \dots, u_m)|^p \|\Omega\Gamma_{(u_1, u_2, \dots, u_m)}\|_p^p \\ &\leq \max_{(u_1, u_2, \dots, u_m) \in V(G)} \|\Omega\Gamma_{(u_1, u_2, \dots, u_m)}\|_p^p. \end{aligned} \quad (23)$$

FIGURE 1: Strong product of three  $K_2$  graphs.

It completes the proof.

□ and if  $1 < p < \infty$ , then

**Theorem 1.** If  $0 < p \leq 1$ , then

$$\|M_K^\phi\|_p = \left( \frac{1}{\phi^p(1)} + \frac{(n_1 \times n_2 \times \dots \times n_m) - 1}{\phi^p(n_1 \times n_2 \times \dots \times n_m)} \right)^{(1/p)}, \quad (24)$$

$$\begin{aligned} & \left( \frac{1}{\phi^p(1)} + \frac{(n_1 \times n_2 \times \dots \times n_m) - 1}{\phi^p(n_1 \times n_2 \times \dots \times n_m)} \right)^{(1/p)} \\ & \leq \|M_K^\phi\|_p \leq \max \left( \frac{(n_1 \times n_2 \times \dots \times n_m)^p}{\phi^p(n_1 \times n_2 \times \dots \times n_m)}, \right. \\ & \left. \left\{ \frac{1}{\phi^p(1)} + \frac{((n_1 \times n_2 \times \dots \times n_m) - 1)(n_1 \times n_2 \times \dots \times n_m)^{(p-1)}}{\phi^p(n_1 \times n_2 \times \dots \times n_m)} \right\} \right)^{(1/p)}. \end{aligned} \quad (25)$$

*Proof.* Let  $f: V(K) \rightarrow \mathbb{R}$  be a function such that  $\|f\|_p = 1$ . Define  $m$  Dirac delta function  $\Gamma_{(u_1, u_2, \dots, u_m)}$ , where

$u_1 \in V(K_{n_1}), u_2 \in V(K_{n_2}), \dots, u_m \in V(K_{n_m})$ . Then, for  $0 < p < \infty$ , we have

$$\begin{aligned} \|M_K^\phi \Gamma_{(u_1, u_2, \dots, u_m)}\|_p &= \left( \left( M_K^\phi \Gamma_{(u_1, u_2, \dots, u_m)}(u_1, u_2, \dots, u_m) \right)^p + \sum_{v_1 \neq u_1} \sum_{v_2 \neq u_2} \dots \sum_{v_m \neq u_m} \left( M_K^\phi \Gamma_{(u_1, u_2, \dots, u_m)}(v_1, v_2, \dots, v_m) \right)^p \right)^{(1/p)} \\ &= \left( \frac{1}{\phi^p(1)} + \frac{(n_1 \times n_2 \times \dots \times n_m) - 1}{\phi^p(n_1 \times n_2 \times \dots \times n_m)} \right)^{(1/p)}. \end{aligned} \quad (26)$$

As  $\|\Gamma\|_p = 1$ , so we have, for  $0 < p < \infty$ ,

$$\left( \frac{1}{\phi^p(1)} + \frac{(n_1 \times n_2 \times \dots \times n_m) - 1}{\phi^p(n_1 \times n_2 \times \dots \times n_m)} \right)^{(1/p)} \leq \|M_K^\phi\|_p. \quad (27)$$

For  $0 < p \leq 1$ , using Lemma 1, we have

$$\left( \frac{1}{\phi^p(1)} + \frac{(n_1 \times n_2 \times \dots \times n_m) - 1}{\phi^p(n_1 \times n_2 \times \dots \times n_m)} \right)^{(1/p)} = \|M_K^\phi\|_p. \quad (28)$$

Now, we will prove upper bound for  $1 < p < \infty$ :

$$\begin{aligned} \|M_K^\phi f\|_p &= \left( \sum_{u_1 \in B_{G_1}} \sum_{u_2 \in B_{G_2}} \cdots \sum_{u_m \in B_{G_m}} \max \left\{ \frac{1}{\phi(1)} |f(u_1, u_2, \dots, u_m)|, \right. \right. \\ &\quad \left. \left. \frac{1}{\phi(n_1 \times n_2 \times \cdots \times n_m)} \sum_{v_1 \in B_{G_1}} \sum_{v_2 \in B_{G_2}} \cdots \sum_{v_m \in B_{G_m}} |f(v_1, v_2, \dots, v_m)|^p \right\} \right)^{(1/p)}. \end{aligned} \quad (29)$$

After applying Hölder's inequality, we have

$$\|M_K^\phi\|_p \leq \sup \left( \sum_{u_1 \in B_{G_1}} \sum_{u_2 \in B_{G_2}} \cdots \sum_{u_m \in B_{G_m}} \max \left\{ \frac{1}{\phi^p(1)} |f(u_1, u_2, \dots, u_m)|^p, \frac{1}{\phi^p(n_1 \times n_2 \times \cdots \times n_m)} (n_1 \times n_2 \times \cdots \times n_m)^{(p-1)} \right\} \right)^{(1/p)}. \quad (30)$$

If  $(|f(u_1, u_2, \dots, u_m)|^p / \phi^p(1)) \leq ((n_1 \times n_2 \times \cdots \times n_m)^{(p-1)} / \phi^p(n_1 \times n_2 \times \cdots \times n_m))$  for all vertices, then we have

$$\|M_K^\phi\|_p \leq \left( \frac{(n_1 \times n_2 \times \cdots \times n_m)^p}{\phi^p(n_1 \times n_2 \times \cdots \times n_m)} \right)^{(1/p)}. \quad (31)$$

If  $(|f(u'_1, u'_2, \dots, u'_m)|^p / \phi^p(1)) > ((n_1 \times n_2 \times \cdots \times n_m)^{(p-1)} / \phi^p(n_1 \times n_2 \times \cdots \times n_m))$  for some  $(u'_1, u'_2, \dots, u'_m) \in V(K)$ , then we have

$$\begin{aligned} \|M_K^\phi\|_p &\leq \left( \frac{1}{\phi^p(1)} |f(u'_1, u'_2, \dots, u'_m)|^p + \frac{((n_1 \times n_2 \times \cdots \times n_m) - 1)(n_1 \times n_2 \times \cdots \times n_m)^{p-1}}{\phi^p(n_1 \times n_2 \times \cdots \times n_m)} \right)^{(1/p)} \\ &\leq \left( \frac{1}{\phi^p(1)} + \frac{((n_1 \times n_2 \times \cdots \times n_m) - 1)(n_1 \times n_2 \times \cdots \times n_m)^{(p-1)}}{\phi^p(n_1 \times n_2 \times \cdots \times n_m)} \right)^{(1/p)}, \end{aligned} \quad (32)$$

which completes our arguments.

The graph of the result of Theorem 1 is shown in Figure 2, where  $\phi(x) = x$ ,  $n_1 \times n_2 \times \cdots \times n_m$  is from 4 to 10, and  $p = 2$  and  $p = 3$ .

3D solution region for Theorem 1 is shown in Figure 3, where  $\phi(x) = x$ ,  $n_1 \times n_2 \times \cdots \times n_m$  is from 4 to 12, and  $p$  is from 1 to 10.

The graph presented in Figure 3 shows the results of Theorem 1 that are not optimal. It is quite difficult task to calculate the exact value of  $\|M_K^\phi\|_p$  for the case  $1 < p < \infty$ . The following example explains the situation.  $\square$

*Example 2.* The estimates we obtained in Theorem 1 for  $1 < p < \infty$  is not optimal in general. For example, if we take graph  $K_2 \times K_2$  and  $\phi(x) = x$ . Consider the function  $f: \{(1,3), (1,4), (2,3), (2,4)\} \rightarrow \mathbb{R}$ . We suppose that  $|f(1,3)| = |f(1,2)| = |f(2,3)|$ ,  $M_{K_2 \times K_2}^x f(1,3) = M_{K_2 \times K_2}^x f(1,4) = M_{K_2 \times K_2}^x f(2,3) = (3|f(1,3)| + |f(1,4)|/4)$ , and  $M_{K_2 \times K_2}^x f(2,4) = |f$

$(2,4)|$ . Then,  $|f(2,4)| \geq |f(1,3)|$ . If we denote  $(|f(1,3)|/|f(2,4)|)$  by  $\lambda$ , then, for every  $0 < p < \infty$ , we have

$$\begin{aligned} \frac{\|M_{K_2 \times K_2}^x f\|_p}{\|f\|_p} &= \left( \frac{3(3|f(1,3)| + |f(1,4)|/4)^p + |f(1,4)|^p}{3|f(1,3)|^p + |f(1,4)|^p} \right)^{(1/p)} \\ &= \frac{1}{4} \left( \frac{3(3\lambda + 1)^p + 4^p}{3\lambda^p + 1} \right)^{(1/p)}, \end{aligned} \quad (33)$$

which leads to

$$\|M_{K_2 \times K_2}^x\|_p = \frac{1}{4} \left( \sup_{0 \leq \lambda \leq 1} \frac{3(3\lambda + 1)^p + 4^p}{3\lambda^p + 1} \right)^{(1/p)}. \quad (34)$$

It is easy to see that, for  $1 < p < \infty$ , the supremum is attained at the unique root  $\lambda_p \in (0, 1)$  of the equation



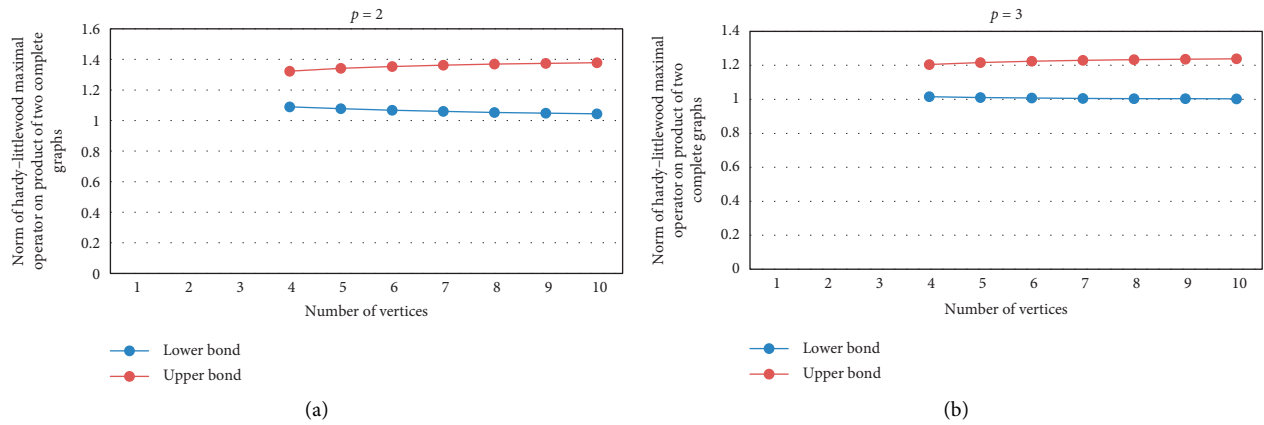


FIGURE 2: Estimation for  $p = 2$  and  $p = 3$ .

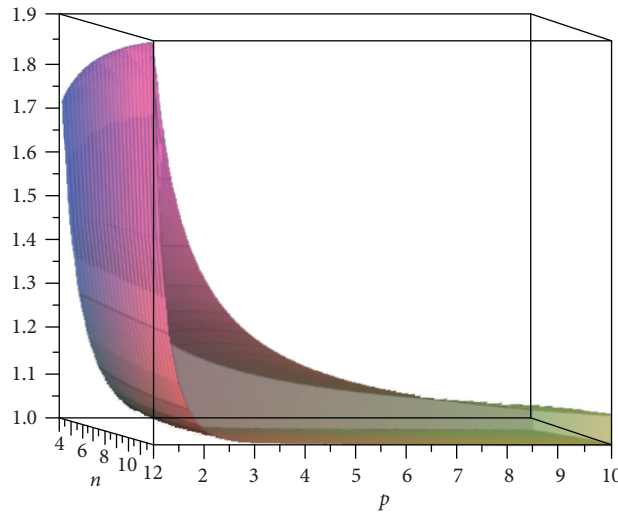


FIGURE 3: 3D view of estimation for  $n = 4 \dots 12$  and  $p = 1 \dots 10$ .

$$(1 + 3\lambda)^{p-1} = \frac{3\lambda^{p-1}(3\lambda + 1)^p + 4^p\lambda^{p-1}}{9\lambda^p + 3}. \quad (35)$$

In particular, if we take  $p = 2$ , then we get  $\lambda = 0.246$ , and from equation (34), we get  $\|M_{K_2 \times K_2}^x\|_2 = 1.151$ . If we calculate it from Theorem 1, we get  $1.090 \leq \|M_{K_2 \times K_2}^x\|_2 \leq 1.323$ . This shows that the estimation in Theorem 1 is not optimal in general for  $1 < p < \infty$ . Now, in the next theorem, we find the estimates of  $G$ .

**Theorem 2.** Let  $G$  be the strong product of  $m$  graphs and  $0 < p \leq 1$ ; then, we have

$$\begin{aligned} & \left( \frac{1}{\phi^p(1)} + \frac{(n_1 \times n_2 \times \dots \times n_m) - 1}{\phi^p(n_1 \times n_2 \times \dots \times n_m)} \right)^{(1/p)} \\ & \leq \|M_G^\phi\|_p \leq \left( \frac{1}{\phi^p(1)} + \frac{(n_1 \times n_2 \times \dots \times n_m) - 1}{\phi^p(2^m)} \right)^{(1/p)}. \end{aligned} \quad (36)$$

*Proof.* Lower bound is trivial. For the upper bound, let  $(u_1, u_2, \dots, u_m) \in V(G)$  and consider the  $m$  Dirac delta function  $\Gamma_{(u_1, u_2, \dots, u_m)}$ . Then, we have

$$\begin{aligned} \|M_G^\phi \Gamma(u_1, u_2, \dots, u_m)\|_p &= \left( \left( M_G^\phi \Gamma(u_1, u_2, \dots, u_m)(u_1, u_2, \dots, u_m) \right)^p + \sum_{v_1 \neq u_1} \sum_{v_2 \neq u_2} \dots \sum_{v_m \neq u_m} \left\{ M_G^\phi \Gamma(u_1, u_2, \dots, u_m)(v_1, v_2, \dots, v_m) \right\}^p \right)^{(1/p)} \\ &= \left( \frac{1}{\phi^p(1)} + \sum_{v_1 \neq u_1} \sum_{v_2 \neq u_2} \dots \sum_{v_m \neq u_m} \left\{ \frac{1}{\phi(|B_{G_1}| \times |B_{G_2}| \times \dots \times |B_{G_m}|)} \sum_{w_1} \sum_{w_2} \dots \sum_{w_m} \Gamma(u_1, u_2, \dots, u_m)(w_1, w_2, \dots, w_m) \right\}^p \right)^{(1/p)}. \end{aligned} \tag{37}$$

As each  $G_i$  is connected,  $|B_{G_i}| \geq 2$  for each  $i$  and radius  $r \geq 1$ . Hence,

$$\|M_G^\phi \Gamma(u_1, u_2, \dots, u_m)\|_p \leq \left( \frac{1}{\phi^p(1)} + \frac{(n_1 \times n_2 \times \dots \times n_m) - 1}{\phi^p(2^m)} \right)^{(1/p)}. \tag{38}$$

By using Lemma 1, we obtain

$$\|M_G^\phi\|_p \leq \left( \frac{1}{\phi^p(1)} + \frac{(n_1 \times n_2 \times \dots \times n_m) - 1}{\phi^p(2^m)} \right)^{(1/p)}. \tag{39}$$

If we take  $\phi(x) = x$  and  $m = 1$ , then Theorems 1 and 2, respectively, yields the same results obtained in [9]. This shows that the results presented in this paper are the generalized form of the results in [6].

We have graph for the result of Theorem 2 in Figure 4, where  $p = 0.5$ ,  $\phi(x) = x$ , and  $n_1 \times n_2 \times \dots \times n_m$  is from 4 to 10.

Some particular examples to support the result of Theorem 2 are given below.  $\square$

*Example 3.* Let  $W_5$  be a wheel graph on five vertices and consider the strong product  $K_2 \times W_5$  of  $K_2$  with  $W_5$ . Take  $\phi(x) = x$ ,  $f = \Gamma$ , and  $p = 1$ . Then,  $\|M_{K_2 \times W_5}^x\| = 2.100$ .

Let  $V(K_2) = \{1, 2\}$  and  $V(W_5) = \{3, 4, 5, 6, 7\}$ , where 7 is the central vertex of  $W_5$ . Now,  $6 \notin N_{W_5}(3)$  and  $5 \notin N_{W_5}(4)$ . Then, the strong product  $K_2 \times W_5$  has a vertex set

$$\begin{aligned} V(K_2 \times W_5) &= \{(1, 3), (1, 4), (1, 5), (1, 6), (1, 7), (2, 3), \\ &\quad (2, 4), (2, 5), (2, 6), (2, 7)\}. \end{aligned} \tag{40}$$

Note that  $K_2 \times W_5$  has 37 edges and  $d_{(1,7)}(K_2 \times W_5) = d_{(2,7)}(K_2 \times W_5) = 9$ , while all other vertices of this graph have degree 7. Hence,

$$M_{K_2 \times W_5}^x \Gamma_{(1,3)} = \begin{cases} 1, & \text{for } \{(1, 3)\}, \\ \frac{1}{10}, & \text{for } \{(1, 6), (1, 7), (2, 6), (2, 7)\}, \\ \frac{1}{8}, & \text{otherwise,} \end{cases} \tag{41}$$

with  $\|M_{K_2 \times W_5}^x \Gamma_{(1,3)}\| = 2.025$ . It is easy to see that  $\|M_{K_2 \times W_5}^x \Gamma_{(1,4)}\| = \|M_{K_2 \times W_5}^x \Gamma_{(1,5)}\| = \|M_{K_2 \times W_5}^x \Gamma_{(1,6)}\| = \|M_{K_2 \times W_5}^x \Gamma_{(2,3)}\| = \|M_{K_2 \times W_5}^x \Gamma_{(2,4)}\| = \|M_{K_2 \times W_5}^x \Gamma_{(2,5)}\| = \|M_{K_2 \times W_5}^x \Gamma_{(2,6)}\| = 2.025$ .

Also,

$$M_{K_2 \times W_5}^x \Gamma_{(1,7)} = \begin{cases} 1, & \text{for } \{(1, 7)\}, \\ \frac{1}{10}, & \text{for } \{(2, 7)\}, \\ \frac{1}{8}, & \text{otherwise,} \end{cases} \tag{42}$$

with  $\|M_{K_2 \times W_5}^x \Gamma_{(1,7)}\| = 2.100$ ,  $\|M_{K_2 \times W_5}^x \Gamma_{(2,7)}\| = 2.100$ , and  $\|M_{K_2 \times W_5}^x\| = 2.100$ .

*Example 4.* Consider the graph used in Example 3. Take  $\phi(x) = x^2$ ,  $f = \Gamma$ , and  $p = 1$ . Then,  $\|M_{K_2 \times W_5}^{x^2}\| = 1.135$ . We have

$$M_{K_2 \times W_5}^{x^2} \Gamma_{(1,3)} = \begin{cases} 1, & \text{for } \{(1, 3)\}, \\ \frac{1}{100}, & \text{for } \{(1, 6), (1, 7), (2, 6), (2, 7)\}, \\ \frac{1}{64}, & \text{otherwise,} \end{cases} \tag{43}$$

with  $\|M_{K_2 \times W_5}^{x^2} \Gamma_{(1,3)}\| = 1.118$  and  $\|M_{K_2 \times W_5}^{x^2} \Gamma_{(1,4)}\| = \|M_{K_2 \times W_5}^{x^2} \Gamma_{(1,5)}\| = \|M_{K_2 \times W_5}^{x^2} \Gamma_{(1,6)}\| = \|M_{K_2 \times W_5}^{x^2} \Gamma_{(2,3)}\| = \|M_{K_2 \times W_5}^{x^2} \Gamma_{(2,4)}\| = \|M_{K_2 \times W_5}^{x^2} \Gamma_{(2,5)}\| = \|M_{K_2 \times W_5}^{x^2} \Gamma_{(2,6)}\| = 1.118$ .

In a similar way, we have

$$M_{K_2 \times W_5}^{x^2} \Gamma_{(1,7)} = \begin{cases} 1, & \text{for } \{(1, 7)\}, \\ \frac{1}{100}, & \text{for } \{(2, 7)\}, \\ \frac{1}{64}, & \text{otherwise,} \end{cases} \tag{44}$$

with  $\|M_{K_2 \times W_5}^{x^2} \Gamma_{(1,7)}\| = 1.135$  and  $\|M_{K_2 \times W_5}^{x^2} \Gamma_{(2,7)}\| = 1.135$ . This implies that  $\|M_{K_2 \times W_5}^{x^2}\| = 1.135$ .

*Example 5.* Let  $S_3$  be star graph on three vertices and consider the strong product  $K_2 \times K_2 \times S_3$ . Take  $\phi(x) = x$ ,  $f = \Gamma$ , and  $p = 1$ . Then,  $\|M_{K_2 \times K_2 \times S_3}^x\| = 2.250$ .

Let  $V(K_2) = \{1, 2\}$ ,  $V(K_2) = \{3, 4\}$ , and  $V(S_3) = \{5, 6, 7\}$  with 7 as a central vertex of  $S_3$ . Then, the strong product  $K_2 \times K_2 \times S_3$  is a graph with vertex set

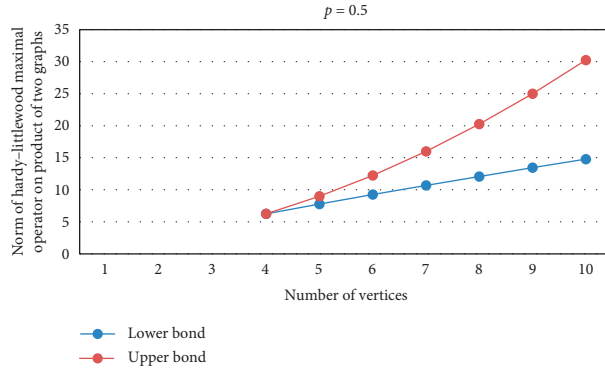


FIGURE 4: Estimation for  $p = 0.5$ .

$$V(K_2 \times K_2 \times S_3) = \{(1, 3, 5), (1, 3, 6), (1, 3, 7), (1, 4, 5), (1, 4, 6), (1, 4, 7), (2, 3, 5), (2, 3, 6), (2, 3, 7), (2, 4, 5), (2, 4, 6), (2, 4, 7)\}. \tag{45}$$

Note that there are 50 edges in this graph and  $d_{(1,3,7)}(K_2 \times K_2 \times S_3) = d_{(1,4,7)}(K_2 \times K_2 \times S_3) = d_{(2,3,7)}(K_2 \times K_2 \times S_3) = d_{(2,4,7)}(K_2 \times K_2 \times S_3) = 11$ , while all the other vertices of the graph have degree 7. We have

$$M_{K_2 \times K_2 \times S_3}^x \Gamma_{(1,3,5)} = \begin{cases} 1, & \text{for } \{(1, 3, 5)\}, \\ \frac{1}{8}, & \text{for } \{(1, 4, 5), (2, 3, 5), (2, 4, 5)\}, \\ \frac{1}{12}, & \text{otherwise,} \end{cases} \tag{46}$$

with  $\|M_{K_2 \times K_2 \times S_3}^x \Gamma_{(1,3,5)}\| = 2.042$ . It is easy to see that  $\|M_{K_2 \times K_2 \times S_3}^x \Gamma_{(1,3,6)}\| = \|M_{K_2 \times K_2 \times S_3}^x \Gamma_{(1,4,5)}\| = \|M_{K_2 \times K_2 \times S_3}^x \Gamma_{(1,4,6)}\| = \|M_{K_2 \times K_2 \times S_3}^x \Gamma_{(2,3,5)}\| = \|M_{K_2 \times K_2 \times S_3}^x \Gamma_{(2,3,6)}\| = \|M_{K_2 \times K_2 \times S_3}^x \Gamma_{(2,4,5)}\| = \|M_{K_2 \times K_2 \times S_3}^x \Gamma_{(2,4,6)}\| = 2.042$ .

Also,

$$M_{K_2 \times K_2 \times S_3}^x \Gamma_{(1,3,7)} = \begin{cases} 1, & \text{for } \{(1, 3, 7)\}, \\ \frac{1}{12}, & \text{for } \{(1, 4, 7), (2, 3, 7), (2, 4, 7)\}, \\ \frac{1}{8}, & \text{otherwise,} \end{cases} \tag{47}$$

with  $\|M_{K_2 \times K_2 \times S_3}^x \Gamma_{(1,3,7)}\| = 2.250$ . Similarly,  $\|M_{K_2 \times K_2 \times S_3}^x \Gamma_{(1,4,7)}\| = \|M_{K_2 \times K_2 \times S_3}^x \Gamma_{(2,3,7)}\| = \|M_{K_2 \times K_2 \times S_3}^x \Gamma_{(2,4,7)}\| = 2.250$ . This implies that  $\|M_{K_2 \times K_2 \times S_3}^x\| = 2.250$ .

*Example 6.* Consider the graph used in example 4,  $\phi(x) = 1 + \ln(x)$ ,  $f = \Gamma$ , and  $p = 1$ ; then,  $\|M_{K_2 \times K_2 \times S_3}^{1+\ln(x)}\| = 4.459$ .

Here, we have

$$M_{K_2 \times K_2 \times S_3}^{1+\ln(x)} \Gamma_{(1,3,5)} = \begin{cases} 1, & \text{for } \{(1, 3, 5)\}, \\ \frac{1}{1 + \ln(8)}, & \text{for } \{(1, 4, 5), (2, 3, 5), (2, 4, 5)\}, \\ \frac{1}{1 + \ln(12)}, & \text{otherwise,} \end{cases} \tag{48}$$

with  $\|M_{K_2 \times K_2 \times S_3}^{1+\ln(x)} \Gamma_{(1,3,5)}\| = 4.271$ . Similarly,  $\|M_{K_2 \times K_2 \times S_3}^{1+\ln(x)} \Gamma_{(1,3,6)}\| = \|M_{K_2 \times K_2 \times S_3}^{1+\ln(x)} \Gamma_{(1,4,5)}\| = \|M_{K_2 \times K_2 \times S_3}^{1+\ln(x)} \Gamma_{(1,4,6)}\| = \|M_{K_2 \times K_2 \times S_3}^{1+\ln(x)} \Gamma_{(2,3,5)}\| = \|M_{K_2 \times K_2 \times S_3}^{1+\ln(x)} \Gamma_{(2,3,6)}\| = \|M_{K_2 \times K_2 \times S_3}^{1+\ln(x)} \Gamma_{(2,4,5)}\| = \|M_{K_2 \times K_2 \times S_3}^{1+\ln(x)} \Gamma_{(2,4,6)}\| = 4.271$ .

Now,

$$M_{K_2 \times K_2 \times S_3}^{1+\ln(x)} \Gamma_{(1,3,7)} = \begin{cases} 1, & \text{for } \{(1, 3, 7)\}, \\ \frac{1}{1 + \ln(12)}, & \text{for } \{(1, 4, 7), (2, 3, 7), (2, 4, 7)\}, \\ \frac{1}{1 + \ln(8)}, & \text{otherwise.} \end{cases} \tag{49}$$

So,  $\|M_{K_2 \times K_2 \times S_3}^{1+\ln(x)} \Gamma_{(1,3,7)}\| = 4.459$ . Similarly,  $\|M_{K_2 \times K_2 \times S_3}^{1+\ln(x)} \Gamma_{(1,4,7)}\| = \|M_{K_2 \times K_2 \times S_3}^{1+\ln(x)} \Gamma_{(2,3,7)}\| = \|M_{K_2 \times K_2 \times S_3}^{1+\ln(x)} \Gamma_{(2,4,7)}\| = 4.459$ .  $\Rightarrow \|M_{K_2 \times K_2 \times S_3}^{1+\ln(x)}\| = 4.459$ .

If we take the same conditions which we used in examples 3–6 in the result of Theorem 2, then we get  $1.900 \leq \|M_{G_1 \times G_2}^x\| \leq 3.250$ ,  $1.090 \leq \|M_{G_1 \times G_2}^x\| \leq 1.563$ ,  $1.917 \leq \|M_{G_1 \times G_2 \times G_3}^x\| \leq 2.375$ , and  $4.156 \leq \|M_{G_1 \times G_2 \times G_3}^{1+\ln(x)}\| \leq 4.572$ . This implies that the examples 3–6 verify the result of Theorem 2.

### 4. Conclusion

In this paper, we have considered the action of generalized maximal operator on  $\ell^p$  spaces and calculated the quasinorm  $\|M_K^\phi\|_p$  for  $0 < p \leq 1$ . We gave the lower bound and

upper bound for the quasi-norm  $\|M_K^\phi\|_p$ , where  $1 < p < \infty$ . Finally, we have proved that  $((1/\phi^p(1)) + ((n_1 \times n_2 \times \dots \times n_m) - 1/\phi^p(n_1 \times n_2 \times \dots \times n_m)))^{(1/p)}$  and  $((1/\phi^p(1)) + ((n_1 \times n_2 \times \dots \times n_m) - 1/\phi^p(2^m)))^{(1/p)}$  are the lower bound and upper bound, respectively.

## Data Availability

No data were used to support this study.

## Conflicts of Interest

The authors declare that they have no conflicts of interest.

## Acknowledgments

The second author and third author thank University of Management and Technology, Lahore, and National Textile University, Faisalabad, for their support.

## References

- [1] B. Bollobás, *Modern Graph Theory, Graduate Texts in Mathematics*, vol. 184, Springer-Verlag, New York, NY, USA.
- [2] A. Bondy and U. S. R. Murty, *Graph Theory, Graduate Texts in Mathematics*, vol. 244, Springer-Verlag, New York, NY, USA.
- [3] R. Hammack, W. Imrich, and S. Klavžar, *Handbook of Product Graphs*, CRC Press, Boca Raton, FL, USA, 2011.
- [4] M. Cowling, S. Meda, and A. G. Setti, "Estimates for functions of the Laplace operator on homogeneous trees," *Transactions of the American Mathematical Society*, vol. 352, no. 9, pp. 4271–4293, 2000.
- [5] C. Gonzalez-Riquelme and J. Madrid, "Sharp P-bounds for maximal operators on finite graphs," 2020, <http://arxiv.org/abs/2005.03146>.
- [6] J. Soria and P. Tradacete, "Best constants for the hardy-littlewood maximal operator on finite graphs," *Journal of Mathematical Analysis and Applications*, vol. 436, no. 2, pp. 661–682, 2016.
- [7] J. Soria and P. Tradacete, "Geometric properties of infinite graphs and the hardy-littlewood maximal operator," *Journal d'Analyse Mathématique*, vol. 1–25, 2016.
- [8] C. Capone, D. Cruz-Urbe, A. Fiorenza, and A. Fiorenza, "The fractional maximal operator and fractional integrals on variable  $L^p$  spaces," *Revista Matemática Iberoamericana*, vol. 23, no. 3, pp. 743–770, 2007.
- [9] I. Ahmad and W. Nazeer, "Optimal couples of rearrangement invariant spaces for generalized maximal operators," *Journal of Function Spaces*, vol. 2014, Article ID 647123, 5 pages, 2014.
- [10] Z. Hussain and S. Talib, "A note on the paper "best constants for the hardy-littlewood maximal operator on finite graphs"" *Hacettepe Journal of Mathematics and Statistics*, vol. 49, no. 2, pp. 498–504, 2020.
- [11] D. Aalto and J. Kinnunen, "The discrete maximal operator in metric spaces," *Journal d'Analyse Mathématique*, vol. 111, no. 1, pp. 369–390, 2010.
- [12] N. Badr and J. M. Martell, "Weighted norm inequalities on graphs," *Journal of Geometric Analysis*, vol. 22, no. 4, pp. 1173–1210, 2012.
- [13] A. Koranyi and M. A. Picardello, "Boundary behaviour of eigenfunctions of the Laplace operator on trees," *Annali della Scuola Normale Superiore. Classe di Scienze*, vol. 13, no. 3, pp. 389–399, 1986.

## Research Article

# Improving Neural Machine Translation with AMR Semantic Graphs

Long H. B. Nguyen <sup>1,2</sup>, Viet H. Pham,<sup>1,2</sup> and Dien Dinh <sup>1,2</sup>

<sup>1</sup>Faculty of Information Technology, University of Science, Ho Chi Minh City, Vietnam

<sup>2</sup>Vietnam National University, Ho Chi Minh City, Vietnam

Correspondence should be addressed to Long H. B. Nguyen; [long.hb.nguyen@gmail.com](mailto:long.hb.nguyen@gmail.com)

Received 15 March 2021; Revised 18 June 2021; Accepted 23 June 2021; Published 8 July 2021

Academic Editor: Ali Ahmad

Copyright © 2021 Long H. B. Nguyen et al. This is an open access article distributed under the Creative Commons Attribution License, which permits unrestricted use, distribution, and reproduction in any medium, provided the original work is properly cited.

The Seq2Seq model and its variants (ConvSeq2Seq and Transformer) emerge as a promising novel solution to the machine translation problem. However, these models only focus on exploiting knowledge from bilingual sentences without paying much attention to utilizing external linguistic knowledge sources such as semantic representations. Not only do semantic representations can help preserve meaning but they also minimize the data sparsity problem. However, to date, semantic information remains rarely integrated into machine translation models. In this study, we examine the effect of abstract meaning representation (AMR) semantic graphs in different machine translation models. Experimental results on the IWSLT15 English-Vietnamese dataset have proven the efficiency of the proposed model, expanding the use of external language knowledge sources to significantly improve the performance of machine translation models, especially in the application of low-resource language pairs.

## 1. Introduction

Neural machine translation (NMT) [1–4] has proven its effectiveness and thus has gained researchers' attention in recent years. In practical applications, the typical inputs to NMT systems are sentences in which words are represented as individual vectors in a word embedding space. This word embedding space does not show any connection among words within a sentence such as dependency or semantic role relationships. Recent studies [5–8] found that semantic information is essential to generate concise and appropriate translations in machine translation. Although these models have made a significant progress, their design and functions are limited to statistical machine translation systems only. Consequently, the tasks of surveying, analyzing, and applying additional semantic information to NMT systems have not received comprehensive attention.

In this study, we present the method of integrating abstract meaning representation (AMR) graphs (<https://amr.isi.edu>) as additional semantic information into the current popular NMT systems such as Seq2Seq,

ConvSeq2Seq, and Transformer. AMR graphs are rooted, labeled, directed, and acyclical graphs representing the entire content of a sentence. They are also abstracted from related syntactic representations in the sense that sentences with similar meanings will have the same AMR graph, even if the words used in these sentences are different. Figure 1 illustrates an AMR graph in which the nodes (e.g., want-01, girl) symbolize concepts, while the edges (e.g., ARG0 and ARG1) represent the relationship between the concepts that they connect. Compared to semantic role graphs, AMR graphs contain more relationships (e.g., between boy and girl). Besides, AMR graphs directly hold entity relations while excluding the alternating variables (i.e., using lemma) and the function words. Therefore, AMR graphs can be combined with the input text to generate better contextual representations. Moreover, the structured information from AMR graphs can help minimize the problem of data sparsity in resource-poor settings. First, the AMR graph representations are combined with the word embedding to create a better context representation for a sentence. Then, multihead attention can focus on all positions of

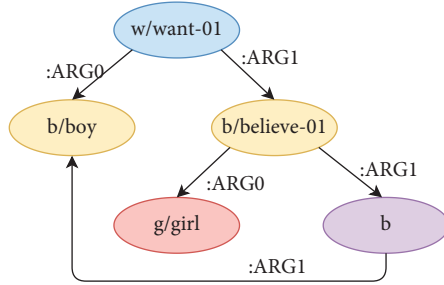


FIGURE 1: The AMR graph for the multiple sentences.

The boy desires the girl to believe him.  
 The boy wants the girl to believe him.  
 The boy has a desire to be believed by the girl.  
 The boy is desirous of the girl believing him.

contextual features with the outputs of the AMR graph representations.

Integrating AMR graphs into NMT yields several benefits. First, this addresses the problems of data sparsity and semantic ambiguity. Second, structured semantic information constructed from AMR graphs could help complement the input text by providing high-level abstract information, thereby improving the encoding of the input word embedding. Last, multihead attention can also take advantage of semantic information to improve the dependency among words within a sentence.

Recent studies have applied semantic representation to NMT models. For instance, Marcheggiani et al. [9] exploited the semantic role labeling (SRL) information for NMT, indicating that the predicate-argument structure from SRL can help increase the quality of an attention-based sequence-to-sequence model. Meanwhile, Song et al. [10] proved that semantic information structured from AMR graphs can complement input text by incorporating high-level abstract information. In this approach, the graph recurrent network (GRN) was utilized to encode AMR graphs without breaking the original graph structure, and a sequential long short-term memory (LSTM) was used to encode the source input. The decoder was a doubly attentive LSTM, taking the encoding results of both the graph encoder and the sequential encoder as attention memories. Song et al. had also argued that the results of an AMR integration is significantly greater than those of a sole SRL integration because AMR graphs include both SRL and the relationships between the nodes (i.e., words). However, Song’s approach has encountered some drawbacks such as failed to address the problem of the correlation between nodes in AMR graphs and investigated only on the machine translation system using the recurrent neural network (RNN).

The contributions of our work are as follows:

- (i) First, instead of adding a node to represent an edge in the graph and assigning properties of the edge as those of the documents, we extend the node embedding algorithm [11] to use direct edge information
- (ii) Second, instead of using the graph recurrent network in [10], we propose an architecture that binds an inductive graph encoder
- (iii) Finally, we examined and analyzed the results on the English-Vietnamese bilingual set, which is considered a low-resource language pair. Through

experiments, we demonstrate the effectiveness of integrating AMR into neural network machine translation and draw insightful conclusions for future studies.

The organization for the remaining of the article is as follows. Section 2 introduces current popular machine translation architectures such as Seq2Seq, ConvSeq2Seq, and Transformer. Next, Section 3 presents the method of representing AMR graphs in the vector form as well as proposing a method to integrate AMR graphs into different NMT models. Then, Sections 4 and 5 discuss the corpus used in the experiment and the experimental configuration for the model, respectively. Afterward, Section 6 presents the experimental results of the machine translation model with an integrated AMR and analyzes the effect of an AMR on the model along with some translation errors generated by the model. Section 7 summarizes our work.

## 2. Neural Machine Translation

In this section, we provide a brief introduction about the Seq2Seq model and its variants such as ConvSeq2Seq and Transformer.

*2.1. Seq2Seq.* We take the attention-based sequence-to-sequence model of [1] as the baseline model, but we use LSTM [12] in both encoder and decoder.

*2.1.1. Encoder.* Given a sentence,  $x = (x_1, x_2, \dots, x_n)$ .

(i) *Uni-LSTM.* As usual, the RNN reads an input sequence  $x$  in order starting from the first token  $x_1$  to  $x_n$  and computes a sequence of hidden state  $[\vec{h}_1, \vec{h}_2, \dots, \vec{h}_n]$  to generate input representation from left to right.

$$H = [\vec{h}_1, \vec{h}_2, \dots, \vec{h}_n]. \quad (1)$$

(ii) *Bi-LSTM.* Consists of forward and backward LSTM’s. The forward LSTM works similar to Uni-LSTM and the backward LSTM reads the sequence in the reverse order from the last token  $x_n$  to  $x_1$ , resulting a sequence of backward hidden states  $[h_1, h_2, \dots, h_n]$ . We obtain the word embedding  $x_i$  by concatenating the forward  $\vec{h}_i$  and backward  $h_i$  hidden state,  $h_i = [\vec{h}_i, h_i]$ .

$$H = [h_1, h_2, \dots, h_n]. \quad (2)$$

**2.1.2. Decoder.** The decoder predicts the next word  $y_t$ , given the context vector  $c$  and all previously predicted words  $(y_0, y_1, \dots, y_{t-1})$ . We used an attention-based LSTM decoder [1], with attention memory as the concatenation of the attention vectors among all source tokens.

For each decoding step  $t$ , the decoder feeds the concatenation of the embedding of current input  $e_{y_t}$  and previous context vector  $c_{t-1}$  into LSTM to update the hidden state:

$$s_t = \text{LSTM}(s_{t-1}, [e_{y_t}, c_{t-1}]). \quad (3)$$

Then, the new context vector is computed as

$$\begin{aligned} \epsilon_{t,i} &= a(s_t, h_i), \\ \alpha_{ti} &= \frac{\exp(\epsilon_{t,i})}{\sum_{k=1}^n \exp(\epsilon_{t,k})}, \\ c_i &= \sum_{i=1}^n \alpha_{t,i} h_i, \end{aligned} \quad (4)$$

where  $a$  is the alignment model which is a feed forward network, scores how well the inputs surround position  $i$ , and the input at position  $t$  match.

The output probability over target vocabulary is calculated:

$$P_{\text{vocab}} = \text{soft max}(W_o[s_t; c_i] + b_o), \quad (5)$$

where  $W_o$  and  $b_o$  are the model parameters.

## 2.2. ConvSeq2Seq

**2.2.1. ConvSeq2Seq.** This architecture is proposed by Gehring et al. [2] to completely replace the RNN with the CNN with the following components:

The ConvS2S model followed the encoder-decoder architecture. Both encoder and decoder blocks share an identical structure that computes hidden states based on a fixed number of input elements. To enlarge the context size, we stack several blocks over each other. Each block comprises a one-dimensional convolution and a nonlinearity. In each convolution kernel, parameters are  $W \in \mathcal{R}^{2 \times k \times d}$  and  $b_w \in \mathcal{R}^{2 \times d}$ . The input is represented as  $\epsilon \in \mathcal{R}^{k \times d}$ , which is a concatenation of  $k$  input elements with dimension of  $d$  and maps them to get the single output  $Y \in \mathcal{R}^{2 \times d}$  with dimension twice of that of the input. Then, the  $k$  output elements will be fed into subsequent layers. We leverage the gated linear unit (GLU) as nonlinearity which applied on the output of the convolution  $Y = [AB] \in \mathcal{R}^{2 \times d}$ :

$$v([AB]) = A \otimes \sigma(B), \quad (6)$$

where  $A, B \in \mathcal{R}^d$  are the inputs to the nonlinearity,  $\otimes$  denotes the element-wise multiplication, the output  $Y = [AB] \in \mathcal{R}^{2 \times d}$  has a half of size compared to  $Y$ , and  $\sigma B$

the gate that control which inputs  $A$  of the current contexts are relevant.

In order to enable deep convolutional blocks, we adopt the residual connections which connect the input of each convolutional layer with the output:

$$h_i^l = v(W^l [h_{i-(k/2)}^{l-1}, \dots, h_{i+(k/2)}^{l-1}] + B_w^l) + h_i^{l-1}, \quad (7)$$

where  $h^l$  is the hidden state of  $l^{\text{th}}$  layer.

**2.2.2. LightConvSeq2Seq.** As a variant of a CNN called lightweight convolution [13] which allows computation with linear complexity,  $O(n)$ , with  $n$  being the length of the input string.

The structure of LightConvSeq2Seq consists of the elements similar to Conv2Seq but using lightweight convolution operation rather than convolution operation.

**Depthwise Convolution (DConv).** Perform a convolution operation independently over every channel; thereby, the number of parameters reduce significantly from  $d^2 k$  to  $dk$ , where  $k$  is the kernel width. In general, at position  $i$  and direction  $c$ , the output  $O_{i,c}$  is calculated as follows:

$$O_{i,c} = \sum_{j=1}^k W_{c,j} \cdot X \left( \frac{k+1}{2} \right)_{x+j-\frac{k+1}{2},c}. \quad (8)$$

**2.3. Transformer.** Transformer [4] also includes an encoder and a decoder. The encoder generates a vector representation of the input sentence. Assuming an input of the form  $x = (x_1, x_2, \dots, x_n)$  and a representation of  $x$  of the form  $z = (z_1, z_2, \dots, z_n)$ , the decoder produces sequentially for a translation of  $y = (y_1, y_2, \dots, y_m)$  based on  $z$  and the previous outputs.

**2.3.1. The Encoder.** There are  $N$  stacked similar blocks. Each of these blocks consists of 2 subblocks: a self-attention mechanism and a feed forward network. A residual connection surrounds each subblock, followed by layer normalization. The general representation formula for the encoder is as follows:

$$\begin{aligned} \hat{z} &= \text{LayerNorm}(x + \text{self-attention}(x)), \\ z &= \text{LayerNorm}(\hat{z} + \text{feed forward}(\hat{z})). \end{aligned} \quad (9)$$

**2.3.2. The Decoder.** There are also  $N$  blocks. However, each block consists of 3 subblocks: a self-attention block, a feed forward block, and an encoder-decoder attention block inserted between them. The residual connection and layer normalization are used similarly to the encoder. The encoder generates outputs step by step. The self-attention block only pays attention to the positions generated in the previous steps by using a mask. The mask prevents the decoder from paying attention to locations that have not been generated,

so outputs can only be predicted based on the result  $z$  of the encoder and previous outputs.

2.3.3. *Self-Attention.* There are 3 components as follows: query ( $Q$ ), key ( $K$ ), and value ( $V$ ), defined as follows:

$$\text{Attention}(Q, K, V) = \text{softmax}\left(\frac{QK^T}{\sqrt{d_k}}V\right), \quad (10)$$

where  $Q, K$ , and  $V$  are the parameters with the number of dimensions  $d_k, d_k$ , and  $d_v$  respectively.

### 3. The Proposed Method

In this section, we present the graph embedding algorithm and propose our method to integrate the AMR graph embedding representation to various well-known NMT systems such as Seq2Seq, ConvSeq2Seq, and Transformer.

3.1. *Graph-Level Information Representation.* Figure 2 depicts the graph encoder architecture based on the model of Xu et al. [11], with some enhancements to integrate more information about the edge of the graph.

The directional graph  $\mathcal{G} = (\mathcal{V}, \mathcal{E})$  with the label on the edge  $e_{u,v} \in \mathcal{E}$  presents the relationship between the nodes  $u$  and  $v$  to which it connects. The process of learning to represent the node  $v \in \mathcal{V}$  is as follows:

- (1) We first transform the text attribute of node  $v$  into a feature vector  $\mathbf{a}_v$  by looking up the embedding matrix  $W_E$
- (2) Next, we categorize the neighbors of  $v$  into two subsets: forward neighbors,  $\mathcal{N}_{\rightarrow}(v)$  and backward neighbors,  $\mathcal{N}_{\leftarrow}(v)$ . Particularly,  $\mathcal{N}_{\rightarrow}(v)$  returns the nodes that  $v$  directs to and vice versa. The information about the edge  $e_{u,v}$  associated between the node  $v$  and the adjacent node  $u$  is combined as follows:

$$\begin{aligned} u_{\leftarrow} &= u_{\leftarrow} + e_{u,v}, \forall u \in \mathcal{N}_{\leftarrow}(v), \\ u_{\rightarrow} &= u_{\rightarrow} + e_{u,v}, \quad \forall u \in \mathcal{N}_{\rightarrow}(v). \end{aligned} \quad (11)$$

- (3) We aggregate the forward information of  $v$ 's forward neighbors  $\{\mathbf{h}_{u_{\rightarrow}}^{k-1}, \forall u \in \mathcal{N}_{\rightarrow}(v)\}$  into a single vector,  $\mathbf{h}_{\mathcal{N}_{\rightarrow}(v)}^k$ , where  $k \in \{1, \dots, K\}$  is the iteration index. We do this by using one of three  $\text{AGG}_{\rightarrow}$  mentioned.
- (4) Then, we concatenate  $v$ 's current forward representation,  $\mathbf{h}_{v_{\rightarrow}}^{k-1}$ , with the new neighborhood vector,  $\mathbf{h}_{\mathcal{N}_{\rightarrow}(v)}^k$ . The result is passed to a feed forward layer, followed by a nonlinearity activation function  $\sigma$ , which updates the forward representation of  $v$ , to be used in the next iteration.
- (5) Update the backward representation of  $v$ ,  $\mathbf{h}_{v_{\leftarrow}}^k$ , using similar procedure in steps (3) and (4), but this time, we utilize backward representations rather than the forward representations and use  $\text{AGG}_{\leftarrow}$  to aggregate neighbor information.

- (6) Repeat steps (3) ~ (5)  $K$  times, and the concatenation of the final forward and backward representation is used as the final bidirectional representation of  $v$ .

$$z_v = \text{CONCAT}(\mathbf{h}_{v_{\rightarrow}}^K, \mathbf{h}_{v_{\leftarrow}}^K), \quad \forall v \in \mathcal{V}. \quad (12)$$

As mentioned in steps (3) and (5), the representation association operation of node  $v$  is performed with one of the following aggregation functions:

- (i) Mean aggregator: performs the average calculation on each element of  $\{\mathbf{h}_{u_{\rightarrow}}^{k-1}, \forall u \in \mathcal{N}_{\rightarrow}(v)\}$  và  $\{\mathbf{h}_{u_{\leftarrow}}^{k-1}, \forall u \in \mathcal{N}_{\leftarrow}(v)\}$
- (ii) GCN aggregator: it is quite similar to mean aggregator, except that the result is fed into a fully connected layer and a nonlinear activation function [14].

$$\begin{aligned} \text{AGG}_k^{\rightarrow} &= \sigma(\mathbf{W}\text{MEAN}(\mathbf{h}_{u_{\rightarrow}}^k) + \mathbf{b}), u \in \mathcal{N}_{\rightarrow}(v), \\ \text{AGG}_k^{\leftarrow} &= \sigma(\mathbf{W}\text{MEAN}(\mathbf{h}_{u_{\leftarrow}}^k) + \mathbf{b}), u \in \mathcal{N}_{\leftarrow}(v), \end{aligned} \quad (13)$$

with MEAN as the function returning the average value, and  $\sigma$  as the nonlinear activation function.

- (iii) Pooling aggregator: each node embedding vector is passed through a feed forward layer followed by the pooling operation (which can be max, min, and average):

$$\begin{aligned} \text{AGG}_k^{\rightarrow} &= \max(\{\sigma(\mathbf{W}_p \mathbf{h}_{u_{\rightarrow}}^k + \mathbf{b}), u \in \mathcal{N}_{\rightarrow}(v)\}), \\ \text{AGG}_k^{\leftarrow} &= \max(\{\sigma(\mathbf{W}_p \mathbf{h}_{u_{\leftarrow}}^k + \mathbf{b}), u \in \mathcal{N}_{\leftarrow}(v)\}), \end{aligned} \quad (14)$$

with max as the maximum operation, and  $\sigma$  as the nonlinear activation function.

3.1.1. *Graph Embedding.* Graph embedding  $Z$  contains all the information on the graph and is calculated by one of the following two methods:

- (i) Pooling based: the node embeddings  $z_v, v \in \mathcal{V}$  are passed through a linear transform network and performs pooling.

$$Z = \text{pooling}(\{z_v, \forall v \in \mathcal{V}\}). \quad (15)$$

- (ii) Adding a super node: node  $v_s$  is pointed by all nodes in the graph. Using the algorithm in Section 3.1, the representation of  $v_s$  is  $z_{v_s}$ . The representation of  $v_s$  contains all information of the nodes that should be considered as representations of the graph or graph embedding.

3.2. *Dual Attention Mechanism.* The architecture of an integrated AMR machine translation model is illustrated in



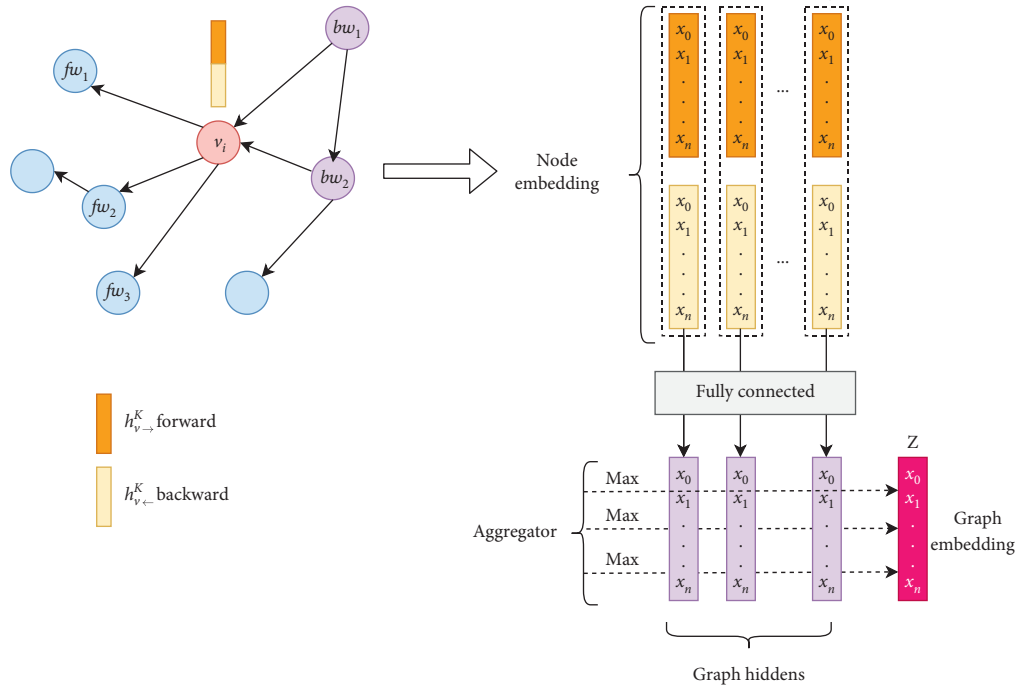


FIGURE 2: The graph encoder architecture.

Figure 3 with an English sentence input and a corresponding AMR graph. The proposed architecture consists of an encoder for the input sentence and a decoder with the input value resulting from the encoder. The main difference from the traditional decoder-encoder model is that there is an additional graph encoder to process information on graphs and to represent this information in a vector format. This vector is then combined with the hidden states of the encoder and fed into the decoder to find the corresponding representation in Vietnamese.

We propose a specific integration method for the Seq2Seq model with sequential processing in Section 3.2.1 and focus on models with parallel processing such as ConvSeq2Seq, LightConvSeq2Seq, and Transformer in Section 3.2.2.

**3.2.1. Seq2Seq Model with the Sequential Processing Mechanism.** The model (Figure 4(a)) consists of two attention mechanisms operating independently: the original attention (left) learns the alignment between the result  $y_{i-1}$  and the hidden states  $h_j$ ,  $j \in [1, n]$  of the encoder and the graph attention learns to align between the output and the nodes in the AMR graph, yielding a context vector  $\hat{c}_{i-1}$ . In particular, the computation of  $\hat{c}_{i-1}$  is as follows:

$$\begin{aligned} \hat{e}_{ij} &= a(s_{i-1}, z_j), \\ \hat{\alpha}_{ij} &= \frac{\exp(\hat{e}_{ij})}{\sum_{k=1}^{\mathcal{V}} \exp(\hat{e}_{ik})} \\ \hat{c}_i &= \sum_{j=1}^{\mathcal{V}} \hat{\alpha}_{ij} z_j, \end{aligned} \quad (16)$$

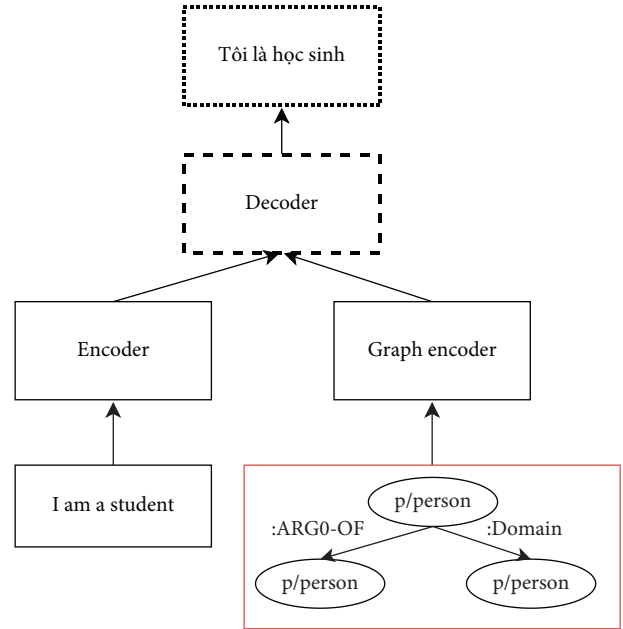


FIGURE 3: Recommended architecture for AMR integration.

where  $a$  is a feed forward network, evaluating the matching between the nodes surrounding the position  $j$  and the input  $i$ .

These two context vectors are then combined with the decoder's state  $s_i$  and the embedding vector of  $y_{i-1}$  to calculate a probability distribution that determines  $y_i$ .

$$P_{\text{vocab}} = \text{Softmax}(W_o[s_i, y_{i-1}, c_i, \hat{c}_i] + b_o). \quad (17)$$

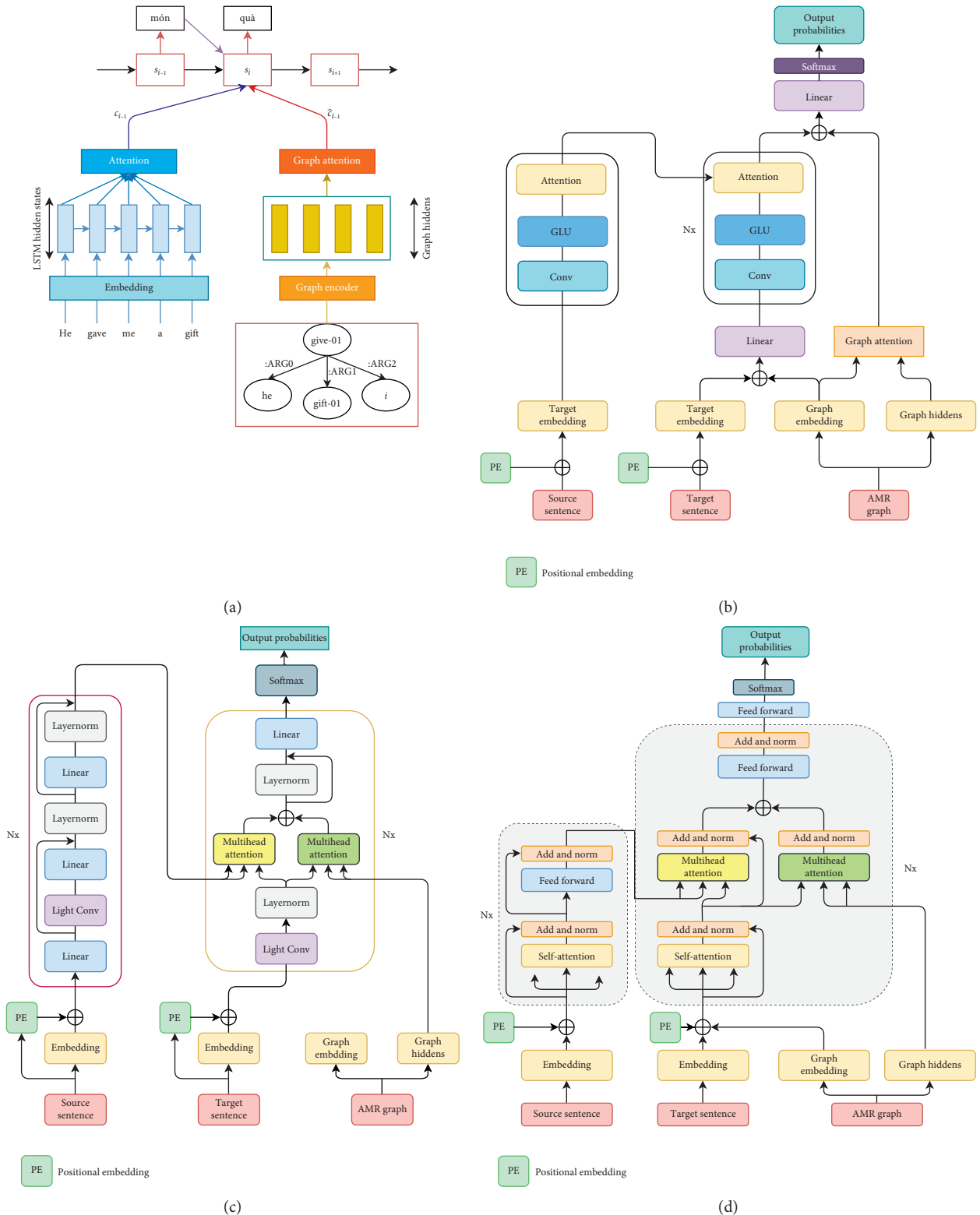


FIGURE 4: Integrating AMR to models with a parallel processing mechanism. (a) Seq2Seq (LSTM) model with the AMR. (b) ConvSeq2Seq-AMR model. (c) LightConvSeq2Seq-AMR model. (d) Transformer-AMR model.

**3.2.2. Models with a Parallel Processing Mechanism.** On the contrary, with parallel processing, the model has no information about the state  $s_{i-1}$  of the decoder. In other words, except  $z_v$ , no information about the graph is included in the

calculation of attention. Besides, using only the states  $z_v$ ,  $v \in \mathcal{V}$  along with the parallel computation leaves the model with no information about the association between the output and the AMR graph in step  $i - 1$ . Consequently,

the model cannot effectively learn the connection between the input sentence, the output sentence, and AMR graph, with a small increase of about 0.2 (experiments with LightConvSeq2Seq and Transformer). Therefore, the use of the graph embedding of  $Z$  should help the model obtain more information about the graph before the attention calculation. This has been proven with experimental results, which show an increase of the BLEU score by 0.6.

Figures 4(b)–4(d) describe the proposed model that integrates AMR with a dual attention mechanism. Regarding the LightConvSeq2Seq-AMR and Transformer-AMR models, the self-attention mechanism for the graph is similar to the description of the self-attention mechanism in Section 2.3 with the input being representations of nodes  $z_v$ ,  $\forall v \in \mathcal{V}$  instead of the state  $h_i$ ,  $\forall i \in n$ . Regarding the ConvSeq2Seq-AMR model, experimental results show that utilizing Luong’s attention mechanism to learn the alignment between the graph and the output produced better results than the multistep attention.

#### 4. The Corpus

The corpus used to evaluate the model is IWSLT15 [15], which includes approximately 130,000 English-Vietnamese bilingual sentences taken from TED Talks presentations for the training set. For fine-tuning, we use the set called tst2012, which includes 1553 parallel pairs language. Besides, the test sets consist of tst2013 and tst2015, which include 1268 and 1080 English-Vietnamese bilingual pairs, respectively. The statistical information is given in Table 1.

For the preprocessing phase, byte-pair encoding (BPE) (<https://github.com/rsennrich/subword-nmt>) [16] with 8000 operations is utilized to deal with rare words and compound words for both English and Vietnamese, thereby significantly reducing the vocabulary size in English from 54111 to 5208 and in Vietnamese from 25335 to 3336.

For AMR parsing, we use NeuralAmr toolkit (<https://github.com/sinantie/NeuralAmr>) [17] which implements the sequence-to-sequence models to the tasks of AMR parsing and AMR generation. Their model achieves competitive results of 62.1 SMATCH [18], the current best score (at the time doing this work, Jan 2020) reported without the significant use of external semantic resources. This tool produces AMR graphs represented in the PENMAN notation (<https://www.isi.edu/natural-language/penman/penman.html>) and in a linear form, as demonstrated in the AMR preprocessing example.

#### 5. Experimental Configuration

The models are implemented in Python 3 and use the library Fairseq (<https://fairseq.readthedocs.io/en/latest/#>) [19].

The configuration of the base models is as follows:

- (i) Seq2Seq: we investigate the MT model with two types of LSTM which are uni-LSTM (one-directional) and bi-LSTM (two-directional). There are 512-word embedding dimensions, which utilize 512 LSTM hidden units in both the encoder and the decoder.

- (ii) ConvSeq2Seq: it comprises 4 convolutional blocks and 512 hidden units for both the encoder and the decoder. The kernel size is 3.
- (iii) LightConvSeq2Seq: it consists of 4 convolutional blocks with the kernel size of 3, 7, 15, and 31 for each block and applies to both the encoder and the decoder. Self-attention is adopted with  $H = 8$  heads.
- (iv) Transformer: it has  $N = 6$  blocks for both the encoder and the decoder. The word embedding dim is set to 512 and 2048 for the feed forward network. Self-attention used with the number of heads was 8.

The proposed models have the same configuration as the base model. Besides, the graph encoder used 128-dimensional embedding for the representation of both edge and node. We stacked 2 layers of the graph encoder and aggregating information from neighboring nodes with the mean aggregator for LSTM and max pooling with the rest of the models.

During training, Adam optimizer [20] is used with a fixed learning rate of 0.001 for LSTM and ConvSeq2Seq, 0.0002 for LightConvSeq2Seq, and 0.0005 for Transformer.

Besides the basic models presented above, the results of the proposed model are also compared with the method of Song et al. [10]. To make a fair comparison, we have retrained Song’s model with the same preprocessed dataset and tuned hyperparameters.

After the models are trained, the BLEU score [21] was used to evaluate the translation quality. We also apply the bootstrap resampling method [22] to measure the statistical significance ( $p < 0.05$ ) of BLEU score differences between translation outputs of proposed models compared to the baseline.

#### 6. Results and Discussion

In this section, we present our experimental results and our analyzes on the results.

**6.1. Results.** Once the models have been trained, a beam search with the size of 5 is utilized to find a translation that maximizes the conditional probabilities.

With both the test sets tst2013 and tst2015, the proposed models are proven to be superior to the corresponding base model. In particular, as given in Table 2, with uni-LSTM-AMR-F and bi-LSTM-AMR, the BLEU scores are 27.21 and 29.29, respectively, which are 1.09 and 3.17 higher than Song’s method [10]. Similarly, with the set tst2015, bi-LSTM-AMR improved BLEU by 2.83, compared to Song’s method. This shows that despite using the double attention mechanism, bi-LSTM-AMR and uni-LSTM-AMR can integrate the information from AMR more effectively, thereby producing better translation results.

Meanwhile, when LightConvSeq2Seq is run on tst2013 and tst 2015, the BLEU scores are only 27.47 and 25.09, respectively. However, when integrating the AMR into the system, the BLEU score increased significantly by 1.0 and 0.58 on tst2013 and tst2015, respectively. Besides, LightConvSeq2Seq-AMR-F and LightConvSeq2Seq-AMR-B,

TABLE 1: Statistics on the corpus.

Corpus	#Sentences	#Tokens (English)	#Tokens (Vietnamese)
Training	133K	2.44 M	2.87 M
Fine tuning (tst2012)	1553	28 K	34 K
Test 1 (tst2013)	1268	26.7 K	33.6 K
Test 2 (tst2015)	1080	21 K	26.2 K

TABLE 2: Experimental results on Seq2Seq using one- and two-directional LSTMs.

Model	BLEU	
	tst2013	tst2015
Song’s method	26.12	23.58
Uni-LSTM-AMR	26.97	24.80
Uni-LSTM-AMR-F	<b>27.21</b>	<b>24.86</b>
Uni-LSTM-AMR-B	26.61	24.66
Bi-LSTM-AMR	<b>29.29</b>	<b>26.41</b>
Bi-LSTM-AMR-F	28.67	26.20
Bi-LSTM-AMR-B	28.36	26.04

The bold values are the highest results for each group of models.

which were integrated graph information from one direction, also outperform LightConvSeq2Seq, as given in Table 3.

As given in Table 4, ConvSeq2Seq also shows an improvement in machine translation quality with an increase in the BLEU score to about 0.3 for ConvSeq2Seq-AMR with tst2013. However, there is a BLEU decrease of 0.08 with tst2015. However, the ConvSeq2Seq-AMR-F model achieves the best results when integrating information from the forward neighbors. An increase of 0.1 in BLEU is observed with tst2013 and 0.5 with tst2015. Similar to Transformer, integrating information from the forward and backward neighbors in Transformer-AMR is not effective, with only an increase of 0.09 over the base model with tst2013. Only combining information from the forward neighbors in Transformer-AMR-F achieves a noticeable BLEU score of 28.88 and 26.28 with tst2013 and tst2015, respectively, which signal an increase of 0.28 and 0.52 compared to Transformer.

*6.2. The Effect of AMR on the NMT Model.* According to the results presented in Section 6.1, the bi-LSTM-AMR and LightConvSeq2Seq-AMR models improve BLEU more than the other two models, ConvSeq2Seq and Transformer. Therefore, to analyze the impact of AMR on the machine translation system, bi-LSTM-AMR and LightConvSeq2Seq-AMR models are selected for further training to examine graph elements such as information integration directions, graph encoding layers, and aggregators.

### 6.2.1. Bi-LSTM-AMR

(i). *Direction and Depth.* Figure 5 depicts the change in performance when adjusting the number of graph encoding layers. The mean aggregator is used to combine information from neighbors. In general, bi-LSTM-AMR and uni-LSTM-AMR-B show the highest translation quality throughout the 30 examined layers. However, an increase in the number of

TABLE 3: Experimental results on LightConvSeq2Seq.

Model	BLEU	
	tst2013	tst2015
LightConvSeq2Seq	27.47	25.09
LightConvSeq2Seq-AMR-F	27.71	25.05
LightConvSeq2Seq-AMR-B	27.84	25.27
LightConvSeq2Seq-AMR	<b>28.46</b>	<b>25.67</b>

The bold values are the highest results when evaluating each model for the “tst2013” and “tst2015” testsets.

TABLE 4: Experimental results on ConvSeq2Seq and Transformer.

Model	BLEU	
	tst2013	tst2015
ConvSeq2Seq	26.98	24.78
ConvSeq2Seq-AMR	27.30	24.70
ConvSeq2Seq-AMR-F	<b>27.40</b>	<b>25.20</b>
ConvSeq2Seq-AMR-B	26.73	24.53
Transformer	28.60	25.76
Transformer-AMR	28.69	25.91
Transformer-AMR-F	<b>28.88</b>	<b>26.28</b>
Transformer-AMR-B	28.69	26.01

The bold values are the highest results for each group of models.

layers does not always help the model achieve a higher BLEU. A decrease in BLEU scores is also observed. The more stacked layers there are, the greater the amount of information the model could learn, which ultimately leads to the overfitting problem due to saturated information. All models obtain the best results with only 2 or 3 graph coding layers. As the number of layers increases, the BLEU scores decrease. Nevertheless, the results seem more consistent and less fluctuating with bi-LSTM than with uni-LSTM.

There are three aggregators used for aggregating information from neighboring nodes: mean aggregator (MA), max-pooling (MP) aggregator, and GCN aggregator (GCN-A). The strategy of using information from one direction (forward or backward) is also considered to make more accurate statements about the effect of the aggregator on the effectiveness of the model. The results in Table 5 show that Bi-LSTM-AMR-MA achieved the highest result on the two test sets with the BLEU scores of 29.29 and 26.41, respectively. Meanwhile, uni-LSTM-AMR-MA, which uses information from both sides, achieved lower BLEU scores than the variants uni-LSTM-AMR-F and uni-LSTM-AMR-B, which only combines information from the forward and the backward neighbors, respectively. Moreover, bi-LSTM-AMR-MA outperforms bi-LSTM-AMR-F and bi-LSTM-AMR-B due to its ability to capture information from two directions during the node embedding learning and combine with information

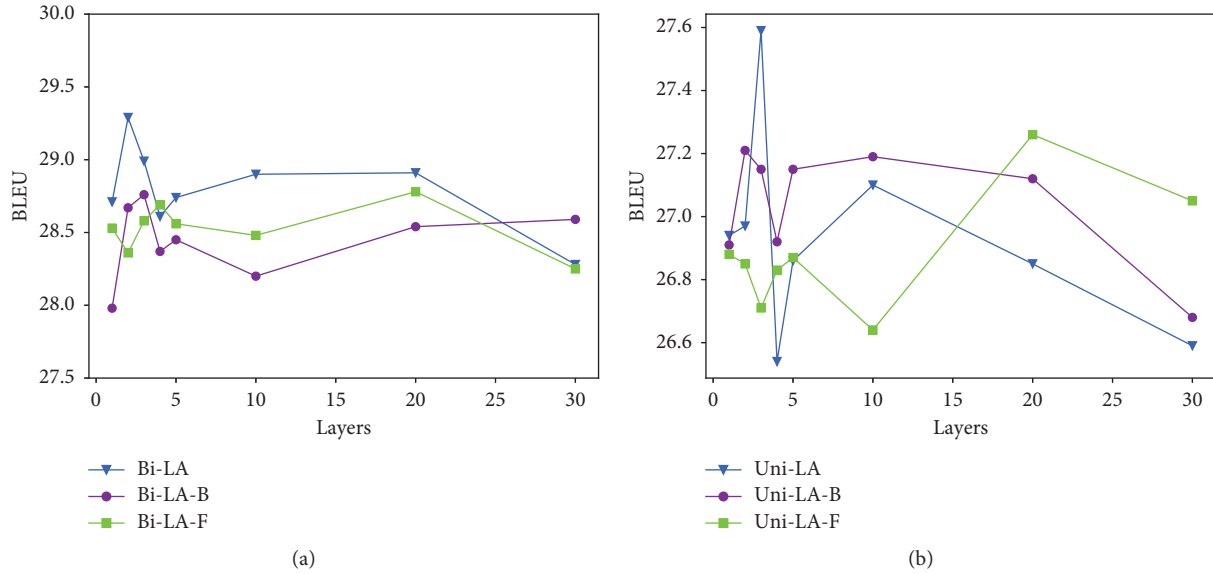


FIGURE 5: Experimental results on tst2013 with a change in the number of graph encoding layers.

TABLE 5: The effect of aggregators on the machine translation quality.

Model	tst2013			tst2015		
	MA	MP	GCN-A	MA	MP	GCN-A
Uni-LSTM-AMR	26.97	26.54	26.55	24.81	24.22	24.47
Uni-LSTM-AMR-F	26.85	27.21	26.76	24.59	<b>24.86</b>	24.48
Uni-LSTM-AMR-B	26.61	<b>27.22</b>	26.42	24.66	24.85	24.47
Bi-LSTM-AMR	<b>29.29</b>	28.94	28.38	<b>26.41</b>	26.24	25.59
Bi-LSTM-AMR-F	28.67	28.99	28.43	26.20	25.81	25.70
Bi-LSTM-AMR-B	28.36	28.40	28.41	26.04	25.90	25.81

TABLE 6: Experimental results of aggregators on LightConvSeq2Seq-AMR.

Model	tst2013			tst2015		
	MA	MP	GCN-A	MA	MP	GCN-A
LightConvSeq2Seq-AMR	28.20	<b>28.46</b>	27.76	<b>25.49</b>	25.05	25.33
LightConvSeq2Seq-AMR-F	<b>27.82</b>	27.71	27.59	<b>25.96</b>	25.27	25.39
LightConvSeq2Seq-AMR-B	<b>28.25</b>	27.84	28.27	25.66	<b>25.67</b>	25.52

The bold values are the highest results when evaluating each model on aggregators (i.e., MA, MP, and GCN-A) for testset (i.e., tst2013 or tst2015).

from the bi-LSTM encoder. Therefore, the LSTM decoder can leverage information from the graph more efficiently to improve the machine translation quality. This shows that bidirectional aggregation is more useful when combined with a bidirectional LSTM encoder. Accordingly, uni-LSTM-AMR-F-MP and uni-LSTM-AMR-B-MP, which only combine information from one direction, achieve good results when used with a unidirectional LSTM encoder.

6.2.2. *LightConvSeq2Seq-AMR*. Similar to bi-LSTM-AMR, the *LightConvSeq2Seq-AMR* model is also affected by different aggregators. In particular, as given in Table 6, the mean aggregator (MA) yields better results on average values than the rest. The results with tst2015 show that all the three modes with MA both achieve much higher results than the rest of models.

On the contrary, the GCN-A results are the lowest, similar to Seq2Seq. This proves that the information combination of GCN-A is not as efficient as those of MA and MP.

Figure 6 shows the change of BLEU when stacking convolutional blocks in the encoder and the decoder and the effect of heads  $H$  in self-attention. On both sides, the BLEU scores increase when the number of heads increases. In particular, the figure on the left shows the *LightConvSeq2Seq-AMR* model with the configuration (4, 4), which stacked 4 convolutional blocks at the encoder and 4 convolutional blocks at the decoder, and (6, 6) yields the best results. The BLEU scores are approximately 28 and 27.6 with just 1 head and then increases to 28.46 and 28.2 when  $H = 8$ . However, with an additional graph encoding layer, the (4, 4) configuration is inferior to the (6, 6) configuration. This configuration yields the highest

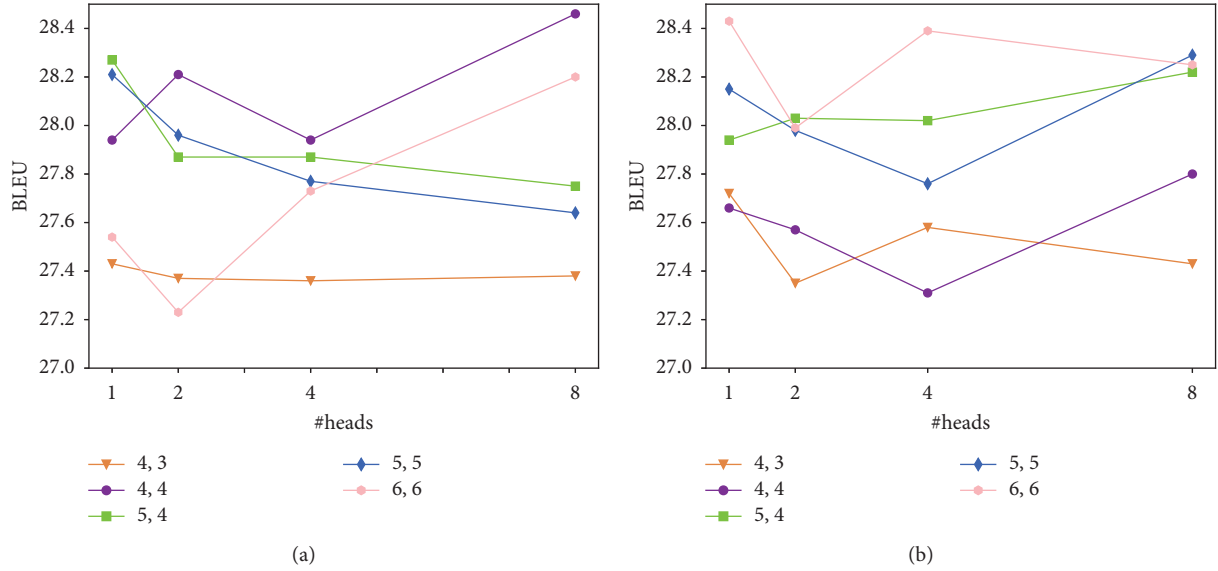


FIGURE 6: Experimental results on the effect of heads  $H$  of the graph attention and the depth of the LightConvSeq2Seq-AMR model. (a) LightConvSeq2Seq-AMR with two graph coding layers. (b) The model with three layers.

TABLE 7: Example 1.

SRC	Here is me on the soccer team and in V Magazine.
REF	Đây là tôi với đội bóng đá trong tạp chí V.
Bi-LSTM-AMR	Đây là tôi trên đội bóng đá và V là Magazine.
ConvSeq2Seq-AMR	Đây là tôi trên đội bóng đá, và trong V.
LightConvSeq2Seq-AMR	Đây là tôi đang ở trong đội bóng đá và V Magazine.
Transformer-AMR	Đây là tôi trong đội bóng đá và ở Magazine.

TABLE 8: Example 2.

SRC	The internal combustion engine is not sustainable.
REF	Động cơ đốt trong không bền vững.
Bi-LSTM-AMR	Động cơ nội tạng không bền vững.
ConvSeq2Seq-AMR	Loại động cơ bên trong không bền vững.
LightConvSeq2Seq-AMR	Động cơ đốt nội không bền vững.
Transformer-AMR	Động cơ đốt trong không bền vững.

TABLE 9: Example 3.

SRC	But it is not only about me.
REF	Nhưng những thông tin đó không chỉ nói về tôi.
Bi-LSTM-AMR	Nhưng nó không chỉ là về tôi.
ConvSeq2Seq-AMR	Nhưng đó không chỉ là tôi.
LightConvSeq2Seq-AMR	Nhưng nó không chỉ là tôi.
Transformer-AMR	Nhưng nó không chỉ là tôi.

results at  $H = 1$  with BLEU approximately 28.4 and observes a slight decrease as  $H$  approaches 8. Meanwhile, (5, 4) and (5, 5) configurations tend to decline sharply as  $H$  increases from 1 to 2 ( $\approx -0.3$ ) and continues to

decline slightly until  $H = 8$ . Meanwhile, the two reconstructions tend to be the opposite when adding a graph encoding layer, as shown on the right figure in Figure 6. The remaining (4, 3) configuration yields the lowest

TABLE 10: More example translation outputs.

AMR	' :arg we:arg (work:arg we:arg office:degree total)
SRC	We do not work from offices.
REF	Chúng tôi không làm việc từ những văn phòng.
Song's method	Chúng tôi không làm việc trong văn phòng.
Bi-LSTM	Chúng tôi không làm việc.
Bi-LSTM-AMR	Chúng tôi không làm việc từ các văn phòng.
AMR	eat:arg they:arg tomatoes:condition (grow:arg they)
SRC	If they grow tomatoes, they eat tomatoes.
REF	Nếu chúng trồng cà chua, chúng sẽ ăn cà chua.
Song's method	Nếu họ phát triển, họ sẽ ăn.
Bi-LSTM	Nếu họ trồng cà chua, họ ăn cà chua.
Bi-LSTM-AMR	Nếu chúng trồng cà chua, chúng ăn cà chua.
AMR	assure:arg i:arg i:arg (thing:arg-of (think:arg you:arg i:duration forever) ): degree total:mod just
SRC	I just totally transformed what you thought of me in six seconds.
REF	Tôi vừa mới thay đổi hoàn toàn những gì bạn nghĩ về tôi trong vòng 6 giây.
Song's method	Tôi không chỉ là những gì bạn nghĩ về tôi trong vòng 6 giây.
Bi-LSTM	Tôi hoàn toàn thay đổi những gì bạn nghĩ trong vòng sáu giây.
Bi-LSTM-AMR	Tôi hoàn toàn thay đổi những gì bạn nghĩ về tôi trong 6 giây.

results for the 2 graph encoding layer options. The results also fluctuate more with 3 layers, as opposed to being nearly constant at 2 layers.

## 7. Conclusions

We proposed a method to integrate the AMR graphs into popular machine translation architectures such as Seq2-Seq, ConvSeq2Seq, and Transformer. Structured semantic information from AMR graphs can supplement the context information in the translation model for a better representation of abstract information. Experimental results show that AMR graphs yield better results than other representations such as dependency trees or semantic roles.

For future studies, we plan to examine other methods to integrate more complex semantic graphs, such as Prague Semantic Dependencies, Elementary Dependency Structures, and Universal Conceptual Cognitive Annotation, and investigate different encoding methods suitable for a range of semantic graphs.

## Appendix

### A. Error Analysis

This section presents some translation errors of the proposed model.

In the first example in Table 7, with bi-LSTM-AMR, the model incorrectly predicts the phrase “and in V Magazine” to be “và V là Magazine.” Although the translation is incorrect, the model still recognizes “V Magazine” as a proper noun and that V is a magazine (“V là Magazine”). Meanwhile, both ConvSeq2Seq-AMR and Transformer-AMR cannot recognize this pattern and

omit the word “Magazine” when translating. Light-ConvSeq2Seq-AMR is the only model that provides a relatively complete translation.

Example 2 in Table 8 illustrates the case in which the model still understands the meaning but selects the wrong representation. The English word “internal” is meant to complement the phrase “combustion engine,” which already entailed the meaning of “động cơ đốt trong.” In this case, ConvSeq2Seq-AMR and bi-LSTM-AMR has taken “internal” to mean “inside” as an adjective that modifies the location information of the engine and ignores the word “combustion” when translated into Vietnamese. Meanwhile, Light-ConvSeq2Seq-AMR and Transformer-AMR prove a better performance in capturing information, as they produce accurate translations.

Table 9 describes the case in which the model retains the meaning correctly, but the reference data are incorrect. The word “it” is translated to “những thông tin đó” in the data. This is an inaccurate translation because the word “it” refers to a singular entity, while the translation is in the plural form. Besides, there is only one sentence and no information about the surrounding context, so the results obtained from the proposed models are similar to one another. The Vietnamese word “nó” can be used to refer to previously mentioned things or events. It is thus highly ambiguous, causing difficulty in interpreting even for humans.

### B. More Illustrative Results

Table 10 illustrates some sample translations of the models: Song's method, bi-LSTM (base model), and bi-LSTM-AMR (proposed model).

## Data Availability

The datasets used to support the findings of this study are from <https://wit3.fbk.eu/>.

## Conflicts of Interest

The authors declare that they have no conflicts of interest.

## Authors' Contributions

Long H. B. Nguyen and Viet H. Pham contributed equally to this work.

## Acknowledgments

This research is funded by University of Science, VNU-HCM under grant number CNTT 2020-06.



## References

- [1] D. Bahdanau, K. Cho, and Y. Bengio, "Neural machine translation by jointly learning to align and translate," in *Conference Track Proceedings 3rd International Conference on Learning Representations, ICLR 2015*, San Diego, CA, USA, May 2015.
- [2] J. Gehring, M. Auli, D. Grangier, D. Yarats, and Y. N. Dauphin, "Convolutional sequence to sequence learning," in *ICML'17*, Sydney, Australia, August 2017.
- [3] I. Sutskever, O. Vinyals, and V. L. Quoc, "Sequence to sequence learning with neural networks," in *NIPS'14*, pp. 3104–3112, MIT Press, Cambridge, MA, USA, March 2014.
- [4] A. Vaswani, N. Shazeer, N. Parmar et al., "Attention is all you need," in *Proceedings of the 31st International Conference on Neural Information Processing Systems (NIPS'17)*, pp. 6000–6010, Curran Associates Inc., Long Beach, California, USA, May 2017.
- [5] M. Bazrafshan and D. Gildea, "Semantic roles for string to tree machine translation," in *Proceedings of the 51st Annual Meeting of the Association for Computational Linguistics (Volume 2: Short Papers)*, pp. 419–423, Association for Computational Linguistics, Sofia, Bulgaria, July 2013, <https://www.aclweb.org/anthology/P13-2074>.
- [6] L. Ding and D. Gildea, "Semantic role features for machine translation," in *Proceedings of the 23rd International Conference on Computational Linguistics (Coling 2010)*, pp. 716–724, Coling 2010 Organizing Committee, Beijing, China, August 2010, <https://www.aclweb.org/anthology/C10-1081>.
- [7] D. Wu and P. Fung, "Semantic roles for SMT: a hybrid two-pass model," in *Proceedings of Human Language Technologies: The 2009 Annual Conference of the North American Chapter of the Association for Computational Linguistics, Companion Volume: Short Papers*, Association for Computational Linguistics, Boulder, Colorado, June 2009, <https://www.aclweb.org/anthology/N09-2004>.
- [8] D. Xiong, M. Zhang, and H. Li, "Modeling the translation of predicate-argument structure for SMT," in *Proceedings of the 50th Annual Meeting of the Association for Computational Linguistics (Volume 1: Long Papers)*, Association for Computational Linguistics, pp. 902–911, July 2012, <https://www.aclweb.org/anthology/P12-1095>.
- [9] D. Marcheggiani, J. Bastings, and I. Titov, "Exploiting semantics in neural machine translation with graph convolutional networks," in *Proceedings of the 2018 Conference of the North American Chapter of the Association for Computational Linguistics: Human Language Technologies, Volume 2 (Short Papers)*, pp. 486–492, Association for Computational Linguistics, New Orleans, Louisiana, 2018.
- [10] L. Song, D. Gildea, Y. Zhang, Z. Wang, and J. Su, "Semantic neural machine translation using AMR," *Transactions of the Association for Computational Linguistics*, vol. 7, pp. 19–31, 2019.
- [11] K. Xu, L. Wu, Z. Wang, Y. Feng, and V. Sheinin, "Graph2Seq: graph to sequence learning with attention-based neural networks," 2018, <https://arxiv.org/abs/1804.00823>.
- [12] S. Hochreiter and J. Schmidhuber, "Long short-term memory," *Neural Computation*, vol. 9, no. 8, pp. 1735–1780, 1997.
- [13] F. Wu, A. Fan, A. Baevski, Y. N. Dauphin, and M. Auli, "Pay less attention with Lightweight and dynamic convolutions," 2019, <https://arxiv.org/abs/1901.10430>.
- [14] W. L. Hamilton, R. Ying, and J. Leskovec, "Inductive representation learning on large graphs," in *NIPS'17*, Curran Associates Inc., Long Beach, CA, USA, May 2017.
- [15] M. Cettolo, J. Niehues, S. Stüker, L. Bentivogli, R. Cattoni, and M. Federico, "The IWSLT 2015 evaluation campaign," 2015.
- [16] R. Sennrich, B. Haddow, and A. Birch, "Neural machine translation of rare words with subword units," in *Proceedings of the 54th Annual Meeting of the Association for Computational Linguistics (Volume 1: Long Papers)*, pp. 1715–1725, Association for Computational Linguistics, Berlin, Germany, June 2016.
- [17] I. Konstas, S. Iyer, M. Yatskar, Y. Choi, and L. Zettlemoyer, "Neural AMR: sequence-to-sequence models for parsing and generation," in *Proceedings of the 55th Annual Meeting of the Association for Computational Linguistics (Volume 1: Long Papers)*, pp. 146–157, Association for Computational Linguistics, Vancouver, Canada, July 2017.
- [18] S. Cai and K. Knight, "Smatch: an evaluation metric for semantic feature structures," in *Proceedings of the 51st Annual Meeting of the Association for Computational Linguistics (Volume 2: Short Papers)*, pp. 748–752, Association for Computational Linguistics, Sofia, Bulgaria, July 2013, <https://www.aclweb.org/anthology/P13-2131>.
- [19] M. Ott, S. Edunov, A. Baevski et al., "Fairseq: a fast, extensible toolkit for sequence modeling," in *Proceedings of NAACL-HLT 2019: Demonstrations*, Minneapolis, MN, USA, February 2019.
- [20] D. P. Kingma and Ba Jimmy, "Adam: a method for stochastic optimization," in *Conference Track Proceedings 3rd International Conference on Learning Representations, ICLR 2015*, San Diego, CA, USA, May 2015.
- [21] K. Papineni, S. Roukos, T. Ward, and W.-J. Zhu, "Bleu," in *Proceedings of the 40th Annual Meeting of the Association for Computational Linguistics*, pp. 311–318, Association for Computational Linguistics, Philadelphia, PA, USA, July 2001.
- [22] P. Koehn, "Statistical significance tests for machine translation evaluation," in *Proceedings of the 2004 Conference on Empirical Methods in Natural Language Processing*, pp. 388–395, Association for Computational Linguistics, Barcelona, Spain, July 2004, <https://www.aclweb.org/anthology/W04-3250>.



## Research Article

# Some Bounds on Bond Incident Degree Indices with Some Parameters

Muhammad Rizwan,<sup>1</sup> Akhlaq Ahmad Bhatti,<sup>1</sup> Muhammad Javaid <sup>2</sup> and Fahd Jarad <sup>3,4</sup>

<sup>1</sup>National University of Computer and Emerging Sciences, Lahore, Pakistan

<sup>2</sup>Department of Mathematics, School of Science, University of Management and Technology, Lahore 54770, Pakistan

<sup>3</sup>Department of Mathematics, Çankaya University, Etimesgut 06790, Ankara, Turkey

<sup>4</sup>Department of Medical Research, China Medical University Hospital, China Medical University, Taichung, Taiwan

Correspondence should be addressed to Fahd Jarad; [fahd@cankaya.edu.tr](mailto:fahd@cankaya.edu.tr)

Received 23 April 2021; Accepted 14 June 2021; Published 8 July 2021

Academic Editor: Nouman Ali

Copyright © 2021 Muhammad Rizwan et al. This is an open access article distributed under the Creative Commons Attribution License, which permits unrestricted use, distribution, and reproduction in any medium, provided the original work is properly cited.

It is considered that there is a fascinating issue in theoretical chemistry to predict the physicochemical and structural properties of the chemical compounds in the molecular graphs. These properties of chemical compounds (boiling points, melting points, molar refraction, acentric factor, octanol-water partition coefficient, and motor octane number) are modeled by topological indices which are more applicable and well-used graph-theoretic tools for the studies of quantitative structure-property relationships (QSPRs) and quantitative structure-activity relationships (QSARs) in the subject of cheminformatics. The  $\pi$ -electron energy of a molecular graph was calculated by adding squares of degrees (valencies) of its vertices (nodes). This computational result, afterwards, was named the first Zagreb index, and in the field of molecular graph theory, it turned out to be a well-swotted topological index. In 2011, Vukicevic introduced the variable sum exdeg index which is famous for predicting the octanol-water partition coefficient of certain chemical compounds such as octane isomers, polyaromatic hydrocarbons (PAH), polychlorobiphenyls (PCB), and phenethylamines (Phenet). In this paper, we characterized the conjugated trees and conjugated unicyclic graphs for variable sum exdeg index in different intervals of real numbers. We also investigated the maximum value of SEI<sub>a</sub> for bicyclic graphs depending on  $a > 1$ .

## 1. Introduction

In chemical graph theory, molecules and macromolecules (such as organic compounds, nucleic acids, and proteins) are represented by graphs wherein vertices correspond to the atoms, whereas edges represent the bonds between atoms [1, 2]. A topological index is a numerical value associated with chemical constitution for correlation of chemical structure with various physicochemical properties [3]. Topological indices play a significant role in organic chemistry and particularly in pharmacology [4, 5]. Physicochemical properties of chemical compounds such as relative enthalpy of formation, biological activity, boiling points, melting points, molar refraction, acentric factor, octanol-water partition coefficient, and motor octane number are modeled

by topological indices in quantitative structure-property relation (QSPR) and quantitative structure-activity relation (QSAR) studies [4, 6–8].

In chemistry, the usage of topological index started in 1947 when the chemist Wiener developed the Wiener index (a distance-based topological index) to predict boiling points of paraffins [9]. Platt index (the oldest degree-based topological index) was proposed in 1952 for predicting paraffin properties [10]. The  $\pi$ -electron energy of a molecular graph was calculated by adding square of degrees (valencies) of its vertices (nodes) in the year 1972. The same computational result, afterwards, was named the first Zagreb index, and in the field of molecular graph theory, it turned out to be a well-swotted topological index [11]. For more details about the topological indices in the field of chemistry, we refer to [6, 8, 12–15].

Many well-known topological indices such as hyper Zagreb index [16], variable sum exdeg index [17], and Zagreb indices [18, 19] have been used to find out sharp bounds for unicyclic, bicyclic, and tricyclic graphs. Vukićević [15] propounded variable sum exdeg index for a graph  $G$  and defined it as

$$SEI_a(G) = \sum_{uv \in E(G)} (a^{d_u} + a^{d_v}) = \sum_{u \in V(G)} (d_u a^{d_u}), \quad (1)$$

where  $a$  is a positive integer other than 1. This topological index is correlated well with octane-water partition coefficient [15] and is employed to the study of octane isomers (see [20–22]). This topological index in the form of polynomial was proposed by Yarahmadi and Ashrafi, and they find its application in nanoscience [23]. Chemical application of this index can be seen in the papers [12, 13, 15].

In this paper, we mainly targeted three main problems. First of all, we find the extremal values of variable sum exdeg index ( $SEI_a$ ) for conjugated trees. After that, we investigated lower and upper bounds of unicyclic conjugated graphs with respect to the length of this cycle in different intervals. At the end of this paper, we find upper bounds of  $SEI_a$  for bicyclic graphs. This paper contains seven sections. In the first section, we have given introduction while in Section 2, we have given the proofs of some lemmas and preliminary results. In Section 3, we discovered the bounds of a conjugated trees and this section helps us to find out lower and upper bounds of unicyclic conjugated graphs with respect to the length of this cycle in Section 4. In Section 5, we discussed an important theorem related with conjugated unicyclic graphs. In Section 6, we discovered the upper bounds of bicyclic graphs. In the last section, we have drawn the conclusion.

## 2. Preliminary Results

All graphs under consideration in this paper will be connected, simple, and finite. Suppose  $G = (V(G), E(G))$  is a simple and finite graph, whereas set of vertices is denoted by  $V(G)$  and the set of edges is denoted by  $E(G)$ . Let  $v \in V(G)$  for which  $d_v$  is defined as the cardinality of edges incident with the vertex  $v$ . Suppose  $N_G(v)$  denotes the set of all vertices which are adjacent with the vertex  $v$  and  $N_G[v] = N_G(v) \cup \{v\}$ . Note that  $\Delta(G)$  and  $\delta(G)$  represent the maximum and minimum degree of a graph  $G$ ,

respectively. A pendent vertex is a vertex of degree one. An edge whose one end is a pendent vertex is called pendent edge. Let  $B \subseteq V(G)$  and  $B' \subseteq E(G)$ ; then,  $G - B$  and  $G - B'$  are subgraphs of  $G$  which are obtained by deleting the vertices and edges from  $G$ , respectively. An edge between the vertices  $x$  and  $y$  is denoted by  $e = xy$ . If  $B = \{v\}$  and  $B' = \{xy\}$ , then  $G - B$  and  $G - B'$  can be expressed as  $G - v$  and  $G - xy$ , respectively.

In a graph  $G$ , if the vertices  $x$  and  $y$  are nonadjacent, then  $G + xy$  means there is an addition of an edge between the vertices  $x$  and  $y$  in a graph  $G$ . We use  $S_n, C_n$ , and  $P_n$  to denote the star graph, cycle graph, and path graph on  $n$  vertices, respectively. We assume that graphs  $(G^*, w_1)$  and  $(G^{**}, w_2)$  be rooted at  $w_1$  and  $w_2$ , respectively. Then,  $(G^*, w_1) \cup (G^{**}, w_2)$  is obtained by identifying  $w_1$  and  $w_2$  as the same vertex. A graph which has no cycle is called a tree. A graph  $G$  is said to be unicyclic graph if it has a unique cycle. A graph  $G$  is said to be bicyclic graph if  $G$  has exactly  $n + 1$  edges. Let  $\mathcal{U}_l(n)$  represent the collection of all those graphs which have order  $n$  and a unique cycle of length  $l$ . We denote  $\mathcal{U}_l(2m, m)$  the collection of all conjugated unicyclic graphs of order  $n$  in which length of its cycle is  $l$ , whereas  $m$  is the matching number of  $G$ . Let  $G \in \mathcal{U}_l(2m, m)$  be a unicyclic graph of length  $l$  and it is denoted by  $C_l$ . Let  $G \in \mathcal{U}_l(2m, m)$ ; if  $n = 2m = l$  or  $n = 2m = l + 1$ , then its  $SEI_a(G)$  is unique. That is why in this paper we will assume  $n = 2m \geq l + 2$ . One can find terminologies and expressions “indefinito” in [24–26].

Suppose that  $G'$  is a graph acquired from another graph  $G$  by using some graph alteration such that  $V(G) = V(G')$ . In all sections of this paper, whenever such two graphs are under debate, we always mean the vertex degree  $d_x$  the degree of the vertex  $x$  in  $G$ .

**Lemma 1.** *Let  $G$  be a graph of order  $n$  if  $G$  contains the vertices  $u, v \in V(G)$  such that  $d_u = s > 1$ ,  $d_v = t > 1$  and  $s \geq t$ ; then, there exists a graph  $G'$  such that  $SEI_a(G') > SEI_a(G)$  for  $a > 1$ .*

*Proof.* Let  $u, v \in V(G)$  and  $v_1, v_2, v_3, \dots, v_k$  be the pendent vertices adjacent to the vertex  $v$ . We define a new graph  $G'$ , i.e.,  $G' = G - \{v_1v, v_2v, \dots, v_kv\} + \{v_1u, v_2u, \dots, v_ku\}$  as in Figure 1. By the definition of  $SEI_a(G)$ , we have

$$\begin{aligned} SEI_a(G) - SEI_a(G') &= [d_u a^{d_u} + d_v a^{d_v}] - [(d_u + k) a^{d_u+k} + (d_v - k) a^{d_v-k}] \\ &= [d_v a^{d_v} - (d_v - k) a^{d_v-k}] - [(d_u + k) a^{d_u+k} - d_u a^{d_u}] \\ &= k [a^{\mu_1} (1 + \mu_1 \ln a) - a^{\mu_2} (1 + \mu_2 \ln a)] < 0, \end{aligned} \quad (2)$$

where  $\mu_1 \in (t - k, t)$ ,  $\mu_2 \in (s, s + k)$ ,  $\mu_2 > \mu_1$  for  $a > 1$ . Thus, the proof of the above lemma is accomplished.  $\square$

**Lemma 2.** *Let  $G$  be a graph having two components  $G_1$  and  $T_1$ , where  $G_1$  is a cycle graph and  $T_1$  is a star graph with*

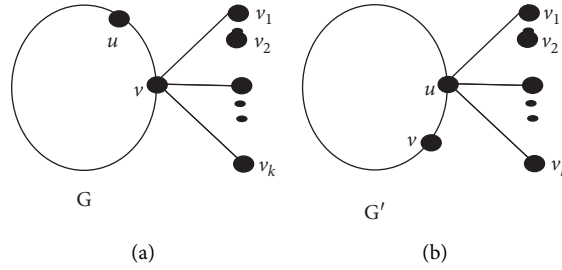


FIGURE 1: (a) G and (b) G' is constructed from G.

central vertex  $v$ . Let  $u \in V(G_1)$  and  $d_u = p$ , such that  $uv$  is an edge in  $G$ . Let  $v_1, v_2, v_3, \dots, v_k$  be the pendent vertices adjacent with the vertex  $v$ , i.e.,  $N_G(v) - \{u\} = \{v_1, v_2, v_3, \dots, v_k\}$ . We define  $G' = G - \{v_1v, v_2v, \dots, v_kv\} + \{v_1u, v_2u, \dots, v_ku\}$  such that  $SEI_a(G') > SEI_a(G)$ .

*Proof.* Let  $G$  be a graph having two components  $G_1$  and  $T_1$  where  $G_1$  is a cycle graph and  $T_1$  is a star graph with central vertex  $v$ . Let  $u \in V(G_1)$ ,  $d_u = p$ , such that  $uv$  is an edge in  $G$ . Let  $v_1, v_2, v_3, \dots, v_k$  be the pendent vertices adjacent with the vertex  $v$ , i.e.,  $N_G(v) - \{u\} = \{v_1, v_2, v_3, \dots, v_k\}$ . We define  $G' = G - \{v_1v, v_2v, \dots, v_kv\} + \{v_1u, v_2u, \dots, v_ku\}$  as in Figure 2. By the definition of  $SEI_a$ , we have

$$SEI_a(G) - SEI_a(G') = [d_u a^{d_u} + d_v a^{d_v}] - [(d_u + k) a^{d_u+k} + (d_v - k) a^{d_v-k}] = [d_v a^{d_v} - (d_v - k) a^{d_v-k} - [(d_u + k) a^{d_u+k} - d_u a^{d_u}]] \tag{3}$$

If  $p \geq k + 1$ , then

$$SEI_a(G) - SEI_a(G') = [d_v a^{d_v} - (d_v - k) a^{d_v-k}] - [(d_u + k) a^{d_u+k} - d_u a^{d_u}] = k[a^{\mu_1} (1 + \mu_1 \ln a) - a^{\mu_2} (1 + \mu_2 \ln a)] < 0, \tag{4}$$

where  $\mu_1 \in (1, k + 1)$ ,  $\mu_2 \in (p, p + k)$ ,  $\mu_2 > \mu_1$ , and  $a > 1$   $SEI_a(G') > SEI_a(G)$ .

If  $p \leq k + 1$ , then

$$SEI_a(G) - SEI_a(G') = [d_u a^{d_u} - (d_v - k) a^{d_v-k}] - [(d_u + k) a^{d_u+k} - d_v a^{d_v}] = z[a^{\mu_1} (1 + \mu_1 \ln a) - a^{\mu_2} (1 + \mu_2 \ln a)] < 0, \tag{5}$$

where  $\mu_1 \in (1, p)$ ,  $\mu_2 \in (k + 1, k + p)$ ,  $\mu_2 > \mu_1$ ,  $z = p - 1$  and  $a > 1$ . Thus, we have  $SEI_a(G') > SEI_a(G)$ .  $\square$

### 3. Extremal Values of Variable Sum Exdeg Index for Conjugated Trees

First we introduce some notations which will be used in the following lemmas and theorems. Suppose that  $\mathbb{T}(n, m)$  be the collection of all trees with  $n$  vertices and  $m$ -matching number with  $n \geq 2m$ . When  $m - 1$  pendent vertices are attached with each certain non-central vertices of  $S_{n-m+1}$ , then

the resulting graph is denoted by  $\mathbb{T}^0(n, m)$ . If we choose  $n = 2m$ , then it means every tree from  $\mathbb{T}(n, m)$  and  $\mathbb{T}^0(n, m)$  contains perfect matching.

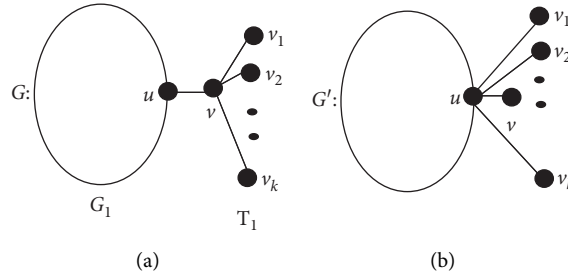
**Lemma 3** (see [26]). *If an  $n$ -vertex tree  $T$  has perfect matching, then there must exist at least two vertices of degree one with neighbouring vertices of degree two, where  $n \geq 3$ .*

**Lemma 4** (see [26]). *If an  $n$ -vertex tree  $T$  has an  $m$ -matching with  $n > 2m$ , then there must exist a pendent vertex  $u$  which is not saturated by  $m$ -matching.*

In the following, we will find two theorems which will give extreme values of  $SEI_a$  for all trees  $T$  in  $\mathbb{T}(2m, m)$ .

**Theorem 1.** *Let  $m \geq 1$ ,  $n \geq 4$ , and  $a > 1$  be integers and  $T \in \mathbb{T}(2m, m)$ ; then,  $SEI_a(T) \leq m a^m + 2(m - 1)a^2 + am$ , where equality meets when  $T \cong \mathbb{T}^0(2m, m)$ .*

*Proof.* Suppose  $T \in \mathbb{T}(2m, m)$ . If the tree  $T$  is isomorphic to  $\mathbb{T}^0(2m, m)$ , then  $SEI_a(T) = SEI_a(\mathbb{T}^0(2m, m))$ . On the other hand, if  $T$  is not isomorphic to  $\mathbb{T}^0(2m, m)$ , then we assume that the vertex  $u \in V(T)$ , i.e.,  $d_u = \Delta(T)$  where  $d_u \geq 2$ . Lemma 3 assures that there exist vertices  $u_1$  and  $v_1$  adjacent by an edge with  $d_{u_1} = 2$  and  $d_{v_1} = 1$ . Let  $N(u_1) - \{v_1\} = w_1$ . We define  $T^{(1)} = T - u_1w_1 + u_1u$ . It is clear that  $T^{(1)} \in \mathbb{T}(2m, m)$ . By the definition of  $SEI_a$ , we have

FIGURE 2: (a) Graph  $G$ ; (b) the graph  $G'$  is obtained from  $G$ .

$$\begin{aligned}
 \text{SEI}_a(T) - \text{SEI}_a(T^{(1)}) &= [d_u \cdot a^{d_u} + d_{w_1} \cdot a^{d_{w_1}}] \\
 &\quad - \left[ (d_u + 1) \cdot a^{d_u+1} + (d_{w_1-1}) \cdot a^{(d_{w_1-1})} \right] \\
 &= \left[ d_{w_1} \cdot a^{d_{w_1}} - (d_{w_1-1}) \cdot a^{(d_{w_1-1})} \right] \\
 &\quad - \left[ (d_u + 1) \cdot a^{d_u+1} - d_u \cdot a^{d_u} \right] \\
 &= a^{\mu_1} (1 + \mu_1 \ln a) - a^{\mu_2} (1 + \mu_2 \ln a) < 0,
 \end{aligned} \tag{6}$$

where  $\mu_1 \in (d_{w_1} - 1, d_{w_1})$ ,  $\mu_2 \in (d_u, d_u + 1)$ , and  $\mu_2 > \mu_1$  for  $a > 1$ .

Note that  $T^* = T^1 - \{u_1, v_1\}$ ; then, obviously  $T^* \in \mathbb{T}(2(m-1), m-1)$ . Then, by the construction of  $T^*$  and keeping Lemma 3 in our mind, we can choose  $u_2$  and  $v_2$  in  $T^*$  where  $d_{u_2} = 2$  and  $d_{v_2} = 1$ . It is clear that  $d_u(T^*) = \Delta(T) = \Delta(T^*)$ . Let  $N(u_2) - \{v_2\} = w_2$ . We set  $T^{**} = T^* - u_2 w_2 + u_2 u$ . Similarly,  $\text{SEI}_a(T^{**}) > \text{SEI}_a(T^*)$ . We define  $T^2 = T^1 - u_2 w_2 + u_2 u$ ; then,

$$\begin{aligned}
 \text{SEI}_a(T^{(2)}) - \text{SEI}_a(T^{(1)}) &= [(d_u + 2) \cdot a^{d_u+2} + (d_{w_2} - 1) \cdot a^{d_{w_2}-1}] \\
 &\quad - [(d_u + 1) \cdot a^{d_u+1} + d_{w_2} \cdot a^{d_{w_2}}] \\
 &= [(d_u + 2) \cdot a^{d_u+2} - (d_u + 1) \cdot a^{d_u+1}] \\
 &\quad - [d_{w_2} \cdot a^{d_{w_2}} - (d_{w_2} - 1) \cdot a^{d_{w_2}-1}] \\
 &= a^{\mu_4} (1 + \mu_4 \ln a) - a^{\mu_3} (1 + \mu_3 \ln a) > 0,
 \end{aligned} \tag{7}$$

where  $\mu_3 \in (d_{w_2} - 1, d_{w_2})$ ,  $\mu_4 \in (d_u + 1, d_u + 2)$ , and  $\mu_4 > \mu_3$  for  $a > 1$ .

This implies that  $\text{SEI}_a(T^{(2)}) - \text{SEI}_a(T^{(1)}) > 0$ . We repeat the above process on the graph  $T$  again and again and we obtain a sequence of graphs  $T^1, T^2, \dots, T^{(s)}, \dots$  with the relation  $\text{SEI}_a(T^{(1)}) < \text{SEI}_a(T^{(2)}) < \dots < \text{SEI}_a(T^{(s)}) < \dots$

For some positive integer  $p$ , we have  $T^{(p)} \cong T^{(p+1)}$  and  $T^{(p)} \cong (\mathbb{T}^0(2m, m))$ .

Hence,  $\text{SEI}_a(T) < \text{SEI}_a(\mathbb{T}^0(2m, m))$ .  $\square$

**Theorem 2.** Suppose that  $m \geq 1$ ,  $n \geq 4$ , and  $a > 1$  be integers. If  $T \in \mathbb{T}(2m, m)$ , then  $\text{SEI}_a(T) \geq 2a + 2(2m-2)a^2$ , where equality meets when  $T \cong P_{2m}$ .

*Proof.* We claim that  $T \cong P_{2m}$ ; then,  $\text{SEI}_a(T) = \text{SEI}_a(P_{2m})$ . If we apply the above-defined process (in previous Theorem

1) on  $T$ , then we will obtain the expression  $\text{SEI}_a(T^{(1)}) < \text{SEI}_a(T^{(2)}) < \dots < \text{SEI}_a(T^{(s)}) < \dots$  for some positive integer  $p \geq 1$   $\text{SEI}_a(T)^p > \text{SEI}_a(P_{2m})$ . Hence,  $\text{SEI}_a(T) \geq \text{SEI}_a(P_{2m}) = 2a + 2(2m-2)a^2$  equality meets when  $T \cong P_{2m}$ .  $\square$

#### 4. Extremal Values of Variable Sum Exdeg Index for Conjugated Unicyclic Graphs

In this portion of the paper, we will find extreme values for  $\text{SEI}_a(G)$  among all the conjugated unicyclic graphs in  $\mathbb{U}_1(2m, m)$  for  $a > 1$ . In this concern, we will prove some lemmas which will support our main theorems.

**Lemma 5** (see [26]). For any tree  $T$  from  $T(2m+1, m)$ , we find at least one vertex of degree 1 which will be adjacent with a vertex  $v$  of degree 2, i.e.,  $d_v = 2$ .

**Lemma 6.** Suppose that  $m \geq 1$ ,  $a > 1$  and  $T \in T(2m+1, m)$ ; then,  $\text{SEI}_a(T) \geq \text{SEI}_a(P_{2m+1})$ , where sign of equality meets when  $T \cong P_{2m+1}$ .

*Proof.* Let  $T \in T(2m+1, m)$ ; then, by Lemma 4, we find a pendent vertex  $u$  in  $T$  which is not saturated by an  $m$ -matching of  $T$ . Obviously, the vertices in  $T - \{u\}$  are saturated by the maximal  $m$ -matching. This implies that  $T - \{u\} \in T(2m, m)$ . Assume that  $N(u) = \{w\}$ ; then,  $\text{SEI}_a(T) = \text{SEI}_a(T - \{u\}) + d_w a^{d_w} + d_u a^{d_u} - (d_w - 1) a^{d_w-1}$ . According to Theorem 2, we have

$$\begin{aligned}
 \text{SEI}_a(T) &\geq \text{SEI}_a(P_{2m}) + d_w a^{d_w} + a - (d_w - 1) a^{d_w-1} \\
 &= 2a + 2(2m-2)a^2 + d_w a^{d_w} + a - (d_w - 1) a^{d_w-1} \\
 &= 2a + 2(2m-1)a^2 - 2a^2 + d_w a^{d_w} + a - (d_w - 1) a^{d_w-1} \\
 &\geq 2a + 2(2m-1)a^2 \\
 &= \text{SEI}_a(P_{2m+1}).
 \end{aligned} \tag{8}$$

The above inequality holds if  $d_w a^{d_w} - (d_w - 1) a^{d_w-1} - (2a^2 - a) \geq 0$ .

If  $d_w = 2$ , then

$$d_w a^{d_w} - (d_w - 1) a^{d_w-1} - (2a^2 - a) = 0. \tag{9}$$

If  $d_w \geq 3$ , then we have

$$a^{\mu_2} (1 + \mu_2 \ln a) - a^{\mu_1} (1 + \mu_1 \ln a) > 0, \quad (10)$$

where  $\mu_1 \in (1, 2)$ ,  $\mu_2 \in (d_w - 1, d_w)$ , and  $\mu_2 > \mu_1$  for  $a > 1$ . Finally, we have  $SEI_a(T) \geq SEI_a(P_{2m+1})$ .  $\square$

**Lemma 7.** Let  $T \in \mathbb{T}(2m+1, m)$ ; then,  $SEI_a(T) \leq SEI_a(\mathbb{T}^0(2m+1, m))$  equality meets when  $T \cong \mathbb{T}^0(2m+1, m)$  where  $m \geq 1$ ,  $a > 1$ .

*Proof.* Let  $T \in \mathbb{T}(2m+1, m)$ ; then, by Lemma 4, we find a pendent vertex  $u$  in  $T$  which is not saturated by a maximal  $m'$ -matching of  $T$ . Suppose that  $N(u) = \{z_1\}$ . Suppose  $v$  is a vertex in  $T$ , i.e.,  $d_v = \Delta(T)$ . Define  $T' = T - uz_1 + uv$ ; then, clearly  $T' - \{u\} \in \mathbb{T}(2m, m)$ . With the help of Theorem 1, we have  $SEI_a(T') - \{u\} \leq SEI_a(\mathbb{T}^0(2m, m))$ , so we have

$$\begin{aligned} SEI_a(T') &= SEI_a(T' - u) + d_u a^{d_u} + (d_v + 1)a^{d_v+1} - d_v a^{d_v} \\ &\leq a + SEI_a(\mathbb{T}^0(2m, m)) + (d_v + 1)a^{d_v+1} - d_v a^{d_v} \\ &*** < a + SEI_a(\mathbb{T}^0(2m, m)) + (m+1)a^{m+1} - ma^m \\ &= a + ma^m + 2a^2(m-1) + a.m + (m+1)a^{m+1} - ma^m \\ &= a + ma^m + 2a^2(m-1) + a.m + (m+1)a^{m+1} - ma^m \\ &= 2a^2(m-1) + (1+m)a + (m+1)a^{m+1} \\ &= SEI_a(\mathbb{T}^0(2m+1, m)). \end{aligned} \quad (11)$$

If we show that  $(d_v + 1)a^{d_v+1} - d_v a^{d_v} < (m+1)a^{m+1} - ma^m$ , then it will be enough for the existence of the expression  $***$ . Since we know that  $\Delta(\mathbb{T}^0(2m, m)) = m$ ,  $T$  is not isomorphic to  $\mathbb{T}^0(2m+1, m)$  and  $d_v \leq m$ . If we assume  $d_v = m$ , then  $(d_v + 1)a^{d_v+1} - d_v a^{d_v} - (m+1)a^{m+1} + ma^m = 0$ . If we assume  $d_v < m$ , then

$$\begin{aligned} &= [(d_v + 1)a^{d_v+1} - d_v a^{d_v}] - [(m+1)a^{m+1} - ma^m] \\ &= a^{\mu_1} (1 + \mu_1 \ln a) - a^{\mu_2} (1 + \mu_2 \ln a) < 0, \end{aligned} \quad (12)$$

where  $\mu_1 \in (d_v, d_v + 1)$ ,  $\mu_2 \in (m, m + 1)$ ,  $\mu_2 > \mu_1$  and  $a > 1$ .

Hence,  $SEI_a(T) < SEI_a(T') < SEI_a(\mathbb{T}^0(2m+1, m))$ . So, we conclude that  $SEI_a(T) < SEI_a(\mathbb{T}^0(2m+1, m))$ , and sign of equality meets when  $T \cong \mathbb{T}^0(2m+1, m)$ .

We define a set  $B = \{x_i \in V(C_l): d_{x_i} \geq 3\}$ . Remember that  $T(x_i)$  represents the connected component having the vertex  $x_i$  of the graph  $G - \{x_{i-1}x_i, x_i x_{i+1}\}$ .  $\square$

**Lemma 8** (see [26]). Let  $G \in \mathbb{U}_l(2m, m)$ ; then, for every  $x_i \in B$ ,  $T(x_i) \in T(n_i, n_i/2)$  or  $T(x_i) \in T(n_i, n_i - 1/2)$ .

**Lemma 9.** Let  $G \in \mathbb{U}_l(2m, m)$  such that  $SEI_a(G)$  is minimum if  $T(x_i) \cong P_{n_i}$  where  $x_i \in B$ ,  $n_i = n(T(x_i))$ ,  $a > 1$  and  $x_i$  is one of the pendent vertices of  $P_{n_i}$ .

*Proof.* Suppose  $G \in \mathbb{U}_l(2m, m)$  with minimum variable sum exdeg index. We also assume that  $x_i \in B$  and the vertices  $x_{i-1}$  and  $x_{i+1}$  are the neighbouring vertices of the vertex  $x_i$  along  $C_l$ . Here we consider the expression

$$\begin{aligned} Q &= [d_{x_i} a^{d_{x_i}} - (d_{x_i} - 2)a^{d_{x_i}-2}] + [d_{x_{i-1}} a^{d_{x_{i-1}}} - (d_{x_{i-1}} - 1)a^{d_{x_{i-1}}-1}] \\ &\quad + [d_{x_{i+1}} a^{d_{x_{i+1}}} - (d_{x_{i+1}} - 1)a^{d_{x_{i+1}}-1}]. \end{aligned} \quad (13)$$

We assume that  $G^*$  is the connected component of  $G - \{x_i x_{i-1}, x_i x_{i+1}\}$  which does not contain the vertex  $x_i$ . We can write the expression,  $SEI_a(G) = SEI_a(G^*) + Q + SEI_a(T_{x_i})$ . According to Lemma 8,  $T(x_i) \in T(n_i, n_i/2)$  or  $T(x_i) \in T(n_i, n_i - 1/2)$ . In either situation, there exists the following relation:  $SEI_a(G) \geq SEI_a(G^*) + Q + SEI_a(P_{n_i})$  according to Theorem 2 and Lemma 6. Furthermore, the sign of equality meets iff  $T(x_i) \cong P_{n_i}$ . Next we will prove that the vertex  $x_i$  is one of the pendent vertices of  $P_{n_i}$  such that  $d_{x_i} = 3$ . We suppose that  $d_{x_i} \geq 4$ , so there must exist two vertices  $u$  and  $v$ , i.e.,  $N(x_i) - \{x_{i-1}, x_{i+1}\} = \{u, v\}$ . Then, there must be one edge of  $x_i u$ , or  $x_i v$  which is not included in  $m$ -matching. Without loss of generality, suppose that  $x_i u$  does not belong to the  $m$ -matching. Let  $P(v) = v_1, v_2, \dots, v_q$  where  $q \geq 2$  represents the path with  $v = v_1$  as a pendent vertex of  $P(v)$ . Define  $G' = G - x_i u + uv_q$ ; it is clear that  $G' \in \mathbb{U}_l(2m, m)$ . By the definition of  $SEI_a$ , we have

$$\begin{aligned} SEI_a(G') - SEI_a(G) &= [(d_{x_i} - 1)a^{d_{x_i}-1} + (d_{v_q} + 1)a^{d_{v_q}+1}] \\ &\quad - [(d_{x_i})a^{d_{x_i}} + d_{v_q} a^{d_{v_q}}] \\ &= [(d_{v_q} + 1)a^{d_{v_q}+1} - (d_{v_q})a^{d_{v_q}}] \\ &\quad - [d_{x_i} a^{d_{x_i}} - (d_{x_i} - 1)a^{d_{x_i}-1}] \\ &= a^{\mu_1} (1 + \mu_1 \ln a) - a^{\mu_2} (1 + \mu_2 \ln a) < 0, \end{aligned} \quad (14)$$

where  $\mu_1 \in (d_{v_q}, d_{v_q} + 1)$ ,  $\mu_2 \in (d_{x_i} - 1, d_{x_i})$ ,  $\mu_2 > \mu_1$  and  $a > 1$ .

$SEI_a(G') < SEI_a(G)$  which contradicts our choice of  $G$ .  $\square$

**Lemma 10.** If  $G \in \mathbb{U}_l(2m, m)$ ,  $a > 1$  with maximum  $SEI_a(G)$ ; then, for every vertex  $x_i \in B$ , there exist  $T(x_i)$  which will be isomorphic to  $\mathbb{T}^0(n_i, n_i/2)$  or  $\mathbb{T}^0(n_i, n_i - 1/2)$ . If  $T(x_i)$  is isomorphic to  $\mathbb{T}^0(n_i, n_i/2)$ , then  $d_{x_i} - 2$  will be equal to  $\Delta(\mathbb{T}^0(n_i, n_i/2))$ . If  $T(x_i)$  is isomorphic to  $\mathbb{T}^0(n_i, n_i - 1/2)$ , then the vertex  $x_i$  will be the one end vertex of  $\mathbb{T}^0(n_i, n_i - 1/2)$  and  $(x_i)$  will be adjacent to some maximum degree vertex of  $\mathbb{T}^0(n_i, n_i - 1/2)$ .

*Proof.* Let  $G \in \mathbb{U}_l(2m, m)$  with maximum variable sum exdeg index. We also assume that  $x_i \in B$  and the vertices  $x_{i-1}$  and  $x_{i+1}$  are the neighbouring vertices of the vertex  $x_i$  along  $C_l$ . Here we consider the expression

$$\begin{aligned} Q &= [d_{x_i} a^{d_{x_i}} - (d_{x_i} - 2)a^{d_{x_i}-2}] + [d_{x_{i-1}} a^{d_{x_{i-1}}} - (d_{x_{i-1}} - 1)a^{d_{x_{i-1}}-1}] \\ &\quad + [d_{x_{i+1}} a^{d_{x_{i+1}}} - (d_{x_{i+1}} - 1)a^{d_{x_{i+1}}-1}]. \end{aligned} \quad (15)$$

We assume that  $G^*$  is the connected component of  $G - \{x_i x_{i-1}, x_i x_{i+1}\}$  which does not contain the vertex  $x_i$ . We

can write the expression  $SEI_a(G) = SEI_a(G^*) + Q + SEI_a(T(x_i))$ .

According to Theorem 1, Lemma 7, and Lemma 8, we have

$$SEI_a(G) \leq SEI_a(G^*) + Q + SEI_a\left(\mathbb{T}^0\left(n_i, \frac{n_i}{2}\right)\right), \quad (16)$$

or

$$SEI_a(G) \leq SEI_a(G^*) + Q + SEI_a\left(\mathbb{T}^0\left(n_i, \frac{n_i - 1}{2}\right)\right), \quad (17)$$

for  $n_i$  being even or odd, respectively. Above two inequalities hold iff  $T(x_i) \cong \mathbb{T}^0(n_i, n_i/2)$  and  $T(x_i) \cong \mathbb{T}^0(n_i, n_i - 1/2)$ , respectively. Next we will prove that

(1) If  $T(x_i) \cong \mathbb{T}^0(n_i, n_i/2)$ , then  $d_{x_i} - 2 = \Delta(\mathbb{T}^0(n_i, n_i/2))$ .

(2) If  $T(x_i) \cong \mathbb{T}^0(n_i, n_i - 1/2)$ , then  $(\mathbb{T}^0(n_i, n_i - 1/2))$  has the vertex  $x_i$  as a pendent vertex that is adjacent to the vertex of maximum degree in  $\mathbb{T}^0(n_i, n_i - 1/2)$ .

For the proof of (i), we assume that  $d_{x_i} - 2 < \Delta(\mathbb{T}^0(n_i, n_i/2))$ . Let  $y \in V(T)$ , i.e.,  $d_y = \Delta(\mathbb{T}^0(n_i, n_i/2))$ . We define  $G' = G - x_i x_{i-1} - x_i x_{i+1} + x_{i-1} y + x_{i+1} y$ . By the definition of  $SEI_a(G)$ ,

$$\begin{aligned} SEI_a(G) - SEI_a(G') &= [d_{x_i} a^{d_{x_i}} + d_y a^{d_y}] \\ &\quad - [(d_{x_i} - 2) a^{d_{x_i} - 2} + (d_y + 2) a^{d_y + 2}] \\ &= [d_{x_i} a^{d_{x_i}} - (d_{x_i} - 2) a^{d_{x_i} - 2}] \\ &\quad - [(d_y + 2) a^{d_y + 2} - d_y a^{d_y}]. \end{aligned} \quad (18)$$

If  $d_{x_i} \geq d_y$ , then

$$\begin{aligned} SEI_a(G) - SEI_a(G') &= [d_y a^{d_y} - (d_{x_i} - 2) a^{d_{x_i} - 2}] \\ &\quad - [(d_y + 2) a^{d_y + 2} - d_{x_i} a^{d_{x_i}}] \\ &= z \cdot [a^{\mu_1} (1 + \mu_1 \ln a) - a^{\mu_2} (1 + \mu_2 \ln a)] < 0, \end{aligned} \quad (19)$$

where  $\mu_1 \in (d_x - 2, d_y)$ ,  $\mu_2 \in (d_{x_i}, d_y + 2)$ ,  $\mu_2 > \mu_1$ ,  $a > 1$ , and  $z = d_y - d_{x_i} + 2$ .

$SEI_a(G') > SEI_a(G)$  which contradicts our choice of  $G$ . If  $d_{x_i} < d_y$ , then

$$\begin{aligned} SEI_a(G) - SEI_a(G') &= [d_{x_i} a^{d_{x_i}} - (d_{x_i} - 2) a^{d_{x_i} - 2}] \\ &\quad - [(d_y + 2) a^{d_y + 2} - (d_y) a^{d_y}] \\ &= 2 \cdot [a^{\mu_1} (1 + \mu_1 \ln a) - a^{\mu_2} (1 + \mu_2 \ln a)] < 0, \end{aligned} \quad (20)$$

where  $\mu_1 \in (d_{x_i} - 2, d_{x_i})$ ,  $\mu_2 \in (d_y, d_y + 2)$ ,  $\mu_2 > \mu_1$ , and  $a > 1$ .

$SEI_a(G') > SEI_a(G)$  which contradicts our choice of  $G$ .

For the proof of (ii), we will just show that  $d_{x_i} = 3$  and  $d_{w_1} = \Delta(T(v_i))$  where  $w_1 = N(x_i) - \{x_{i+1}, x_{i-1}\}$ .

Since  $G \in \mathbb{U}_l(2m, m)$  and  $T(x_i)$  is isomorphic to  $\mathbb{T}^0(n_i, n_i - 1/2)$ ,  $d_{x_i} - 2 < \Delta(\mathbb{T}^0(n_i, n_i - 1/2))$ .

Note that any vertex  $w_2$  other than the vertex of maximum degree in  $\mathbb{T}^0(n_i, n_i - 1/2)$  has the degree 2 or 1. If  $d_{x_i} - 2 = 2$ , this implies that in  $\mathbb{T}^0(n_i, n_i - 1/2)$ , there will be a vertex which is not saturated by the maximal matching of  $G$ . Here a contradiction arises for  $d_{x_i} - 2 = 1$ . This implies  $d_{x_i} = 3$ . If we assume  $d_{w_1} < \Delta(\mathbb{T}^0(n_i, n_i - 1/2))$ , then once again we find a vertex in  $\mathbb{T}^0(n_i, n_i - 1/2)$  which is not saturated by the maximal matching in  $G$  and again we will find a contradiction. From the above discussion, the proof is accomplished.  $\square$

**Theorem 3.** Suppose  $G \in \mathbb{U}_l(2m, m)$ ; then,  $SEI_a \geq 1 + 3a^3 + 2(2m - 2)a^2$  for  $a > 1$  and the sign of equality meets when  $G \cong (C_l, x_i) \uplus (P_{2m-k+1}, x_i)$  where  $x_i \in C_l$  is a pendent vertex of  $P_{2m-k+1}$ .

*Proof.* Suppose  $G \in \mathbb{U}_l(2m, m)$  having minimum  $SEI_a$ . According to Lemma 9, for the minimum  $SEI_a(G)$ ,  $T(x_{s_t})$  will be isomorphic to  $P_{n_{s_t}}$  for every  $x_{s_t} \in B$  where  $n_{s_t} = n(T(x_{s_t}))$ . For  $|B| = 1$ , the above result holds. Now we discuss the above result for  $|B| \geq 2$ . We have  $T(x_{s_t}) \cong P_{n_{s_t}}(t = 1, 2, \dots, |B|)$ . So, we denote  $T(x_{s_t}) = y_0^t y_1^t \dots y_{b_t}^t$  ( $b_t \geq 1$ ), where  $y_0^t = x_{s_t}$  ( $t = 1, 2, \dots, |B|$ ). We define  $G^* = G - y_0^2 y_1^2 - y_0^3 y_1^3 \dots - y_0^{|B|} y_1^{|B|} + y_{b_1}^1 y_1^1 + y_{b_2}^2 y_1^2 + \dots + y_{b_{|B|-1}}^{|B|-1} y_1^{|B|-1}$ . It is clear that  $G^* \in \mathbb{U}_l(2m, m)$ ; then, by the definition of  $SEI_a$ ,

$$\begin{aligned} SEI_a(G^*) - SEI_a(G) &= (|B| - 1)[(2a^2 - a) - (3a^3 - 2a^2)] \\ &= (|B| - 1)[a^{\mu_1} (1 + \mu_1 \ln a) - a^{\mu_2} (1 + \mu_2 \ln a)] < 0, \end{aligned} \quad (21)$$

where  $\mu_1 \in (1, 2)$ ,  $\mu_2 \in (2, 3)$ ,  $\mu_2 > \mu_1$ , and  $a > 1$ .

$SEI_a(G^*) < SEI_a(G)$  which contradicts our choice of  $G$ . Hence, the proof of above theorem is finished.  $\square$

## 5. Main Result

**Theorem 4.** Let  $G \in \mathbb{U}_l(2m, m)$  and  $a > 1$ ; then, the following results must hold:

- (1) If  $2m = l + 2$ , then  $SEI_a \leq 2a + 2(l - 2)a^2 + 3a^3$  and the sign of equality meets when  $G$  is not isomorphic to  $(C_l, P_3)$ .
- (2) If  $2m \geq l + 3$  and  $l$  is odd, then  $SEI_a(G) \leq (m - l - 1/2)a + 2(m + l - 3/2)a^2 + (m - l - 5/2)a^{m-l-5/2}$  sign of equality meets iff  $G \cong (C_l, x_i) \uplus (\mathbb{T}^0(2m - l + 1, 2m - l + 1/2), x_i)$ .
- (3) If  $2m \geq l + 3$  and  $l$  is even, then  $SEI_a(G) \leq (m - l/2)a + 2(m + l/2 - 2)a^2 + 3a^3 + (m - l/2 + 1)a^{m-l/2+1}$  sign of equality meets iff  $G \cong (C_l, x_i) \uplus (\mathbb{T}^0(2m - l + 1, 2m - l/2), x_i)$ , where  $d_{x_i} = 3$ ,  $N(x_i) - \{x_{i-1}, x_{i+1}\} = y$ , and  $y = \Delta(\mathbb{T}^0(2m - l + 1, 2m - l/2), x_i)$ .

*Proof.* Let  $G \in \mathbb{U}_l(2m, m)$ ,  $a > 1$  with maximum  $SEI_a(G)$ . According to Lemma 8, we are sure that  $T(x_i)$  is isomorphic to  $\mathbb{T}^0(n_i, n_i - 1/2)$  or  $\mathbb{T}^0(n_i, n_i/2)$  where  $x_i \in B$ .

For  $|B| = 1$ , we have no graph  $G \not\cong (C_l, P_3)$  for which  $2m = l + 2$ . Whenever  $2m = l + 2$ , then  $G$  must be isomorphic to  $(C_l, P_3)$  where  $G \in \cup_l(2m, m)$ . According to Theorem 3, we can find a graph  $G'$  such that  $SEI_a(G') > SEI_a(C_l, P_3) = SEI_a(G)$  for  $G' \neq (C_l, P_3)$  which contradicts the choice of  $G$ . With the help of Lemma 10, the proof of (2) or (3) is satisfied. For  $|B| \geq 2$ , we may have the below cases.

*Case 1.* Let  $2m = l + 2$ ; then, for any two graphs  $G^*$  and  $G^{**}$ , both graphs are not isomorphic to  $(C_l, P_3)$  and  $SEI_a(G^*) = SEI_a(G^{**})$ . According to Theorem 3, we have  $SEI_a(G) > SEI_a((C_l, P_3))$  where  $G \not\cong (C_l, P_3)$ , and hence (1) satisfies.

*Case 2.* For  $2m \geq l + 3$ , we make the following subcases. Let  $x_{s_t} \in B, t = 1, 2, \dots, |B|$  and  $n(T(x_{s_t})) = n_t$ .

*Subcase 2.1.* Let  $n_t = 2$  for every  $x_{s_t} \in B$ ; then, we have the following set of vertices:  $V(G) - V(C_l) = \{y_1, y_2, \dots, y_{|B|}\}$  and  $N(y_t) = x_{s_t}, t = 1, 2, \dots, |B|$ . Let  $N(x_{s_t}) - \{y_t\} = \{x_{s_t} - 1, x_{s_t} + 1\}, t = 1, 2, \dots, |B|$ . Choose  $|B| \geq 3$ . If  $|B| = 3$ , we define  $G^* = G - x_{s_2}y_2 - x_{s_3}y_3 + x_{s_1}y_2 + y_2y_3$ . If  $|B| \geq 4$ , we define  $G^* = G - x_{s_2}y_2 - x_{s_3}y_3 - x_{s_{2-1}}x_{s_2} - x_{s_2}x_{s_{2+1}} - x_{s_3}x_{s_{3+1}} + x_{s_{2-1}}x_{s_{2+1}} + x_{s_2}x_{s_3} + x_{s_2}x_{s_{3+1}} + x_{s_1}y_2 + y_2y_3$

In both above  $G^*$ , we have  $G^* \in \cup_l(2m, m)$  and we have the expression

$$\begin{aligned} SEI_a(G^*) - SEI_a(G) &= (4a^4 - 3a^3) + (2a^2 - a) \\ &\quad - 2(3a^3 - 2a^2) = (4a^4 - 3.3a^3) \\ &\quad + (3.2a^2 - a) > 0, \end{aligned} \tag{22}$$

which contradicts our choice of  $G$ .

*Subcase 2.2.* Let  $x_{s_{l'}} \in B$ , i.e.,  $n_{l'} = 3$ ; here we have  $|B| \geq 2$ ; there must exist a vertex  $x_{s_{l'}}$  in  $B - \{x_{s_{l'}}\}$ . We define  $G^* = G - x_{s_{l'}}y_{l'} + x_{s_{l'}}y_{l'}$ ; then, clearly  $G^* \in \cup_l(2m, m)$ . By the definition of  $SEI_a(G)$ , we have

$$\begin{aligned} SEI_a(G^*) - SEI_a(G) &= \left[ (d_{x_{s_{l'}}} + 1)a^{d_{x_{s_{l'}}} + 1} + 2a^2 \right] \\ &\quad - \left[ d_{x_{s_{l'}}}a^{d_{x_{s_{l'}}} + 3a^3} \right] \\ &= \left[ (d_{x_{s_{l'}}} + 1)a^{d_{x_{s_{l'}}} + 1} - (d_{x_{s_{l'}}}a^{d_{x_{s_{l'}}})} \right] \\ &\quad - \left[ 3a^3 - 2a^2 \right]. \end{aligned} \tag{23}$$

Since  $d_{x_{s_{l'}}} \geq 3$  and  $a > 1$ , this implies that  $SEI_a(G^*) - SEI_a(G) > 0$  which is a contradiction to the choice of  $G$ .

*Subcase 2.3.* Let  $x_{s_t} \in B$  and  $n_t \geq 4$ . In this concern, two subcases arise.

*Subcase 2.3.1.* Suppose that  $d_{x_{s_i}} = \Delta(G)$  for some  $x_{s_i} \in B$ ; since we have  $|B| \geq 2$ , there exists a vertex  $x_{s_j}$  in  $B - \{x_{s_i}\}$ . According to Lemma 8, Lemma 3, and Lemma 5, there must exist some adjacent vertices say  $u_s$  and  $v_s$  in  $T(x_{s_i})$ , i.e.,  $d_{u_s} = 2$  and  $d_{v_s} = 1$ . Let  $N(u_s) - \{v_s\} = \{w_s\}$ . We define  $G^* = G - w_su_s + x_{s_i}u_s$ ; then, clearly  $G^* \in \cup_l(2m, m)$  and

$$\begin{aligned} SEI_a(G^*) - SEI_a(G) &= \left[ (d_{x_{s_i}} + 1)a^{d_{x_{s_i}} + 1} - (d_{w_s} - 1)a^{d_{w_s} - 1} \right] - \left[ d_{x_{s_i}}a^{d_{x_{s_i}}} + d_{w_s}a^{d_{w_s}} \right] \\ &= \left[ (d_{x_{s_i}} + 1)a^{d_{x_{s_i}} + 1} - d_{x_{s_i}}a^{d_{x_{s_i}}} \right] - \left[ d_{w_s}a^{d_{w_s}} - (d_{w_s} - 1)a^{d_{w_s} - 1} \right] \\ &= [a^{\mu_2}(1 + \mu_2 \ln a) - a^{\mu_1}(1 + \mu_1 \ln a)] > 0, \end{aligned} \tag{24}$$

where  $\mu_1 \in (d_{w_s} - 1, d_{w_s}), \mu_2 \in (d_{x_{s_i}}, d_{x_{s_i}} + 1), \mu_2 > \mu_1$ , and  $a > 1$ .

$SEI_a(G^*) > SEI_a(G)$  which contradicts our choice of  $G$ .

*Subcase 2.3.2.* Suppose that  $d_{x_{s_i}} < \Delta(G)$  for some  $x_{s_i} \in B$ . Let  $y$  be a vertex in  $G$  with  $d_y = \Delta(G)$ , so this implies that  $y \in T(x_{s_i})$  where  $l$  is a positive integer. Since we have  $|B| \geq 2$ , then there exists some vertex  $x_{s_j}$  in  $B - \{x_{s_i}\}$ . According to Lemma 8, Lemma 3, and Lemma 5, there must exist some adjacent vertices say  $u_s$  and  $v_s$  in  $T(x_{s_i})$ , i.e.,  $d_{u_s} = 2$  and  $d_{v_s} = 1$ . Let  $N(u_s) - \{v_s\} = \{w_s\}$ .

Remaining portion of the under discussion subcase is similar to subcase 2.3.1 and once again we find the

contradiction. According to all above discussion and argument, we follow the desired result.  $\square$

**Theorem 5.** Let  $G \in \cup_l(2m, m), a > 1$ , and  $n(T(x_i)) \geq 3$  for every  $x_i \in B$ ; then,

- (1) If  $2m \geq l + 3$  and  $l$  is odd, then  $SEI_a(G) \leq (m - l - 1/2)a + 2(m + l - 3/2)a^2 + (m - l - 5/2)a^{m-l-5/2}$  sign of equality meets iff  $G \cong (C_l, x_i) \cup (\mathbb{T}^0(2m - l + 1, 2m - l + 1/2), x_i)$ .
- (2) If  $2m \geq l + 3$  and  $l$  is even, then  $SEI_a(G) \leq (m - l/2)a + 2(m + l/2 - 2)a^2 + 3a^3 + (m - l/2 + 1)a^{m-l/2+1}$  sign of equality meets iff  $G \cong (C_l, x_i) \cup (\mathbb{T}^0(2m - l + 1, 2m - l + 1/2), x_i)$ , where

$$d_{x_i} = 3, \quad N(x_i) - \{x_{i-1}, x_{i+1}\} = y, \quad \text{and} \\ y = \Delta(\mathbb{T}^0(2m - l + 1, 2m - l/2), x_i).$$

## 6. Extremal Values of Variable Sum Exdeg Index for Bicyclic Graphs

Here we are going to define some notations. Let  $\mathbb{G}(n, n+1)$  be the collection of bicyclic graphs or all those graphs which have  $n$  vertices and  $n+1$  number of edges. Note that if  $G \in \mathbb{G}(n, n+1)$ , then there exist two cycles say  $C_i$  and  $C_j$  in  $G$ .

- (i)  $\mathbb{A}(i, j)$  is the collection of graphs  $G \in \mathbb{G}(n, n+1)$  in which cycles  $C_i$  and  $C_j$  share a single vertex only.
- (ii)  $\mathbb{B}(i, j)$  is the collection of graphs  $G \in \mathbb{G}(n, n+1)$  in which cycles  $C_i$  and  $C_j$  share no common vertex.
- (iii)  $\mathbb{C}(i, j, l)$  is the collection of graphs  $G \in \mathbb{G}(n, n+1)$  in which cycles  $C_i$  and  $C_j$  share a common path of length  $l$ .

**6.1. Extremal Graphs in  $\mathbb{A}(i, j)$ .** Suppose  $\mathbb{S}_n(i, j)$  is a graph from the collection  $\mathbb{A}(i, j)$ , i.e., there are  $k = n - i - j + 1$  pendent vertices adjacent to a common vertex of  $C_i$  and  $C_j$  as shown in Figure 3.

**Lemma 11.** Let  $G \in \mathbb{A}(i, j)$ ; if  $G \notin \mathbb{S}_n(i, j)$ , then  $SEI_a(G) < SEI_a(\mathbb{S}_n(i, j))$  for  $a > 1$ .

*Proof.* Let  $G \in \mathbb{A}(i, j)$ ; then, by Lemma 2, we obtain another graph say  $G'$  for which  $SEI_a(G') > SEI_a(G)$ . Further by Lemma 1, the graph  $G'$  can be changed into another graph say  $G''$  in which pendent vertices will be attached with some common vertex  $u$ , of  $C_i$  and  $C_j$ . If  $u$  is not a common vertex of  $C_i$  and  $C_j$ , then  $G'' \notin \mathbb{S}_n(i, j)$ . By the definition of  $SEI_a(G)$ , we have

$$SEI_a(\mathbb{S}_n(i, j)) - SEI_a(G'') = [(k+4).a^{k+4} + 2a^2] - [(k+2).a^{k+2} + 4a^4]. \quad (25)$$

where  $\mu_1 \in (1, 2), \mu_2 \in (k+4, k+5), \mu_2 > \mu_1$  and  $a > 1 \Rightarrow SEI_a(G') > SEI_a(G)$ .

Proof of (ii) is the same as proof of (i).  $\square$

**Theorem 6.** If  $G \in \mathbb{A}(i, j)$ , then  $SEI_a(G)$  will be maximal if  $G \cong \mathbb{S}_n(i, j)$  and for all  $i \geq 3, j \geq 3$ , the graph from  $\mathbb{A}(i, j)$  with maximum  $SEI_a$  is  $\mathbb{S}_n(3, 3)$ .

*Proof.* Proof of this theorem can be obtained by Lemma 11 and Lemma 12.  $\square$

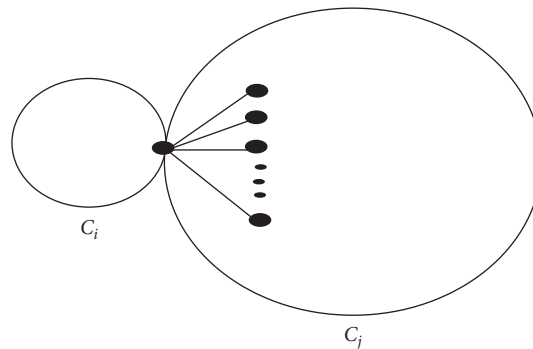


FIGURE 3:  $\mathbb{S}_n(i, j)$  graphs.

Case - 1: for  $k = n + 1 - i - j = 1, a > 1$ , we have

$$SEI_a(\mathbb{S}_n(i, j)) - SEI_a(G'') = [(k+4).a^{k+4} - 4a^4] - [(k+2).a^{k+2} - 2a^2] \\ = [a^{\mu_2}(1 + \mu_2 \ln a) - a^{\mu_1}(1 + \mu_1 \ln a)] > 0, \quad (26)$$

where  $\mu_1 \in (2, k+2), \mu_2 \in (4, k+4), \mu_2 > \mu_1, a > 1$ .

Case - 2: for  $k = n + 1 - i - j \geq 2, a > 1$ , we have

$$SEI_a(\mathbb{S}_n(i, j)) - SEI_a(G'') = [(k+4).a^{k+4} - (k+2).a^{k+2}] - [4a^4 - 2a^2] \\ = k.[a^{\mu_2}(1 + \mu_2 \ln a) - a^{\mu_1}(1 + \mu_1 \ln a)] > 0, \quad (27)$$

where  $\mu_1 \in (2, 4), \mu_2 \in (k+2, k+4), \mu_2 > \mu_1, a > 1$ .

From the above two cases, we conclude that  $SEI_a(\mathbb{S}_n(i, j)) > SEI_a(G'')$ .  $\square$

**Lemma 12.** Let  $\mathbb{S}_n(i, j) \in \mathbb{A}(i, j)$ ; then,

- (a)  $SEI_a(\mathbb{S}_n(i, j)) < SEI_a(\mathbb{S}_n(i-1, j))$ ,  $a > 1, i > 3$ .
- (b)  $SEI_a(\mathbb{S}_n(i, j)) < SEI_a(\mathbb{S}_n(i, j-1))$ ,  $a > 1, j > 3$ .

*Proof.* By the definition of  $SEI_a(G)$ , we have

$$SEI_a(\mathbb{S}_n(i, j)) - SEI_a(\mathbb{S}_n(i-1, j)) = [2a^2 - a] - [(k+5)a^{k+5} - (k+4)a^{k+4}] \\ = a^{\mu_1}(1 + \mu_1 \ln a) - a^{\mu_2}(1 + \mu_2 \ln a) < 0, \quad (28)$$

**6.2. Extremal Graphs in  $\mathbb{B}(i, j)$ .** Here we define that  $\mathbb{T}_n^r(i, j)$  is a graph which is obtained by joining  $C_i$  and  $C_j$  by a path  $P$  of length  $r$  and the remaining number of vertices  $k = n - i - j - r + 1$  are attached to the same end vertex of  $P$  as shown in Figure 4.

**Lemma 13.** Let  $G \in \mathbb{B}(i, j)$ ; if  $G \notin \mathbb{T}_n^r(i, j)$ , then  $SEI_a(G) < SEI_a(\mathbb{T}_n^r(i, j))$  for  $a > 1$ .

*Proof.* Let  $G \in \mathbb{B}(i, j)$ ; then, by Lemma 2, we obtain another graph say  $G'$  for which  $SEI_a(G') > SEI_a(G)$ . Further by



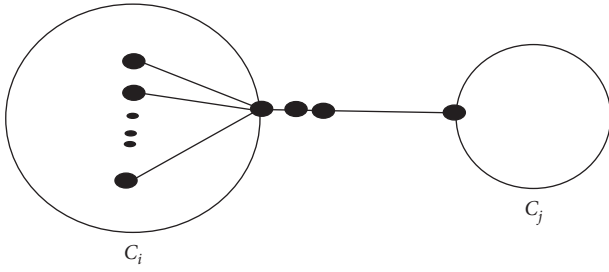


FIGURE 4:  $\mathcal{T}_r(i, j)$  graphs.

Lemma 1, the graph  $G'$  can be changed into another graph say  $G''$  in which pendent edges are attached with same vertex  $u$ , i.e.,  $SEI_a(G'') > SEI_a(G')$ . If  $u$  is not end vertex of path  $P$ , then we will show  $SEI_a(\mathbb{T}_n^r) > SEI_a(G'')$ . By the definition of  $SEI_a$ , we have

$$\begin{aligned} SEI_a(\mathbb{T}_n^r) - SEI_a(G'') &= [(k+3)a^{k+3} - (k+2)a^{k+2}] - [3a^3 - 2a^2] \\ &= a^{\mu_2}(1 + \mu_2 \ln a) - a^{\mu_1}(1 + \mu_1 \ln a) > 0, \end{aligned} \quad (29)$$

where  $\mu_1 \in (2, 3), \mu_2 \in (k+2, k+3), \mu_2 > \mu_1, a > 1$ , and  $k = n+1-i-j-r$ .  $\square$

**Lemma 14.** Let  $\mathbb{T}_n^r \in \mathbb{B}(i, j)$ ; then,

- (a)  $SEI_a(\mathbb{T}_n^r(i-1, j)) > SEI_a(\mathbb{T}_n^r(i, j)), a > 1, i > 3$ .
- (b)  $SEI_a(\mathbb{T}_n^r(i, j-1)) > SEI_a(\mathbb{T}_n^r(i, j)), a > 1, j > 3$ .
- (c)  $SEI_a(\mathbb{T}_n^{r-1}(i, j)) > SEI_a(\mathbb{T}_n^r(i, j)), a > 1, r > 1$ .

*Proof.* By the definition of  $SEI_a(G)$ ,

$$\begin{aligned} \theta &= SEI_a(\mathbb{T}_n^r(i-1, j)) - SEI_a(\mathbb{T}_n^r(i, j)) \\ &= [(k+4)a^{k+4} - (k+3)a^{k+3}] - [2a^2 - a] \\ &= a^{\mu_2}(1 + \mu_2 \ln a) - a^{\mu_1}(1 + \mu_1 \ln a) > 0, \end{aligned} \quad (30)$$

where  $\mu_1 \in (1, 2), \mu_2 \in (k+3, k+4), \mu_2 > \mu_1, a > 1$ , and  $k = n+1-i-j-r$ . This implies that  $\theta > 0$ .

Proof of (ii) is the same as proof of (i).  $\square$

*Proof.* By the definition of  $SEI_a(G)$ ,

$$\begin{aligned} \theta &= SEI_a(\mathbb{T}_n^{r-1}(i, j)) - SEI_a(\mathbb{T}_n^r(i, j)) \\ &= [(k+4)a^{k+4} - (k+3)a^{k+3}] - [2a^2 - a] \\ &= a^{\mu_2}(1 + \mu_2 \ln a) - a^{\mu_1}(1 + \mu_1 \ln a) > 0, \end{aligned} \quad (31)$$

where  $\mu_1 \in (1, 2), \mu_2 \in (k+3, k+4), \mu_2 > \mu_1, a > 1$ . This implies that  $\theta > 0$ .

$SEI_a(\mathbb{T}_n^{r-1}(i, j)) > SEI_a(\mathbb{T}_n^r(i, j))$ . After proving Lemma 13 and Lemma 14, we are able to present the following theorem.  $\square$

**Theorem 7.** If  $G \in \mathbb{B}(i, j)$ , then  $SEI_a(G)$  will be maximal if  $G \cong \mathbb{T}_n(i, j)$  and for all  $i \geq 3, j \geq 3$ , the graph from  $\mathbb{B}(i, j)$  with maximum  $SEI_a$  is  $\mathbb{T}_n(3, 3)$ .

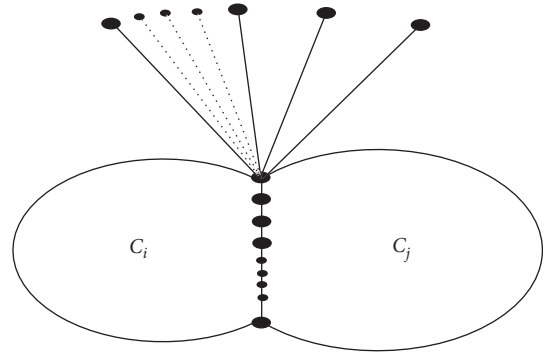


FIGURE 5:  $\Lambda_n^l(i, j)$  graphs.

**6.3. Extremal Graphs in  $\mathbb{C}(i, j, l)$ .** Here we define that  $\Lambda_n^l(i, j)$  is a graph which is obtained by attaching  $n+l+1-i-j$  edges to one of the vertices of degree 3 in  $G \in \mathbb{C}(i, j, l)$  (see Figure 5). Here we define some lemmas but skip their proofs. We refer Lemma 13 and Lemma 14 for the proof of following lemmas.

**Lemma 15.** Let  $G \in \mathbb{C}(i, j, l)$ ; if  $G \neq \Lambda_n^l(i, j)$ , then  $SEI_a(G) < SEI_a(\Lambda_n^l(i, j))$  for  $a > 1$ .

**Lemma 16.** Let  $\Lambda_n^l(i, j) \in \mathbb{C}(i, j, l)$ ; then,

- (a)  $SEI_a(\Lambda_n^l(i-1, j)) > SEI_a(\Lambda_n^l(i, j)), i > 3$ .
- (b)  $SEI_a(\Lambda_n^l(i, j-1)) > SEI_a(\Lambda_n^l(i, j)), j > 3$ .
- (c)  $SEI_a(\Lambda_n^{l-1}(i, j)) > SEI_a(\Lambda_n^l(i, j)), l > 1$ .

**Theorem 8.** For  $a > 1$  and the graph from the collection  $\mathbb{C}(i, j, l)$  with maximum  $SEI_a(G)$  for all  $i \geq 3, j \geq 3$  and  $l > 1$  is  $\Lambda_n^1(3, 3)$ .

**Theorem 9.** A graph  $G \in \mathbb{G}(n, n+1)$  has maximum variable sum exdeg index if and only if  $G \cong \Lambda_n^1(3, 3)$  for  $a > 1$ .

*Proof.* Since  $\mathbb{S}_n(3, 3), \mathbb{T}_n^1(3, 3)$ , and  $\Lambda_n^1(3, 3)$  belong to  $\mathbb{G}(n, n+1)$ . All the previous lemmas and theorems make it very clear and easy to understand that  $\mathbb{S}_n(3, 3), \mathbb{T}_n^1(3, 3)$ , and  $\Lambda_n^1(3, 3)$  have maximum  $SEI_a(G)$ , and  $\mathbb{S}_n(3, 3), \mathbb{T}_n^1(3, 3)$ , and  $\Lambda_n^1(3, 3)$  belong to  $\mathbb{A}(i, j), \mathbb{B}(i, j)$ , and  $\mathbb{C}(i, j, l)$ , respectively, for  $n \geq 6$ . Now we just need to compare the  $SEI_a$  of  $\mathbb{S}_n(3, 3), \mathbb{T}_n^1(3, 3)$ , and  $\Lambda_n^1(3, 3)$ .

$$\begin{aligned} \theta_1 &= SEI_a(\Lambda_n^1(3, 3)) - SEI_a(\mathbb{S}_n(3, 3)) \\ &= [(n-1)a^{n-1} + 3a^3 + 2.2a^2 + (n-4)a] \\ &\quad - [(n-1)a^{n-1} + 4.2a^2 + (n-5)a] \\ &= 3a^3 - 2.2a^2 + (n-5)a > 0. \end{aligned} \quad (32)$$

This implies that  $\theta_1 > 0$ .

$$\begin{aligned}
\theta_2 &= \text{SEI}_a(\mathbb{S}_n(3, 3)) - \text{SEI}_a(\mathbb{T}_n^1(3, 3)) \\
&= [(n-1)a^{n-1} + 4.2a^2 + (n-5)a] \\
&\quad - [(n-3)a^{n-3} + 4.2a^2 + 3a^3 + (n-6)a] \quad (33) \\
&= [(n-1)a^{n-1} - (n-3)a^{n-3}] - [3a^3 - a] \\
&= 2[a^{\mu_2}(1 + \mu_2 \ln a) - a^{\mu_1}(1 + \mu_1 \ln a)] > 0,
\end{aligned}$$

where  $\mu_1 \in (1, 3)$ ,  $\mu_2 \in (n-3, n-1)$ ,  $\mu_2 > \mu_1$ ,  $a > 1$ . This implies that  $\theta_2 > 0$ . From the above discussion, we conclude that  $\Lambda_n^1(3, 3) > \mathbb{S}_n(3, 3) > \mathbb{T}_n^1(3, 3)$ .  $\square$

## 7. Conclusion

Ascertaining the upper and lower bounds on any molecular structure descriptor with regard to various graph parameters is a significant job. We have sought the maximum value of  $\text{SEI}_a$  for unicyclic graphs. Sharp bounds have also been investigated for conjugated trees and conjugated unicyclic graphs. We also investigated the extremal graphs for each upper and lower bounds. Following are the main points of conclusion.

- (i) We have provided maximum and minimum values of  $\text{SEI}_a$  for conjugated trees.
- (ii) We have also provided lower and upper bounds of  $\text{SEI}_a$  for unicyclic conjugated graphs with respect to the length of this cycle.
- (iii) At the end of this paper, we have determined the maximum value of  $\text{SEI}_a$  for bicyclic graphs or  $(n, n+1)$  – graphs.

## Data Availability

The data used to support the findings of this study are included within the article. However, the reader may contact the corresponding author for more details of the data.

## Conflicts of Interest

The authors declare that they have no conflicts of interest.

## References

- [1] E. Estrada and D. Bonchev, "Chemical graph theory," in *Handbook of Graph Theory*, Y. Gross, Ed., pp. 1538–1558, CRC Press, Boca Raton, FL, USA, 2nd edition, 2013.
- [2] N. Trinajstić, *Chemical Graph Theory*, CRC Press, Boca Raton, FL, USA, 2nd edition, 1992.
- [3] H. Van De Waterbeemd, R. E. Carter, G. Grassy et al., "Glossary of terms used in computational drug design (IUPAC Recommendations 1997)," *Pure and Applied Chemistry*, vol. 69, no. 5, pp. 1137–1152, 1997.
- [4] I. Gutman and B. Furtula, *Novel Molecular Structure Descriptors Theory and Applications, I-II*, Kragujevac university Kragujevac, Kragujevac, Serbia, 2010.
- [5] R. Todeschini and V. Consonni, *Handbook of Molecular Descriptors*, Wiley VCH, Hoboken, NY, USA, 2000.
- [6] M. V. Diudea, *QSPR/QSAR Studies by Molecular Descriptors*, NOVA, Nagoya, Japan, 2001.
- [7] J. Devillers and A. T. Balaban, *Topological Indices and Related Descriptors in QSAR and QSPR*, Gordon & Breach, Amsterdam, Netherlands, 1999.
- [8] L. A. J. Muller, K. G. Kugler, A. Graber, and Dehmer, "A network-base approach to classify the three domains of life," *Biology Direct*, vol. 6, pp. 140–141, 2011.
- [9] H. Wiener, "Structural determination of paraffin boiling points," *Journal of the American Chemical Society*, vol. 69, pp. 17–20, 1947.
- [10] J. R. Platt, "Prediction of isomeric differences in paraffin properties," *Journal of Physical Chemistry*, vol. 56, pp. 328–336, 1952.
- [11] I. Gutman and N. Trinajstić, "Graph theory and molecular orbitals. Total  $\phi$ -electron energy of alternant hydrocarbons," *Chemical Physics Letters*, vol. 17, no. 4, pp. 535–538, 1972.
- [12] A. Ali and D. Dimitrov, "On the extremal graphs with respect to bond incident degree indices," *Discrete Applied Mathematics*, vol. 238, pp. 32–40, 2018.
- [13] A. Ghalavand and A. R. Ashra, "Extremal graph with respect to variable sum exdeg index via majorization," *Applied Mathematics and Computation*, vol. 303, pp. 19–23, 2017.
- [14] A. Mehler, P. Wei, and A. Lucking, "A network model of interpersonal alignment entropy," *Entropy*, vol. 12, pp. 1440–1483, 2010.
- [15] D. Vukicevic, "Bond additive modelling 4. QSPR and QSAR studies of the variable Adriatic indices," *Croatica Chemica Acta*, vol. 41, no. 1, pp. 87–91, 2011.
- [16] W. Gao, M. K. Jamil, A. Javed, M. R. Farhani, S. Wang, and J. B. Liu, "Sharp bounds of the hyper-zagreb index on acyclic, unicyclic and bicyclic graphs," *Discrete Dynamics in Nature and Society*, vol. 2017, Article ID 6079450, 5 pages, 2017.
- [17] A. Ghalavand and A. R. Ashrafi, "Extremal graphs with respect to variable sum exdeg index via majorization," *Applied Mathematics and Computation*, vol. 303, pp. 19–23, 2017.
- [18] A. Ilic and B. Zhou, "On reformulated Zagreb indices," *Discrete Applied Mathematics*, vol. 160, pp. 204–209, 2012.
- [19] S. Ji, X. Li, and B. Huo, "On reformulated zagreb indices with respect to acyclic, unicyclic and bicyclic graphs," *MATCH Communications in Mathematical and in Computer Chemistry*, vol. 72, no. 3, pp. 723–732, 2014.
- [20] D. Vukicevic, "Bond additive modelling 5. Mathematical properties of the variable sum exdeg index," *Croatica Chemica Acta*, vol. 84, no. 1, pp. 93–101, 2011.
- [21] D. Vukicevic, "Bond additive modelling 1. Mathematical properties of the variable sum exdeg index," *Croatica Chemica Acta*, vol. 83, pp. 243–260, 2010.
- [22] D. Vukicevic, "Bond additive modelling 6. randomness vs. design," *Communications in Mathematical and in Computer Chemistry*, vol. 65, pp. 415–426, 2011.
- [23] Z. Yarahmadi and A. R. Ashrafi, "The exdeg polynomial of some graph operations and applications in nanoscience," *Journal of Computational and Eoretical Nanoscience*, vol. 12, pp. 45–51, 2015.
- [24] J. A. Bondy, *Murty Graph Theory*, Springer, Berlin, Germany, 2008.
- [25] R. Diestel, *Graph Theory*, Springer, Berlin, Germany, 2005.
- [26] H. Hua, M. Wang, and H. Wang, "On zeroth order general Randić index of conjugated unicyclic graphs," *Journal of Mathematical Chemistry*, vol. 43, pp. 737–748, 2007.

## Research Article

# On Computation and Analysis of Entropy Measures for Crystal Structures

Muhammad Kamran Siddiqui,<sup>1</sup> Shazia Manzoor,<sup>1</sup> Sarfraz Ahmad,<sup>1</sup>  
and Mohammed K. A. Kaabar <sup>2</sup>

<sup>1</sup>Department of Mathematics, COMSATS University Islamabad, Lahore Campus, Lahore 54000, Pakistan

<sup>2</sup>Jabalia Camp, United Nations Relief and Works Agency (UNRWA) Palestinian Refugee Camp, Gaza Strip, Jabalya, State of Palestine

Correspondence should be addressed to Mohammed K. A. Kaabar; mohammed.kaabar@wsu.edu

Received 28 March 2021; Accepted 10 June 2021; Published 28 June 2021

Academic Editor: Kamal Shah

Copyright © 2021 Muhammad Kamran Siddiqui et al. This is an open access article distributed under the Creative Commons Attribution License, which permits unrestricted use, distribution, and reproduction in any medium, provided the original work is properly cited.

In recent years, the study of topological indices associated to different molecular tubes and structures gained a lot of attention of the researchers—working in Chemistry and Mathematics. These descriptors play an important role in describing different properties associated to the objects of study. Moreover, Shannon's entropy concept—a slightly different but more effective approach—provides structural information related to the molecular graphs. In this article, we have computed and analyzed different entropy measures associated to different crystallographic structures. In particular, we have worked on the Zagreb entropies, hyper and augmented Zagreb entropies, and forgotten and Balaban entropies for the crystallographic structures of the cuprite  $\text{Cu}_2\text{O}$  and titanium difluoride  $\text{TiF}_2$ .

## 1. Introduction

The role of Graph Theory has been significantly improvised as applications in other areas of sciences, particularly in the direction of Chemical Graph Theory. Many researchers have been able to explore many new directions during last few years. However, there are plenty of gaps which need to be fixed in. The study of topological indices plays an important role in identifying many physical and chemical properties of the molecular structures of study. In recent time, another approach which is a bit different—but more effective—has been introduced in the literature, namely, using the concept of Shannon's entropy [1, 2]. Concoction graph hypothesis is a part of numerical science wherein devices of graph hypothesis are applied to demonstrate the compound wonder scientifically. In addition, it has been identified with the insignificant uses of graph postulate for subatomic disputes. This hypothesis contributes a noticeable job in the field of compound sciences; for details, see [3–5].

The graph entropy gauges that partner likelihood dissemination with components (vertices, edges, and so forth) of a diagram can be delegated inherent and outward measures. There are a few distinct kinds of such chart entropy measures [6]. The degree powers are very critical invariants and concentrated broadly in chart hypothesis and system science, and they are utilized as the data functionals to investigate the systems [7, 8]. Dehmer presented chart entropies dependent on data functionals, which catch auxiliary data and contemplate their properties [9, 10]. For increasingly broad exploration, Estrada and Hatano recommended a truly solid entropy ration for systems/charts [11] and considered the walk-based diagram entropies [12].

The idea of entropy was presented first in Shannon's celebrated paper [13] as “the entropy of a likelihood dissemination is known as a proportion of the unusualness of data content or a proportion of the liability of a framework.” Afterward, entropy was started to be applied to diagrams and substance systems. It was created for estimating the auxiliary

data of diagrams and substance systems. In 1955, Rashevsky [14] presented the idea of graph entropy dependent on the orders of vertex circles. As of late, diagram entropies have been broadly applied in a wide range of fields, for example, science, biology, and humanism [15, 16].

The entropy measures for diagrams have been generally applied in art, chemical engineering, and basic science (see [17]). This issue is mind boggling as it is not sure about which diagram class the ration ought to be assessed. We guess that the presented degree-based entropy can be utilized to quantify organize heterogeneity. It is important to note that the mentioned applications have been identified by taking into account the hidden information investigation issue [18, 19]. Be that as it may, the purported auxiliary translation should be examined too. Comprehensively, the applications for entopic organize measures extend from assessable erection portrayal in basic science or programming innovation to investigate natural or synthetic properties of subatomic charts [20]. This calls to look at what sort of basic multifaceted nature does the measure identify. Comparable entropy measures which depend on vertex-degrees to identify arrange heterogeneity have been presented by Solé and Valverde [21] and Tan and Wu [22].

Shannon's fundamental work [13] in the late nineteen-forties denotes the beginning stage of present day data hypothesis. Succeeding primary solicitations in semantics

and electrical building, data hypothesis was applied broadly in science (see [23, 24]). Subsequently, this strategy has been utilized for investigating living frameworks, e.g., natural and concoction frameworks by methods for charts. These applications have been discussed by both Rashevsky [14] and Trucco [25]. Here, the fundamental oddity was thinking about a structure as a result of a subjective correspondence [26]. With the guide of this knowledge, Shannon's entropy equations [13] were utilized to decide the basic data substance of a system [21]. In what follows, we survey in sequential request diagram entropy quantifies that have been utilized for considering organic and compound complexes [27–29].

In 2014, Chen et al. [30] presented the meaning of the entropy of edge prejudiced graph. At that point, the entropy of edge slanted graph is given as follows:

$$\text{ENT}_{\mathfrak{F}}(G) = - \sum_{r's' \in E(G)} \frac{\mathfrak{F}(r's')}{\sum_{rs \in E(G)} \mathfrak{F}(rs)} \log \left[ \frac{\mathfrak{F}(r's')}{\sum_{rs \in E(G)} \mathfrak{F}(rs)} \right]. \quad (1)$$

- (i) *The First Zagreb Entropy.* If  $\mathfrak{F}(rs) = \Theta(r) + \Theta(s)$ , then equation (1) is reduced and is called the first Zagreb entropy:

$$\text{ENT}_{M_1}(G) = \log(M_1(G)) - \frac{1}{(M_1(G))} \log \left[ \prod_{rs \in E(G)} [\Theta(r) + \Theta(s)]^{[\Theta(r) + \Theta(s)]} \right]. \quad (2)$$

- (ii) *The Second Zagreb Entropy.* If  $\mathfrak{F}(rs) = \Theta(r) \times \Theta(s)$ , then equation (1) is reduced and is called the second Zagreb entropy:

$$\text{ENT}_{M_2}(G) = \log(M_2(G)) - \frac{1}{(M_2(G))} \log \left[ \prod_{rs \in E(G)} [\Theta(r) \times \Theta(s)]^{[\Theta(r) \times \Theta(s)]} \right]. \quad (3)$$

- (iii) *The Hyper Zagreb Entropy.* If  $\mathfrak{F}(rs) = [\Theta(r) + \Theta(s)]^2$ , then equation (1) is reduced and is called the hyper Zagreb entropy:

$$\text{ENT}_{\text{HM}}(G) = \log(\text{HM}(G)) - \frac{1}{(\text{HM}(G))} \log \left[ \prod_{rs \in E(G)} [(\Theta(r) + \Theta(s))^2]^{[(\Theta(r) + \Theta(s))^2]} \right]. \quad (4)$$

- (iv) *The Forgotten Entropy.* If  $\mathfrak{F}(rs) = [(\Theta(r))^2 + (\Theta(s))^2]$ , then equation (1) is reduced and is called the forgotten entropy:

$$\text{ENT}_F(G) = \log(F(G)) - \frac{1}{(F(G))} \log \left[ \prod_{rs \in E(G)} [(\Theta(r))^2 + (\Theta(s))^2]^{[(\Theta(r))^2 + (\Theta(s))^2]} \right]. \quad (5)$$

(v) *The Augmented Zagreb Entropy.* If  $\mathfrak{F}(rs) = (\Theta(r)\Theta(s)/\Theta(r) + \Theta(s) - 2)^3$ , then equation (1)

is reduced and is called the augmented Zagreb entropy:

$$ENT_{AZI}(G) = \log(AZI(G)) - \frac{1}{(AZI(G))} \log \left[ \prod_{rs \in E(G)} \left[ \left( \frac{\Theta(r)\Theta(s)}{\Theta(r) + \Theta(s) - 2} \right)^3 \right]^{[(\Theta(r)\Theta(s)/\Theta(r) + \Theta(s) - 2)^3]} \right]. \quad (6)$$

(vi) *The Balaban Entropy.* If  $\mathfrak{F}(rs) = (q/q - p + 2) \times (1/\sqrt{\Theta(r)\Theta(s)})$ , then equation (1) is reduced and is called the Balaban entropy:

$$ENT_J(G) = \log(J(G)) - \frac{1}{(J(G))} \log \left[ \prod_{rs \in E(G)} \left[ \frac{q}{q - p + 2} \times \frac{1}{\sqrt{\Theta(r)\Theta(s)}} \right]^{[(q/q - p + 2) \times (1/\sqrt{\Theta(r)\Theta(s)})]} \right]. \quad (7)$$

For further details about these entropy measures, see [31–34].

graph of crystallographic erection of  $Cu_2O$  is depicted in Figures 1 and 2; see subtleties in [37].

## 2. Crystallographic Structure of $Cu_2O[m, n, t]$

The vertex partition and edge partition are depicted in Tables 1 and 2, respectively.

Among different progress metal oxides,  $Cu_2O$  has pulled in huge consideration as of late attributable to its predictable assets and nonpoisonous nature and rudimentary establishment progression [35]. These days, the promising utilizations of  $Cu_2O$  are particularly seen nearby mixture beams, sunlight-based cells, and catalysis [36]. The invention

### 2.1. Results for Crystallographic Structure of $Cu_2O[m, n, t]$

(i) *The First Zagreb Entropy.* We computed the first Zagreb index and first Zagreb entropy as follows:

$$M_1(G) = (48mnt - 8(mn + mt + nt) + 4m + 4n + 4t),$$

$$\begin{aligned} ENT_{M_1}(Cu_2O) &= \log(M_1) - \frac{1}{(M_1)} \log \left[ \prod_{rs \in E_1(G)} [\Theta(r) + \Theta(s)]^{[\Theta(r) + \Theta(s)]} \times \prod_{rs \in E_2(G)} [\Theta(r) + \Theta(s)]^{[\Theta(r) + \Theta(s)]} \right. \\ &\quad \left. \times \prod_{rs \in E_3(G)} [\Theta(r) + \Theta(s)]^{[\Theta(r) + \Theta(s)]} \right] \\ &= \log(M_1) - \frac{1}{(M_1)} \log [(4n + 4m + 4t - 8) \times (27)] \\ &\quad \times [(4nt + 4nm - 8m + 4mt - 8t - 8n + 12) \times (256)] \\ &\quad \times [(8nmt - 4nm + 4n + 4m - 4nt - 4mt + 4t - 4) \times (46656)], \end{aligned} \quad (8)$$

$$\begin{aligned} ENT_{M_1}(Cu_2O) &= \log((48mnt - 8mn - 8mt - 8nt + 4m + 4n + 4t)) \\ &\quad - \frac{\log([(4n + 4m + 4t - 8) \times (27)])}{((48mnt - 8mn - 8mt - 8nt + 4m + 4n + 4t))} \\ &\quad - \frac{\log([(4nt + 4nm - 8m + 4mt - 8t - 8n + 12) \times (256)])}{((48mnt - 8mn - 8mt - 8nt + 4m + 4n + 4t))} \\ &\quad - \frac{\log([(8nmt - 4nm + 4n + 4m - 4nt - 4mt + 4t - 4) \times (46656)])}{((48mnt - 8mn - 8mt - 8nt + 4m + 4n + 4t))}. \end{aligned}$$

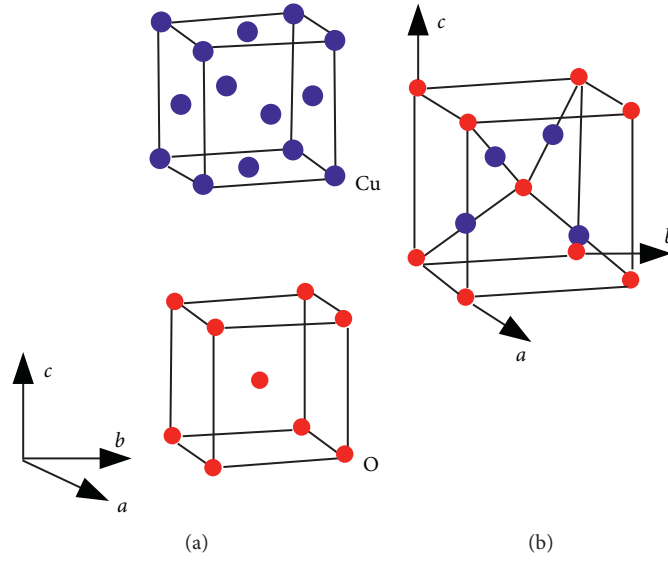


FIGURE 1: (a)  $\text{Cu}_2\text{O}$  lattice. (b) Unit cell of  $\text{Cu}_2\text{O}$ .

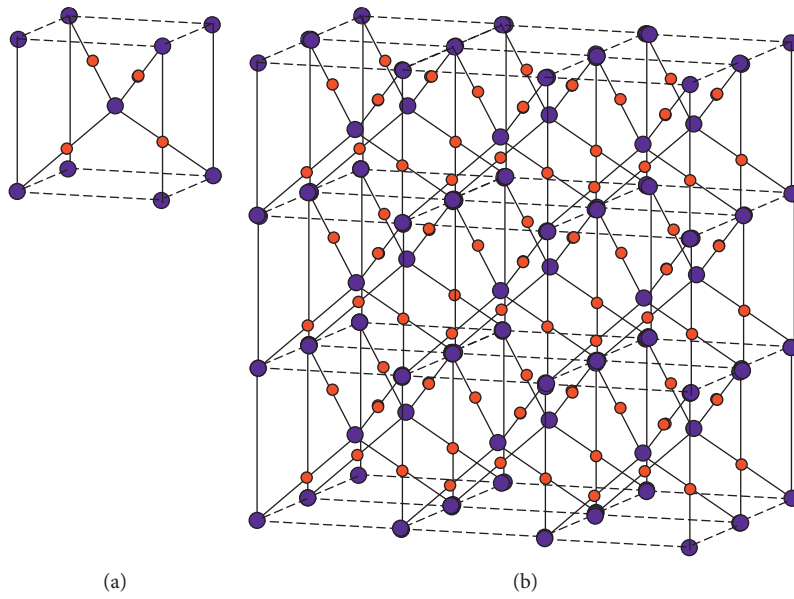


FIGURE 2: Crystallographic structure of  $\text{Cu}_2\text{O}[3, 2, 3]$ .

TABLE 1: Vertex partition of  $\text{Cu}_2\text{O}[m, n, t]$ .

$\Theta(r)$	Frequency	Set of vertices
1	$4t + 4m + 4n - 8$	$V_1$
2	$2mt - 4t + 2mn - 4n - 4mnt + 4m + 2nt + 6$	$V_2$
4	$n + m + t + 2mnt - mt - nm - nt - 1$	$V_3$

TABLE 2: Edge partition of  $\text{Cu}_2\text{O}[m, n, t]$ .

$(\Theta(r), \Theta(s))$	Frequency	Set of edges
(1, 2)	$4t + 4n + 4m - 8$	$E_1$
(2, 2)	$4mt + 4nt + 4nm - 8m - 8t - 8n + 12$	$E_2$
(2, 4)	$4m + 4n + 8mnt - 4nm - 4nt - 4mt + 4t - 4$	$E_3$

(ii) *The Second Zagreb Entropy.* We computed the second Zagreb index and second Zagreb entropy as follows:

$$\begin{aligned}
 M_2(G) &= (64mnt - 16mn - 16mt - 16nt + 8m + 8n + 8t), \\
 ENT_{M_2}(Cu_2O) &= \log(M_2) - \frac{1}{(M_2)} \log \left[ \prod_{rs \in E_1(G)} [\Theta(r) \times \Theta(s)]^{[\Theta(r) \times \Theta(s)]} \right. \\
 &\quad \left. \times \prod_{rs \in E_2(G)} [\Theta(r) \times \Theta(s)]^{[\Theta(r) \times \Theta(s)]} \times \prod_{rs \in E_3(G)} [\Theta(r) \times \Theta(s)]^{[\Theta(r) \times \Theta(s)]} \right] \\
 &= \log(M_2) - \frac{1}{(M_2)} \log [ [(4n + 4m + 4t - 8) \times (4)] \\
 &\quad \times [(4nt + 4nm - 8m + 4mt - 8t - 8n + 12) \times (256)] \\
 &\quad \times [(8rmt - 4nm + 4n + 4m - 4nt - 4mt + 4t - 4) \times (16777216)] ], \\
 ENT_{M_2}(Cu_2O) &= \log((64mnt + 8m - 16mn - 16nt + 8n - 16mt + 8t)) \\
 &\quad - \frac{\log [ [(4n + 4m + 4t - 8) \times (4)] ]}{((64mnt + 8m - 16mn - 16nt + 8n - 16mt + 8t))} \\
 &\quad - \frac{\log [(4nt + 4nm - 8m + 4mt - 8t - 8n + 12) \times (256)]}{((64mnt + 8m - 16mn - 16nt + 8n - 16mt + 8t))} \\
 &\quad - \frac{\log [ [(8rmt - 4nm + 4n + 4m - 4nt - 4mt + 4t - 4) \times (16777216)] ]}{((64mnt + 8m - 16mn - 16nt + 8n - 16mt + 8t))}.
 \end{aligned} \tag{9}$$

(iii) *The Hyper Zagreb Entropy of Cu<sub>2</sub>O[m, n, t].* We computed the hyper Zagreb index and hyper Zagreb entropy as follows:

$$\begin{aligned}
 HM(G) &= [8mnt - 80mn - 80mt - 80nt + 52m + 52n + 52t - 24], \\
 ENT_{HM}(Cu_2O) &= \log(HM) - \frac{1}{(HM)} \log \left[ \prod_{rs \in E_1(G)} [(\Theta(r) + \Theta(s))^2]^{[(\Theta(r) + \Theta(s))^2]} \right. \\
 &\quad \left. \times \prod_{rs \in E_2(G)} [(\Theta(r) + \Theta(s))^2]^{[(\Theta(r) + \Theta(s))^2]} \times \prod_{rs \in E_3(G)} [(\Theta(r) + \Theta(s))^2]^{[(\Theta(r) + \Theta(s))^2]} \right] \\
 &= \log(HM) - \frac{1}{(HM)} \log [ [(4n + 4m + 4t - 8) \times (9)] \\
 &\quad \times [(4nt + 4nm - 8m + 4mt - 8t - 8n + 12) \times (16)] \\
 &\quad \times [(8rmt - 4nm + 4n + 4m - 4nt - 4mt + 4t - 4) \times (36)] ], \\
 ENT_{HM}(Cu_2O) &= \log(8mnt - 80mn - 80mt - 80nt + 52m + 52n + 52t - 24) \\
 &\quad - \frac{\log [ [(4n + 4m + 4t - 8) \times (9)] ]}{(8mnt - 80mn - 80mt - 80nt + 52m + 52n + 52t - 24)} \\
 &\quad - \frac{\log [(4nt + 4nm - 8m + 4mt - 8t - 8n + 12) \times (16)]}{(8mnt - 80mn - 80mt - 80nt + 52m + 52n + 52t - 24)} \\
 &\quad - \frac{\log [ [(8rmt - 4nm + 4n + 4m - 4nt - 4mt + 4t - 4) \times (36)] ]}{(8mnt - 80mn - 80mt - 80nt + 52m + 52n + 52t - 24)}.
 \end{aligned} \tag{10}$$

(iv) *The Forgotten Entropy of Cu<sub>2</sub>O[m, n, t].* We computed the forgotten index and forgotten entropy as follows:

$$\begin{aligned}
 F(G) &= 36n + 36m + 36t - 24 - 48nm - 48nt - 48mt + 160nmt, \\
 ENT_F(Cu_2O) &= \log(F(G)) - \frac{1}{(F(G))} \log \left[ \prod_{rs \in E_1(G)} [(\Theta(r))^2 + (\Theta(s))^2]^{[(\Theta(r))^2 + (\Theta(s))^2]} \right. \\
 &\quad \times \prod_{rs \in E_2(G)} [(\Theta(r))^2 + (\Theta(s))^2]^{[(\Theta(r))^2 + (\Theta(s))^2]} \times \left. \prod_{rs \in E_3(G)} [(\Theta(r))^2 + (\Theta(s))^2]^{[(\Theta(r))^2 + (\Theta(s))^2]} \right] \\
 &= \log(F(G)) - \frac{1}{(F(G))} \log [ (4n + 4m + 4t - 8) \times (3125) ] \\
 &\quad \times [ (4nt + 4nm - 8m + 4mt - 8t - 8n + 12) \times (16777216) ] \\
 &\quad \times [ (8nmt - 4nm + 4n + 4m - 4nt - 4mt + 4t - 4) \times (1.048576 \times 10^{26}) ],
 \end{aligned} \tag{11}$$

$$\begin{aligned}
 ENT_F(Cu_2O) &= \log(36n + 36m + 36t - 24 - 48nm - 48nt - 48mt + 160nmt) \\
 &\quad - \frac{\log [ (4n + 4m + 4t - 8) \times (3125) ]}{(36n + 36m + 36t - 24 - 48nm - 48nt - 48mt + 160nmt)} \\
 &\quad - \frac{\log [ (4nt + 4nm - 8m + 4mt - 8t - 8n + 12) \times (16777216) ]}{(36n + 36m + 36t - 24 - 48nm - 48nt - 48mt + 160nmt)} \\
 &\quad - \frac{\log [ (8nmt - 4nm + 4n + 4m - 4nt - 4mt + 4t - 4) \times (1.048576 \times 10^{26}) ]}{(36n + 36m + 36t - 24 - 48nm - 48nt - 48mt + 160nmt)}.
 \end{aligned}$$

(v) *The Augmented Zagreb Entropy of Cu<sub>2</sub>O[m, n, t].* We computed the augmented Zagreb index and

augmented Zagreb entropy as follows:  
 $AZI(G) = 64nmt.$

$$\begin{aligned}
 ENT_{AZI}(Cu_2O) &= \log(AZI(G)) - \frac{1}{(AZI(G))} \\
 &\quad \cdot \log \left[ \prod_{rs \in E_1(G)} \left[ \left( \frac{\Theta(r)\Theta(s)}{\Theta(r) + \Theta(s) - 2} \right)^3 \right]^{[(\Theta(r)\Theta(s)/\Theta(r) + \Theta(s) - 2)^3]} \right. \\
 &\quad \times \prod_{rs \in E_2(G)} \left[ \left( \frac{\Theta(r)\Theta(s)}{\Theta(r) + \Theta(s) - 2} \right)^3 \right]^{[(\Theta(r)\Theta(s)/\Theta(r) + \Theta(s) - 2)^3]} \\
 &\quad \times \left. \prod_{rs \in E_3(G)} \left[ \left( \frac{\Theta(r)\Theta(s)}{\Theta(r) + \Theta(s) - 2} \right)^3 \right]^{[(\Theta(r)\Theta(s)/\Theta(r) + \Theta(s) - 2)^3]} \right] \\
 &= \log(AZI(G)) - \frac{1}{(AZI(G))} \log [ (4n + 4m + 4t - 8) \times (16777216) ] \\
 &\quad \times [ (4nt + 4nm - 8m + 4mt - 8t - 8n + 12) \times (16777216) ] \\
 &\quad \times [ (8nmt - 4nm + 4n + 4m - 4nt - 4mt + 4t - 4) \times (16777216) ], \\
 ENT_{AZI}(Cu_2O) &= \log(64nmt) - \frac{\log [ (4n + 4m + 4t - 8) \times (16777216) ]}{(64nmt)} \\
 &\quad - \frac{\log [ (4nt + 4nm - 8m + 4mt - 8t - 8n + 12) \times (16777216) ]}{(64nmt)} \\
 &\quad - \frac{\log [ (8nmt - 4nm + 4n + 4m - 4nt - 4mt + 4t - 4) \times (16777216) ]}{(64nmt)}.
 \end{aligned} \tag{12}$$



(vi) *The Balaban Entropy of Cu<sub>2</sub>O [m, n, t].* We computed the Balaban index and Balaban entropy as follows:

$$\begin{aligned}
 J(G) &= \frac{8mnt}{2mnt - mt - nt - t + 1 - mn - m - n} \\
 &\times \left[ \frac{1}{\sqrt{2}} (4n + 4m + 4t - 8) + \frac{1}{2} (4nt + 4nm - 8m + 4mt - 8t - 8n + 12) \right] \\
 &+ \frac{8mnt}{2mnt - mt - nt - t + 1 - mn - m - n} \times \left[ \frac{1}{\sqrt{8}} ((8mnt - 4nm + 4n + 4m - 4nt - 4mt + 4t - 4)) \right] \\
 &= \frac{8mnt}{2mnt - mt - nt - t + 1 - mn - m - n} \times \left[ \frac{\sqrt{2}}{2} (4n + 4m + 4t - 8) \right] \\
 &+ \frac{8mnt}{2mnt - mt - nt - t + 1 - mn - m - n} \times [2mn + 2nt + 2mt - 4n - 4m - 4t + 6] \\
 &+ \frac{8mnt}{2mnt - mt - nt - t + 1 - mn - m - n} \times \left[ \frac{\sqrt{2}}{2} (2nmt - nm - nt - mt + n + m + t - 1) \right],
 \end{aligned}$$

$$\text{ENT}_J(\text{Cu}_2\text{O}) = \log(J(G))$$

$$\begin{aligned}
 & - \frac{1}{(J(G))} \log \left[ \prod_{rs \in E_1(G)} \left[ \frac{q}{q-p+2} \times \frac{1}{\sqrt{\Theta(r)\Theta(s)}} \right]^{[(q/q-p+2) \times (1/\sqrt{\Theta(r)\Theta(s)})]} \right] \\
 & \times \prod_{rs \in E_2(G)} \left[ \frac{q}{q-p+2} \times \frac{1}{\sqrt{\Theta(r)\Theta(s)}} \right]^{[(q/q-p+2) \times (1/\sqrt{\Theta(r)\Theta(s)})]} \\
 & \times \prod_{rs \in E_3(G)} \left[ \frac{q}{q-p+2} \times \frac{1}{\sqrt{\Theta(r)\Theta(s)}} \right]^{[(q/q-p+2) \times (1/\sqrt{\Theta(r)\Theta(s)})]} \Bigg],
 \end{aligned} \tag{13}$$

$$\begin{aligned}
 \text{ENT}_J(\text{Cu}_2\text{O}) &= \log(J(G)) - \frac{1}{(J(G))} \log \left[ \left[ (4n + 4m + 4t - 8) \times \left[ \frac{q}{\sqrt{2}(q-p+2)} \right]^{[(q/\sqrt{2}(q-p+2))]} \right] \right. \\
 & \times \left[ (4nt + 4nm - 8m + 4mt - 8t - 8n + 12) \times \left[ \frac{q}{2(q-p+2)} \right]^{[(q/2(q-p+2))]} \right] \\
 & \left. \times \left[ (8mnt - 4nm + 4n + 4m - 4nt - 4mt + 4t - 4) \times \left[ \frac{q}{2\sqrt{2}(q-p+2)} \right]^{[(q/2\sqrt{2}(q-p+2))]} \right] \right],
 \end{aligned}$$

$$\begin{aligned}
 \text{ENT}_J(\text{Cu}_2\text{O}) &= \log(J(G)) - \frac{\log \left[ \left[ (4n + 4m + 4t - 8) \times [(q/\sqrt{2}(q-p+2))]^{[(q/\sqrt{2}(q-p+2))]} \right] \right]}{(J(G))} \\
 & - \frac{\log \left[ (4nt + 4nm - 8m + 4mt - 8t - 8n + 12) \times [(q/2(q-p+2))]^{[(q/2(q-p+2))]} \right]}{(J(G))} \\
 & - \frac{\log \left[ \left[ (8mnt - 4nm + 4n + 4m - 4nt - 4mt + 4t - 4) \times [(q/2\sqrt{2}(q-p+2))]^{[(q/2\sqrt{2}(q-p+2))]} \right] \right]}{(J(G))}.
 \end{aligned}$$

### 3. Crystallographic Structure of TiF<sub>2</sub> [m, n, t]

Titanium difluoride is a water inexplicable titanium cradle for use in oxygen-sensitive solicitations, such as iron invention. Fluoride mixtures have assorted solicitations in

existing machineries and science, from oil sanitizing and engraving to unreal animate chemistry and the fabrication of pharmaceuticals. The substance graph of mineral erection of titanium difluoride TiF<sub>2</sub> [m, n, t] is designated in Figure 3; for more details, see [38].

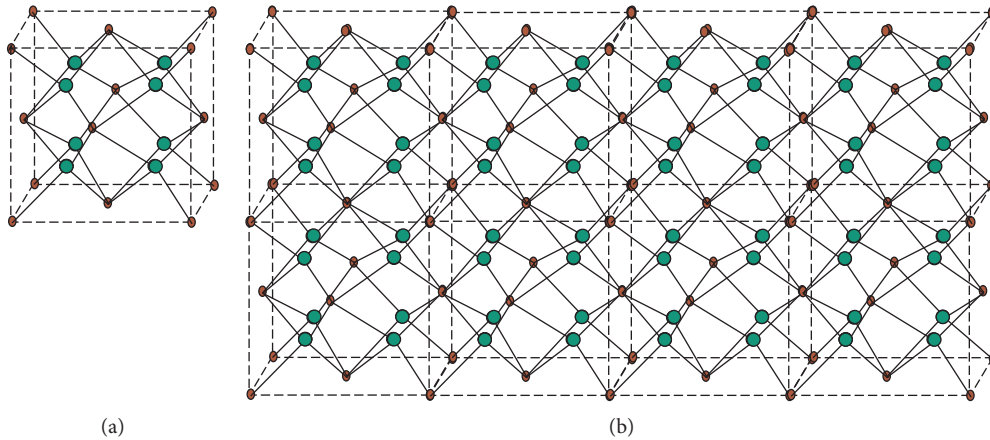


FIGURE 3: Crystal structure titanium difluoride  $\text{TiF}_2[m, n, t]$ : (a) unit cell of  $\text{TiF}_2[m, n, t]$ ; (b) crystal structure of  $\text{TiF}_2[4, 1, 2]$ .

The vertex partition and edge partition of  $\text{TiF}_2[m, n, t]$  are depicted in Tables 3 and 4.

### 3.1. Results for Crystallographic Structure of $\text{TiF}_2[m, n, t]$

(i) *The First Zagreb Entropy of  $\text{TiF}_2[m, n, t]$ .* We calculated the first Zagreb index and first Zagreb entropy as follows:

$$\begin{aligned}
 M_1(G) &= [384mnt - 64mn - 64mt - 64nt + 16m + 16n + 16t - 8], \\
 \text{ENT}_{M_1}(\text{TiF}_2) &= \log(M_1) - \frac{1}{(M_1)} \log \left[ \prod_{rs \in E_1(G)} [\Theta(r) + \Theta(s)]^{[\Theta(r) + \Theta(s)]} \right. \\
 &\quad \times \prod_{rs \in E_2(G)} [\Theta(r) + \Theta(s)]^{[\Theta(r) + \Theta(s)]} \\
 &\quad \times \left. \prod_{rs \in E_3(G)} [\Theta(r) + \Theta(s)]^{[\Theta(r) + \Theta(s)]} \times \prod_{rs \in E_4(G)} [\Theta(r) + \Theta(s)]^{[\Theta(r) + \Theta(s)]} \right] \\
 &= \log(M_1) - \frac{1}{(M_1)} \log [ [(8) \times (3125)] \times [((8m + 8t - 24 + 8n)) \times (46656)] \\
 &\quad \times [((16mn + 16mt + 16nt - 16m - 16n - 16t + 24)) \times (16777216)] \\
 &\quad \times [(32mnt - 16mt - 16mn - 16nt + 8m + 8n + 8t - 8) \times (8916100448456)] ], \\
 \text{ENT}_{M_1}(\text{TiF}_2) &= \log(384mnt - 64mn - 64mt - 64nt + 16m + 16n + 16t - 8) \\
 &\quad - \frac{\log [ [(8) \times (3125)] ]}{(384mnt - 64mn - 64mt - 64nt + 16m + 16n + 16t - 8)} \\
 &\quad - \frac{\log [ ((8m + 8n + 8t - 24)) \times (46656) \times (256) ]}{(384mnt - 64mn - 64mt - 64nt + 16m + 16n + 16t - 8)} \\
 &\quad - \frac{\log [ (((16mn + 16nt - 16n - 16t + 24 + 16mt - 16m)) \times (16777216)) ]}{(384mnt - 64mn - 64mt - 64nt + 16m + 16n + 16t - 8)} \\
 &\quad - \frac{\log [ [(32mnt - 16mt - 16mn - 16nt + 8m + 8n + 8t - 8) \times (8916100448456)] ]}{(384mnt - 64mn - 64mt - 64nt + 16m + 16n + 16t - 8)}.
 \end{aligned} \tag{14}$$

TABLE 3: Vertex partition of  $TiF_2[m, n, t]$ .

$\Theta(r)$	Frequency	Set of vertices
1	8	$V_1$
2	$4m + 4n + 4t - 12$	$V_2$
4	$4mn + 4mt - 4m - 4t + 6 + 8mnt + 4nt - 4n$	$V_3$
8	$n + t - 2(mn + mt + nt) - 1 + 4mnt + m$	$V_4$

TABLE 4: Edge partition of  $TiF_2[m, n, t]$ .

$(\Theta(r), \Theta(s))$	Frequency	Set of edges
(1, 4)	8	$E_1$
(2, 4)	$(8m + 8n + 8t - 24)$	$E_2$
(4, 4)	$16mn + 16mt - 16n - 16m + 16nt - 16t + 24$	$E_3$
(4, 8)	$8m + 8n + 16mn - 16nt + 8t - 8 + 32mnt - 16mt$	$E_4$

(ii) *The Second Zagreb Entropy of  $TiF_2[m, n, t]$ .* We computed the second Zagreb index and second Zagreb entropy as follows:

$$M_2(G) = [1024mnt - 256mn - 256mt - 256nt + 64m + 64n + 64t - 32],$$

$$ENT_{M_2}(TiF_2) = \log(M_2)$$

$$\begin{aligned}
 & - \frac{1}{(M_2)} \log \left[ \prod_{rs \in E_1(G)} [\Theta(r) \times \Theta(s)]^{[\Theta(r) \times \Theta(s)]} \times \prod_{rs \in E_2(G)} [\Theta(r) \times \Theta(s)]^{[\Theta(r) \times \Theta(s)]} \right. \\
 & \left. \times \prod_{rs \in E_3(G)} [\Theta(r) \times \Theta(s)]^{[\Theta(r) \times \Theta(s)]} \times \prod_{rs \in E_4(G)} [\Theta(r) \times \Theta(s)]^{[\Theta(r) \times \Theta(s)]} \right] \quad (15) \\
 & = \log(M_2) - \frac{1}{(M_2)} \log [ (8) \times (256) \times [ (8m + 8n + 8t - 24) \times (16777216) ] \\
 & \quad \times [ (16mn + 16nt - 16n - 16t + 24 + 16mt - 16m) \times (16)^{(16)} ] \\
 & \quad \times [ (32mnt - 16mt - 16mn - 16nt + 8m + 8n + 8t - 8) \times (32)^{(32)} ] ],
 \end{aligned}$$

$$ENT_{M_2}(TiF_2) = \log(1024mnt - 256mn - 256mt - 256nt + 64m + 64n + 64t - 32)$$

$$\begin{aligned}
 & - \frac{\log [ (8) \times (256) ]}{(1024mnt - 256mn - 256mt - 256nt + 64m + 64n + 64t - 32)} \\
 & - \frac{\log [ (8m + 8n + 8t - 24) \times (16777216) ]}{(1024mnt - 256mn - 256mt - 256nt + 64m + 64n + 64t - 32)} \quad (16) \\
 & - \frac{\log [ [ (16mn + 16nt - 16m + 16mt - 16n - 16t + 24) \times (16)^{(16)} ] ]}{(1024mnt - 256mn - 256mt - 256nt + 64m + 64n + 64t - 32)} \\
 & - \frac{\log [ [ (32mnt - 16mt - 16mn - 16nt + 8m + 8n + 8t - 8) \times (32)^{(32)} ] ]}{(1024mnt - 256mn - 256mt - 256nt + 64m + 64n + 64t - 32)}.
 \end{aligned}$$

- (iii) *The Hyper Zagreb Entropy of  $TiF_2[m, n, t]$ .* We computed the hyper Zagreb index and hyper Zagreb entropy as follows:

$$HM(G) = [4608mnt - 1280mn - 1280mt - 1280nt + 416m + 416n + 416t - 280],$$

$$ENT_{HM}(TiF_2) = \log(HM) - \frac{1}{(HM)}$$

$$\cdot \log \left[ \prod_{rs \in E_1(G)} [(\Theta(r) + \Theta(s))^2]^{[(\Theta(r) + \Theta(s))^2]} \times \prod_{rs \in E_2(G)} [(\Theta(r) + \Theta(s))^2]^{[(\Theta(r) + \Theta(s))^2]} \right. \\ \left. \times \prod_{rs \in E_3(G)} [(\Theta(r) + \Theta(s))^2]^{[(\Theta(r) + \Theta(s))^2]} \times \prod_{rs \in E_4(G)} [(\Theta(r) + \Theta(s))^2]^{[(\Theta(r) + \Theta(s))^2]} \right],$$

$$ENT_{HM}(TiF_2) = \log(HM) - \frac{1}{(HM)} \log \left[ [(8) \times (25)^{(25)}] \times [(8m + 8n + 8t - 24) \times (36)^{(36)}] \right.$$

$$\times [((16mn + 16nt - 16m + 16mt - 16n - 16t + 24)) \times (64)^{(64)}]$$

(17)

$$\times [(32mnt - 16mt - 16mn - 16nt + 8m + 8n + 8t - 8) \times (144)^{(144)}],$$

$$ENT_{HM}(TiF_2) = \log(4608mnt - 1280mn - 1280mt - 1280nt + 416m + 416n + 416t - 280)$$

$$- \frac{\log \left[ [(8) \times (25)^{(25)}] \right]}{(4608mnt - 1280mn - 1280mt - 1280nt + 416m + 416n + 416t - 280)}$$

$$- \frac{\log \left[ ((8m + 8n + 8t - 24) \times (36)^{(36)}) \right]}{(4608mnt - 1280mn - 1280mt - 1280nt + 416m + 416n + 416t - 280)}$$

$$- \frac{\log \left[ ((16mn + 16nt - 16m + 16mt - 16n - 16t + 24)) \times (64)^{(64)} \right]}{(4608mnt - 1280mn - 1280mt - 1280nt + 416m + 416n + 416t - 280)}$$

$$- \frac{\log \left[ ((32mnt - 16mt - 16mn - 16nt + 8m + 8n + 8t - 8) \times (144)^{(144)}) \right]}{(4608mnt - 1280mn - 1280mt - 1280nt + 416m + 416n + 416t - 280)}$$

(iv) *The Forgotten Entropy of  $TiF_2[m, n, t]$ .* We computed the forgotten index and forgotten entropy as follows:

$$F(G) = 2560mnt - 216 + 288m + 288n + 288t - 768mn - 768mt - 768nt,$$

$$\begin{aligned} ENT_F(TiF_2) &= \log(F(G)) - \frac{1}{(F(G))} \log \left[ \prod_{rs \in E_1(G)} [(\Theta(r))^2 + (\Theta(s))^2]^{[(\Theta(r))^2 + (\Theta(s))^2]} \right. \\ &\quad \times \prod_{rs \in E_2(G)} [(\Theta(r))^2 + (\Theta(s))^2]^{[(\Theta(r))^2 + (\Theta(s))^2]} \\ &\quad \times \prod_{rs \in E_3(G)} [(\Theta(r))^2 + (\Theta(s))^2]^{[(\Theta(r))^2 + (\Theta(s))^2]} \times \left. \prod_{rs \in E_4(G)} [(\Theta(r))^2 + (\Theta(s))^2]^{[(\Theta(r))^2 + (\Theta(s))^2]} \right] \\ &= \log(F(G)) - \frac{1}{(F(G))} \log \left[ [(8) \times (17)^{(17)}] \times [(8m + 8n + 8t - 24) \times (20)^{(20)}] \right] \\ &\quad \times [(16mn + 16nt - 16n - 16t + 24 + 16mt - 16m) \times (32)^{(32)}] \\ &\quad \times [(32mnt - 16mt - 16mn - 16nt + 8m + 8n + 8t - 8) \times (80)^{(80)}], \end{aligned} \tag{18}$$

$$ENT_F(TiF_2) = \log(2560mnt - 216 + 288m + 288n + 288t - 768mn - 768mt - 768nt)$$

$$\begin{aligned} &- \frac{\log \left[ [(8) \times (17)^{(17)}] \right]}{(2560mnt - 216 + 288m + 288n + 288t - 768mn - 768mt - 768nt)} \\ &- \frac{\log \left[ ((8m + 8n + 8t - 24) \times (20)^{(20)}) \right]}{(2560mnt - 216 + 288m + 288n + 288t - 768mn - 768mt - 768nt)} \\ &- \frac{\log \left[ ((16mn + 16nt - 16n - 16t + 24 + 16mt - 16m) \times (32)^{(32)}) \right]}{(2560mnt - 216 + 288m + 288n + 288t - 768mn - 768mt - 768nt)} \\ &- \frac{\log \left[ [(32mnt - 16mt - 16mn - 16nt + 8m + 8n + 8t - 8) \times (80)^{(80)}] \right]}{(2560mnt - 216 + 288m + 288n + 288t - 768mn - 768mt - 768nt)}. \end{aligned}$$

- (v) *The Augmented Zagreb Entropy of  $\text{TiF}_2[m, n, t]$ .*  
We computed the augmented Zagreb index and augmented Zagreb entropy as follows:

$$\begin{aligned}
 \text{AZI}(\text{TiF}_2) &= \frac{67264}{3375} + \frac{76736}{3375}m + \frac{76736}{3375}n + \frac{76736}{3375}t - \frac{745472}{3375}mn - \frac{745472}{3375}mt - \frac{745472}{3375}nt + \frac{131072}{125}mnt, \\
 \text{ENT}_{\text{AZI}}(\text{TiF}_2) &= \log(\text{AZI}(G)) \\
 &\quad - \frac{1}{(\text{AZI}(G))} \log \left[ \prod_{rs \in E_1(G)} \left[ \left( \frac{\Theta(r)\Theta(s)}{\Theta(r) + \Theta(s) - 2} \right)^3 \right]^{(\Theta(r)\Theta(s)/\Theta(r) + \Theta(s) - 2)^3} \right] \\
 &\quad \times \prod_{rs \in E_2(G)} \left[ \left( \frac{\Theta(r)\Theta(s)}{\Theta(r) + \Theta(s) - 2} \right)^3 \right]^{(\Theta(r)\Theta(s)/\Theta(r) + \Theta(s) - 2)^3} \\
 &\quad \times \prod_{rs \in E_3(G)} \left[ \left( \frac{\Theta(r)\Theta(s)}{\Theta(r) + \Theta(s) - 2} \right)^3 \right]^{(\Theta(r)\Theta(s)/\Theta(r) + \Theta(s) - 2)^3} \\
 &\quad \times \prod_{rs \in E_4(G)} \left[ \left( \frac{\Theta(r)\Theta(s)}{\Theta(r) + \Theta(s) - 2} \right)^3 \right]^{(\Theta(r)\Theta(s)/\Theta(r) + \Theta(s) - 2)^3} \\
 &= \log(\text{AZI}(G)) - \frac{1}{(\text{AZI}(G))} \log \left[ \left[ (8) \times \left( \frac{64}{27} \right)^{(64/27)} \right] \times [(8m + 8n + 8t - 24) \times (8)^{(8)}] \right. \\
 &\quad \times \left[ ((16mn + 16nt - 16n - 16t + 24 + 16mt - 16m)) \times \left( \frac{512}{27} \right)^{(512/27)} \right] \\
 &\quad \left. \times \left[ (32mnt - 16mt - 16mn - 16nt + 8m + 8n + 8t - 8) \times \left( \frac{4096}{125} \right)^{(4096/125)} \right] \right], \\
 \text{ENT}_{\text{AZI}}(\text{TiF}_2) &= \log(\text{AZI}(\text{TiF}_2)) - \frac{\log \left[ \left[ (8) \times \left( \frac{64}{27} \right)^{(64/27)} \right] \right]}{(\text{AZI}(\text{TiF}_2))} \\
 &\quad - \frac{\log \left[ ((8m + 8n + 8t - 24) \times (8)^{(8)}) \right]}{(\text{AZI}(\text{TiF}_2))} \\
 &\quad - \frac{\log \left[ ((16mn + 16nt - 16n - 16t + 24 + 16mt - 16m)) \times \left( \frac{512}{27} \right)^{(512/27)} \right]}{(\text{AZI}(\text{TiF}_2))} \\
 &\quad - \frac{\log \left[ (32mnt - 16mt - 16mn - 16nt + 8m + 8n + 8t - 8) \times \left( \frac{4096}{125} \right)^{(4096/125)} \right]}{(\text{AZI}(\text{TiF}_2))}.
 \end{aligned} \tag{19}$$

#### 4. Comparisons and Discussion for $\text{Cu}_2\text{O}[m, n, t]$

We develop Tables 5 and 6 for tiny estimations of  $m, n, t$  for the structure of  $\text{Cu}_2\text{O}[m, n, t]$ . The graphical portrayals of registered outcomes area unit as described in Figures 4–6 for specific estimations of  $m, n, t$ .

#### 5. Comparisons and Discussion for $\text{TiF}_2[m, n, t]$

Presently, from Tables 7 and 8, we are able to notice that while there is not much of a stretch, we see that each one of the estimations of entropy is in increasing request because the estimations of  $m, n, t$  are increments. The graphical portrayals

TABLE 5: Comparison of  $ENT_{M_1}$  and  $ENT_{M_2}$  for  $Cu_2O[m, n, t]$ .

$[m, n, t]$	$ENT_{M_1}$	$ENT_{M_2}$
[1, 1, 1]	1.12	1.21
[2, 2, 2]	1.42	1.61
[3, 3, 3]	1.82	1.91
[4, 4, 4]	2.12	2.51
[5, 5, 5]	3.41	3.32

TABLE 6: Comparison of  $ENT_{HM}$ ,  $ENT_F$ ,  $ENT_{AZI}$ , and  $ENT_J$  entropies for  $Cu_2O[m, n, t]$ .

$[m, n, t]$	$ENT_{HM}$	$ENT_F$	$ENT_{AZI}$	$ENT_J$
[1, 1, 1]	2.12	2.41	2.22	2.42
[2, 2, 2]	3.65	3.52	3.52	3.41
[3, 3, 3]	4.54	4.65	4.42	4.81
[4, 4, 4]	5.25	5.74	5.32	5.51
[5, 5, 5]	6.43	6.68	6.21	6.72

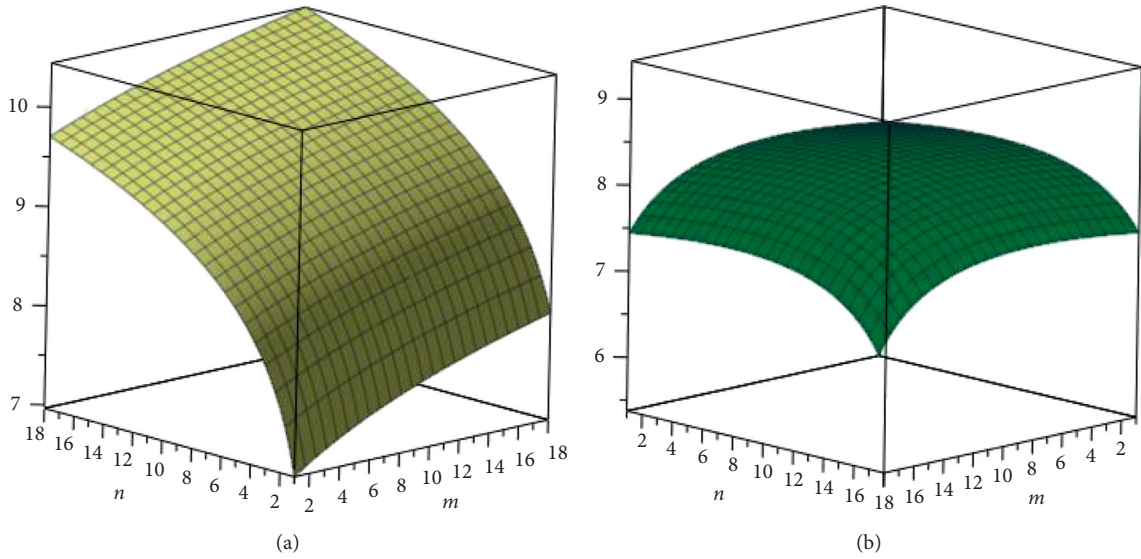


FIGURE 4: (a) The first Zagreb entropy. (b) The second Zagreb entropy.

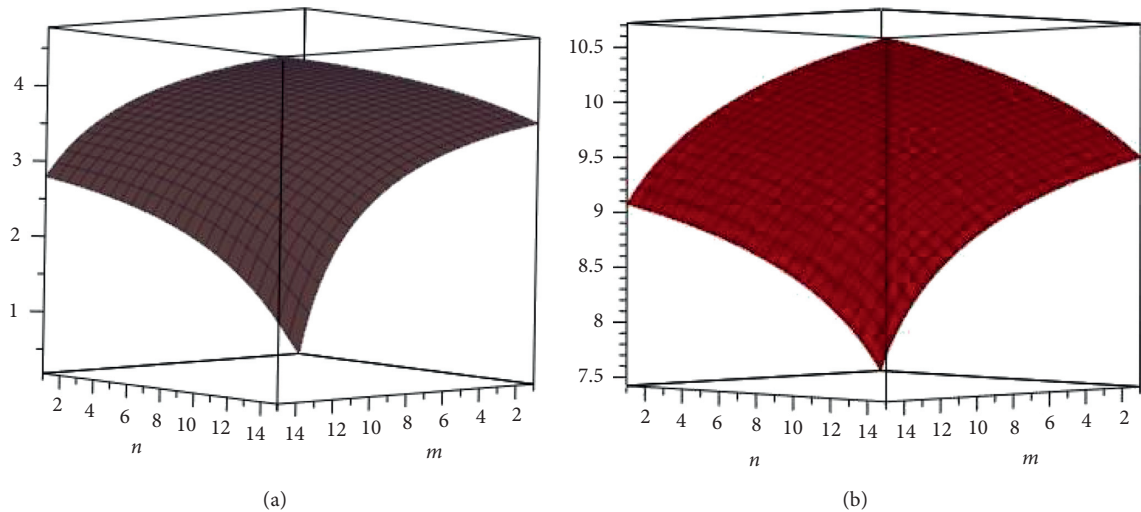


FIGURE 5: (a) The hyper Zagreb entropy. (b) The forgotten entropy.

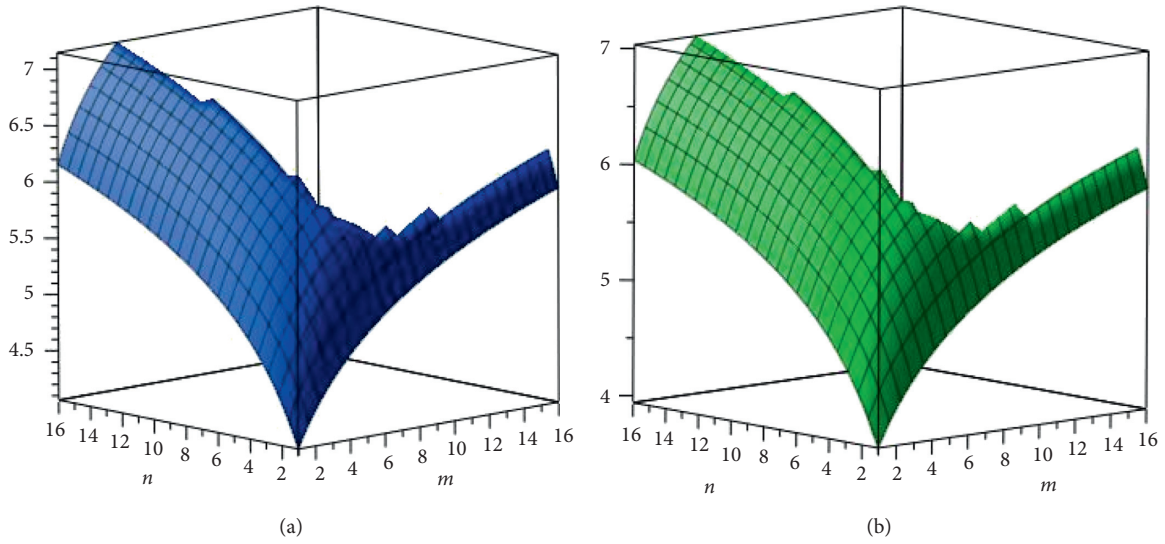


FIGURE 6: (a) The augmented Zagreb entropy. (b) The Balaban entropy.

TABLE 7: Comparison of  $ENT_{M_1}$  and  $ENT_{M_2}$  for  $TiF_2[m, n, t]$ .

$[m, n, t]$	$ENT_{M_1}$	$ENT_{M_2}$
[1, 1, 1]	1.22	1.31
[2, 2, 2]	1.62	1.81
[3, 3, 3]	1.92	2.31
[4, 4, 4]	2.32	2.91
[5, 5, 5]	3.61	3.42

TABLE 8: Comparison of  $ENT_{HM}$ ,  $ENT_F$ ,  $ENT_{AZI}$ , and  $ENT_j$  entropies for  $TiF_2[m, n, t]$ .

$[m, n, t]$	$ENT_{HM}$	$ENT_F$	$ENT_{AZI}$	$ENT_j$
[1, 1, 1]	2.02	2.21	2.12	2.32
[2, 2, 2]	3.45	3.32	3.42	3.51
[3, 3, 3]	4.34	4.45	4.52	4.71
[4, 4, 4]	5.55	5.54	5.62	5.41
[5, 5, 5]	6.63	6.88	6.31	6.22

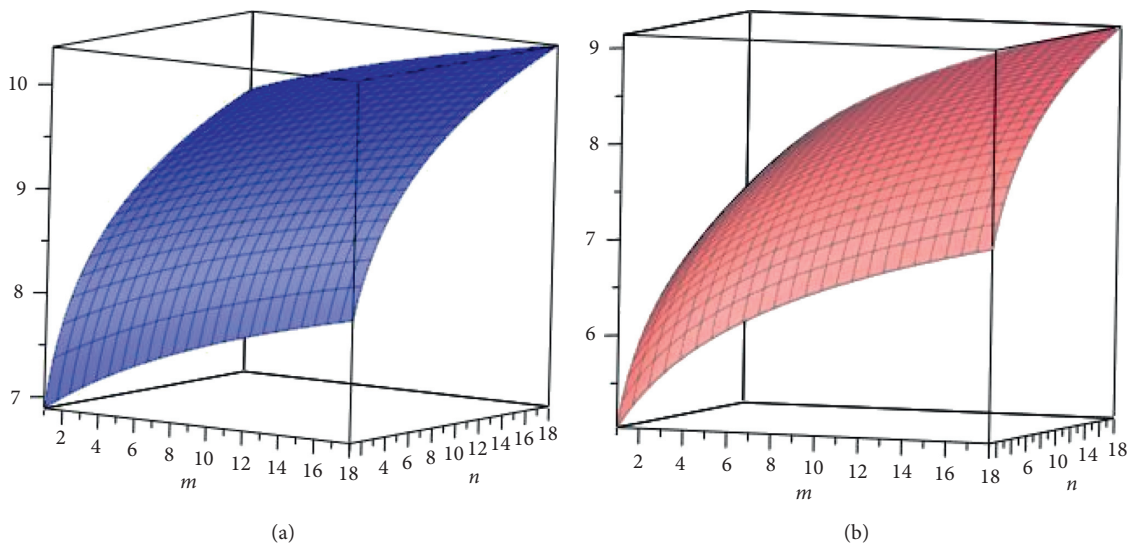


FIGURE 7: (a) The first Zagreb entropy. (b) The second Zagreb entropy.



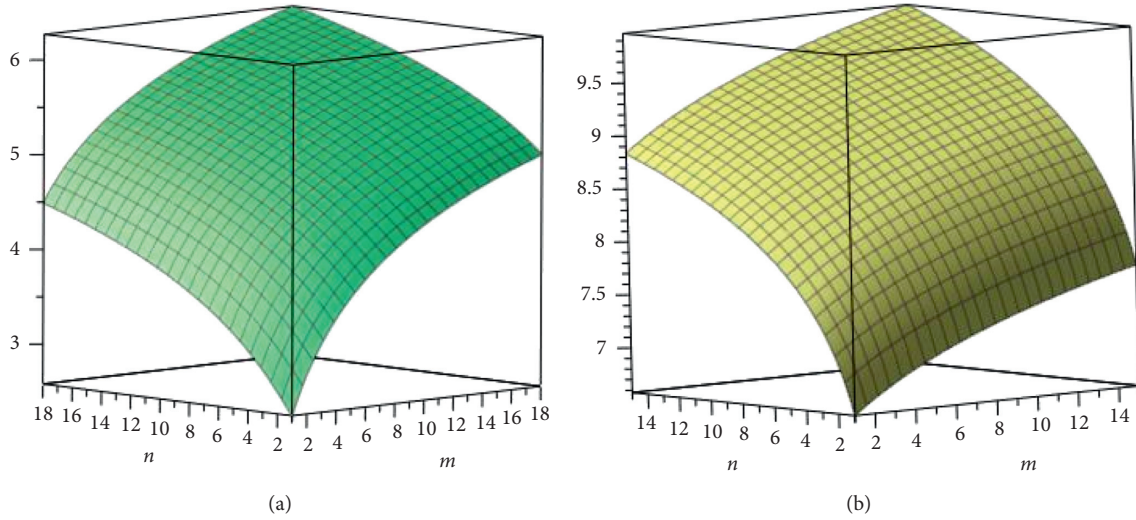


FIGURE 8: (a) The hyper Zagreb entropy. (b) The forgotten entropy.

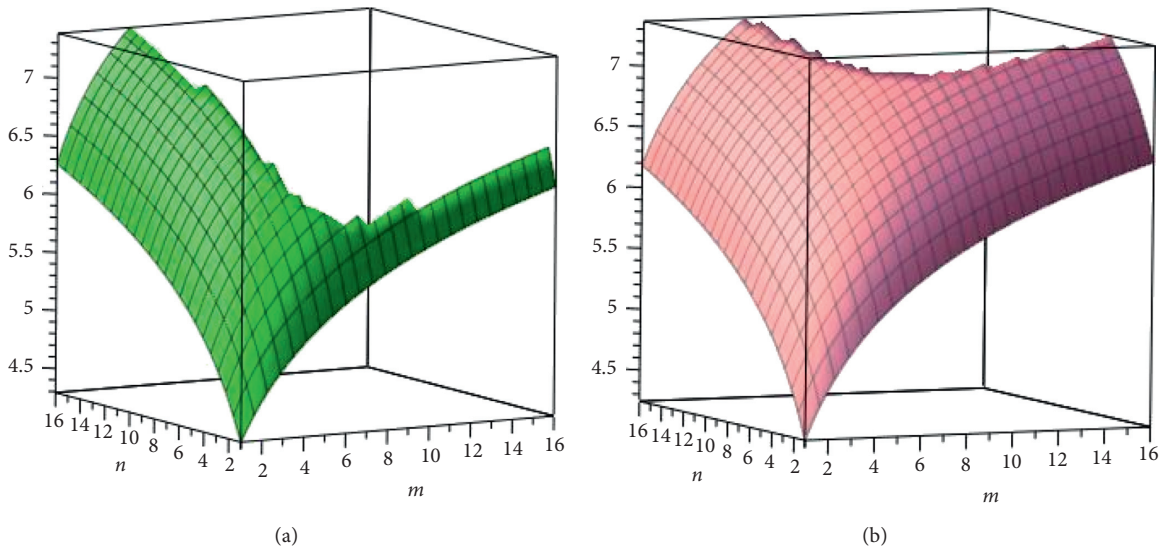


FIGURE 9: (a) The augmented Zagreb entropy. (b) The Balaban entropy.

of registered outcomes are diagrammatic in Figures 7–9 for specific estimations of  $m, n, t$ .

### 6. Conclusion

In this paper, in lightweight of applied scientist,  $s$  entropy, we have a tendency to study the graph entropies known with another information work. We have a tendency to present an association between the gradation established topological indices with gradation established entropies. We are particularly interested in forming the gradation that is based on entropies for crystallographic erection of oxide  $\text{Cu}_2\text{O}[m, n, t]$  and metal difluoride  $\text{TiF}_2[m, n, t]$ . In addition, the arithmetic estimations of these entropies have been registered in tables that provide the correlation between the gradation focused topological lists and gradation established

entropies that drives the United States of America to differentiate the physio-substance possessions of those crystallographic erection of  $\text{Cu}_2\text{O}[m, n, t]$  and  $\text{TiF}_2[m, n, t]$ .

### Data Availability

No data were used to support this study.

### Conflicts of Interest

The authors declare that they have no conflicts of interest.

### References

[1] W. Gao, M. K. Siddiqui, M. Naeem, and N. A. Rehman, “Topological characterization of carbon graphite and crystal

- cubic carbon structures," *Molecules*, vol. 22, no. 9, pp. 1496–1507, 2017.
- [2] M. Imran, M. K. Siddiqui, M. Naeem, and M. A. Iqbal, "On topological properties of symmetric chemical structures," *Symmetry*, vol. 10, pp. 1–21, 2018.
  - [3] W. Gao, H. Wu, M. K. Siddiqui, and A. Q. Baig, "Study of biological networks using graph theory," *Saudi Journal of Biological Sciences*, vol. 25, no. 6, pp. 1212–1219, 2018.
  - [4] M. K. Siddiqui, M. Imran, and A. Ahmad, "On zagreb indices, zagreb polynomials of some nanostar dendrimers," *Applied Mathematics and Computation*, vol. 280, pp. 132–139, 2016.
  - [5] M. K. Siddiqui, M. Naeem, N. A. Rahman, and M. Imran, "Computing topological indices of certain networks," *Journal of Optoelectronics and Advanced Materials*, vol. 18, no. 9-10, pp. 884–892, 2016.
  - [6] A. Mowshowitz and M. Dehmer, "Entropy and the complexity of graphs revisited," *Entropy*, vol. 14, no. 3, pp. 559–570, 2012.
  - [7] S. Cao, M. Dehmer, and Y. Shi, "Extremality of degree-based graph entropies," *Information Sciences*, vol. 278, pp. 22–33, 2014.
  - [8] S. Cao and M. Dehmer, "Degree-based entropies of networks revisited," *Applied Mathematics and Computation*, vol. 261, pp. 141–147, 2015.
  - [9] M. Dehmer, "Information processing in complex networks: graph entropy and information functionals," *Applied Mathematics and Computation*, vol. 201, no. 1-2, pp. 82–94, 2008.
  - [10] M. Dehmer, L. Sivakumar, and K. Varmuza, "Uniquely discriminating molecular structures using novel eigenvalue-based descriptors," *MATCH Communications in Mathematical and in Computer Chemistry*, vol. 67, pp. 147–172, 2012.
  - [11] E. Estrada and N. Hatano, "Statistical-mechanical approach to subgraph centrality in complex networks," *Chemical Physics Letters*, vol. 439, no. 1–3, pp. 247–251, 2007.
  - [12] E. Estrada, "Generalized walks-based centrality measures for complex biological networks," *Journal of Theoretical Biology*, vol. 263, no. 4, pp. 556–565, 2010.
  - [13] C. E. Shannon, "A mathematical theory of communication," *Bell System Technical Journal*, vol. 27, no. 3, pp. 379–423, 1948.
  - [14] N. Rashevsky, "Life, information theory, and topology," *The Bulletin of Mathematical Biophysics*, vol. 17, no. 3, pp. 229–235, 1955.
  - [15] M. Dehmer and M. Graber, "The discrimination power of molecular identification numbers revisited," *MATCH Communications in Mathematical and in Computer Chemistry*, vol. 69, pp. 785–794, 2013.
  - [16] R. E. Ulanowicz, "Quantitative methods for ecological network analysis," *Computational Biology and Chemistry*, vol. 28, no. 5-6, pp. 321–339, 2004.
  - [17] M. Dehmer and A. Mowshowitz, "A history of graph entropy measures," *Information Sciences*, vol. 181, no. 1, pp. 57–78, 2011.
  - [18] B. Furtula and I. Gutman, "A forgotten topological index," *Journal of Mathematical Chemistry*, vol. 53, no. 4, pp. 1184–1190, 2015.
  - [19] B. Furtula, A. Graovac, and D. Vukičević, "Augmented zagreb index," *Journal of Mathematical Chemistry*, vol. 48, no. 2, pp. 370–380, 2010.
  - [20] W. Wu, C. Zhang, W. Lin et al., "Quantitative structure-property relationship (QSPR) modeling of drug-loaded polymeric micelles via genetic function approximation," *PLoS One*, vol. 10, no. 3, Article ID e0119575, 2015.
  - [21] R. V. Solé and S. I. Valverde, "Information theory of complex networks: on evolution and architectural constraints," *Complex Networks*, vol. 650, pp. 189–207, 2004.
  - [22] Y. J. Tan and J. Wu, "Network structure entropy and its application to scale-free networks," *Systems Engineering-Theory & Practice*, vol. 6, pp. 1–3, 2004.
  - [23] H. Morowitz, "Some order-disorder considerations in living systems," *Bulletin of Mathematical Biophysics*, vol. 17, pp. 81–86, 1953.
  - [24] H. Quastler, "Information theory in biology," *Bulletin of Mathematical Biology*, vol. 8, pp. 183–185, 1954.
  - [25] E. Trucco, "A note on the information content of graphs," *The Bulletin of Mathematical Biophysics*, vol. 18, no. 2, pp. 129–135, 1956.
  - [26] D. Bonchev, *Complexity in Chemistry, Introduction and Fundamentals*, Taylor and Francis, Boca Raton, FL, USA, 2003.
  - [27] I. Gutman and N. Trinajstić, "Graph theory and molecular orbitals., total  $\pi$ -electron energy of alternant hydrocarbons," *Chemical Physics Letters*, vol. 17, no. 4, pp. 535–538, 1972.
  - [28] I. Gutman and K. C. Das, "The first zagreb index 30 years after," *MATCH Communication in Mathematical Computer Chemistry*, vol. 50, pp. 83–92, 2004.
  - [29] G. H. Shirdel, H. RezaPour, and A. M. Sayadi, "The hyper zagreb index of graph operations," *Iranian Journal of Mathematical Chemistry*, vol. 4, no. 2, pp. 213–220, 2013.
  - [30] Z. Chen, M. Dehmer, and Y. Shi, "A note on distance based graph entropies," *Entropy*, vol. 16, no. 10, pp. 5416–5427, 2014.
  - [31] S. Manzoor, M. K. Siddiqui, and S. Ahmad, "On physical analysis of degree-based entropy measures for metal-organic superlattices," *The European Physical Journal Plus*, vol. 136, no. 3, pp. 1–22, 2021.
  - [32] S. Manzoor, M. K. Siddiqui, and S. Ahmad, "Degree-based entropy of molecular structure of hyaluronic acid-curcumin conjugates," *The European Physical Journal Plus*, vol. 136, no. 1, pp. 1–21, 2021.
  - [33] S. Manzoor, Y. M. Chu, M. K. Siddiqui, and S. Ahmad, "On topological aspects of degree based entropy for two carbon nanosheets," *Main Group Metal Chemistry*, vol. 43, no. 1, pp. 205–218, 2020.
  - [34] S. Manzoor, M. K. Siddiqui, and S. Ahmad, "On entropy measures of molecular graphs using topological indices," *Arabian Journal of Chemistry*, vol. 13, no. 8, pp. 6285–6298, 2020.
  - [35] K. Chen, C. Sun, S. Song, and D. Xue, "Polymorphic crystallization of Cu<sub>2</sub>O compound," *CrystEngComm*, vol. 16, pp. 52–57, 2014.
  - [36] B. D. Yuhás and P. Yang, "Nanowire-based all-oxide solar cells," *Journal of the American Chemical Society*, vol. 131, no. 10, pp. 3756–3761, 2009.
  - [37] J. Zhang, J. Liu, Q. Peng, X. Wang, and Y. Li, "Nearly monodisperse Cu<sub>2</sub>O and NCuO nanospheres: preparation and applications for sensitive gas sensors," *Chemistry of Materials*, vol. 18, no. 4, pp. 867–871, 2006.
  - [38] F. A. Cotton, G. Wilkinson, C. A. Murillo, and M. Bochmann, *Advanced Inorganic Chemistry*, John Wiley and Sons, Hoboken, NJ, USA, 1999.

## Research Article

# Hypergraphical Metric Spaces and Fixed Point Theorems

Xiaodong Li <sup>1</sup>, Farhan Khan,<sup>2</sup> Gohar Ali <sup>3</sup>, Lubna Gul,<sup>3</sup> and Muhammad Sarwar <sup>2</sup>

<sup>1</sup>Huanghe Jiaotong University, Jiaozuo 454950, Henan, China

<sup>2</sup>Department of Mathematics, University of Malakand, Chakdara Dir (L), Khyber Pakhtunkhwa, Pakistan

<sup>3</sup>Department of Mathematics, Islamia College Peshawar, Khyber Pakhtunkhwa, Pakistan

Correspondence should be addressed to Xiaodong Li; [li-xiaodong-li@outlook.com](mailto:li-xiaodong-li@outlook.com), Gohar Ali; [gohar.ali@icp.edu.pk](mailto:gohar.ali@icp.edu.pk), and Muhammad Sarwar; [sarwarswati@gmail.com](mailto:sarwarswati@gmail.com)

Received 23 March 2021; Accepted 6 June 2021; Published 27 June 2021

Academic Editor: Ali Ahmad

Copyright © 2021 Xiaodong Li et al. This is an open access article distributed under the Creative Commons Attribution License, which permits unrestricted use, distribution, and reproduction in any medium, provided the original work is properly cited.

Hypergraph is a generalization of graph in which an edge can join any number of vertices. Hypergraph is used for combinatorial structures which generalize graphs. In this research work, the notion of hypergraphical metric spaces is introduced, which generalizes many existing spaces. Some fixed point theorems are studied in the corresponding spaces. To show the authenticity of the established work, nontrivial examples and applications are also provided.

## 1. Introduction

Graph theory has been used to study the various concepts of navigation in an arbitrary space. A work place can be denoted as a vertex in the language of graph theory, and edges denote the connections between these places (vertices). Hypergraph is a generalization of graph in which an edge can join any number of vertices. Hypergraph is used for combinatorial structures which generalize graphs. The applications of hypergraph can be found in Engineering sciences, many areas of Computer Science, and almost all areas of Mathematics.

Moreover, directed hypergraphs are used in computer science, particularly in the development of data mining, software testing, image segmentation and processing, information security, and communication networks.

## 2. Preliminaries

Frechet et al. initiated the concept of metric spaces in 1906, which open the door for entering into a more waste and new field in the world of mathematics. Upon this foundation, different researchers introduced different generalized metric spaces and studied various fixed point results with

applications. In this way, we refer some recent developments in [1–3]. About basic notions of graph theory, we refer to the readers [4–6] and references therein.

In 1736, Leonhard Euler put the framework of graph theory by studying the historical problem of seven bridges of Konigsberg and prefigured the concept of topology. Echinique [7] deliberated fixed point theory by using graph. Jachymsky [8] replaced the order structure with a graph structure on a metric space and studied the well-known Banach contraction principle. Aleomraninejad et al. [9] gave the concept of some fixed point results on metric space with a graph, in which they presented some iterative results for G-contractive and G-nonexpansive mappings on graphs. Samreen et al. [10] investigated some fixed point theorems in b-metric space endowed with graph. Argoubi et al. [11] presented some fixed point results and its applications by considering self-mappings defined on a metric space endowed with a finite number of graphs.

Shukhla et al. [12] gave the concept of graphical metric space which is a generalized setting in fixed point theory and established some fixed point results with applications. Abbas et al. [13] presented some fixed point results for set contractions on metric spaces with a directed graph. In 2017, Debanath and Neog [14] initiated the concept of start point

on a metric space endowed with a directed graph. They offered the alternate concept of start point in a directed graph and provided the characterizations which are necessary for a directed graph having start point. Kumam et al. [15] presented graphic contraction mapping in b-metric space and established some fixed point results with applications.

Motivated by the above results, combining the notion of hypergraph and metric, we introduced hypergraphical metric space which generalized the concept of graphical metric space. In hypergraphical metric space, vertices of graph are replaced by edges. Some conclusions, examples, and an application to integral equation are also presented to authenticate the acceptance and unifying power of obtained generalizations. For iterative numerical schemes, the interesting readers can refer the recent papers [16, 17].

### 3. Hypergraph and Hypergraphical Metrics

*Definition 1.* Hypergraph is real generalization of graph. The edges of hypergraph connect any number of nodes. Formally it is a pair, i.e.,  $G_H = (\zeta, \xi)$  in which  $\zeta$  represents set of vertices and  $\xi$  is a set of nonempty subsets of  $\zeta$  called hyperedges or simply edges.

*Definition 2.* Hypergraph  $G_H$  is said to be directed hypergraph if  $G_H = (V, \xi)$  where  $V \neq \emptyset$  is a finite set and is known as the set of nodes of  $G_H$  and  $\xi$  is the set of directed hyperedges, where a hyperedge or hyperarc  $e = (T(e), H(e))$  is a directed hyperedge with  $|T(e)| > 0$  and  $|H(e)| > 0$  and both are disjoint.  $H(e)$  and  $T(e)$  represent head and tail, respectively, where hyperedge ends and starts and contains set of nodes.

*Definition 3.* The size of directed hypergraph  $G_H$  is defined as the sum of the tail and head nodes of each hyperedge together with the number of nodes of the hypergraph, i.e.,  $|G_H| = |V| + \sum_{e \in \xi} (|T(e)| + |H(e)|)$ .

*Definition 4.* A directed path in a directed hypergraph is a sequence of nodes and hyperedges such that each edge points from a node in the sequence to its successor in the sequence.

Let  $G_H = (v, \xi)$  be a directed hypergraph and  $(v_i, v_j \in v)$  is a directed path from  $s$  to  $t$  in  $G_H$ , which represent the sequence  $(\pi_{s,t})$  of the form  $\pi_{s \rightarrow t} = (v_1, e_1, v_2, e_2, \dots, e_{n-1}, v_n)$ :  $n > 0$  such that  $v_i \in v, \forall i \in \{1, 2, 3, \dots, n\}$  and  $e_j \in \xi, \forall j \in \{1, 2, 3, \dots, n-1\}$ .  $v_1 \in s \implies v_1 \in T(e_1)$  and  $v_n = t \implies v_n \in H(e_{n-1}) \cap T(e_n), \forall i \in \{2, \dots, n-1\}$ .

*Definition 5.* The edges which connect other edges are called hyperdelta edges; that is, vertices of these edges are also edges and denoted by  $\Delta$ .

*Definition 6.* A hypergraph in which we assign numerical value, i.e., nonnegative real numbers  $[0, \infty)$  to their edges is called labeled graph.

*Definition 7* (see [12]). Let  $\zeta \neq \emptyset$  set endowed with graph  $G_m$  and  $d_{G_m}: \zeta * \zeta \rightarrow R$  be a function satisfying the following condition:

$$\begin{aligned} (GM_1). & d_{G_m}(a, b) = 0, \text{ if } a = b \\ (GM_2). & d_{G_m}(a, b) > 0, \text{ if } a \neq b \\ (GM_3). & d_{G_m}(a, b) = d_{G_m}(b, a), \forall a, b \in \zeta \\ (GM_4). & (apb)_{G_m}, \\ & c \in (apb)_{G_m} \text{ implies } d_{G_m}(a, b) \leq d_{G_m}(a, c) + \\ & d_{G_m}(c, b), \forall a, b, c \in \zeta \end{aligned}$$

Then, the mapping  $d_{G_m}$  is called a graphical metric on  $\zeta$ , and the pair  $(\zeta, d_{G_m})$  is called graphical metric space.

By combining the concept of hypergraph and graphical metric space, we introduced the following notion of hypergraphical metric spaces.

*Definition 8.* Suppose  $\zeta$  be a nonempty set endowed with hypergraph  $G_H$  such that  $V(G_H) = \zeta$  and let  $\xi$  represent hyperedges of  $G_H$  such that each hyperedge  $e$  represents nonempty subset of  $\zeta$ . Suppose the mapping  $d_{G_H}: \xi * \xi \rightarrow R$  satisfying the following condition:

$$\begin{aligned} (HGM_1). & d_{G_H}(e_i, e_j) = 0, \text{ if } e_i = e_j \\ (HGM_2). & d_{G_H}(e_i, e_j) > 0, \text{ if } e_i \neq e_j \\ (HGM_3). & d_{G_H}(e_i, e_j) = d_{G_H}(e_j, e_i), \forall e_i, e_j \in \xi \\ (HGM_4). & (e_i p e_j)_{G_H} \\ & e_k \in (e_i p e_j)_{G_H} \text{ implies } d_{G_H}(e_i, e_j) \leq d_{G_H}(e_i, e_k) + \\ & d_{G_H}(e_k, e_j), \forall e_i, e_j, e_k \in \xi \end{aligned}$$

Then,  $d_{G_H}$  is called a hypergraphical metric on  $\xi$ , and  $(\xi, d_{G_H})$  is said to be hypergraphical metric space.

*Remark 1.* We noted that hypergraphical metric space is the real generalization of graphical metric space; that is, every graphical metric space is hypergraphical metric but converse is not true.

*Example 1.* Let  $\zeta = \{v_1, v_2, v_3, v_4, v_5, v_6\}$  be the set of vertices, and let  $\xi = \{\{v_1\}, \{v_2\}, \{v_3\}, \{v_4, v_5, v_6\}\}$  which is composed by edges of hypergraph  $G_H$ . Now, let us define a function  $d_{G_H}: \xi * \xi \rightarrow R^+$  by

$$d_{G_H}(e_i, e_j) = \begin{cases} 0, & \text{if } e_i = e_j, \\ 5A, & \text{if } e_i, e_j \in \{\{v_1\}, \{v_2\}\} e_i \neq e_j, \\ 3A, & \text{if } e_i, e_j \in \{\{v_1\}, \{v_3\}\} e_i \neq e_j, \\ A, & \text{if } e_i, e_j \in \{\{v_2\}, \{v_3\}\} e_i \neq e_j, \\ 4A, & \text{if } e_i, e_j \in \{\{v_1\}, \{v_4, v_5, v_6\}\} e_i \neq e_j, \\ 6A, & \text{if } e_i, e_j \in \{\{v_2\}, \{v_4, v_5, v_6\}\} e_i \neq e_j, \\ 2A, & \text{if } e_i, e_j \in \{\{v_4, v_5, v_6\}, \{v_2\}\} e_i \neq e_j, \end{cases} \quad (1)$$

where  $A > 1$  is the positive real number. Evidently  $d_{G_H}$  is not a graphical metric because

$$d_{G_H}(\{v_1\}, \{v_2\}) \not\leq d_{G_H}(\{v_1\}, \{v_3\}) + d_{G_H}(\{v_3\}, \{v_2\}), \quad (2)$$

since  $5A > 3A + A$ .

On the other hand,

$$d_{G_H}(\{v_1\}, \{v_2\}) \leq d_{G_H}(\{v_1\}, \{v_4, v_5, v_6\}) + d_{G_H}(\{v_4, v_5, v_6\}, \{v_2\}). \quad (3)$$

In this case, we have  $5A \leq 4A + 6A$ . Therefore,  $d_{G_H}$  is the hypergraphical metric space.

Not every hypergraphical metric space is metric. Let us provide an example as follows.

*Example 2.* Let  $X = [0, 1]$ ; here,  $X$  interval means the weight of edges of  $G_H$ , where  $G_H$  be the hypergraph such that its edges can be defined as  $\xi_{G_H} = \Delta U\{e_i, e_j: e_i, e_j \in (1, 1)e_i \leq e_j \wedge i, j \in \mathbb{N}\}$ . Define a mapping  $d_{G_H}: \xi * \xi \rightarrow R^+$  by

$$d_{G_H}(e_i, e_j) = \begin{cases} 0, & \text{if } e_i = e_j; \\ e_i * e_j, & \text{if } e_i, e_j \in (0, 1]e_i \neq e_j; \\ e_i + e_j, & \text{otherwise.} \end{cases} \quad (4)$$

Then,  $d_{G_H}$  is a hypergraphical metric on  $\xi$  and  $(\xi, d_{G_H})$  is a hypergraphical metric space obviously where  $d_{G_H}$  not a metric on  $\xi$ .

*Definition 9.* Let  $(\xi, d_{G_H})$  be hypergraphical metric space. An open ball  $B_{G_H}(e, \epsilon)$  with center  $e$  and radius  $\epsilon$  is defined as

$$B_{G_H}(e, \epsilon) = \{e': (epe')_{G_H}, d_{G_H}(e, e') < \epsilon\}. \quad (5)$$

Since  $\xi(G_H) \supseteq \Delta$ , therefore, we have  $e \in B_{G_H}(e, \epsilon)$ . Hence,  $B_{G_H}(e, \epsilon)$  is nonempty  $\forall e \in \xi$  and  $\epsilon > 0$ . The collection

$$B = \{B_{G_H}(e, \epsilon): e \in \xi, \epsilon > 0\}, \quad (6)$$

which is the neighborhood system for the topology  $T_{G_H}$  on  $\xi$  induced by the hypergraphical metric  $d_{G_H}$ . A subset  $S$  of  $\xi$  is called open if for every  $e \in S$  there exist an  $\epsilon > 0$  such that  $B_{G_H}(e, \epsilon) \subset S$ ; of course, a subset  $T$  of  $\xi$  is called closed if its complement  $T^c$  is open.

**Lemma 1.** Every open ball in  $\xi$  is an open set.

*Proof.* Let  $e' \in B_{G_H}(e, \epsilon)$  for some  $e \in \xi$  and  $\epsilon > 0$ . Let  $\alpha = \epsilon - d_{G_H}(e, e') > 0$  and  $e'' \in B_{G_H}(e', \alpha)$ ; by definition, we have  $(epe')_{G_H}$  and  $(e'pe'')_{G_H}$  and so that  $(epe'')_{G_H}$ . Now, from Property (4) of hypergraphical metric space,  $d_{G_H}(e'', e) \leq d_{G_H}(e'', e') + d_{G_H}(e', e) < \alpha + d_{G_H}(e', e) = \epsilon - d_{G_H}(e', e) + d_{G_H}(e', e) = \epsilon$ . Hence,  $B_{G_H}(e', \alpha) \subset B_{G_H}(e, \epsilon)$ . Hence, every open ball in  $\xi$  is an open set.  $\square$

*Definition 10.* Suppose  $(\xi, d_{G_H})$  is hypergraphical metric space and  $\{e_n\}$  be a sequence in  $\xi$ , then  $\{e_n\}$  is called convergent and converges to  $e \in \xi$  if for given  $\epsilon > 0$  there  $\exists n_0 \in \mathbb{N}$  such that  $d_{G_H}(e_n, e) \leq \epsilon, \forall n > n_0$ . Obviously the sequence  $\{e_n\}$  is convergent and converges to  $e$  if and only if  $\lim_{n \rightarrow \infty} d_{G_H}(e_n, e) = 0$ .

*Remark 2.* The limit of a sequence in hypergraphical metric space may not be unique as clear from the following example.

*Example 3.* let  $X$  be the set of vertices of hypergraph, and we take  $\xi(G_H)$  to be the set of subsets of  $X$  such that each subset represents an edge of the hypergraph  $G_H$ . Now, we labeled some edges from the set  $2_A \cup \{0\}$ , where  $2_A = \{1/2^n: n \in \mathbb{N}\}$ . We define  $\xi(G_H) = \{e_i, e_j: e_i \leq e_j, i, j \in \mathbb{N}\}$ . Define a mapping  $d_{G_H}: \xi \times \xi \rightarrow \mathbb{R}^+$  by

$$d_{G_H}(e_i, e_j) = \begin{cases} 0, & \text{if } e_i = e_j; \\ e_i \times e_j, & \text{if } e_i, e_j \in 2_A e_i \neq e_j; \\ \frac{1}{2}, & \text{otherwise.} \end{cases} \quad (7)$$

Clearly,  $d_{G_H}$  is a hypergraphical metric on  $\xi$ . Now, let us consider the sequence  $\{e_n\}$  in  $\xi$  where  $e_n = 1/2^n, \forall n \in \mathbb{N}$ ; then, for any fixed  $k \in \mathbb{N}$ , we have

$$d_{G_H}\left(\frac{1}{2^n}, \frac{1}{2^k}\right) = \frac{1}{2^{n+k}} \rightarrow 0, \quad n \rightarrow \infty. \quad (8)$$

Therefore, the sequence  $\{1/2^n\}$  converges to  $1/2^k$  for every fixed  $k \in \mathbb{N}$ .

**Lemma 2.** Let  $(\xi, d_{G_H})$  be a hypergraphical metric space with induced hypergraphical topology  $T_{G_H}$ . Then,  $T_{G_H}$  is  $T_1$  but not generally Hausdorff, i.e.,  $T_2$ .

*Proof.* We want to show that for every  $e \in \xi$ , the singleton set  $\{e\}$  is a closed subset of  $\xi$  or the set  $\xi - \{e\}$  is an open subset of  $\xi$ . For this, let us suppose  $e' \in \xi - \{e\}$ , then clearly  $e' \neq e$  and  $d_{G_H}(e, e') > 0$ . Now, let us take  $d_{G_H}(e, e') = 2\epsilon > 0 \rightarrow (*)$ . Then, clearly  $e$  does not belong to  $B_{G_H}(e', \epsilon)$ . Suppose on contrary that  $e \in B_{G_H}(e', \epsilon)$ , then  $d_{G_H}(e, e') < \epsilon$  which is contradiction to  $(*)$ . Hence,  $B_{G_H}(e', \epsilon) \subset \xi - \{e\}$  is open, and hence hypergraphical metric space is not Hausdorff.  $\square$

*Remark 3.* Let  $(\xi, d_{G_H})$  be hypergraphical metric space in previous remark, then  $1/2$  is limit point of the sequence  $e_n = \{1/2^n\} \in \xi$ , but for any  $k \in \mathbb{N}$ , if  $k > 1$ , we have  $\lim_{n \rightarrow \infty} d_{G_H}(1/2^n, 1/2^k) = 0 \neq d_{G_H}(1/2, 1/2^k)$ . Therefore, a hypergraphical metric does not need to be continuous.

*Definition 11.* Let  $(\xi, d_{G_H})$  be hypergraphical metric space, and  $\{e_n\} \in \xi$  is a sequence. Then,  $\{e_n\}$  is called Cauchy if for given  $\epsilon > 0$  there exist  $n_0$  belong to  $\mathbb{N}$  such that  $d_{G_H}(e_n, e_m) < \epsilon, \forall n, m > n_0$ ; obviously the sequence  $\{e_n\}$  is Cauchy sequence  $\Leftrightarrow \lim_{n \rightarrow \infty} d_{G_H}(e_n, e_m) = 0$ .

*Definition 12.* A hypergraphical metric space  $(\xi, d_{G_H})$  is called complete if each Cauchy sequence in  $\xi$  converges in  $\xi$ . Suppose  $G'_H$  is another hypergraph such that each  $e \in \xi(G'_H)$  is subset of  $V(G'_H)$ , that is,  $e \subseteq V(G'_H)$ , then  $(\xi, d_{G_H})$  is called

$G'_H$ -complete if every  $G'_H$  termwise connected Cauchy sequence in  $\xi$  converges in  $\xi$ .

In this paper, we suppose that hypergraph  $G_H$  is considered to be directed. We include directed path (p) between edges and denote by  $[e]_{G_H}^l = \{e' \in \xi: \text{directed path from } e \text{ to } e' \text{ of length } l\}$ .

#### 4. Main Results

In this section, we provide fixed point results in hypergraphical metric space; for this, we need various definitions to support our main results.

**Definition 13.** Suppose  $(\xi, d_{G_H})$  is hypergraphical metric space and  $F: \xi \rightarrow \xi$  is a mapping and  $G_H^*$  is subhypergraph of  $G_H$  such that  $\xi(G_H^*) \supseteq \Delta$ . Then,  $F$  is said  $(G_H, G_H^*)$ -hypergraphical contraction on  $\xi$  if the conditions given below are satisfied.

$G_{HC1}$ :  $F$  preserves edges in  $G_H^*$  such that  $e \in \xi(G_H^*) \Rightarrow Fe \in \xi(G_H^*)$

$G_{HC2}$ : there exists  $\alpha \in [0, 1)$ , such that for  $e_i, e_j \in \xi(G_H^*)$  and  $F_{e_i}, F_{e_j} \in \xi(G_H^*)$ ,  $d_{G_H}(F_{e_i}, F_{e_j}) \leq \alpha d_{G_H}(e_i, e_j)$  for all  $e_i, e_j \in \xi(G_H^*)$

Here, we assign the hypergraphical distance between the edges of  $G_H^*$ , and hypergraphical contraction decreases the distance by factor  $\alpha \in [0, 1)$ . The sequence  $\{e_n\}$  having earliest value  $e_0 \in \xi$  is called  $F$ -picard sequence if  $e_n = F_{e_{n-1}}, \forall n \in \mathbb{N}$ . Further, we suppose that  $G_H^*$  is a subhypergraph of  $G_H$  such that  $\xi(G_H^*) \supseteq \Delta$ . The next theorem is the dominant outcome which gives sufficient conditions for the convergence of picard sequence yielded by  $(G_H, G_H^*)$ -hypergraphical contraction on  $G'_H$ -complete hypergraphical metric space.

**Theorem 1.** Suppose  $(\xi, d_{G_H})$  is  $G'_H$ -complete hypergraphical metric space and  $F: \xi \rightarrow \xi$  be a  $(G_H, G_H^*)$ -hypergraphical contraction and also satisfies the following conditions. (1) There exist  $e_0 \in \xi$  such that  $F_{e_0} \in [e_0]_{G_H^*}^l$ , for some  $l \in \mathbb{N}$ . (2) If  $G'_H$ -termwise connected  $F$ -picard sequence  $\{e_n\}$  converges in  $\xi$ , then a limit  $e' \in \xi$  of  $\{e_n\}$  exists and  $n_0 \in \mathbb{N}$ , such that  $(e_n, e') \in \xi(G_H^*), \forall n > n_0$ .

Then, there exist  $e^* \in \xi$  such that the  $F$ -picard sequence  $\{e_n\}$  of initial value  $e_0$  is  $G'_H$ -termwise connected and converges to  $e^*$  and  $Fe^*$ .

*Proof.* Suppose  $e_0 \in \xi$  such that  $F_{e_0} \in [e_0]_{G_H^*}^l$  for some  $l \in \mathbb{N}$  and  $\{e_n\}$  is  $F$ -picard sequence having initial value  $e_0$ , then  $[\{e'_i\}]_{i=0}^l$  is a path such that  $e_0 = e'_0, Fe_0 = e'_1$ , and  $(e_{i-1}', e'_i) \in \xi(G_H^*)$  for  $i = 1, 2, 3, \dots, l$ . As  $F$  is a  $(G_H, G_H^*)$ -hypergraphical contraction, we have

$$(Fe_{i-1}', Fe'_i) \in \xi(G_H^*), \quad \text{for } i = 1, 2, 3, \dots, l. \quad (9)$$

Therefore,  $[\{Te'_i\}]_{i=0}^l$  represent a path from  $Fe'_0 = Fe_0 = e_1$  to  $Te'_l = F^2e_0 = e_2$  of length  $l$  and so  $e_2 \in [e_1]_{G_H^*}^l$ ; proceeding similarly, we get the path  $[\{T^m e'_i\}]_{i=0}^l$  from  $F^m e'_0 =$

$F^m e_0 = e_n$  to  $F^n e'_l = F^n Fe_0 = e_{n+1}$  of length  $l$ . Hence,  $e_{n+1} \in [e_n]_{G_H^*}^l, \forall n \in \mathbb{N}$ ; thus,  $\{e_n\}$  is a  $G'_H$ -termwise connected sequence. Since  $(F^n e'_{i-1}, F^n e'_i) \in \xi(G_H^*)$  for  $i = 1, 2, 3, \dots, l$  and  $n \in \mathbb{N}$ . Using condition  $(G_H C_2)$ , we have

$$d_{G_H}(F^n e'_{i-1}, F^n e'_i) \leq \alpha^n (d_{G_H}(e'_{i-1}, e'_i)). \quad (10)$$

Since  $G'_H$  is a subgraph of  $G_H$ ,  $\{e_n\}$  and is a termwise connected sequence in  $G'_H$ , by using (10), the following relation holds  $\forall n \in \mathbb{N}, m > n$ :

$$d_{G_H}(e_n, e_{n+1}) = d_{G_H}(F^n e_0, F^{n+1} e_0) \leq \sum_{i=1}^l \alpha^n d_{G_H}(e'_{i-1}, e'_i) = \alpha^n F_l. \quad (11)$$

where  $F_l = \sum_{i=1}^l d_{G_H}(e'_{i-1}, e'_i)$ . Again as the sequence  $\{e_n\}$  is  $G'_H$ -termwise connected, therefore,  $n, m \in \mathbb{N}$  with  $m > n$ , we have

$$\begin{aligned} d_{G_H}(e_n, e_m) &\leq \sum_{i=n}^{m-1} d_{G_H}(e_i, e_{i+1}) \leq \sum_{i=n}^{m-1} \alpha^i F_l = \sum_{i=n}^{m-1} \alpha^{i-n+n} F_l \\ &= \alpha^n \left[ \sum_{i=n}^{m-1} \alpha^{i-n} F_l \right] = \frac{\alpha^n}{1-\alpha}. \end{aligned} \quad (12)$$

Since  $\alpha \in (0, 1]$ , we obtain  $\lim_{n,m \rightarrow \infty} d_{G_H}(e_n, e_m) = 0$ . Therefore,  $\{e_n\}$  is a Cauchy sequence in  $\xi$ . From  $G'_H$ -completeness of  $\xi$ , the sequence  $\{e_n\}$  converges in  $\xi$ . And from condition (2), there exist  $e^* \in \xi$  and  $n_0 \in \mathbb{N}$ , such that  $(e_n, e^*) \in \xi(G_H^*), \forall n > n_0$  and  $\lim_{n \rightarrow \infty} d_{G_H}(e_n, e^*) = 0$ . Thus, the sequence  $\{e_n\}$  converges to  $e^* \in \xi$ . Now, if  $(e_n, e^*) \in \xi(G_H^*)$  for all  $n > n_0$  by using  $(G_H C_2)$ , we obtain

$$d_{G_H}(e_{n+1}, Fe^*) = d_{G_H}(Fe_n, Fe^*) \leq \alpha d_{G_H}(e_n, e^*), \quad \text{for all } n > n_0, \quad (13)$$

since  $\lim_{n \rightarrow \infty} d_{G_H}(e_n, e^*) = 0$ .

Therefore,

$$\lim_{n \rightarrow \infty} d_{G_H}(e_{n+1}, Fe^*) = 0. \quad (14)$$

A similar result holds if  $(e^*, e_n) \in \xi(G_H^*)$ , and hence the sequence  $\{e_n\}$  converges to both  $e^*$  and  $Fe^*$ .  $\square$

If we replace  $\xi$  by the set of vertices instead of edges, we get the following corollary.

**Corollary 1.** Suppose  $(\xi, d_{G_H})$  is  $G'_H$ -complete graphical metric space and  $F: \xi \rightarrow \xi$  be a  $(G_H, G_H^*)$ -graphical contraction and also satisfies the following conditions.

- (1) There exist  $x_0 \in \xi$  such that  $F_{x_0} \in [x_0]_{G_H^*}^l$ . For some  $l \in \mathbb{N}$ .
- (2) If  $G'_H$ -termwise connected,  $F$ -picard sequence  $\{x_n\}$  converges in  $\xi$ . Then, a limit  $x' \in \xi$  of  $\{x_n\}$  exists and  $n_0 \in \mathbb{N}$ , such that  $(x_n, x') \in \xi(G_H^*), \forall n > n_0$ .

Then, there exist  $x^* \in \xi$  such that the  $F$ -picard sequence  $\{e_n\}$  of earliest value  $x_0$  is  $G'_H$ -termwise connected and converges to  $x^*$  and  $Fx^*$ .

**Remark 4**

Corollary 1 is the result of Shukla [12].

**Remark 5.** Theorem 1 confirms only convergent of a picard sequence yielded from a  $(G_H, G'_H)$ -hypergraphical contraction on a  $G'_H$ -complete hypergraphical metric space. Next example displays that no one should appreciate this theorem as an existence theorem in  $G'_H$ -complete hypergraphical metric space.

**Example 4.** Suppose  $\zeta$  be the nonempty set of vertices of hypergraph  $G_H$  and  $\xi(G_H)$  be the set of subset of  $\zeta$  such that each subset represents an edge of the hypergraph  $G_H$ . Note (here,  $G_H$  means weighted hypergraph) that we labeled some edges of  $G_H$  from set  $2_A \cup \{0\}$ . Here,  $2_A$  is the set, that is,  $2_A = \{1/2^n: n \in N\}$  and  $\xi(G_H) = \{e_i, e_j: e_i \leq e_j \text{ and } i, j \in N\}$ . Define a mapping  $d_{G_H}: \xi^* \xi \rightarrow \mathbf{R}^+$  by

$$d_{G_H}(e_i, e_j) = \begin{cases} 0, & \text{if } e_i = e_j; \\ e_i * e_j, & \text{if } e_i, e_j \in 2_A e_i \neq e_j; \\ \frac{1}{2}, & \text{otherwise.} \end{cases} \quad (15)$$

Then,  $d_{G_H}$  is hypergraphical metric on  $\xi$  and  $(\xi, d_{G_H})$  is  $G_H$ -complete hypergraphical metric space; now, here we define a mapping.

$F: \xi \rightarrow \xi$  by

$$Fe = \begin{cases} \frac{e}{2}, & \text{if } e \in 2_A; \\ \frac{1}{2}, & \text{if } e = 0; \end{cases} \quad (16)$$

It should be noted that  $F$  is hypergraphical contraction having  $\alpha = 1/4, \forall e \in 2_A$ , and we have  $(e, Fe) \in \xi(G_H)$ , which implies that  $Fe \in [e]_{G'_H}$ . Also any  $G_H$ -termwise connected and convergent sequence in  $\xi$  is constant or monotonic decreasing subsequence with respect to usual order of the sequence  $\{1/2^n\}$  and having at least one limit  $e'$  such that property (2) of contraction theorem hold surely. However, there is no fixed point in  $\xi$  of  $F$ . As mentioned, that convergent sequence's limit may not be unique in hypergraphical metric space  $G_H$ . Therefore, we provide one more definition that is as follows.

**Definition 14.** Suppose  $(\xi, d_{G_H})$  is hypergraphical metric space and  $F: \xi \rightarrow \xi$  is a mapping, then property (P) holds for the quadruple  $(x, d_{G_H}, G'_H, T)$ , that is:

(P): whenever a  $G'_H$ -termwise connected, F-picard sequence  $\{x_n\}$  having limits  $e_i$  and  $e_j$  where  $e_i \in \xi$  and  $e_j \in F(\xi)$ , then  $e_i = e_j$ .

We represent all fixed point of a set by  $\text{Fix} * F$ , and notation for this is  $\xi_F = \{e \in \xi: (e, Fe) \in \xi(G'_H)\}$ .

**Remark 6.** If we chose  $\xi(G_H) = \xi^* \xi$ , then it is clear to check that quadruple  $(\xi, d_{G_H}, G'_H, F)$  satisfies property (P) for arbitrary subhypergraph  $G'_H$ .

**Example 5.** Let  $X, G_H$ , and  $d_{G_H}$  be those which is used in Example 1. And  $\xi(G'_H) = \Delta \cup \{e_i, e_j: e_i, e_j \in (0, 1), e_i \leq e_j \wedge i, j \in N\}$ .

$$Fe = \begin{cases} e, & \text{if } e \in Q \cap [0, 1]; \\ 1, & \text{otherwise;} \end{cases} \quad (17)$$

Then, the quadruple  $(\xi, d_{G_H}, G'_H, F)$  has the property (P). In the next theorem, we want to give enough condition for the existence of fixed point of a  $(G_H, G'_H)$ -graphical contraction.

**Theorem 2.** Suppose  $(\xi, d_{G_H})$  is  $G'_H$ -complete hypergraphical metric space and  $F: \xi \rightarrow \xi$  is  $(G_H, G'_H)$ -hypergraphical contraction, it holds the following: (1) there exist  $e_0 \in \xi$  such that  $T_{e_0} \in [e_0]_{G'_H}$  for some  $l \in N$ ; (2) if a  $G'_H$ -termwise connected T-picard sequence  $\{e_n\}$  converges in  $\xi$ , then there  $\exists e' \in \xi$  of  $\{e_n\}$  which is limit point and  $n_0 \in N$  such that  $(e_n, e') \in \xi(G'_H)$  for all  $n > n_0$ ; then, there exist  $e^* \in \xi$  such that the T-picard sequence  $\{e_n\}$  having earliest value  $e_0$  is  $G'_H$ -termwise connected and converges to  $e^*$  and  $Te^*$ . Also, if the quadruple  $(\xi, d_{G_H}, G'_H, F)$  satisfies property (P), then there must be fixed point of  $F$  in  $\xi$ .

**Proof.** From Theorem 3.2, F-picard sequence  $\{e_n\}$  having earliest value  $e_0$  converges to  $e^*$  and  $Te^*$ . As  $e^* \in \xi$  and  $Fe^* \in F(\xi)$ , therefore, by property (P), it is essential that  $Te^* = e^*$ . Hence, F has fixed point  $e^*$  which is a fixed point of T.  $\square$

**Remark 7.** In the above result, fixed point of F exists due to property (P); it is very important to note that in Example 5, every condition of above result holds except property (P). However,  $\text{Fix}(F) = \Phi$ . Therefore, in the above theorem property, (P) remains unused.

### 5. Applications

Let  $I > 0$  and  $\zeta = C([0, 1], R)$  represent set of weights of edges which is in the form of real continuous function on weighted interval  $[0, I]$ . We give a special application of fixed point theory for examining integral equations of  $\zeta$ ; we show that according to certain condition, the actuality of a lower or upper solution of an integral equation ensures the solution of integral equation. Let  $B_H = \{e \in X: 0 < \inf_{p \in [0, I]} e(p) \text{ and } e(p) \leq 1, t \in [0, I]\}$ . Here, we have  $G_H = G'_H$  and  $\xi(G_H) = \Delta \{e_i, e_j\} \{e_i, e_j \in B_H e_i(p) \leq e_j(p) \forall p$

$\in [0, I]$ . Consider that hypergraphical metric space which is given below, that is,  $d_{G_H}: \xi * \xi \rightarrow R$  is given by

$$d_{G_H}(e_i, e_j) = \begin{cases} 0, & \text{if } e_i = e_j, \\ \sup_{p \in [0, I]} \left\{ \ln \left( \frac{1}{e_i(p) \cdot e_j(p)} \right) \right\}, & \text{if } e_i, e_j \in B_H, e_i \neq e_j, \\ 1, & \text{otherwise.} \end{cases} \tag{18}$$

So,  $(\xi, d_{G_H})$  is  $G_H^I$ -complete hypergraphical metric space. Here, we suppose following integral equation:

$$e_i(p) = \int_0^I g(p, q)h(q, e_i(q))dq, \tag{19}$$

where  $g: [0, I] * [0, I] \rightarrow [0, +\infty)$  and  $h: [0, I] * R \rightarrow R$  are continuous functions. Mapping  $\beta \in C([0, I], R)$  is called lower solution of (19) if  $\beta(p) \leq \int_0^I g(p, q)h(q, \beta(q))dq$ ,  $p \in [0, I]$ . Here, we want to prove that the existence of lower solution of (Z1) confirms the existence of solution of (19). Let us suppose that the operator  $F: \xi \rightarrow \xi$  is defined by

$$Fe_i(p) = \int_0^I g(p, q)h(q, e_i(q))dq, \tag{20}$$

and sufficient conditions are provided for existence of fixed point of (20) in  $\xi$ , and obviously that fixed point is solution of (19).

**Theorem 3.** Consider that coming conditions hold the following:

- (a) ...  $h(q, *): R \rightarrow R$  is increasing function on  $(0, I]$  for every  $q \in [0, I]$ . Moreover,  $\inf_{p \in [0, I]} g(p, q) > 0$  and  $g(p, q)h(q, 1) \leq I^{-1}$ .
- (b) There exist  $\alpha \in (0, 1)$  and  $\rho \in [1, +\infty)$  such that for  $e_i, e_j \in \xi$  and  $(e_i, e_j) \in \xi, \forall q, r \in [0, I]$ .

$$h(q, e_i(q))h(r, e_j(r)) \geq [e_i(q)e_j(r)]^\alpha, \tag{21}$$

$$\int_0^I \int_0^I g(p, q)g(p, r)dqdr \geq \rho, \quad \forall p \in [0, I].$$

Then, existence of a lower solution of (19) in  $B_H$  confirms the existence of solution of (19) in  $\xi$ .

*Proof.* By condition (b), for  $e_i, e_j \in \xi$  also  $(e_i, e_j) \in \xi$ , and  $P \in [0, I]$ , we derived

$$\begin{aligned} & \ln \left( \frac{1}{F(e_i)(p) \cdot F(e_j)(p)} \right) \\ &= \ln \left( \frac{1}{\int_0^I \int_0^I g(p, q)g(p, r)h(q, e_i(q))h(r, e_j(r))dqdr} \right) \\ &\leq \ln \left( \frac{1}{\inf_{p \in [0, I]} [e_i(p)e_j(p)]^\alpha \int_0^I \int_0^I g(p, q)g(p, r)dqdr} \right) \\ &= \ln \left( \frac{1}{F(e_i)(p) \cdot F(e_j)(p)} \right) \\ &= \ln \left( \frac{1}{\int_0^I \int_0^I g(p, q)g(p, r)h(q, e_i(q))h(r, e_j(r))dqdr} \right) \\ &\leq \ln \left( \frac{1}{\int_0^I \int_0^I g(p, q)g(p, r)[e_i(q)e_j(r)]^\alpha dqdr} \right) \\ &\leq \ln \left( \frac{1}{\inf_{p \in [0, I]} [e_i(p)e_j(p)]^\alpha \int_0^I \int_0^I g(p, q)g(p, r)dqdr} \right) \\ &\leq \ln \left( \frac{1}{\rho \inf_{p \in [0, I]} [e_i(p)e_j(p)]^\alpha} \right) \\ &\leq \alpha d_{G_H}(e_i(p), e_j(p)) \rho. \end{aligned} \tag{22}$$

Then, we have

$$d_{G_H}(Fe_i, Fe_j) = \sup_{p \in [0, I]} \ln \left( \frac{1}{F(e_i)(p)F(e_j)(p)} \right) \tag{23}$$

$$\leq \alpha d_{G_H}(e_i(P), e_j(P)).$$

Further, for  $e_i, e_j \in B_H$ , and  $e_i(p) \leq e_j(p), \forall p \in [0, I]$  and from condition (a) we have  $\inf_{p \in [0, I]} F(e_i)(p) > 0$  and

$$\begin{aligned} F(e_i)(p) &= \int_0^I g(p, q)h(q, e_i(q))dq \\ &\leq \int_0^I g(p, q)h(1, 1)dq \leq 1, \\ F(e_1)(p) &= \int_0^I g(p, q)f(q, e_i(q))dq \\ &\leq \int_0^I g(p, q)h(q, e_j(q))dq = F(e_j)(p). \end{aligned} \tag{24}$$



Consequently, the existence of lower solution of equation (19), i.e.,  $\beta \in B_H$  implies that property of Theorem 3 holds. Also, the quadruple  $(\xi, d_{G_H}, G_H', F)$  has property (p). Hence, all conditions of Theorem 2.8 are satisfied. Thus, the operator F has a fixed point which is solution of integral equation (19) in  $\xi$ .  $\square$

## Data Availability

The data used to support this research are included within the paper.

## Conflicts of Interest

The authors declare that they have no conflicts of interest.

## Authors' Contributions

X. Li analyzed the results and finalized the paper. G. Ali supervised the work. L. Gul proved the main results. F. Khan wrote the first draft of the paper. M. Sarwar verified the results.

## References

- [1] I. Altun and H. Simsek, "Some fixed point theorems on ordered metric spaces and application," *Fixed Point Theory and Applications*, vol. 2010, no. 1, 11 pages, Article ID 621469, 2010.
- [2] W. Sintunavarat, "Fixed point results in b-metric spaces approach to the existence of a solution for nonlinear integral equations," *Serie A. Matemáticas*, vol. 110, no. 2, pp. 585–600, 2016.
- [3] E. Karapinar and M. Noorwali, "Dragomir and Gosa type inequalities on b-metric spaces," *Journal of Inequalities and Applications*, vol. 29, 2019.
- [4] H. M. Nagesh and V. R. Girish, "On the entire Zagreb indices of the line graph and line cut-vertex graph of the subdivision graph," *Open Journal of Mathematical Sciences*, vol. 4, no. 1, pp. 470–475, 2020.
- [5] M. Numan, S. I. Butt, and A. Taimur, "Super cyclic antimagic covering for some families of graphs," *Open Journal of Mathematical Sciences*, vol. 5, no. 1, 2021.
- [6] F. Asif, Z. Zahid, and S. Zafar, "Leap Zagreb and leap hyper-Zagreb indices of Jahangir and Jahangir derived graphs," *Engineering and Applied Science Letter*, vol. 3, no. 2, p. 18, 2020.
- [7] F. echenique, "A short and constructive proof of Tarski's fixed-point theorem," *International Journal of Game Theory*, vol. 33, no. 2, pp. 215–218, 2005.
- [8] J. Jacek, "The contraction principle for mappings on a metric with a graph," *Proceeding of the American Mathematical Society*, vol. 136, no. 4, pp. 1359–1373, 2008.
- [9] S. Aleomraninejad, S. Rezapour, and N. Shahzad, "Some fixed point results on a metric space with a graph," *Topology and its Applications*, vol. 159, no. 3, 2012.
- [10] M. Samreen, T. Kamran, and N. Shahzad, "Some fixed point theorems in b-Metric space endowed with graph," *Abstract and Applied Analysis*, vol. 2013, Article ID 967132, 9 pages, 2013.
- [11] H. Argoubi, B. Samet, M. Turinici, B. Samet, and M. Turinici, "Fixed Point results on a metric space endowed with a finite number of graphs and applications," *Czechoslovak Mathematical Journal*, vol. 64, no. 1, pp. 241–250, 2014.
- [12] S. Shukla, "Graphical metric space: a generalized setting in fixed point theory," *Serie A, Matematicas*, vol. 111, no. 3, 2016.
- [13] M. Abbas, M. R. Alfuraidan, A. R. Khan, and T. Nazir, "Fixed point results for set-contractions on metric spaces with a directed graph," *Fixed Point Theory and Applications*, vol. 2015, no. 1, 2015.
- [14] M. Neog and P. Debnath, "Fixed points of set valued mappings in terms of start point on a metric space endowed with a directed graph," *Mathematics*, vol. 5, 2017.
- [15] N. Chuensupantharat, P. Kumam, V. Chauhan, and D. Singh, "Graphic contraction mapping via graphical b-metric spaces with applications," *Article in the Bulletin of the Malaysian Society Series*, vol. 2, 2018.
- [16] S. Regmi, I. K. Argyros, and S. George, "Convergence analysis for a fast class of multi-step Chebyshev-Halley-type methods under weak conditions," *Open Journal of Mathematical Sciences*, vol. 4, no. 1, pp. 34–43, 2021.
- [17] S. Regmi, C. Argyros, C. Argyros, I. K. Argyros, and S. George, "On some iterative methods with frozen derivatives for solving equations," *Open Journal of Mathematical Sciences*, vol. 5, no. 1, pp. 209–217, 2021.

## Research Article

# Extremal Values of Randić Index among Some Classes of Graphs

Ali Ghalavand <sup>1</sup>, Ali Reza Ashrafi <sup>1</sup>, and Marzieh Pourbabae <sup>2</sup>

<sup>1</sup>Department of Pure Mathematics, Faculty of Mathematical Sciences, University of Kashan, Kashan 87317-53153, Iran

<sup>2</sup>Department of Applied Mathematics, Faculty of Mathematical Sciences, University of Kashan, Kashan 87317-53153, Iran

Correspondence should be addressed to Ali Ghalavand; [alighalavand@grad.kashanu.ac.ir](mailto:alighalavand@grad.kashanu.ac.ir)

Received 18 April 2021; Accepted 31 May 2021; Published 14 June 2021

Academic Editor: Roslan Hasni

Copyright © 2021 Ali Ghalavand et al. This is an open access article distributed under the Creative Commons Attribution License, which permits unrestricted use, distribution, and reproduction in any medium, provided the original work is properly cited.

Suppose  $G$  is a simple graph with edge set  $E(G)$ . The Randić index  $R(G)$  is defined as  $R(G) = \sum_{uv \in E(G)} (1/\sqrt{\deg_G(u)\deg_G(v)})$ , where  $\deg_G(u)$  and  $\deg_G(v)$  denote the vertex degrees of  $u$  and  $v$  in  $G$ , respectively. In this paper, the first and second maximum of Randić index among all  $n$ -vertex  $c$ -cyclic graphs was computed. As a consequence, it is proved that the Randić index attains its maximum and second maximum on two classes of chemical graphs. Finally, we will present new lower and upper bounds for the Randić index of connected chemical graphs.

## 1. Mathematical Notions and Notations

In this section, we first describe some mathematical notions that will be kept throughout. A pair  $G = (V, E)$  in which  $V$  is a finite nonempty set and  $E$  is a subset of 2-elements subsets of  $V$  is called a simple graph. Throughout this paper, the term graph means simple graph and the sets  $V = V(G)$  and  $E = E(G)$  in definition of  $G$  are called the vertex set and edge set of  $G$ , respectively.

Suppose  $G$  is a graph. For simplicity of our argument, an edge  $e = \{a, b\}$  in  $G$  is simply written as  $e = ab$ . Choose a vertex  $v$  in  $G$ . The vertex degree of  $v$ ,  $\deg_G(v)$ , is defined as the number of edges in the form  $ax$ . A chemical graph is a graph in which all vertices have degrees less than or equal to 4 [1]. The reason for this name is from quantum chemistry in which it is convenient to model a molecule  $M$  in such a way that vertices are used to denote atoms and edges are for chemical bonds.

The set of all vertices adjacent to a vertex  $v$  is denoted by  $N[v, G]$  and notations  $\Delta = \Delta(G)$ ,  $n_i = n_i(G)$ , and  $\varepsilon_i = \varepsilon_i(G)$  are used for the maximum degree, the number of vertices of degree  $i$ , and the number of edges of degree  $i$  in  $G$ , respectively. The number of edges connecting a vertex of degree  $i$  with a vertex of degree  $j$  in  $G$  is denoted by  $m_{i,j}(G)$ . A connected  $n$ -vertex graph  $G$  is called to be  $c$ -cyclic if it has  $n + c - 1$  edges and the number  $c = c(G)$  is said to be the cyclomatic number of  $G$ .

Suppose  $W$  is a nonempty subset of vertices in a graph  $G$ . The subgraph of  $G$  obtained by deleting the vertices of  $W$  is denoted by  $G - W$ , and similarly, if  $F \subseteq E(G)$ , then the subgraph obtained by deleting all edges in  $F$  is denoted by  $G - F$ . In the case that  $W = \{v\}$  or  $F = \{xy\}$ , the subgraphs  $G - W$  and  $G - F$  will shortly be written as  $G - v$  or  $G - xy$ , respectively. Furthermore, if  $x$  and  $y$  are nonadjacent vertices in  $G$ , then the notation  $G + xy$  is used for the graph obtained from  $G$  by adding an edge  $xy$ .

The Randić index of a graph  $G$  is defined as

$$R(G) = \sum_{uv \in E(G)} \frac{1}{\sqrt{\deg_G(u)\deg_G(v)}}. \quad (1)$$

This topological index was proposed by Milan Randić [2] under the name “branching index.” The Randić index is suitable for measuring the extent of branching of the carbon-atom skeleton of saturated hydrocarbons. We encourage the interested readers to consult the books [3,4] for more information on this topic.

## 2. Background Materials

This section aims to briefly review the literature on ordering graphs concerning the Randić index. By referring to Theorems 2.2 and 2.3 in [5], among all  $n$ -vertex trees, the star  $S_n$

has the minimum Randić index and the path  $P_n$  attains the maximum Randić index. Caporossi et al. [6] proved that among all 1-cyclic graphs of order  $n$ , the cycle  $C_n$  attains the maximum value, and the unicyclic graphs obtained by attaching a pendant path to a vertex of a cycle attain the second maximum Randić index. These are the starting point of the following problem.

*Question 1.* Find  $n$ -vertex  $c$ -cyclic graphs with maximum and minimum Randić index.

Shiu and Zhang [7] obtained the maximum value of Randić index in the class of all  $n$ -vertex chemical trees with  $k$  pendants such that  $n < 3k - 2$ . Shi [8] obtained some interesting results for chemical trees with respect to two generalizations of Randić index. Dehghan-Zadeh et al. [9, 10] obtained the first and second maximum of Randić index in the class of all  $n$ -vertex  $c$ -cyclic graphs when  $c = 3, 4$ .

Deng et al. [11] considered various degree mean rates of an edge and gave some tight bounds for the variation of the Randić index of a graph  $G$  in terms of its maximum and minimum degree mean rates over its edges. Gutman et al. in a recent interesting paper [12] investigated the connection between Randić index and the degree-based information content of molecular and also general graphs. This connection is based on the linear correlation between Randić index and the logarithm of the multiplicative version of the Randić index.

The aim of this paper is to proceed with Question 1. We will obtain the first and second maximum of Randić index among all  $c$ -cyclic graphs. This extends some results in [6, 9, 10].

### 3. Five Graph Transformations

In this section, five graph transformations will be presented which are useful in computing Randić index of graphs. The transformations I and II were introduced in [13].

- (1) *Transformation I.* Suppose that  $G$  is a graph with a given vertex  $w$ . In addition, we assume that  $P: v_1, v_2, \dots, v_k$  and  $Q: u_1 u_2 \dots u_l$  are two paths of lengths  $k - 1$  and  $l - 1$ , respectively. Let  $G_1$  be the graph obtained from  $G$ ,  $P$ , and  $Q$  by attaching edges  $v_1 w$  and  $w u_1$ . Define  $G_2 = G_1 - v_1 w + u_1 v_1$ . The above-referred graphs are illustrated in Figure 1.
- (2) *Transformation II.* Suppose that  $G$  is a graph with given vertices  $x$  and  $y$  such that  $\deg_G(x), \deg_G(y) \geq 2$  and for all  $v \in N[x, G]$ ,  $\deg_G(x) \geq 2$ . In addition, we assume that  $P: v_1, v_2, \dots, v_l$  and  $Q: u_1, u_2, \dots, u_k$  are two paths of lengths  $l - 1$  and  $k - 1$ , respectively. Define  $G_1$  be the graph obtained from  $G$ ,  $P$ , and  $Q$  by attaching vertices  $y v_1, u_1 x$ , and  $G_2 = G_1 - u_1 x + v_1 u_1$ . See Figure 2 for more details.
- (3) *Transformation III.* Suppose that  $G$  is a graph with vertices  $x, y, w$ , and  $z$  such that  $\{xy, wz\} \subseteq E(G)$ . In

addition, we assume that  $G'$  is a trivial graph with vertex set  $\{v\}$ . Define  $G_1 = G - \{xy\} + \{xv, vy\}$  and  $G_2 = G - \{wz\} + \{wv, vz\}$ . The above-referred graphs are illustrated in Figure 3.

- (4) *Transformation IV.* Suppose that  $G$  is a graph with given vertex  $w$  such that  $\deg_G(w) = \Delta(G) \geq 4$ ,  $N[w, G] = \{w_1, \dots, w_{\deg_G(w)}\}$  and  $\deg_G(w_1) = \deg_G(w_2) = 2$ . In addition, we assume that  $v \in V(G)$ ,  $\deg_G(v) \geq 2$ , and  $vw_1 \in E(G)$ . Define  $G' = G - ww_2 + w_1 w_2$ . See Figure 4 for more details.
- (5) *Transformation V.* Suppose that  $G$  is a graph with vertices  $x_1, x_2, x_3, x_4, x_5, x_6$ , and  $w$  such that  $\{x_1 x_2, x_2 x_3, x_2 w, x_4 x_5, x_5 x_6\} \subseteq E(G)$ ,  $\deg_G(x_1) = \deg_G(x_2) = \deg_G(x_3) = 3$ ,  $\deg_G(x_4) = 4$ ,  $\deg_G(x_5) = 2$ , and  $\deg_G(x_6) = 1$  or 2. Define  $G' = G - \{x_2 w\} + \{x_5 w\}$ . The above-referred graphs are illustrated in Figure 5.

It is well-known that if the derivative  $f'(x)$  of a continuous function  $f(x)$  satisfies  $f'(x) > 0$  on an open interval  $(a, b)$ , then  $f(x)$  is increasing on  $(a, b)$ .

**Lemma 1.** *The following hold:*

- (1) Let  $G_1$  and  $G_2$  be two graphs satisfying the conditions of Transformation I. If  $\deg_G(w) \geq 3$  or  $\deg_G(w) = 2$  and  $\min_{uw \in E(G)} \deg_G(u) \leq 168$  or  $\deg_G(w) = 1$  and  $\min_{uw \in E(G)} \deg_G(u) \leq 30$ , then  $R(G_2) > R(G_1)$ .
- (2) Let  $G_1$  and  $G_2$  be two graphs satisfying the conditions of Transformation II and let  $\deg_G(x) = a$ ,  $N[x, G] = \{h_1, \dots, h_a\}$ ,  $\deg_G(h_i) = d_i$ ,  $\deg_G(h_i) = d_i$ ,  $1 \leq i \leq a$ ,  $d_i \leq d_{i+1}$ ,  $1 \leq i \leq a - 1$ . If  $a \geq 5$  or  $a = 4$  and  $d_2 \leq 20$  or  $a = 3$  and  $d_2 \leq 6$  or  $a = 2$  and  $d_2 \leq 5$ , then  $R(G_2) > R(G_1)$ .
- (3) Let  $G_1$  and  $G_2$  be two graphs as shown in Transformation III.
  - (a) If  $\deg_G(x), \deg_G(y) \geq 3$ , and  $\deg_G(z) \in \{1, 2\}$ , then  $R(G_2) > R(G_1)$
  - (b) If  $\deg_G(x) = 2$ ,  $\deg_G(w) \geq 3$ , and  $\deg_G(z) = 1$ , then  $R(G_2) > R(G_1)$
  - (c) If  $\deg_G(x) = 2$  and  $\deg_G(w) = 2$ , then  $R(G_2) = R(G_1)$
- (4) Let  $G$  and  $G'$  be two graphs satisfying the conditions of Transformation IV. Then,  $R(G') \geq R(G)$ .
- (5) Let  $G$  and  $G'$  be two graphs satisfying the conditions of Transformation V. Then,  $R(G') > R(G)$ .

*Proof*

- (1) Let  $x = \deg_G(w)$ ,  $N[w, G] = \{l_1, \dots, l_x\}$ ,  $d_G(l_i) = d_i$ ,  $1 \leq i \leq x$ ,  $\min_{i=1}^x d_i = d_1$ , and  $k, l \geq 2$ . Then, by definition,

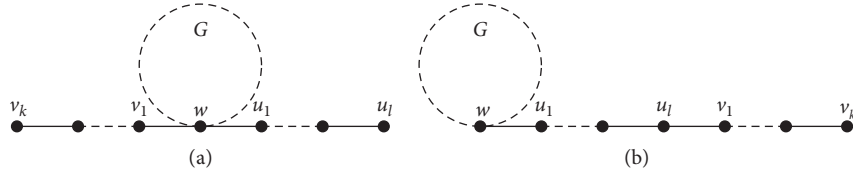


FIGURE 1: The graphs (a)  $G_1$  and (b)  $G_2$  in Transformation I.

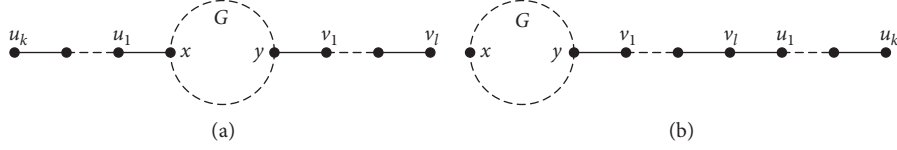


FIGURE 2: The graph (a)  $G_1$  and (b)  $G_2$  in Transformation II.

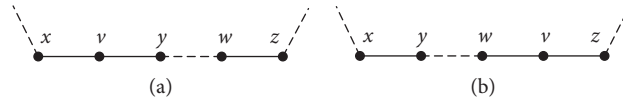


FIGURE 3: The graph (a)  $G_1$  and (b)  $G_2$  in Transformation III.

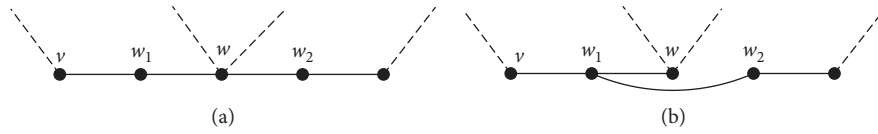


FIGURE 4: The graph (a)  $G$  and (b)  $G'$  in Transformation IV.

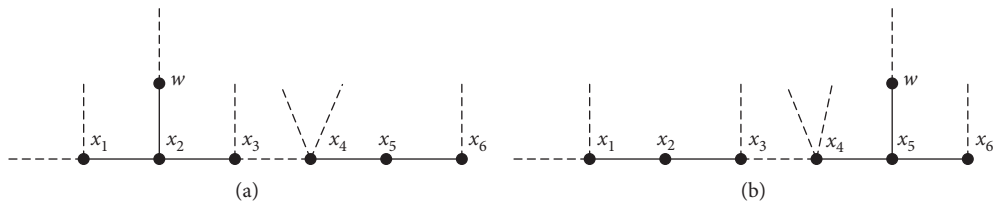


FIGURE 5: The graph (a)  $G$  and (b)  $G'$  in Transformation V.

$$\begin{aligned}
 R(G_2) - R(G_1) &= \left( \frac{1}{\sqrt{2(x+1)}} + 1 + \sum_{i=1}^x \frac{1}{\sqrt{d_i(x+1)}} \right) - \left( \frac{2}{\sqrt{2(x+2)}} + \frac{1}{\sqrt{2}} + \sum_{i=1}^x \frac{1}{\sqrt{d_i(x+2)}} \right) \\
 &\geq \left[ \frac{1}{\sqrt{2}} + \frac{1}{\sqrt{d_1}} \right] \left[ \frac{1}{\sqrt{x+1}} - \frac{1}{\sqrt{x+2}} \right] - \frac{1}{\sqrt{2}} \frac{1}{\sqrt{x+2}} + 1 - \frac{1}{\sqrt{2}}.
 \end{aligned} \tag{2}$$

Now, by Equality (2),

$R(G_2) - R(G_1) \geq (1/\sqrt{2})[(1/\sqrt{x+1}) - (1/\sqrt{x+2})]$   
 $+ (1/\sqrt{2})(1/\sqrt{x+2}) + 1 - (1/\sqrt{2}) > 0.013$ , for  $x \geq 3$ ,  
 $R(G_2) - R(G_1) \geq 0.0000024$ , for  $x = 2$  and  $d_1 \leq 168$ ,  
 and  $R(G_2) - R(G_1) \geq 0.000086$ , for  $x = 1$  and

$d_1 \leq 30$ . The proof of other cases of  $k$  and  $l$  is similar,  
 and we omit them.

(2) Let  $\deg_G(x) = a$ ,  $N[x, G] = \{h_1, \dots, h_a\}$ ,  $\deg_G(h_i) = d_i$ ,  $1 \leq i \leq a$ ,  $d_i \leq d_{i+1}$ ,  $1 \leq i \leq a - 1$  and  $k, l \geq 2$ . Then, by definition,

$$\begin{aligned}
 R(G_2) - R(G_1) &= \left( 1 + \sum_{i=1}^a \frac{1}{\sqrt{d_i a}} \right) - \left( \frac{1}{\sqrt{2(a+1)}} + \frac{1}{\sqrt{2}} + \sum_{i=1}^a \frac{1}{\sqrt{d_i(a+1)}} \right) \\
 &\geq 1 - \frac{1}{\sqrt{2(a+1)}} - \frac{1}{\sqrt{2}} + \left[ \frac{1}{\sqrt{d_1}} + \frac{1}{\sqrt{d_2}} \right] \left[ \frac{1}{\sqrt{a}} - \frac{1}{\sqrt{a+1}} \right].
 \end{aligned} \tag{3}$$

And, by last equality,

$R(G_2) - R(G_1) > 0.0042$  for  $a \geq 5$ ,  $R(G_2) - R(G_1) > 0.00027$  for  $a = 4$  and  $d_2 \leq 20$ ,  $R(G_2) - R(G_1) > 0.0024$  for  $a = 3$  and  $d_2 \leq 6$ , and  $R(G_2) - R(G_1) >$

0.0007 for  $a = 3$  and  $d_2 \leq 5$ . The proof of other cases of  $k$  and  $l$  is similar, and we omit them.

(3) Suppose  $\deg_G(x) = s, \deg_G(y) = r, \deg_G(w) = l$ , and  $\deg_G(z) = t$ . To prove (a), we note that

$$\begin{aligned}
 R(G_2) - R(G_1) &= \left( \frac{1}{\sqrt{sr}} + \frac{1}{\sqrt{2l}} + \frac{1}{\sqrt{2t}} \right) - \left( \frac{1}{\sqrt{2s}} + \frac{1}{\sqrt{2r}} + \frac{1}{\sqrt{lt}} \right) \\
 &= \left( \frac{1}{\sqrt{sr}} - \frac{1}{\sqrt{2s}} - \frac{1}{\sqrt{2r}} \right) + \left( \frac{1}{\sqrt{2l}} - \frac{1}{\sqrt{2t}} - \frac{1}{\sqrt{lt}} \right) > -0.48 + 0.50 > 0.
 \end{aligned} \tag{4}$$

To prove (b), we first calculate the difference between  $R(G_2)$  and  $R(G_1)$ .

$$R(G_2) - R(G_1) = \left( \frac{1}{\sqrt{2}} + \frac{1}{\sqrt{2l}} \right) - \left( \frac{1}{2} + \frac{1}{\sqrt{l}} \right). \tag{5}$$

Let  $h(x) = (1/\sqrt{2x}) - (1/\sqrt{x})$ , for  $x \in (0, \infty)$ . Then,  $h$  is increasing on  $(0, \infty)$ , and hence by

equation (5),  $R(G_2) - R(G_1) > 0.038$ . For the proof of (c), it is enough to notice that  $m_{i,j}(G_1) = m_{i,j}(G_2)$ ,  $1 \leq i \leq j \leq n - 1$ . Thus,  $R(G_2) = R(G_1)$ , as desired.

(4) Suppose that  $\deg_G(v) = s, \deg_G(w) = q$ , and  $\deg_G(w_i) = d_i, 2 \leq i \leq q$ . Then,

$$\begin{aligned}
 R(G') - R(G) &= \left( \frac{1}{\sqrt{3s}} + \frac{1}{\sqrt{3(q-1)}} + \frac{1}{\sqrt{6}} + \sum_{i=3}^q \frac{1}{\sqrt{(q-1)d_i}} \right) - \left( \frac{1}{\sqrt{2s}} + \frac{2}{\sqrt{2q}} + \sum_{i=3}^q \frac{1}{\sqrt{qd_i}} \right) \\
 &\geq \left( \frac{2}{\sqrt{6}} + \frac{1}{\sqrt{3(q-1)}} + \frac{q-2}{\sqrt{(q-1)q}} \right) - \left( \frac{1}{\sqrt{4}} + \frac{2}{\sqrt{2q}} - \frac{q-2}{\sqrt{q^2}} \right) > 0.02,
 \end{aligned} \tag{6}$$

as desired.

(5) Suppose that  $\deg_G(x_6) = r$ . Then, by definition,

$$R(G') - R(G) = \left( \frac{2}{\sqrt{9}} + \frac{1}{\sqrt{8}} + \frac{1}{\sqrt{2r}} \right) - \left( \frac{2}{\sqrt{6}} + \frac{1}{\sqrt{12}} + \frac{1}{\sqrt{3r}} \right) > 0.0068. \tag{7}$$

Hence, the result.

For a graph  $G$ , its first Zagreb index  $M_1(G)$  is defined as  $M_1(G) = \sum_{v \in V(G)} \deg_G(v)^2$ .  $\square$

$$\varepsilon_1(G) = 4m - M_1(G) + \sum_{i=3}^{2n-4} \varepsilon_i(G)(i-2), \tag{8}$$

$$\varepsilon_2(G) = M_1(G) - 3m - \sum_{i=3}^{2n-4} \varepsilon_i(G)(i-1).$$

**Lemma 2** (see [14]). *If  $G$  is a connected graph with  $n$  vertices and  $m$  edges, then*

**Theorem 1.** Let  $G$  be a connected graph with  $n \geq 3$  vertices and  $m$  edges.

- (1) If  $\Delta(G) \leq 3$  or ( $\Delta(G) \leq 11$  and  $m_{1,4}(G) = m_{2,3}(G) = 0$ ), then  $R(G) \geq (4m - M_1(G)/\sqrt{2}) + (M_1(G) - 3m/2)$ . The equality holds if and only if  $G \cong P_n$ .
- (2) If  $\Delta(G) \leq 3$  and  $m_{2,2}(G) = m_{1,4}(G) = m_{2,3}(G) = 0$  or ( $\Delta(G) \leq 5$  and  $m_{2,2}(G) = m_{1,4}(G) = m_{2,3}(G) = m_{1,5}(G) = m_{2,4}(G) = m_{3,3}(G) = 0$ ), then  $R(G) \geq (4m - M_1(G)/\sqrt{2}) + (M_1(G) - 3m/\sqrt{3})$ , with equality if and only if  $G \cong S_4$ .

*Proof.* By definition,

$$R(G) = \sum_{1 \leq i < j \leq n-1} m_{i,j} \frac{1}{\sqrt{ij}} \geq m_{1,2} \frac{1}{\sqrt{2}} + m_{1,3} \frac{1}{\sqrt{3}} + m_{2,2} \frac{1}{2} + \sum_{i=3}^{2n-4} \varepsilon_i(G) \frac{1}{\Delta(G)}. \quad (9)$$

---


$$\begin{aligned}
 R(G) &\geq \frac{1}{\sqrt{2}} \left[ 4m - M_1(G) + \sum_{i=3}^4 \varepsilon_i(G) (i-2) \right] \\
 &\quad + \frac{1}{2} \left[ M_1(G) - 3m - \sum_{i=3}^4 \varepsilon_i(G) (i-1) \right] + \sum_{i=3}^4 \varepsilon_i(G) \frac{1}{3} \\
 &= \frac{4m - M_1(G)}{\sqrt{2}} + \frac{M_1(G) - 3m}{2} + \left[ \frac{1}{\sqrt{2}} - \frac{1}{2} \right] \sum_{i=3}^4 \varepsilon_i(G) (i-1) - \left[ \frac{1}{\sqrt{2}} - \frac{1}{3} \right] \sum_{i=3}^4 \varepsilon_i(G) \\
 &\geq \frac{4m - M_1(G)}{\sqrt{2}} + \frac{M_1(G) - 3m}{2} + 2 \left[ \frac{1}{\sqrt{2}} - \frac{1}{2} \right] \sum_{i=3}^4 \varepsilon_i(G) - \left[ \frac{1}{\sqrt{2}} - \frac{1}{3} \right] \sum_{i=3}^4 \varepsilon_i(G) \\
 &= \frac{4m - M_1(G)}{\sqrt{2}} + \frac{M_1(G) - 3m}{2} + \left[ \frac{1}{\sqrt{2}} - 1 + \frac{1}{3} \right] \sum_{i=3}^4 \varepsilon_i(G) \\
 &\geq \frac{4m - M_1(G)}{\sqrt{2}} + \frac{M_1(G) - 3m}{2}.
 \end{aligned} \quad (11)$$


---

Equality holds if and only if  $G \cong P_n$ . Let  $\Delta(G) \leq 11$  and  $m_{1,4}(G) = m_{2,3}(G) = 0$ . Then, by Equality (9),

1. The last equality for  $\Delta(G) \leq 3$  gives

$$\begin{aligned}
 R(G) &\geq m_{1,2} \frac{1}{\sqrt{2}} + \frac{1}{2} [m_{1,3} + m_{2,2}] + \sum_{i=3}^4 \varepsilon_i(G) \frac{1}{3} \\
 &= \frac{1}{\sqrt{2}} \varepsilon_1(G) + \frac{1}{2} \varepsilon_2(G) + \sum_{i=3}^4 \varepsilon_i(G) \frac{1}{3},
 \end{aligned} \quad (10)$$

and by Lemma 2,

$$\begin{aligned}
 R(G) &\geq m_{1,2} \frac{1}{\sqrt{2}} + \frac{1}{2} [m_{1,3} + m_{2,2}] + \sum_{i=4}^{20} \varepsilon_i(G) \frac{1}{11} \\
 &= \frac{1}{\sqrt{2}} \varepsilon_1(G) + \frac{1}{2} \varepsilon_2(G) + \sum_{i=4}^{20} \varepsilon_i(G) \frac{1}{11},
 \end{aligned}
 \tag{12}$$

and by Lemma 2 and some simple calculations,

$$\begin{aligned}
 R(G) &\geq \frac{4m - M_1(G)}{\sqrt{2}} + \frac{M_1(G) - 3m}{2} + 3 \left[ \frac{1}{\sqrt{2}} - \frac{1}{2} \right] \sum_{i=4}^{20} \varepsilon_i(G) - \left[ \frac{1}{\sqrt{2}} - \frac{1}{11} \right] \sum_{i=4}^{20} \varepsilon_i(G) \\
 &= \frac{4m - M_1(G)}{\sqrt{2}} + \frac{M_1(G) - 3m}{2} + \left[ \frac{2}{\sqrt{2}} - \frac{3}{2} + \frac{1}{11} \right] \sum_{i=4}^{20} \varepsilon_i(G) \\
 &\geq \frac{4m - M_1(G)}{\sqrt{2}} + \frac{M_1(G) - 3m}{2},
 \end{aligned}
 \tag{13}$$

with equality if and only if  $G \cong P_n$ .

(2) A similar argument as the case 1, it can be proved that for  $\Delta(G) \leq 3$  and  $m_{2,2}(G) = m_{1,4}(G) = m_{2,3}(G) = 0$ ,

$$\begin{aligned}
 R(G) &\geq \frac{4m - M_1(G)}{\sqrt{2}} + \frac{M_1(G) - 3m}{\sqrt{3}} + \left[ \frac{2}{\sqrt{2}} - \frac{3}{\sqrt{3}} + \frac{1}{3} \right] \varepsilon_4(G) \\
 &\geq \frac{4m - M_1(G)}{\sqrt{2}} + \frac{M_1(G) - 3m}{\sqrt{3}},
 \end{aligned}
 \tag{14}$$

with equality if and only if  $G \cong S_4$ . For  $\Delta(G) \leq 5$  and  $m_{2,2}(G) = m_{1,4}(G) = m_{2,3}(G) = m_{1,5}(G) = m_{2,4}(G) = m_{3,3}(G) = 0$ ,

$$\begin{aligned}
 R(G) &\geq \frac{4m - M_1(G)}{\sqrt{2}} + \frac{M_1(G) - 3m}{\sqrt{3}} + \left[ \frac{3}{\sqrt{2}} - \frac{4}{\sqrt{3}} + \frac{1}{5} \right] \sum_{i=5}^8 \varepsilon_i(G) \\
 &\geq \frac{4m - M_1(G)}{\sqrt{2}} + \frac{M_1(G) - 3m}{\sqrt{3}},
 \end{aligned}
 \tag{15}$$

with equality if and only if  $G \cong S_4$ . This completes the proof.  $\square$

**Theorem 2** (see [6]). *Let  $G$  be a graph with  $n$  vertices. Then,*

$$R(G) = \frac{n}{2} - \frac{1}{2} \sum_{uv \in E(G)} \left( \frac{1}{\sqrt{\deg_G(u)}} - \frac{1}{\sqrt{\deg_G(v)}} \right)^2. \tag{16}$$

**Lemma 3** (see [15]). *If  $G$  is a connected graph with  $n$  vertices and cyclomatic number  $c$ , then  $n_1(G) = 2 - 2c + \sum_{i=3}^{\Delta(G)} (i - 2)n_i$  and  $n_2(G) = 2c + n - 2 - \sum_{i=3}^{\Delta(G)} (i - 1)n_i$ .*

**Corollary 1.** *Let  $G$  be a connected graph with  $n$  vertices and cyclomatic number  $c$ .*

(1) *If  $c = 5$ , then  $n_1(G) = \sum_{i=3}^{\Delta(G)} (i - 2)n_i - 8$  and  $n_2(G) = n + 8 - \sum_{i=3}^{\Delta(G)} (i - 1)n_i$*

(2) *If  $c = 6$ , then  $n_1(G) = \sum_{i=3}^{\Delta(G)} (i - 2)n_i - 10$  and  $n_2(G) = n + 10 - \sum_{i=3}^{\Delta(G)} (i - 1)n_i$*

*Define  $Y_1(n) = \{G | n_3 = 8, n_2 = n - 8\}$ ,  $Y_2(n) = \{G | n_1 = 1, n_3 = 9, n_2 = n - 10\}$ ,  $Y_3(n) = \{G | n_3 = 10, n_2 = n - 10\}$ , and  $Y_4(n) = \{G | n_1 = 1, n_3 = 11, n_2 = n - 12\}$ .*

**Lemma 4.** Let  $G$  be a connected graph with  $n$  vertices,  $m$  edges, and cyclomatic number  $c$ .

- (1) Suppose  $n_1 = 0$  and  $0 < n_i < n$  for some  $3 \leq i \leq n - 1$ . Then,  $m_{i,i}(G) \leq n_i(G) - 2 + c$ .
- (2) Suppose  $n_1 \geq 1$  and  $0 < n_i < n$  for some  $3 \leq i \leq n - 1$ . Then,  $m_{i,i}(G) \leq n_i(G) - 1 + c$ .

*Proof.* Since  $n_1 = 0$ ,  $c(G - v) \leq c(G) - 1$ , for all  $v \in V(G)$ . Now, the proof follows from this fact that  $m = n - 1 + c$ . The part (2) is similar.

Let  $n$  be a positive integer. Define

$$\begin{aligned} \Omega_1(n) &= \{G \in Y_1(n) \mid m_{3,3} = 11, m_{2,3} = 2, m_{2,2} = n - 9\}, \\ \Omega_2(n) &= \{G \in Y_2(n) \mid m_{3,3} = 13, m_{2,3} = 1, m_{1,2} = 1, m_{2,2} = n - 11\}, \\ \Omega_3(n) &= \{G \in Y_3(n) \mid m_{3,3} = 14, m_{2,3} = 2, m_{2,2} = n - 11\}, \\ \Omega_4(n) &= \{G \in Y_4(n) \mid m_{3,3} = 16, m_{2,3} = 1, m_{1,2} = 1, m_{2,2} = n - 13\}. \end{aligned} \tag{17}$$

If  $G_i \in \Omega_i(n)$  for  $1 \leq i \leq 4$ , then  $R(G_1) = (1/2)n - (5 - 2\sqrt{6}/6)$ ,  $R(G_2) = (1/2)n - (7 - (\sqrt{6} + 3\sqrt{2})/6)$ ,  $R(G_3) = (1/2)n - (5 - 2\sqrt{6}/6)$ , and  $R(G_4) = (1/2)n - (7 - (\sqrt{6} + 3\sqrt{2})/6)$ .  $\square$

**Theorem 3.** The following hold:

- (1) Let  $G$  be a connected graph with  $n \geq 9$  vertices and cyclomatic number 5. Then,  $R(G) \leq (1/2)n - (5 - 2\sqrt{6}/6)$ , with equality if and only if  $G \in \Omega_1(n)$ .
- (2) Let  $G$  be a connected graph with  $n \geq 11$  vertices and cyclomatic number 6. Then,  $R(G) \leq (1/2)n - (5 - 2\sqrt{6}/6)$ , with equality if and only if  $G \in \Omega_3(n)$ .

*Proof*

- (1) If  $n_1(G) = 0$ , then by Corollary 1 and Theorem 2,  $R(G) \leq (1/2)n - (5 - 2\sqrt{6}/6)$ , with equality if and

only if  $G \in \Omega_1(n)$ . For  $n_1(G) = 1$ ,  $R(G) \leq (1/2)n - (7 - (\sqrt{6} + 3\sqrt{2})/6) < (1/2)n - (5 - 2\sqrt{6}/6)$ . Let  $n_1(G) \geq 2$ . Then, again by Corollary 1 and Theorem 2,  $R(G) \leq (1/2)n - (3 - 2\sqrt{2}/2) < (1/2)n - (5 - 2\sqrt{6}/6)$ .

(2) Proof is similar to the last case, and we omit it.  $\square$

*Remark 1*

- (1) Let  $G$  be a connected graph with  $n = 8$  vertices and cyclomatic number 5. Then,  $R(G) \leq 4$ , with equality if and only if  $G$  is a 3-regular graph.
- (2) Let  $G$  be a connected graph with  $n = 10$  vertices and cyclomatic number 6. Then,  $R(G) \leq 5$ , with equality if and only if  $G$  is a 3-regular graph.

For a positive number  $c \geq 3$ , we define

$$\begin{aligned} \Lambda_c^1(n) &= \{G \mid m_{3,3} = 3c - 4, m_{2,3} = 2, m_{2,2} = n - (2c - 1)\}, \\ \Gamma_c^1(n) &= \{G \mid m_{3,3} = 3c - 2, m_{2,3} = 1, m_{1,2} = 1, m_{2,2} = n - (2c + 1)\}. \end{aligned} \tag{18}$$

If  $G_1 \in \Lambda_c^1(n)$  and  $G_2 \in \Gamma_c^1(n)$ , then  $R(G_1) = (1/2)n - (5 - 2\sqrt{6}/6)$  and  $R(G_2) = (1/2)n - (7 - (\sqrt{6} + 3\sqrt{2})/6)$ .

**Proposition 1.** Let  $G$  be a connected graph with  $n$  vertices,  $m$  edges, and cyclomatic number  $c$ , where  $c \geq 3$  is a positive integer. If  $n \geq 2c - 1$  and  $n_1(G) = 0$ , then  $n_2(G) \geq 1$ .

*Proof.* Those are well-known that  $c = m - n + 1$  and  $\sum_{i=1}^n n_i(G)i = 2m$ . Therefore,  $2c = 2n_2(G) + \sum_{i=3}^n n_i(G)i - 2n + 2$ . Thus,  $2c \geq 2n_2(G) + 3(n - n_2(G)) - 2n + 2 = n - n_2(G) + 2$ , and this implies that  $n_2(G) \geq n - 2c + 2$ . Now, since  $n \geq 2c - 1$ ,  $n_2(G) \geq 1$ .

By Proposition 1 and a similar argument as the proof of Theorem 3, we will have the following general result.  $\square$

**Theorem 4.** Let  $G$  be a connected graph with  $n$  vertices and cyclomatic number  $c$ , where  $c \geq 3$  is a positive integer.

- (1) If  $n \geq 2c - 1$ , then  $R(G) \leq (1/2)n - (5 - 2\sqrt{6}/6)$ , with equality if and only if  $G \in \Lambda_c^1(n)$ .
- (2) If  $n = 2c - 2$ , then  $R(G) \leq (1/2)n$ , with equality if and only if  $G$  is a 3-regular graph.

Let  $n$  be a positive number,  $Y_5(n) = \{G \mid n_1 = 0, n_4 = 1, n_3 = 6, n_2 = n - 7\}$  and  $Y_6(n) = \{G \mid n_1 = 0, n_4 = 1, n_3 = 8, n_2 = n - 9\}$ . Define



$$\begin{aligned}
\Omega_5(n) &= \{G \in Y_5(n) | m_{4,3} = 4, m_{3,3} = 6, m_{2,3} = 2, m_{2,2} = n - 8\}, \\
\Omega_6(n) &= \{G \in Y_1(n) | m_{3,3} = 10, m_{2,3} = 4, m_{2,2} = n - 10\}, \\
\Omega_7(n) &= \{G \in Y_6(n) | m_{4,3} = 4, m_{3,3} = 9, m_{2,3} = 2, m_{2,2} = n - 10\}, \\
\Omega_8(n) &= \{G \in Y_3(n) | m_{3,3} = 13, m_{2,3} = 4, m_{2,2} = n - 12\}.
\end{aligned} \tag{19}$$

If  $G_i \in \Omega_5(n)$  for  $1 \leq i \leq 4$ , then  $R(G_1) = (1/2)n - (6 - (2\sqrt{3} + \sqrt{6})/3)$ ,  $R(G_2) = (1/2)n - (5 - 2\sqrt{6}/3)$ ,  $R(G_3) = (1/2)n - (6 - (2\sqrt{3} + \sqrt{6})/3)$  and  $R(G_4) = (1/2)n - (5 - 2\sqrt{6}/3)$ .

**Theorem 5.** *The following hold:*

- (1) Let  $G$  be a connected graph with  $n \geq 9$  vertices and cyclomatic number 5. If  $G \notin \Omega_1(n)$ , then  $R(G) \leq (1/2)n - (6 - (2\sqrt{3} + \sqrt{6})/3)$ , with equality if and only if  $G \in \Omega_5(n)$ .
- (2) Let  $G$  be a connected graph with  $n \geq 11$  vertices and cyclomatic number 6. If  $G \notin \Omega_3(n)$ , then  $R(G) \leq (1/2)n - (6 - (2\sqrt{3} + \sqrt{6})/3)$ , with equality if and only if  $G \in \Omega_7(n)$ .

*Proof*

- (1) Let  $n_1(G) = 0$  and  $G \notin \Omega_1(n)$ . For  $\Delta(G) = 3$ ,  $m_{2,3} \geq 4$  and Corollary 1 and Theorem 2 give  $R(G) \leq (1/2)n - (5 - 2\sqrt{6}/3) < (1/2)n - (6 - (2\sqrt{3} + \sqrt{6})/3)$ . For  $\Delta(G) \geq 4$ ,  $R(G) \leq (1/2)n - (6 - (2\sqrt{3} + \sqrt{6})/3)$ , with equality if and only if  $G \in \Omega_5(n)$ . If  $n_1(G) \geq 1$ ,

then  $R(G) \leq (1/2)n - (7 - (\sqrt{6} + 3\sqrt{2})/6) < (1/2)n - (6 - (2\sqrt{3} + \sqrt{6})/3)$ .

(2) Proof is similar to Case 1, and we omit it.

By a simple calculation, one can easily see that Theorem 5 (1) holds for  $n = 8$  and Theorem 5 (2) holds for  $n = 10$ . On the other hand, Theorems 3 and 5 imply the following result.  $\square$

**Corollary 2.** *The following hold:*

- (1) Suppose  $n \geq 9$ . The connected graphs with cyclomatic number 5 in the sets  $\Omega_1(n)$  and  $\Omega_5(n)$  have the first and second maximum Randić index among all  $n$ -vertex connected graphs with cyclomatic number 5, respectively.
- (2) Suppose  $n \geq 11$ . The connected graphs with cyclomatic number 6 in the sets  $\Omega_7(n)$  and  $\Omega_8(n)$  have the first and second maximum Randić index among all  $n$ -vertex connected graphs with cyclomatic number 6, respectively.

Suppose  $c \geq 4$  is a positive integer. Define

$$\begin{aligned}
\Lambda_c^2(n) &= \{G | m_{3,3} = 3c - 5, m_{2,3} = 4, m_{2,2} = n - 2c\}, \\
\Gamma_c^2(n) &= \{G | m_{4,3} = 4, m_{3,3} = 3c - 9, m_{2,3} = 2, m_{2,2} = n - (2c - 2)\}.
\end{aligned} \tag{20}$$

If  $H_1 \in \Lambda_c^2(n)$  and  $H_2 \in \Gamma_c^2(n)$ , then  $R(H_1) = (1/2)n - (5 - 2\sqrt{6}/3)$  and  $R(H_2) = (1/2)n - (6 - (2\sqrt{3} + \sqrt{6})/3)$ .

**Theorem 6.** *Let  $G$  be a connected graph with  $n$  vertices and cyclomatic number  $c \geq 4$ .*

- (1) If  $n \geq 2c - 1$  and  $G \notin \Lambda_c^1(n)$ , then  $R(G) \leq (1/2)n - (6 - (2\sqrt{3} + \sqrt{6})/3)$ , with equality if and only if  $G \in \Gamma_c^2(n)$ .
- (2) If  $n = 2c - 2$  and  $G$  is not a 3-regular graph, then  $R(G) \leq (1/2)n - (6 - (2\sqrt{3} + \sqrt{6})/3)$ , with equality if and only if  $G \in \Gamma_c^2(n)$ .

*Proof.* The result follows from Proposition 1 and a similar argument as Theorem 3.

We end this section with the following result that follows from Theorems 4 and 6.  $\square$

**Theorem 7.** *Let  $G$  be a connected graph with  $n$  vertices and cyclomatic number  $c \geq 4$ .*

- (1) If  $n \geq 2c - 1$ , then the connected graphs with cyclomatic number  $c$  in the sets  $\Lambda_c^1(n)$  and  $\Gamma_c^2(n)$  have the first and second maximum Randić index among all  $n$ -vertices connected graphs with cyclomatic number  $c$ , respectively.
- (2) If  $n = 2c - 2$ , then the 3-regular connected graphs and the connected graphs in the set  $\Gamma_c^2(n)$  with cyclomatic number  $c$  have the first and second maximum Randić index among all  $n$ -vertices connected graphs with cyclomatic number  $c$ , respectively.

#### 4. Connected Chemical Graphs

Let  $G$  be a connected chemical graph with  $n$  vertices and  $m$  edges. By Lemma 3,

$$\begin{aligned} n_1 &= 2n - 2m + n_3 + 2n_4, \\ n_2 &= 2m - n - 2n_3 - 3n_4, \end{aligned} \quad (21)$$

and by Lemma 2,

$$\begin{aligned} \varepsilon_1(G) &= 4m - [n_1 + 4n_2 + 9n_3 + 16n_4] + \varepsilon_3(G) + 2\varepsilon_4(G) + 3\varepsilon_5(G) + 4\varepsilon_6(G), \\ \varepsilon_2(G) &= n_1 + 4n_2 + 9n_3 + 16n_4 - 3m - [2\varepsilon_3(G) + 3\varepsilon_4(G) + 4\varepsilon_5(G) + 5\varepsilon_6(G)]. \end{aligned} \quad (22)$$

Now, by some calculations, we have

$$\begin{aligned} \varepsilon_1(G) &= 2n - 2m - 2n_3 - 6n_4 + \varepsilon_3(G) + 2\varepsilon_4(G) + 3\varepsilon_5(G) + 4\varepsilon_6(G), \\ \varepsilon_2(G) &= 3m - 2n + 2n_3 + 6n_4 - [2\varepsilon_3(G) + 3\varepsilon_4(G) + 4\varepsilon_5(G) + 5\varepsilon_6(G)]. \end{aligned} \quad (23)$$

Suppose  $M_k = \{m_{i,j} | 1 \leq i \leq j \leq 4 \text{ and } i + j = k + 2\}$ ,  $1 \leq k \leq 4$ . Since  $\varepsilon_k = \sum_{x \in M_k} x$ ,  $1 \leq k \leq 4$ ,

$$\begin{aligned} m_{1,2} &= 2n - 2m - 2n_3 - 6n_4 + m_{1,4} + m_{2,3} + 2m_{2,4} + 2m_{3,3} + 3m_{3,4} + 4m_{4,4}, \\ m_{2,2} &= 3m - 2n + 2n_3 + 6n_4 - [m_{1,3} + 2m_{1,4} + 2m_{2,3} + 3m_{2,4} + 3m_{3,3} + 4m_{3,4} + 5m_{4,4}], \end{aligned} \quad (24)$$

and since  $m_{1,3} = 3n_3 - m_{2,3} - 2m_{3,3} - m_{3,4}$  and  $m_{1,4} = 4n_4 - m_{2,4} - m_{3,4} - 2m_{4,4}$ ,

$$\begin{aligned} m_{1,2} &= 2n - 2m - 2n_3 - 2n_4 + m_{2,3} + m_{2,4} + 2m_{3,3} \\ &\quad + 2m_{3,4} + 2m_{4,4}, \end{aligned} \quad (25)$$

$$\begin{aligned} m_{2,2} &= 3m - 2n - n_3 - 2n_4 - m_{2,3} - m_{2,4} - m_{3,3} \\ &\quad - m_{3,4} - m_{4,4}. \end{aligned} \quad (26)$$

On the other hand,

$$R(G) = \frac{1}{\sqrt{2}}m_{1,2} + \frac{1}{\sqrt{3}}m_{1,3} + \frac{1}{2}m_{1,4} + \frac{1}{2}m_{2,2} + \frac{1}{\sqrt{6}}m_{2,3} + \frac{1}{\sqrt{8}}m_{2,4} + \frac{1}{3}m_{3,3} + \frac{1}{\sqrt{12}}m_{3,4} + \frac{1}{4}m_{4,4}. \quad (27)$$

By equations (25)–(27), we have

$$\begin{aligned} R(G) &= \frac{1}{2}(3 - 2\sqrt{2})(m + 2\sqrt{2}n + 2n) - \frac{1}{2}(1 - 2\sqrt{3} + 2\sqrt{2})n_3 \\ &\quad - (\sqrt{2} - 1)n_4 + \frac{1}{6}(\sqrt{3}\sqrt{2} + 3\sqrt{2} - 2\sqrt{3} - 3)m_{2,3} + \frac{1}{4}(3\sqrt{2} - 4)m_{2,4} \\ &\quad + \frac{1}{6}(6\sqrt{2} - 4\sqrt{3} - 1)m_{3,3} + \frac{1}{6}(6\sqrt{2} - \sqrt{3} - 6)m_{3,4} + \frac{1}{4}(4\sqrt{2} - 5)m_{4,4}. \end{aligned} \quad (28)$$

**Theorem 8.** Let  $G$  be a connected chemical graph with  $n > 5$  vertices and  $m$  edges. Then,

(1)  $R(G) \leq (1/2)(3 - 2\sqrt{2})(m + 2\sqrt{2}n + 2n)$ , with equality if and only if  $G \cong P_n$  or  $C_n$

$$(2) R(G) \geq (1/6)(2\sqrt{2} - 3)((\sqrt{3}\sqrt{2} + 2\sqrt{3} - 3\sqrt{2} - 3)n - \sqrt{3}\sqrt{2} - 2\sqrt{3} + 3\sqrt{2} - 3m + 3)$$

*Proof.* It is easy to see that  $n_3 \geq (1/3)(m_{2,3} + 2m_{3,3} + m_{3,4})$  and  $n_4 \geq (1/4)(m_{2,4} + m_{3,4} + 2m_{4,4})$ . Therefore, by equation (28), we have

$$\begin{aligned} R(G) &\leq \frac{1}{2}(3 - 2\sqrt{2})(m + 2\sqrt{2}n + 2n) - \frac{1}{6}(4 - \sqrt{3}\sqrt{2} - \sqrt{2})m_{2,3} \\ &\quad - \frac{1}{4}(3 - 2\sqrt{2})m_{2,4} - \frac{1}{6}(3 - 2\sqrt{2})m_{3,3} - \frac{1}{12}(11 - 2\sqrt{3} - 5\sqrt{2})m_{3,4} \\ &\quad - \frac{1}{4}(3 - 2\sqrt{2})m_{4,4} \leq \frac{1}{2}(3 - 2\sqrt{2})(m + 2\sqrt{2}n + 2n), \end{aligned} \quad (29)$$

with equality if and only if  $G \cong P_n$  or  $C_n$ . On the other hand,  $n_3 + n_4 \leq n$  and  $m_{2,3} + m_{2,4} + m_{3,3} + m_{3,4} + m_{4,4} \geq n_3 + n_4 - 1$ . Therefore, by equation (28),

$$\begin{aligned} R(G) &\geq \frac{1}{2}(3 - 2\sqrt{2})(m + 2\sqrt{2}n + 2n) - (\sqrt{2} - 1)(n_3 + n_4) \\ &\quad + \frac{1}{6}(\sqrt{3}\sqrt{2} + 3\sqrt{2} - 2\sqrt{3} - 3)(n_3 + n_4 - 1) \\ &\geq \frac{1}{2}(3 - 2\sqrt{2})(m + 2\sqrt{2}n + 2n) - \frac{1}{6}(3\sqrt{2} + 2\sqrt{3} - 3 - \sqrt{3}\sqrt{2})(n_3 + n_4 + 5 - 2\sqrt{3}\sqrt{2}) \\ &\geq \frac{1}{6}(2\sqrt{2} - 3)((\sqrt{3}\sqrt{2} + 2\sqrt{3} - 3\sqrt{2} - 3)n - \sqrt{3}\sqrt{2} - 2\sqrt{3} + 3\sqrt{2} - 3m + 3). \end{aligned} \quad (30)$$

This completes the proof.  $\square$

## Data Availability

All data generated or analyzed during this study are included in this published article. There are no experimental data in this article.

## Conflicts of Interest

The authors declare that there are no conflicts of interest regarding the publication of this article.

## References

- [1] M. Ö. Turaci, "On vertex and edge eccentricity-based topological indices of a certain chemical graph that represents bidentate ligands," *Journal of Molecular Structure*, vol. 1207, Article ID 127766, 2020.
- [2] M. Randić, "On characterization of molecular branching," *Journal of the American Chemical Society*, vol. 97, pp. 6609–6661, 1975.
- [3] I. Gutman and B. Furtula, *Recent Results in the Theory of Randić Index*, University of Kragujevac, Kragujevac, Serbia, 2008.
- [4] X. Li and I. Gutman, *Mathematical Aspects of Randić-type Molecular Structure Descriptors*, University of Kragujevac, Kragujevac, Serbia, 2006.
- [5] X. Li and Y. Shi, "A survey on the Randić index," *MATCH Communications in Mathematical and in Computer Chemistry*, vol. 59, no. 1, pp. 127–156, 2008.
- [6] G. Caporossi, I. Gutman, P. Hansen, and L. Pavlović, "Graphs with maximum connectivity index," *Computational Biology and Chemistry*, vol. 27, pp. 85–90, 2003.
- [7] W. C. Shiu and L. Z. Zhang, "The maximum Randić index of chemical trees with  $k$  pendants," *Discrete Mathematics*, vol. 309, pp. 4409–4416, 2009.
- [8] Y. Shi, "Note on two generalizations of the Randić index," *Applied Mathematics and Computation*, vol. 265, pp. 1019–1025, 2015.
- [9] T. Dehghan-Zadeh, A. R. Ashrafi, and N. Habibi, "Maximum and second maximum of Randić index in the class of tricyclic graphs," *MATCH Communications in Mathematical and in Computer Chemistry*, vol. 74, pp. 137–144, 2015.
- [10] T. Dehghan-Zadeh, A. R. Ashrafi, and N. Habibi, "Tetracyclic graphs with extremal values of Randić index," *Bollettino dell'Unione Matematica Italiana*, vol. 8, pp. 9–16, 2015.
- [11] H. Deng, S. Balachandran, and S. Elumalai, "Some tight bounds for the harmonic index and the variation of the Randić index of graphs," *Discrete Mathematics*, vol. 342, no. 7, pp. 2060–2065, 2019.
- [12] I. Gutman, B. Furtula, and V. Katanić, "Randić index and information," *AKCE International Journal of Graphs and Combinatorics*, vol. 15, no. 3, pp. 307–312, 2018.
- [13] A. Ghalavand and A. R. Ashrafi, "Ordering chemical graphs by Randić and sum-connectivity numbers," *Applied Mathematics and Computation*, vol. 331, pp. 160–168, 2018.

- [14] A. Ghalavand and A. R. Ashrafi, "Bounds on the entire Zagreb indices of graphs," *MATCH Communications in Mathematical and in Computer Chemistry*, vol. 81, pp. 371–381, 2019.
- [15] A. Ghalavand, A. R. Ashrafi, and I. Gutman, "Extremal graphs for the second multiplicative Zagreb index," *Bulletin of the International Mathematical Virtual Institute*, vol. 8, no. 2, pp. 369–383, 2018.

## Research Article

# Sharp Bounds for the Inverse Sum Indeg Index of Graph Operations

Anam Rani,<sup>1</sup> Muhammad Imran ,<sup>2</sup> and Usman Ali <sup>3,4</sup>

<sup>1</sup>Department of Basic Sciences, Deanship of Preparatory Year, King Faisal University, Al Hofuf, Al Ahsa, Saudi Arabia

<sup>2</sup>Department of Mathematical Sciences, United Arab Emirates University, P.O. Box 15551, Al Ain, UAE

<sup>3</sup>Institute de Mathematiques de Jussieu-Paris Rive Gauche, (Universite de Paris/Sorbonne Universite), Paris, France

<sup>4</sup>CASPAM, Bahauddin Zakariya University, Multan 66000, Pakistan

Correspondence should be addressed to Usman Ali; [uali@bzu.edu.pk](mailto:uali@bzu.edu.pk)

Received 8 February 2021; Accepted 22 May 2021; Published 9 June 2021

Academic Editor: Toqeer Mahmood

Copyright © 2021 Anam Rani et al. This is an open access article distributed under the Creative Commons Attribution License, which permits unrestricted use, distribution, and reproduction in any medium, provided the original work is properly cited.

Vukičević and Gasperov introduced the concept of 148 discrete Adriatic indices in 2010. These indices showed good predictive properties against the testing sets of the International Academy of Mathematical Chemistry. Among these indices, twenty indices were taken as beneficial predictors of physicochemical properties. The inverse sum indeg index denoted by  $ISI(\mathbf{G}_k)$  of  $\mathbf{G}_k$  is a notable predictor of total surface area for octane isomers and is presented as  $ISI(\mathbf{G}_k) = \sum_{g_k, g'_k \in E(\mathbf{G}_k)} (d_{\mathbf{G}_k}(g_k)d_{\mathbf{G}_k}(g'_k)/d_{\mathbf{G}_k}(g_k) + d_{\mathbf{G}_k}(g'_k))$ , where  $d_{\mathbf{G}_k}(g_k)$  represents the degree of  $g_k \in V(\mathbf{G}_k)$ . In this paper, we determine sharp bounds for ISI index of graph operations, including the Cartesian product, tensor product, strong product, composition, disjunction, symmetric difference, corona product, Indu-Bala product, union of graphs, double graph, and strong double graph.

## 1. Introduction

Let  $\mathbf{G}_k$  be a connected and simple graph whose vertex and edge sets are  $V(\mathbf{G}_k)$  and  $E(\mathbf{G}_k)$ , respectively. The order  $k$  and size  $k'$  of  $\mathbf{G}_k$  are the cardinalities of  $|V(\mathbf{G}_k)|$  and  $|E(\mathbf{G}_k)|$ , respectively. The degree formula of  $g_k \in V(\mathbf{G}_k)$  is the cardinality of linked vertices to  $g_k$  in  $\mathbf{G}_k$  and represented by  $d_{\mathbf{G}_k}(g_k)$ . The largest (or smallest) degree of  $\mathbf{G}_k$  is the degree of a vertex of  $\mathbf{G}_k$  with the greatest (or least) number of edges incident to it and represented by  $\Delta(\mathbf{G}_k)$  (or  $\delta(\mathbf{G}_k)$ ).

A molecular descriptor is a numerical parameter of a graph that distinguished its topology. In organic chemistry, topological descriptors have investigated many applications in pharmaceutical drug design, QSAR/QSPR study, chemical documentation, and isomer discrimination. Some of these topological indices are Wiener index, Zagreb indices, Szeged index, and Randić index. The set of 148 discrete Adriatic descriptors [1] have been defined in 2010. These descriptors showed well predictive characteristics on the testing sets given by International Academy of Mathematical Chemistry. Twenty of these descriptors were taken as

noteworthy predictors of physicochemical properties. One such index is inverse sum indeg index, denoted by  $ISI(\mathbf{G}_k)$ , of  $\mathbf{G}_k$  that was investigated in [1] as a noteworthy predictor of total surface area for octane isomers and is presented as follows:

$$ISI(\mathbf{G}_k) = \sum_{g_k, g'_k \in E(\mathbf{G}_k)} \frac{d_{\mathbf{G}_k}(g_k)d_{\mathbf{G}_k}(g'_k)}{d_{\mathbf{G}_k}(g_k) + d_{\mathbf{G}_k}(g'_k)}. \quad (1)$$

Sedlar et al. [2] investigated graph-theoretical characteristics of ISI index. Falahati-Nezhad et al. [3] computed some sharp bounds of inverse sum indeg (ISI) index.

The Zagreb indices of  $\mathbf{G}_k$  are presented by Gutman and Trinajstić [4] as follows:

$$\begin{aligned} M_1(\mathbf{G}_k) &= \sum_{g_k \in V(\mathbf{G}_k)} d_{\mathbf{G}_k}(g_k)^2, \\ M_2(\mathbf{G}_k) &= \sum_{g_k, g'_k \in E(\mathbf{G}_k)} d_{\mathbf{G}_k}(g_k)d_{\mathbf{G}_k}(g'_k). \end{aligned} \quad (2)$$

Let  $\mathbf{G}_k$  be  $k$ -vertex and  $\mathbf{H}_l$  be  $l$ -vertex graphs with size  $k'$  and  $l'$ , respectively. The Cartesian product  $\mathbf{G}_k \triangleright \mathbf{H}_l$ , whose vertex set is  $V(\mathbf{G}_k) \times V(\mathbf{H}_l)$  and  $(g_k, h_l)$  and  $(g'_k, h'_l)$  are adjacent when  $g_k = g'_k$  and  $h_l h'_l \in E(\mathbf{H}_l)$  or  $g_k g'_k \in E(\mathbf{G}_k)$  and  $h_l = h'_l$ , is a graph. The order and size of  $\mathbf{G}_k \triangleright \mathbf{H}_l$  are  $kl$  and  $k'l + kl'$ , respectively. The degree formula for  $(g_k, h_l) \in V(\mathbf{G}_k \triangleright \mathbf{H}_l)$  is  $d_{\mathbf{G}_k}(g_k) + d_{\mathbf{H}_l}(h_l)$ .

The tensor product  $\mathbf{G}_k \times \mathbf{H}_l$ , whose set of vertices is  $V(\mathbf{G}_k) \times V(\mathbf{H}_l)$  and  $(g_k, h_l)$  and  $(g'_k, h'_l)$  are linked when  $g_k g'_k \in E(\mathbf{G}_k)$  and  $h_l h'_l \in E(\mathbf{H}_l)$ , is a graph. The order and size of  $\mathbf{G}_k \times \mathbf{H}_l$  are  $kl$  and  $2k'l'$ , respectively. The degree formula for  $(g_k, h_l)$  in  $\mathbf{G}_k \times \mathbf{H}_l$  is  $d_{\mathbf{G}_k}(g_k) d_{\mathbf{H}_l}(h_l)$ .

The strong product  $\mathbf{G}_k \boxtimes \mathbf{H}_l$ , whose vertex set and edge set are  $V(\mathbf{G}_k) \times V(\mathbf{H}_l)$  and  $E(\mathbf{G}_k \triangleright \mathbf{H}_l) \cup E(\mathbf{G}_k \times \mathbf{H}_l)$ , respectively, is a graph. The order and size of  $\mathbf{G}_k \boxtimes \mathbf{H}_l$  are  $kl$  and  $kl' + lk' + 2k'l'$ , respectively. The degree formula for  $(g_k, h_l)$  in  $\mathbf{G}_k \boxtimes \mathbf{H}_l$  is  $d_{\mathbf{G}_k}(g_k) + d_{\mathbf{H}_l}(h_l) + d_{\mathbf{G}_k}(g_k) d_{\mathbf{H}_l}(h_l)$ .

The composition  $\mathbf{G}_k[\mathbf{H}_l]$ , whose vertex set  $V(\mathbf{G}_k) \times V(\mathbf{H}_l)$  and  $(g_k, h_l)$  and  $(g'_k, h'_l)$  are linked when  $g_k g'_k \in E(\mathbf{G}_k)$  or  $g_k = g'_k$  and  $h_l h'_l \in E(\mathbf{H}_l)$ , is a graph. The order and size of  $\mathbf{G}_k[\mathbf{H}_l]$  are  $kl$  and  $k'l^2 + kl'$ , respectively. The degree formula for  $(g_k, h_l)$  in  $\mathbf{G}_k[\mathbf{H}_l]$  is  $ld_{\mathbf{G}_k}(g_k) + d_{\mathbf{H}_l}(h_l)$ .

The disjunction  $\mathbf{G}_k \vee \mathbf{H}_l$ , whose vertex set is  $V(\mathbf{G}_k) \times V(\mathbf{H}_l)$  and  $(g_k, h_l)$  and  $(g'_k, h'_l)$  are linked when  $g_k g'_k \in E(\mathbf{G}_k)$  or  $h_l h'_l \in E(\mathbf{H}_l)$  is a graph. The order and size of  $\mathbf{G}_k \vee \mathbf{H}_l$  are  $kl$  and  $kl^2 + lk^2 - 2kl$ , respectively. The degree formula for  $(g_k, h_l)$  in  $\mathbf{G}_k \vee \mathbf{H}_l$  is  $ld_{\mathbf{G}_k}(g_k) + kd_{\mathbf{H}_l}(h_l) - d_{\mathbf{G}_k}(g_k) d_{\mathbf{H}_l}(h_l)$ .

The symmetric difference  $\mathbf{G}_k \oplus \mathbf{H}_l$  is a graph with vertex set  $V(\mathbf{G}_k) \times V(\mathbf{H}_l)$  and  $(g_k, h_l)(g'_k, h'_l) \in E(\mathbf{G}_k \oplus \mathbf{H}_l)$  whenever  $[g_k g'_k \in E(\mathbf{G}_k)]$  or  $[h_l h'_l \in E(\mathbf{H}_l)]$  but not both. The order and size of  $\mathbf{G}_k \oplus \mathbf{H}_l$  are  $kl$  and  $kl^2 + l'k^2 - 4kl$ , respectively. The degree formula for  $(g_k, h_l) \in V(\mathbf{G}_k \oplus \mathbf{H}_l)$  is  $ld_{\mathbf{G}_k}(g_k) + kd_{\mathbf{H}_l}(h_l) - 2d_{\mathbf{G}_k}(g_k) d_{\mathbf{H}_l}(h_l)$ .

Let  $\mathbf{G}_{k_1}, \mathbf{G}_{k_2}, \dots, \mathbf{G}_{k_n}$  be all vertex disjoint graphs. Then, their join is a graph whose vertex set is  $\cup_{s=1}^n V(\mathbf{G}_{k_s})$  and edge set is  $\cup_{s=1}^n E(\mathbf{G}_{k_s})$  together with the edges linking  $V(\mathbf{G}_{k_1})$  and  $V(\mathbf{G}_{k_2}), V(\mathbf{G}_{k_2})$  and  $V(\mathbf{G}_{k_3})$  so on  $V(\mathbf{G}_{k_{n-1}})$  and  $V(\mathbf{G}_{k_n})$ . The degree formula of  $g_k \in V(\mathbf{G}_{k_1} + \mathbf{G}_{k_2} + \dots + \mathbf{G}_{k_n})$  is  $d_{\mathbf{G}_{k_s}}(g_k) + r - k_s$ ,  $s = 1, 2, \dots, n$  and  $r = k_1 + k_2 + \dots + k_n$ .

The corona product  $\mathbf{G}_k \circ \mathbf{H}_l$  is acquired by taking  $\mathbf{G}_k$  as a single copy and  $k$  copies of  $\mathbf{H}_l$  and by linking  $r$ -th vertex of  $\mathbf{G}_k$  to every vertex of  $r$ -th copy of  $\mathbf{H}_l$ , where  $1 \leq r \leq k$ . The graph  $\mathbf{G}_k \circ \mathbf{H}_l$  has size and order  $k' + kl' + kl$  and  $k(1 + l)$ , respectively. The degree formula of  $g \in V(\mathbf{G}_k \circ \mathbf{H}_l)$  is

$$d_{\mathbf{G}_k \circ \mathbf{H}_l}(g) = \begin{cases} d_{\mathbf{G}_k}(g) + l, & \text{for } g \in V(\mathbf{G}_k), \\ d_{\mathbf{H}_l}(g) + 1, & \text{for } g \in V(\mathbf{H}_l). \end{cases} \quad (3)$$

The Indu-Bala product  $\mathbf{G}_k \blacktriangledown \mathbf{H}_l$  is obtained from two disjoint copies of  $\mathbf{G}_k + \mathbf{H}_l$  by linking the corresponding vertices of two copies of  $\mathbf{H}_l$ . The order and size of  $\mathbf{G}_k \blacktriangledown \mathbf{H}_l$  are  $2(k + l)$  and  $2k' + 2l' + 2kl + l$ , respectively. The degree of  $g \in V(\mathbf{G}_k \blacktriangledown \mathbf{H}_l)$  is

$$d_{\mathbf{G}_k \blacktriangledown \mathbf{H}_l}(g) = \begin{cases} d_{\mathbf{G}_k}(g) + l, & \text{for } g \in V(\mathbf{G}_k), \\ d_{\mathbf{H}_l}(g) + k + 1, & \text{for } g \in V(\mathbf{H}_l). \end{cases} \quad (4)$$

The double graph  $D[\mathbf{G}_k]$  is acquired by taking original edge set of two copies  $V_1(\mathbf{G}_k)$  and  $V_2(\mathbf{G}_k)$  of  $V(\mathbf{G}_k)$  and linking each vertex in  $V_1(\mathbf{G}_k)$  with the linked vertices of corresponding vertex in  $V_2(\mathbf{G}_k)$ . The strong double graph  $SD[\mathbf{G}_k]$  is acquired by taking two copies of  $V_1(\mathbf{G}_k)$  and  $V_2(\mathbf{G}_k)$  of  $V(\mathbf{G}_k)$  and linking each vertex in  $V_1(\mathbf{G}_k)$  with closed neighborhood of corresponding vertex in  $V_2(\mathbf{G}_k)$ .

Figure 1 depicts some graph operations. For more details on these graph operations, see [5–14]. Also, we refer some recent articles [15–19] on different kinds of descriptors. It is an important and well-reputed problem to study and explore the molecular topological descriptors of the graph operations in terms of the original graphs, say  $\mathbf{G}_k$  and  $\mathbf{H}_l$ , and this also helps to explore the physicochemical properties of the complex chemical structures which arise from these graph operations. The upper and lower bounds of any molecular descriptors are the important information related to a chemical graph. They determine the approximate possible range of the invariant in the form of molecular structural parameters. There are some bounds already available for the inverse sum indeg (ISI) index regarding the number of pendant vertices, size, radius, smallest and largest vertex degrees, and smallest nonpendent vertex degree of a graph computed in [3]. The objective of this article is to determine the bounds for inverse sum indeg index of some graph operations including Cartesian product, tensor product, strong product, composition, disjunction, symmetric difference, corona product, Indu-Bala product, union of graphs, double graph, and strong double graph in the form of original graphs, say  $\mathbf{G}_k$  and  $\mathbf{H}_l$ .

## 2. Applications of Graph Theory Concept and Topological Indices in Chemistry

In 1936, Hosoya introduced the concept of graph terminologies in chemistry and provided a modeling for molecules. This modeling contents lead to predict the chemical properties of molecules, easy classification of chemical compounds, computer simulations, and computer-assisted design of new chemical compounds. As in current century, chemists manipulate graphs on a daily basis using Table 1 terminologies for recent development in their research.

Graph hypothesis had investigated an interesting exercise around in research. Compound graph speculation has provided a collection of beneficial indices, for instance, topological indices. The Zagreb indices are the topological indices that are correlated to a substantial computation of fabricated characteristics of the particles and have been investigated parallel to establishing the Kovats constants and limit of the particles [20]. The hyper Zagreb descriptor has a strong bound between the security of direct dendrimers besides the expanded medication stores and for establishing the strain criticalness of cyclo alkanes [21]. To connect with various physico-mix characteristics, Zagreb indices have required deep control upon the essentialness of the dendrimers [22]. The Zagreb polynomials were determined to happen for computation of the  $\pi$ -electron imperativeness of the particles inside specific brutal verbalizations [23, 24].

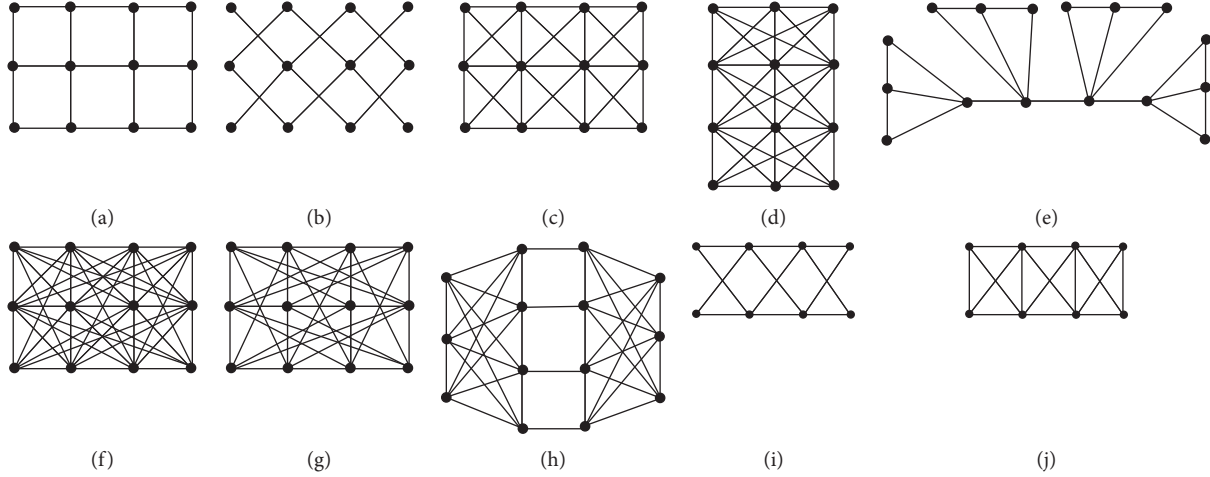


FIGURE 1: Graph operations: (a)  $P_3 \square P_4$ ; (b)  $P_3 \times P_4$ ; (c)  $P_3 \boxtimes P_4$ ; (d)  $P_4[P_3]$ ; (e)  $P_4 \circ P_3$ ; (f)  $P_3 \vee P_4$ ; (g)  $P_3 \oplus P_4$ ; (h)  $P_3 \blacktriangledown P_4$ ; (i)  $D[P_4]$ ; (j)  $SD[P_4]$ .

TABLE 1: Graph theory and chemistry dictionary.

Graph theory	Chemistry
Graph	Structural formula
Vertex	Atom
Edge	Chemical bond
Vertex degree	Valency of atom
Tree	Acyclic structure
Bipartite graph	Alternant structure
Perfect matching	Kekule structure
Adjacency matrix	Huckel matrix

### 3. Inverse Sum Indeg Index of Graph Operations

In this section, we compute the inverse sum indeg index of the Cartesian product, tensor product, strong product, composition, disjunction, symmetric difference, corona product, Indu-Bala product, double graph, and strong double graph. The relation between largest and

smallest degree of  $\mathbf{G}_k$  to the degree of  $g_k \in V(\mathbf{G}_k)$  is as follows:

$$\begin{aligned} d_{\mathbf{G}_k}(g_k) &\leq \Delta_{\mathbf{G}_k}, \\ d_{\mathbf{G}_k}(g_k) &\geq \delta_{\mathbf{G}_k}. \end{aligned} \quad (5)$$

In the upcoming theorem, we calculate the bounds for inverse sum indeg (ISI) index of Cartesian product.

**Theorem 1.** Let  $\mathbf{G}_k$  and  $\mathbf{H}_l$  be two graphs. Then,

$$\frac{M_2(\mathbf{G}_k \triangleright \mathbf{H}_l)}{2(\Delta_{\mathbf{G}_k} + \Delta_{\mathbf{H}_l})} \leq \text{ISI}(\mathbf{G}_k \triangleright \mathbf{H}_l) \leq \frac{M_2(\mathbf{G}_k \triangleright \mathbf{H}_l)}{2(\delta_{\mathbf{G}_k} + \delta_{\mathbf{H}_l})}. \quad (6)$$

The equalities hold if and only if  $\mathbf{G}_k$  and  $\mathbf{H}_l$  are regular.

*Proof.* Using the degree formula for a vertex of  $\mathbf{G}_k \triangleright \mathbf{H}_l$  in equation (1),

$$\begin{aligned} \text{ISI}(\mathbf{G}_k \triangleright \mathbf{H}_l) &= \sum_{(g_k, h_l)(g'_k, h'_l) \in E(\mathbf{G}_k \triangleright \mathbf{H}_l)} \frac{d_{\mathbf{G}_k \triangleright \mathbf{H}_l}(g_k, h_l) d_{\mathbf{G}_k \triangleright \mathbf{H}_l}(g'_k, h'_l)}{d_{\mathbf{G}_k \triangleright \mathbf{H}_l}(g_k, h_l) + d_{\mathbf{G}_k \triangleright \mathbf{H}_l}(g'_k, h'_l)} \\ &= \sum_{(g_k, h_l)(g'_k, h'_l) \in E(\mathbf{G}_k \triangleright \mathbf{H}_l)} \frac{d_{\mathbf{G}_k \triangleright \mathbf{H}_l}(g_k, h_l) d_{\mathbf{G}_k \triangleright \mathbf{H}_l}(g'_k, h'_l)}{d_{\mathbf{G}_k}(g_k) + d_{\mathbf{H}_l}(h_l) + d_{\mathbf{G}_k}(g'_k) + d_{\mathbf{H}_l}(h'_l)} \\ &\leq \frac{1}{2(\delta_{\mathbf{G}_k} + \delta_{\mathbf{H}_l})} \sum_{(g_k, h_l)(g'_k, h'_l) \in E(\mathbf{G}_k \triangleright \mathbf{H}_l)} d_{\mathbf{G}_k \triangleright \mathbf{H}_l}(g_k, h_l) d_{\mathbf{G}_k \triangleright \mathbf{H}_l}(g'_k, h'_l) \\ &= \frac{M_2(\mathbf{G}_k \triangleright \mathbf{H}_l)}{2(\delta_{\mathbf{G}_k} + \delta_{\mathbf{H}_l})}. \end{aligned} \quad (7)$$

Similarly, we can evaluate

$$\text{ISI}(\mathbf{G}_k \triangleright \mathbf{H}_l) \geq \frac{M_2(\mathbf{G}_k \triangleright \mathbf{H}_l)}{2(\Delta_{\mathbf{G}_k} + \Delta_{\mathbf{H}_l})}. \quad (8)$$

The above equalities hold if and only if factor graphs are regular.

In the next theorem, we calculate the bounds for ISI index of tensor product of  $\mathbf{G}_k$  and  $\mathbf{H}_l$ .  $\square$

**Theorem 2.** Let  $\mathbf{G}_k$  and  $\mathbf{H}_l$  be two graphs. Then,

$$\frac{M_2(\mathbf{G}_k)M_2(\mathbf{H}_l)}{\Delta_{\mathbf{G}_k}\Delta_{\mathbf{H}_l}} \leq \text{ISI}(\mathbf{G}_k \times \mathbf{H}_l) \leq \frac{M_2(\mathbf{G}_k)M_2(\mathbf{H}_l)}{\delta_{\mathbf{G}_k}\delta_{\mathbf{H}_l}}. \quad (9)$$

The above equalities hold if and only if both graphs are regular.

*Proof.* Using the degree formula for a vertex in tensor product of graphs in (1),

$$\begin{aligned} \text{ISI}(\mathbf{G}_k \times \mathbf{H}_l) &= \sum_{(g_k, h_l), (g'_k, h'_l) \in E(\mathbf{G}_k \times \mathbf{H}_l)} \frac{d_{\mathbf{G}_k \times \mathbf{H}_l}(g_k, h_l)d_{\mathbf{G}_k \times \mathbf{H}_l}(g'_k, h'_l)}{d_{\mathbf{G}_k \times \mathbf{H}_l}(g_k, h_l) + d_{\mathbf{G}_k \times \mathbf{H}_l}(g'_k, h'_l)} \\ &= \sum_{(g_k, h_l), (g'_k, h'_l) \in E(\mathbf{G}_k \times \mathbf{H}_l)} \frac{d_{\mathbf{G}_k \times \mathbf{H}_l}(g_k, h_l)d_{\mathbf{G}_k \times \mathbf{H}_l}(g'_k, h'_l)}{d_{\mathbf{G}_k}(g_k)d_{\mathbf{H}_l}(h_l) + d_{\mathbf{G}_k}(g'_k)d_{\mathbf{H}_l}(h'_l)} \\ &\leq \frac{1}{2\delta_{\mathbf{G}_k}\delta_{\mathbf{H}_l}} \sum_{(g_k, h_l), (g'_k, h'_l) \in E(\mathbf{G}_k \times \mathbf{H}_l)} d_{\mathbf{G}_k \times \mathbf{H}_l}(g_k, h_l)d_{\mathbf{G}_k \times \mathbf{H}_l}(g'_k, h'_l) \\ &= \frac{M_2(\mathbf{G}_k \times \mathbf{H}_l)}{2\delta_{\mathbf{G}_k}\delta_{\mathbf{H}_l}} \\ &= \frac{M_2(\mathbf{G}_k)M_2(\mathbf{H}_l)}{\delta_{\mathbf{G}_k}\delta_{\mathbf{H}_l}}. \end{aligned} \quad (10)$$

See Theorem 2.1 in [25]. Similarly, we can compute

$$\text{ISI}(\mathbf{G}_k \times \mathbf{H}_l) \geq \frac{M_2(\mathbf{G}_k)M_2(\mathbf{H}_l)}{\Delta_{\mathbf{G}_k}\Delta_{\mathbf{H}_l}}. \quad (11)$$

The above equalities hold if and only if factor graphs are regular.

We derive the bounds of inverse sum indeg (ISI) index of  $\mathbf{G}_k \boxtimes \mathbf{H}_l$  in the upcoming theorem.  $\square$

**Theorem 3.** Let  $\mathbf{G}_k$  and  $\mathbf{H}_l$  be two graphs. Then,

$$\frac{M_2(\mathbf{G}_k \boxtimes \mathbf{H}_l)}{2(\Delta_{\mathbf{G}_k} + \Delta_{\mathbf{H}_l} + \Delta_{\mathbf{G}_k}\Delta_{\mathbf{H}_l})} \leq \text{ISI}(\mathbf{G}_k \boxtimes \mathbf{H}_l) \leq \frac{M_2(\mathbf{G}_k \boxtimes \mathbf{H}_l)}{2(\delta_{\mathbf{G}_k} + \delta_{\mathbf{H}_l} + \delta_{\mathbf{G}_k}\delta_{\mathbf{H}_l})}. \quad (12)$$

The equalities hold if and only if both graphs are regular.

*Proof.* Using the degree formula of a vertex in strong product of graphs in (1),

$$\begin{aligned} \text{ISI}(\mathbf{G}_k \times \mathbf{H}_l) &= \sum_{(g_k, h_l), (g'_k, h'_l) \in E(\mathbf{G}_k \boxtimes \mathbf{H}_l)} \frac{d_{\mathbf{G}_k \boxtimes \mathbf{H}_l}(g_k, h_l)d_{\mathbf{G}_k \boxtimes \mathbf{H}_l}(g'_k, h'_l)}{d_{\mathbf{G}_k \boxtimes \mathbf{H}_l}(g_k, h_l) + d_{\mathbf{G}_k \boxtimes \mathbf{H}_l}(g'_k, h'_l)} \\ &= \sum_{(g_k, h_l), (g'_k, h'_l) \in E(\mathbf{G}_k \boxtimes \mathbf{H}_l)} \frac{d_{\mathbf{G}_k \boxtimes \mathbf{H}_l}(g_k, h_l)d_{\mathbf{G}_k \boxtimes \mathbf{H}_l}(g'_k, h'_l)}{d_{\mathbf{G}_k}(g_k) + d_{\mathbf{H}_l}(h_l) + d_{\mathbf{G}_k}(g_k)d_{\mathbf{H}_l}(h_l) + d_{\mathbf{G}_k}(g'_k)d_{\mathbf{H}_l}(h'_l) + d_{\mathbf{G}_k}(g_k) + d_{\mathbf{H}_l}(h'_l)} \\ &\leq \frac{1}{2(\delta_{\mathbf{G}_k} + \delta_{\mathbf{H}_l} + \delta_{\mathbf{G}_k}\delta_{\mathbf{H}_l})} \sum_{(g_k, h_l), (g'_k, h'_l) \in E(\mathbf{G}_k \boxtimes \mathbf{H}_l)} d_{\mathbf{G}_k \boxtimes \mathbf{H}_l}(g_k, h_l)d_{\mathbf{G}_k \boxtimes \mathbf{H}_l}(g'_k, h'_l) \\ &= \frac{M_2(\mathbf{G}_k \times \mathbf{H}_l)}{2(\delta_{\mathbf{G}_k} + \delta_{\mathbf{H}_l} + \delta_{\mathbf{G}_k}\delta_{\mathbf{H}_l})}. \end{aligned} \quad (13)$$

In a similarly way,



$$\text{ISI}(\mathbf{G}_k \boxtimes \mathbf{H}_l) \geq \frac{M_2(\mathbf{G}_k \boxtimes \mathbf{H}_l)}{2(\Delta_{\mathbf{G}_k} + \Delta_{\mathbf{H}_l} + \Delta_{\mathbf{G}_k} \Delta_{\mathbf{H}_l})}. \quad (14)$$

The above equalities satisfy if and only if factor graphs are regular.

In the upcoming theorem, we evaluate the bounds for inverse sum indeg (ISI) index of  $\mathbf{G}_k[\mathbf{H}_l]$ .  $\square$

**Theorem 4.** Let  $\mathbf{G}_k$  and  $\mathbf{H}_l$  be two graphs. Then,

$$\begin{aligned} \text{ISI}(\mathbf{G}_k[\mathbf{H}_l]) &= \sum_{(g_k, h_l), (g'_k, h'_l) \in E(\mathbf{G}_k[\mathbf{H}_l])} \frac{d_{\mathbf{G}_k[\mathbf{H}_l]}(g_k, h_l) d_{\mathbf{G}_k[\mathbf{H}_l]}(g'_k, h'_l)}{d_{\mathbf{G}_k[\mathbf{H}_l]}(g_k, h_l) + d_{\mathbf{G}_k[\mathbf{H}_l]}(g'_k, h'_l)} \\ &= \sum_{(g_k, h_l), (g'_k, h'_l) \in E(\mathbf{G}_k[\mathbf{H}_l])} \frac{d_{\mathbf{G}_k[\mathbf{H}_l]}(g_k, h_l) d_{\mathbf{G}_k[\mathbf{H}_l]}(g'_k, h'_l)}{ld_{\mathbf{G}_k}(g_k) + d_{\mathbf{H}_l}(h_l) + ld_{\mathbf{G}_k}(g'_k) + d_{\mathbf{H}_l}(h'_l)} \\ &\leq \frac{1}{2(ld_{\mathbf{G}_k} + \delta_{\mathbf{H}_l})} \sum_{(g_k, h_l), (g'_k, h'_l) \in E(\mathbf{G}_k[\mathbf{H}_l])} d_{\mathbf{G}_k[\mathbf{H}_l]}(g_k, h_l) d_{\mathbf{G}_k[\mathbf{H}_l]}(g'_k, h'_l) \\ &= \frac{M_2(\mathbf{G}_k[\mathbf{H}_l])}{2(ld_{\mathbf{G}_k} + \delta_{\mathbf{H}_l})}. \end{aligned} \quad (16)$$

In a similar way,

$$\text{ISI}(\mathbf{G}_k[\mathbf{H}_l]) \geq \frac{M_2(\mathbf{G}_k[\mathbf{H}_l])}{2(l\Delta_{\mathbf{G}_k} + \Delta_{\mathbf{H}_l})}. \quad (17)$$

The above equalities hold if and only if factor graphs are regular.

In the following theorem, we present the bounds for inverse sum indeg (ISI) index of disjunction of  $\mathbf{G}_k$  and  $\mathbf{H}_l$ .  $\square$

**Theorem 5.** Let  $\mathbf{G}_k$  and  $\mathbf{H}_l$  be two graphs. Then,

$$\begin{aligned} \text{ISI}(\mathbf{G}_k \vee \mathbf{H}_l) &= \sum_{(g_k, h_l), (g'_k, h'_l) \in E(\mathbf{G}_k \vee \mathbf{H}_l)} \frac{d_{\mathbf{G}_k \vee \mathbf{H}_l}(g_k, h_l) d_{\mathbf{G}_k \vee \mathbf{H}_l}(g'_k, h'_l)}{d_{\mathbf{G}_k \vee \mathbf{H}_l}(g_k, h_l) + d_{\mathbf{G}_k \vee \mathbf{H}_l}(g'_k, h'_l)} \\ &= \sum_{(g_k, h_l), (g'_k, h'_l) \in E(\mathbf{G}_k \vee \mathbf{H}_l)} \frac{d_{\mathbf{G}_k \vee \mathbf{H}_l}(g_k, h_l) d_{\mathbf{G}_k \vee \mathbf{H}_l}(g'_k, h'_l)}{ld_{\mathbf{G}_k}(g_k) + kd_{\mathbf{H}_l}(h_l) - d_{\mathbf{G}_k}(g_k) d_{\mathbf{H}_l}(h_l) + ld_{\mathbf{G}_k}(g'_k) + kd_{\mathbf{H}_l}(h'_l) - d_{\mathbf{G}_k}(g'_k) d_{\mathbf{H}_l}(h'_l)} \\ &\leq \frac{1}{2(l\delta_{\mathbf{G}_k} + k\delta_{\mathbf{H}_l} - \delta_{\mathbf{G}_k} \delta_{\mathbf{H}_l})} \sum_{(g_k, h_l), (g'_k, h'_l) \in E(\mathbf{G}_k \vee \mathbf{H}_l)} d_{\mathbf{G}_k \vee \mathbf{H}_l}(g_k, h_l) d_{\mathbf{G}_k \vee \mathbf{H}_l}(g'_k, h'_l) \\ &= \frac{M_2(\mathbf{G}_k \vee \mathbf{H}_l)}{2(l\delta_{\mathbf{G}_k} + k\delta_{\mathbf{H}_l} - \delta_{\mathbf{G}_k} \delta_{\mathbf{H}_l})}. \end{aligned} \quad (19)$$

$$\frac{M_2(\mathbf{G}_k[\mathbf{H}_l])}{2(l\Delta_{\mathbf{G}_k} + \Delta_{\mathbf{H}_l})} \leq \text{ISI}(\mathbf{G}_k[\mathbf{H}_l]) \leq \frac{M_2(\mathbf{G}_k[\mathbf{H}_l])}{2(l\delta_{\mathbf{G}_k} + \delta_{\mathbf{H}_l})}. \quad (15)$$

The equalities hold if and only if both graphs are regular.

*Proof.* Using the degree formula of an element of  $V(\mathbf{G}_k[\mathbf{H}_l])$  in (1),

$$\begin{aligned} \frac{M_2(\mathbf{G}_k \vee \mathbf{H}_l)}{2(l\Delta_{\mathbf{G}_k} + k\Delta_{\mathbf{H}_l} - \Delta_{\mathbf{G}_k} \Delta_{\mathbf{H}_l})} &\leq \text{ISI}(\mathbf{G}_k \vee \mathbf{H}_l) \\ &\leq \frac{M_2(\mathbf{G}_k \vee \mathbf{H}_l)}{2(l\delta_{\mathbf{G}_k} + k\delta_{\mathbf{H}_l} - \delta_{\mathbf{G}_k} \delta_{\mathbf{H}_l})}. \end{aligned} \quad (18)$$

The equalities hold when factor graphs are regular.

*Proof.* Using the degree formula of an element of  $V(\mathbf{G}_k \vee \mathbf{H}_l)$  in (1),

Similarly, we compute

$$\text{ISI}(\mathbf{G}_k \vee \mathbf{H}_l) \geq \frac{M_2(\mathbf{G}_k \vee \mathbf{H}_l)}{2(l\Delta_{\mathbf{G}_k} + k\Delta_{\mathbf{H}_l} - \Delta_{\mathbf{G}_k} \Delta_{\mathbf{H}_l})}. \quad (20)$$

The above equalities hold when both graphs are regular.

Next, we derive the bounds of inverse sum indeg (ISI) index of  $\mathbf{G}_k \oplus \mathbf{H}_l$ .  $\square$

**Theorem 6.** Let  $\mathbf{G}_k$  and  $\mathbf{H}_l$  be two graphs. Then,

$$\begin{aligned} \frac{M_2(\mathbf{G}_k \oplus \mathbf{H}_l)}{2(l\Delta_{\mathbf{G}_k} + k\Delta_{\mathbf{H}_l} - 2\Delta_{\mathbf{G}_k} \Delta_{\mathbf{H}_l})} &\leq \text{ISI}(\mathbf{G}_k \oplus \mathbf{H}_l) \\ &\leq \frac{M_2(\mathbf{G}_k \oplus \mathbf{H}_l)}{2(l\delta_{\mathbf{G}_k} + k\delta_{\mathbf{H}_l} - 2\delta_{\mathbf{G}_k} \delta_{\mathbf{H}_l})}. \end{aligned} \quad (21)$$

$$\begin{aligned} \text{ISI}(\mathbf{G}_k \oplus \mathbf{H}_l) &= \sum_{(g_k, h_l) (g'_k, h'_l) \in E(\mathbf{G}_k \oplus \mathbf{H}_l)} \frac{d_{\mathbf{G}_k \oplus \mathbf{H}_l}(g_k, h_l) d_{\mathbf{G}_k \oplus \mathbf{H}_l}(g'_k, h'_l)}{d_{\mathbf{G}_k \oplus \mathbf{H}_l}(g_k, h_l) + d_{\mathbf{G}_k \oplus \mathbf{H}_l}(g'_k, h'_l)} \\ &= \sum_{(g_k, h_l) (g'_k, h'_l) \in E(\mathbf{G}_k \oplus \mathbf{H}_l)} \frac{d_{\mathbf{G}_k \oplus \mathbf{H}_l}(g_k, h_l) d_{\mathbf{G}_k \oplus \mathbf{H}_l}(g'_k, h'_l)}{ld_{\mathbf{G}_k}(g_k) + kd_{\mathbf{H}_l}(h_l) - 2d_{\mathbf{G}_k}(g_k) d_{\mathbf{H}_l}(h_l) + ld_{\mathbf{G}_k}(g'_k) + kd_{\mathbf{H}_l}(h'_l) - 2d_{\mathbf{G}_k}(g'_k) d_{\mathbf{H}_l}(h'_l)} \\ &\leq \frac{1}{2(l\delta_{\mathbf{G}_k} + k\delta_{\mathbf{H}_l} - 2\delta_{\mathbf{G}_k} \delta_{\mathbf{H}_l})} \sum_{(g_k, h_l) (g'_k, h'_l) \in E(\mathbf{G}_k \oplus \mathbf{H}_l)} d_{\mathbf{G}_k \oplus \mathbf{H}_l}(g_k, h_l) d_{\mathbf{G}_k \oplus \mathbf{H}_l}(g'_k, h'_l) \\ &= \frac{M_2(\mathbf{G}_k \oplus \mathbf{H}_l)}{2(l\delta_{\mathbf{G}_k} + k\delta_{\mathbf{H}_l} - 2\delta_{\mathbf{G}_k} \delta_{\mathbf{H}_l})}. \end{aligned} \quad (22)$$

Similarly,

$$\text{ISI}(\mathbf{G}_k \oplus \mathbf{H}_l) \geq \frac{M_2(\mathbf{G}_k \oplus \mathbf{H}_l)}{2(l\Delta_{\mathbf{G}_k} + k\Delta_{\mathbf{H}_l} - 2\Delta_{\mathbf{G}_k} \Delta_{\mathbf{H}_l})}. \quad (23)$$

The above equalities hold if and only if both graphs are regular.  $\square$

The equalities hold if and only if factor graphs are regular.

*Proof.* Using the degree formula of a vertex of  $V(\mathbf{G}_k \oplus \mathbf{H}_l)$  in (1),

Next, we evaluate the bounds of inverse sum indeg (ISI) index of join of  $n$  graphs.  $\square$

**Theorem 7.** Let  $\mathbf{G}_k = \mathbf{G}_{k_1} + \mathbf{G}_{k_2} + \dots + \mathbf{G}_{k_n}$ . Then,

$$\begin{aligned} &\sum_{s=1}^n \frac{M_2(\mathbf{G}_{k_s}) + (r - k_s)M_1(\mathbf{G}_{k_s}) + k'_s(r - k_s)^2}{2(\Delta_{\mathbf{G}_{k_s}} + r - k_s)} + \frac{1}{2} \sum_{s \neq j, s, j=1}^n \frac{(2k'_s + k_s(r - k_s))(2k'_j + k_j(r - k_j))}{\Delta_{\mathbf{G}_{k_s}} + \Delta_{\mathbf{G}_{k_j}} + 2r - k_s - k_j} \\ &\leq \text{ISI}(\mathbf{G}_k) \leq \sum_{s=1}^n \frac{M_2(\mathbf{G}_{k_s}) + (r - k_s)M_1(\mathbf{G}_{k_s}) + k'_s(r - k_s)^2}{2(\delta_{\mathbf{G}_{k_s}} + r - k_s)} \\ &\quad + \frac{1}{2} \sum_{i \neq j, s, j=1}^n \frac{(2k'_s + k_s(r - k_s))(2k'_j + k_j(r - k_j))}{\delta_{\mathbf{G}_{k_s}} + \delta_{\mathbf{G}_{k_j}} + 2r - k_s - k_j}. \end{aligned} \quad (24)$$

The equalities hold if and only if  $\mathbf{G}_{k_s}$ , for  $s = 1, 2, \dots, n$ , are regular graphs.

*Proof.* We assume that  $|V(\mathbf{G}_{k_s})| = k_s$ ,  $|E(\mathbf{G}_{k_s})| = k'_s$  for  $s = 1, 2, \dots, n$  and  $r = k_1 + k_2 + \dots + k_n$ . By using the degree formula of a vertex in  $\mathbf{G}_k$  given in (1),

$$\begin{aligned}
 \text{ISI}(\mathbf{G}_k) &= \sum_{g_k, g'_k \in E(\mathbf{G}_k)} \frac{d_{\mathbf{G}_k}(g_k)d_{\mathbf{G}_k}(g'_k)}{d_{\mathbf{G}_k}(g_k) + d_{\mathbf{G}_k}(g'_k)} \\
 &= \sum_{s=1}^n \sum_{g_k, g'_k \in E(\mathbf{G}_{k_s})} \frac{(d_{\mathbf{G}_{k_s}}(g_k) + r - k_s)(d_{\mathbf{G}_{k_s}}(g'_k) + r - k_s)}{d_{\mathbf{G}_{k_s}}(g_k) + d_{\mathbf{G}_{k_s}}(g'_k) + 2r - 2k_s} + \frac{1}{2} \sum_{\substack{s \neq j, \\ s, j=1}}^n \sum_{g_k \in V(\mathbf{G}_{k_s})} \sum_{g'_k \in V(\mathbf{G}_{k_j})} \frac{(d_{\mathbf{G}_{k_s}}(g_k) + r - k_s) - (d_{\mathbf{G}_{k_j}}(g'_k) + r - k_j)}{d_{\mathbf{G}_{k_s}}(g_k) + d_{\mathbf{G}_{k_j}}(g'_k) + 2r - k_s - k_j} \\
 &\leq \sum_{s=1}^n \sum_{g_k, g'_k \in E(\mathbf{G}_{k_s})} \frac{(d_{\mathbf{G}_{k_s}}(g_k) + r - k_s)(d_{\mathbf{G}_{k_s}}(g'_k) + r - k_s)}{\delta_{\mathbf{G}_{k_s}} + \delta_{\mathbf{G}_{k_s}} + 2r - 2k_s} + \frac{1}{2} \sum_{\substack{s \neq j, \\ s, j=1}}^n \sum_{g_k \in V(\mathbf{G}_{k_s})} \sum_{v \in V(\mathbf{G}_{k_j})} \frac{(d_{\mathbf{G}_{k_s}}(g_k) + r - k_s)(d_{\mathbf{G}_{k_j}}(v) + r - k_j)}{\delta_{\mathbf{G}_{k_s}} + \delta_{\mathbf{G}_{k_j}} + 2r - k_s - k_j} \\
 &= \sum_{s=1}^n \frac{M_2(\mathbf{G}_{k_s}) + (r - k_s)M_1(\mathbf{G}_{k_s}) + k'_s(r - k_s)^2}{2(\delta_{\mathbf{G}_{k_s}} + r - k_s)} + \frac{1}{2} \sum_{\substack{s \neq j, \\ s, j=1}}^n \frac{(2k'_s + k_s(r - k_s))(2k'_j + k_j(r - k_j))}{\delta_{\mathbf{G}_{k_s}} + \delta_{\mathbf{G}_{k_j}} + 2r - k_s - k_j}.
 \end{aligned} \tag{25}$$

Similarly

$$\text{ISI}(\mathbf{G}_k) \geq \sum_{s=1}^n \frac{M_2(\mathbf{G}_{k_s}) + (r - k_s)M_1(\mathbf{G}_{k_s}) + k'_s(r - k_s)^2}{2(\Delta_{\mathbf{G}_{k_s}} + r - k_s)} + \frac{1}{2} \sum_{\substack{s \neq j, \\ s, j=1}}^n \frac{(2k'_s + k_s(r - k_s))(2k'_j + k_j(r - k_j))}{\Delta_{\mathbf{G}_{k_s}} + \Delta_{\mathbf{G}_{k_j}} + 2r - k_s - k_j}. \tag{26}$$

The above equalities hold if and only if  $\mathbf{G}_{k_s}$ ,  $s = 1, 2, \dots, n$ , are regular.

In the following theorem, we calculate the bounds for ISI index of  $\mathbf{G}_k \circ \mathbf{H}_l$ .  $\square$

**Theorem 8.** Let  $\mathbf{G}_k$  and  $\mathbf{H}_l$  be  $k$ -vertex and  $l$ -vertex graphs. Then,

$$\begin{aligned}
 &\frac{k(M_2(\mathbf{H}_l) + M_1(\mathbf{H}_l) + l)}{2(\Delta_{\mathbf{H}_l} + 1)} + \frac{(2l' + l)(2k' + kl)}{\Delta_{\mathbf{G}_k} + \Delta_{\mathbf{H}_l} + l + 1} + \frac{M_2(\mathbf{G}_k) + lM_1(\mathbf{G}_k) + l^2l'}{2(\Delta_{\mathbf{G}_k} + l)} \leq \text{ISI}(\mathbf{G}_k \circ \mathbf{H}_l) \\
 &\leq \frac{k(M_2(\mathbf{H}_l) + M_1(\mathbf{H}_l) + l)}{2(\delta_{\mathbf{H}_l} + 1)} + \frac{(2l' + l)(2k' + kl)}{\delta_{\mathbf{G}_k} + \delta_{\mathbf{H}_l} + l + 1} + \frac{M_2(\mathbf{G}_k) + lM_1(\mathbf{G}_k) + l^2l'}{2(\delta_{\mathbf{G}_k} + l)}.
 \end{aligned} \tag{27}$$

The equalities hold if and only if both graphs are regular.

*Proof.* Using the degree formula of a vertex in corona product in (1),

$$\begin{aligned} \text{ISI}(\mathbf{G}_k \circ \mathbf{H}_l) &= k \sum_{h_i, h'_i \in E(\mathbf{H}_l)} \frac{(d_{\mathbf{H}_l}(h_i) + 1)(d_{\mathbf{H}_l}(h'_i) + 1)}{d_{\mathbf{H}_l}(h_i) + d_{\mathbf{H}_l}(h'_i) + 2} + \sum_{s=1}^k \sum_{j=1}^l \frac{(d_{\mathbf{H}_l}(h_{l_j}) + 1)(d_{\mathbf{G}_k}(g_{k_s}) + l)}{d_{\mathbf{H}_l}(h_{l_j}) + d_{\mathbf{G}_k}(g_{k_s}) + l + 1} \\ &+ \sum_{g_k, g'_k \in E(\mathbf{G}_k)} \frac{(d_{\mathbf{G}_k}(g_k) + l)(d_{\mathbf{G}_k}(g'_k) + l)}{d_{\mathbf{G}_k}(g_k) + d_{\mathbf{G}_k}(g'_k) + 2l}. \end{aligned} \quad (28)$$

From equation (2), we obtain

$$\begin{aligned} \text{ISI}(\mathbf{G}_k \circ \mathbf{H}_l) &\leq k \sum_{h_i, h'_i \in E(\mathbf{H}_l)} \frac{(d_{\mathbf{H}_l}(h_i) + 1)(d_{\mathbf{H}_l}(h'_i) + 1)}{2(\delta_{\mathbf{H}_l} + 1)} + \sum_{s=1}^k \sum_{j=1}^l \frac{(d_{\mathbf{H}_l}(h_{l_j}) + 1)(d_{\mathbf{G}_k}(g_{k_s}) + l)}{\delta_{\mathbf{G}_k} + \delta_{\mathbf{H}_l} + l + 1} \\ &+ \sum_{g_k, g'_k \in E(\mathbf{G}_k)} \frac{(d_{\mathbf{G}_k}(g_k) + l)(d_{\mathbf{G}_k}(g'_k) + l)}{2(\delta_{\mathbf{G}_k} + l)} \\ &= \frac{k(M_2(\mathbf{H}_l) + M_1(\mathbf{H}_l) + l)}{2(\delta_{\mathbf{H}_l} + 1)} + \frac{(2l' + l)(2k' + kl)}{\delta_{\mathbf{G}_k} + \delta_{\mathbf{H}_l} + l + 1} + \frac{M_2(\mathbf{G}_k) + lk'(\mathbf{G}_k) + l^2 l'}{2(\delta_{\mathbf{G}_k} + l)}. \end{aligned} \quad (29)$$

Similarly, we calculate

$$\text{ISI}(\mathbf{G}_k \circ \mathbf{H}_l) \geq \frac{k(M_2(\mathbf{H}_l) + M_1(\mathbf{H}_l) + l)}{2(\Delta_{\mathbf{H}_l} + 1)} + \frac{(2l' + l)(2k' + kl)}{\Delta_{\mathbf{G}_k} + \Delta_{\mathbf{H}_l} + l + 1} + \frac{M_2(\mathbf{G}_k) + lM_1(\mathbf{G}_k) + l^2 l'}{2(\Delta_{\mathbf{G}_k} + l)}. \quad (30)$$

The above equalities hold only when  $\mathbf{G}_k$  and  $\mathbf{H}_l$  are regular graphs.

Next, we evaluate the bounds for inverse sum indeg (ISI) index of Indu–Bala product.  $\square$

**Theorem 9.** Let  $\mathbf{G}_k$  and  $\mathbf{H}_l$  be  $k$ -vertex and  $l$ -vertex graphs. Then,

$$\begin{aligned}
 & \frac{M_2(\mathbf{G}_k) + lM_1(\mathbf{G}_k) + l^2k'}{\Delta_{\mathbf{G}_k} + l} + \frac{2M_2(\mathbf{H}_l) + (2l + 3)M_1(\mathbf{H}_l) + (2l' + l)(k + 1)^2 + 4l'(k + 1)}{2(\Delta_{\mathbf{H}_l} + k + 1)} \\
 & + \frac{2(4k'l' + 2k'l(k + 1) + 2l'kl + l^2k(k + 1))}{\Delta_{\mathbf{G}_k} + \Delta_{\mathbf{H}_l} + k + l + 1} \leq \text{ISI}(\mathbf{G}_k \blacktriangledown \mathbf{H}_l) \leq \frac{M_2(\mathbf{G}_k) + lM_1(\mathbf{G}_k) + l^2k'}{\delta_{\mathbf{G}_k} + l} \\
 & + \frac{2M_2(\mathbf{H}_l) + (2l + 3)M_1(\mathbf{H}_l) + (2l' + l)(k + 1)^2 + 4l'(k + 1)}{2(\delta_{\mathbf{H}_l} + k + 1)} \\
 & + \frac{2(4k'l' + 2k'l(k + 1) + 2l'kl + l^2k(k + 1))}{\delta_{\mathbf{G}_k} + \delta_{\mathbf{H}_l} + k + l + 1}.
 \end{aligned} \tag{31}$$

The equalities hold only when  $\mathbf{G}_k$  and  $\mathbf{H}_l$  are regular.

*Proof.* Using the degree formula of a vertex in Indu–Bala product in (1),

$$\begin{aligned}
 \text{ISI}(\mathbf{G}_k \blacktriangledown \mathbf{H}_l) &= 2 \left[ \sum_{g_k, g'_k \in E(\mathbf{G}_k)} \frac{(d_{\mathbf{G}_k}(g_k) + l)(d_{\mathbf{G}_k}(g'_k) + l)}{(d_{\mathbf{G}_k}(g_k) + d_{\mathbf{G}_k}(g'_k)) + 2l} + \sum_{h_l, h'_l \in E(\mathbf{H}_l)} \frac{(d_{\mathbf{H}_l}(h_l) + k + 1)(d_{\mathbf{H}_l}(h'_l) + k + 1)}{d_{\mathbf{H}_l}(h_l) + d_{\mathbf{H}_l}(h'_l) + 2k + 2} \right. \\
 & \left. + \sum_{g_k \in V(\mathbf{G}_k)} \sum_{h_l \in V(\mathbf{H}_l)} \frac{(d_{\mathbf{G}_k}(g_k) + l)(d_{\mathbf{H}_l}(h_l) + k + 1)}{d_{\mathbf{G}_k}(g_k) + d_{\mathbf{H}_l}(h_l) + k + l + 1} \right] + \sum_{h_l \in V(\mathbf{H}_l)} \frac{(d_{\mathbf{H}_l}(h_l) + k + 1)^2}{2(d_{\mathbf{H}_l}(h_l) + k + 1)}.
 \end{aligned} \tag{32}$$

Using equation (2), then we have

$$\begin{aligned}
 \text{ISI}(\mathbf{G}_k \blacktriangledown \mathbf{H}_l) &\leq 2 \left[ \sum_{g_k, g'_k \in E(\mathbf{G}_k)} \frac{(d_{\mathbf{G}_k}(g_k) + l)(d_{\mathbf{G}_k}(g'_k) + l)}{2(\delta_{\mathbf{G}_k} + l)} + \sum_{h_l, h'_l \in E(\mathbf{H}_l)} \frac{(d_{\mathbf{H}_l}(h_l) + k + 1)(d_{\mathbf{H}_l}(h'_l) + k + 1)}{2(\delta_{\mathbf{H}_l} + k + 1)} \right. \\
 & \left. + \sum_{g_k \in V(\mathbf{G}_k)} \sum_{h_l \in V(\mathbf{H}_l)} \frac{(d_{\mathbf{G}_k}(g_k) + l)(d_{\mathbf{H}_l}(h_l) + k + 1)}{\delta_{\mathbf{G}_k} + \delta_{\mathbf{H}_l} + k + l + 1} \right] + \sum_{h_l \in V(\mathbf{H}_l)} \frac{(d_{\mathbf{H}_l}(h_l) + k + 1)^2}{2(\delta_{\mathbf{H}_l} + k + 1)} \\
 &= \frac{M_2(\mathbf{G}_k) + lM_1(\mathbf{G}_k) + l^2k'}{\delta_{\mathbf{G}_k} + l} + \frac{2M_2(\mathbf{H}_l) + (2l + 3)M_1(\mathbf{H}_l) + (2l' + l)(k + 1)^2 + 4l'(k + 1)}{2(\delta_{\mathbf{H}_l} + k + 1)} \\
 &+ \frac{2(4k'l' + 2k'l(k + 1) + 2l'kl + l^2k(k + 1))}{\delta_{\mathbf{G}_k} + \delta_{\mathbf{H}_l} + k + l + 1}.
 \end{aligned} \tag{33}$$

Similarly, we calculate

$$\begin{aligned}
 \text{ISI}(\mathbf{G}_k \blacktriangledown \mathbf{H}_l) \geq & \frac{M_2(\mathbf{G}_k) + lM_1(\mathbf{G}_k) + l^2k'}{\Delta_{\mathbf{G}_k} + l} + \frac{2M_2(\mathbf{H}_l) + (2l + 3)M_1(\mathbf{H}_l) + (2l' + l)(k + 1)^2 + 4l'(k + 1)}{2(\Delta_{\mathbf{H}_l} + k + 1)} \\
 & + \frac{2(4k'l' + 2k'l(k + 1) + 2l'kl + l^2k(k + 1))}{\Delta_{\mathbf{G}_k} + \Delta_{\mathbf{H}_l} + k + l + 1}.
 \end{aligned} \tag{34}$$

The equalities hold only when  $\mathbf{G}_k$  and  $\mathbf{H}_l$  are regular graphs.

In the next theorem, we find the inverse sum indeg (ISI) index of double graph.  $\square$

**Theorem 10.** Let  $\mathbf{G}_k$  be a  $k$ -vertex graph. Then,

$$\text{ISI}(D[\mathbf{G}_k]) = 8\text{ISI}(\mathbf{G}_k). \tag{35}$$

*Proof.* Using the degree formula of a vertex in  $D[\mathbf{G}_k]$  in equation (1), we acquire

$$\begin{aligned}
 \text{ISI}(D[\mathbf{G}_k]) &= \sum_{g_k, g'_k \in E(D[\mathbf{G}_k])} \frac{d_{D[\mathbf{G}_k]}(g_k)d_{D[\mathbf{G}_k]}(g'_k)}{d_{D[\mathbf{G}_k]}(g_k) + d_{D[\mathbf{G}_k]}(g'_k)} \\
 &= 4 \sum_{g_k, g'_k \in E(\mathbf{G}_k)} \frac{(2d_{\mathbf{G}_k}(g_k))(2d_{\mathbf{G}_k}(g'_k))}{2d_{\mathbf{G}_k}(g_k) + 2d_{\mathbf{G}_k}(g'_k)} \\
 &= 8 \sum_{g_k, g'_k \in E(\mathbf{G}_k)} \frac{d_{\mathbf{G}_k}(g_k)d_{\mathbf{G}_k}(g'_k)}{d_{\mathbf{G}_k}(g_k) + d_{\mathbf{G}_k}(g'_k)} = 8\text{ISI}(\mathbf{G}_k).
 \end{aligned} \tag{36}$$

In the upcoming theorem, we calculate the bounds for inverse sum indeg (ISI) index of strong double graph.  $\square$

**Theorem 11.** Let  $\mathbf{G}_k$  be an  $k$ -vertex graph. Then,

$$\frac{M_2(\text{SD}[\mathbf{G}_k])}{2(2\Delta_{\mathbf{G}_k} + 1)} \leq \text{ISI}(\text{SD}[\mathbf{G}_k]) \leq \frac{M_2(\text{SD}[\mathbf{G}_k])}{2(2\delta_{\mathbf{G}_k} + 1)}. \tag{37}$$

The equalities hold only when  $\mathbf{G}_k$  is regular.

*Proof.* Using the degree formula of a vertex in  $\text{SD}[\mathbf{G}_k]$  in (1),

$$\begin{aligned}
 \text{ISI}(\text{SD}[\mathbf{G}_k]) &= \sum_{g_k, g'_k \in E(\text{SD}[\mathbf{G}_k])} \frac{d_{(\text{SD}[\mathbf{G}_k])}(g_k)d_{(\text{SD}[\mathbf{G}_k])}(g'_k)}{d_{(\text{SD}[\mathbf{G}_k])}(g_k) + d_{(\text{SD}[\mathbf{G}_k])}(g'_k)} \\
 &= \sum_{g_k, g'_k \in E(\mathbf{G}_k)} \frac{d_{(\text{SD}[\mathbf{G}_k])}(g_k)d_{(\text{SD}[\mathbf{G}_k])}(g'_k)}{2d_{\mathbf{G}_k}(g_k) + 1 + 2d_{\mathbf{G}_k}(g'_k) + 1} \\
 &\leq \sum_{uv \in E(\text{SD}[\mathbf{G}_k])} \frac{d_{(\text{SD}[\mathbf{G}_k])}(g_k)d_{(\text{SD}[\mathbf{G}_k])}(g'_k)}{2(\delta_{\mathbf{G}_k} + 1)} \\
 &= \frac{M_2(\text{SD}[\mathbf{G}_k])}{2(2\delta_{\mathbf{G}_k} + 1)}.
 \end{aligned} \tag{38}$$

Similarly, we compute

$$\text{ISI}(\text{SD}[\mathbf{G}_k]) \geq \frac{M_2(\text{SD}[\mathbf{G}_k])}{2(2\Delta_{\mathbf{G}_k} + 1)}. \tag{39}$$

The above equalities hold only when  $\mathbf{G}_k$  is a regular graph.  $\square$

#### 4. Conclusion

In this paper, some graph operations including different products, differences, union of graphs, double graph, and strong double graph are studied. In particular, we have found the sharp bounds for inverse sum indeg (ISI) index of these operations of graphs. The investigation related to other significant predictors is still open.

#### Data Availability

All kinds of data and materials, used to compute the results, are provided in Section 1.

#### Conflicts of Interest

The authors declare that they have no conflicts of interest.

## Acknowledgments

This project was sponsored by the Deanship of Scientific Research under Nasher Proposal No. 216006, King Faisal University.

## References

- [1] D. Vuki, ević and M. Nazlić, “Bond additive modelling 1. Aromatic indices,” *Croatica Chemica Acta*, vol. 83, pp. 243–260, 2010.
- [2] J. Sedlar, D. Stevanović, and A. Vasilyev, “On the inverse sum indeg index,” *Discrete Applied Mathematics*, vol. 184, pp. 202–212, 2015.
- [3] F. Falahati-Nezhad, M. Azari, and T. Došlić, “Sharp bounds on the inverse sum indeg index,” *Discrete Applied Mathematics*, vol. 217, pp. 185–195, 2017.
- [4] I. Gutman and N. Trinajstić, “Graph theory and molecular orbitals. Total  $\varphi$ -electron energy of alternant hydrocarbons  $\pi$  electron energy of alternant hydro-carbons,” *Chemical Physics Letters*, vol. 17, no. 4, pp. 535–538, 1972.
- [5] A. R. Ashrafi, M. H. Khalifeh, and H. Yousefi-Azari, “The first and second zagreb indices of some graphs operations,” *Discrete Applied Mathematics*, vol. 157, pp. 804–811, 2009.
- [6] A. R. Ashrafi and Z. Yarahmadi, “The szeged, vertex PI, first and second zagreb indices of corona product of graphs,” *Filomat*, vol. 3, no. 3, pp. 467–472, 2012.
- [7] A. R. Ashrafi, T. Došlić, and A. Hamzeh, “The zagreb coincides of graph operations,” *Discrete Applied Mathematics*, vol. 158, no. 15, pp. 1571–1578, 2010.
- [8] M. Aaari and A. Iranmanesh, “Some inequalities for the multiplicative sum zagreb index of graph operations,” *Journal of Mathematical Inequalities*, vol. 9, pp. 727–738, 2015.
- [9] B. Basavanagoud, S. Patil, V. R. Desai, and S. M. Hosamani, “Computing certain topological indices of indu-bala product of graphs,” 2016.
- [10] N. De, S. M. A. Nayeem, and A. Pal, “F-index of some graph operations,” *Discrete Mathematics, Algorithms and Applications*, vol. 8, no. 2, p. 1650025, 2016.
- [11] G. Indulal and R. Balakrishnan, “Distance spectrum of Indu-Bala product of graphs,” *AKCE International Journal of Graphs and Combinatorics*, vol. 13, no. 3, pp. 230–234, 2016.
- [12] E. Munarini, A. Scagliola, C. P. Cippo, and N. Salvi, “Double graphs,” *Discrete Mathematics*, vol. 308, no. 2-3, pp. 242–254, 2008.
- [13] M. S. Marino and N. Z. Salvi, “Generalizing double graphs,” *Atti della Accademia Peloritana dei Pericolanti-Classe di Scienze Fisiche Matematiche e Naturali*, vol. 85, no. 2, 2006.
- [14] S. Pirzada and H. A. Ganie, “Spectra, energy and laplacian energy of strong double graphs,” *Mathematical Technology of Networks*, vol. 128, pp. 175–189, 2015.
- [15] S. Akhter, Z. Iqbal, A. Aslam, and W. Gao, “Mostar index of graph operations,” 2020, <https://arxiv.org/abs/2005.09416>.
- [16] W. Gao, Z. Iqbal, Z. Iqbal, S. Akhter, M. Ishaq, and A. Aslam, “On irregularity descriptors of derived graphs,” *AIMS Mathematics*, vol. 5, no. 5, pp. 4085–4107, 2020.
- [17] M. Imran, S. Akhter, and Z. Iqbal, “Edge Mostar index of chemical structures and nanostructures using graph operations,” *Int. J. Quantum. Chem.*, vol. 120, no. 15, Article ID e26259, 2020.
- [18] M. Imran, S. Akhter, and Z. Iqbal, “On the eccentric connectivity polynomial of  $F$ -sum of connected graphs,” *Complexity*, vol. 2020, Article ID 5061682, 9 pages, 2020.
- [19] H. Yang, M. Imran, S. Akhter, Z. Iqbal, and M. K. Siddiqui, “On distance-based topological descriptors of subdivision vertex-edge join of three graphs,” *IEEE Access*, vol. 7, pp. 143381–143391, 2019.
- [20] S. Akhter and M. Imran, “The sharp bounds on general sum-connectivity index of four operations on graphs,” *Journal of Inequalities and Applications*, vol. 2016, no. 1, pp. 241–250, 2016.
- [21] S. Akhter, M. Imran, and Z. Raza, “On the general sum-connectivity index and general randić index of cacti,” *Journal of Inequalities and Applications*, vol. 2016, no. 1, pp. 300–309, 2016.
- [22] S. Akhter and M. Imran, “Computing the forgotten topological index of four operations on graphs,” *AKCE International Journal of Graphs and Combinatorics*, vol. 14, no. 1, pp. 70–79, 2017.
- [23] M. Imran, S. Baby, H. M. A. Siddiqui, and M. K. Shafiq, “On the bounds of degree-based topological indices of the cartesian product of  $F$ -sum of connected graphs,” *Journal of Inequalities and Applications*, vol. 2017, no. 1, pp. 305–315, 2017.
- [24] H. M. A. Siddiqui, S. Baby, and M. K. Shafiq, “The sharp bounds of topological indices of strong product of new  $F$ -sum on connected graphs,” *Utilitas Mathematica*, vol. 112, pp. 139–156, 2017.
- [25] Z. Yarahmadi, “Computing some topological indices of tensor product of graphs,” *Iranian Journal of Mathematical Chemistry*, vol. 2, no. 1, pp. 109–118, 2011.

## Research Article

# On the Spectrum of Laplacian Matrix

Akbar Jahanbani , Seyed Mahmoud Sheikholeslami , and Rana Khoeilar

Department of Mathematics, Azarbaijan Shahid Madani University, Tabriz, Iran

Correspondence should be addressed to Akbar Jahanbani; akbar.jahanbani92@gmail.com

Received 12 April 2021; Accepted 19 May 2021; Published 4 June 2021

Academic Editor: Andrea Semaničová-Feňovčíková

Copyright © 2021 Akbar Jahanbani et al. This is an open access article distributed under the Creative Commons Attribution License, which permits unrestricted use, distribution, and reproduction in any medium, provided the original work is properly cited.

Let  $G$  be a simple graph of order  $n$ . The matrix  $\mathcal{L}(G) = D(G) - A(G)$  is called the Laplacian matrix of  $G$ , where  $D(G)$  and  $A(G)$  denote the diagonal matrix of vertex degrees and the adjacency matrix of  $G$ , respectively. Let  $l_1(G)$ ,  $l_{n-1}(G)$  be the largest eigenvalue, the second smallest eigenvalue of  $\mathcal{L}(G)$  respectively, and  $\lambda_1(G)$  be the largest eigenvalue of  $A(G)$ . In this paper, we will present sharp upper and lower bounds for  $l_1(G)$  and  $l_{n-1}(G)$ . Moreover, we investigate the relation between  $l_1(G)$  and  $\lambda_1(G)$ .

## 1. Introduction

We begin with the preliminaries which are required throughout this paper. Let  $G$  be a simple graph with vertex set  $V = V(G)$  and edge set  $E(G)$ . The integers  $n = n(G) = |V(G)|$  and  $\varepsilon = \varepsilon(G) = |E(G)|$  are the order and the size of the graph  $G$ , respectively. The open neighborhood of vertex  $v_i$  is  $N_G(v_i) = N(v_i) = \{v_j \in V(G) \mid v_i v_j \in E(G)\}$ , and the degree of  $v_i$  is  $d_G(v_i) = d_i = |N(v_i)|$ . Let  $K_n$  be the complete graph of order  $n$  and  $\bar{G}$  be the complement of the graph  $G$ . Let  $\Delta$  and  $\delta$  be the maximum degree and the minimum degree of the vertices of  $G$ , respectively. The eigenvalues of the adjacency matrix  $A(G)$ , are denoted by  $\lambda_1(G) \geq \lambda_2(G) \geq \dots \geq \lambda_n(G)$ . The matrix  $\mathcal{L}(G) = D(G) - A(G)$ , where  $D(G)$  is the diagonal matrix of vertex degrees, is called the Laplacian matrix of  $G$  and rarely appears in the literature. The eigenvalues of Laplacian matrix  $G$  are denoted as  $l_1(G) \geq l_2(G) \geq \dots \geq l_n(G) = 0$ . The Laplacian matrix of a graph and its eigenvalues can be used in several areas of mathematical research and have a physical interpretation in various physical and chemical theories. The adjacency matrix of a graph and its eigenvalues were much more investigated in the past than the Laplacian matrix. Many related physical quantities have the same relation to  $\mathcal{L}(G)$ ; also, there are many problems in physics and chemistry where the Laplacian matrices of graphs and their spectra play the central role. Recently, its applications to several difficult problems in graph theory were discovered (see [1–7]).

Merris [8] discussed the Laplacian matrices of graphs. In [9], some bounds are established for Laplacian eigenvalues of graphs. Taheri et al. [10] presented some bounds for the largest Laplacian eigenvalue of graphs. Patra et al. [11] obtained bounds for the Laplacian spectral radius of graphs. In [12], the authors investigated some bounds for the Laplacian spectral radius of an oriented hypergraph. Chen [13] established some bounds for  $\lambda_1(G)$ .

In this paper, we first present sharp upper and lower bounds for  $l_1(G)$  and  $l_{n-1}(G)$ , and then we investigate the relation between  $l_1(G)$  and  $\lambda_1(G)$ .

## 2. Preliminaries

In this section, some fundamental results that are used in this paper are recalled. We begin with the following result, which plays a key role in this section.

**Lemma 1** (see [14]). Let  $G$  be a graph of order  $n$  and size  $\varepsilon$ . Then,

$$\begin{aligned} \sum_{i=1}^{n-1} l_i &= \sum_{i=1}^n l_i = \text{tr} \mathcal{L}(G) = 2\varepsilon, \\ \sum_{i=1}^{n-1} l_i^2 &= \sum_{i=1}^n l_i^2 = \text{tr} \mathcal{L}^2(G) = 2\varepsilon + M_1(G), \end{aligned} \quad (1)$$



where  $M_1(G) = \sum_{i=1}^n d_i^2$  is the well-known graph invariant called the first Zagreb index [15].

Favaron and Mahéo [16] proved the following result:

**Lemma 2** (see [16]). Let  $G$  be a graph of order  $n$ . Then,

$$\lambda_1 \geq \sqrt{\frac{\sum_{i=1}^n d_i^2}{n}}. \tag{2}$$

The proof of the next result can be found in [17].

**Lemma 3.** Let  $G$  be a graph of order  $n$ . Then,  $l_1 = l_2 = \dots = l_{n-1}$  if and only if  $G \cong K_n$  or  $G \cong \overline{K}_n$ .

Das in [18] proved the following lemma.

**Lemma 4.** Let  $G$  be a connected graph of order  $n \geq 3$ . Then,  $l_2 = l_3 = \dots = l_{n-1}$  if and only if  $G \cong K_n$ .

In [14], a class of real polynomials  $P_n(x) = x^n + a_1x^{n-1} + a_2x^{n-2} + b_3x^{n-3} + \dots + b_n$ , denoted as  $\mathcal{P}_n(a_1, a_2)$ , where  $a_1$  and  $a_2$  are fixed real numbers, was considered.

**Theorem 1.** For the roots  $y_1 \geq y_2 \geq \dots \geq y_n$  of an arbitrary polynomial  $\varphi_n(y)$  from this class, the following values were introduced:

$$\begin{aligned} \bar{y} &= \frac{1}{n} \sum_{i=1}^n y_i, \\ \Gamma &= n \sum_{i=1}^n y_i^2 - \left( \sum_{i=1}^n y_i \right)^2. \end{aligned} \tag{3}$$

Then upper and lower bounds for the polynomial roots,  $y_i, i = 1, 2, \dots, n$ , were determined in terms of the introduced values

$$\begin{aligned} \bar{y} + \frac{1}{n} \sqrt{\frac{\Gamma}{n-1}} &\leq y_1 \leq \bar{y} + \frac{1}{n} \sqrt{(n-1)\Gamma}, \\ \bar{y} - \frac{1}{n} \sqrt{\frac{(i-1)}{n-i+1} \Gamma} &\leq y_i \leq \bar{y} + \frac{1}{n} \sqrt{\frac{(n-i)}{i} \Gamma}, \quad \text{for } i = 2, 3, \dots, n-1. \end{aligned} \tag{4}$$

### 3. Main Results

In this section, we will obtain some sharp upper and lower bounds for  $l_1(G)$  and  $l_{n-1}(G)$  involving the first Zagreb index and order and size of graphs. Moreover, we investigate the relation between  $l_1(G)$  and  $\lambda_1(G)$ . The first result is an immediate consequence of Theorem 1 and Lemma 1.

**Lemma 5.** Let  $G$  be a graph of order  $n \geq 2$  and size  $\varepsilon$ . Then,

$$\frac{2\varepsilon + \sqrt{(n-1)(2\varepsilon + M_1(G)) - 4\varepsilon^2/n - 2}}{n-1} \leq l_1 \tag{5}$$

$$\leq \frac{2\varepsilon + \sqrt{(n-2)((n-1)(2\varepsilon + M_1(G)) - 4\varepsilon^2)}}{n-1},$$

$$\frac{2\varepsilon - \sqrt{(n-2)((n-1)(2\varepsilon + M_1(G)) - 4\varepsilon^2)/2}}{n-1} \leq l_{n-1} \leq \frac{2\varepsilon}{n-1}. \tag{6}$$

Here, we will obtain a lower and an upper bound for the largest Laplacian eigenvalue  $l_1$  and the second smallest Laplacian eigenvalue  $l_{n-1}$ , respectively.

**Theorem 2.** Let  $G$  be a graph of order  $n \geq 3$  and size  $\varepsilon$ . Then,

$$l_1 \geq \frac{2\varepsilon}{n-1} + \sqrt{\frac{1}{(n-1)(n-2)} \left( \frac{2\varepsilon(n-1+2\varepsilon)}{n-1} + \sum_{i=1}^n d_i^2 \right)}, \tag{7}$$

$$l_{n-1} \leq \frac{2\varepsilon}{n-1} - \sqrt{\frac{1}{(n-1)(n-2)} \left( \frac{2\varepsilon(n-1+2\varepsilon)}{n-1} + \sum_{i=1}^n d_i^2 \right)}, \tag{8}$$

and the equalities hold if and only if  $G \cong K_n$  or  $G \cong \overline{K}_n$ .

*Proof.* For every fixed number  $t$ , we can write that

$$\begin{aligned} \left( \sum_{i=1}^{n-1} l_i - (n-1)l_t \right)^2 &= \left( \sum_{i=1}^{n-1} (l_i - l_t) \right)^2 \\ &= \sum_{i=1}^{n-1} (l_i - l_t)^2 + 2 \sum_{1 \leq i < j \leq n-1} (l_i - l_t)(l_j - l_t). \end{aligned} \tag{9}$$

It is not hard to see that when  $t = 1$  or  $t = n - 1$ , we get

$$\sum_{1 \leq i < j \leq n-1} (l_i - l_t)(l_j - l_t) \geq 0. \tag{10}$$

Hence, we have

$$\left( \sum_{i=1}^{n-1} l_i - (n-1)l_t \right)^2 \geq \sum_{i=1}^{n-1} (l_i - l_t)^2. \tag{11}$$

So, we can write

$$\begin{aligned} & \left( \sum_{i=1}^{n-1} l_i \right)^2 - 2(n-1)l_t \sum_{i=1}^{n-1} l_i + (n-1)^2 l_t^2 \\ & \geq \sum_{i=1}^{n-1} l_i^2 - 2l_t \sum_{i=1}^{n-1} l_i + (n-1)l_t. \end{aligned} \quad (12)$$

This is equivalent to

$$l_t^2 - \frac{2l_t \sum_{i=1}^{n-1} l_i}{n-1} + \frac{\left( \sum_{i=1}^{n-1} l_i \right)^2}{(n-1)^2 - (n-1)} \geq \frac{\sum_{i=1}^{n-1} l_i^2}{(n-1)^2 - (n-1)}, \quad (13)$$

or

$$\left( l_t - \frac{\sum_{i=1}^{n-1} l_i}{n-1} \right)^2 - \frac{\left( \sum_{i=1}^{n-1} l_i \right)^2}{(n-1)^2} + \frac{\left( \sum_{i=1}^{n-1} l_i \right)^2}{(n-1)(n-2)} \geq \frac{\sum_{i=1}^{n-1} l_i^2}{(n-1)(n-2)}. \quad (14)$$

Therefore, we have

$$\left( l_t - \frac{\sum_{i=1}^{n-1} l_i}{n-1} \right)^2 \geq \frac{1}{(n-1)(n-2)} \left( \sum_{i=1}^{n-1} l_i^2 - \frac{1}{n-1} \left( \sum_{i=1}^{n-1} l_i \right)^2 \right). \quad (15)$$

Hence, by using Lemma 1, we have

$$\sum_{i=1}^{n-1} l_i = \sum_{i=1}^n l_i = \text{tr} \mathcal{L}(G) = 2\varepsilon, \quad (16)$$

$$\sum_{i=1}^{n-1} l_i^2 = \sum_{i=1}^n l_i^2 = \text{tr} \mathcal{L}^2(G) = 2\varepsilon + M_1(G). \quad (17)$$

By combining inequalities (15)–(17), we get the following inequality:

$$\left( l_1 - \frac{2\varepsilon}{n-1} \right)^2 \geq \frac{1}{(n-1)(n-2)} \left( 2\varepsilon - \frac{4\varepsilon^2}{n-1} + \sum_{i=1}^n d_i^2 \right). \quad (18)$$

By inequalities (5) and (6), we have

$$l_1 - \frac{2\varepsilon}{n-1} \geq 0, l_{n-1} - \frac{2\varepsilon}{n-1} \leq 0. \quad (19)$$

Therefore, we have

$$\begin{aligned} l_1 & \geq \frac{2\varepsilon}{n-1} + \sqrt{\frac{1}{(n-1)(n-2)} \left( \frac{2\varepsilon(n-1+2\varepsilon)}{n-1} + \sum_{i=1}^n d_i^2 \right)} \\ l_{n-1} & \leq \frac{2\varepsilon}{n-1} - \sqrt{\frac{1}{(n-1)(n-2)} \left( \frac{2\varepsilon(n-1+2\varepsilon)}{n-1} + \sum_{i=1}^n d_i^2 \right)}. \end{aligned} \quad (20)$$

If the equality in (7) holds, then the inequality in (10) must hold, and hence we have  $l_1 = l_2 = \dots = l_{n-1} = 2\varepsilon/n - 1$ ; thus, by Lemma 3, we have  $G \cong K_n$  or  $G \cong \overline{K}_n$ . Conversely, if

$G \cong K_n$  or  $G \cong \overline{K}_n$ , then it is not difficult to see that the equalities in (7) and (8) hold.

Next, we present an upper bound for spectral radius of the Laplacian matrix.  $\square$

**Theorem 3.** Let  $G$  be a connected graph of order  $n \geq 2$  and size  $\varepsilon$ . Then,

$$l_1 \leq \frac{\sqrt{(16n-16)((2\varepsilon + M_1(G))(n-2) - 4\varepsilon^2)} + 8\varepsilon}{8n-8}. \quad (21)$$

*Proof.* Applying Lemma 1, we can write

$$\beta := \sum_{i=1}^{n-1} l_i^2 = 2\varepsilon + \sum_{i=1}^{n-1} d_i^2 = 2\varepsilon + M_1(G), \quad (22)$$

or

$$l_1^2 = \beta - \sum_{i=2}^{n-1} l_i^2 \leq \beta - \frac{1}{n-2} \left( \sum_{i=2}^{n-1} l_i \right)^2 = \beta - \frac{(2\varepsilon - l_1)^2}{n-2}. \quad (23)$$

By inequality (23), we have

$$l_1^2 \leq \beta - \frac{4\varepsilon^2 + l_1^2 - 4\varepsilon l_1}{n-2}. \quad (24)$$

Using inequality (24), we get

$$l_1^2 \left( 1 + \frac{1}{n-2} \right) + \frac{4\varepsilon^2}{n-2} - \frac{4\varepsilon l_1}{n-2} - \beta \leq 0, \quad (25)$$

or

$$l_1^2(n-1) + 4\varepsilon^2 - 4\varepsilon l_1 - (n-2)\beta \leq 0. \quad (26)$$

By inequality (26), we can write

$$l_1^2(n-1) + 4\varepsilon^2 - 4\varepsilon l_1 - 2\varepsilon(n-2) - M_1(G)(n-2) \leq 0. \quad (27)$$

Solving this inequality leads to

$$l_1 \leq \frac{\sqrt{(16n-16)((2\varepsilon + M_1(G))(n-2) - 4\varepsilon^2)} + 8\varepsilon}{8n-8}. \quad (28)$$

Finally, we will describe a relationship between spectral radius ( $l_1$ ) of the Laplacian matrix and the spectral radius ( $\lambda_1$ ) of the adjacency matrix.  $\square$

**Theorem 4.** Let  $G$  be a connected graph of order  $n \geq 3$  and size  $\varepsilon$ . Then,

$$\lambda_1 \geq \sqrt{\frac{l_1^2(n-1)}{n(n-2)} + \frac{4\varepsilon^2}{n(n-2)} - \frac{4\varepsilon l_1}{n(n-2)} - \frac{2\varepsilon}{n}}, \quad (29)$$

and the equality holds if and only if  $G \cong K_n$ .

*Proof.* By inequality (26) and Lemma 2, we have

$$l_1^2(n-1) + 4\epsilon^2 - 4\epsilon l_1 \leq (n-2)\beta = (n-2)\left(2\epsilon + \sum_{i=1}^n d_i^2\right), \quad (30)$$

$$\leq (n-2)(2\epsilon + n\lambda_1^2) = 2\epsilon(n-2) + n(n-2)\lambda_1^2. \quad (31)$$

Now suppose that the equality holds in (29). Then, all the inequalities in the proof must be equalities.

If the equality holds in (30), then inequality (23) must be equality; in other words,

$$\beta - \sum_{i=2}^{n-1} l_i^2 = \beta - \frac{1}{n-2} \left( \sum_{i=2}^{n-1} l_i \right)^2, \quad (32)$$

or

$$\sum_{i=2}^{n-1} l_i^2 = \frac{1}{n-2} \left( \sum_{i=2}^{n-1} l_i \right)^2. \quad (33)$$

Therefore, by equality (33), we get

$$l_2 = l_3 = \dots = l_{n-1}. \quad (34)$$

Hence, by Lemma 4, we get  $G \cong K_n$ . Conversely, one can easily see that equality holds in (29) when  $G \cong K_n$ .  $\square$

#### 4. Conclusion

In this paper, we established some sharp upper and lower bounds for the largest eigenvalue and the second smallest eigenvalues of Laplacian matrix involving the first Zagreb index and order and size of graphs. Moreover, we investigate a relation between the largest eigenvalues of Laplacian matrix and the adjacency matrix.

There are still open and challenging problems for researchers. For example, the problem of ABC matrix, GA matrix, and so on remains open for further investigation.

#### Data Availability

The data involved in the examples of our manuscript are included within the article.

#### Conflicts of Interest

The authors declare that they have no conflicts of interest.

#### References

- [1] B. E. Eichinger, "An approach to distribution functions for Gaussian molecules," *Macromolecules*, vol. 10, no. 3, pp. 671-675, 1977.
- [2] B. E. Eichinger, "Scattering functions for Gaussian molecules," *Macromolecules*, vol. 11, no. 2, pp. 432-433, 1978.
- [3] B. E. Eichinger, "Scattering functions for Gaussian molecules. 2. Intermolecular correlations," *Macromolecules*, vol. 11, no. 5, pp. 1056-1057, 1978.
- [4] H. A. Ganie, S. Pirzada, and T. Vilmar, "On the sum of k largest laplacian eigenvalues of a graph and clique number," *Mediterranean Journal of Mathematics*, vol. 18, no. 1, pp. 1-13, 2021.
- [5] J. Jost, R. Mulas, and F. Munch, "Spectral gap of the largest eigenvalue of the normalized graph Laplacian," *Communications in Mathematics and Statistics*, vol. 9, pp. 1-11, 2021.
- [6] R. Li, "Combinations of some spectral invariants and Hamiltonian properties of graphs," *Contributions to Mathematics*, vol. 1, pp. 54-56, 2020.
- [7] C. Maas, "Transportation in graphs and the admittance spectrum," *Discrete Applied Mathematics*, vol. 16, no. 1, pp. 31-49, 1987.
- [8] R. Merris, "Laplacian matrices of graphs: a survey," *Linear Algebra and Its Applications*, vol. 197-198, pp. 143-176, 1994.
- [9] S. Buyukkose and S. Basdas, "Bounds for the laplacian eigenvalue of graphs using 2-adjacency," *Journal of Science and Arts*, vol. 18, no. 1, pp. 175-182, 2018.
- [10] H. Taheri and G. H. Fath-Tabar, "New upper bound on the largest laplacian eigenvalue of graphs," *Facta Universitatis, Series: Mathematics and Informatics*, vol. 35, pp. 533-540, 2020.
- [11] K. L. Patra, B. K. Sahoo, and B. K. Sahoo, "Bounds for the Laplacian spectral radius of graphs," *Electronic Journal of Graph Theory and Applications*, vol. 5, no. 2, pp. 276-303, 2017.
- [12] O. Kitouni and R. Nathan, "Lower bounds for the Laplacian spectral radius of an oriented hypergraph," *Australasian Journal of Combinatorics*, vol. 74, no. 3, pp. 408-422, 2019.
- [13] C. Yan, "Properties of spectra of graphs and line graphs," *Applied Mathematics-A Journal of Chinese Universities*, vol. 17, no. 3, pp. 371-376, 2002.
- [14] A. Lupaş, "Inequalities for the roots of a class of polynomials," *Publikacije Elektrotehničkog Fakulteta. Serija Matematika I Fizika*, vol. 577/598, pp. 79-85, 1977.
- [15] I. Gutman and Ch Das Kinkar, "The first Zagreb index 30 years after," *MATCH Commun.*, *Math. Comput. Chem.*, vol. 50, no. 1, pp. 83-92, 2004.
- [16] O. Favaron and M. Mahéo, "Some eigenvalue properties in graphs (conjectures of Graffiti-II)," *Discrete Mathematics*, vol. 111, no. 1-3, pp. 197-220, 1993.
- [17] Bo Zhou, "On sum of powers of the Laplacian eigenvalues of graphs," *Linear Algebra and Its Applications*, vol. 429, no. 8-9, pp. 2239-2246, 2008.
- [18] K. C. Das, "A sharp upper bound for the number of spanning trees of a graph," *Graphs and Combinatorics*, vol. 23, no. 6, pp. 625-632, 2007.

## Research Article

# Distance-Based Topological Polynomials Associated with Zero-Divisor Graphs

Ali Ahmad <sup>1</sup> and S. C. López <sup>2</sup>

<sup>1</sup>College of Computer Science & Information Technology, Jazan University, Jazan, Saudi Arabia

<sup>2</sup>Departament De Matemàtica, Universitat de Lleida, Av. Pla de la Massa, Igualada 8 08700, Spain

Correspondence should be addressed to Ali Ahmad; ahmadsms@gmail.com

Received 18 April 2021; Accepted 21 May 2021; Published 28 May 2021

Academic Editor: Michal Kawulok

Copyright © 2021 Ali Ahmad and S. C. López. This is an open access article distributed under the Creative Commons Attribution License, which permits unrestricted use, distribution, and reproduction in any medium, provided the original work is properly cited.

Let  $R$  be a commutative ring with nonzero identity and let  $Z(R)$  be its set of zero divisors. The zero-divisor graph of  $R$  is the graph  $\Gamma(R)$  with vertex set  $V(\Gamma(R)) = Z(R)^*$ , where  $Z(R)^* = Z(R) \setminus \{0\}$ , and edge set  $E(\Gamma(R)) = \{\{x, y\} : x \cdot y = 0\}$ . One of the basic results for these graphs is that  $\Gamma(R)$  is connected with diameter less than or equal to 3. In this paper, we obtain a few distance-based topological polynomials and indices of zero-divisor graph when the commutative ring is  $\mathbb{Z}_{p^2q^2}$ , namely, the Wiener index, the Hosoya polynomial, and the Shultz and the modified Shultz indices and polynomials.

## 1. Introduction

Algebraic structures have been investigated significantly for their nearby connection with representation theory and number theory; likewise, they have been widely concentrated in combinatorics [1, 2]. Despite the expansive theoretical research in these areas, restricted rings and fields got consideration for their applications to cryptography and coding theory.

In mathematical chemistry, a graphical structure of a chemical compound is a representation of the structural formula. In a chemical graph, vertices and edges represent the atoms and their chemical bonds of the compound, respectively. Molecular descriptors for a particular chemical compound are calculated on basis of the corresponding molecular graph. A topological index is a graph invariant that is obtained from it. In [3], the first topological index, namely, the Wiener index, was introduced. Nowadays, it is widely used in QSAR (“Quantitative Structure Activity Relationship”), whose properties are surveyed in [4, 5].

Topological indices are classified as degree based [6–9] and distance based of graphs. Some well-known topological indices based on the degrees of a graph are the Randić connectivity index, Zagreb indices, Harmonic index, atom bond connectivity, and geometric arithmetic index. The Wiener index, Hosoya index, and Estrada index are distance-based topological

indices [10, 11]. Topological indices formulate the criteria for the development of compound structures, and numerical activities on these structures extend multidisciplinary research. In what follows, we cite some of them.

A relationship among the stability of linear alkanes and the branched alkanes is examined using the ABC index, which helped in computation of strain energy for cycle alkanes [12, 13]. The GA index is more appropriate and efficient to correlate certain physico-chemical characteristics for predictive power than the Randić connectivity index [14, 15]. The Zagreb indices are powerful tools for the calculation of total  $p$ -electron energy of the molecules with precise approximation [16]. The degree-based topological indices are more useful to examine the chemical characteristics of distinct molecular structures. Eccentricity-based topological indices are useful as a key for the judgement of toxicological, physico-chemical, and pharmacological properties of a compound through the structure of its molecules. The study of the QSAR is known for this sort of analysis [17]. By exploring [18, 19], further applications of topological indices can be obtained.

*1.1. Distance-Based Topological Indices and Polynomials.* In this section, we introduce the topological indices and polynomials that will be obtained for the graphs studied in

this paper. We recall some concepts from graph theory. Let  $G$  be a (undirected) graph. If there is a path between any two distinct vertices of  $G$ , then  $G$  is a connected graph. For two distinct vertices  $x, y \in V(G)$ , we denote  $d(x, y)$  the length of a shortest path connecting  $x$  and  $y$  ( $d(x, x) = 0$  and,  $d(x, y) = \infty$  if no such a path exists). The diameter of the graph  $G$  is the maximum length of the shortest path connecting two distinct vertices of  $G$ , that is,  $\text{diam}(G) = \max\{d(x, y) : x \neq y \in V(G)\}$ . The number of edges incidence a vertex  $x$  of simple graph  $G$  is called the degree of the vertex  $x$ , denoted as  $d_x$ .

The Wiener index [11] was introduced by Wiener in 1947 to illustrate the connection between physico-chemical properties of organic compounds and the index of their molecular graphs:

$$W(G) = \frac{1}{2} \sum_{u \in V(G)} \sum_{v \in V(G)} d(u, v). \quad (1)$$

Randić [20] and Randić et al. [21] introduced a modified version of the Wiener index that is used for predicting physico-chemical properties of organic components. The new index was called the hyper-Wiener index and it is defined as follows:

$$WW(G) = \frac{1}{2} \sum_{u \in V(G)} \sum_{v \in V(G)} (d(u, v) + d(u, v)^2). \quad (2)$$

The Hosoya polynomial was introduced in 1989 [22]. The definition is as follows:

$$H(G, x) = \frac{1}{2} \sum_{u \in V(G)} \sum_{v \in V(G)} x^{d(u, v)}. \quad (3)$$

Dobrynin and Kochetova [23], and independently, Gutman [24] introduced a degree distance index, which is known as the Schultz index. Let  $G$  be a connected graph and  $d_u$  be the degree of  $u \in V(G)$ . Then, the Schultz index or the degree distance of  $G$  is defined as follows:

$$\text{Sc}(G) = \frac{1}{2} \sum_{u \in V(G)} \sum_{v \in V(G)} (d_u + d_v)d(u, v). \quad (4)$$

Klavžar and Gutman defined, in [25], the modified Schulz index of a graph as follows:

$$\text{Sc}^*(G) = \frac{1}{2} \sum_{u \in V(G)} \sum_{v \in V(G)} (d_u \cdot d_v)d(u, v). \quad (5)$$

Finally, Gutman, in [24], introduced two topological polynomials, namely, the Schulz polynomial  $\text{Sc}(G, x)$  and the modified Schulz polynomial  $\text{Sc}^*(G, x)$  as follows:

$$\text{Sc}(G, x) = \frac{1}{2} \sum_{u \in V(G)} \sum_{v \in V(G)} (d_u + d_v)x^{d(u, v)}, \quad (6)$$

$$\text{Sc}^*(G, x) = \frac{1}{2} \sum_{u \in V(G)} \sum_{v \in V(G)} (d_u \cdot d_v)x^{d(u, v)}.$$

The connection between the above polynomials and the previous two indices is stated below:

$$\begin{aligned} \text{Sc}(G) &= \left. \frac{\partial \text{Sc}(G, x)}{\partial x} \right|_{x=1}, \\ \text{Sc}^*(G) &= \left. \frac{\partial \text{Sc}^*(G, x)}{\partial x} \right|_{x=1}. \end{aligned} \quad (7)$$

**1.2. Zero-Divisor Graphs.** Let  $R$  be a commutative ring with nonzero identity and let  $Z(R)$  be its set of zero divisors. The zero-divisor graph of  $R$  is the graph  $\Gamma(R)$  with vertex set  $V(\Gamma(R)) = Z(R)^*$ , where  $Z(R)^* = Z(R) \setminus \{0\}$ , and edge set  $E(\Gamma(R)) = \{\{x, y\} : x \cdot y = 0\}$ . As usual, an edge  $\{x, y\}$  is simply denoted as  $xy$ . Zero-divisor graphs were introduced by Beck [2] in 1988 and then studied by Anderson and Naseer in [26]. These authors were interested in colorings and the original definition included all elements in  $R$ , even the zero. Later on, Anderson and Livingston [27] made emphasis on the relationship between ring-theoretical properties and graph-theoretical properties and reformulated the definition as it appears in the lines above. One of the basic results in this relationship is the following one.

**Theorem 1** (see [27]). *Let  $R$  be a commutative ring. Then,  $\Gamma(R)$  is connected with diameter less or equal to 3.*

The study conducted in [28, 29] may serve as a survey that is very interesting to find the relation between ring-theoretic properties and graph-theoretic properties of  $\Gamma(G)$ . Some applications and relation between algebraic theory and chemical graph theory can be seen in [1, 18, 30]. In this paper, we presented some results that interplay in the relation between a zero-divisor graph and chemical graph theory. The structure of the paper is as follows. In Section 2, we describe the family of zero-divisor graphs of the form  $\Gamma(\mathbb{Z}_{p^2q^2})$ , where  $p$  and  $q$  are different primes, and we also count pairs of vertices that are exactly at distance  $i$ , for  $i = 1, 2, 3$ . In Section 3, we obtain the Wiener index and the Hosoya, the Shultz, and the modified Shultz polynomials of  $\Gamma(\mathbb{Z}_{p^2q^2})$ . We also obtain the Shultz and the modified Shultz indices of  $\Gamma(\mathbb{Z}_{p^2q^2})$ .

## 2. The Zero-Divisor Graph on $\Gamma(\mathbb{Z}_{p^2q^2})$

Let us start by introducing some notation that will be used along the paper. We assume that  $p$  and  $q$  are different positive primes.

**Lemma 1.** *Let  $0 \leq i, j \leq 2$ . Let  $A_{i,j} = (p^i q^j) \subset \mathbb{Z}_{p^2q^2}$ , for  $0 \leq i + j \leq 4$  and  $A_{i,j} = \emptyset$ , otherwise. Then,*

- (i)  $|A_{i,j}| = p^{2-i} q^{2-j}$
- (ii)  $A_{i+1,j} \cup A_{i,j+1} \subset A_{i,j}$
- (iii)  $A_{i+1,j} \cap A_{i,j+1} = A_{i+1,j+1}$ , whenever  $i + j + 2 \leq 4$

*The vertices of  $\Gamma(\mathbb{Z}_{p^2q^2})$  can be split into blocks such that all vertices in the same block have the same behavior. From this partition, we can easily describe the structure of  $\Gamma(\mathbb{Z}_{p^2q^2})$ , that is, the content of the following lemma.*

**Lemma 2.** *For  $0 \leq i, j \leq 2$  and  $0 < i + j < 4$ , let  $B_{i,j} = A_{i,j} \setminus (A_{i+1,j} \cup A_{i,j+1})$ . Then,*

$$|B_{i,j}| = \begin{cases} p^{2-i}q^{2-j} - p^{1-i}q^{2-j} - p^{2-i}q^{1-j} + p^{1-i}q^{1-j}, & \text{if } \max\{i, j\} = 1, \\ q^{2-j} - q^{1-j}, & \text{if } i = 2, \\ p^{2-i} - p^{1-i}, & \text{if } j = 2. \end{cases} \quad (8)$$

Moreover,

- (i) If  $i, j \geq 1$ , then  $\Gamma[B_{i,j}]$  is a clique. Otherwise,  $\Gamma[B_{i,j}]$  is a set of independent vertices.
- (ii) Let  $B_{i,j}$  and  $B_{i',j'}$  such that  $i + i' = j + j' = 2$ . Then, the edges  $uv, u \in B_{i,j}$  and  $v \in B_{i',j'}$ , define a complete bipartite graph.

According to the definition, all vertices in the same block of the zero-divisor graph on  $\mathbb{Z}_{p^2q^2}$  have the same degree. For more details on this graph, see [30]. Let  $d_{ij}$  be the degree of any vertex in  $B_{i,j}$ . Following the notation of the previous lemma, we also conclude the following information.

**Lemma 3.** For  $0 \leq i, j \leq 2$  and  $0 < i + j < 4$ , then

$$d_{ij} = \begin{cases} p^i q^j - i - j, & \text{if } \max\{i, j\} = 1, \\ p^2 q^j - j - 1, & \text{if } i = 2, \\ p^i q^2 - i - 1, & \text{if } j = 2. \end{cases} \quad (9)$$

Figure 1 shows the structure of the zero-divisor graph  $\mathbb{Z}_{p^2q^2}$ . White vertices represent blocks of independent vertices in  $\mathbb{Z}_{p^2q^2}$ , whereas black vertices represent cliques.

The structure shown in Lemmas 2 and 3 can be completed by showing the distance between pairs of vertices, which only depends on the block they belong to. This information appears in Table 1.

Let  $\text{TP}_i(G)$ ,  $i \in \mathbb{Z}$  and  $i > 0$ , the number of pairs of vertices at distance  $i$  in a graph  $G$ .

**Lemma 4.** Let  $\Gamma(\mathbb{Z}_{p^2q^2})$  be a zero-divisor graph; then,

$$\text{TP}_1(\Gamma(\mathbb{Z}_{p^2q^2})) = 3pq(p-1)(q-1) + \frac{1}{2}(pq-1)(pq-2). \quad (10)$$

*Proof.* The size of  $\Gamma(\mathbb{Z}_{p^2q^2})$  is given by

$$\begin{aligned} & |B_{1,2}|(|B_{2,0}| + |B_{1,0}|) + |B_{2,1}|(|B_{0,2}| + |B_{0,1}|) + |B_{2,0}||B_{0,2}| \\ & + \left| E(K_{|B_{1,2}|+|B_{1,1}|+|B_{2,1}|}) \right|. \end{aligned} \quad (11)$$

That is, by introducing the values described in Lemma 2, the result follows.  $\square$

**Lemma 5.** Let  $\Gamma(\mathbb{Z}_{p^2q^2})$  be a zero-divisor graph; then,

$$\text{TP}_2(\Gamma(\mathbb{Z}_{p^2q^2})) = pq \left( \frac{p(q+2)(q-1)-1}{2} (q-1) + \frac{q(p+2)(p-1)-1}{2} (p-1) \right). \quad (15)$$

Hence, after simplification, the result follows.  $\square$

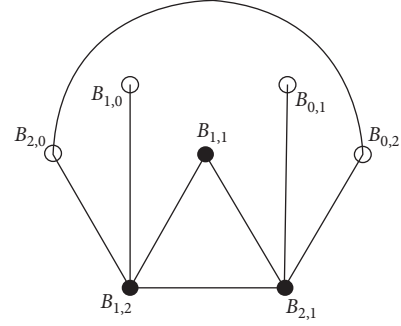


FIGURE 1: The structure of  $\mathbb{Z}_{p^2q^2}$ .

TABLE 1: Distance between pair of vertices, according to the block they belong to 1.

	$B_{1,0}$	$B_{0,1}$	$B_{2,0}$	$B_{1,1}$	$B_{0,2}$	$B_{1,2}$	$B_{2,1}$
$B_{1,0}$	2	3	2	2	3	1	2
$B_{0,1}$	3	2	3	2	2	2	1
$B_{2,0}$	2	3	2	2	1	1	2
$B_{1,1}$	2	2	2	1	2	1	1
$B_{0,2}$	3	2	1	2	2	2	1
$B_{1,2}$	1	2	1	1	2	1	1
$B_{2,1}$	2	1	2	1	1	1	1

$$\text{TP}_2(\Gamma(\mathbb{Z}_{p^2q^2})) = \frac{1}{2}pq(pq(p^2 + q^2 - 6) + p + q + 2). \quad (12)$$

*Proof.* The number of pairs of vertices at distance 2 is given by the formula that follows:

$$\begin{aligned} \text{TP}_2(\Gamma(\mathbb{Z}_{p^2q^2})) &= \binom{|B_{2,0}| + |B_{1,0}|}{2} + \binom{|B_{0,2}| + |B_{0,1}|}{2} \\ &+ |B_{1,1}|(|B_{2,0}| + |B_{1,0}| + |B_{0,2}| + |B_{0,1}|) \\ &+ |B_{2,1}|(|B_{2,0}| + |B_{1,0}|) + |B_{1,2}|(|B_{0,2}| + |B_{0,1}|), \end{aligned} \quad (13)$$

that is,

$$\begin{aligned} \text{TP}_2(\Gamma(\mathbb{Z}_{p^2q^2})) &= (|B_{2,0}| + |B_{1,0}|) \left( \frac{|B_{2,0}| + |B_{1,0}| - 1}{2} + |B_{1,1}| + |B_{2,1}| \right) \\ &+ (|B_{0,2}| + |B_{0,1}|) \left( \frac{|B_{0,2}| + |B_{0,1}| - 1}{2} + |B_{1,1}| + |B_{1,2}| \right). \end{aligned} \quad (14)$$

Thus, by Lemma 2, we obtain the following expression:

**Lemma 6.** Let  $\Gamma(\mathbb{Z}_{p^2q^2})$  be a zero-divisor graph; then,

$$TP_3(\Gamma(\mathbb{Z}_{p^2q^2})) = pq(p-1)(q-1)(pq-1). \quad (16)$$

*Proof.* The number of pairs at distance exactly 3,  $TP_3$ , is given by the following expression:

$$TP_3(\Gamma(\mathbb{Z}_{p^2q^2})) = |B_{0,1}||B_{2,0}| + |B_{0,1}||B_{1,0}| + |B_{0,2}||B_{1,0}|. \quad (17)$$

Thus, by Lemma 2, we get the result.  $\square$

### 3. Distance-Based Topological Indices and Polynomials of $\Gamma(\mathbb{Z}_{p^2q^2})$

Now, we are ready to state and prove the following theorems.

**Theorem 2.** *The Winner index of  $\Gamma(\mathbb{Z}_{p^2q^2})$  is*

$$W(\Gamma(\mathbb{Z}_{p^2q^2})) = 3p^2q^2(p-1)(q-1) + pq(pq(p^2+q^2-6) + p+q+2) + \frac{1}{2}(pq-1)(pq-2). \quad (18)$$

*Proof.* The diameter of  $\Gamma(\mathbb{Z}_{p^2q^2})$  is 3. Thus, there are pairs of vertices at distance 1, 2, and 3, and the Winner index can be obtained as follows:

$$W(\Gamma(\mathbb{Z}_{p^2q^2})) = TP_1 + 2TP_2 + 3TP_3. \quad (19)$$

By Lemmas 4–6, we get  $TP_1$ ,  $TP_2$ , and  $TP_3$ , respectively. Thus, by introducing these values in (19), we get, after simplification, the required result.  $\square$

**Lemma 7.** *The Hosoya polynomial of  $\Gamma(\mathbb{Z}_{p^2q^2})$  is  $((p^2q^2-1)/2) + (TP_1)x + (TP_2)x^2 + (TP_3)x^3$ .*

**Theorem 3.** *The Hosoya polynomial of  $\Gamma(\mathbb{Z}_{p^2q^2})$  is*

$$\begin{aligned} H(\Gamma(\mathbb{Z}_{p^2q^2}), x) &= \frac{p^2q^2-1}{2} + \left(3pq(p-1)(q-1) + \frac{1}{2}(pq-1)(pq-2)\right)x \\ &+ \frac{1}{2}pq(pq(p^2+q^2-6) + p+q+2)x^2 \\ &+ pq(p-1)(q-1)(pq-1)x^3. \end{aligned} \quad (20)$$

*Proof.* The result follows by Lemma 7 and by Lemmas 4–6.  $\square$

**Lemma 8.** *The Hyper-Wiener index of  $\Gamma(\mathbb{Z}_{p^2q^2})$  is  $2TP_1 + 6TP_2 + 12TP_3$ .*

**Theorem 4.** *The Hyper-Wiener index of  $\Gamma(\mathbb{Z}_{p^2q^2})$  is*

$$WW(\Gamma(\mathbb{Z}_{p^2q^2})) = 12p^2q^2(p-1)(q-1) + pq(pq(3p^2+3q^2-23) + 9p+9q-3) + 2. \quad (21)$$

*Proof.* The result follows by Lemma 8 and by Lemmas 4–6, after some simplifications.  $\square$

**Lemma 9.** *Let  $\alpha_{ij} = |B_{i,j}|d_{ij}$ , where  $d_{ij}$  is the degree of any vertex in  $B_{i,j}$ ,  $0 \leq i, j \leq 2$  and  $0 < i + j < 4$ . Then, the Schultz polynomial of  $\Gamma = \Gamma(\mathbb{Z}_{p^2q^2}) = (V, E)$  is equal to*

$$\begin{aligned} Sc(\Gamma, x) &= \{\alpha_{10}(|B_{0,1}| + |B_{0,2}|) + \alpha_{01}(|B_{1,0}| + |B_{2,0}|) + \alpha_{20}|B_{0,1}| + \alpha_{02}|B_{1,0}|\}x^3 \\ &+ \{(|B_{0,1}| + |B_{0,2}|)(\alpha_{12} + \alpha_{11}) + (|B_{1,0}| + |B_{2,0}|)(\alpha_{21} + \alpha_{11}) + (d_{12} - |B_{1,2}|)(\alpha_{20} + \alpha_{10}) + (d_{21} - |B_{2,1}|)(\alpha_{02} + \alpha_{01})\}x^2 \\ &+ \sum_{u \in V(\Gamma)} d_u^2x + 2|E(\Gamma)|. \end{aligned} \quad (22)$$

*Proof.* Since the diameter of  $\Gamma$  is 3, 3 is by definition the degree of  $\text{Sc}(\Gamma, x)$ . The 3rd coefficient of the polynomial is given by

$$|B_{0,1}||B_{1,0}|(d_{10} + d_{01}) + |B_{2,0}||B_{0,1}|(d_{20} + d_{01}) + |B_{0,2}||B_{1,0}|(d_{02} + d_{10}). \quad (23)$$

That is,  $\alpha_{10}|B_{0,1}| + \alpha_{01}|B_{1,0}| + \alpha_{20}|B_{0,1}| + \alpha_{01}|B_{2,0}| + \alpha_{02}|B_{1,0}| + \alpha_{10}|B_{0,2}|$ . From this expression, we clearly obtain the 3rd coefficient that appears in the statement.

The coefficients of  $x^2$  and  $x$  (see Table 1) are given, respectively, by

$$\begin{aligned} s_2 = & 2 \binom{|B_{1,0}|}{2} d_{10} + 2 \binom{|B_{2,0}|}{2} d_{20} + 2 \binom{|B_{0,1}|}{2} d_{01} + 2 \binom{|B_{0,2}|}{2} d_{02} \\ & + |B_{2,0}||B_{1,0}|(d_{20} + d_{10}) + |B_{1,1}||B_{1,0}|(d_{11} + d_{10}) + |B_{1,1}||B_{0,1}|(d_{11} + d_{01}) \\ & + |B_{1,1}||B_{2,0}|(d_{11} + d_{20}) + |B_{0,2}||B_{0,1}|(d_{02} + d_{01}) + |B_{0,2}||B_{1,1}|(d_{02} + d_{11}) \\ & + |B_{1,2}||B_{0,1}|(d_{12} + d_{01}) + |B_{1,2}||B_{0,2}|(d_{12} + d_{02}) + |B_{2,1}||B_{1,0}|(d_{21} + d_{10}) \\ & + |B_{2,1}||B_{2,0}|(d_{21} + d_{20}), \\ s_1 = & 2 \binom{|B_{1,1}|}{2} d_{11} + 2 \binom{|B_{1,2}|}{2} d_{12} + 2 \binom{|B_{2,1}|}{2} d_{21} + |B_{1,2}||B_{2,0}|(d_{12} + d_{20}) \\ & + |B_{2,1}||B_{0,2}|(d_{21} + d_{02}) + |B_{1,2}||B_{1,0}|(d_{12} + d_{10}) + |B_{2,1}||B_{0,1}|(d_{21} + d_{01}) \\ & + |B_{0,2}||B_{2,0}|(d_{02} + d_{20}) + |B_{1,1}||B_{1,2}|(d_{11} + d_{12}) + |B_{1,1}||B_{2,1}|(d_{11} + d_{21}) \\ & + |B_{2,1}||B_{1,2}|(d_{21} + d_{12}). \end{aligned} \quad (24)$$

By doing similar transformations as above, we obtain the  $2^n$  and the 1st coefficient, respectively, that appears in the statement. Finally, the independent term appears when we apply the formula to each vertex.  $\square$

**Theorem 5.** Let  $p$  and  $q$  be different primes. Then, the Schultz polynomial of  $\Gamma = \Gamma(\mathbb{Z}_{p^2q^2})$  is equal to

$$\begin{aligned} \text{Sc}(\Gamma, x) = & \{p(p-1)q(q-1)(2p^2q + 2pq^2 - 4pq - p^2 - q^2 + 2)\}x^3 \\ & + \{pq(4p^3q^2 + 4p^2q^3 - 3p^3q - 12p^2q^2 - 3pq^3 + 2pq^2 + 2p^2q + 6pq + 2p^2 + 2q^2 - 4)\}x^2 \\ & + \{(p-1)(q-1)(p^3q + p^2q^2 + pq^3 + 2p^2q + 2pq^2 - 10pq + 4) + (p-1)(pq^2 - 2)^2 \\ & + (q-1)(pq^2 - 2)^2\}x + (p-1)(q-1)(5pq - 2) + (p-1)(pq^2 - 2) \\ & + (q-1)(p^2q - 2). \end{aligned} \quad (25)$$

*Proof.* Consider the formula obtained in Lemma 9. Note that

$$\begin{aligned} \sum_{u \in V(\Gamma)} d_u^2 = & \alpha_{20}d_{20} + \alpha_{02}d_{02} + \alpha_{10}d_{10} + \alpha_{01}d_{01} + \alpha_{11}d_{11} \\ & + \alpha_{12}d_{12} + \alpha_{21}d_{21} \end{aligned} \quad (26)$$

and  $2|E(\Gamma)| = \alpha_{20} + \alpha_{02} + \alpha_{10} + \alpha_{01} + \alpha_{11} + \alpha_{12} + \alpha_{21}$ . By introducing the values of  $|B_{i,j}|$ ,  $d_{ij}$  (collected in Lemmas 2 and 3), and  $\alpha_{ij}$  in terms of  $p$  and  $q$ , the result follows.  $\square$

**Corollary 1.** The Schultz index or the degree distance of  $\Gamma = \Gamma(\mathbb{Z}_{p^2q^2})$  is equal to



$$\begin{aligned}
\text{Sc}(\Gamma, x) &= 3p(p-1)q(q-1)(2p^2q + 2pq^2 - 4pq - p^2 - q^2 + 2) + 2pq \\
&\quad \cdot (4p^3q^2 + 4p^2q^3 - 3p^3q - 12p^2q^2 - 3pq^3 + 2pq^2 + 2p^2q + 6pq + 2p^2 + 2q^2 - 4) \\
&\quad + (p-1)(q-1)(p^3q + p^2q^2 + pq^3 + 2p^2q + 2pq^2 - 10pq + 4) + (p-1)(pq^2 - 2)^2 \\
&\quad + (q-1)(pq^2 - 2)^2.
\end{aligned} \tag{27}$$

**Lemma 10.** Let  $\alpha_{ij} = |B_{i,j}|d_{ij}$ , where  $d_{ij}$  is the degree of any vertex in  $B_{i,j}$ ,  $0 \leq i, j \leq 2$  and  $0 < i + j < 4$ . Then, the modified Schultz polynomial of  $\Gamma = \Gamma(\mathbb{Z}_{p^2q^2}) = (V, E)$  is equal to

$$\begin{aligned}
\text{Sc}^*(\Gamma, x) &= \{\alpha_{10}\alpha_{01} + \alpha_{20}\alpha_{01} + \alpha_{02}\alpha_{10}\}x^3 + \left\{ \frac{\alpha_{10}(\alpha_{10} - d_{10})}{2} + \frac{\alpha_{20}(\alpha_{20} - d_{20})}{2} \right. \\
&\quad + \frac{\alpha_{01}(\alpha_{01} - d_{01})}{2} + \frac{\alpha_{02}(\alpha_{02} - d_{02})}{2} + \alpha_{20}\alpha_{10} + \alpha_{11}\alpha_{10} + \alpha_{11}\alpha_{01} + \alpha_{11}\alpha_{20} + \\
&\quad + \alpha_{02}\alpha_{01} + \alpha_{02}\alpha_{11} + \alpha_{12}\alpha_{01} + \alpha_{12}\alpha_{02} + \alpha_{21}\alpha_{10} + \alpha_{21}\alpha_{20} \} x^2 + \left\{ \frac{\alpha_{11}(\alpha_{11} - d_{11})}{2} \right. \\
&\quad + \frac{\alpha_{12}(\alpha_{12} - d_{12})}{2} + \frac{\alpha_{21}(\alpha_{21} - d_{21})}{2} + \alpha_{12}\alpha_{20} + \alpha_{21}\alpha_{02} + \alpha_{12}\alpha_{10} + \alpha_{21}\alpha_{01} \\
&\quad + \alpha_{02}\alpha_{20} + \alpha_{11}\alpha_{12} + \alpha_{11}\alpha_{21} + \alpha_{21}\alpha_{12} \} x + \sum_{u \in V} d_u^2.
\end{aligned} \tag{28}$$

*Proof.* Since the diameter of  $\Gamma$  is 3, 3 is by definition the degree of  $\text{Sc}^*(\Gamma, x)$ . The 3rd coefficient of the polynomial is given by

$$|B_{0,1}| |B_{1,0}| d_{10} d_{01} + |B_{2,0}| |B_{0,1}| d_{20} d_{01} + |B_{0,2}| |B_{1,0}| d_{02} d_{10}, \tag{29}$$

that is,  $\alpha_{10}\alpha_{01} + \alpha_{20}\alpha_{01} + \alpha_{02}\alpha_{10}$ .

The coefficients of  $x^2$  and  $x$  (see Table 1) are given, respectively, by

$$\begin{aligned}
s_2^* &= \binom{|B_{1,0}|}{2} d_{10}^2 + \binom{|B_{2,0}|}{2} d_{20}^2 + \binom{|B_{0,1}|}{2} d_{01}^2 + \binom{|B_{0,2}|}{2} d_{02}^2 + |B_{2,0}| |B_{1,0}| d_{20} d_{10} \\
&\quad + |B_{1,1}| |B_{1,0}| d_{11} d_{10} + |B_{1,1}| |B_{0,1}| d_{11} d_{01} + |B_{1,1}| |B_{2,0}| d_{11} d_{20} + |B_{0,2}| |B_{0,1}| d_{02} d_{01} \\
&\quad + |B_{0,2}| |B_{1,1}| d_{02} d_{11} + |B_{1,2}| |B_{0,1}| d_{12} d_{01} + |B_{1,2}| |B_{0,2}| d_{12} d_{02} + |B_{2,1}| |B_{1,0}| d_{21} d_{10} \\
&\quad + |B_{2,1}| |B_{2,0}| d_{21} d_{20}, \\
s_1^* &= \binom{|B_{1,1}|}{2} d_{11}^2 + \binom{|B_{1,2}|}{2} d_{12}^2 + \binom{|B_{2,1}|}{2} d_{21}^2 + |B_{1,2}| |B_{2,0}| d_{12} d_{20} \\
&\quad + |B_{2,1}| |B_{0,2}| d_{21} d_{02} + |B_{1,2}| |B_{1,0}| d_{12} d_{10} + |B_{2,1}| |B_{0,1}| d_{21} d_{01} + |B_{0,2}| |B_{2,0}| d_{02} d_{20} \\
&\quad + |B_{1,1}| |B_{1,2}| d_{11} d_{12} + |B_{1,1}| |B_{2,1}| d_{11} d_{21} + |B_{2,1}| |B_{1,2}| d_{21} d_{12}.
\end{aligned} \tag{30}$$

By doing similar transformations as above, we obtain the  $2^n$  and the 1st coefficient, respectively, that appears in the

statement. Finally, the independent term appears when we apply the formula to each vertex.  $\square$

**Theorem 6.** Let  $p$  and  $q$  be different primes. Then, the modified Schultz polynomial of  $\Gamma = \Gamma(\mathbb{Z}_{p^2q^2})$  is equal to

$$\begin{aligned} Sc^*(\Gamma, x) &= \{p(p-1)^2q(q-1)^2(3pq-p-q-1)\}x^3 \\ &+ \left\{ (p-1)^2(q-1)^2 \left( 8p^2q^2 + \frac{(p^2q+pq^2)}{2} - p^2 - q^2 - 11pq - p - q \right) \right. \\ &+ \frac{1}{2}(p-1)(q-1)(6p^3q^3 - 2p^3q - 2pq^3 - 6p^2q^2 - 4p^2q - 4pq^2 - p^3 - q^3 - 3p^2 \\ &- 3q^2 + 10pq + 5p + 5q)\}x^2 + \{(p-1)(q-1)(13p^3q^3 - 5p^3q^2 - 2p^3q - p^2q^3 \\ &- 8p^2q^2 - 8p^2q - 6pq^3 - 4pq^2 + 14pq + 4p + 4q) + \frac{1}{2}(p-1)(p-2)(pq^2-2)^2 \\ &+ \frac{1}{2}(q-1)(q-2)(p^2q-2)^2\}x + (p-1)(pq^2-2)^2 + (q-1)(p^2q-2)^2 \\ &+ (p-1)(q-1)(p^3q + p^2q^2 + pq^3 + p^2q + pq^2 - 8pq + 4). \end{aligned} \tag{31}$$

*Proof.* Consider the formula obtained in Lemma 10. Recall that  $\sum_{u \in V(\Gamma)} d_u^2 = \alpha_{20}d_{20} + \alpha_{02}d_{02} + \alpha_{10}d_{10} + \alpha_{01}d_{01} + \alpha_{11}d_{11} + \alpha_{12}d_{12} + \alpha_{21}d_{21}$ . By introducing the values of  $|B_{i,j}|$ ,  $d_{i,j}$  (collected in Lemmas 2 and 3), and  $\alpha_{ij}$  in terms of  $p$  and  $q$ , the result follows.  $\square$

**Corollary 2.** The modified Schultz index of  $\Gamma = \Gamma(\mathbb{Z}_{p^2q^2})$  is equal to

$$\begin{aligned} Sc(\Gamma, x) &= (p-1)^2(q-1)^2(25p^2q^2 - 2p^2q - 2pq^2 - p^2 - q^2 - 14pq - p - q) \\ &+ (p-1)(q-1)(19p^3q^3 - 5p^3q^2 - 4p^3q - p^3 - 14p^2q^2 - 12p^2q - 3p^2 - 8pq^3 \\ &- 8pq^2 + 24pq + 9p - q^3 - 3q^2 + 9q) + \frac{1}{2}(p-1)(p-2)(pq^2-2)^2 \\ &+ \frac{1}{2}(q-1)(q-2)(p^2q-2)^2. \end{aligned} \tag{32}$$

#### 4. Conclusion

The structure of zero-divisor graphs of the form of  $\Gamma(\mathbb{Z}_{p^2q^2})$  is particularly interesting for studying distance-based topological indices. First, because its diameter is exactly 3, but also because there are defined blocks, with a complete bipartite connection between them, of either independent vertices or complete graphs (cliques). In this paper, we have focused on the Wiener index and the Hosoya, the Shultz, and the modified Shultz polynomials of  $\Gamma(\mathbb{Z}_{p^2q^2})$  and, finally, on the Shultz and the modified Shultz indices of  $\Gamma(\mathbb{Z}_{p^2q^2})$ . For that reason, we have introduced some notation that could be useful not only for studying other distance-base topological indices of  $\Gamma(\mathbb{Z}_{p^2q^2})$  but also for other graphs of the form  $\Gamma(\mathbb{Z}_{p^mq^n})$ ,

for  $m, n$  positive integers. A key point in this notation is the study of pairs that are exactly a distance one (the size of the graph), two, or three. We think that a possible line of future research should include the study of paths connecting pairs of vertices a different distances and the extension to other indices, as for instance, the Estrada index.

#### Data Availability

All the data are provided within the manuscript.

#### Conflicts of Interest

The authors declare that they have no conflicts of interest.

## Acknowledgments

The research conducted by the second author has been supported by Ministerio de Ciencia, Innovación y Universidades (Spain), under project PGC2018-095471-B-I00.

## References

- [1] A. Ahmad and A. Haider, "Computing the radio labeling associated with zero-divisor graph of a commutative ring," *UPB Scientific Bulletin Series A*, vol. 81, no. 1, pp. 65–72, 2019.
- [2] I. Beck, "Coloring of commutative rings," *Journal of Algebra*, vol. 116, no. 1, pp. 208–226, 1988.
- [3] R. C. Entringer, D. E. Jackson, and D. A. Snyder, "Distance in graphs," *Czechoslovak Mathematical Journal*, vol. 26, no. 2, pp. 283–296, 1976.
- [4] A. A. Dobrynin, R. Entringer, and I. Gutman, "Wiener index of trees: theory and applications," *Acta Applicandae Mathematicae*, vol. 66, no. 3, pp. 211–249, 2001.
- [5] A. A. Dobrynin, I. Gutman, S. Klavžar, and P. Žigert, "Wiener index of hexagonal systems," *Acta Applicandae Mathematicae*, vol. 72, no. 3, pp. 247–294, 2002.
- [6] A. Ahmad, "On the degree based topological indices of benzene ring embedded in P-type-surface in 2D network," *Hacetatepe Journal of Mathematics and Statistics*, vol. 47, no. 1, pp. 9–18, 2018.
- [7] A. Ahmad, "Computation of certain topological properties of honeycomb networks and Graphene," *Discrete Mathematics, Algorithms and Applications*, vol. 9, no. 5, 2017.
- [8] S. Akhter, W. Gao, M. Imran, and M. R. Farahani, "On topological indices of honeycomb networks and graphene networks," *Hacetatepe Journal of Mathematics and Statistics*, vol. 47, no. 1, pp. 19–35, 2018.
- [9] M. F. Nadeem, S. Zafar, and Z. Zahid, "On topological properties of the line graphs of subdivision graphs of certain nanostructures," *Applied Mathematics and Computation*, vol. 273, pp. 125–130, 2016.
- [10] S. Wang, M. R. Farahani, M. R. R. Kanna, M. K. Jamil, and R. P. Kumar, "The Wiener index and the Hosoya polynomial of the Jahangir graphs," *Applied and Computational Mathematics*, vol. 5, no. 3, pp. 138–141, 2016.
- [11] H. Wiener, "Structural determination of paraffin boiling points," *Journal of the American Chemical Society*, vol. 69, pp. 17–20, 1947.
- [12] E. Estrada, L. Torres, L. Rodriguez, and I. Gutman, "An atom-bond connectivity index: modelling the enthalpy of formation of alkanes," *Indian Journal Chemistry*, vol. 37A, pp. 849–855, 1998.
- [13] M. K. Siddiqui, M. Naeem, N. A. Rehman, and M. Imran, "Computing topological indices of certain networks," *Journal of Optoelectronics and Advanced Materials*, vol. 18, pp. 884–892, 2016.
- [14] Z. Shao, P. Wu, Y. Gao, I. Gutman, and X. Zhang, "On the maximum ABC index of graphs without pendent vertices," *Applied Mathematics and Computation*, vol. 315, pp. 298–312, 2017.
- [15] M. K. Siddiqui, M. Imran, and A. Ahmad, "On Zagreb indices, Zagreb polynomials of some nanostar dendrimers," *Applied Mathematics and Computation*, vol. 280, pp. 132–139, 2016.
- [16] Z. Shao, M. K. Siddiqui, and M. H. Muhammad, "Computing Zagreb indices and Zagreb polynomials for symmetrical nanotubes," *Symmetry*, vol. 10, no. 244, 2018.
- [17] S. Gupta, M. Singh, and A. K. Madan, "Application of graph theory: relationship of eccentric connectivity index and Wiener's index with anti-inflammatory activity," *Journal of Mathematical Analysis and Applications*, vol. 266, no. 2, pp. 259–268, 2002.
- [18] K. Elahi, A. Ahmad, and R. Hasni, "Construction algorithm for zero-divisor graphs of finite commutative rings and their vertex-based eccentric topological indices," *Mathematics*, vol. 6, no. 12, p. 301, 2018.
- [19] M. Imran, M. K. Siddiqui, A. A. E. Abunamous, D. Adi, S. H. Rafique, and A. Q. Baig, "Eccentricity based topological indices of an oxide network," *Mathematics*, vol. 6, no. 126, 2018.
- [20] M. Randić, "Novel molecular descriptor for structure-property studies," *Chemical Physics Letters*, vol. 211, pp. 478–483, 1993.
- [21] M. Randić, X. Guo, T. Oxley, H. Krishnapriyan, and L. Naylor, "Wiener matrix invariants," *Journal of Chemical Information and Computer Sciences*, vol. 34, no. 2, pp. 361–367, 1994.
- [22] H. Hosoya, "On some counting polynomials in chemistry," *Discrete Applied Mathematics*, vol. 19, pp. 239–257, 1989.
- [23] A. A. Dobrynin and A. A. Kochetova, "Degree distance of a graph: a degree analog of the Wiener index," *Journal of Chemical Information and Computer Sciences*, vol. 34, no. 5, pp. 1082–1086, 1994.
- [24] I. Gutman, "Selected properties of the Schultz molecular topological index," *Journal of Chemical Information and Computer Sciences*, vol. 34, no. 5, pp. 1087–1089, 1994.
- [25] S. Klavžar and I. Gutman, "A comparison of the Schultz molecular topological index with the Wiener index," *Journal of Chemical Information and Computer Sciences*, vol. 36, pp. 1001–1003, 2018.
- [26] D. D. Anderson and M. Naseer, "Beck's coloring of a commutative ring," *Journal of Algebra*, vol. 159, no. 2, pp. 500–514, 1993.
- [27] D. F. Anderson and P. S. Livingston, "The zero-divisor graph of a commutative ring," *Journal of Algebra*, vol. 217, no. 2, pp. 434–447, 1999.
- [28] D. F. Anderson, R. Levy, and J. Shapiro, "Zero-divisor graphs, von Neumann regular rings, and Boolean algebras," *Journal of Pure and Applied Algebra*, vol. 180, no. 3, pp. 221–241, 2003.
- [29] F. DeMeyer and L. DeMeyer, "Zero divisor graphs of semi-groups," *Journal of Algebra*, vol. 283, no. 1, pp. 190–198, 2005.
- [30] A. N. A. Kaom, A. Ahmad, and A. Haider, "On eccentric topological indices based on edges of zero-divisor graphs," *Symmetry*, vol. 11, no. 7, p. 907, 2019.

## Research Article

# New Results on Zagreb Energy of Graphs

Seyed Mahmoud Sheikholeslami , Akbar Jahanbani , and Rana Khoeilar

Department of Mathematics, Azarbaijan Shahid Madani University, Tabriz, Iran

Correspondence should be addressed to Akbar Jahanbani; akbar.jahanbani92@gmail.com

Received 2 April 2021; Accepted 6 May 2021; Published 24 May 2021

Academic Editor: Roslan Hasni

Copyright © 2021 Seyed Mahmoud Sheikholeslami et al. This is an open access article distributed under the Creative Commons Attribution License, which permits unrestricted use, distribution, and reproduction in any medium, provided the original work is properly cited.

Let  $G$  be a graph with vertex set  $V(G) = \{v_1, \dots, v_n\}$ , and let  $d_i$  be the degree of  $v_i$ . The Zagreb matrix of  $G$  is the square matrix of order  $n$  whose  $(i, j)$ -entry is equal to  $d_i + d_j$  if the vertices  $v_i$  and  $v_j$  are adjacent, and zero otherwise. The Zagreb energy  $ZE(G)$  of  $G$  is the sum of the absolute values of the eigenvalues of the Zagreb matrix. In this paper, we determine some classes of Zagreb hyperenergetic, Zagreb borderenergetic, and Zagreb equienergetic graphs.

## 1. Introduction

In this paper,  $G$  is a simple undirected graph, with vertex set  $V = V(G)$  and edge set  $E = E(G)$ . The integers  $n = n(G) = |V(G)|$  and  $m = m(G) = |E(G)|$  are the *order* and the *size* of the graph  $G$ , respectively. For a vertex  $v \in V$ , the *open neighborhood* of  $v$  is the set  $N(v) = \{u \in V | uv \in E\}$  and the *degree* of  $v$  is  $d(v) = |N(v)|$ . We write  $P_n$ ,  $C_n$ , and  $K_n$  for the path, cycle, and complete graph of order  $n$ , respectively. A *bipartite* graph is a graph such that its vertex set can be partitioned into two sets  $X$  and  $Y$  (called the partite sets) such that every edge meets both  $X$  and  $Y$ . A *complete bipartite graph* is a bipartite graph such that any vertex of a partite set is adjacent to all vertices of the other partite set. A complete bipartite graph with partite set of cardinalities  $p$  and  $q$  is denoted by  $K_{p,q}$ . The complement  $\bar{G}$  of  $G$  is the simple graph whose vertex set is  $V$  and whose edges are the pairs of nonadjacent vertices of  $G$ . The line graph of a graph  $G$ , written  $L(G)$ , is the graph whose vertices are the edges of  $G$ , with  $ef \in E(L(G))$  when  $e = uv$  and  $f = vw$  in  $G$ . The line graph  $L(G)$  of a  $r$ -regular graph  $G$  with  $n$  vertices is  $(2r - 2)$ -regular with  $nr/2$  vertices.

For each vertex  $v$  of a graph  $G$ , take a new vertex  $v'$  and join  $v'$  to all vertices of  $G$  adjacent to  $v$ . The graph  $S'(G)$  thus obtained is called the splitting graph of  $G$ . The *cocktail party*

graph  $CP(a)$  (for  $a \geq 3$ ) is a graph obtained from the complete graph  $K_{2a}$  by deleting a perfect matching.

Any graph on  $n$  vertices, with  $n \geq 2$ , has at least two vertices with the same degree. The graphs with at most two vertices with the same degree are called *antiregular*; for more information, see [1, 17]. For any positive integer  $n$ , there exists only one connected antiregular graph on  $n$  vertices, denoted by  $A_n$  (see Figure 1).

The adjacency matrix  $A(G)$  of  $G$  is defined by its entries as  $a_{ij} = 1$  if  $v_i v_j \in E(G)$  and 0 otherwise. Let  $\lambda_1 \geq \lambda_2 \geq \dots \geq \lambda_n$  denote the eigenvalues of  $A(G)$ . The energy of the graph  $G$  is defined as

$$\mathcal{E} = \mathcal{E}(G) = \sum_{i=1}^n |\lambda_i|, \quad (1)$$

where  $\lambda_i$ ,  $i = 1, 2, \dots, n$ , are the eigenvalues of graph  $G$ .

This concept was introduced by Gutman and is intensively studied in chemistry, since it can be used to approximate the total  $\pi$ -electron energy of a molecule (see, e.g., [8, 9]). Since then, numerous other bounds for  $\mathcal{E}$  were found (see, e.g., [11–14]).

The Zagreb indices are widely studied degree-based topological indices and were introduced by Gutman and Trinajstić [7] in 1972. The *Zagreb matrix* of a graph  $G$  is a

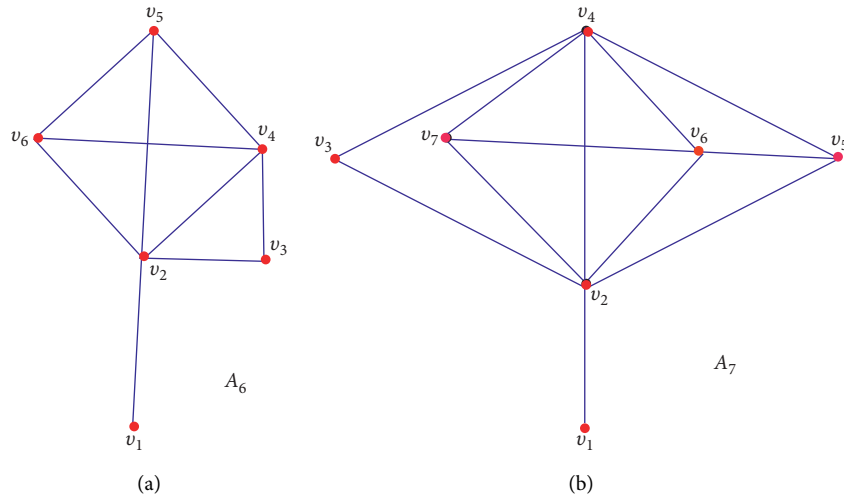


FIGURE 1: Two antiregular graph with vertices  $n = 6$  and  $n = 7$ .

square matrix  $A_z(G) = [m_{ij}]$  of order  $n$ , defined in [10], as follows:

$$m_{ij} = \begin{cases} d_i + d_j, & \text{if the vertices } v_i \text{ and } v_j \text{ of } G \text{ are adjacent,} \\ 0, & \text{otherwise.} \end{cases} \quad (2)$$

The eigenvalues of  $A_z(G)$  labeled as  $z_1 \geq z_2 \geq \dots \geq z_n$  are said to be the Zagreb eigenvalues or  $A_z$ -eigenvalues of  $G$  and their collection is called Zagreb spectrum or  $A_z$ -spectrum of  $G$ .

If  $z_1, z_2, \dots, z_s$  are the distinct Zagreb eigenvalues of  $G$  having the multiplicities  $m_1, m_2, \dots, m_s$ , then the Zagreb spectrum of  $G$  is denoted as

$$\text{Spec}(A_z) = \left( \begin{matrix} z_1 & z_2 & \dots & z_s \\ m_1 & m_2 & \dots & m_s \end{matrix} \right), \quad (3)$$

where  $m_1 + m_2 + \dots + m_s = n$ .

The sum of all absolute Zagreb eigenvalues is the Zagreb energy denoted by  $\text{ZE}(G)$  and defined in [10] as follows:

$$\text{ZE} = \text{ZE}(G) = \sum_{i=1}^n |z_i|. \quad (4)$$

Now, we prove the next lemma that will be needed to obtain our results.

**Lemma 1.** For a complete graph  $K_n$ , the Zagreb eigenvalues are  $-2(n-1)$  and  $2(n-1)^2$  with multiplicities  $(n-1)$  and  $1$ , respectively, and  $\text{ZE}(K_n) = 4(n-1)^2$ .

*Proof.* Let  $G$  be a graph with vertices  $v_1, v_2, v_3, \dots, v_n$ . Then, the Zagreb matrix is as follows:

$$A_z(G) = \begin{matrix} & v_1 & v_2 & v_3 & \dots & v_p \\ \begin{matrix} v_1 \\ v_2 \\ v_3 \\ \vdots \\ v_p \end{matrix} & \begin{pmatrix} 0 & d_1 + d_2 & d_1 + d_3 & \dots & d_1 + d_n \\ d_2 + d_1 & 0 & d_2 + d_3 & \dots & d_2 + d_n \\ d_3 + d_1 & d_3 + d_2 & 0 & \dots & d_3 + d_n \\ \vdots & \vdots & \vdots & \ddots & \vdots \\ d_n + d_1 & d_n + d_2 & d_n + d_3 & \dots & 0 \end{pmatrix} \end{matrix}. \quad (5)$$

Since,  $K_n$  is a regular graph of degree  $n-1$ , we have

$$A_z(K_n) = \begin{bmatrix} 0 & 2n-2 & 2n-2 & \dots & 2n-2 \\ 2n-2 & 0 & 2n-2 & \dots & 2n-2 \\ 2n-2 & 2n-2 & 0 & \dots & 2n-2 \\ \vdots & \vdots & \vdots & \ddots & \vdots \\ 2n-2 & 2n-2 & 2n-2 & \dots & 0 \end{bmatrix}. \quad (6)$$

It can be easily seen that the Zagreb spectrum of  $K_n$  is as follows:

$$\text{Spec}A_z(K_n) = \left( \begin{matrix} 2(n-1)^2 & -2(n-1) \\ 1 & n-1 \end{matrix} \right). \quad (7)$$

Therefore, by the definition of the Zagreb energy, we have

$$\text{ZE}(K_n) = 4(n-1)^2. \quad (8)$$

Gutman [5] introduced energy in 1978 and conjectured that the complete graph  $K_n$  possesses the maximum energy among all graphs with  $n$  vertices. Gutman [6] also proved this to be false leading to the new concept of hyperenergetic graphs.

A graph is *hyperenergetic* [6] if  $\mathcal{E}(G) > 2n - 2$ , *non-hyperenergetic* if  $\mathcal{E}(G) < 2n - 2$ , and *broderenergetic* [4] (other than  $K_n$ ) if  $\mathcal{E}(G) = 2n - 2$ . If  $\mathcal{E}(G) = \mathcal{E}(H)$ , then graphs  $G$  and  $H$  are *equienergetic* [2].

Following the above ideas, a graph  $G$  of order  $n$  is said to be *Zagreb hyperenergetic* if  $ZE(G) > 4(n - 1)^2$ , *Zagreb non-hyperenergetic* if  $ZE(G) < 4(n - 1)^2$ , and *Zagreb broderenergetic* (other than  $K_n$ ) if  $ZE(G) = 4(n - 1)^2$ . If  $ZE(G) = ZE(H)$ , then two graphs  $G$  and  $H$  are called *Zagreb equienergetic*.

In [10], the authors obtained some lower and upper bounds for Zagreb energy, Das [3] presented some new bounds for Zagreb energy, Rakshith [16] discussed the new bounds for Zagreb energy, and Jahanbani et al. [15] obtained new bounds for Zagreb energy.

In this paper, we study the Zagreb energy of line graphs, Zagreb energy of complement graphs, and Zagreb hyperenergetic, Zagreb borderenergetic, and Zagreb equienergetic graphs.  $\square$

## 2. Main Results

In this section, we provide Zagreb energy of complement  $\bar{G}$  and Zagreb energy of line graph  $L(G)$  of a graph  $G$ , and furthermore, we develop results to determine the nature of graphs like complement  $\bar{G}$ , line graph  $L(G)$ , and splitting graph  $S'(G)$  to be Zagreb hyperenergetic and Zagreb borderenergetic.

We start with the following proposition that helps us to obtain our results.

**Proposition 1.** *Let  $G$  be an  $r$ -regular graph ( $r \geq 3$ ) of order  $n$  with Zagreb eigenvalues  $z_1 \geq z_2 \geq \dots \geq z_n$ . The Zagreb eigenvalues of  $A_z(\bar{G})$  are  $2(n - r - 1)^2$  with multiplicity one and  $2(n - r - 1)(-z_i/2r - 1)$ , for  $i = 2, 3, \dots, n$ .*

**Theorem 1.** *Let  $G$  be an  $r$ -regular graph ( $r \geq 3$ ) of order  $n$  with Zagreb eigenvalues  $z_1 \geq z_2 \geq \dots \geq z_n$ . The Zagreb energy of complement  $\bar{G}$  is*

$$ZE(\bar{G}) = 2(n - r - 1) \left( |(n - r - 1)| + \left| \sum_{i=2}^n \left( \frac{-z_i}{2r} - 1 \right) \right| \right). \tag{9}$$

*Proof.* Since  $G$  is  $r$ -regular, the complement  $\bar{G}$  is  $(n - r - 1)$ -regular. By Equality (4) and Proposition 1, we obtain

$$\begin{aligned} ZE(\bar{G}) &= 2|(n - r - 1)(n - r - 1)| \\ &\quad + \left| \sum_{i=2}^n 2(n - r - 1) \left( \frac{-z_i}{2r} - 1 \right) \right| \\ &= 2(n - r - 1) \left( |(n - r - 1)| + \left| \sum_{i=2}^n \left( \frac{-z_i}{2r} - 1 \right) \right| \right). \end{aligned} \tag{10}$$

$\square$

**Theorem 2.** *For an  $r$ -regular graph  $G$  of order  $n$ , the complement  $\bar{G}$  is Zagreb non-hyperenergetic if  $r \geq 3$ .*

*Proof.* From Equality (10), we have

$$ZE(\bar{G}) = 2(n - r - 1) \left( |(n - r - 1)| + \left| \sum_{i=2}^n \left( \frac{-z_i}{2r} - 1 \right) \right| \right). \tag{11}$$

It is easy to verify that

$$2(n - r - 1) \left( |(n - r - 1)| + \left| \sum_{i=2}^n \left( \frac{-z_i}{2r} - 1 \right) \right| \right) < 4(n - 1)^2. \tag{12}$$

Hence, the complement  $\bar{G}$  is a Zagreb non-hyperenergetic graph.  $\square$

**Proposition 2.** *Let  $G$  be an  $r$ -regular graph ( $r \geq 3$ ) of order  $n$  with Zagreb eigenvalues  $z_1 \geq z_2 \geq \dots \geq z_n$ . The Zagreb eigenvalues of  $A_z(L(G))$  are  $(8 - 8r)$  with multiplicity  $n(r - 2)/2$  and  $4(r - 1)(z_i/2r + r - 2)$  for  $i = 1, 2, \dots, n$ .*

**Theorem 3.** *Let  $G$  be an  $r$ -regular graph ( $r \geq 3$ ) of order  $n$  with Zagreb eigenvalues  $z_1 \geq z_2 \geq \dots \geq z_n$ . The Zagreb energy of line graph  $L(G)$  is*

$$\begin{aligned} ZE(L(G)) &= 4(r - 1) \left| \sum_{i=1}^n \left( \frac{z_i}{2r} + r - 2 \right) \right| \\ &\quad + |8 - 8r| \left( \frac{n(r - 2)}{2} \right). \end{aligned} \tag{13}$$

*Proof.* The line graph  $L(G)$  of a  $r$ -regular graph  $G$  is a  $(2r - 2)$ -regular graph of order  $nr/2$ . By definition of Zagreb energy and Proposition 2, we have

$$\begin{aligned} ZE(L(G)) &= \left| \sum_{i=1}^n 4(r - 1) \left( \frac{z_i}{2r} + r - 2 \right) \right| \\ &\quad + |(8 - 8r)| \left( \frac{n(r - 2)}{2} \right) \\ &= 4(r - 1) \left| \sum_{i=1}^n \left( \frac{z_i}{2r} + r - 2 \right) \right| \\ &\quad + |(8 - 8r)| \left( \frac{n(r - 2)}{2} \right). \end{aligned} \tag{14}$$

$\square$

**Theorem 4.** *Let  $G$  be an  $r$ -regular graph ( $r \geq 3$ ) of order  $n$  different from  $K_2$  and  $K_3$ . Then,  $L(G)$  is Zagreb non-hyperenergetic.*

*Proof.* Applying Theorem 3, we have

$$\begin{aligned}
 \text{ZE}(L(G)) &= 4(r-1) \left| \sum_{i=1}^n \left( \frac{z_i}{2r} + r - 2 \right) \right| \\
 &\quad + |(8-8r)| \left( \frac{n(r-2)}{2} \right).
 \end{aligned}
 \tag{15}$$

It is not hard to see that

$$\begin{aligned}
 4(r-1) \left| \sum_{i=1}^n \left( \frac{z_i}{2r} + r - 2 \right) \right| + |(8-8r)| \left( \frac{n(r-2)}{2} \right) \\
 < 4 \left( \frac{nr}{2} - 1 \right)^2.
 \end{aligned}
 \tag{16}$$

Thus,  $L(G)$  is a Zagreb non-hyperenergetic graph.  $\square$

*Remark 1.* Note that the graphs  $K_2$  or  $K_3$  are Zagreb borderenergetic.

*Example 1.* The antiregular graphs  $A_6$  and  $A_7$  illustrated in Figure 1 are non-hyperenergetic.

Let  $A_6$  be a graph with vertices  $v_1, v_2, v_3, v_4, v_5,$  and  $v_6$ . The Zagreb matrix of  $A_6$  is

$$\begin{matrix}
 & v_1 & v_2 & v_3 & v_4 & v_5 & v_6 \\
 \begin{matrix} v_1 \\ v_2 \\ v_3 \\ v_4 \\ v_5 \\ v_6 \end{matrix} & \begin{pmatrix} 0 & 6 & 0 & 0 & 0 & 0 \\ 6 & 0 & 7 & 9 & 8 & 8 \\ 0 & 7 & 0 & 6 & 0 & 0 \\ 0 & 9 & 6 & 0 & 7 & 7 \\ 0 & 8 & 0 & 7 & 0 & 6 \\ 0 & 8 & 0 & 7 & 6 & 0 \end{pmatrix} & & & & & 
 \end{matrix}
 \tag{17}$$

Therefore, the Zagreb spectrum of  $A_6$  is as follows:

$$\text{Spec}_{A_z}(A_6) = \begin{pmatrix} 25.02 & 2.339 & 1.087 & -6 & -13.149 & -9.297 \\ 1 & 1 & 1 & 1 & 1 & 1 \end{pmatrix}.
 \tag{18}$$

By the definition of the Zagreb energy, we have

$$\text{ZE}(A_6) = 56.892.
 \tag{19}$$

Analogously, we can see that

$$\begin{matrix}
 & v_1 & v_2 & v_3 & v_4 & v_5 & v_6 & v_7 \\
 \begin{matrix} v_1 \\ v_2 \\ v_3 \\ v_4 \\ v_5 \\ v_6 \\ v_7 \end{matrix} & \begin{pmatrix} 0 & 7 & 0 & 0 & 0 & 0 & 0 \\ 7 & 0 & 9 & 11 & 9 & 19 & 9 \\ 0 & 9 & 0 & 7 & 0 & 0 & 0 \\ 0 & 11 & 7 & 0 & 8 & 9 & 8 \\ 0 & 9 & 0 & 8 & 0 & 7 & 0 \\ 0 & 10 & 0 & 9 & 7 & 0 & 7 \\ 0 & 9 & 0 & 8 & 0 & 7 & 0 \end{pmatrix} & & & & & & 
 \end{matrix}
 \tag{20}$$

Therefore, the Zagreb spectrum of  $A_7$  is as follows:

$$\text{Spec}_{A_z}(A_7) = \begin{pmatrix} 34.501 & -17.57 & 3.189 & -11.737 & 1.094 & -9.477 & 0 \\ 1 & 1 & 1 & 1 & 1 & 1 & 1 \end{pmatrix}.
 \tag{21}$$

Hence, by the definition of the Zagreb energy, we have

$$\text{ZE}(A_7) = 77.568.
 \tag{22}$$

By definition and Equalities (19) and (22), we deduce that  $A_6$  and  $A_7$  are non-hyperenergetic.

*2.1. Some Classes of Zagreb Hyperenergetic and Zagreb Equienergetic Graphs.* This section contributes some results towards Zagreb hyperenergetic and Zagreb equienergetic graphs.

**Theorem 5.** For a regular graph  $G$ , the splitting graph  $S'(G)$  is a Zagreb hyperenergetic graph.

*Proof.* Let  $G$  be a graph with vertices  $v_1, v_2, v_3, \dots, v_p$ . Then, the Zagreb matrix is as follows:

$$\begin{matrix}
 & v_1 & v_2 & v_3 & \dots & v_p \\
 \begin{matrix} v_1 \\ v_2 \\ v_3 \\ \vdots \\ v_p \end{matrix} & \begin{pmatrix} 0 & d_1 + d_2 & d_1 + d_3 & \dots & d_1 + d_p \\ d_2 + d_1 & 0 & d_2 + d_3 & \dots & d_2 + d_p \\ d_3 + d_1 & d_3 + d_2 & 0 & \dots & d_3 + d_p \\ \vdots & \vdots & \vdots & \ddots & \vdots \\ d_p + d_1 & d_p + d_2 & d_p + d_3 & \dots & 0 \end{pmatrix} & & & & 
 \end{matrix}
 \tag{23}$$

Let  $v'_1, v'_2, v'_3, \dots, v'_p$  be the vertices added in  $G$  corresponding to  $v_1, v_2, v_3, \dots, v_p$  to obtain  $S'(G)$  such that  $N(v_i) = N(v'_i)$ . Note that the degree of  $v'_i$  is  $d_i$ . Then, the

Zagreb matrix of  $S'(G)$  can be written as a block matrix as follows:

$$A_z(S'(G)) = \begin{bmatrix} 2A_z(G) & \frac{3}{2}A_z(G) \\ \frac{3}{2}A_z(G) & 0 \end{bmatrix} \quad (24)$$

or

$$A_z(S'(G)) = \begin{bmatrix} 2 & \frac{3}{2} \\ \frac{3}{2} & 0 \end{bmatrix} \otimes A_z(G). \quad (25)$$

Therefore, the Zagreb spectrum of  $S'(G)$  is as follows

$$\text{Spec}_{A_z}(S'(G)) = \begin{pmatrix} \left(\frac{2-\sqrt{13}}{2}\right)z_i & \left(\frac{2+\sqrt{13}}{2}\right)z_i \\ p & p \end{pmatrix}, \quad (26)$$

where  $z_i$  for  $i = 1, 2, 3, \dots, p$  are the eigenvalues of  $A_z(G)$  and  $2 \pm \sqrt{13}/2$  are the eigenvalues of  $\begin{bmatrix} 2 & 3/2 \\ 3/2 & 0 \end{bmatrix}$ . Therefore, by the definition of the Zagreb energy, we can write

$$\begin{aligned} \text{ZE}(S'(G)) &= \sum_{i=1}^p \left| \left(\frac{2-\sqrt{13}}{2}\right)z_i \right| \\ &= \sum_{i=1}^p |z_i| \left( \frac{2-\sqrt{13}}{2} + \frac{2+\sqrt{13}}{2} \right) \\ &= 2\text{ZE}(G). \end{aligned} \quad (27)$$

Hence, we have

$$\text{ZE}(S'(G)) = 2\text{ZE}(G). \quad (28)$$

Equality (28) gives the desired result.  $\square$

**Theorem 6.** For  $n \geq 3$ ,  $\text{ZE}(K_n) = \text{ZE}(K_{n-1,n-1})$ .

*Proof.* Consider the complete graph  $K_n$  and the complete bipartite graph  $K_{n-1,n-1}$  for  $n \geq 3$ . The Zagreb spectrum of  $K_n$  is

$$\text{Spec}_{A_z}(K_n) = \begin{pmatrix} 2(n-1)^2 & -2(n-1) \\ 1 & n-1 \end{pmatrix}. \quad (29)$$

Therefore, by the definition of Zagreb energy, we have

$$\text{ZE}(K_n) = 2(n-1)^2 + |-2(n-1)|(n-1) = 4(n-1)^2. \quad (30)$$

On the other hand, the Zagreb spectrum of  $K_{n-1,n-1}$  is

$$\text{Spec}_{A_z}(K_{n-1,n-1}) = \begin{pmatrix} 0 & 2(n-1)^2 & 2(n-1)(1-n) \\ 2n-4 & 1 & 1 \end{pmatrix}. \quad (31)$$

By the definition of Zagreb energy, we can write

$$\text{ZE}(K_{n-1,n-1}) = 2(n-1)^2 + |2(1-n)|(n-1) = 4(n-1)^2. \quad (32)$$

Thus, from Equalities (30) and (32), the required result follows.  $\square$

**Theorem 7.** For  $a \geq 3$ ,  $\text{ZE}(K_{2a-1}) = \text{ZE}(CP(a))$ .

*Proof.* The Zagreb spectrum of the complete graph  $K_{2a-1}$  is

$$\text{Spec}_{A_z}(K_{2a-1}) = \begin{pmatrix} 8(a-1)^2 & -4(a-1) \\ 1 & 2(a-1) \end{pmatrix}. \quad (33)$$

Also, the Zagreb spectrum of the cocktail party graph  $CP(a)$  is

$$\text{Spec}_{A_z}(CP(a)) = \begin{pmatrix} -8(a-1) & 8(a-1)^2 \\ (a-1) & 1 \end{pmatrix}. \quad (34)$$

Therefore,

$$\text{ZE}(K_{2a-1}) = 8(a-1)^2 + |8(1-a)|(a-1) = 16(a-1)^2, \quad (35)$$

$$\text{ZE}(CP(a)) = 8(a-1)^2 + |-8(a-1)|(a-1) = 16(a-1)^2. \quad (36)$$

Now, Equalities (35) and (36) lead to the result.  $\square$

### Data Availability

The data used to support the findings of this study are included within the article.

### Conflicts of Interest

The authors declare that they have no conflicts of interest.

### References

- [1] A. Ali, "A survey of antiregular graphs," *Contributions to Discrete Mathematics*, vol. 1, pp. 67–79, 2020.
- [2] V. Brankov, D. Stevanovic, and I. Gutman, "Equienergetic chemical trees," *Journal of the Serbian Chemical Society*, vol. 69, no. 7, pp. 549–554, 2004.
- [3] K. C. Das, "On the Zagreb energy and Zagreb Estrada index of graphs," *MATCH Communications in Mathematical and in Computer*, vol. 82, pp. 529–542, 2019.
- [4] S. Gong, X. Li, G. Xu, I. Gutman, and B. Furtula, "Border-energetic graphs," *MATCH Communications in Mathematical and in Computer*, vol. 74, pp. 321–332, 2015.
- [5] I. Gutman, "The energy of a graph," *Ber. Math. Stat. Sect. Forschungs. Graz*, vol. 103, pp. 1–22, 1978.



- [6] I. Gutman, "Hyperenergetic molecular graphs," *Journal of the Serbian Chemical Society*, vol. 64, pp. 199–205, 1999.
- [7] I. Gutman and N. Trinajstić, "Graph theory and molecular orbitals. Total  $\pi$ -electron energy of alternant hydrocarbons $\pi$ ," *Chemical Physics Letters*, vol. 17, no. 4, pp. 535–538, 1972.
- [8] I. Gutman and O. E. Polansky, *Mathematical Concepts in Organic Chemistry*, Springer, Berlin, 1986.
- [9] I. Gutman, "The energy of a graph: old and new results," in *Algebraic Combinatorics and Applications*, A. Betten, A. Kohnert, R. Laue, and A. Wassermann, Eds., Springer-Verlag, Berlin, Germany, pp. 196–211, 2001.
- [10] N. J. Rad, A. Jahanbani, and I. Gutman, "Zagreb energy and Zagreb estrada index of graphs," *MATCH Communications in Mathematical and in Computer*, vol. 79, pp. 371–386, 2018.
- [11] A. Jahanbani, "Lower bounds for the energy of graphs," *AKCE International Journal of Graphs and Combinatorics*, vol. 15, no. 1, pp. 88–96, 2018.
- [12] A. Jahanbani, "Upper bounds for the energy of graphs," *MATCH Communications in Mathematical and in Computer*, vol. 79, pp. 275–286, 2018.
- [13] A. Jahanbani, "Some new lower bounds for energy of graphs," *Applied Mathematics and Computation*, vol. 296, pp. 233–238, 2017.
- [14] A. Jahanbani and J. R. Zambrano, "Koolen-Moulton-type upper bounds on the energy of a graph," *MATCH Communications in Mathematical and in Computer*, vol. 83, pp. 497–518, 2020.
- [15] A. Jahanbani, R. Khoeilari, and H. Shooshtari, "On the Zagreb matrix and Zagreb energy," *Asian-European Journal of Mathematics*, In press.
- [16] B. R. Rakshith, "On Zagreb energy and edge-Zagreb energy," *Communications in Combinatorics and Optimization*, vol. 6, pp. 155–169, 2021.
- [17] E. Munarini, "Characteristic, admittance and matching polynomials of an antiregular graph," *Applicable Analysis and Discrete Mathematics*, vol. 3, no. 1, pp. 157–176, 2009.

## Research Article

# Grid Partition Variable Step Alpha Shapes Algorithm

Zhenxiu Liao , Jun Liu, Guodong Shi, and Junxia Meng

*School of Civil Engineering, Anhui Jianzhu University, Hefei, Anhui Province 230601, China*

Correspondence should be addressed to Zhenxiu Liao; [liao@ahjzu.edu.cn](mailto:liao@ahjzu.edu.cn)

Received 26 March 2021; Accepted 3 May 2021; Published 18 May 2021

Academic Editor: Sakander Hayat

Copyright © 2021 Zhenxiu Liao et al. This is an open access article distributed under the Creative Commons Attribution License, which permits unrestricted use, distribution, and reproduction in any medium, provided the original work is properly cited.

On the basis of Alpha Shapes boundary extraction algorithm for discrete point set, a grid partition variable step Alpha Shapes algorithm is proposed to deal with the shortcomings of the original Alpha Shapes algorithm in the processing of nonuniform distributed point set and multiconcave point set. Firstly, the grid partition and row-column index table are established for the point set, and the point set of boundary grid partition is quickly extracted. Then, the average distance of the  $k$ -nearest neighbors of the point is calculated as the value of  $\alpha$ . For the point set of boundary grid partition extracted in the previous step, Alpha Shapes algorithm is used to quickly construct the point set boundary. The proposed algorithm is verified by experiments of simulated point set and measured point set, and it has high execution efficiency. Compared with similar algorithms, the larger the number of point sets is, the more obvious the execution efficiency is.

## 1. Introduction

From the traditional electronic total station, handheld satellite positioning collector, to mobile (vehicle-mounted/airborne) three-dimensional laser radar, modern spatial information acquisition technology has entered the era of massive data at the GB and TB level. How to store, process, and express massive data efficiently has become a new challenge to the related fields such as computer information technology (IT), computer-aided design/manufacturing (CAD/CAM), geographic information (GIS) and remote sensing (RS), and even building information modeling (BIM) [1–4]. The boundary information of the discrete point set is composed of discrete points representing the original contour features of the measured object. It is a basic and important technical work in spatial data processing to quickly and efficiently construct the boundary information from the discrete point set. Two-dimensional point set boundary information is the basic data of land area statistics, road earthwork calculation, and other engineering applications [5, 6]. Three-dimensional point set boundary information plays an important role in the process of 3D model reconstruction [7–10].

To construct the boundary information of point set, it is necessary to study the shape of point set composed of two-dimensional or three-dimensional discrete points. From the

literature reading analysis, it is known that, since the 1970s, scholars and experts at home and abroad have successively carried out research work in this field and got good research results. Graham [11] proposed a scanning algorithm for determining the convex hull of a planar set, but the algorithm is only effective for convex hull boundary and cannot deal with the case of concave boundary; Jarvis [12] proposed a numerical method based on two-dimensional convex hull point set to express the contour geometry of two-dimensional point set, but again it can only deal with convex hull boundary; Sampath and Shan [13] improved R. A. Jarvis's algorithm, which can be used to deal with two-dimensional discrete point concave boundary, but the algorithm is not as efficient as the new algorithm proposed by subsequent researchers. In the 1980s, Edelsbrunner et al. [14] gave a rigorous mathematical definition on the "shape of a set of points" based on two-dimensional plane point set and proposed a point set boundary construction algorithm called Alpha Shapes (AS). Based on rigorous mathematical definition, this algorithm can deal with complex discrete point set boundaries including convex hull, concave points, and holes. Ten years later, H Edelsbrunner extended the AS algorithm [15] to be applied to three-dimensional point set surface reconstruction, thus greatly expanding the scope of the application of the algorithm. Jochem et al. [16] used the

AS algorithm to automatically extract the building roof from airborne LiDAR point cloud; Shen et al. [17] and Li et al. [18] used the improved AS algorithm to extract building contour; Wang et al. [19] used the improved algorithm to extract edges from massive point cloud data in mountainous areas; Li and Li [20] used the improved algorithm to reconstruct the 3D surface model from the point cloud data of handicrafts; Sun et al. [5] applied the improved algorithm to extract the plot boundary from the trajectory data points collected by the vehicle-mounted satellite navigation receiver of agricultural machinery and then finely measured the farmland area; Li et al. [21] applied the algorithm to construct the tree crown three-dimensional model; Fu et al. [22] applied the algorithm to construct a three-dimensional model from jujube tree point cloud.

## 2. Alpha Shapes Algorithm

**2.1. Algorithm Content.** In literature [14], Edelsbrunner gave a rigorous mathematical definition of the geometric shape of a two-dimensional plane point set, namely,  $\alpha$ -Shape. Let  $S$  be a two-dimensional planar point set, and give any parameter  $\alpha$ ; the polygon  $\partial S$  extracted from  $S$  by the AS algorithm rule is  $\alpha$ -Shape, which can be used to express the boundary contour of the point set, and its precision is determined by the value of the parameter  $\alpha$ .

Simplified AS algorithm steps are as follows:

Step 1: Input two-dimensional point set  $S = \{P_1, P_2, \dots, P_n\}$ , and calculate the point set average point spacing  $d$  as the value of  $\alpha$ .

Step 2: Traverse  $S$ , take  $P_i$  ( $i \leq n$ ) as the center of the circle, and take the length not greater than  $2\alpha$  as the radius  $R$  to construct the search circle, and search the point set  $S_i = \{P_1^i, P_2^i, \dots, P_m^i\}$  ( $m \leq n$ ),  $S_i \subseteq S$ .

Step 3: Traverse  $S_i$  and construct  $\alpha$ -shape criterion to determine whether line segment  $P_i P_j$  ( $j \leq m$ ) is a boundary edge. If so, add it to  $\alpha$ -shape set and return to Step 2. If not, proceed to the next point until the traversal is complete and return to Step 2.

Step 4: After traversing  $S$  is complete, output  $\alpha$ -Shape collection.

The simplified flow chart of Alpha Shapes algorithm is shown in Figure 1.

Among these steps, the third step, “construct  $\alpha$ -shape criterion,” is the core step of the algorithm, and the rules are as follows.

Draw a circle with radius  $R = \alpha$  through two points  $P_i, P_j$  (as  $P_1$  and  $P_2$  in Figure 2). If no point in point set  $S$  falls into the circle, the line segment  $P_i P_j$  is the boundary line; otherwise, it is the nonboundary line. The judgment method of whether a point in the point set  $S$  falls into the circle is shown in Figure 2. According to formula (1), the center point  $P_c$  is calculated, the point set  $S$  is traversed, and the distance  $d_k$  between each point (as  $P_k$  in Figure 2) and the center point  $P_c$  is calculated. If  $d_k < \alpha$ , it indicates that a point falls into the circle.

The formula for calculating the coordinates of the center point  $P_c$  can be obtained via the “distance intersection algorithm” in Geomatics [23]:

$$\begin{cases} x_c = x_1 + 0.5(x_2 - x_1) + H(y_2 - y_1) \\ y_c = y_1 + 0.5(y_2 - y_1) + H(x_1 - x_2) \end{cases} \quad (1)$$

In the formula,  $H = \pm \sqrt{(\alpha/d)^2 - (1/4)}$ ,  $d = \sqrt{(x_2 - x_1)^2 + (y_2 - y_1)^2}$ .

The process of constructing point set boundary by AS algorithm can be understood as a circle with radius  $R = \alpha$  rolling outside the edge of the point set  $S$ . When the value of  $\alpha$  is appropriate, the trajectory that the circle rolls through is the boundary of point set  $S$ , as shown in Figure 3. At the range of  $\alpha \in (0, \infty)$ , when  $\alpha \rightarrow 0$ , all points in  $S$  are boundary points; when  $\alpha \rightarrow \infty$ , the convex hull of  $S$  is the boundary; when the value of  $\alpha$  is reasonable and the distribution of points in  $S$  is uniform, the AS algorithm can construct the boundary of point set  $S$  in an ideal way. If the value of  $\alpha$  is too large, the turning angle of the lines connecting the boundary points would be replaced by a larger blunt angle, resulting in a blunted effect at the corner, as shown in the shaded area in Figure 3.

**2.2. Algorithm Shortcomings.** Compared with the previous similar algorithms, AS algorithm has the advantages of rigorous mathematical definition, the ability to deal with complex two-dimensional point set boundary and three-dimensional point set surface, and a wide range of applications, but there are also shortcomings. The only parameter  $\alpha$  in the algorithm determines the fineness of the point set shape, which needs to be manually input and adjusted according to different scenarios. At the same time, the unicity of parameter  $\alpha$  determines that the algorithm is very suitable for processing convex hull point sets with uniform distribution density but cannot ideally deal with the two following scenarios:

- (1) For point sets with nonuniform density distribution per unit area, such as the discrete points at the farmland boundary collected by handheld or vehicle-mounted satellite navigation receiver, and the three-dimensional laser point cloud of bare tree branches, the processing effect is not very ideal.
- (2) For the point set composed of many concaves, such as complex buildings, roads, water flow, and other linear features, the processing effect in the concave corner area is not perfect. Therefore, it is necessary to improve and perfect the algorithm.

When applying AS algorithm to extracting building contour, it is found in [17] that if the value of  $\alpha$  is too small, the building contour point set will be very fragmented; if it is too large, the concave corner area of the building will be distorted due to being excessively blunted (Figure 3). According to different application scenarios, literatures [5, 18] put forward an improved algorithm called “dual threshold Alpha Shapes,” aiming at the specific problems caused by the excessively single value of  $\alpha$ . Based on the AS

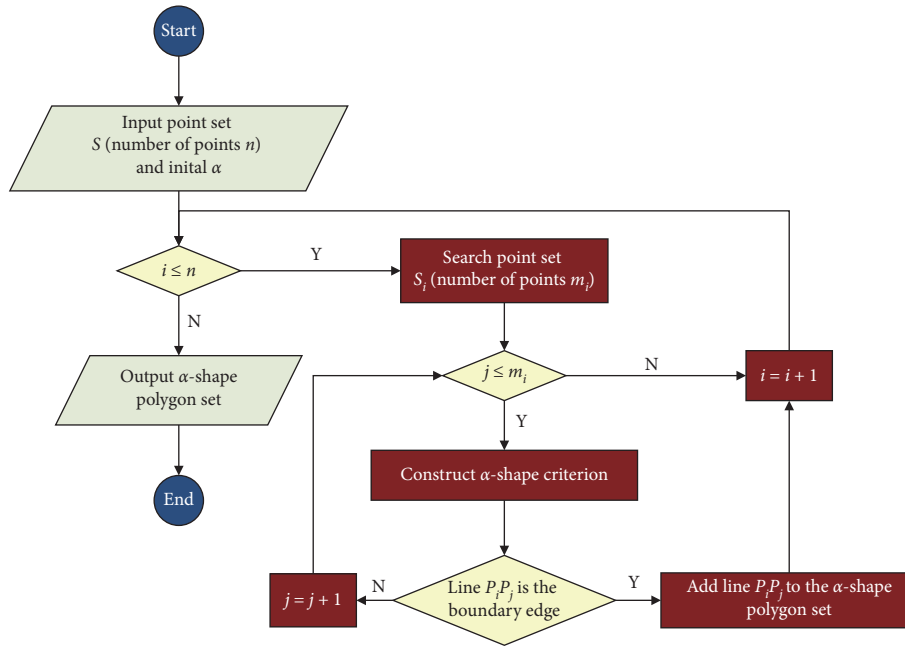


FIGURE 1: Simplified flow chart of Alpha Shapes algorithm.

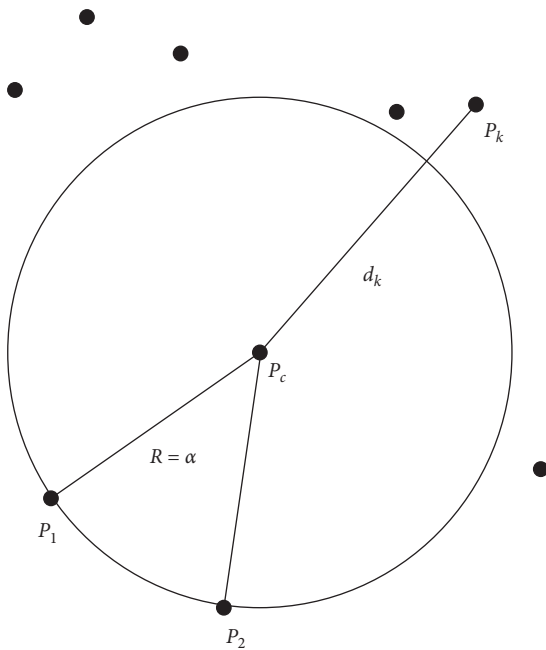


FIGURE 2: Sketch map of  $\alpha$ -Shapes criterion.

algorithm, literature [19] used the grid detection method to quickly filter nonboundary points and proposed an algorithm for fast extracting edges from massive point clouds. However, the  $\alpha$  value of the algorithm is fixed, which still cannot overcome the specific problems caused by the single value of  $\alpha$ . Literature [20] proposed a surface reconstruction algorithm using “self-adaptive step Alpha Shapes algorithm,” which can automatically calculate different values according to the point density of different regions of the point set and better deal with the problem caused by

nonuniform point distribution. However, this algorithm requires that every point in the point set has the same status to participate in the search calculation, and there is still room for the improvement of the execution efficiency. Based on the algorithms proposed in literatures [14, 15], this paper puts forward a grid partition variable step Alpha Shapes (GPVAS) algorithm, which has higher computational efficiency while solving the problems caused by nonuniform distribution of point sets.

### 3. Grid Partition Variable Step Alpha Shapes Algorithm

#### 3.1. Algorithm Overview

The main improvements of the GPVAS algorithm are as follows:

- (1) The point set  $S$  is partitioned, the nonboundary grid area is removed by fast filtering, and the boundary grid point set  $S_G$  is extracted.
- (2) For points in point set  $S_G$ , within the range of point set  $S$ , variable step Alpha Shapes (VAS) algorithm [20] is applied to construct the boundary shape of point set  $S$ . Figure 4 shows the simplified flow chart of GPVAS algorithm.

3.2. *Extracting Boundary Grid Partition Point Set.* This step consists of two steps: “grid partition” and “extracting point set of boundary grid partition.” The steps are as follows.

3.2.1. *Grid Partitions.* The envelop rectangle  $G$  of point set  $S$  is constructed, and its inflexion points are  $G_1(X_{\min}, Y_{\min})$ ,  $G_2(X_{\min}, Y_{\max})$ ,  $G_3(X_{\max}, Y_{\max})$  and  $G_4(X_{\max}, Y_{\min})$ , respectively.

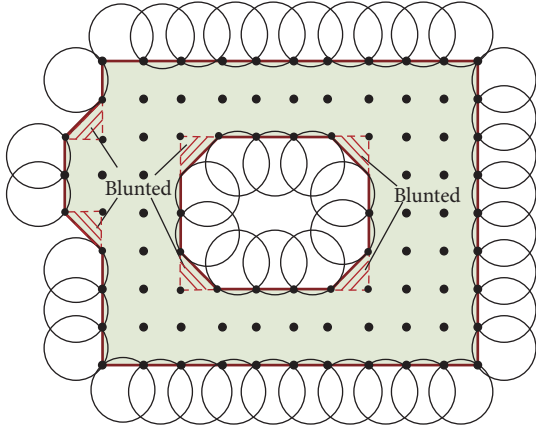


FIGURE 3: Building boundary of point set by Alpha Shapes algorithm.

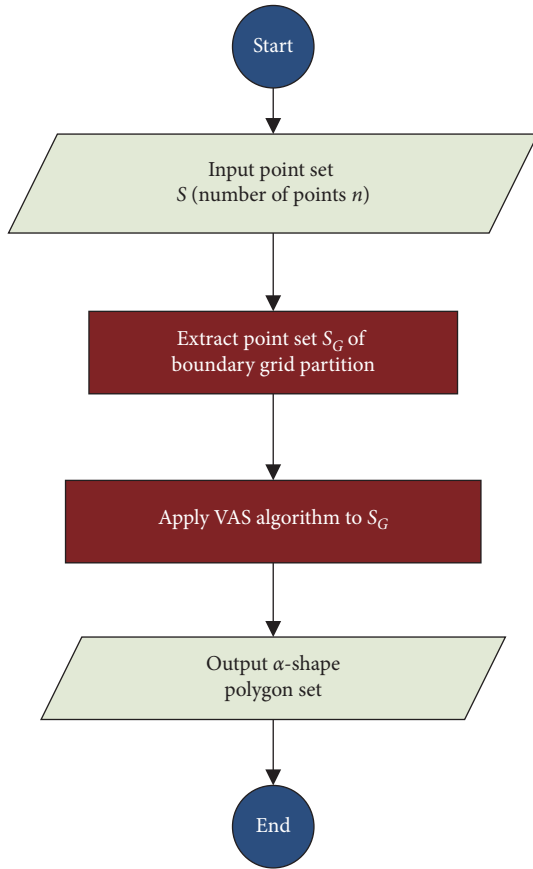


FIGURE 4: Simplified flow chart of GPVAS algorithm.

The envelop rectangle  $G$  is divided into  $M \times N$  grid partition set  $G_0$  by the square grid with side length of  $d$  (usually 2-3 times the average point spacing of point set  $S$ ), where

$$\begin{cases} M = \left\lceil \frac{Y_{\max} - Y_{\min}}{a} \right\rceil + 1, \\ N = \left\lceil \frac{X_{\max} - X_{\min}}{a} \right\rceil + 1, \end{cases} \quad (2)$$

where  $M$  is the number of rows,  $N$  is the number of columns, and the symbol  $\lceil \cdot \rceil$  is the integer of real numbers.

3.2.2. *Extracting Point Set of Boundary Grid Partition.* A row-column index table is established for the point set  $S$ , and the formula for calculating the row-column index value of point  $P_i$  is as follows:

$$\begin{cases} r_i = \left\lceil \frac{Y_i - Y_{\min}}{a} \right\rceil, \\ c_i = \left\lceil \frac{X_i - X_{\min}}{a} \right\rceil, \end{cases} \quad (3)$$

where  $r_i$  is the row number in the grid partition where point  $P_i$  is located and  $c_i$  is the column number in the grid partition where point  $P_i$  is located. Thus, the mapping relationship between point and grid partition is established, as shown in Figure 5.

Traverse the grid, and quickly determine whether the grid contains a point from the row-column index table of point set  $S$ . If it contains a point, it is 1; otherwise, it is 0.

Traverse the grid, extract the point set  $G_1$  of boundary grid partition (the diagonal filling grid shown in Figure 5), and then quickly obtain the boundary grid point set  $S_G$  through the row-column index table of the point set  $S$ . The judgment rule of the boundary grid is that the boundary grid contains points, and at least one of its eight adjacent grids does not contain any point.

3.3. *Extracting Boundary Grid Partition Point Set.* Once the value of parameter  $\alpha$  in AS algorithm (i.e., the search step in constructing  $\alpha$ -shape) is set, it is constant throughout the boundary construction process, which is the reason for the unsatisfactory effect of the algorithm in dealing with the nonuniform distribution point set or point set containing concave points. Literature [20] proposed VAS algorithm and used kd-tree to calculate the average distance of  $k$ -nearest neighbors of the point as  $\alpha$  value to participate in the construction of  $\alpha$ -shape. The average distance of  $k$ -nearest neighbors of a point is the average distance between the nearest  $k$  number of points and the point in a point set. At this point, the value of  $\alpha$  is variable; when the point density is large, the  $\alpha$  value is small, which ensures the continuity of the boundary and the high  $\alpha$ -shape construction efficiency into account; when the point density is small, the  $\alpha$  value becomes larger, which can prevent boundary fragmentation caused by the excessively small  $\alpha$  value. However, in the process of calculating  $\alpha$  value and applying  $\alpha$  value to construct  $\alpha$ -shape, the VAS algorithm needs to search the entire  $S$  point set under the worst condition. The time complexity is  $O(n^3)$ , and the efficiency of the algorithm is not ideal.

The GPVAS algorithm proposed in this paper still adopts the calculation steps of VAS algorithm, first calculating the  $\alpha$  value and then applying the  $\alpha$  value to construct the  $\alpha$ -shape. The biggest improvement of GPVAS algorithm lies in the grid partition and point set row-column index table

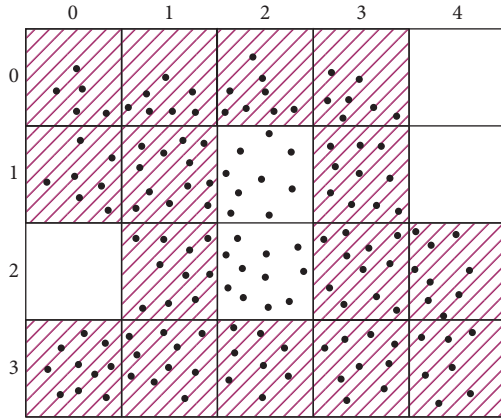


FIGURE 5: Extracting point set of boundary grid partition by GPVAS algorithm.

constructed based on the above steps. No matter whether it is calculating  $\alpha$  value or constructing  $\alpha$ -shape, it is convenient to take the grid where the target point or center point is located as the center and search layer by layer from small to large distance (as shown in Figure 6), which is equivalent to arranging the point set  $S$  in ascending sort order according to the distance value from the target point or center point. The experimental results show that the efficiency of the algorithm is significantly improved.

#### 4. Comparative Experiments

To intuitively verify the time efficiency of the algorithm, two kinds of data are designed for experimental verification based on AS algorithm, VAS algorithm and GPVAS algorithm: one is the data point set of computer numerical simulation (hereinafter referred to as the simulated point set), and the other is the data point set of engineering measurement (hereinafter referred to as the measured point set).

**4.1. Comparison of Simulated Point Sets.** The data of random point set generated randomly by circular analytic formula (4) according to the density of the upper semicircle point is 3 times that of the lower semicircle point, and the inner point of the upper and lower semicircle is generated randomly according to the uniform distribution, as shown in Figure 7.

$$S = \{(x, y) | (x - 1)^2 + (y - 1)^2 \leq 1\}. \quad (4)$$

The effective range of parameter  $k$  in the calculation of the average distance of  $k$ -nearest neighbors in VAS algorithm and GPVAS algorithm is [9, 24]. According to the experimental statistics in literature [20],  $k = 20$  is considered to be more ideal. In this paper,  $k = 20$  is also used to calculate the nearest neighbor average distance as  $\alpha$ , and  $2\alpha$  is taken as the grid edge length. The experimental laptop is configured as Intel(R) Core(TM) i7-10750H CPU@2.60 GHz, 16 G memory, and 64-bit Windows 10 operating system; experimental algorithm program is based on Microsoft Visual Studio 2010 IDE, C# language; the simulation point set is

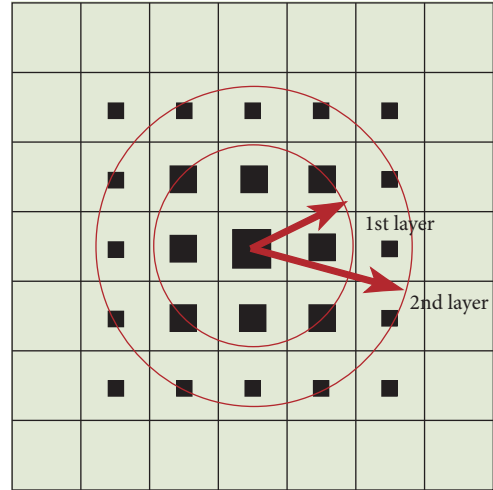


FIGURE 6: Sketch map of layer-by-layer search by GPVAS algorithm.

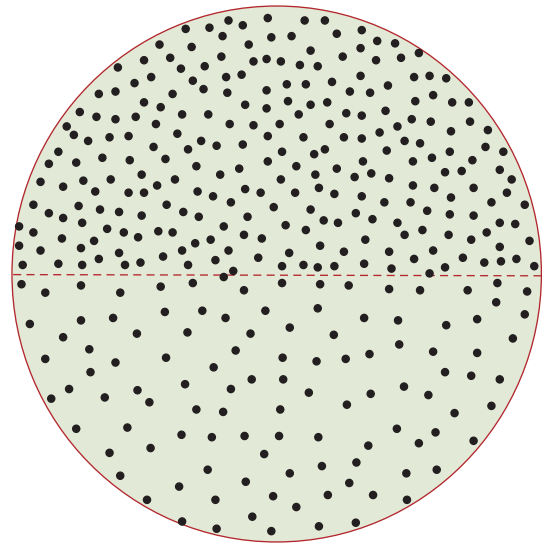


FIGURE 7: Circular nonuniform simulation point set.

divided into four control groups (1000, 5000, 10000, and 20000) according to the number of points. The experimental results are shown in Table 1.

According to the comparison of experimental results in Table 1, when the number of point sets is small, the efficiency of VAS algorithm and GPVAS algorithm is lower than that of AS algorithm. The order of efficiency is as follows: AS > VAS > GPVAS. This is because the VAS algorithm and GPVAS algorithm need to spend some time to dynamically calculate the average distance of  $k$ -nearest neighbors as  $\alpha$  value before each execution of the  $\alpha$ -shape criterion to filter the boundary points. In addition, GPVAS also needs to establish a grid partition and row-column index table for the point set. As the number of points increases, the execution efficiency of VAS algorithm and GPVAS algorithm begins to improve. Compared with AS algorithm, the execution efficiency of VAS algorithm can be improved by 20%~30%. When the number of points increases, the efficiency of

TABLE 1: Comparison table of experimental results of different algorithms (simulated point set).

Algorithm	Number of points	$\alpha$ value (min/max)	Execution time (ms)
AS algorithm	1000	0.360	245
	5000	0.072	5128
	10,000	0.036	26124
	20,000	0.018	128356
VAS algorithm	1000	0.240/0.781	326
	5000	0.048/0.156	4289
	10,000	0.024/0.075	19356
	20,000	0.012/0.039	96786
GPVAS algorithm	1000	0.240/0.781	861
	5000	0.048/0.156	3243
	10,000	0.024/0.075	6934
	20,000	0.012/0.039	10189

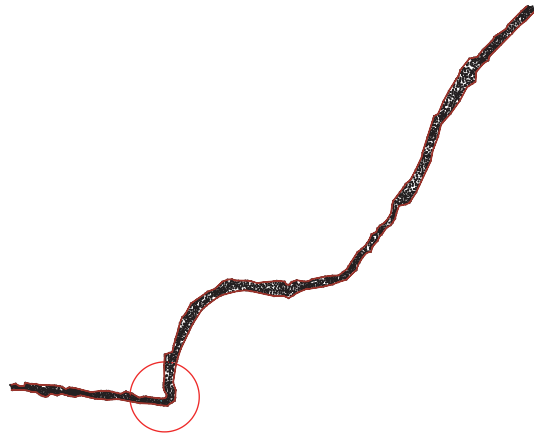


FIGURE 8: Boundary of strip terrain points on mountain highway.

TABLE 2: Comparison table of experimental results of different algorithms (measured point set).

Algorithm	$\alpha$ value (min/max)	Execution time (ms)
AS algorithm	10 m	16287
AS algorithm	30 m	21458
VAS algorithm	8.6 m/41.2 m	11356
GPVAS algorithm	8.6 m/41.2 m	7127

GPVAS algorithm increases rapidly. When the number of points is 20,000, the execution efficiency increases by more than 10 times. The order of the execution efficiency of the algorithm is  $GPVAS > VAS > AS$ . This is because the time-consuming distance budget time complexity of the AS algorithm is  $O(n^3)$ , and the GPVAS algorithm is able to construct the grid partition and row-column index table of the point set with negligible extra storage space before the  $\alpha$ -shape criterion filtering the boundary point set with the time complexity of  $O(n^2)$ , so as to quickly extract the boundary point set. Compared with the increase in the total number of point sets, the increase in the number of boundary point sets constructed by grid partitioning is very limited.

#### 4.2. Comparative Study of Strip Terrain Points on Mountain Highway.

In order to verify the effectiveness of the

algorithm applied to the measured point set, this paper selects the highway strip terrain data (Figure 8), which is composed of more than 8000 GPS measuring points with a total length of about 17 km in the mountainous area of southern Anhui, and the average distance between the measuring points is 28.513 m. There are many curves in the strip terrain data in mountainous areas, dense collection points in undulating sections, and sparse collection points in flat sections. The density distribution of point set is not uniform, and there are many concave areas, so it is an ideal experimental data to verify the algorithm. The experimental results are shown in Table 2; Figures 8 and 9(a) to Figure 9(c) (Figures 9(a)–9(c)) are the enlarged images of the boundaries extracted by different algorithms at highway curve in Figure 8.

The experimental results show that all the three algorithms can be used to construct the boundary of experimental data, and the construction efficiency is

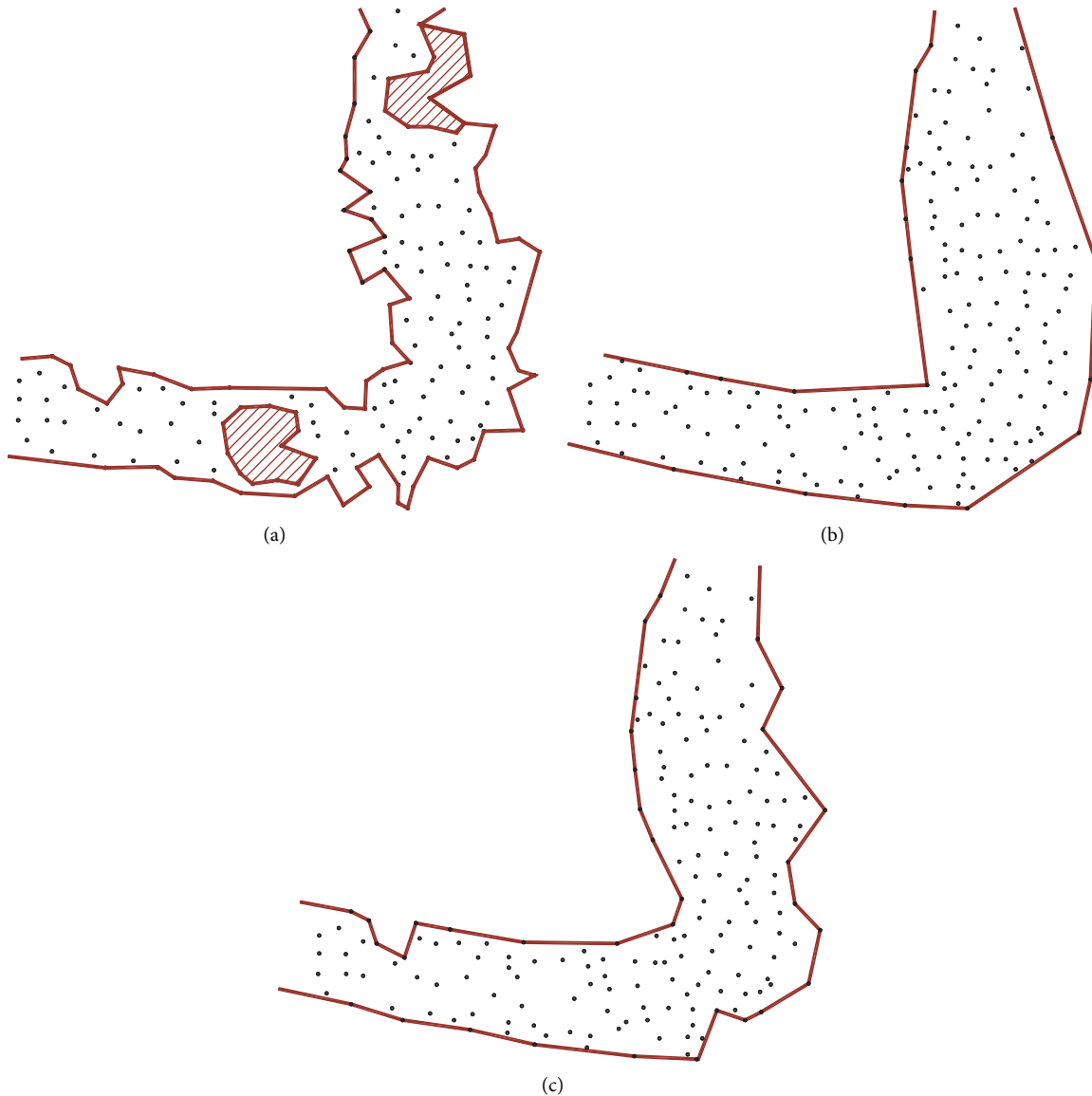


FIGURE 9: Boundaries extracted by different algorithms at highway curve. (a) AS algorithm,  $\alpha = 10$  m. (b) AS algorithm,  $\alpha = 30$  m. (c) VAS, GPVAS algorithm,  $\alpha_{\min} = 8.6$  m,  $\alpha_{\max} = 41.2$  m.

GPVAS > VAS > AS. Regarding the construction results, GPVAS algorithm and VAS algorithm are almost the same with good effect (Figure 9(c)), while the AS algorithm is greatly affected by the set value of  $\alpha$ . When the value of  $\alpha$  is small (10 m in the experiment), the boundary is relatively fine, and it is easy to form the boundary of holes in the area of sparse points (Figure 9(a), where the diagonal filling area is determined as the hole). When the value of  $\alpha$  is large (30 m in the experiment), the boundary is relatively crude (Figure 9(b)), and the algorithm execution efficiency is lower than that when the value of  $\alpha$  is small.

## 5. Conclusions

Based on the Alpha Shapes algorithm for extracting the boundary of discrete point sets, this paper analyzes and

summarizes the previous research work. In view of the shortcomings of Alpha Shapes algorithm in processing non-uniform distributed point sets and multiconcave point sets, this paper proposes the grid partition variable step Alpha Shapes algorithm, which is used to quickly construct the boundary of point sets. This algorithm has two main advantages:

- (1) Establish grid partition and row-column index table for point set, quickly filter nonboundary point partition, and extract boundary grid partition point set involved in subsequent  $\alpha$ -shape construction; compared with the increase in the total number of point sets, the increase in the number of point sets of boundary grid partition constructed by grid partition is very limited, which is the main reason why GPVAS algorithm can effectively deal with a large number of point sets.



- (2) The average distance of  $k$ -nearest neighbors of the point calculated by kd-tree is used as the  $\alpha$  value. In the region with dense point distribution, the  $\alpha$  value is small, and, in the region with sparse point distribution, the  $\alpha$  value is large, so that the algorithm can well deal with the regional boundary with nonuniform point distribution.

The algorithm is verified by simulated point set and measured point set, and the execution efficiency of the algorithm is very high. Compared with similar algorithms, the larger the number of point sets is, the more obvious the efficiency improvement is. As an alternative algorithm, this algorithm has been effectively verified in engineering scenarios such as land area statistics and road earthwork calculation. In the field of 3D point cloud surface reconstruction with broader application scenarios, this algorithm has not been verified, which is also the follow-up research direction of this paper.

### Data Availability

The data used to support the findings of this research were generated from experiments.

### Conflicts of Interest

The authors declare that there are no conflicts of interest regarding the publication of this paper.

### Acknowledgments

This research was funded by the National Natural Science Foundation of China (41906168), Natural Science Research Project of Anhui Education Department (KJ2018JD04), and AHJZU-Anhui Huali Construction Co., Ltd., Joint Research Project (HYB20190152).

### References

- [1] B. Xiong, M. Jancosek, S. O. Elberink, and G. Vosselman, "Flexible building primitives for 3D building modeling," *ISPRS Journal of Photogrammetry and Remote Sensing*, vol. 101, pp. 275–290, 2015.
- [2] B. Yang, R. Huang, Z. Dong, Y. Zang, and J. Li, "Two-step adaptive extraction method for ground points and breaklines from lidar point clouds," *ISPRS Journal of Photogrammetry and Remote Sensing*, vol. 119, pp. 373–389, 2016.
- [3] B. S. Yang, W. X. Dai, Z. Dong, and Y. Liu, "Automatic forest mapping at individual tree levels from terrestrial laser scanning point clouds with a hierarchical minimum cut method," *Remote Sensing*, vol. 8, no. 5, 372 pages, 2016.
- [4] B. S. Yang, F. X. Liang, and R. G. Huang, "Progress, challenges and perspectives of 3D lidar point cloud processing," *Acta Geodaetica et Cartographica Sinica*, vol. 46, no. 10, pp. 1509–1516, 2017.
- [5] Y. Z. Sun, J. Li, B. Liu et al., "Measurement of agricultural machinery operation area based on improved alpha shapes algorithm," *Journal of Chinese Agricultural Mechanization*, vol. 40, no. 8, pp. 144–148, 2019.
- [6] Z. X. Liao and D. L. Wang, "Research on DTM TIN generation algorithm considering border restriction," *Journal of Hefei University of Technology (Natural Science Edition)*, vol. 34, no. 9, pp. 1381–1384, 2011.
- [7] W. T. Freeman, T. R. Jones, and E. C. Pasztor, "Example-based super-resolution," *IEEE Computer Graphics and Applications*, vol. 22, no. 2, pp. 56–65, 2002.
- [8] X. Xu and K. Harada, "Automatic surface reconstruction with alpha-shape method," *The Visual Computer*, vol. 19, no. 7–8, pp. 431–443, 2003.
- [9] S. N. Karl and Q. N. Truong, "Image super-resolution using support vector regression," *IEEE Transactions on Image Processing*, vol. 16, no. 6, pp. 1596–1610, 2007.
- [10] H. Ganapathy, P. Ramu, and R. Muthuganapathy, "Alpha shape based design space decomposition for island failure regions in reliability based design," *Structural and Multidisciplinary Optimization*, vol. 52, no. 1, pp. 121–136, 2015.
- [11] R. Graham, "An efficient algorithm for determining the convex hull of a planar set," *Information Processing Letters*, vol. 1, no. 1, pp. 132–133, 1972.
- [12] R. A. Jarvis, "Computing the Shape Hull of Points in the Plane," in *Proceedings of the IEEE Computing Society Conference on Pattern Recognition and Image Processing*, pp. 231–241, IEEE, Troy, NY, USA, 1977.
- [13] A. Sampath and J. Shan, "Building boundary tracing and regularization from airborne LiDAR point clouds," *Photogrammetric Engineering & Remote Sensing*, vol. 73, no. 7, pp. 805–812, 2007.
- [14] H. Edelsbrunner, D. Kirkpatrick, and R. Seidel, "On the shape of a set of points in the plane," *IEEE Transactions on Information Theory*, vol. 29, no. 4, pp. 551–559, 1983.
- [15] H. Edelsbrunner and E. P. Mücke, "Three-dimensional alpha shapes," *ACM Transactions on Graphics*, vol. 13, no. 1, pp. 43–72, 1994.
- [16] A. Jochem, B. Höfle, M. Rutzinger, and N. Pfeifer, "automatic roof plane detection and analysis in airborne lidar point clouds for solar potential assessment," *Sensors*, vol. 9, no. 7, pp. 5241–5262, 2009.
- [17] W. Shen, J. Li, Y. H. Chen, D. Lei, and G. X. Peng, "Algorithms study of building boundary extraction and normalization based on lidar data," *Journal of Remote Sensing*, vol. 12, no. 5, pp. 692–698, 2008.
- [18] Y. F. Li, D. B. Tan, G. Gao, and L. Rui, "Extraction of building contour from point clouds using dual threshold alpha shapes algorithm," *Journal of Yangtze River Scientific Research Institute*, vol. 33, no. 11, pp. 1–4, 2016.
- [19] Z. Y. Wang, H. C. Ma, H. G. Xu, and Y. Zhiwei, "Novel algorithm for fast extracting edges from massive point clouds," *Computer Engineering and Applications*, vol. 46, no. 36, pp. 213–215, 2010.
- [20] S. L. Li and H. J. Li, "Surface reconstruction algorithm using self-adaptive step alpha-shape," *Journal of Data Acquisition and Processing*, vol. 34, no. 3, pp. 491–499, 2019.
- [21] Q. Li, X. W. Gao, X. Y. Fei et al., "Construction of tree crown three-dimensional model of using alpha-shape algorithm," *Bulletin of Surveying and Mapping*, vol. 2018, no. 12, pp. 91–95, 2018.
- [22] Y. X. Fu, C. M. Li, J. Zhu, W. Baolong, Z. Bin, and F. Wei, "Three-dimensional model construction method and experiment of jujube tree point cloud using alpha-shape algorithm," *Transactions of the Chinese Society of Agricultural Engineering*, vol. 36, no. 22, pp. 214–221, 2020.
- [23] H. Zhang, Y. N. Wen, A. L. Liu et al., *GIS Algorithm Basis*, Science Press, Beijing, China, 2006.
- [24] H. J. Li, X. Y. Liu, X. P. Zhang, and D. Yan, "A semi-automatic 3D point cloud classification method based on the probability mixture of local shape features," *Journal of Zhejiang University: Science Edition*, vol. 44, no. 1, pp. 1–9, 2017.

## Research Article

# The Behavior of Weighted Graph's Orbit and Its Energy

Ali A. Shukur <sup>1,2</sup>, Akbar Jahanbani <sup>3</sup>, and Haider Shelash<sup>4</sup>

<sup>1</sup>Computer Technical Engineering Department, College of Technical Engineering, The Islamic University, Najaf, Iraq

<sup>2</sup>Mechanics-Mathematics Faculty, Belarusian State University, Minsk, Belarus

<sup>3</sup>Department of Mathematics, Azarbaijan Shahid Madani University, Tabriz, Iran

<sup>4</sup>Department of Mathematics, University of Kufa, Najaf, Iraq

Correspondence should be addressed to Akbar Jahanbani; akbar.jahanbani92@gmail.com

Received 29 March 2021; Revised 17 April 2021; Accepted 5 May 2021; Published 17 May 2021

Academic Editor: Andrea Semaničová-Feňovčíková

Copyright © 2021 Ali A. Shukur et al. This is an open access article distributed under the Creative Commons Attribution License, which permits unrestricted use, distribution, and reproduction in any medium, provided the original work is properly cited.

Studying the orbit of an element in a discrete dynamical system is one of the most important areas in pure and applied mathematics. It is well known that each graph contains a finite (or infinite) number of elements. In this work, we introduce a new analytical phenomenon to the weighted graphs by studying the orbit of their elements. Studying the weighted graph's orbit allows us to have a better understanding to the behaviour of the systems (graphs) during determined time and environment. Moreover, the energy of the graph's orbit is given.

## 1. Introduction

Let  $G$  be a graph of order  $N$ ,  $E(G) = \{u_1, u_2, \dots, u_N\}$  be the set of edges, and  $V(G) = \{v_1, v_2, \dots, v_N\}$  be the set of vertices. We consider connected graphs with weights. An (edge)-weighted graph  $W(G)$  is defined to be an ordered pair  $(G, f)$ , where  $G_N$  is the underlying graph of order  $N$  and

$$f: E \longrightarrow \mathbb{R}, \quad (1)$$

is the weight function, which assigns to each edge  $u \in E(G)$  a nonzero weight  $f(u)$ . Every graph can be regarded as the weighted graph with weight of each edge equal to one. Thus, weighted graphs are generalizations of graphs.

In this paper, we study the orbit of weighted graph for given initial weight-edge  $u: = u_1 = u_2 = \dots = u_N$  such as

$$\text{Orb}(G_N, f(u)) = \{u, f(u), f^2(u), \dots, f^n(u) : n \in \mathbb{N}, u \in E(G)\}, \quad (2)$$

and by  $G^n(W(G), f(u))$  we denote the system graph's orbit of order  $N$  but in short, we will use only  $G^n$ . Usually, the algebraic and topological peculiarities of graphs bring

information about it in present time, but studying graph's orbit shows how does graph behave during the time. For more details about discrete dynamical systems, we refer [1, 2].

## 2. Linear and Chaotic Behavior of Weighted Graphs

In this section, we discuss properties of the weighted graphs necessary for other discussions.

We recall basic definitions.

A metric space defined over a set of points in terms of distances in a graph defined over the  $V(G)$  is called a graph metric. The vertex set (of an undirected graph) and the distance function form a metric space, if and only if the graph is connected.

Let us assume that the function in (1) represents the distance between  $v_i$  and  $v_j$  where  $i \neq j$  such as  $f(u) = \max|\text{dist}(v_i, v_j)|$ , i.e., metric edge map over metric space. One can easily check the following statement.

**Proposition 1.** Let  $G_N$  be a connected weighted graph of order  $N$  and  $f(u)$  be a metric edge map. Then,

Case I. If  $f(u)$  is linear decreasing map, then the graph's orbit behaves like

$$G^n \longrightarrow 0 \text{ as } n \longrightarrow \infty. \quad (3)$$

In this case, we say that the graph is attracted and denote it by  $G_A^n$ .

Case II. If  $f(u)$  is linear increasing map, then the graph's orbit behaves like

$$G^n \longrightarrow \infty \text{ as } n \longrightarrow \infty. \quad (4)$$

In this case, we say that the graph is repelled and denote it by  $G_R^n$ .

*Example 1.* Let  $G \cong K_3$  and  $f(u) = (1/2)u$  with initial edges  $u: = u_1 = u_2 = u_3 = (1/2)$ . Then, the orbit of  $(K_3)^n$  is as follows:

$$\text{Orb}\left((K_3)^n, \frac{1}{2}u\right) = \left\{\frac{1}{2}, \frac{1}{4}, \frac{1}{16}, \frac{1}{64}, \frac{1}{256}, \frac{1}{1024}, n = 0, 1, 2, \dots, 5\right\}, \quad (5)$$

and the attracted graph's orbit  $(K_3)^n$  for  $n = 1, 2, \dots, 5$  is shown in Figure 1.

Similar to the above considered techniques, we will check the orbit of  $K_3$  where  $f(u) = 2u$  with initial edges:

$$\text{Orb}\left((K_3)^n, 2u\right) = \{2, 4, 16, 64, 256, 1024; n = 0, 1, 2, \dots, 5\}, \quad (6)$$

and the repelled graph's orbit of  $(K_3)^n$  for  $n = 1, 2, \dots, 5$  is shown in Figure 2.

In what follows, we will consider a special case when function (1) is a nonlinear chaotic map; here, the graph's orbit  $G^n$  shows unpredictable behavior. We say that the graph's orbit has chaotic index.

Since Lorenz discovered his nonlinear system in 1964 [3], chaos had been studied as a system with conditions. After that, chaotic maps find their way in many scientific branches.

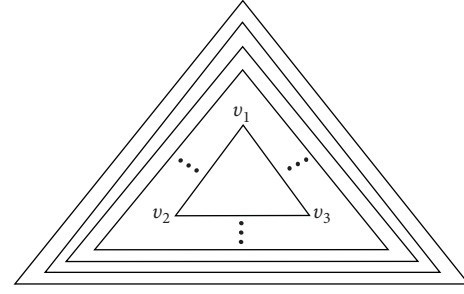


FIGURE 1: Attracted graph's orbit of  $K_3$ .

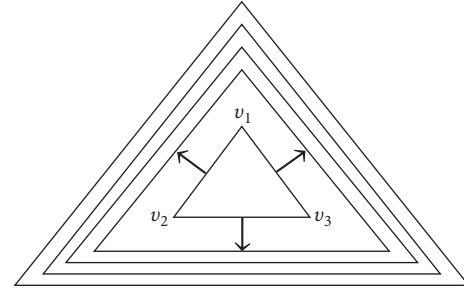


FIGURE 2: Repelled graph's orbit of  $K_3$ .

Among the chaotic maps, a logistic map is the most studied one.

The logistic map is a polynomial mapping, and it was popularized in 1976 [4] by the biologist Robert May as an analogous discrete-time demographic model. Nowadays, the logistic map is considered as the simplest nonlinear dynamical system in dimension one which is given by the following expression:

$$x_{n+1} = \mu x_n (1 - x_n), \quad (7)$$

for  $x \in (0, 1)$  and  $\mu \in [0, 4]$ . The logistic map shows a very special behavior which is complex and chaotic as one can see in Figure 3.

Coming back to our issue, we will assume that the function in (1) is logistic map such that  $u_{n+1} = f(u)$  and

$$u_{n+1} = \mu u_n (1 - u_n). \quad (8)$$

To better understand, we give the following examples.

*Example 2.* Let the parameter of (8)  $\mu = 3.56995$ . In Table 1 and Figure 4, we observed that the graph's orbit of  $(K_3)^n$  for  $n = 1, 2, \dots, 7$  with initial edges  $u: = u_1 = u_2 = u_3 = 0.25$  shows a nonlinear behaviour under the action of logistic map settled with the mentioned  $\mu$ .

*Example 3.* The Cayley's orbit graph  $\text{Cay}(D_{16}, S)$  of the Dihedral group of order 16 when

$$S = \{a, a^7, b\}, \quad (9)$$

generated by logistic map considered in Example 2, is shown in Figure 5.

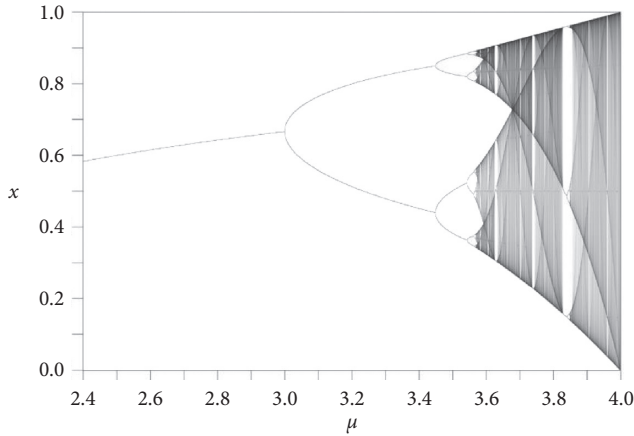


FIGURE 3: The bifurcation diagram of logistic map for  $x \in (0, 1)$  and  $\mu \in [0, 4]$ .

TABLE 1: The values of graph's orbit of  $K_3$  under the action of logistic map.

$x_0 = 0.24$	$x_1 \approx 0.6$
$x_2 \approx 0.8$	$x_3 \approx 0.5$
$x_4 \approx 0.8$	$x_5 \approx 0.5$
$x_6 \approx 0.8$	$x_7 \approx 0.5$

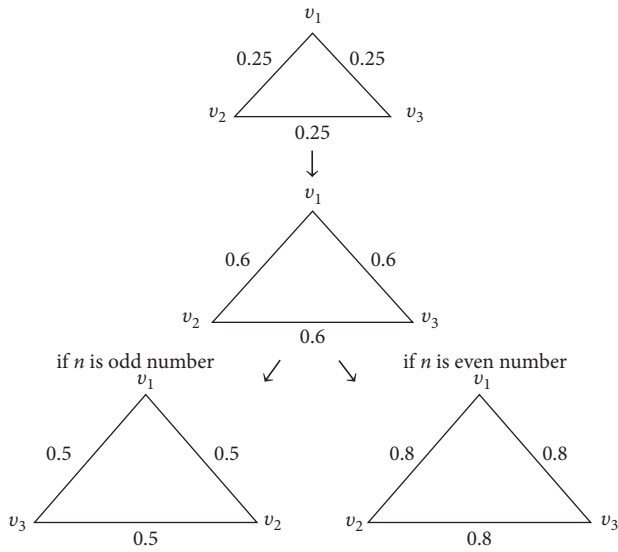


FIGURE 4: Chaotic graph's orbit of  $K_3$ .

### 3. Energy of Weighted Graph's Orbit

In this section, we are interested in studying one of the most important topological graph indices for  $G^n$  which was termed by graph energy.

Let  $W(G)$  be a graph of order  $N$ , and the adjacency matrix of a weighted graph  $W(G)$  is the  $N \times N$  matrix  $A(W(G)) = (w_{i,j})$ , where

$$w_{ij} = \begin{cases} w(v_i, v_j), & \text{if } v_i v_j \in E(W(G)), \\ 0, & \text{otherwise.} \end{cases} \quad (10)$$

The matrix  $A(W(G))$  is real symmetric, so all its eigenvalues are real. The characteristic polynomial  $\Phi(W(G), \lambda) = |\lambda I - A(W(G))|$  of the matrix  $A(W(G))$  is called the characteristic polynomial of the weighted graph  $W(G)$ . The eigenvalues of  $A(W(G))$  are called the eigenvalues of  $W(G)$ . The set of distinct eigenvalues of  $W(G)$  together with their multiplicities is called the spectrum of  $W(G)$ . The energy of weighted graph was defined in [5] as follows:

$$E(W(G)) = \sum_{i=1}^N |\lambda_i|, \quad (11)$$

where  $\lambda_1, \lambda_2, \dots, \lambda_N$  are the eigenvalues of  $A(W(G))$ .

This graph invariant in (11) has important applications in chemical graph theory and has been extensively studied. Moreover, in chemical graph theory, if the underlying molecule is a hydrocarbon, then  $G$  is a simple, unweighted graph but if the conjugated molecule contains atoms different from carbon and hydrogen (in chemistry referred to as "heteroatoms"), then  $G$  must possess pertinently weighted edges (see [6]). These weights are usually positive valued, but they may also be negative (for more details, we refer to [7–12]).

Let us denote by  $\mathbb{M}(A(G^n))$  the set of the adjacency matrices of graph's orbit  $G^n$  for  $n \in \mathbb{N}$  such that the elements of each adjacency matrix depends on the order of considered map and its nature (linear or nonlinear). Therefore, the energy of  $G^n$  is the sum of the energies which is calculated by the adjacency matrices in graph's orbit that can be given by the following formula:

$$\sum_{l=0}^n \left[ \sum_{i=0}^N |\lambda_i| \right]^l. \quad (12)$$

In particular, one can see that we have 5 different values in graph's orbit of  $(K_3)^n$  considered in Example 1; this means that we almost have 5 adjacency matrices for each one and the energy of graph's orbit is the sum of all energies calculated for each adjacency matrix belonging to the calculated orbit. Thus, we have

$$E(K_{3,A}^n) \approx 2 + 1 + 0.25 + 0.0624 + 0.0156 + 0.004 = 3.332, \quad (13)$$

while the energy in case II is

$$E(K_{3,R}^n) \approx 8 + 16 + 64 + 256 + 1024 + 4096 = 5464. \quad (14)$$

It is obvious that

$$E(G_A^n) < E(G_R^n). \quad (15)$$

More precisely, if map (1) is logistic map given by (8) where  $\mu = 3.56995$  with initial edge  $u \in [0, 1]$ , it follows that the graph's orbit  $G^n$  is chaotic and unpredictable. To have more, we assume that the graph's orbit  $G^n$  contains the following adjacency matrices:

- (1)  $A_1(G(W))$  is the adjacency matrix of the initial weight edges of weighted graph  $G(W)$ .

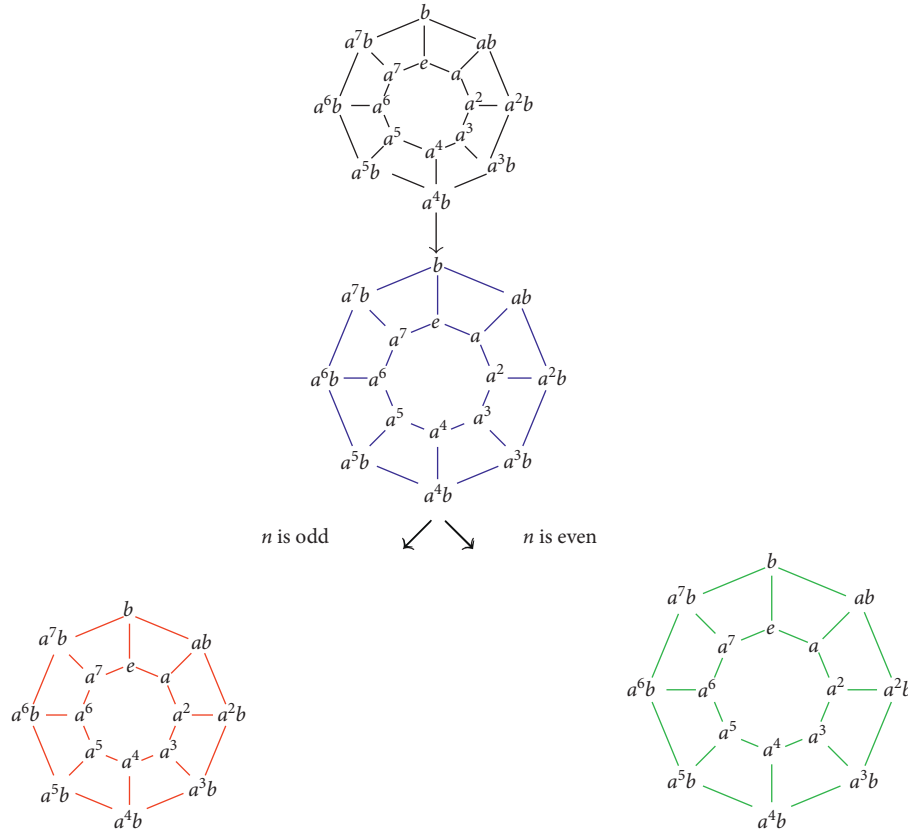


FIGURE 5: Graph's orbit of Cay ( $D_16, S$ ) in which the black color represents the graph status at the initial edge, the blue color represents the graph status at the first order, the red color shows the graph status for odd orders, and green color shows the graph status for even orders.

- (2)  $A_2(G(W))$  is the adjacency matrix of weighted graph  $G(W)$  obtained by the action of  $f(u)$ .
- (3)  $A_\alpha(G(W))$  is the adjacency matrix of weighted graph  $G(W)$  obtained by the action of  $f^{2n}(u) (n \in \mathbb{N})$ .
- (4)  $A_\beta(G(W))$  is the adjacency matrix of weighted graph  $G(W)$  obtained by the action of  $f^{2n+1}(u) (n \in \mathbb{N})$ .

Hence, we can calculate the energy of graph  $G^n$  as follows:

- (1) If  $n$  is even, then

$$E(G^n) = \left[ \sum_{i=1}^N |\lambda_{i_1}| + \sum_{i=1}^N |\lambda_{i_2}| + \left(\frac{n}{2}\right) \sum_{i=1}^N |\lambda_{i_\alpha}| + \left(\frac{n}{2} - 1\right) \sum_{i=1}^N |\lambda_{i_\beta}| \right]. \tag{16}$$

- (2) If  $n$  is odd, then

$$E(G^n) = \left[ \sum_{i=1}^N |\lambda_{i_1}| + \sum_{i=1}^N |\lambda_{i_2}| + \left(\frac{n-1}{2}\right) \sum_{i=1}^N |\lambda_{i_\alpha}| + \left(\frac{n-1}{2}\right) \sum_{i=1}^N |\lambda_{i_\beta}| \right], \tag{17}$$

where  $\lambda_{i_1}, \lambda_{i_2}, \lambda_{i_\alpha}$ , and  $\lambda_{i_\beta}$  are the eigenvalues of  $A_1, A_2, A_\alpha$ , and  $A_\beta$ , respectively. In particular, the energy of  $(K_3)^n$  considered in Example 2 is

$$E((K_3)^n) \approx 1 + 2.4 + (3)3.2 + (3)2 = 19. \tag{18}$$

Moreover, by using formula (19), one can apply the earlier results of weighted graph energy to their orbit's graph, i.e., to the set  $\mathbb{M}(A(G^n))$ . Here, we are considering a special class called bipartite weighted graphs for which the characteristic polynomials are determined in the following.

**Lemma 1.** Let  $G$  be a bipartite weighted graph with  $n$  vertices. Then,

$$\Phi(G, q) = \sum_0^{n/2} b(G, k) q^{2k} (-1)^k q^{n-2k}, \tag{19}$$

where  $b(G, k) \geq 0$  for all  $k$ .

Equation (19) is widely used in the theory of graph energy for unweighted graphs and weighted bipartite graphs. In [13], it was shown that if the graph  $G$  is a bipartite graph with the characteristic polynomial as in (19), then from the Coulson integral formula follows the energy of  $G$ :

$$E(G) = \frac{2}{\pi} \int_0^\infty \frac{1}{q^2} \ln \left( \sum_0^{n/2} b(G, k) q^{2k} \right) dq. \tag{20}$$

The energy in (20) holds equally for simple and bipartite weighted graph. Moreover, the energy of weighted graphs orbit can be calculated by using (20). In [14], it was shown

TABLE 2: Energy of some chemical systems represented by weighted graphs in Figure 6.

Object	$u$	$N$	$n$	$E(G^n)$	Graph
Vinyl-chloride-like systems	0.4	3	2	6	$\Gamma_1$
			5	12.2	
			9	20.4	
Pyrrole-like systems	0.2	5	2	19.6	$\Gamma_2$
			4	30.8	
			7	50.4	
Pyridine-like systems	0.9	6	2	32.7	$\Gamma_3$
			5	47.4	
			8	71.1	
1,1-Dichloro-ethylene-like systems	0.4	4	2	10.8	$\Gamma_4$
			5	20.2	
			8	30.9	

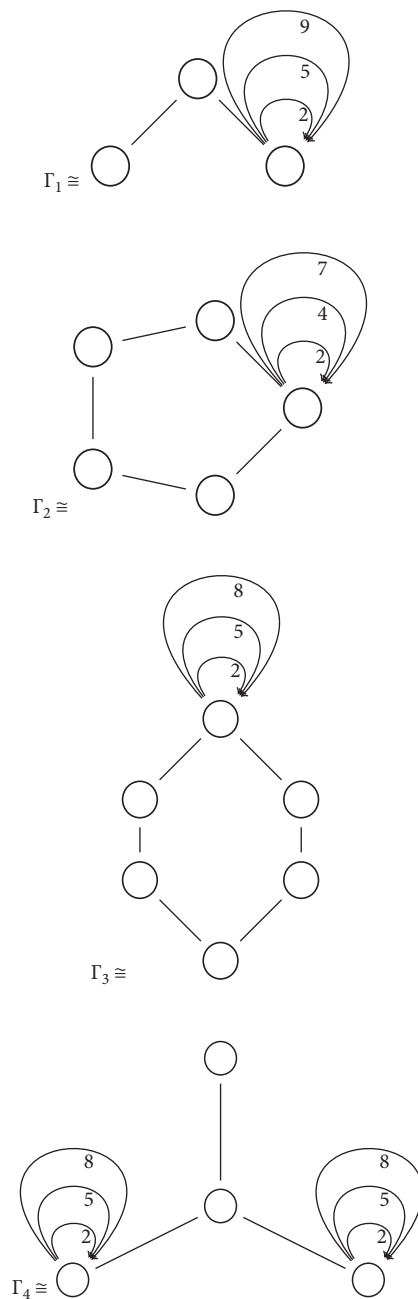


FIGURE 6: The graphs  $\Gamma_i, i = 1, 2, 3, 4$ .

that the weighted star  $W(K_{1,N-1})$  on  $N$  vertices with  $w_{ij}$  on the edge  $e_k = (v_i, v_j)$ , where  $1 \leq i, j \leq N$  and  $1 \leq k \leq N-1$ , can be obtained by the following.

$$E(W(K_{1,N-1})) = 2\sqrt{w_{12}^2 + w_{13}^2 + \dots + w_{1N}^2}. \quad (21)$$

**Proposition 2.** *The energy of weighted star graph orbit is*

$$E((W(K_{1,N-1}))^n) = 2n \sum_{l=0}^n \left[ \sqrt{\sum_{r=1}^N w_{1r}^2} \right]^l. \quad (22)$$

The proof is direct from (19) and (21).

#### 4. Computational Studies on Weighted Graph Orbit

Studying the dynamics of such physical element (molecular) allows us to understand the behavior of it during determined time and environment. To have a better insight into the particularities of the weighted graph orbit, we investigate the orbit of some chemical systems (as mentioned above, the heteroatom systems can be represented by graphs with weights) under the action of the logistic map given in (8) with different times as shown in Table 2.

#### 5. Conclusion

The weighted graphs are very important in representing many problems in complex networks, data structure, chemical systems, urban engineering, and others. In Proposition 1, we show that the introduced method of studying the orbit of each weighted edge belongs to weighted graph brings us more information about the behavior of the consider dynamical systems. We show the relationship between the weight function and the graph's orbit with three possible cases and compute some examples for better understanding their properties. By computing the energy of graph's orbit, we show the change of the energy of such a system during the time which was given in Proposition 2. Finally, we computed the energy of graph's orbit of some popular chemical systems.

#### Data Availability

The data used to support the findings of this study are included within the article.

#### Conflicts of Interest

The authors declare that they have no conflicts of interest.

#### References

- [1] H. S. Mortveit, *An Introduction to Sequential Dynamical Systems*, Springer, New York, NY, USA, 2008.
- [2] A. B. Antonevich and A. A. Shukur, "On powers of operator generated by rotation," *Journal of Analysis and Applications*, vol. 16, pp. 57–67, 2018.

- [3] E. N. Lorenz, "Deterministic nonperiodic flow," *Journal of the Atmospheric Sciences*, vol. 20, no. 2, pp. 130–141, 1963.
- [4] R. M. May, "Simple mathematical models with very complicated dynamics," *Nature*, vol. 261, no. 5560, pp. 459–467, 1976.
- [5] I. Gutman and J.-Y. Shao, "The energy change of weighted graphs," *Linear Algebra and Its Applications*, vol. 435, no. 10, pp. 2425–2431, 2011.
- [6] R. B. Mallion, A. J. Schwenk, and N. Trinajstich, "A graphical study of heteroconjugated molecules," *Croatica Chemica Acta*, vol. 46, pp. 171–182, 1974.
- [7] E. Andrade, M. Robbiano, and B. San Martín, "A lower bound for the energy of symmetric matrices and graphs," *Linear Algebra and Its Applications*, vol. 513, pp. 264–275, 2017.
- [8] D. Cvetkovic, M. Doob, and H. Sachs, *Spectra of Graphs—Theory and Application*, Academic Press, Cambridge, MA, USA, 1980.
- [9] I. Gutman, "The energy of a graph," *Ber Math-Statist Sekt Forschungsz Graz*, vol. 103, pp. 1–22, 1978.
- [10] I. Gutman, "Comparative studies of graph energies," *Bulletin Classe de Sciences Mathematiques et Naturelles, Sciences Mathematiques*, vol. 144, pp. 1–17, 2012.
- [11] I. Gutman, "Census of graph energies," *MATCH Communications in Mathematical and in Computer Chemistry*, vol. 74, pp. 219–221, 2015.
- [12] S. Ali and I. Gutman, "Energy of monad graphs," *Bulletin of the International Mathematical Virtual Institute*, vol. 11, no. 2, pp. 261–268, 2021.
- [13] I. Gutman, "Acyclic systems with extremal Hückel  $\pi$ -electron energy," *Theoretica Chimica Acta*, vol. 45, no. 2, pp. 79–87, 1977.
- [14] H. A. Ganie and B. A. Chat, "Bounds for the energy of weighted graphs," *Discrete Applied Mathematics*, vol. 268, pp. 91–101, 2019.

## Research Article

# Study of Carbon Nanocones $CNC_k(n)$ via Connection Zagreb Indices

Muhammad Asif <sup>1</sup>, Muhammad Hussain <sup>1</sup>, Hamad Almohamedh <sup>2</sup>,  
Khalid M Alhamed <sup>3</sup>, Rana Alabdan <sup>4</sup>, Abdulrazaq A. Almutairi <sup>5</sup>,  
and Sultan Almotairi <sup>6</sup>

<sup>1</sup>Department of Mathematics, COMSATS University Islamabad, Lahore Campus, Lahore 54000, Pakistan

<sup>2</sup>Faculty of King Abdulaziz City for Science and Technology (KACST) Riyadh, Riyadh, Saudi Arabia

<sup>3</sup>IT Programs Center, Faculty of IT Department, Institute of Public Administration, Riyadh 11141, Saudi Arabia

<sup>4</sup>Department of Information Systems, Faculty of Computer and Information Sciences College, Majmaah University, Majmaah 11952, Saudi Arabia

<sup>5</sup>Information and Computer Center, The Public Authority for Applied Education and Training, The Ministry of Education, Adailiyah, Kuwait

<sup>6</sup>Department of Natural and Applied Sciences, Faculty of Community College, Majmaah University, Majmaah 11952, Saudi Arabia

Correspondence should be addressed to Hamad Almohamedh; [halmohamedh@kacst.edu.sa](mailto:halmohamedh@kacst.edu.sa), Rana Alabdan; [r.alabdan@mu.edu.sa](mailto:r.alabdan@mu.edu.sa), and Sultan Almotairi; [almotairi@mu.edu.sa](mailto:almotairi@mu.edu.sa)

Received 25 January 2021; Revised 27 March 2021; Accepted 30 April 2021; Published 12 May 2021

Academic Editor: Ali Ahmad

Copyright © 2021 Muhammad Asif et al. This is an open access article distributed under the Creative Commons Attribution License, which permits unrestricted use, distribution, and reproduction in any medium, provided the original work is properly cited.

Topology of fullerenes, carbon nanotubes, and nanocones has considerable worth due to their effective applications in nanotechnology. These are emerging materials of practical application in gas storage devices, nanoelectronics devices, energy storage, biosensor, and chemical probes. The topological indices are graph invariant used to investigate the physical and chemical properties of the compounds such as boiling point, stability, and strain energy through associated chemical graph of the underlying compound. We computed recently modified Zagreb connection indices of nanocones  $CNC_4(n)$ ,  $CNC_5(n)$ , and  $CNC_6(n)$  and generalized our findings up to a large class of  $CNC_k(n)$ . Topological characterization of nanocones via these indices is mathematically novel and assists to enable its emerging use in nanotechnology. For computation and verification of results, we use Mathematica software.

## 1. Introduction

Carbon nanomaterials received considerable attention due to their effective physical applications in nanotechnology [1] as emerging materials of practical application. However, carbon nanocones (CNCs) received considerable attention after the discovery of free-standing structures or canonical topology as cap on one end of nanotubes (CNTs) [2, 3]. CNCs are considered as alternatives of (CNTs) due to the absence of potentially poisonous metal catalyst in synthesis and mass production at room temperature [4]. Generally, during the declamation of CNTs, strong acids are used in

order to close out metal catalysts. In this process, deficiency is introduced with the hindrance of destructing the graphite structure. On the contrary, the applications and properties of CNCs are easy to approach. CNCs' application as drug delivery capsules [5] and gas storage devices increased their significance. Throughout the years, this subject has been developing scientific obsession with planar, curved, and wrapped nanoscale structures, such as graphene, fullerenes, and nanotubes. It has a strong technological interest just because of their innovative structural, electronic, and mechanical properties. Curved carbon structures are used to investigate growth and nucleation. Especially, pentagon



presence in CNCs plays a vital role [6]. The 60 declination defect is detected when pentagon inserted in the graphite sheet. This is the key of CNCs' formation with pentagon as tip apex which leads us to the existence of nanotubes with tip topology. This type of defects in graphite networks is theoretically considered for study of electronic states [7]. CNCs have free-standing structures with sharp edges because these properties have applications in technology and electronics [8]. In Figure 1, the canonical form of CNCs is shown in Figure 1(a) and associated chemical graph is shown in Figure 1(b). We are interested in the characterization of CNCs using chemical graph theory.

**1.1. Graph.** Let  $G = (V, E)$  be a graph comprising set of vertices  $V$  and  $E \subseteq \binom{V}{2}$  as the set of edges. A graph is called the directed graph if the edges have some orientations. In a multigraph, two vertices can share more than one edge. A loop in a graph is an edge joining a vertex to itself. Graph is called simple if it is not directed or multigraph and has no loops.

**1.2. Chemical Graph Theory.** Graph theory is considered as a powerful tool in different areas of research such as in coding theory, database management system, circuit design, secret sharing schemes, and theoretical chemistry. Chemical graph theory is the combination of chemistry and graph theory. It develops a relationship between structure of organic substances and their physio-chemical properties through some useful graph invariants with the help of their associated molecular graph. The molecular graph is a simple graph on vertices which are representatives of atoms of corresponding chemical substance and edges placed against the bonds between atoms. Figure 2 depicts chemical graphs of some hydrocarbons as benzene in Figure 2(a) and naphthalene in Figure 2(b). The theoretical study of underlying substance using molecular graphs through graph invariants has effective applications in quantitative structure properties relationship (QSPR) or quantitative structure activities relationship (QSAR) investigation [9].

## 2. Topological Indices

Topological indices among graph invariants have a special place and are used to estimate the physio-chemical properties of chemical compound. A topological index is considered as a function  $f: G \rightarrow R$  which maps each graph of chemical structures into a numerical value and have special place among other graph invariants due to its estimation applicability for physio-chemical properties of chemical compound. The idea of topological indices was first introduced by Wiener in 1947 during the work on paraffin's boiling points [10]. In 1972, Zagreb indices were introduced by Ivan Gutman and Trinajstić [11]. Second Zagreb index was thought of by Hosoya et al. in 1975 [12]. The first and second Zagreb indices are defined as

$$\begin{aligned} M_1(\Gamma) &= \sum_{uv \in E(\Gamma)} (\deg_u + \deg_v), \\ M_2(\Gamma) &= \sum_{uv \in E(\Gamma)} (\deg_u \times \deg_v). \end{aligned} \quad (1)$$

Recently, modified versions of Zagreb indices were introduced and studied independently in [13–15]. These indices based on connection number are assigned to the vertices of graph. For more detail of topological indices, one can refer to [16–18].

**2.1. Connection Number.** Let  $G$  be a graph. The connection number associated to the vertex  $u \in V(G)$  is the number of distinct vertices at distance two from vertex  $u$ . It is denoted by  $\tau_u$ :

$$\tau_u = |\{v \in V(G) : d(u, v) = 2\}|. \quad (2)$$

**2.2. Connection Zagreb Indices.** The first  $ZC_1(G)$  and second  $ZC_2(G)$  connection Zagreb indices are defined as

$$\begin{aligned} ZC_1(G) &= \sum_{u \in V(G)} \tau_u^2, \\ ZC_2(G) &= \sum_{uv \in E(G)} \tau_u \times \tau_v, \end{aligned} \quad (3)$$

where  $ZC_1^*$  is another recently introduced graph invariant over connection number [19]:

$$ZC_1^*(G) = \sum_{u \in V(G)} (\deg_u \tau_u) = \sum_{uv \in E(G)} (\tau_u + \tau_v), \quad (4)$$

where  $\deg_u$  stands for degree of  $u \in (G)$  and  $\tau_u$  is the connection number assigned to  $u$ . Ali et al. [19] proved that, for triangle and rectangle free graphs, connection number  $\tau_u$  assigned to a vertex  $u$  is  $\tau_u = \sum_{uv \in E(G)} \deg_v - \deg_u$ .

**2.3. Applications of Connection Zagreb Indices in Chemistry.** Applicability of  $ZC_1(G)$ ,  $ZC_2(G)$ , and  $ZC_1^*(G)$  is observed by its good correlation with entropy of octane isomers [19]. Ali et al. [20] concluded that  $ZC_1^*$  has correlation coefficient approximately 0.949 and 0.892 for acentric factor and entropy, respectively, and  $ZC_1$  has a good correlation with enthalpy. Javaid et al. studied T-sum graphs and graphs constructed through graph operation using connection indices [21–25]. This contemplation recommends chemical applicability of these indices as useful descriptor in QSAR and QSPR investigation.

## 3. Materials and Methods

In this work, we use graph theoretic techniques adopted in [21–25] to study the topology of the corresponding molecular graph of underlying compound for their insight investigation. We used investigative procedure, vertex segment strategy, edge segment procedure, and degree tallying strategy along with combinatorial enlisting techniques, number theoretic logics, and edges and vertices partition

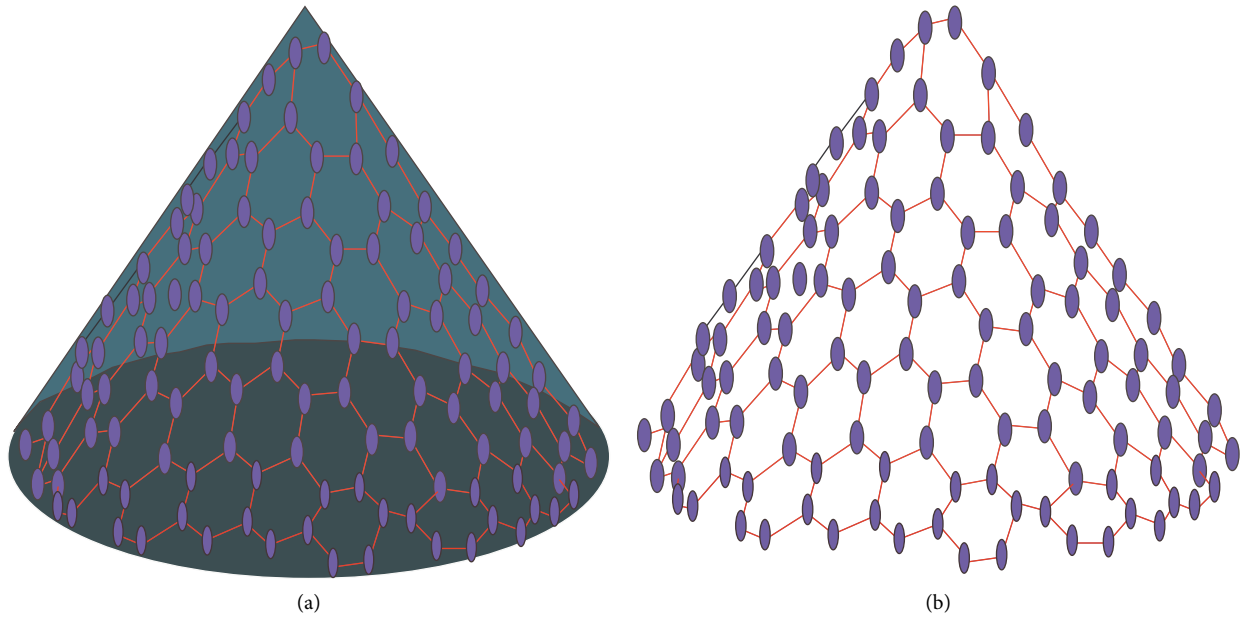


FIGURE 1: Carbon nanocones with associated chemical graph. (a) Canonical form of carbon nanocones. (b) Chemical Graph of carbon nanocones.

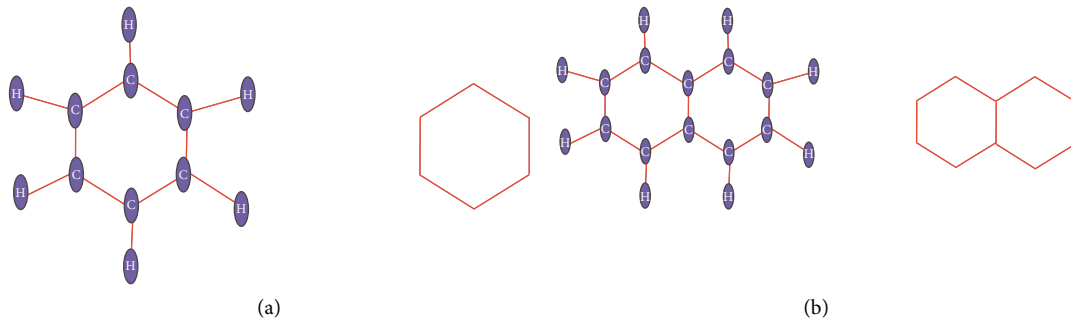


FIGURE 2: Some hydrocarbons with associated chemical graphs. (a) Benzene with chemical graph. (b) Naphthalene with chemical graph.

according to the values associated to the vertices for desired computation.

Throughout this work, we use standard graph theoretic notations, graph  $G = (V, E)$ , set of vertices  $V(G)$  and the set of edges  $E(G)$  of a graph  $G$  with  $|V|$  order and  $|E|$  size of  $G$ ,  $\text{deg}_{v_i}$  as degree for vertex  $v_i$ , and the number of edges incident to  $v_i$ . We draw graph of  $\text{CNC}_k(n)$  using Mathematica software for  $k = 4, 5, 6$  and compute degree sequence for different values of  $n$ . Through observations, we listed possibilities for connection numbers assigned to the vertices and determined vertex petition as well as edge partitions with respect to connection number assigned to the vertices of these graphs.

#### 4. Results and Discussion

In this work, we compute connection Zagreb indices  $ZC_1(G)$ ,  $ZC_2(G)$ , and  $ZC_1^*(G)$  of CNCs which are helpful in their topological investigation and generalize our findings up to a large class of  $\text{CNC}_k(n)$ .  $\text{CNC}_k(n)$  are classified on the basis of  $k$ , where  $k$  is the number of carbon atoms present in

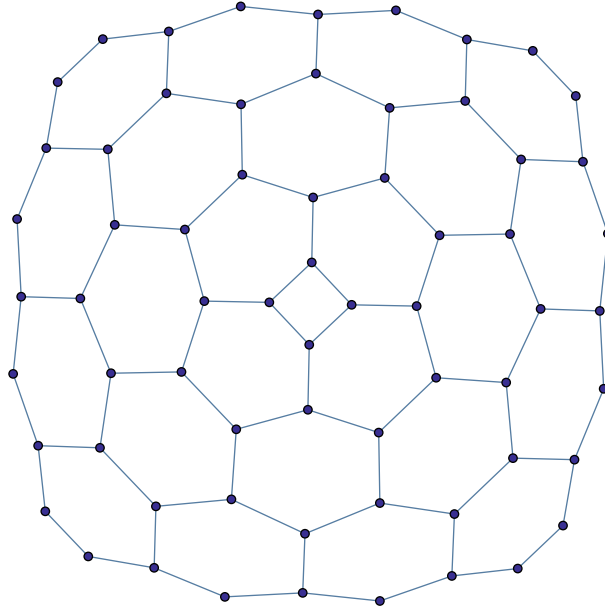
the core of nanocones and  $n$  is the number of hexagon layers around the core [26].

4.1. Results for  $\text{CNC}_4(n)$ . In [27], Ghorbani and Jalali compute vertex PI index, Szeged index, and Omega Polynomials, and Hayat and Imran [28] computed  $\text{ABC}_4$  and  $\text{GA}_5$  of  $\text{CNC}_4(n)$ . In Theorem 1, we computed connection Zagreb indices of  $\text{CNC}_4(n)$ .  $\text{CNC}_4(n)$  for  $n = 3$  is shown in Figure 3.

**Theorem 1.** The  $ZC_1, ZC_2$ , and  $ZC_1^*$  of  $\text{CNC}_4(n)$  are

$$\begin{aligned} ZC_1(\text{CNC}_4(n)) &= 144n^2 + 128n + 8, \\ ZC_2(\text{CNC}_4(n)) &= 216n^2 + 152n + 4, \\ ZC_1^*(\text{CNC}_4(n)) &= 72n^2 + 80n + 16. \end{aligned} \tag{5}$$

*Proof.* Let  $G = \text{CNC}_4(n)$  be the graph of under consideration CNCs. The total number of vertices of  $\text{CNC}_4(n)$  are  $4(n + 1)^2$  and  $2(3n^2 + 5n + 2)$  edges. We made partition of

FIGURE 3:  $CNC_4(3)$ .

vertex set with respect to the connection number  $\tau_u$  as  $V_{\tau_u}(G)$ . For this purpose, we draw graphs of  $CNC_4(n)$  for  $n = 1, 2, 3$  using Mathematica and compute degree sequence as  $\{2, 3\}$ . Degree sequence  $\{2, 3\}$  of  $CNC_4(n)$  implies 3, 4, and 6 are the only possibilities of the connection numbers associated to the vertices of  $G$  and  $(3, 3)$ ,  $(3, 4)$ ,  $(4, 4)$ ,  $(4, 6)$ , and  $(6, 6)$  are the possibilities for the edges. For partition of edges having the same end vertices connection numbers, we use edge and vertex segment strategy along with edges and vertex listing technique. The following tabular calculation enables us for this partition through induction.

The numerical results of Table 1 depict  $|V_3(G)| = 8$ ,  $|V_4(G)| = 8n - 4$ , and  $|V_6(G)| = 4n^2$ . By using this partition, we computed  $ZC_1(CNC_4(n))$ :

$$ZC_1(G) = \sum_{u \in V(G)} \tau_u^2. \quad (6)$$

Let  $N_\tau = \{\tau_u : u \in V(G)\}$ , and from vertex partition  $V_{\tau_u}(G)$ , we obtain

$$\begin{aligned} ZC_1(G) &= \sum_{\tau_u \in N_\tau} \sum_{u \in V_{\tau_u}(G)} \tau_u = \sum_{u \in V_3(G)} \tau_u + \sum_{u \in V_4(G)} \tau_u + \sum_{u \in V_6(G)} \tau_u, \\ ZC_1(G) &= 8(3)^2 + (8n - 4)(4)^2 + 4n^2(6)^2, \end{aligned} \quad (7)$$

$$ZC_1(CNC_4(n)) = 144n^2 + 16(8n - 4) + 72.$$

In Table 2, we list our observation for the number of edges with similar end vertex connection number and generalize our findings for arbitrary value of  $n$ .

The generalization based on Table 2 provides edge partitions as  $E_{(\tau_u, \tau_v)}(G)$ :  $|E_{(3,3)}(G)| = 4$ ,  $|E_{(3,4)}(G)| = 8$ ,  $|E_{(4,4)}(G)| = 8(n - 1)$ ,  $|E_{(4,6)}(G)| = 4n$ , and  $|E_{(6,6)}(G)| = 2n$

$(3n - 1)$ . Using this partition, we computed  $ZC_2(CNC_k(n))$  defined as

$$ZC_2(G) = \sum_{uv \in E(G)} \tau_u \tau_v. \quad (8)$$

Let  $M_\tau = \{(\tau_u, \tau_v) : uv \in G\}$ :

$$\begin{aligned}
 ZC_2(G) &= \sum_{(\tau_u, \tau_v) \in M_\tau} \sum_{uv \in E_{(\tau_u, \tau_v)}(G)} \tau_u \tau_v = \sum_{uv \in E_{(3,3)}(G)} \tau_u \tau_v + \sum_{uv \in E_{(3,4)}(G)} \tau_u \tau_v + \sum_{uv \in E_{(4,4)}(G)} \tau_u \tau_v + \sum_{uv \in E_{(4,6)}(G)} \tau_u \tau_v + \sum_{uv \in E_{(6,6)}(G)} \tau_u \tau_v, \\
 ZC_2(G) &= 4(3 \times 3) + 8(3 \times 4) + (8n - 8)(4 \times 4) + 4n(4 \times 6) + 2n(3n - 1)(6 \times 6), \\
 ZC_2(G) &= 216n^2 + 152n + 4.
 \end{aligned} \tag{9}$$

Now, we compute  $ZC_1^*(G)$  which is defined as

$$ZC_1^*(G) = \sum_{u \in V(G)} \tau_u \deg_u = \sum_{uv \in E_{(u,v)}(G)} (\tau_u + \tau_v). \tag{10}$$

Let  $O_\tau = \{(\tau_u, \tau_v): uv \in E(G)\}$  and

$$\begin{aligned}
 ZC_1^*(G) &= \sum_{(\tau_u, \tau_v) \in O_\tau} \sum_{uv \in E_{(\tau_u, \tau_v)}(G)} (\tau_u + \tau_v) = \sum_{uv \in E_{(3,3)}(G)} (\tau_u + \tau_v) + \sum_{uv \in E_{(3,4)}(G)} (\tau_u + \tau_v) + \sum_{uv \in E_{(4,4)}(G)} (\tau_u + \tau_v) \\
 &\quad + \sum_{uv \in E_{(4,6)}(G)} (\tau_u + \tau_v) + \sum_{uv \in E_{(6,6)}(G)} (\tau_u + \tau_v), s, \\
 ZC_1^*(G) &= 4(3 + 3) + 8(3 + 4) + (8n - 8)(4 + 4) + 4n(4 + 6) + 2n(3n - 1)(6 + 6), \\
 ZC_1^*(G) &= 72n^2 + 80n + 16.
 \end{aligned} \tag{11}$$

4.2. Results for  $CNC_5(n)$ . A. R. Ashrafi in [29] computed winner index of  $CNC_5(n)$ . In Theorem 2, we computed connection Zagreb indices of  $CNC_5(n)$  whose chemical graph for  $n = 3$  is shown in Figure 4.

**Theorem 2.** The  $ZC_1, ZC_2,$  and  $ZC_1^*$  of  $CNC_5(n)$  are equal to

$$\begin{aligned}
 ZC_1(CNC_5(n)) &= 180n^2 + 160n + 10, \\
 ZC_2(CNC_5(n)) &= 270n^2 + 190n + 5, \tag{12} \\
 ZC_1^*(CNC_5(n)) &= 90n^2 + 100n + 20.
 \end{aligned}$$

*Proof.* The total number of vertices of  $G = CNC_5(n)$  are  $5(n + 1)^2$  and edges  $5/2(3n^2 + 5n + 2)$ . Like  $CNC_4(n)$ , we partitioned the vertex set as  $V_{\tau_u}(G)$  and the edge set as  $E_{(\tau_u, \tau_v)}(G)$  by using edge and vertex segment strategy along with edges and vertex listing technique for desired partition.

The computations in Table 3 depict  $|V_3(G)| = 10, |V_4(G)| = 10n - 5,$  and  $|V_6(G)| = 5n^2$ . By using this partition, we compute  $ZC_1(CNC_5(n)) = ZC_1(G)$  as

$$ZC_1(G) = \sum_{u \in V(G)} \tau_u^2. \tag{13}$$

Let  $N_\tau = \{\tau_u: u \in V(G)\}$ ; then, by using vertex set partition  $V(\tau_u)$ , we obtain

$$\begin{aligned}
 ZC_1(G) &= \sum_{\tau_u \in N_\tau} \sum_{u \in V_{\tau_u}(G)} \tau_u = \sum_{u \in V_3(G)} \tau_u + \sum_{u \in V_4(G)} \tau_u + \sum_{u \in V_6(G)} \tau_u, \\
 ZC_1(G) &= 10(3)^2 + (10n - 5)(4)^2 + 5n^2(6)^2, \\
 ZC_1(CNC_5(n)) &= 180n^2 + 160n + 10.
 \end{aligned} \tag{14}$$

In Table 4, we list our observation for the number of edges with similar end vertex connection number and generalize our findings for  $n$ .

The generalization based on Table 4 provides edge partitions as  $E_{(\tau_u, \tau_v)}(G): |E_{(3,3)}(G)| = 5, |E_{(3,4)}(G)| = 10, |E_{(4,4)}(G)| = 10(n - 1), |E_{(4,6)}(G)| = 5n,$  and  $|E_{(6,6)}$

TABLE 1: Vertex partition of  $CNC_4(n)$  with respect to connection number  $\tau$ .

$n$	1	2	3	4	5	6	7	8	9	10	...	$p$
$\tau_u = 3$	8	8	8	8	8	8	8	8	8	8	...	8
$\tau_u = 4$	4	12	20	28	38	44	52	60	68	76	...	$8p - 4$
$\tau_u = 6$	4	16	36	64	100	144	196	256	324	400	...	$4p^2$

TABLE 2: Edge partition of  $CNC_4(n)$  with respect to connection number  $\tau$ .

$n/ E_{(\tau_u, \tau_v)} $	1	2	3	4	5	6	7	8	9	10	...	$n = p$
$ E_{(3,3)} $	4	4	4	4	4	4	4	4	4	4	...	4
$ E_{(3,4)} $	8	8	8	8	8	8	8	8	8	8	...	8
$ E_{(4,4)} $	0	8	16	24	32	40	48	56	64	72	...	$8(p-1)$
$ E_{(4,6)} $	4	8	12	16	20	24	28	32	36	40	...	$4p$
$ E_{(6,6)} $	4	20	48	88	140	204	280	368	468	580	...	$2p(3p - 1)$

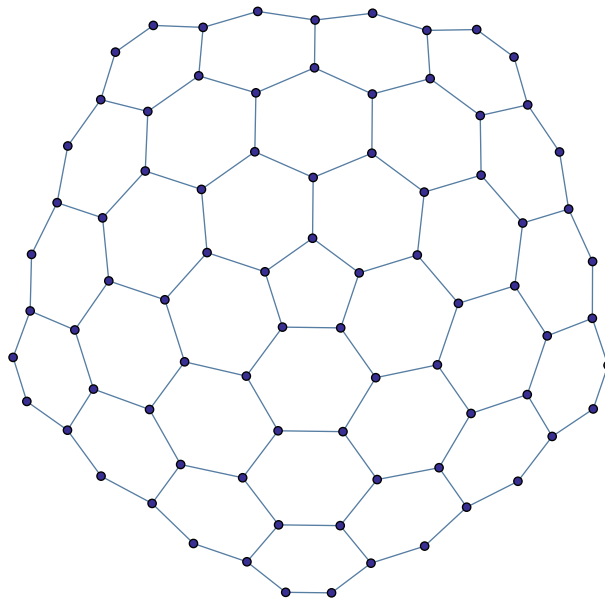


FIGURE 4: Chemical graph of  $CNC_5(n)$  for  $n = 3$ .

TABLE 3: Vertex partition of  $CNC_5(n)$  with respect to connection number  $\tau$ .

$n$	1	2	3	4	5	6	7	8	9	10	...	$p$
$\tau = 3$	10	10	10	10	10	10	10	10	10	10	...	10
$\tau = 4$	5	15	25	35	45	55	65	75	85	95	...	$10p - 5$
$\tau = 6$	5	20	45	80	125	180	245	320	405	500	...	$5p^2$

TABLE 4: Edge partition of  $CNC_5(n)$  with respect to connection number  $\tau$ .

$n/ E_{(\tau_u, \tau_v)} $	1	2	3	4	5	6	7	8	9	10	...	$n = p$
$ E_{(3,3)} $	5	5	5	5	5	5	5	5	5	5	...	5
$ E_{(3,4)} $	10	10	10	10	10	10	10	10	10	10	...	10
$ E_{(4,4)} $	0	10	20	30	40	50	60	70	80	90	...	$10(p-1)$
$ E_{(4,6)} $	5	10	15	20	25	30	35	40	45	50	...	$5p$
$ E_{(6,6)} $	5	25	60	110	175	255	350	460	585	725	...	$5p/2(3p - 1)$

$|G| = 5/2n(3n - 1)$ . Using this partition, we computed  $ZC_2$  ( $CNC_5(n)$ ) and  $ZC_1^*$  ( $CNC_5(n)$ ):

$$ZC_2(G) = \sum_{uv \in E(G)} \tau_u \tau_v. \tag{15}$$

Let  $M_\tau = \{(\tau_u, \tau_v): uv \in G\}$ ; then, by using vertex edge partition  $E_{(\tau_u, \tau_v)}(G)$ , we obtain

$$\begin{aligned} ZC_2(G) &= \sum_{(\tau_u, \tau_v) \in M_\tau} \sum_{uv \in E_{(\tau_u, \tau_v)}(G)} \tau_u \tau_v = \sum_{uv \in E_{(3,3)}(G)} \tau_u \tau_v + \sum_{uv \in E_{(3,4)}(G)} \tau_u \tau_v + \sum_{uv \in E_{(4,4)}(G)} \tau_u \tau_v + \sum_{uv \in E_{(4,6)}(G)} \tau_u \tau_v + \sum_{uv \in E_{(6,6)}(G)} \tau_u \tau_v \\ &= 5(3 \times 3) + 10(3 \times 4) + (10n - 10)(4 \times 4) + 5n(4 \times 6) + 5/2n(3n - 1)(6 \times 6) \\ &= 270n^2 + 190n + 5. \end{aligned} \tag{16}$$

For  $ZC_1^*(G)$ ,

$$ZC_1^*(G) = \sum_{u \in V(G)} \tau_u \deg_u = \sum_{uv \in E_{(u,v)}(G)} (\tau_u + \tau_v). \tag{17}$$

Let  $O_\tau = \{(\tau_u, \tau_v): uv \in E(G)\}$ :

$$\begin{aligned} ZC_1^*(G) &= \sum_{(\tau_u, \tau_v) \in O_\tau} \sum_{uv \in E_{(\tau_u, \tau_v)}(G)} (\tau_u + \tau_v) = \sum_{uv \in E_{(3,3)}(G)} (\tau_u + \tau_v) + \sum_{uv \in E_{(3,4)}(G)} (\tau_u + \tau_v) + \sum_{uv \in E_{(4,4)}(G)} (\tau_u + \tau_v) \\ &+ \sum_{uv \in E_{(4,6)}(G)} (\tau_u + \tau_v) + \sum_{uv \in E_{(6,6)}(G)} (\tau_u + \tau_v) \\ &= 5(3 + 3) + 10(3 + 4) + (10n - 10)(4 + 4) + 5n(4 + 6) + \frac{5}{2}n(3n - 1)(6 + 6) = 90n^2 + 100n + 20. \end{aligned} \tag{18}$$

4.3. Results for  $CNC_6(n)$ . In Theorem 3, we computed connection Zagreb indices of  $CNC_k(n)$ , for  $k = 6$ .  $CNC_6(n)$  for  $n = 4$  is shown in Figure 5.

**Theorem 3.** The  $ZC_1, ZC_2$ , and  $ZC_1^*$  of  $CNC_5(n)$  are equal to

$$\begin{aligned} ZC_1(CNC_6(n)) &= 180n^2 + 160n + 10, \\ ZC_2(CNC_6(n)) &= 270n^2 + 190n + 5, \\ ZC_1^*(CNC_6(n)) &= 108n^2 + 100n + 20. \end{aligned} \tag{19}$$

*Proof.* The total number of vertices of  $G = CNC_6(n)$  are  $6(n + 1)^2$  and  $3(3n^2 + 5n + 2)$  edges. Similar technique is

used as in  $CNC_4(n)$  and  $CNC_5(n)$  computation. We partitioned the vertex set as  $V_{\tau_u}(G)$  and the edge set as  $E_{(\tau_u, \tau_v)}(G)$ .

The computations in Table 5 give vertex partition  $|V_3(G)| = 10, |V_4(G)| = 10n - 5$ , and  $|V_6(G)| = 5n^2$ . By using this partition, we compute  $ZC_1(CNC_6(n)) = ZC_1(G)$ :

$$ZC_1(G) = \sum_{u \in V(G)} \tau_u^2. \tag{20}$$

Let  $N_\tau = \{\tau_u: u \in V(G)\}$ :

$$\begin{aligned} ZC_1(G) &= \sum_{\tau_u \in N_\tau} \sum_{u \in V_{\tau_u}(G)} \tau_u = \sum_{u \in V_3(G)} \tau_u + \sum_{u \in V_4(G)} \tau_u + \sum_{u \in V_6(G)} \tau_u, \\ ZC_1(G) &= 12(3)^2 + (12n - 6)(4)^2 + 6n^2(6)^2, \\ ZC_1(CNC_6(n)) &= 216n^2 + 192n + 12. \end{aligned} \tag{21}$$

In Table 6, we list our observation for the number of edges with similar end vertex connection number of  $CNC_6(n)$  and generalize for arbitrary value of  $n$ .

The generalization based on Table 6 provides edge partitions as  $E_{(\tau_u, \tau_v)}(G), |E_{(3,3)}(G)| = 6, |E_{(3,4)}(G)| = 12, |E_{(4,4)}(G)| = 12(n - 1), |E_{(4,6)}(G)| = 6n$ , and  $|E_{(6,6)}(G)|$

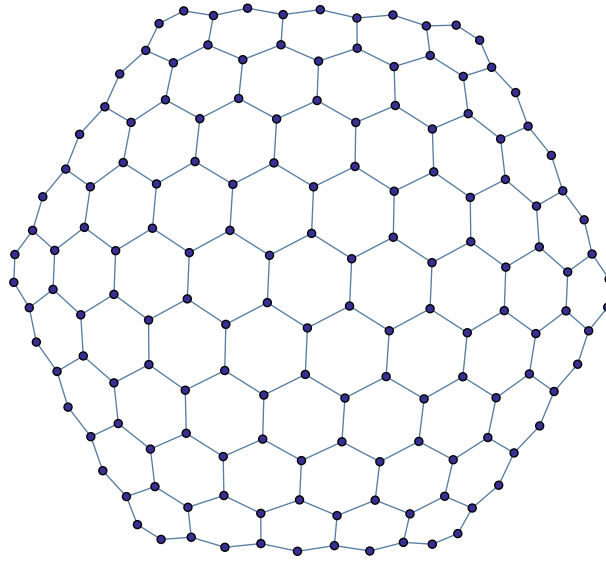


FIGURE 5: Graphical representation of  $CNC_6(n)$ .

$= 3n(3n - 1)$ . Using this partition, we computed  $ZC_2(CNC_6(n))$  and  $ZC_1^*(CNC_6(n))$ :

Let  $M_\tau = \{(\tau_u, \tau_v) : uv \in G\}$ ,

$$ZC_2(G) = \sum_{uv \in E(G)} \tau_u \tau_v, \tag{22}$$

---


$$\begin{aligned} ZC_2(G) &= \sum_{(\tau_u, \tau_v) \in M_\tau} \sum_{uv \in E_{(\tau_u, \tau_v)}(G)} \tau_u \tau_v = \sum_{uv \in E_{(3,3)}(G)} \tau_u \tau_v + \sum_{uv \in E_{(3,4)}(G)} \tau_u \tau_v + \sum_{uv \in E_{(4,4)}(G)} \tau_u \tau_v + \sum_{uv \in E_{(4,6)}(G)} \tau_u \tau_v + \sum_{uv \in E_{(6,6)}(G)} \tau_u \tau_v \\ &= 6(3 \times 3) + 12(3 \times 4) + (12n - 12)(4 \times 4) + 6n(4 \times 6) + 3n(3n - 1)(6 \times 6), \end{aligned} \tag{23}$$

$$ZC_2(CNC_6(n)) = 324n^2 + 228n + 6.$$

Now, for  $ZC_1^*(G)$ ,

Let  $O_\tau = \{(\tau_u, \tau_v) : uv \in E(G)\}$ :

$$ZC_1^*(G) = \sum_{u \in V(G)} \tau_u \deg_u = \sum_{uv \in E_{(u,v)}(G)} (\tau_u + \tau_v). \tag{24}$$

---


$$\begin{aligned} ZC_*(G) &= \sum_{(\tau_u, \tau_v) \in O_\tau} \sum_{uv \in E_{(\tau_u, \tau_v)}(G)} (\tau_u + \tau_v) = \sum_{uv \in E_{(3,3)}(G)} (\tau_u + \tau_v) + \sum_{uv \in E_{(3,4)}(G)} (\tau_u + \tau_v) + \sum_{uv \in E_{(4,4)}(G)} (\tau_u + \tau_v) \\ &\quad + \sum_{uv \in E_{(4,6)}(G)} (\tau_u + \tau_v) + \sum_{uv \in E_{(6,6)}(G)} (\tau_u + \tau_v) \\ &= 6(3 + 3) + 12(3 + 4) + (12n - 12)(4 + 4) + 6n(4 + 6) + 3n(3n - 1)(6 + 6), \end{aligned} \tag{25}$$

$$ZC_1^*(CNC_6(n)) = 108n^2 + 192n + 24.$$

□

TABLE 5: Vertex partition of  $CNC_6(n)$  with respect to connection number  $\tau$ .

$n$	1	2	3	4	5	6	7	8	9	10	...	$p$
$\tau = 3$	12	12	12	12	12	12	12	12	12	12	...	12
$\tau = 4$	6	18	30	42	54	66	78	90	102	114	...	$12p - 6$
$\tau = 6$	5	24	54	96	150	216	294	384	486	600	...	$6p^2$

TABLE 6: Edge partition of  $CNC_6(n)$  with respect to connection number  $\tau$ .

$n/ E_{(\tau_u, \tau_v)} $	1	2	3	4	5	6	7	8	9	10	...	$n = p$
$ E_{(3,3)} $	6	6	6	6	6	6	6	6	6	6	...	6
$ E_{(3,4)} $	12	12	12	12	12	12	12	12	12	12	...	12
$ E_{(4,4)} $	0	12	24	36	48	60	72	84	96	108	...	$12(p-1)$
$ E_{(4,6)} $	6	12	18	24	30	36	42	48	54	60	...	$6p$
$ E_{(6,6)} $	6	30	72	132	210	306	420	552	702	870	...	$3p(3p - 1)$

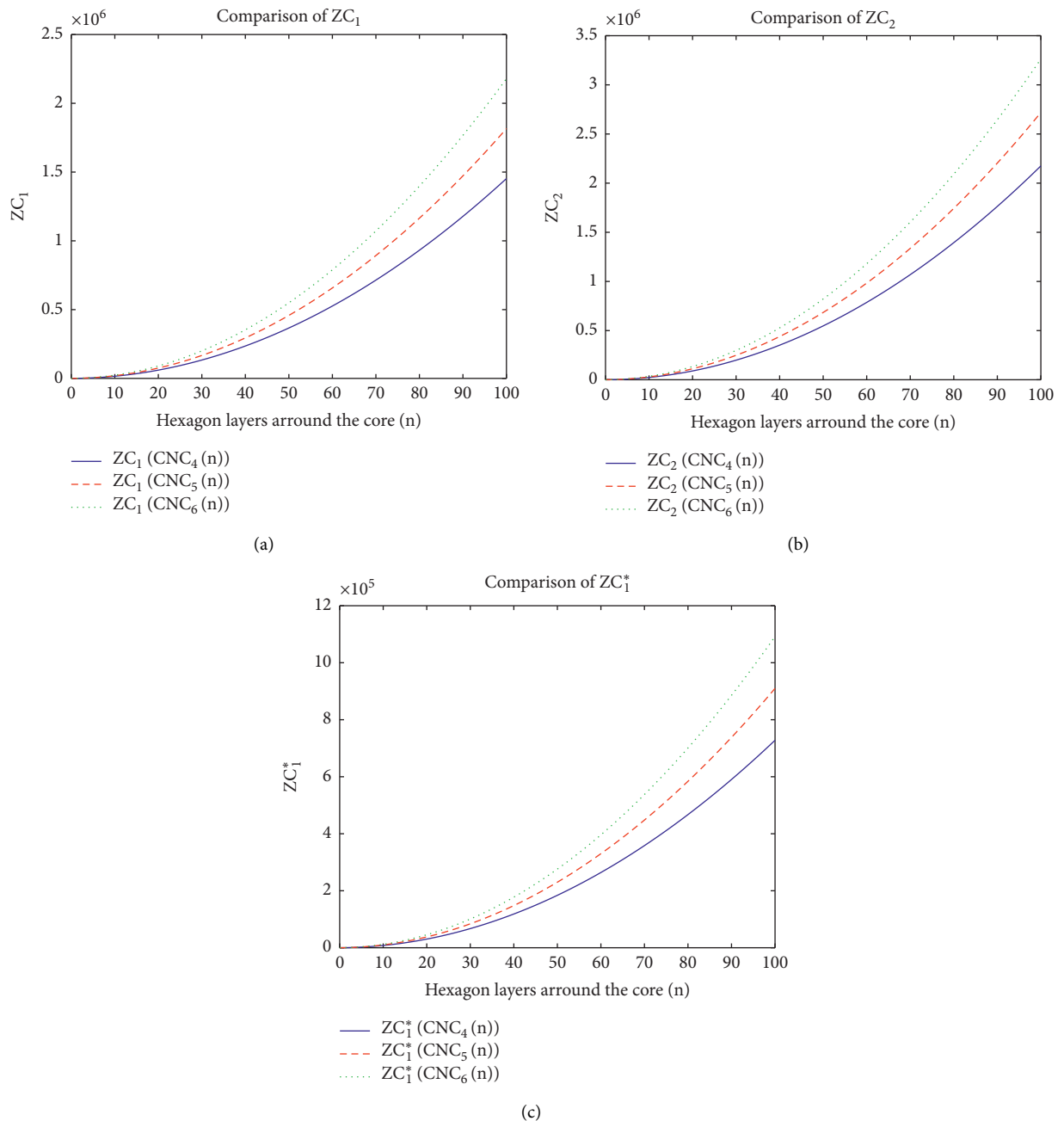


FIGURE 6: Comparison of results computed in Theorems 1–3. (a) Comparison of results regarding  $ZC_1$ . (b) Comparison of results regarding  $ZC_2$ . (c) Comparison of results regarding  $ZC_1^*$ .



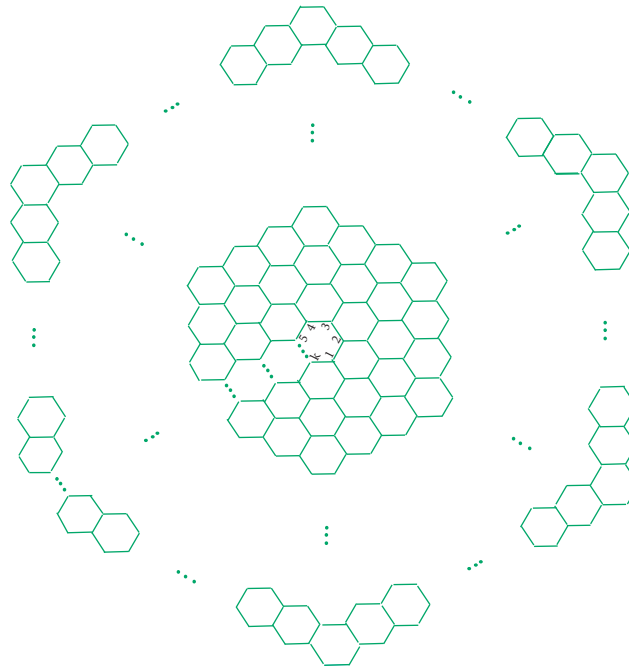


FIGURE 7: The chemical graph of generalized carbon nanocone  $CNC_k(n)$ .

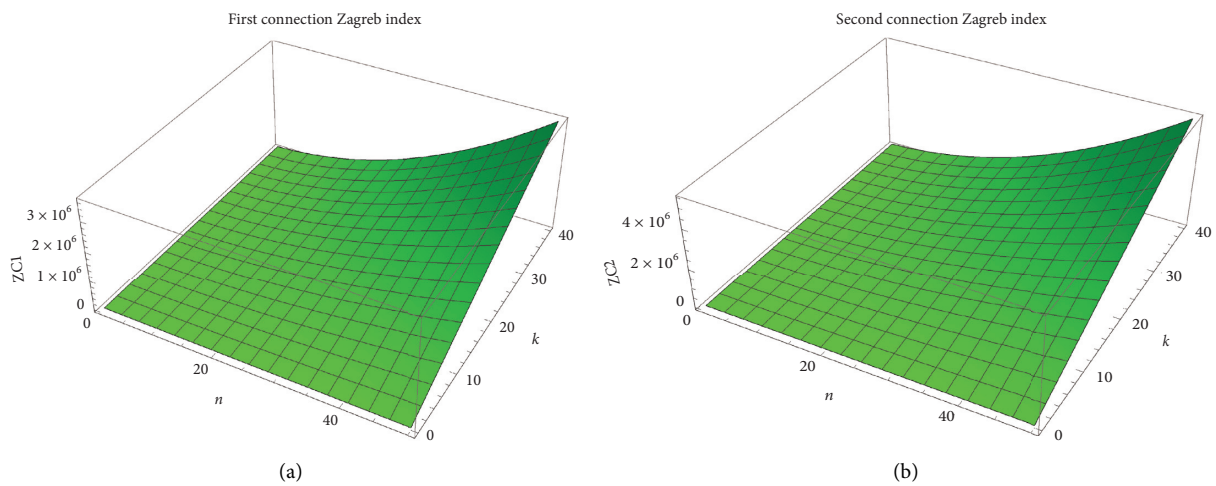


FIGURE 8: The graphical representation of connection Zagreb indices for generalized values of  $n$  and  $k$ . (a) The graphical representation of  $ZC_1(CNC_k(n))$ . (b) The graphical representation of  $ZC_2(CNC_k(n))$ .

4.4. *Comparison of Results.* In Figure 6, Figure 6(a) interprets behavior of  $ZC_1(G)$ , Figure 6(b) of  $ZC_2(G)$ , and Figure 6(c) of  $ZC_1^*(G)$  for  $k = 4, 5, 6$ .

4.5. *Results for  $CNC_k(n)$ .* Graph shown in Figure 7 is the associated chemical graph of  $CNC_k(n)$  for arbitrary value of  $k$ . It consists of a  $k$ -gon as the central core cycle with  $n$  layers of hexagons around the core.

**Theorem 4.** *The  $ZC_1, ZC_2$ , and  $ZC_1^*$  of  $CNC_k(n)$  are*

$$\begin{aligned} ZC_1(CNC_k(n)) &= 36kn^2 + 32kn + 2k, \\ ZC_2(CNC_k(n)) &= 54kn^2 + 38kn + k, \\ ZC_1^*(CNC_k(n)) &= 18kn^2 + 20kn + 4k. \end{aligned} \tag{26}$$

*Proof.* The chemical graph of  $CNC_k(n)$  has cycle of length  $k$  corresponding to core of  $CNC_k(n)$ , where  $n$  represent the number of layers of hexagons around the core. Total vertices of  $CNC_k(n)$  is  $k(n + 1)^2$  and edges is  $k/2(3n^2 + 5n + 2)$  [30].

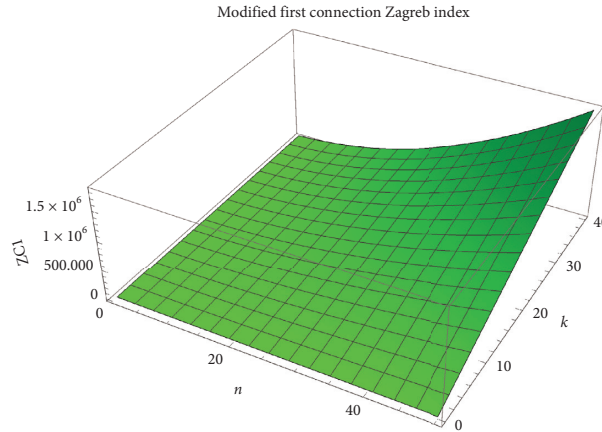


FIGURE 9: The graphical representation of  $ZC_1^*(CNC_k(n))$  for generalized values  $k$ .

For computation of  $ZC_1$  for generalized nanocone  $CNC_k(n)$ , we used their edges and vertex partition. From the construction of  $CNC_k(n)$ , it is clear that the connection number associated to the vertices is 6 except the  $k(2n + 1)$  vertices of outer layer of hexagons. So, the number of vertices with connection number 6 is  $|V_6(CNC_k(n))| = k(n + 1)^2 - k(2n + 1) = kn^2 = kn^2$ .

In the outer layer of hexagons, two vertices at each corner have connection number  $\tau_u = 3$  and all other have  $\tau_u = 4$ . So,  $|V_3(CNC_k(n))| = 2k$  and  $|V_4(CNC_k(n))| =$

$k(2n + 1) - 2k = k(2n - 1)$ . Similarly, all the edges other than edges of the outer layer of hexagons have (6,6) as end vertex connection number, i.e.,  $|E_{(6,6)}(CNC_k(n))| = k/2(3n^2 + 5n + 2) - (3kn + k) = k/2(3n^2 - 1)$ . The edges in the outer layer of hexagons are partitioned as  $|E_{(3,3)}(CNC_k(n))| = k$ ,  $|E_{(3,4)}(CNC_k(n))| = 2k$ ,  $|E_{(4,4)}(CNC_k(n))| = k(2n - 2)$ , and  $|E_{(4,6)}(CNC_k(n))| = kn$ . We use this vertex and edge partition and technique as used in Theorems 1–3 for proof. Let  $G = CNC_k(n)$  and  $N_\tau = \{\tau_u; u \in V(G)\}$ :

$$ZC_1(G) = \sum_{u \in V(G)} \tau_u^2,$$

$$ZC_1(G) = \sum_{\tau_u \in N_\tau} \sum_{u \in V_{\tau_u}(G)} \tau_u = \sum_{u \in V_3(G)} \tau_u + \sum_{u \in V_4(G)} \tau_u + \sum_{u \in V_6(G)} \tau_u, \tag{27}$$

$$ZC_1(G) = 2k(3)^2 + k(2n - 1)(4)^2 + kn^2(6)^2,$$

$$ZC_1(CNC_k(n)) = 36kn^2 + 32kn + 2k,$$

$$ZC_2(G) = \sum_{uv \in E(G)} \tau_u \tau_v,$$

$$ZC_2(G) = \sum_{(\tau_u, \tau_v) \in M_\tau} \sum_{uv \in E_{(\tau_u, \tau_v)}(G)} \tau_u \tau_v = \sum_{uv \in E_{(3,3)}(G)} \tau_u \tau_v + \sum_{uv \in E_{(3,4)}(G)} \tau_u \tau_v + \sum_{uv \in E_{(4,4)}(G)} \tau_u \tau_v + \sum_{uv \in E_{(4,6)}(G)} \tau_u \tau_v + \sum_{uv \in E_{(6,6)}(G)} \tau_u \tau_v,$$

$$ZC_2(G) = k(3 \times 3) + 2k(3 \times 4) + (2kn - 2k)(4 \times 4) + kn(4 \times 6) + \frac{k}{2}(3n^2 - 1)(6 \times 6),$$

$$ZC_1(CNC_k(n)) = 54kn^2 + 38kn + k,$$

(28)

$$\begin{aligned}
ZC_1^*(G) &= \sum_{u \in V(G)} \tau_u \deg_u = \sum_{uv \in E_{(u,v)}(G)} (\tau_u + \tau_v), \\
ZC_1^*(G) &= \sum_{(\tau_u, \tau_v) \in O_\tau} \sum_{uv \in E_{(\tau_u, \tau_v)}(G)} (\tau_u + \tau_v) = \sum_{uv \in E_{(3,3)}(G)} (\tau_u + \tau_v) + \sum_{uv \in E_{(3,4)}(G)} (\tau_u + \tau_v) + \sum_{uv \in E_{(4,4)}(G)} (\tau_u + \tau_v) \\
&\quad + \sum_{uv \in E_{(4,6)}(G)} (\tau_u + \tau_v) + \sum_{uv \in E_{(6,6)}(G)} (\tau_u + \tau_v), \tag{29}
\end{aligned}$$

$$ZC_1^*(G) = k(3+3) + 2k(3+4) + (2kn-2k)(4+4) + kn(4+6) + \frac{k}{2}(3n^2-1)(6+6),$$

$$ZC_1^*(CNC_k(n)) = 18kn^2 + 20kn + 4k.$$

Hence, the proof is completed.

Theorem 4 shows that connection Zagreb indices of  $CNC_k(n)$  increased by a factor  $k$  (number of carbon atoms in the core). In Figure 8, Figures 8(a) and 8(b) interpret computed results of  $ZC_1(CNC_k(n))$  and  $ZC_2(CNC_k(n))$ , respectively, for any value of  $k$  and 9 of  $ZC_1^*(CNC_k(n))$ .  $\square$

## 5. Conclusion

The International Academy of Theoretical Chemistry explored that any topological index is acceptable to estimate chemical properties of compounds if it has a sound correlation with actual physio-chemical property of octane isomers. Customarily, octane isomers are adopted for such investigations due to the huge number of structural isomers of octane [31] for the acceptable statistical conclusion. Ali et al. [32] studied the correlation efficiency of  $ZC_1^*$  for the physio-chemical properties of octane isomers: entropy, boiling point, density, enthalpies, acentric factor, etc. They concluded that  $ZC_1^*$  has a correlation coefficient approximately 0.949 and 0.892 for acentric factor and entropy, respectively. Correlation of  $ZC_1$  with physical properties was studied by Jakkannavar and Basavanagoud [33] and found good with enthalpy. Possibility of large-scale production of CNCs [34] and predictive ability of topological indices [35] encourages theoretical study of  $CNC_k(n)$ . We computed connection Zagreb indices  $ZC_1(G)$ ,  $ZC_2(G)$ , and  $ZC_1^*(G)$  of  $CNC_k(n)$  for  $k = 4, 5, 6$  in Theorems 1–3 and generalized our finding up to large value of  $K$  in 4.4. These results facilitate topological characterization of  $CNC_k(n)$  which is helpful in finding new applications in the emerging field of nanotechnology.

## Data Availability

No data were used to support this study.

## Conflicts of Interest

The authors of this paper declare that they have no conflicts of interest.

## Authors' Contributions

All authors have contributed equally.

## Acknowledgments

The authors extend their appreciation to the Deanship of Scientific Research at Majmaah University for funding this work under project number no. R-2021-103.

## References

- [1] N. Tagmatarchis, *Advances in Carbon Nanomaterials: Science and Applications*, CRC Press, Boca Raton, FL, USA, 2012.
- [2] S. Iijima, P. M. Ajayan, and T. Ichihashi, "Growth model for carbon nanotubes," *Physical Review Letters*, vol. 69, no. 21, pp. 3100–3103, 1992.
- [3] M. Ge and K. Sattler, "Observation of fullerene cones," *Chemical Physics Letters*, vol. 220, no. 3–5, pp. 192–196, 1994.
- [4] O. O. Adisa, B. J. Cox, and J. M. Hill, "Open carbon nanocones as candidates for gas storage," *The Journal of Physical Chemistry C*, vol. 115, no. 50, pp. 24528–24533, 2011.
- [5] K. Ajima, T. Murakami, Y. Mizoguchi et al., "Enhancement of in vivo anticancer effects of cisplatin by incorporation inside single-wall carbon nanohorns," *ACS Nano*, vol. 2, no. 10, pp. 2057–2064, 2008.
- [6] A. Krishnan, E. Dujardin, M. M. J. Treacy, J. Huggdahl, S. Lynum, and T. W. Ebbesen, "Graphitic cones and the nucleation of curved carbon surfaces," *Nature*, vol. 388, no. 6641, pp. 451–454, 1997.
- [7] D. L. Carroll, P. Redlich, P. M. Ajayan et al., "Electronic structure and localized states at carbon nanotube tips," *Physical Review Letters*, vol. 78, no. 14, pp. 2811–2814, 1997.
- [8] R. Tamura and M. Tsukada, "Electronic states of the cap structure in the carbon nanotube," *Physical Review B*, vol. 52, no. 8, pp. 6015–6026, 1995.
- [9] G. Rücker and C. Rücker, "On topological indices, boiling points, and cycloalkanes," *Journal of Chemical Information and Computer Sciences*, vol. 39, no. 5, pp. 788–802, 1999.
- [10] H. Wiener, "Structural determination of paraffin boiling points," *Journal of the American Chemical Society*, vol. 69, no. 1, pp. 17–20, 1947.
- [11] I. Gutman and N. Trinajstić, "Graph theory and molecular orbitals. Total  $\phi$ -electron energy of alternant hydrocarbons," *Chemical Physics Letters*, vol. 17, no. 4, pp. 535–538, 1972.
- [12] H. Hosoya, K. Hosoi, and I. Gutman, "A topological index for the total  $\pi$ -electron energy," *Theoretica Chimica Acta*, vol. 38, no. 1, pp. 37–47, 1975.
- [13] A. Ali and N. Trinajstić, "A novel/old modification of the first Zagreb index," *Molecular Informatics*, vol. 37, no. 1–8, Article ID 1800008, 2018.
- [14] S. Manzoor, N. Fatima, A. A. Bhatti, and A. Ali, "Zagreb connection indices of some nanostructures," *Acta Chemica Iasi*, vol. 26, no. 2, pp. 169–180, 2018.

- [15] G. Ducoffe, R. Marinescu-Ghemeci, C. Obreja, A. Popa, and R. Tache, *Extremal Graphs with Respect to the Modified First Zagreb Connection Index*, HAL, Bangalore, India, 2018.
- [16] A. N. A. Koam, A. Ahmad, and M. F. Nadeem, "Comparative study of valency-based topological descriptor for hexagon star network," *Computer Systems Science and Engineering*, vol. 36, no. 2, pp. 293–306, 2021.
- [17] A. Ahmad, R. Hasni, K. Elahi, and M. A. Asim, "Polynomials of degree-based indices for swapped networks modeled by optical transpose interconnection system," *IEEE Access*, vol. 8, pp. 214293–214299, 2020.
- [18] A. Ahmad, "On the degree based topological indices of Benzene ring embedded in the P-type-surface in 2D network," *Hacettepe Journal of Mathematics and Statistics*, vol. 47, no. 1, pp. 9–18, 2018.
- [19] Z. Du, A. Ali, and N. Trinajstić, "Alkanes with the first three maximal/minimal modified first Zagreb connection indices," *Molecular Informatics*, vol. 38, no. 4, Article ID 1800116, 2019.
- [20] A. Ali and N. Trinajstić, "A novel/old modification of the first Zagreb index," *Molecular Informatics*, vol. 37, no. 1–8, Article ID 1800008, 2018.
- [21] U. Ali, M. Javaid, and A. M. Alanazi, "Computing analysis of connection-based indices and coindices for product of molecular networks," *Symmetry*, vol. 12, no. 8, p. 1320, 2020.
- [22] U. Ali, M. Javaid, and A. Kashif, "Modified Zagreb connection indices of the T-sum graphs," *Main Group Metal Chemistry*, vol. 43, no. 1, pp. 43–55, 2020.
- [23] J. Cao, U. Ali, M. Javaid, and C. Huang, "Zagreb connection indices of molecular graphs based on operations," *Complexity*, vol. 2020, Article ID 7385682, 15 pages, 2020.
- [24] J.-H. Tang, U. Ali, M. Javaid, and K. Shabbir, "Zagreb connection indices of subdivision and semi-total point operations on graphs," *Journal of Chemistry*, vol. 2019, Article ID 9846913, 14 pages, 2019.
- [25] M. Ahmad, M. Saeed, M. Javaid, and M. Hussain, "Exact formula and improved bounds for general sum-connectivity index of graph-operations," *IEEE Access*, vol. 7, pp. 167290–167299, 2019.
- [26] W. Nazeer, A. Farooq, M. Younas, M. Munir, and S. Kang, "On molecular descriptors of carbon nanocones," *Biomolecules*, vol. 8, no. 3, p. 92, 2018.
- [27] M. Ghorbani and M. Jalali, "The vertex PI, szeged and omega polynomials of carbon nanocones  $CNC_4(n)$ ," *Match*, vol. 62, p. 353, 2009.
- [28] S. Hayat and M. Imran, "On topological properties of nanocones  $CNC_k$ ," *Studia UBB Chemia*, vol. 59, pp. 113–128, 2014.
- [29] M. Alipour and A. Ashrafi, "Computer calculation of the wiener index of one-pentagonal carbon nanocone" *Digest Journal of Nanomaterials and Biostructures (DJNB)*, vol. 4, 2009.
- [30] M. Arockiaraj, J. Clement, and K. Balasubramanian, "Topological properties of carbon nanocones," *Polycyclic Aromatic Compounds*, vol. 41, pp. 1–15, 2018.
- [31] S. Hayat and M. Imran, "Computation of certain topological indices of nanotubes covered by  $C_5$  and  $C_7$ ," *Journal of Computational and Theoretical Nanoscience*, vol. 12, no. 4, pp. 533–541, 2015.
- [32] N. Fatima, A. A. Bhatti, A. Ali, and W. Gao, "Zagreb connection indices of two dendrimer nanostars," *Acta Chemica Iasi*, vol. 27, no. 1, pp. 1–14, 2019.
- [33] B. Basavanagoud and P. Jakkannavar, "Computing first leap Zagreb index of some nano structures," *International Journal of Applied Mathematics*, vol. 55, no. 7, 2018.
- [34] S. N. Naess, A. Elgsaeter, G. Helgesen, and K. D. Knudsen, "Carbon nanocones: wall structure and morphology," *Science and Technology of Advanced Materials*, vol. 10, Article ID 065002, 2009.
- [35] I. Gutman and J. Tosovic, "Testing the quality of molecular structure descriptors. Vertex-degree-based topological indices," *Journal of the Serbian Chemical Society*, vol. 78, no. 6, pp. 805–810, 2013.

## Research Article

# Cayley Graphs over LA-Groups and LA-Polygroups

Nabilah Abughazalah <sup>1</sup>, Naveed Yaqoob <sup>2</sup>, and Asif Bashir<sup>2</sup>

<sup>1</sup>Mathematical Sciences Department, College of Science, Princess Nourah Bint Abdulrahman University, P.O. Box 84428, Riyadh 11671, Saudi Arabia

<sup>2</sup>Department of Mathematics and Statistics, Riphah International University, I-14, Islamabad, Pakistan

Correspondence should be addressed to Nabilah Abughazalah; [nhabughazala@pnu.edu.sa](mailto:nhabughazala@pnu.edu.sa)

Received 6 April 2021; Accepted 27 April 2021; Published 10 May 2021

Academic Editor: Roslan Hasni

Copyright © 2021 Nabilah Abughazalah et al. This is an open access article distributed under the Creative Commons Attribution License, which permits unrestricted use, distribution, and reproduction in any medium, provided the original work is properly cited.

The purpose of this paper is the study of simple graphs that are generalized Cayley graphs over LA-polygroups (GCLAP – graphs). In this regard, we construct two new extensions for building LA-polygroups. Then, we define Cayley graph over LA-group and GCLAP-graph. Further, we investigate a few properties of them to show that each simple graph of order three, four, and five (except cycle graph of order five which may or may not be a GCLAP-graph) is a GCLAP-graph and then we prove this result.

## 1. Introduction

The origins of graph theory can be traced back to Euler's work [1] on the Königsberg bridges problem (1735), which thusly prompted the idea of an Eulerian graph. Graph is a mathematical portrayal of a grid and it portrays the relationship between lines and points.

The idea of Cayley graph was introduced by Cayley [2] in 1878. Cayley graph has been widely studied in both directed and undirected forms. To study the characteristics of Cayley graphs, refer the papers [3–6].

First time Marty [7] introduced the concept of algebraic hyperstructures, which is a suitable extension of classical algebraic structures. Since then, a lot of works have been written on this topic. For a brief analysis of this theory, see [8,9]. In the books [10–13], we can see the applications of hyperstructures in lattices, cryptography, graph, automata, probability, geometry, and hypergraphs. A very good presentation of polygroup theory is in [14], which is utilized to consider color algebra [15–17] and hypergraph theory in [18] by Berge.

The theory of left almost structures was first defined by Kazim and Naseeruddin [19] in 1972. Subsequently, Mushtaq and Kamran [20] established a new concept of left almost group (nonassociative group) called LA-group. The theory of left almost hyperstructures was first introduced by

Hila and Dine [21] in the form of left almost semi-hypergroups, which was further investigated by Yaqoob et al. [22] and Amjad et al. [23]. In [24], Yaqoob et al. introduced the concept of LA-polygroups.

Recently, Heidari et al. [25] introduced a suitable generalization of Cayley graphs that is defined over polygroups (GCP – graphs) and showed that each simple graph of order  $\geq 5$  is a GCP-graph.

In this paper, we construct two new extensions for building LA-polygroups. Then, we define the idea of Cayley graph over LA-group and GCLAP-graph. In particular, we proved some properties of them in order to show that each simple graph of order three, four, and five (except cycle graph of order five which may or may not be a GCLAP-graph) is a GCLAP-graph.

## 2. Preliminaries and Notations

This section contains some basic definitions of graph theory (see [26]) and left almost theory (see [24]).

A graph is represented by  $\Phi = (R, D)$ , where  $R$  is the set of vertices and  $D$  is the set of edges. Note that  $|R|$  is the order of a graph and  $|D|$  in a graph is its size. The graph  $K_n$  is known as complete graph if every couple of vertices form an edge, where  $n$  is the number of vertices. In specific,  $K_1$  is

known as trivial graph and  $N_n$  is known as null graph having no edges and  $n$  vertices.

If  $\Phi = (R, D)$  is a graph such that  $R = R' \cup R''$  and  $R' \cap R'' = \emptyset$ , where  $R'$  and  $R''$  are subsets of  $R$  and edges of the form  $\{\{d, f\} | d \in R' \text{ and } f \in R''\}$ , then  $\Phi = K_{m,n}$  is known as complete bipartite graph, where  $|R'| = m$  and  $|R''| = n$ . In specific,  $K_{1,n}$  is known as star graph. The complement of a simple graph  $\Phi = (R, D)$  is denoted by  $\overline{\Phi}$ , where  $\overline{\Phi} = (R, \overline{D})$  such that  $\overline{D} = \{\{d, f\} | \{d, f\} \notin D\}$ . Let  $\Phi = (R, D)$  and  $\Phi' = (R', D')$  be two graphs. Then,  $\Phi'$  is known as subgraph of  $\Phi$ , if  $R' \subseteq R$  and  $D' \subseteq D$ . A subgraph  $\Phi' \subseteq \Phi$  is known as induced subgraph, if  $\Phi'$  contains each and every edge  $\{d, f\} \in D$  with  $d, f \in R'$ . Two graphs  $\Phi = (R, D)$  and  $\Phi' = (R', D')$  are said to be isomorphic, if  $\exists$ , a bijection,  $\gamma: R \rightarrow R'$  such that  $\{z, a\} \in D \Leftrightarrow \{\gamma(z), \gamma(a)\} \in D'$ . We denote this by  $\Phi \cong \Phi'$ . Let  $\Phi = (R, D)$  and  $\Phi' = (R', D')$  be two graphs. Then,  $\Phi \cup \Phi' = (R'', D'')$ , where  $R'' = R \cup R'$  and  $D'' = D \cup D'$  and joint of two graphs  $\Phi \vee \Phi' = (R'', D'')$  with  $R'' = R \cup R'$  and  $D'' = D \cup D' \cup \{\{d, f\} | d \in R, f \in R'\}$ . A graph  $\Phi = (R, D)$  having no self edges and no multiple edges is known as simple graph.

*Definition 1* (see [27]). If  $\Phi = (R, D)$  is a graph and we form a sequence of vertices (ordered from left to right)  $d_1, d_2, d_3, \dots, d_n$  such that there is just one edge between every two successive vertices and there are no other edges known as path. A path on  $n$  vertices is denoted by  $P_n$ .

*Definition 2* (see [27]). A graph is said to be a connected graph if there exists at least one path between every two vertices.

*Definition 3* (see [27]). If all vertices have degree two of a connected graph, then it is called a cycle. A cycle graph has  $n$  vertices, represented by  $C_n$ .

*Definition 4* (see [20]). A groupoid  $G$  is called a left almost group, i.e., LA-group, if

- (i)  $\exists e \in G$  such that  $e d = d$  for all  $d \in G$ ,
- (ii)  $\forall d \in G, \exists d^* \in G$  such that  $d d^* = e$ ,
- (iii)  $(w f) d = (d f) w, \forall d, f, w \in G$ .

*Example 1* (see [20]). Let  $G_n = \{t_1, t_2, \dots, t_n\}$  where  $n \geq 3$ , under binary operation  $*$  which is defined as

$$t_i * t_j = t_k, \quad k \equiv (j + 1) - i \pmod{n}. \quad (1)$$

Then,  $(G_n, *)$  is an LA-group. For  $n = 5$ , we have the Cayley (Table 1).

*Definition 5* (see [24]). A multivalued system  $\langle L, \circ, e^{-1} \rangle$ , where  $e \in L^{-1}$ , is a unitary operation and  $\circ$  maps  $L \times L$  into the family of nonempty subsets of  $L$  which is called LA-polygroup, if the following postulates hold for all  $d, f, w \in L$ :

- (i) Left invertive law:  $(d \circ f) \circ w = (w \circ f) \circ d$ ,
- (ii) Reproducibility axiom:  $d \circ L = L \circ d = L$ ,

TABLE 1: LA-group.

*	$t_1$	$t_2$	$t_3$	$t_4$	$t_5$
$t_1$	$t_1$	$t_2$	$t_3$	$t_4$	$t_5$
$t_2$	$t_5$	$t_1$	$t_2$	$t_3$	$t_4$
$t_3$	$t_4$	$t_5$	$t_1$	$t_2$	$t_3$
$t_4$	$t_3$	$t_4$	$t_5$	$t_1$	$t_2$
$t_5$	$t_2$	$t_3$	$t_4$	$t_5$	$t_1$

- (iii)  $\exists$  is a left identity  $L \ni e$  such that  $f = e \circ f$ ,
- (iv)  $f^{-1} \circ f \cap f \circ f^{-1} \sum e$ ,
- (v)  $d \in f \circ w \implies f \in d \circ w^{-1}$ .

*Example 2* (see [24]). Consider a finite set  $Q_n = \{t_1, t_2, t_3, \dots, t_n\}$ , where  $n \geq 3$ . Then,  $Q_n$  is an LA-polygroup under the following hyperoperation:

$$t_i * t_j = \begin{cases} t_j, & \text{for } i = 1, \\ t_k, & \text{for } j = 1 \text{ and } k \equiv 2 - i \pmod{|Q_n|}, \\ Q_n, & \text{for } j \neq 1, i \neq 1, i = j, \\ Q_n \setminus \{t_1\}, & \text{for } j \neq 1, i \neq 1, i \neq j. \end{cases} \quad (2)$$

For  $n = 5$ , we have the Cayley (Table 2).

*Example 3* (see [24]). Consider  $L_1 = \{1, 2, 3, 4\}$  with the hyperoperation  $\circ$ , given in Table 3.

Then,  $L_1 = \langle \{1, 2, 3, 4\}, \circ, 1,^{-1} \rangle$  is an LA-polygroup.

*Notations.* All LA-polygroups are represented by  $L, M, N, \dots$  and the underlying sets are represented by  $L, M, N, \dots$ . Also,  $L^* = L \setminus \{e\}$  and  $A^{-1} = \{a^{-1} : a \in A\}$ . Now, we establish two new extensions for making LA-polygroups.

*2.1. (I) Extension of an LA-Polygroup by a Set:  $L\{T\}$ .* Suppose that  $\langle L, \circ, e^{-1} \rangle$  is an LA-polygroup and  $L \cap T = \emptyset$ , where  $T$  is a nonempty set. Put  $M = L \cup T$ ,  $e \cup d = d$ , for every  $d \in M$  and  $\forall d, f \in M^* = \{d \in M : d \neq e\}$ ; we define

$$d^{-1} = \begin{cases} d^{-1}, & \text{if } d \in L, \\ d, & \text{if } d \in T, \end{cases}$$

$$d \cup e = \begin{cases} d \circ e, & \text{if } d \in L, \\ d, & \text{if } d \in T, \end{cases} \quad (3)$$

$$d \cup f = \begin{cases} (d \circ f) \cup T, & \text{if } d, f \in L, \\ L \cup T, & \text{if } d = f \in T, \\ M^*, & \text{otherwise.} \end{cases}$$

The system  $\langle M, \cup, e^{-1} \rangle$  is known as the extension of LA-polygroup  $L$  by a set  $T$  and represented by  $L\{T\}$ .

**Theorem 1.** Let  $\langle L, \circ, e^{-1} \rangle$  be an LA-polygroup and  $T$  be a nonempty set such that  $L \cap T = \emptyset$ . Then,  $L\{T\}$  is an LA-polygroup.

TABLE 2: LA-polygroup.

*	$t_1$	$t_2$	$t_3$	$t_4$	$t_5$
$t_1$	$t_1$	$t_2$	$t_3$	$t_4$	$t_5$
$t_2$	$t_5$	$Q_n$	$Q_n \setminus \{t_1\}$	$Q_n \setminus \{t_1\}$	$Q_n \setminus \{t_1\}$
$t_3$	$t_4$	$Q_n \setminus \{t_1\}$	$Q_n$	$Q_n \setminus \{t_1\}$	$Q_n \setminus \{t_1\}$
$t_4$	$t_3$	$Q_n \setminus \{t_1\}$	$Q_n \setminus \{t_1\}$	$Q_n$	$Q_n \setminus \{t_1\}$
$t_5$	$t_2$	$Q_n \setminus \{t_1\}$	$Q_n \setminus \{t_1\}$	$Q_n \setminus \{t_1\}$	$Q_n$

TABLE 3: LA-polygroup.

$\circ$	1	2	3	4
1	1	2	3	4
2	4	{2, 3, 4}	{2, 4}	{1, 2, 3}
3	3	{2, 4}	{1, 3}	{2, 4}
4	2	{1, 3, 4}	{2, 4}	{2, 3, 4}

*Proof.* Suppose that  $L\{T\} = M$ ,  $L \cup T = M$ ,  $L \cap T = \emptyset$ , and  $d, f, w \in M$ . If  $\{d, f, w\} \subseteq L^*$ , then

$$\begin{aligned} (d \uplus f) \uplus w &= [(d \circ f) \circ w \cup T] \cup M^* \\ &= [(w \circ f) \circ d \cup T] \cup M^* \\ &= (w \uplus f) \uplus d. \end{aligned} \quad (4)$$

If exactly one of  $d, f, w \in L$  is equal to the left identity, then

$$(d \uplus f) \uplus w = (d \circ f) \circ w \cup T = (w \circ f) \circ d \cup T = (w \uplus f) \uplus d. \quad (5)$$

If exactly two of  $d, f, w \in L$  are equal to the left identity, then

$$(d \uplus f) \uplus w = (d \circ f) \circ w = (w \circ f) \circ d = (w \uplus f) \uplus d. \quad (6)$$

If  $\{d, f, w\} \not\subseteq L$ , then  $(d \uplus f) \uplus w = M = (w \uplus f) \uplus d$ . Thus, left invertive law holds. Now, we prove axiom (v) of Definition 5. Let  $d, f, w \in M$  such that  $w \in d \uplus f$ , then

*Case 1.* If  $d, f, w \in L$ , then we have done.

$$\begin{aligned} d^{-1} &= \begin{cases} d^{-1}, & \text{if } d \in L, \\ d, & \text{if } d \in T, \end{cases} \\ d \uplus e &= \begin{cases} d \circ e, & \text{if } d \in L, \\ d, & \text{if } d \in T, \end{cases} \\ d \uplus f &= \begin{cases} d \circ f, & \text{if } d, f \in L, \\ t_i, & \text{if } d \in L, f = t_i \in T \text{ OR } d = t_i \in T, f \in L \text{ where } 1 \leq i \leq n, \\ t_i, & \text{if } d = t_i, f = t_j \in T \text{ where } i > j, \\ t_j, & \text{if } d = t_i, f = t_j \in T \text{ where } i < j, \\ L, & \text{if } d = t_1 = f \in T, \\ L \cup A_i, & \text{if } d = t_{i+1} = f \in T \text{ where } 1 \leq i \leq n-1, \end{cases} \end{aligned} \quad (8)$$

*Case 2. (a)* If  $w \in L^*$ , then we have the following possibilities:

- (i) If  $d \in T$  and  $f \in L^*$ , then  $T \subseteq w \uplus f^{-1} \Rightarrow d \in w \uplus f^{-1}$ ;
- (ii) If  $f \in T$  and  $d \in L^*$ , then  $d \in w \uplus f^{-1} = w \uplus f = M^* \Rightarrow d \in w \uplus f^{-1}$ ;
- (iii) If  $d, f \in T$ , then  $d \in w \uplus f^{-1} = w \uplus f = M^* \Rightarrow d \in w \uplus f^{-1}$ .

*Case 2. (b)* If  $w = e$ , then  $w \in d \uplus f \Rightarrow d = f^{-1}$  and  $w \uplus f^{-1} = e \uplus d = \{d\} \Rightarrow d \in w \uplus f^{-1}$ .

*Case 3. (a)* If  $w \notin L$  and  $d, f \in M^*$ , then

$$\begin{cases} w \uplus f^{-1} = M^*, & \text{if } w \neq f, \\ w \uplus f^{-1} = M, & \text{if } w = f. \end{cases} \quad (7)$$

Hence,  $d \in w \uplus f^{-1}$ .

*Case 3. (b)* If  $w \notin L$  and  $d = e$ , then  $w \in d \uplus f \Rightarrow w = f \in T$  and  $w \uplus f^{-1} = f \uplus f^{-1} = f \uplus f = M$ , hence  $d \in w \uplus f^{-1}$ .

*Case 3. (c)* If  $w \notin L$  and  $f = e$ , then

$w \in d \uplus f = \{d\} \Rightarrow w = d$  and  $w \uplus f^{-1} = \{w\} = \{d\}$ , hence  $d \in w \uplus f^{-1}$ .

Thus, condition (v) of Definition 5 holds and hence the theorem is proved.  $\square$

*Example 4.* Let  $\mathbf{L}_2 = \langle \{1, 2, 3, 4\}, \circ, 1, {}^{-1} \rangle$  be an LA-polygroup with the Cayley (Table 4).

Then,  $\mathbf{M}_2 = \mathbf{L}_2\{\{5, 6\}\}$  is an LA-polygroup with six elements and the Cayley (Table 5), where  $M_2 = \{1, 2, 3, 4, 5, 6\}$ .

*2.2. (II) Extension of an LA-Polygroup by a Set:  $\mathbf{L}\{T\}^\diamond$ .* Suppose that  $\langle L, \circ, e, {}^{-1} \rangle$  is an LA-polygroup and  $L \cap T = \emptyset$ , where  $T$  is a nonempty set such that  $T = \cup_{i=1}^n t_i$  (ordered from left to right, i.e.,  $t_1, t_2, t_3, \dots, t_n$ ). Put  $L \cup T = M$  and  $e \uplus d = d, \forall d \in M$ . We define

TABLE 4: LA-polygroup.

$\circ$	1	2	3	4
1	1	2	3	4
2	3	{2, 3}	{1, 2}	4
3	2	{1, 3}	{2, 3}	4
4	4	4	4	{1, 2, 3}

TABLE 5: LA-polygroup.

$\uplus$	1	2	3	4	5	6
1	1	2	3	4	5	6
2	3	{2, 3, 5, 6}	{1, 2, 5, 6}	{4, 5, 6}	$M_2^*$	$M_2^*$
3	2	{1, 3, 5, 6}	{2, 3, 5, 6}	{4, 5, 6}	$M_2^*$	$M_2^*$
4	4	{4, 5, 6}	{4, 5, 6}	{1, 2, 3, 5, 6}	$M_2^*$	$M_2^*$
5	5	$M_2^*$	$M_2^*$	$M_2^*$	$M_2^*$	$M_2^*$
6	6	$M_2^*$	$M_2^*$	$M_2^*$	$M_2^*$	$M_2^*$

Note that  $M_2^* = M_2 \setminus \{1\} = \{2, 3, 4, 5, 6\}$ .

where  $A_i = \cup_{h=1}^i \{t_h\}$ . The system  $\langle M, \uplus, e, {}^{-1} \rangle$  is known as the extension of LA-polygroup  $\mathbf{L}$  by a set  $T$  and represented by  $\mathbf{L}\{T\}^\diamond$ .

**Theorem 2.** Let  $\langle L, \circ, e, {}^{-1} \rangle$  be an LA-polygroup and  $T$  be a nonempty set such that  $L \cap T = \emptyset$ . Then,  $\mathbf{L}\{T\}^\diamond$  is an LA-polygroup.

$$\begin{aligned} (d \uplus f) \uplus w &= (s_i \uplus s_j) \uplus s_k = s_i \uplus s_i = (s_k \uplus s_j) \uplus s_i = (w \uplus f) \uplus d, & \text{if } k < i = j \neq 1, \\ (d \uplus f) \uplus w &= (s_i \uplus s_j) \uplus s_k = s_k = (s_k \uplus s_j) \uplus s_i = (w \uplus f) \uplus d, & \text{if } k > i = j, \end{aligned} \quad (11)$$

(iii) such that  $j = k$ , then

$$\begin{aligned} (d \uplus f) \uplus w &= (s_i \uplus s_j) \uplus s_k = s_j \uplus s_j = (s_k \uplus s_j) \uplus s_i = (w \uplus f) \uplus d, & \text{if } i < j = k \neq 1, \\ (d \uplus f) \uplus w &= (s_i \uplus s_j) \uplus s_k = s_i = (s_k \uplus s_j) \uplus s_i = (w \uplus f) \uplus d, & \text{if } i > j = k. \end{aligned} \quad (12)$$

Thus, left invertive law holds. Now, we prove axiom (v) of Definition 5. Let  $d, f, w \in M$  such that  $w \in d \uplus f$ . Then, we consider the following cases:

*Case 1.* If  $w \in T$ , then either  $w = d \in T$  or  $w = f \in T$  or  $s_1 \neq d = f \in T$ :

- (i) If  $w = d \in T$ , then  $d \in w \uplus f^{-1} = d \uplus f^{-1} = \{d\}$ ,
- (ii) If  $w = f \in T$  and  $d \in L$ , then  $L \subseteq f \uplus f = w \uplus f^{-1} \Rightarrow d \in w \uplus f^{-1}$ ; if  $w = f \in T$  and  $d \in T$ , then  $w = f = s_j$  ( $j \neq 1$ ) and  $L \cup A_{j-1} \subseteq w \uplus f^{-1} \Rightarrow d \in w \uplus f^{-1}$ ,
- (iii) If  $s_1 \neq d = f \in T$ , then  $w \uplus f^{-1} = w \uplus f = f = d \Rightarrow d \in w \uplus f^{-1}$ .

*Case 2.* If  $w \in L$ , then  $d = f \in T$  and  $w \uplus f^{-1} = w \uplus f = f = d \Rightarrow d \in w \uplus f^{-1}$ .

*Proof.* Suppose that  $\mathbf{L}\{T\}^\diamond$ ,  $L \cup T = M$ ,  $L \cap T = \emptyset$ , and  $d, f, w \in M$ .

If  $\{d, f, w\} \subseteq L$ , then clearly left invertive law holds.

If  $\{d, f, w\} \not\subseteq L$ , then we consider the following cases:

*Case 1.* If  $w \notin L$  and  $d, f \in L$ , then  $(w \uplus f) \uplus d = w = (d \uplus f) \uplus w$ .

*Case 2.* If  $w = s_k$ ,  $f = s_j \notin L$ , and  $d \in L$ , then

$$\begin{aligned} (d \uplus f) \uplus w &= w \uplus w = (w \uplus f) \uplus d, & \text{if } k = j, \\ (d \uplus f) \uplus w &= w = (w \uplus f) \uplus d, & \text{if } k > j, \\ (d \uplus f) \uplus w &= f = (w \uplus f) \uplus d, & \text{if } k < j, \end{aligned} \quad (9)$$

*Case 3.* If  $w = s_k$ ,  $f = s_j$ ,  $d = s_i \notin L$  in the following way:

(i) such that  $k > j > i$ , then

$$\begin{aligned} (d \uplus f) \uplus w &= (s_i \uplus s_j) \uplus s_k = s_k \\ &= (s_k \uplus s_j) \uplus s_i = (w \uplus f) \uplus d, \end{aligned} \quad (10)$$

(ii) such that  $i = j$ , then

Thus, condition (v) of Definition 5 holds and hence the theorem is proved.  $\square$

*Example 5.* Let  $\mathbf{L}_3 = \langle \{1, 2, 3\}, \circ, 1, {}^{-1} \rangle$  be an LA-polygroup with the Cayley (Table 6).

Then,  $\mathbf{M}_3 = \mathbf{L}_3 \{ \{4, 5\} \}^\diamond$  is an LA-polygroup with five elements and the Cayley (Table 7), where  $M_3 = \{1, 2, 3, 4, 5\}$ .

This is an LA-polygroup and not a polygroup.

### 3. Cayley Graphs over LA-Groups and LA-Polygroups

*Definition 6.* Suppose that  $\mathbf{G}$  is an LA-group and  $C$  is a subset of  $G$  such that



TABLE 6: LA-polygroup.

$\circ$	1	2	3
1	1	2	3
2	3	{2, 3}	{1, 2, 3}
3	2	{1, 2, 3}	{2, 3}

TABLE 7: LA-polygroup.

$\circ$	1	2	3	4	5
1	1	2	3	4	5
2	3	{2, 3}	{1, 2, 3}	4	5
3	2	{1, 2, 3}	{2, 3}	4	5
4	4	4	4	{1, 2, 3}	5
5	5	5	5	5	{1, 2, 3, 4}

- (i)  $1 \notin C$ ,
- (ii)  $C^{-1} = C$ ; then, Cayley graph  $\text{Cay}(\mathbf{LAG}, C)$  of  $\mathbf{G}$  relative to  $C$  is the simple graph which has vertex set  $G$  and edge set

$$D = \{\{g, gs\} | g \neq gs, \text{ where } g \in G \text{ and } s \in C\}. \quad (13)$$

*Example 6.* The Cayley graphs of the LA-group  $\mathbf{G}_5 = (\{t_1, t_2, t_3, t_4, t_5\}, *)$  given in Example 1, with connection sets  $\{t_2\}$  and  $\{t_2, t_3\}$ , are shown in Figures 1 and 2. For  $C = \{t_2\}$ , we have

$$\begin{aligned} \{t_1, t_1 * t_2\} &= \{t_1, t_2\} \{t_2, t_2 * t_2\} \\ &= \{t_2, t_1\} \{t_3, t_3 * t_2\} \\ &= \{t_3, t_5\} \{t_4, t_4 * t_2\} \\ &= \{t_4, t_4\} \{t_5, t_5 * t_2\} \\ &= \{t_5, t_3\}. \end{aligned} \quad (14)$$

For  $C = \{t_2, t_3\}$ , we have

$$\begin{aligned} \{t_1, t_1 * t_2\} &= \{t_1, t_2\} \{t_3, t_3 * t_2\} \\ &= \{t_3, t_5\} \{t_1, t_1 * t_3\} \\ &= \{t_1, t_3\} \{t_4, t_4 * t_3\} \\ &= \{t_4, t_5\}. \end{aligned} \quad (15)$$

*Definition 7.* Given an LA-polygroup  $\mathbf{L} = \langle L, \circ, e, {}^{-1} \rangle$  and  $L \subseteq C \neq \emptyset$  such that  $(C = C^{-1})$ , say the connection set. Then, we define the generalized Cayley graph over LA-polygroup  $\text{GCLAP}(\mathbf{L}; C)$  which is the simple graph having vertex set  $L$  and the edge set

$$D = \{\{d, f\} | d \neq f \text{ and } (d \circ e) \circ f \cap C \neq \emptyset\}. \quad (16)$$

If we have an LA-polygroup  $\mathbf{L}$  and a connection set  $C$  such that  $\text{GCLAP}(\mathbf{L}; C) \cong \Lambda$ , then the graph  $\Lambda$  is known as a *GCLAP-graph*.

Here, we give few examples of GCLAP-graphs.

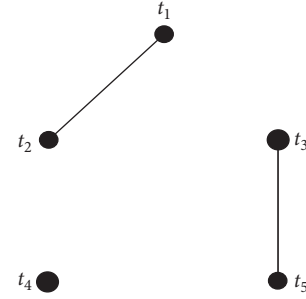


FIGURE 1:  $\text{Cay}(\mathbf{LAG}_5, \{t_2\})$ .

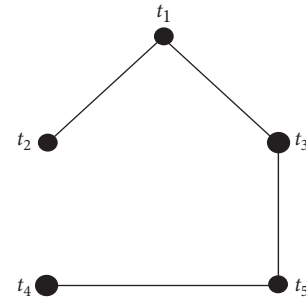


FIGURE 2:  $\text{Cay}(\mathbf{LAG}_5, \{t_2, t_3\})$ .

*Example 7.* The generalized Cayley graph of the left almost polygroup  $\mathbf{L}_4 = \langle \{1, 2, 3, 4\}, \circ, 1, {}^{-1} \rangle$ , with connection set  $C = \{3, 4\}$  which is shown in Figure 3, where " $\circ$ " is defined in Table 8.

*Example 8.* The generalized Cayley graph of the left almost polygroup  $\mathbf{L}_5 = \langle \{1, 2, 3, 4, 5\}, \circ, 1, {}^{-1} \rangle$  with connection set  $\{2, 3\}$  which is shown in Figure 4, where " $\circ$ " is defined in Table 9.

#### 4. Which Simple Graphs Are GCLAP-Graphs?

First, we point out a few types of simple graphs that are GCLAP-graphs. After that, we infer that each simple graph of order three, four, and five (except cycle graph of order five which may or may not be a GCLAP-graph) is a GCLAP-graph.

**Lemma 1.** *Every Cayley graph is a GCLAP-graph.*

*Proof.* Since every LA-group is an LA-polygroup, therefore, by Definition 7, the result holds.  $\square$

**Lemma 2.** *Every complete graph of order at least three is a GCLAP-graph.*

*Proof.* Let  $\langle Q_n, *, t_1^{-1} \rangle$  be an LA-polygroup, where  $n \geq 3$  (as defined in Example 2). Then,  $\text{GCLAP}(Q_n; Q_n \setminus \{t_1\})$  are isomorphic to the complete graphs on  $n$  vertices, where  $n \geq 3$ . Hence, it is proved.  $\square$

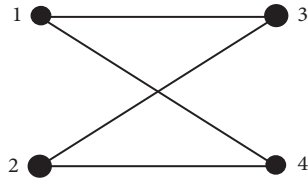


FIGURE 3:  $\text{GCLAP}(\mathbf{L}_4; \{3, 4\})$ .

TABLE 8: LA-polygroup.

$\circ$	1	2	3	4
1	1	2	3	4
2	3	{1, 2, 3}	{2, 3, 4}	2
3	2	{2, 3, 4}	{1, 2, 3}	3
4	4	3	2	1

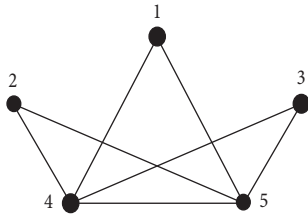


FIGURE 4:  $\text{GCLAP}(\mathbf{L}_5; \{4, 5\})$ .

TABLE 9: LA-polygroup.

$\circ$	1	2	3	4	5
1	1	2	3	4	5
2	3	{2, 3}	{1, 2}	4	5
3	2	{1, 3}	{2, 3}	4	5
4	4	4	4	{1, 2, 3, 4, 5}	{4, 5}
5	5	5	5	{4, 5}	{1, 2, 3, 4, 5}

**Lemma 3.** Show that each star graph of order at least three is a GCLAP-graph.

*Proof.* Suppose that  $\mathbf{L} = \mathbf{G}_n\{t_{n+1}\}^\diamond$ , where  $n \geq 3$  and  $\mathbf{G}_n$  is defined in Example 1. Then, Cayley table for  $\mathbf{L}$  is given in Table 10.

Now, by considering connection set  $C = \{t_{n+1}\}$ , we can see that  $S_n \cong \text{GCLAP}(\mathbf{L}; C)$ .  $\square$

**Lemma 4.** If  $\Phi$  is a GCLAP-graph. Then, show that  $\Phi \cup nK_1$  is also a GCLAP-graph, where  $n \geq 1$ .

*Proof.* Let  $\Phi$  be a GCLAP-graph. Then, we have a left almost polygroup  $\mathbf{L}$  and a connection set  $C$  such that  $\Phi \cong \text{GCLAP}(\mathbf{L}; C)$ . Suppose that  $\Phi_n = \Phi \cup nK_1$  and  $Z_m = \cup_{t=1}^m \{z_t\}$ . By Extension (III) and Definition 7, we have  $\Phi_1 \cong \text{GCLAP}(\mathbf{L}\{Z_1\}^\diamond; C)$ . Now, by using induction,  $\Phi_m \cong \text{GCLAP}(\mathbf{Q}; C)$ , where  $\mathbf{Q} = \mathbf{L}\{Z_m\}^\diamond$  and  $C$  is a connection set. Hence,  $\Phi_{m+1} \cong \text{GCLAP}(\mathbf{Q}\{z_{m+1}\}^\diamond; C)$ . Thus,  $\Phi_n$  is a GCLAP-graph for every  $n \in \mathbb{N}$ .  $\square$

TABLE 10: LA-polygroup.

$\circ$	$t_1$	$t_2$	$\cdot$	$\cdot$	$\cdot$	$t_n$	$t_{n+1}$
$t_1$							$t_{n+1}$
$t_2$							$t_{n+1}$
$\cdot$			$\mathbf{G}_n$				$\cdot$
$\cdot$							$\cdot$
$t_n$							$t_{n+1}$
$t_{n+1}$	$t_{n+1}$	$t_{n+1}$	$\cdot$	$\cdot$	$\cdot$	$t_{n+1}$	$\{t_1, t_2, t_3, \dots, t_n\}$

**Definition 8.** Let  $m \in \{1, 2, 3, \dots\}$  and  $q \in \{2, 3, 4, \dots, m-1\}$ . Then, the  $(m, q)$ -pseudo complete graph is known as the complement of the graph  $S_q \cup N_{m-q}$  and represented by  $\widehat{U}(m, q)$ . A graph  $\Phi$  is known as a pseudocomplete graph if  $\Phi \cong \widehat{U}(m, q)$  for some  $m \in \{1, 2, 3, \dots\}$  and  $q \in \{2, 3, 4, \dots, m-1\}$ .

**Example 9.** Pseudocomplete graphs on five vertices are shown in Figure 5.

**Lemma 5.** If  $m \in \{1, 2, 3, \dots\}$  and  $b, q \in \{2, 3, \dots, m-1\}$ , then the following statements hold:

- (i)  $\widehat{U}(m, q)$  is connected,
- (ii) If  $q \neq b$  then  $\widehat{U}(m, q) \neq \widehat{U}(m, b)$ ,
- (iii) A connected graph  $\Phi$  of order  $m$  is a pseudocomplete graph  $\Leftrightarrow$ ; it contains  $K_{m-1}$  as a subgraph.

**Lemma 6.** All pseudocomplete graphs are GCLAP-graphs.

*Proof.* Let  $\Phi = \widehat{U}(m, q)$  be a pseudocomplete graph, where  $m \geq 1$  and  $q \in \{2, 3, 4, \dots, m-1\}$ . Consider the LA-polygroup  $\mathbf{L} = \mathbf{Q}_3\{\{4, 5, 6, \dots, m\}\}$ , where  $\mathbf{Q}_3 = \langle \{1, 2, 3\}, *, 1,^{-1} \rangle$ , given in Example 2, and the connection set  $C = \{q+1, q+2, \dots, m\}$ . Then,  $\text{GCLAP}(\mathbf{L}; C)$  is isomorphic to the graph  $S_q \cup N_{m-q}$ . Hence,  $\widehat{U}(m, q) \cong \text{GCLAP}(\mathbf{L}; C)$ .  $\square$

**Definition 9.** The expansion of the graph  $\Phi$ , represented by  $\Phi^+$ , is the join of the graph  $\Phi$  and  $K_1$ , i.e.,  $\Phi^+ = \Phi \vee K_1$ .

**Lemma 7.** Show that the expansion of a GCLAP-graph is a GCLAP-graph.

*Proof.* Let  $\Lambda \cong \text{GCLAP}(\mathbf{L}; C)$ , where  $\mathbf{L}$  is a left almost polygroup having  $n$  elements and  $C$  is a connection set. Suppose that  $\mathbf{Q} = \mathbf{L}\{n+1\}^\diamond$  and  $C' = C \cup \{n+1\}$ . Then,  $\Phi^+ \cong \text{GCLAP}(\mathbf{Q}; C')$ .  $\square$

**Definition 10.** Let  $\Phi = (G, D)$  be a graph,  $g \in G$ , and  $f \notin G$ . The faulty join graph, represented by  $\nabla_g$ , is the graph such that  $\nabla_g(\Phi, f) = (G', D')$ , where  $G' = G \cup \{f\}$  and  $D' = D \cup \{\{f, h\} : g \neq h \in G\}$ . Moreover, a graph is known as  $\nabla_1$ -graph if it is isomorphic to  $\nabla_1(\Phi, f)$ , where  $\Phi = \text{GCLAP}(\mathbf{L}; C)$  such that  $\mathbf{L}$  is a left almost polygroup having  $n$  elements,  $f \notin L$ , and  $C$  is a connection set.

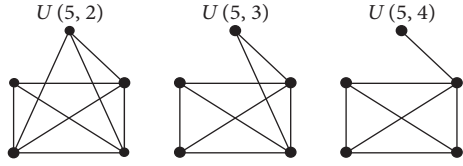


FIGURE 5: Pseudocomplete graphs on five vertices.

**Lemma 8.** Every  $\nabla_1$ -graph is a GCLAP-graph.

*Proof.* Suppose that  $\Lambda$  is a  $\nabla_1$ -graph having  $n$  vertices. So, we have a left almost polygroup  $\mathbf{L}$  having  $n$  elements and a connection set  $C$  such that  $\Lambda \cong \nabla_1(\text{GCLAP}(\mathbf{L}; C), n + 1)$ . Let  $\mathbf{L}\{\{n + 1\}\} = \mathbf{Q}$ , then we have

$$\nabla_1(\text{GCLAP}(\mathbf{L}; C), n + 1) \cong \text{GCLAP}(\mathbf{Q}; C). \quad (17)$$

Hence,  $\Lambda$  is a GCLAP-graph.

Up to here, we have determined a few types of GCLAP-graphs. Now, we confine ourselves to the graphs of order at most five (except cycle graph of order five) and show that every simple graph of order three, four, and five (except cycle graph of order five which may or may not be a GCLAP-graph) is a GCLAP-graph. In Appendix, we have shown all simple connected graphs of order three, four, and five (except cycle graph of order five) and denote them by  $\Omega_1, \Omega_2, \dots, \Omega_{28}$ .

**Theorem 3.** All simple graphs of order three, four, and five (except cycle graph of order five which may or may not be a GCLAP-graph) are GCLAP-graphs.

*Proof.* Suppose that  $\Phi$  is a simple graph of order three, four, and five (except cycle graph of order five). Then, as per the connectivity of  $\Phi$ , two cases can be thought of:

*Case 1.* If  $\Phi$  is a connected graph, then we have six subcases:

- Subcase (i) (cycles and complete graphs): Consider the LA-polygroup  $\mathbf{L}_4$  as in Example 7. Then,  $\text{GCLAP}(\mathbf{L}_4; \{3, 4\}) \cong \Omega_5$ , so  $\Omega_5$  is a GCLAP-graph. Also, since  $\Omega_2, \Omega_8$ , and  $\Omega_{28}$  are complete graphs, therefore, by Lemma 2, they are GCLAP-graphs.
- Subcase (ii) (star graphs): Think about LA-polygroup  $\mathbf{L}_3$  as given in Example 5, then  $\text{GCLAP}(\mathbf{L}_3; \{2\}) \cong \Omega_1$ . Also, since  $\Omega_4$  and  $\Omega_9$  are star graphs, so by Lemma 3, they are GCLAP-graphs.
- Subcase (iii) (path graphs): Consider the LA-polygroup  $\mathbf{L}_4$  and LA-group  $\mathbf{G}_5$  as defined in Examples 7 and 6, respectively. Then,  $\Omega_3 \cong \text{GCLAP}(\mathbf{L}_4; \{2\})$ , so  $\Omega_3$  is a GCLAP-graph. Also, since  $\text{Cay}(\mathbf{LAG}_5, \{t_2, t_3\}) \cong \Omega_{11}$ , therefore, by Lemma 1,  $\Omega_{11}$  is a GCLAP-graph.
- Subcase (iv) (pseudocompleted graphs): Definition 8 implies that  $\Omega_6, \Omega_7, \Omega_{22}, \Omega_{25}$ , and  $\Omega_{27}$  are pseudocomplete graphs and by Lemma 6, they are GCLAP-graphs.

TABLE 11: LA-polygroup.

$\circ$	1	2	3	4
1	1	2	3	4
2	3	{2, 3, 4}	{1, 2, 4}	{2, 3}
3	2	{1, 3, 4}	{2, 3, 4}	{2, 3}
4	4	{2, 3}	{2, 3}	{1, 4}

Subcase (v) (expansion graphs): Think about the LA-polygroup  $\mathbf{L}_4$  as in Example 7 and  $\mathbf{L}_6 = \langle \{1, 2, 3, 4\}, \circ, 1, -^1 \rangle$ , given in Table 11.

$$\begin{aligned} \Omega_{12} &\cong (\text{GCLAP}(\mathbf{L}_4; \{4\}))^+, \\ \Omega_{16} &\cong (\Omega_1 \cup K_1)^+, \\ \Omega_{17} &\cong (\text{GCLAP}(\mathbf{L}_6; \{4\}))^+, \\ \Omega_{21} &\cong \Omega_4^+, \\ \Omega_{23} &\cong \Omega_3^+, \\ \Omega_{26} &\cong \Omega_5^+. \end{aligned} \quad (18)$$

Definition 9 and above cases suggest that the graphs  $\Omega_{12}, \Omega_{16}, \Omega_{17}, \Omega_{21}, \Omega_{23}$ , and  $\Omega_{26}$  are expansion graphs of GCLAP-graphs and by Lemma 7, we infer that they are GCLAP-graphs.

Subcase (vi) ( $\nabla_1 0$  graphs):

Consider three LA-polygroups  $\mathbf{L}_4, \mathbf{L}_2$ , and  $\mathbf{L}_1$  as in Example 7, Example 4, and Example 3, respectively, then the following isomorphisms hold:

$$\begin{aligned} \Omega_{10} &\cong \nabla_1(\text{GCLAP}(\mathbf{L}_4; \{4\}), 5), \\ \Omega_{13} &\cong \nabla_1(\text{GCLAP}(\mathbf{L}_2; \{2\}), 5), \\ \Omega_{14} &\cong \nabla_1(\text{GCLAP}(\mathbf{L}_1; \{3\}), 5), \\ \Omega_{18} &\cong \nabla_1(\text{GCLAP}(\mathbf{L}_4; \{2\}), 5), \\ \Omega_{24} &\cong \nabla_1(\text{GCLAP}(\mathbf{L}_4; \{2, 4\}), 5). \end{aligned} \quad (19)$$

Thus, the graphs  $\Omega_{10}, \Omega_{13}, \Omega_{14}, \Omega_{18}$ , and  $\Omega_{24}$  are  $\nabla_1$ -graphs. By Lemma 8, we conclude that they are GCLAP-graphs. In the end, if we consider the left almost group  $\mathbf{G}_5$  given in Example 6 and LA-polygroup,  $\mathbf{L}_7 = \langle \{1, 2, 3, 4, 5\}, \circ, 1, -^1 \rangle$  with the Cayley (Table 12). Then, by Lemma 1, we conclude that  $\Omega_{19} \cong \text{Cay}(\mathbf{LAG}_5; \{a_2, a_3, a_5\})$  and hence the following isomorphisms hold:

$$\begin{aligned} \Omega_{15} &\cong \text{GCLAP}(\mathbf{L}_7; \{3, 5\}), \\ \Omega_{20} &\cong \text{GCLAP}(\mathbf{L}_7; \{3, 4\}). \end{aligned} \quad (20)$$

Thus, all simple connected graphs of order three, four, and five (except cycle graph of order five which may or may not be a GCLAP-graph) are GCLAP-graphs.

*Case 2.* If  $\Phi$  is not connected. We have two subcases: Subcase (i): if  $\Phi$  contains two nontrivial parts, then  $\Phi$  is isomorphic to  $K_2 \cup K_2, K_2 \cup \Omega_1$ , and  $K_2 \cup \Omega_2$ . We have  $K_2 \cup K_2 \cong \text{GCLAP}(\mathbf{L}_1; \{3\})$ ,  $K_2 \cup \Omega_1 \cong \text{GCLAP}(\mathbf{L}_7;$

TABLE 12: LA-polygroup.

$\circ$	1	2	3	4	5
1	1	2	3	4	5
2	2	1	3	4	5
3	4	4	{1,2}	5	3
4	3	3	5	{1,2}	4
5	5	5	4	3	{1,2}

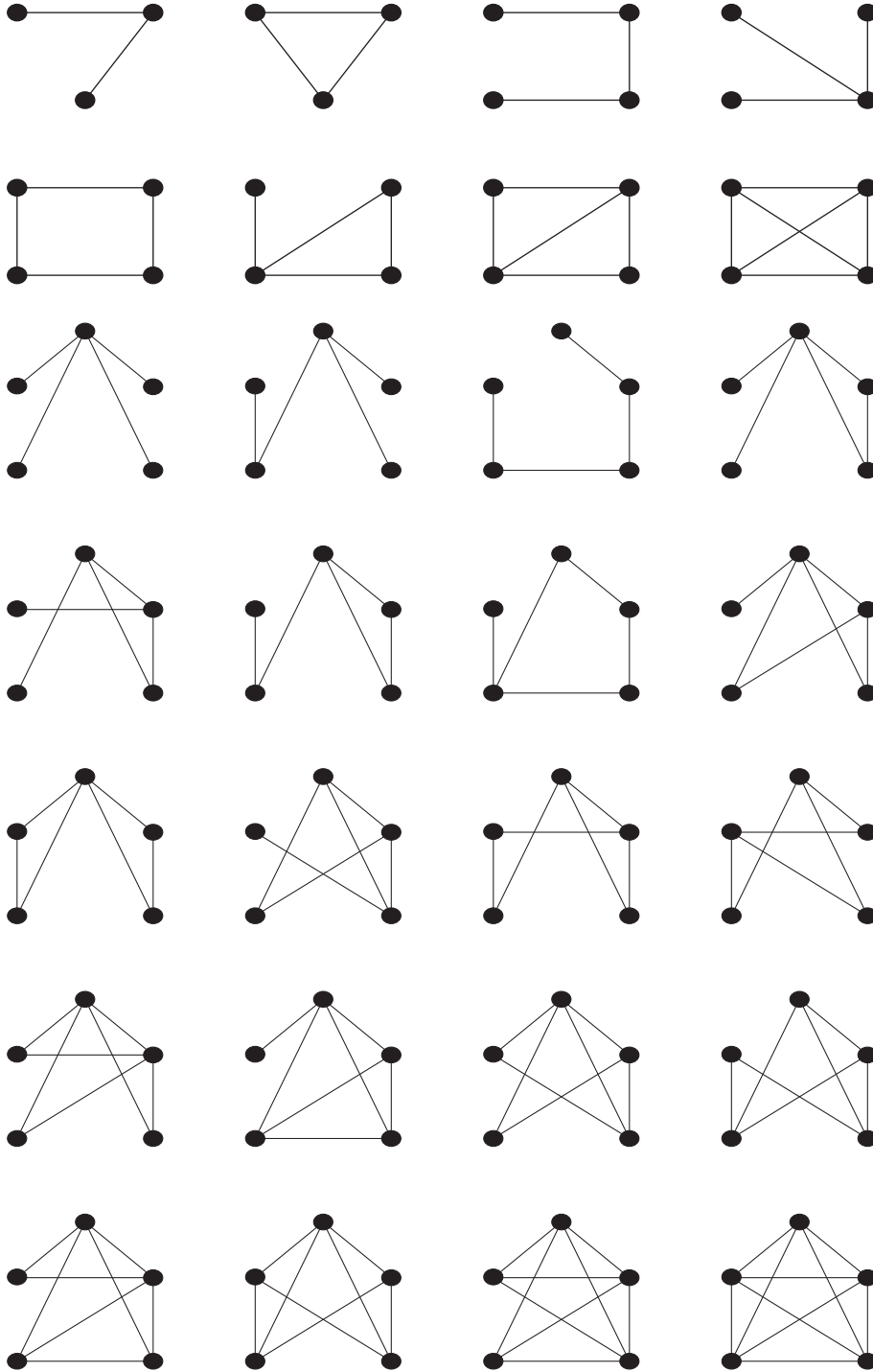


FIGURE 6: Connected simple graphs  $\Omega_1, \Omega_2, \Omega_3, \dots, \Omega_{28}$ .

$\{3\}$ ), and  $K_2 \cup \Omega_2 \cong \text{GCLAP}(\mathbf{L}_7; \{2, 5\})$ , where  $\mathbf{L}_1$  and  $\mathbf{L}_7$  are given in Example 3 and Subcase (vi), respectively. Subcase (ii): if  $K_1$  is a subgraph of  $\Phi$ , then  $\Phi \cong nK_1 \cup \Lambda$ , for  $n \geq 1$  and  $\Lambda$  is isomorphic to  $K_2 \cup K_2$  or isomorphic to  $\text{Cay}(\mathbf{LAG}_3, \{t_2\})$  or a connected graph of order  $< 5$ . By Lemma 4, we conclude that  $\Phi$  is a GCLAP – graph which completes the proof.  $\square$

The question that usually comes to mind is what happens if  $|\Phi| > 5$ ; we present this query as an open problem [28, 29].

## Appendix

There are 28 connected simple graphs of order three, four, and five (except cycle graph of order five) and they are denoted by  $\Omega_1, \Omega_2, \Omega_3, \dots, \Omega_{28}$  as given in Figure 6.

## Data Availability

No data were used to support this study.

## Conflicts of Interest

The authors of this paper declare that they have no conflicts of interest.

## Acknowledgments

This research was funded by the Deanship of Scientific Research at Princess Nourah Bint Abdulrahman University through the Fast-Track Research Funding Program.

## References

- [1] N. Biggs, E. K. Lloyd, and R. J. Wilson, *Graph Theory, 1736-1936*, Oxford University Press, Oxford, UK, 1986.
- [2] A. Cayley, "On the theory of groups," *Proceedings of the London Mathematical Society*, vol. 9, pp. 126–233, 1878.
- [3] P. S. Loh and L. J. Schulman, "Improved expansion of random cayley graphs," *Discrete Mathematics and Theoretical Computer Science*, vol. 6, pp. 523–528, 2004.
- [4] A. Lubotzky, "Cayley graphs: eigenvalues, expanders and random walks," in *Surveys in Combinatorics, 1995*, pp. 155–190, Cambridge University Press, Cambridge, UK, 1995.
- [5] J. Morris, "Connectivity of Cayley graphs: a special family," *Journal of Combinatorial Mathematics and Combinatorial Computing*, vol. 20, pp. 111–120, 1996.
- [6] M. H. Shahzamanian, M. Shirmohammadi, and B. Davvaz, "Roughness in Cayley graphs," *Information Sciences*, vol. 180, no. 17, pp. 3362–3372, 2010.
- [7] F. Marty, "Sur une generalization de la notion de groupe," in *Proceedings of the 8th Congress des Mathematiciens Scandinaves*, pp. 45–49, Stockholm, Sweden, 1934.
- [8] P. Corsini and V. Leoreanu, *Applications of Hyperstructure Theory*, Springer Science & Business Media, Berlin, Germany, 2013.
- [9] B. Davvaz, *Semihypergroup Theory*, Academic Press, Cambridge, MA, USA, 2016.
- [10] P. Corsini, *Prolegomena of Hypergroup Theory*, Aviani editore, Meerut, India, 1993.
- [11] B. Davvaz, *Hyperring Theory and Applications*, Bijan Davvaz Publications, Yazd, Iran, 2007.
- [12] B. Davvaz, *Polygroup Theory and Related Systems*, World Scientific Publishing Co Pte Ltd., Hackensack, NJ, USA, 2013.
- [13] T. Vougiouklis, *Hyperstructures and their representations*, Hadronic Press. Inc., Palm Harbor, FL, USA, 1994.
- [14] S. Ioulidis, "Polygroups et certains de leurs proprietes," *Bulletin of the Malaysian Mathematical Sciences Society*, vol. 39, no. 2, pp. 707–721, 1981.
- [15] S. M. Anvariye, S. Mirvakili, and B. Davvaz, "Combinatorial aspects of n-ary polygroups and n-ary color schemes," *European Journal of Combinatorics*, vol. 34, no. 2, pp. 207–216, 2013.
- [16] S. D. Comer, "Extension of polygroups by polygroups and their representations using color schemes," in *Universal Algebra and Lattice Theory*, pp. 91–103, Springer, Berlin, Germany, 1983.
- [17] S. D. Comer, "Polygroups derived from cogroups," *Journal of Algebra*, vol. 89, no. 2, pp. 397–405, 1984.
- [18] C. Berge and C. Berge, *Graphes et hypergraphes. 1970*, Dunod, Paris, France, 1967.
- [19] M. A. Kazim and M. Naseeruddin, "On almost semigroups," *The Align Bulletin Mathematics*, vol. 2, pp. 1–7, 1972.
- [20] Q. Mushtaq and M. S. Kamran, "On left almost groups," *Proceedings-Pakistan Academy of Sciences*, vol. 33, pp. 53–56, 1996.
- [21] K. Hila and J. Dine, "On hyperideals in left almost semihypergroups," *ISRN Algebra*, vol. 2011, Article ID 953124, 8 pages, 2011.
- [22] N. Yaqoob, P. Corsini, and F. Yousafzai, "On intra-regular left almost semihypergroups with pure left identity," *Journal of Mathematics*, vol. 2013, Article ID 510790, 10 pages, 2013.
- [23] V. Amjad, K. Hila, and F. Yousafzai, "Generalized hyperideals in locally associative left almost semihypergroups," *New York Journal of Mathematics*, vol. 20, 2014.
- [24] N. Yaqoob, I. Cristea, M. Gulistan, and S. Nawaz, "Left almost polygroups," *Italian Journal of Pure and Applied Mathematics*, vol. 39, pp. 465–474, 2018.
- [25] D. Heidari, M. Amooshahi, and B. Davvaz, "Generalized Cayley graphs over polygroups," *Communications in Algebra*, vol. 47, no. 5, pp. 2209–2219, 2019.
- [26] J. A. Bondy and U. S. R. Murty, *Graph Theory with Applications*, Vol. 290, Macmillan, London, UK, 1976.
- [27] V. I. Voloshin, *Introduction to Graph and Hypergraph Theory*, Nova Science Publishers, Hauppauge, New York, USA, 2009.
- [28] D. J. Robinson, *A Course in the Theory of Groups*, Springer Science & Business Media, Berlin, Germany, 2012.
- [29] G. Smith and O. Tabachnikova, *Topics in Group Theory*, Springer Science & Business Media, Berlin, Germany, 2000.

## Research Article

# The Role of Motivation and Desire in Explaining Students' VR Games Addiction: A Cognitive-Behavioral Perspective

Xuesong Zhai <sup>1,2</sup>, Fahad Asmi <sup>3</sup>, Jing Yuan,<sup>4</sup> Muhammad Azfar Anwar,<sup>5</sup>  
Nabia Luqman Siddiquei,<sup>6</sup> Intikhab Ahmad <sup>3,7</sup> and Rongting Zhou <sup>3,8</sup>

<sup>1</sup>College of Education, Zhejiang University, Hangzhou, China

<sup>2</sup>Anhui Province Key Laboratory of Intelligent Building and Building Energy Savings, Anhui Jianzhu University, Hefei, China

<sup>3</sup>University of Science and Technology of China, Hefei, China

<sup>4</sup>Quality-Oriented Education Research Center, Anhui Xinhua University, Hefei, China

<sup>5</sup>Shenzhen University, Shenzhen, China

<sup>6</sup>Virtual University of Pakistan, Lahore, Pakistan

<sup>7</sup>Bahria University Islamabad Campus, Islamabad, Pakistan

<sup>8</sup>Key Laboratory of Immersive Media Technology (Wanxin Media), Ministry of Culture and Tourism, Hefei, China

Correspondence should be addressed to Intikhab Ahmad; [intikhabahmad@mail.ustc.edu.cn](mailto:intikhabahmad@mail.ustc.edu.cn) and Rongting Zhou; [rongting@ustc.edu.cn](mailto:rongting@ustc.edu.cn)

Received 21 January 2021; Revised 7 March 2021; Accepted 9 April 2021; Published 8 May 2021

Academic Editor: Ali Ahmad

Copyright © 2021 Xuesong Zhai et al. This is an open access article distributed under the Creative Commons Attribution License, which permits unrestricted use, distribution, and reproduction in any medium, provided the original work is properly cited.

Virtual Reality games create an interactive platform for gaming and education for young people. While some longitudinal study has studied the beneficial effects of VR games on learning, the problematic use of VR games by a significant number of learners has become increasingly serious. The current study investigated the mediating effect of behavioral desire and moderation of cyber aggression on consumers' VAD, which contributes to behavioral and psychological urge to use VR games. Data are from 367 VR games users collected. Findings suggest that behavioral desire influences addictive behavior in the presence of a positive flow experience. Furthermore, theoretical and practical implications in the context of VR-based games are also discussed in this current research.

## 1. Introduction

Virtual Reality (VR) games consist of devices that monitor the behavior of users and react to the sensory world, intended to replicate the physical world. In recent innovations, VR has been made available to a broad customer market and has widened its coverage to cover fitness, arts, and entertainment as commercial value. It is also believed that the entertainment industry will adopt VR technology more frequently in the near future. Besides, scientific research and theorizing of VR culture are expanding along with VR technology advances [1]. Moreover, the Games industry is intending to adopt immersive technology and it will be a game-changer in the games industry.

The early traces of technology of VR (previously known as Sensoromoa) dates back to the 1960s, a period in which color TV was the most recent advance in major media production. Video game companies were brought to the retail market in the mid-1990s with the first generation of consumer-oriented products, although it took many decades to grow [2]. Though recently the trend of VR use is changed to infotainment and entertainment and it is getting wide attention from the consumers. The global film industry has cleverly adapted its technical innovation to plan, create, and generate content that can provide its customers with the greatest economic and psychological gains [3]. In different sectors, a parallel increase in technical growth can be observed [4]. Ineke also concluded VR as an important aspect of the future entertainment environment. It must be

remembered that even though various fields of education and connectivity have been established by the VR industry, entertainment is still a core element of technical interaction in the face of diverse intentions. Most consumers, therefore, seem to know VR as an interactive platform irrespective of their particular intent [5].

Furthermore, many of the educational intuitions intend to develop a Virtual Learning Environment (VLE) for better results than the traditional way of learning. Moreover, previous studies used the VR tool as a motivational tool for education. Merchant et al. also stated, for example, that VR increases the capacity of young people in schools and colleges to read [6]. Furthermore, Bergin counters the previous statement that the VR environment encourages the students' learning ability because of the media richness of the VR environment. Moreover, Educational games will have a positive impact on the users. Previous papers suggest that VR brain games enhance the cognitive skills of the students more than the traditional way of schooling [7]. Because of the broad geographic penetration and business value, VR technology is now a strategic informatics and entertainment weapon, and many sectors, including e-commerce, real estate, and sport, consider VR technology as an open platform [8]. In the year 2020, the VR industry is projected to hit US\$ 120 trillion [9]. The existence of VR is thus observed to increase over the ITC spectrum [10]. Authors claim that the transition from passive to active in associated sectors will make it easier for relevant stakeholders to reach optimum economic and psychological benefit [11]. In this current study, authors have assumed that VR users will harm their behavior, specifically addictive behavior among users. Therefore, the objective of the current study to emphasize VR driven consumers' addictive behavior, which can help map and recommend preventive measures to avoid addiction and reduce the impact of overuse of VR-based games.

## 2. Literature

Numerous learning experiences have been provided through virtual reality (VR). VR will potentially bring tremendous possibilities in the future and is hence a tool to be regarded and investigated at considerable length. VRs are being used as virtual learning environments (VLE) in which students can communicate with others while performing a variety of tasks [12]. You may even learn new techniques, including spatial socialization, networking, data processing, and even new linguistic capacities. It is a heuristic method for engaging students through real-time and creative concepts. It took several years to reach the consumers' use. In the early 1960s, the first VR technology was introduced due to the high price it was not possible to use for entertainment purposes but for military and medical training, whereas in the mid-1990, it was introduced to mass markets by the Gaming Industries and it can be easily found anywhere in the market with little price.

Previous studies suggested that the companies need to work on the display and the quality of the function to enhance the users of VR gadgets, and it is the need of time to reduce the price so that layman can easily use for their daily uses. Flow is defined by a battle between real and actual challenges [13].

Moreover, a previous study indicated that once the user plays best in both physical and mental states, they usually forget entirely about their surroundings even the time they are passing [14]. "The users work in his/her maximum capacity when they are inflowing. The person works at maximum capacity when they are in flow. If challenges start to surpass skills, one becomes alert first and then anxious; if skills continue to exceed challenges, one relaxes first and then becomes bored" [15]. Furthermore, the dimension of the theory of flow is divided into nine elements: clear purposes, feedback in time, the balance of challenges and skills, integration of behavior and consciousness, removal of interference in consciousness, freedom of control, loss of self-awareness, time-conscious abnormalities, and its purposive knowledge [14]. Over time, this same behavior will cause a person to worry for a moment and then instantly relax in a state of flow [16]. Studies show that perceived gratification occurs in a state of flow [17]. Persons that can interact with the technology and believe that time flows while focusing on its output are more likely to reach a flow state. In reality, when people have fun, a feeling of distortion is especially common [18]. It is assumed that flow in the games will lead to the desire to play more games frequently. Prior research suggested that social games are involved in flow and the fact that flow leads to the overuse of Internet applications that causes addiction to the games [19].

Compulsive gaming has become a significant and growing social issue since the advent of online video games. The prevalence rates for teenagers range between five and ten percent, depending on the definition of gaming addiction [20, 21]. As a "condition to further research" in the Diagnostic and Statistical Manual of Mental Disorders (DSM-5), the American Psychiatric Association (APA) agreed that game dependence might pose a serious threat to adolescent psychosocial development [22]. Addiction is thus a condition of uncontrollable conduct that induces the mind to perform recurring tasks in a way that neglects to do its everyday life acts. Zilberman, Yadid, Efrati, and Rassoovsky stated that addiction might impact the formulation of both positive and negative life events [23]. Furthermore, in the review of addictions and related psychological disorders [24], E-sport (or e-game) is a phenomenon that simultaneously has the same effect as a type of entertainment and sport and is experienced both online and offline [25]. Kuss and Lopez-Fernandez pointed out that digital gaming is another inherently addictive topic.

Gong, Zhang, Cheung, Chen, and Lee stated that online games, social networks games, or Massively Multiplayer Online Role Play Games (MMORP) are the core elements of addictive behavior. Similarly, a previous paper by Mancini, Imperato, and Sibilla stated that VR self-Discrepancy, Avatar identification will also lead to addictive behavior. Furthermore, users wanted to enhance the skills and earn more online outfits and types of equipment which cause them serious addictive behavior.

## 3. Theoretical Framework

Research on Virtual Reality is ongoing through the advancement of VR-Technologies and the growth of the VR-

Industrial, including architecture [26], medicine [27], and training [28]. The TAM was the most narrowly modified model for customers' expectative and system interventions [29]. In multiple experiments, VR technology was used to integrate external influences. Theories of technology acceptance focus primarily on advantages and ignore important consumer risk assessments [30, 31]. The TAM2 [32], UTAUT [33], and UTAUT2 [34] are examples of how models for functional adaptation are built over time. Nonetheless, no behavioral model relevant to technology was appropriate for demonstrating the darker side of technical advancement. In this research, the high media richness appreciates the addictive aspect of consumers of VR games. The cognitive-behavioral model was renamed by (Davis) to "Problematic Internet Use."

The Cognitive Behavioral Model is identified as the problematic IT Use (PIT). In this model, user's cognitions as the main reason for abnormal behavior. Davis concentrated on "pathological Internet usage" and "dysfunctional elements" of maladaptive cognitions. He also explained his concept of two forms of PIU: basic and common. The particular PIU refers to the inappropriate use of the Internet or the reliance on a certain form of utility, such as gaming, the use of personal content, stocks traders, or auction services. People with generalized PIU frequently spend more time on quantities of online chat and e-mail without any reason. They are possibly unadjustable and prefer social contact online in the real world. Davis did not consider the use of the Internet as a source of anxiety and depression but believed PIU as the product of maladaptive, psychologically induced cognitive processes. Caplan, based on the cognitive-behavioral model [35], claims of the problem use of the Internet includes maladaptive cognitions and abnormal behavior and the renaming of "pathological Internet use" to "problematic Internet use." Prior studies demonstrate the potential insight for understanding the role of dilemma IT use of the cognitive-behavioral model [36, 37]. As a result, this theory has been used more and more to investigate various aspects of addictive activity such as online gaming [19], online trading [36], and overuse of the Internet [38]. Authors also presume and try to validate that the cognitive-behavioral paradigm is sufficient to describe addiction to VR games. While the cognitive-compliance approach offers a logical basis for the definition of addiction, clear variations need to be taken into account to achieve a better interpretation of features in various contexts [39].

**3.1. Flow as Construct.** Flow has been described as an ideal experience, the best emotions, the most satisfying human life experiences that derive from people's perceptions of difficulties and abilities in specific situations [13, 40]. Csikszentmihalyi developed the theory of flow, which describes a condition of concentration or complete absorption with activity and the situation [41]. Moreover, cognitive absorption is characterized as a state of deep involvement with IT based on flow theory [42]. Research indicates that cognitive absorption adversely affects the conduct of users in the use of the target information system. Csikszentmihalyi

explains the enjoyment of the citizens who do a thing that gives little clear intrinsic incentive but is highly satisfying and fulfilling. Such behaviors were inherently motivational and their optimum experience was classified as "flow" [43]. The sport is inevitable and the flow interaction of excellence is play [43]. Moreover, flow is characterized as an "experience of the highest," as it is a concentrated psychological condition of pleasure (Enjoyment) and productivity [15, 42]. Performing time flies may be the most striking aspect of the flow experience. This finding was introduced into the flow analysis by Csikszentmihalyi when he suggested that a person's knowledge of time is a predictor of flow. If a work experience is strong and equal to the degree of competence of the individual and whether they are, therefore, in the flow stage, their subjective perception of time is less than the objective time that has elapsed [44]. Moreover, pleasure (enjoyment) motivates the curiosity about the behavioral desire to show certain talent to others [45]. In addition, previous studies indicate that heavy behaviors and loss of self-regulation have a beneficial impact on the addiction to the online game [46]. For instance, from a games perspective, too much involvement in flow through being overabsorbed and involved can damage children as they may obsess the state of pleasure but ignore self-care and interpersonal relations [47]:

H1: individuals' enriched flow experience in VR encourages consumers to have VR games addictive behavior

H2: individuals' enriched flow experience in VR encourages consumers to have a behavioral desire to use VR games

**3.2. Behavioral Desire.** It can be argued that strong desires can be pleasurable experienced if no negative consequences are expected, but if potential benefits are also linked by guilty feelings, a desire may be less pleasurable and even strained. Andrade suggests that mental images are emotive. This claim is reinforced by the idea that neural sensitization mechanisms can switch between love and openness to addictive behaviors [48]. Rose et al. found some evidence that Website (online games) approaches may affect adolescents' diet and physical behavior. This can be partly because of the interaction's uncertainty. Such improvements are not, however, necessarily maintained over the medium or long term [49]. Furthermore, two forms can be conceptualized for a user's desire: the desire for the actions of a person and a desire for the behavior [46]. The second type of want (desire) is a mutual desire rooted in an individual social group's self-concept and represents the drive to socialize with social group members [46, 50]. In addition, previous studies indicate that heavy behaviors and loss of self-regulation have a beneficial impact on the addiction towards technology [46].

H3: behavioral desires of VR game users motivate consumers to have VR games addictive behavior

H4: behavioral desire of VR games mediates the relationship between flow experience and VR game addiction



**3.3. Cyber Aggression.** Cyber aggression has been described as a repetitive course of action involving intentional or unwanted interpersonal violence mediated by ICT in an attempt to threaten, insult, harass, and/or endanger the target [51, 52]. The self-perceived effect on teenagers is also an issue in most conceptions of cyber aggression. Recent studies have found that cyber aggression is not inherently harmful or disturbing, while other studies have shown that cyber aggression intervention can cause significant physical, mental, educational, and social consequences [53]. The young person may contribute to understanding these high rates of development and their initial capacity to awareness of the moral, social, and legal consequences of cyber aggression behaviors [54]. Previously published research articles stated that aggression is directly related to game addiction. Similarly, previous studies also suggest that cyber aggression has nothing to do with game addiction behavior in real life. Formerly, Kim, Namkoong, Ku, and Kim reported Craig's report stated that low self-esteem and negative evaluation of oneself are the good predictors of game addiction and the total time spent on playing video games. Similarly, it is assumed that Cyber Aggression can potentially have a great impact on behavioral desire and simultaneously have influential power on users' addictive behavior towards the game addiction, specifically VR-based games.

H5: the essence of Cyber aggression moderates the relationship between VR games flow experience and its addictive behavior

## 4. Materials and Methods

The study tested the hypothesized model by using the Preacher and Hayes process macro (Model 4). The further methodological aspects are discussed in detail in the following subsections. Although, in the field of quantitative research, the applied mathematical research holds a variety of approaches, i.e., [55, 56]. However, behavioral analysis is mostly comprised of behavior modeling and hypothesis-based study, as observed in the current research.

**4.1. Instrument.** The quantitative research approach adopted the existing sources of literature to make the results credible and valid for further study. Three-item scale for CA is adapted from Zhang and Sun, a five-item scale for EJ is adopted from Ghazali et al., and the three-item scale for TD is adopted from Im and Varma, whereas for BD authors adapted a three-item scale from the study of Hsieh and Liao. Similarly, author's adapted five-item scales for CG from Shapka and Maghsoudi and GA were measured by a three-point scale as suggested by Gong, Yu, and Luqman to emphasize customer VR addiction. To measure each model, a Likert scale (1–Highly Disagree and 5, Highly Agree) was adopted.

**4.2. Data Collection.** The data were gathered from the user of VR games who approached through the social networking

sites (SNS) (in particular Facebook). The authors took the stance of basic random sampling as (1) over the world leading VR-based Facebook pages; as authors not considered any of the controlled variables, i.e., gender and age group. The only condition authors followed is to find potential candidates for the survey who have not restricted themselves to accept unknown friend requests.

It is important to note that SNS limited and suspended many data collector accounts during this data collection process as SNS has stringent rules on submitting requests from friends within a certain amount of time, particularly the data collection period of seven months (mid of February to mid of September 2020). Each of the respondents initially been contacted with a brief introduction and purpose of the study. Moreover, to enhance the data response, the authors announced that the prize amount range from \$1 to \$10 in the form of bitcoin. The history of individuals consuming VR-based games has been researched to check possible sample candidates. The remaining sample was submitted by the only respondents who had a positive response. The authors also assume that the obtained sample is optimal for the analysis. A total of 600 participants were invited for the survey. However, 470 responses have been received after 30 consecutive weeks. During the initial data securitizing, 103 responses were eliminated for the incomplete responses. As a result, only 367 responses were able to be examined. For the nonresponse biases, authors inspected the initial subset of 30 participants with the later participants. In this way, the early and the later responses help authors to conclude that there is no evidence of nonresponse biases found. A short descriptive profile of the user of the VR-based game is shown in Table 1.

## 5. Findings

To examine the reliability and validity of all constructions and models, factor analysis was performed. Factor loading for each variable, Cronbach-alpha ( $\alpha$ ), composite reliability, and extracted average variance (AVE) of each variable computed, as shown in Table 2.

In the next phase of analysis, the structural model is built from the data with the help of SPSS-AMOS. The initial and the second-order index values of the model noted in the satisfactory range as listed in Table 3. The root means estimate noted over the continuum of 0.050 to 0.052 as within a suggested acceptable range [57, 58]. In addition, the chi-squares observed within the range of 3.436–4.319 in both of the cases of CFA (first and second-order) and the model, are as listed in Table 3. Moreover, all other fitness indices are listed in Table 3.

The Variance Inflation Factor (VIF) was estimated for all constructs to analyze the multicollinearity effect. The VIF values recorded in Table 4 were less than the 10 cut-off values as recommended by Hair et al. [59] Specifically, it ranged from 1.287 to 1.451. Therefore, in the current study, multicollinearity was not a problem. The common method bias effect was measured to ensure the findings were reliable as the data collection monoprocess was observed. The Harman single method score was determined as a part of dimension

TABLE 1: Demographics of respondents.

Characteristic	Detail	Frequency	In percentage
Gender	Male	294	80.11
	Female	73	19.89
	Once	19	05.17
Frequency of playing VR games (in a week)	Two or three times	43	11.72
	Four or five times	196	53.41
	More than five times	109	29.70
	Immersion	154	41.96
The most appealing attribute of VR games	Interactivity	117	31.88
	Sensory feedback	96	26.16

TABLE 2: Reliability analysis of the collected survey.

Construct	Items	Loadings	CR	CA	AVE
Cyber aggression (CA)	CG1	0.879	0.923	0.923	0.706
	CG2	0.866			
	CG3	0.858			
	CG4	0.828			
	CG5	0.767			
Enjoyment (EJ)	EJ1	0.872	0.888	0.882	0.615
	EJ2	0.801			
	EJ3	0.790			
	EJ4	0.743			
	EJ5	0.706			
Cognitive absorption (CA)	CA1	0.899	0.924	0.765	0.802
	CA2	0.894			
	CA3	0.893			
Time distortion (TD)	TD1	0.804	0.835	0.906	0.628
	TD2	0.791			
	TD3	0.783			
Behavioral desire (BD)	BD1	0.867	0.885	0.900	0.718
	BD2	0.845			
	BD3	0.831			
VR game addiction (GA)	GA1	0.768	0.791	0.746	0.559
	GA2	0.767			
	GA3	0.706			
Maximum variance explained is 33.074%					

TABLE 3: Fitness indices of the proposed model.

Fitness indices	First order	Second order	Proposed model
Chi-square	625.366	688.084	820.596
Degree of freedom	182	188	190
Chi-square/degree of freedom	3.436	3.660	4.319
GFI	0.947	0.942	0.929
AGFI	0.927	0.922	0.905
NFI	0.956	0.951	0.942
TLI	0.959	0.956	0.945
CFI	0.968	0.964	0.955
RSMEA	0.050	0.052	0.058

Note. \*\*\* = Significance level of 0.001, \*\* = Significance level of 0.01, \* = Significance level of 0.05.

reduction [60]. The highest variance reported for a single factor in the current analysis was 33.074 percent, suggesting that neither any proposed construct controlled the overall model variance and common method biasness is not the problem in this study. The following section will lead to the testing of the proposed hypotheses.

For examining the proposed model, SPSS-Process Macro was used as suggested by Preacher and Hayes, and the study examined the mediating effect of behavioral desire in case of the relationship between the flow experience and VR-based games addiction among youth. The results concluded that the richness of flow experience has the potential to increase

TABLE 4: External reliability analysis.

Construct	Mean (SD)	VIF	CG	EJ	CA	TD	BD	GA
CG	4.047 (0.606)	1.287	<b>0.840</b>					
EJ	3.865 (0.738)	1.451	0.293**	<b>0.784</b>				
CA	3.239 (0.804)	1.218	0.164**	0.362**	<b>0.895</b>			
TD	3.800 (0.815)	1.233	0.271**	0.334**	0.326**	<b>0.792</b>		
BD	3.578 (0.814)	1.420	0.430**	0.442**	0.163**	0.222**	<b>0.845</b>	
GA	3.683 (0.667)	—	0.479**	0.339**	0.153**	0.193**	0.402**	<b>0.747</b>

TABLE 5: Mediation analysis by using bootstrapping with the sampling size = 5000.

Hyp	IV	M	DV	Effect of IV on M	Effect of M on DV	Direct (c')	Indirect (a * b)	Total effect (c)	95% (CI)	Mediation
H	FL	BD	GA	0.501***	0.277***	0.202***	0.139***	0.341***	(0.109, 0.172)	Supported

Note. \*\*\* = Significance level of 0.001, \*\* = Significance level of 0.01, \* = Significance level of 0.05.

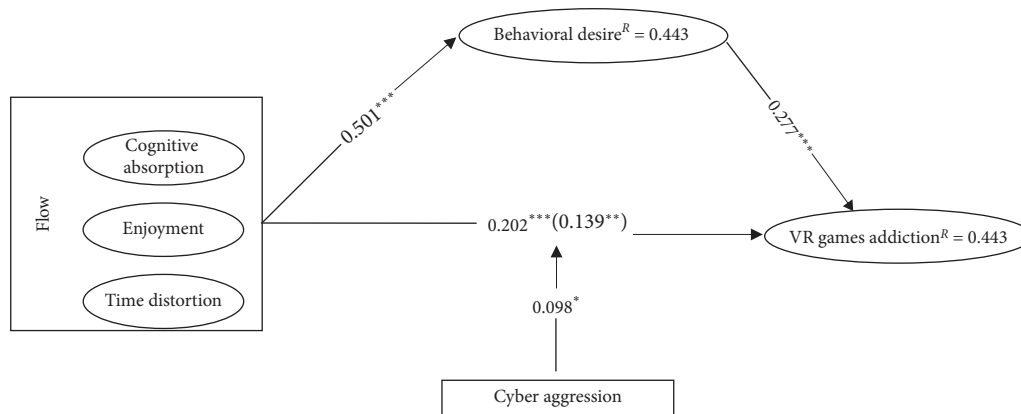


FIGURE 1: Graphical explanation of proposed model of the study.

VR game addiction among youth (H1:  $\beta = 0.501$ ,  $p \leq 0.001$ ) and also helps to elevate the behavioral desire among youth to get involved in VR games (H2:  $\beta = 0.139$ ,  $p \leq 0.01$ ). Moreover, the findings also concluded that the behavioral desire also positively affects VR games addiction among users, which can potentially lead towards valuable practical implications (H3:  $\beta = 0.277$ ,  $p \leq 0.001$ ).

In the meanwhile, the mediating effect of behavioral desire is also noted as significant, which statistically underlines the partial mediating behavior of behavioral desire in the currently proposed settings. Particularly, the bootstrapping results in the tabular format are listed in Table 5 and shown graphically in Figure 1.

The hierarchal regression analysis was adopted to test the proposed moderating effect of Cyber aggression on the association between enriched flow experience and VR games addiction among youth. The findings are listed in Table 6 below. The statistical findings revealed that the presence of cyber aggression strengthens the relationship between flow experience and VR games addiction among users (H5  $\beta = 0.098$ ,  $p \leq 0.05$ ). Further, the slope test examined the strength and nature of the moderating effect, as shown in Figure 2.

TABLE 6: Moderating effect of cyber aggression over the association between flow experience and VR games addiction.

Construct	Model 1	Model 2	Model 3
Flow (FL)	0.341***	0.185***	0.219***
Cyber aggression (CA)		0.470***	0.226***
FL * CA			0.098*
F	97.927	113.081	167.111
R <sup>2</sup>	0.090	0.253	0.256

## 6. Discussion and Conclusion

In this current study, the authors concluded that this study implicates all the stakeholders (i.e., Education, Entertainment, and Infotainment). Authors found that flow creates a high level of addiction among the users when it mediates with the behavioral desire, which means that behavioral desires need to be more bifurcate. Likewise, in previous studies, VR is widely used for entertainment purposes rather than educational purposes; therefore, addiction through behavioral desire also supports the stance of addiction behavior studies. It is worth mentioning that there are dark aspects in VR that need to be sorted out. For entertainment

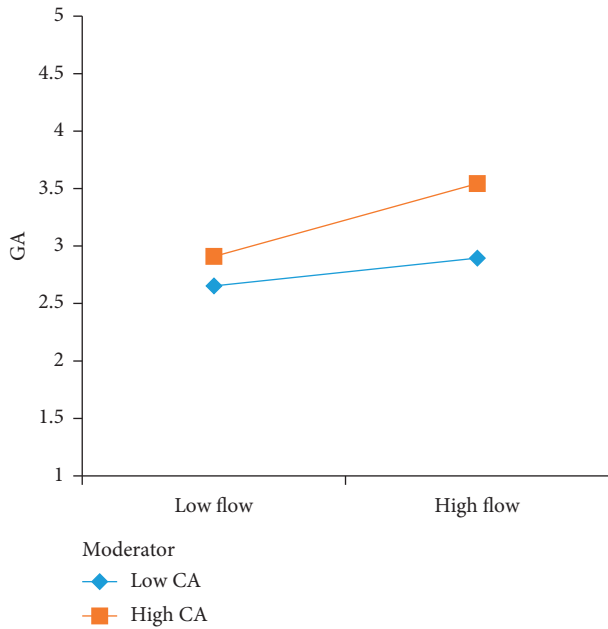


FIGURE 2: Interaction plot for cyber aggression over the association between flow experience and VR games addiction.

purpose as it can be seen that it creates high addictive behavior so all the policymakers and legislators and suppliers have their social responsibility and ethical responsibility to tackle the addiction in the VR products as this study also identify this issue. The entertainment industry is changing and adopting advanced technology like VR, so it is a need time that there should be a proper policy so the dark aspects of the entertainment industry through VR can also be tackled. As in this study, Cyber aggression is needed to study further as in this study; authors have found behavioral desire as a mediator and Cyber Aggression as a moderator has positive effects on addiction. Furthermore, theoretical and practical implications are discussed further in the section below.

**6.1. Theoretical Implications.** This research presented the scholarly literature with in-depth and beneficial contributions. First of all, this research is the first of its kind to understand the actions of VR game addiction. Previous studies have been used other variables whereas in this current study authors approach the gamers' behavioral intentions towards the VR-based Games specifically the addiction behavior. Furthermore, in this paper authors used the attributes of flow as proposed by (Cho) inquire and understand the stance of the users towards the VR-based games. Secondly, behavioral desire is taken as a mediator while explaining the addiction behavior. It is used to check the addictive behavior of gamers. It was not used before in any research where it was used with the game's addiction. Moreover, few researchers adopted addiction with the behavioral model. Previous papers results indicated that excessive use of games is highly risky for the health of the gamers not only physically but mentally [61]. While previous studies also concluded that flow has high influence on users'

addiction behavior. For instance, flow in cognitive absorption has an adverse effect on the users' behavior. It can be both negative and positive from a gaming perspective. The feeling of flow online is appealing to gamers. Therefore, the ability to obtain the flow sensation may influence the pace and length of gaming and therefore be involved in the creation and maintenance of addictive behaviors [20, 62]. Moreover, Sherry indicated that the chance to witness flow online may be a strong gaming motivator. Addiction is sometimes called a desire; the high desire has a high probability of addiction towards anything he wishes for. Likewise, previous papers also support the stance of the current paper, which suggested that flow has a beneficial impact on the games' addiction behavior on the users [63]. Moreover, previous papers also suggest that besides the addiction, there are serious physical health concerns for those who use games excessively [64]. In this current study, authors have used behavioral desire, whereas, in previous papers, authors did not find any evidence where behavior desire has been used specifically in the context of the game's addiction. Moreover, flow-based factors, i.e., cognitive absorption, enjoyment, and time distortion, have been used in the game's addiction, but no study found where it has been used in the context of VR-based game addiction. Therefore, it is worth mentioning that it is also the novelty of this current study. Furthermore, the purposed mediator (behavioral desire) partially mediates the proposed relation of flow to addiction. The study also concluded that Cyber aggression is a psychological perspective that strengthens the addictive behavior of the users in the case of VR. Authors also found that psychological constructs dominate in creating addiction among the users and push them to use it extensively.

**6.2. Practical Implications.** In this current study, the authors found that flow creates a high level of behavioral desires among the users. Similarly, previous papers suggested that flow has a significant role in game addiction. In addition, experts voiced significant questions about wellness and Internet gaming addiction. Online gaming addictions were reportedly causing mental health issues for gamers. In particular, the claim among children is that game addiction can influence learning and thinking. Similarly, the time and demographic use of VR games can be limited. VR applications can be used for information rather than extreme entertainment. As previous papers suggested that its games can be used to develop the skills among the students and youngsters, it can also be said that VR games need to be improved in the context of learning to develop the IQ level of youngsters and students specifically. VR application can revise the algorithms and it can be restricted to a specific time. If the users exceed the time limit, it can be shut down itself. Flow is revolving around the users' satisfaction. Similarly, from the analysis of the current study results, it is found that flow does affect the addiction behavior with the help of behavioral desire. Therefore, the quality of the VR games application can be improved to attract more users to capture the global market. For the attraction of the users,

developers need to develop more exciting characters in the games and make them more realistic to the current world. Balakrishnan and Gri suggested it is difficult to maintain the consumer's commitment to the Internet; thus, advanced features need to be built to draw consumers and allow them to come back and play VR games with technical advances. Moreover, it can harm the users' behavioral desire, which may disturb users' daily behavior. It can be taken into consideration that it will not disturb the users' behavior. Therefore, lust full users may likely to have more experience towards VAD. Moreover, applications can be developing for psychological treatment, medical training assistance and can be used for the learning purpose only. Furthermore, VR-based applications can be designed competitively so that users can have more time and use their cognitive skills to enhance their IQ level and learn new techniques, too, later on, use in their daily life. It is always considered that computer games are mentally oriented, which enhances the users' skills, specifically competitive games. Moreover, game developers can restrict games with age factors as recently, the MPPOG (i.e., PUBG) has put some restrictions on the Under 18 users. In this restriction, users under 1 are only allowed to play for 3 hours' maximum in 24 hours. It is also advised for the VR game developers to put stricter restrictions on the users so they will not get addicted to VR-based games. As mention above, VR applications can be enhancing the cognitive skills of the users by developing more brains using games rather than games that waste the time of the users.

**6.3. Limitation and Conclusion.** In this current study, the authors used the Cognitive-Behavioral model to scrutinize the user's addictive behavior towards VR-based games. In the current context, the authors found that flow has the loftiest probability for the admiring situation. Similarly, flow has shown a significant impact on the user's addiction behavior towards the VR game's addiction. Behavioral desire is also found to be the source of creating addiction among the users. Authors have some limitations while conducting this research which could lead to new and further studies. VR applications can be enhanced and also improved so that users can use them and also recommend them to others. VR should be used for academic and training purposes rather than entertainment. The authors also suggest that further studies can carry out on specific demographic and educational qualifications. In this paper, education did not study, but it is advised that further studies can be done to keep the education level of the users and it can also be divided into developed and underdeveloped nations. Other factors of flow can be studied with other types of game addiction. While mapping the Cyber aggression mediator role, it is found that it is not used before with any type of addiction. At the same time, the present study is the first to use cyber aggression in the context of VR-based game addiction. Furthermore, in this study, authors adopted a quantitative approach, while further researches can also adopt the qualitative approach as well for data collection and analysis.

## Data Availability

Data will be available on request to the corresponding author.

## Disclosure

Jing Yuan, Xuesong Zhai, and Fahad Asmi should be considered as the co-first authors.

## Conflicts of Interest

The authors declare no conflicts of interest.

## Authors' Contributions

Jing Yuan, Xuesong Zhai, and Fahad Asmi contributed equally to this work.

## Acknowledgments

This research work was supported by the National Social Science Fund of China (Grant ID: 17BXW034) and the Youth Foundation of Humanities and Social Sciences Project of the Ministry of Education in China (Grant ID: 20YJC880118).

## References

- [1] D. M. Shafer, C. P. Carbonara, and M. F. Korpi, "Factors affecting enjoyment of virtual reality games: a comparison involving consumer-grade virtual reality technology," *Games for Health Journal*, vol. 8, no. 1, pp. 15–23, 2019.
- [2] T. Hartmann and J. Fox, "Entertainment in virtual reality and beyond: the influence of embodiment, Co-location, and cognitive distancing on users' entertainment experience tilo," in *The Oxford Handbook of Entertainment Theory* Oxford University Press, Oxford, UK, 2020.
- [3] M. Wood, G. Wood, and M. Balaam, "They're just tixel pits, man," in *Proceedings of the 2017 CHI Conference on Human Factors in Computing Systems*, pp. 5439–5451, New York, NY, USA, May 2017.
- [4] J. Zenor, "Sins of the flesh? Obscenity law in the era of virtual reality," *Communication Law and Policy*, vol. 19, no. 4, pp. 563–589, 2014.
- [5] K. E. Jung and H. Lee, "The adoption of virtual reality devices: the technology acceptance model integrating enjoyment, social interaction, and strength of the social ties," *Telematics and Informatics*, vol. 39, pp. 37–48, 2018.
- [6] Z. Merchant, E. T. Goetz, L. Cifuentes, W. Keeney-Kennicutt, and T. J. Davis, "Effectiveness of virtual reality-based instruction on students' learning outcomes in K-12 and higher education: a meta-analysis," *Computers & Education*, vol. 70, pp. 29–40, 2014.
- [7] J. Parong and R. E. Mayer, "Cognitive consequences of playing brain-training games in immersive virtual reality," *Applied Cognitive Psychology*, vol. 34, no. 1, pp. 29–38, 2020.
- [8] Y. Jang and E. Park, "An adoption model for virtual reality games: the roles of presence and enjoyment," *Telematics and Informatics*, vol. 42, Article ID 101239, 2019.
- [9] *Digi-Capital Augmented/Virtual Reality Revenue Forecast Revised to Hit \$120 Billion by 2020*, <https://www.digi-capital.com/news/2020/08/the-ar-vr-ecosystem-are-we-there-yet/>.

- [10] A. Keizer, A. A. Cuperus, J. A. W. Tejjink, A. W. M. Evers, I. J. M. van der Ham, and M. M. L. van den Houten, "Manipulating spatial distance in virtual reality: effects on treadmill walking performance in patients with intermittent claudication," *Computers in Human Behavior*, vol. 79, pp. 211–216, 2017.
- [11] J. W. B. Elsej, K. van Andel, R. B. Kater, I. M. Reints, and M. Spiering, "The impact of virtual reality versus 2D pornography on sexual arousal and presence," *Computers in Human Behavior*, vol. 97, pp. 35–43, 2019.
- [12] D. Marinova, K. de Ruyter, M.-H. Huang, M. L. Meuter, and G. Challagalla, "Getting smart," *Journal of Service Research*, vol. 20, no. 1, pp. 29–42, 2017.
- [13] M. S. Davis and M. Csikszentmihalyi, "Beyond boredom and anxiety: the experience of play in work and games," *Contemporary Sociology*, vol. 6, no. 2, p. 197, 1977.
- [14] Y. Fu and Q. Li, "Flow theory in the interactive design of educational games," *Int. J. Contemp. Humanit.*, 2020.
- [15] J. Nakamura and M. Csikszentmihalyi, "The concept of flow," in *Handbook of Positive Psychology*, pp. 89–105, Oxford University Press, Oxford, UK, 2002.
- [16] Y. Yan, R. M. Davison, and C. Mo, "Employee creativity formation: the roles of knowledge seeking, knowledge contributing and flow experience in Web 2.0 virtual communities," *Computers in Human Behavior*, vol. 29, no. 5, pp. 1923–1932, 2013.
- [17] J. Hamari, D. J. Shernoff, E. Rowe, B. Coller, J. Asbell-clarke, and T. Edwards, "Challenging games help students learn: an empirical study on engagement, flow and immersion in game-based learning," *Computers in Human Behavior*, vol. 54, pp. 170–179, 2016.
- [18] J. Matute-Vallejo and I. Melero-Polo, "Understanding online business simulation games: the role of flow experience, perceived enjoyment and personal innovativeness," *Australasian Journal of Educational Technology*, vol. 35, no. 3, pp. 71–85, 2019.
- [19] E. Hu, V. Stavropoulos, A. Anderson, M. Scerri, and J. Collard, "Internet gaming disorder: feeling the flow of social games," *Addictive Behaviors Reports*, vol. 9, Article ID 100140, 2019.
- [20] M. D. Griffiths, D. J. Kuss, and D. L. King, "Video game addiction: past, present and future," *Current Psychiatry Reviews*, vol. 44, 2012.
- [21] D. J. Kuss and M. D. Griffiths, "Internet addiction in students: prevalence and risk factors," *Journal of Chemical Information and Modeling*, vol. 53, pp. 1689–1699, 2013.
- [22] M. Peeters, I. Koning, and R. van den Eijnden, "Predicting Internet Gaming Disorder symptoms in young adolescents: a one-year follow-up study," *Computers in Human Behavior*, vol. 80, pp. 255–261, 2018.
- [23] N. Zilberman, G. Yadid, Y. Efrati, and Y. Rassovsky, "Negative and positive life events and their relation to substance and behavioral addictions," *Drug and Alcohol Dependence*, vol. 204, p. 107562, 2019.
- [24] C. Varo, A. Murru, E. Salagre et al., "Behavioral addictions in bipolar disorders: a systematic review," *European Neuropsychopharmacology*, vol. 29, no. 1, pp. 76–97, 2019.
- [25] J. Burrell, "Raising the stakes: E-sports and the professionalization of computer games," in *Contemporary Sociology*, pp. 623–624, MIT Press, Cambridge, MA, USA, 2012.
- [26] M. E. Portman, A. Natapov, and D. Fisher-Gewirtzman, "To go where no man has gone before: virtual reality in architecture, landscape architecture and environmental planning," *Computers, Environment and Urban Systems*, vol. 54, pp. 376–384, 2015.
- [27] E. K. Yuen, E. M. Goetter, M. J. Stasio et al., "A pilot of acceptance and commitment therapy for public speaking anxiety delivered with group videoconferencing and virtual reality exposure," *Journal of Contextual Behavioral Science*, vol. 12, pp. 47–54, 2019.
- [28] F. Ke, M. Pachman, and Z. Dai, "Investigating educational affordances of virtual reality for simulation-based teaching training with graduate teaching assistants," *Journal of Computing in Higher Education*, vol. 32, no. 3, pp. 607–627, 2020.
- [29] H. Yang, J. Yu, H. Zo, and M. Choi, "User acceptance of wearable devices: an extended perspective of perceived value," *Telematics and Informatics*, vol. 33, no. 2, pp. 256–269, 2016.
- [30] F. D. Davis, "Perceived usefulness, perceived ease of use, and user acceptance of information technology," *MIS Quarterly*, vol. 13, no. 3, p. 319, 1989.
- [31] R. Agarwal and E. Karahanna, "Time flies when you're having fun: cognitive absorption and beliefs about information technology usage," *MIS Quarterly*, vol. 24, no. 4, pp. 665–694, 2000.
- [32] V. Venkatesh and F. D. Davis, "A theoretical extension of the technology acceptance model: four longitudinal field studies," *Management Science*, vol. 46, no. 2, pp. 186–204, 2000.
- [33] V. Vankatesh, M. G. Morris, M. Hall, G. B. Davis, F. D. Davis, and S. M. Walton, "User acceptance of information technology: toward a unified view 1," *MIS Quarterly*, vol. 27, no. 3, pp. 425–478, 2003.
- [34] V. Venkatesh, Y. L. Thong, and X. Xu, "Consumer acceptance and use of information technology: extending the unified theory of acceptance and use of technology," *MIS Quarterly*, vol. 36, no. 1, pp. 157–178, 2012.
- [35] R. A. Davis, "Cognitive-behavioral model of pathological Internet use," *Computers in Human Behavior*, 2001.
- [36] O. Turel and A. Serenko, "Developing a (bad) habit: antecedents and adverse consequences of social networking website use habit," in *Proceedings of the 17th Americas Conference on Information Systems 2011*, AMCIS, Detroit, MI, USA, August 2011.
- [37] X. Zheng and M. K. O. Lee, "Excessive use of mobile social networking sites: negative consequences on individuals," *Computers in Human Behavior*, vol. 65, pp. 65–76, 2016.
- [38] M. Brand, C. Laier, and K. S. Young, "Internet addiction: coping styles, expectancies, and treatment implications," *Frontiers in Psychology*, vol. 5, pp. 1–14, 2014.
- [39] C. Wang, M. K. O. Lee, and Z. Hua, "A theory of social media dependence: evidence from microblog users," *Decision Support Systems*, vol. 69, pp. 40–49, 2015.
- [40] M. Csikszentmihalyi, *Beyond Boredom and Anxiety*, Jossey-Bass Inc., San Francisco, CA, USA, 2000.
- [41] M. Csikszentmihalyi, "Happiness and creativity: going with the flow," *Futurist*, 1997.
- [42] M. Csikszentmihalyi, "Flow: the psychology of optimal experience," *Academy of Management Review*, vol. 16, pp. 636–640, 1990.
- [43] M. A. Csikszentmihalyi, "Theoretical model for enjoyment," in *Beyond Boredom and Anxiety*, Jossey-Bass Inc., San Francisco, CA, USA, 1975.
- [44] S.-H. Im and S. Varma, "Distorted time perception during flow as revealed by an attention-demanding cognitive task," *Creativity Research Journal*, vol. 30, no. 3, pp. 295–304, 2018.
- [45] E. Ghazali, D. S. Mutum, and M.-Y. Woon, "Exploring player behavior and motivations to continue playing Pokémon GO,"

- Information Technology & People*, vol. 32, no. 3, pp. 646–667, 2019.
- [46] X. Gong, K. Z. K. Zhang, C. M. K. Cheung, C. Chen, and M. K. O. Lee, “Alone or together? Exploring the role of desire for online group gaming in players’ social game addiction,” *Information & Management*, vol. 56, no. 6, Article ID 103139, 2019.
- [47] S. Sanjamsai and D. Phukao, “Flow experience in computer game playing among Thai university students,” *Kasetsart Journal of Social Sciences*, vol. 39, no. 2, pp. 175–182, 2018.
- [48] K. C. Berridge and T. E. Robinson, “Liking, wanting, and the incentive-sensitization theory of addiction,” *American Psychologist*, vol. 71, no. 8, pp. 670–679, 2016.
- [49] T. Rose, M. Barker, C. Maria Jacob et al., “A systematic review of digital interventions for improving the diet and physical activity behaviors of adolescents,” *Journal of Adolescent Health*, vol. 61, no. 6, pp. 669–677, 2017.
- [50] O. Turel and H. Qahri-Saremi, “Problematic use of social networking sites: antecedents and consequence from a dual-system theory perspective,” *Journal of Management Information Systems*, vol. 33, no. 4, pp. 1087–1116, 2016.
- [51] M. F. Wright, “Parental mediation, cyberbullying, and cybertrolling: the role of gender,” *Computers in Human Behavior*, vol. 71, pp. 189–195, 2017.
- [52] F. Pereira, B. H. Spitzberg, and M. Matos, “Cyber-harassment victimization in Portugal: prevalence, fear and help-seeking among adolescents,” *Computers in Human Behavior*, vol. 62, pp. 136–146, 2016.
- [53] E. Larrañaga, S. Yubero, A. Ovejero, and R. Navarro, “Loneliness, parent-child communication and cyberbullying victimization among Spanish youths,” *Computers in Human Behavior*, vol. 65, pp. 1–8, 2016.
- [54] A. Vale, F. Pereira, M. Gonçalves, and M. Matos, “Cyber-aggression in adolescence and internet parenting styles: a study with victims, perpetrators and victim-perpetrators,” *Children and Youth Services Review*, vol. 93, pp. 88–99, 2018.
- [55] J.-B. Liu and S. N. Daoud, “Number of spanning trees in the sequence of some graphs,” *Complexity*, vol. 2019, Article ID 4271783, 22 pages, 2019.
- [56] J. Cao, J.-B. Liu, and S. Wang, “Resistance distances in corona and neighborhood corona networks based on Laplacian generalized inverse approach,” *Journal of Algebra and its Applications*, vol. 18, no. 3, Article ID 1950053, 2019.
- [57] J. C. Anderson and D. W. Gerbing, “Structural equation modeling in practice: a review and recommended two-step approach,” *Psychological Bulletin*, vol. 103, pp. 411–423, 1998.
- [58] R. C. MacCallum, M. W. Browne, and H. M. Sugawara, “Power analysis and determination of sample size for covariance structure modeling,” *Psychological Methods*, vol. 1, no. 2, pp. 130–149, 1996.
- [59] J. F. Hair, W. C. Black, B. J. Babin, and R. E. Anderson, *Multivariate Data Analysis*, CRC Press, Boca Raton, FL, USA, 7th edition, 2014.
- [60] P. M. Podsakoff, S. B. MacKenzie, J.-Y. Lee, and N. P. Podsakoff, “Common method biases in behavioral research: a critical review of the literature and recommended remedies,” *Journal of Applied Psychology*, vol. 88, no. 5, pp. 879–903, 2003.
- [61] P. Dullur and P. Hay, “Problem internet use and internet gaming disorder: a survey of health literacy among psychiatrists from Australia and New Zealand,” *Australasian Psychiatry*, vol. 25, no. 2, pp. 140–145, 2017.
- [62] B. L. M. Adams, V. Stavropoulos, T. L. Burleigh, L. W. L. Liew, C. L. Beard, and M. D. Griffiths, “Internet gaming disorder behaviors in emergent adulthood: a pilot study examining the interplay between anxiety and family cohesion,” *International Journal of Mental Health and Addiction*, vol. 17, pp. 828–844, 2018.
- [63] X. Zhai, F. Asmi, R. Zhou et al., “Investigating the mediation and moderation effect of students’ addiction to virtual reality games: a perspective of structural equation modeling,” *Discrete Dynamics in Nature and Society*, vol. 2020, Article ID 5714546, 13 pages, 2020.
- [64] J. Gackenbach, D. Wijeyaratnam, and C. Flockhart, *The Video Gaming Frontier*, Elsevier, Amsterdam, Netherlands, 2017.

## Research Article

# Improved Lower Bound of LFMD with Applications of Prism-Related Networks

Muhammad Javaid <sup>1</sup>, Hassan Zafar,<sup>1</sup> Q. Zhu,<sup>2,3</sup> and Abdulaziz Mohammed Alanazi <sup>4</sup>

<sup>1</sup>Department of Mathematics, School of Science, University of Management and Technology, Lahore 54770, Pakistan

<sup>2</sup>School of Mathematics and Statistics, Hunan Normal University, Changsha, Hunan 4100081, China

<sup>3</sup>Department of Mathematics, School of Information Science and Engineering, Chengdu University, Chengdu 610106, China

<sup>4</sup>Department of Mathematics, University of Tabuk, Tabuk, Saudi Arabia

Correspondence should be addressed to Muhammad Javaid; [javidmath@gmail.com](mailto:javidmath@gmail.com)

Received 22 March 2021; Revised 10 April 2021; Accepted 19 April 2021; Published 4 May 2021

Academic Editor: Sakander Hayat

Copyright © 2021 Muhammad Javaid et al. This is an open access article distributed under the Creative Commons Attribution License, which permits unrestricted use, distribution, and reproduction in any medium, provided the original work is properly cited.

The different distance-based parameters are used to study the problems in various fields of computer science and chemistry such as pattern recognition, image processing, integer programming, navigation, drug discovery, and formation of different chemical compounds. In particular, distance among the nodes (vertices) of the networks plays a supreme role to study structural properties of networks such as connectivity, robustness, completeness, complexity, and clustering. Metric dimension is used to find the locations of machines with respect to minimum utilization of time, lesser number of the utilized nodes as places of the objects, and shortest distance among destinations. In this paper, lower bound of local fractional metric dimension for the connected networks is improved from unity and expressed in terms of ratio obtained by the cardinalities of the under-study network and the local resolving neighbourhood with maximum order for some edges of network. In the same context, the LFMDs of prism-related networks such as circular diagonal ladder, antiprism, triangular winged prism, and sun flower networks are computed with the help of obtained criteria. At the end, the bounded- and unboundedness of the obtained results is also shown numerically.

## 1. Introduction

For a connected network  $G$ , Salter introduced the concept of resolving (locating) set with the cardinality of minimum resolving set which is called the location number of  $G$  [1]. Harary and Melter introduced the concept of metric dimension for the connected networks [2]. The concept of metric independence number  $mi(G)$  of a graph  $G$  is introduced by Currie and Oellermann [3]. The metric dimension has been applied to solve the problems involving percolation in hierarchical lattice [4], coin weighting, and robot navigation [5]. It is also applied in subject of chemistry to find the structures of chemical compounds having similar characteristics in functional groups. These functional groups play a vital role in chemical and pharmaceutical industries to predict the various chemical properties of the molecular

compounds that are used in the drug discovery [6]. Metric dimension of graph was formulated as integer programming problem by Charterand et al. [6]. Fehar et al. studied the metric dimension of Cayley digraphs [7]. For further studies of metric dimension of convex polytopes, Cayley and Toeplitz networks, see [8–11].

Currie and Oellermann defined the concept of fractional metric dimension (FMD) as an optimal solution of the linear relaxation of the integer programming problem (IPP) [3]. Later, Faher et al. presented the identical calculation of IPP with the help of FMD [7]. Arguman and Matthew introduced many different properties of FMD for connected networks with respect to their order [12]. FMDs of hierarchical product of graphs were computed by Feng and Wang [13]. Liu et al. [14] computed the FMD of generalized Jahangir graph. The concept of local fractional metric



dimension (LFMD) is introduced by Aisyah et al. [15]. They also computed it for the connected networks which are obtained by the operation of the corona product. The results for the LFMDs of some cycle-related networks and rotationally symmetric and planar networks can be found in [16, 17]. Javaid et al. (2020) computed the sharp bounds of LFMD of connected networks and illustrated the obtained results with the help of wheel-related networks. They also compared the bounded- and unboundedness of the obtained results [18].

In this paper, lower bound of LFMD for connected networks is improved from unity and expressed in terms of ratio obtained by the cardinalities of the under-study network and the local resolving neighbourhood with maximum order for some edges of network. In the outcome of the obtained result, the LFMDs of prism-related networks as exact values and sharp bounds are computed. The rest of the article is organised as follows: Section 2 consists the preliminaries, Section 3 consists of main results of LFMD of connected networks, Section 4 deals with the local resolving neighbourhoods of prism-related networks, Section 5 presents LFMD of prism-related networks and Section 6 consists of conclusion and comparison among the main results.

## 2. Preliminaries

Let  $G = (V(G), E(G))$  be a network with  $V(G)$  and  $E(G)$  as set of vertices and edges, respectively. A walk is defined as a sequence of alternating vertices and edges. A walk in which the vertices are all distinct is a path between vertices  $a$  and  $b$  and a closed path is called a cycle. For any two vertices  $a$  and  $b$  of  $G$ , the distance  $d(a, b)$  is the length of shortest path  $a \sim b$  in  $G$ . A pair of vertices  $a$  and  $b$  in a network is a connected pair if there is a path between them and the network is a connected network. For a connected network  $G$  and  $e = ab \in E(G)$ , a vertex  $x \in V(G)$  distinguishes two vertices  $a$  and  $b$  if  $d(x, a) \neq d(x, b)$  is known as symmetric vertex. Moreover,  $x$  resolves the edge  $e$  in  $G$  if  $d(x, a) \neq d(x, b)$ . For  $D = \{a_1, a_2, a_3, \dots, a_n\} \subseteq V(G)$  and  $x \in V(G)$ , the  $k$ -tuple metric form of  $D$  in terms of  $x$  is given by  $r(x|D) = d(x, a_1), d(x, a_2), d(x, a_3), \dots, d(x, a_n)$ . The set  $D$  becomes resolving set having  $n$  elements of graph  $G$  if each pair of vertices in  $G$  bears a distinct metric form with respect to  $D$ . The resolving set with least number of vertices is referred as metric basis for  $G$  and cardinality of such resolving set is called metric dimension of  $G$  defined by

$$\dim(G) = \min\{|D|: D \text{ is resolving set of } G\}. \quad (1)$$

For an edge  $ab \in E(G)$ , the local resolving neighbourhood (LRN) is defined as  $\text{LR}(ab) = \{x \in V(G): d(x, a) \neq d(x, b)\}$ , where  $x \in V(G)$ . A function is called an upper local resolving function (ULRF) if  $f: V(G) \rightarrow [0, 1]$  and  $f(\text{LR}(ab)) \geq 1$  for each  $\text{LR}(ab)$  of  $G$ , where  $f(\text{LR}(ab)) = \sum_{x \in \text{LR}(ab)} f(x)$ . On the other hand, a function is called lower local resolving function (LLRF) if  $\Psi: V(G) \rightarrow [0, 1]$  and  $\Psi(\text{LR}(ab)) \leq 1$  for each  $\text{LR}(ab)$  of  $G$ , where  $\Psi(\text{LR}(ab)) = \sum_{x \in \text{LR}(ab)} \Psi(x)$ . Then, LFMD is

defined as  $\dim_{lf}(G) = \tau$ , where  $\tau$  is  $\min\{|f|: f \text{ which is the upper local minimal resolving function of } G\}$  or  $\max\{|g|: g \text{ is the lower local maximal resolving function of } G\}$ .

For  $1 \leq i \leq n$ , now we present some prism-related networks. The circular diagonal ladder ( $\text{CDL}_n$ ) is obtained from prism network  $D_n$  of order  $2n$  and size  $5n$  by adding some double crossing edges  $a_i b_{(i+1)}$  and  $a_{(i+1)} b_i$ , as shown in Figure 1. The antiprism network ( $A_n$ ) of order  $2n$  and size  $4n$  is obtained by prism network ( $D_n$ ) by adding some crossing edges  $a_i b_{(i+1)}$ , see Figure 2. The sun flower network ( $\text{SF}_n$ ) of order  $2n$  and size  $3n$ , we mean a network, is isomorphic to the network obtained from  $A_n$  by deleting edges  $b_i b_{(i+1)}$ , see Figure 3 [19].

**Theorem 1** (see [18]). *Let  $G = (V(G), E(G))$  be a connected network. Let  $\text{LR}(e)$  be a local resolving neighbourhood for the edge  $e$  of  $G$ . If  $|\text{LR}(e) \cap Z| \geq \alpha$ ,  $\forall e \in E(G)$ , then*

$$1 \leq \dim_{lf}(G) \leq \frac{|Z|}{\alpha}, \quad (2)$$

where  $Z = \cup \{\text{LR}(e): |\text{LR}(e)| = \alpha\}$ ,  $\alpha = \min\{|\text{LR}(e)|: e \in E(G)\}$ , and  $2 \leq \alpha \leq |V(G)|$ .

**Proposition 1** (see [18]). *Let  $G = (V(G), E(G))$  be a connected network. For each  $e \in E(G)$ , if  $|\text{LR}(e) \cap Z| \geq 2$ , then  $\dim_{lf}(G) = (|Z|/2)$ , where  $Z = \cup \{\text{LR}(e): |\text{LR}(e)| = 2\}$ , and  $\text{LR}(e)$  is a LRN set of  $e \in E(G)$ .*

## 3. Main Results

Main results of LFMD are as follows.

**Proposition 2.** *Let  $G = (V(G), E(G))$  be a connected network and  $\text{LR}(e)$  be the local resolving neighbourhood set of the edge  $e$  of  $G$ . For  $\beta = \max\{|\text{LR}(e)|: e \in E(G)\}$ , if  $Y = \cup \{\text{LR}(e): |\text{LR}(e)| = \beta\} \subseteq V(G)$ , then  $|\text{LR}(e) \cap Y| \leq \beta$  for each local resolving neighbourhood  $\text{LR}(e)$  of  $G$ .*

**Theorem 2.** *Let  $G = (V(G), E(G))$  be a connected network and  $\text{LR}(e)$  be the local resolving neighbourhood set. Then,*

$$\frac{|V(G)|}{\beta} \leq \dim_{lf}(G), \quad (3)$$

where  $\beta = \max\{|\text{LR}(e)|: e \in E(G)\}$  and  $2 \leq \beta \leq |V(G)|$ .

*Proof.* Define  $\Phi: V(G) \rightarrow [0, 1]$  as  $\phi(v) = (1/\beta)$  for  $v \in V(G)$ . By Proposition 2, for  $e \in E(G)$ , we have

$$\phi(\text{LR}(e)) = \sum_{x \in \text{LR}(e)} \phi(x) = \sum_{x \in \text{LR}(e) \cap V(G)} \frac{1}{\beta} = |\text{LR}(e) \cap V(G)| \frac{1}{\beta} \leq 1. \quad (4)$$

This shows that  $\phi$  is a lower local resolving function (LLRF). To show that  $\phi$  is maximal, suppose on contrary, there exists another LLRF  $\Psi$  such that  $\Psi(x) \geq \Phi(x)$ , where  $\Psi(x) \neq \Phi(x)$ , for at least one  $x \in V(G)$ .  $\forall x \in \text{LR}(e)$  such that  $|\text{LR}(e)| = \beta$ , we have

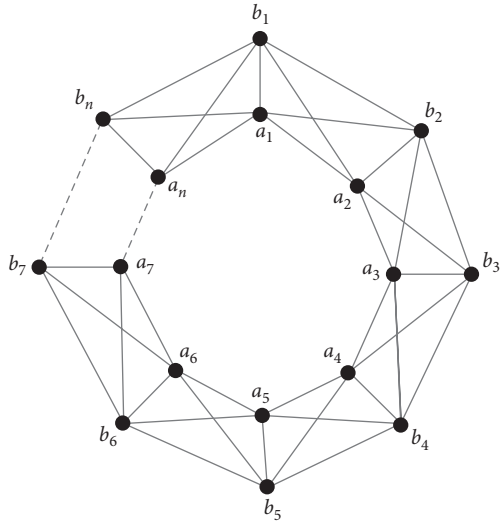


FIGURE 1: Circular diagonal ladder  $CDL_n$ .

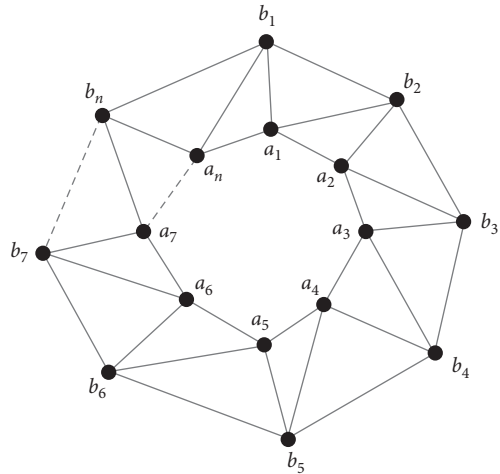


FIGURE 2: Antiprism  $A_n$ .

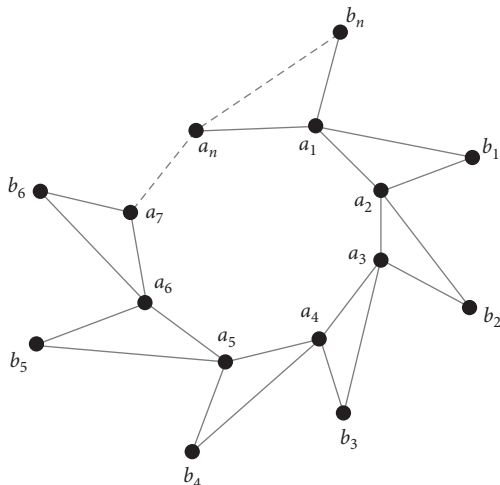


FIGURE 3: Sun flower network  $SF_n$ .

$$\Psi(LR(e)) = \sum_{x \in LR(e)} \Psi(x) > \sum_{x \in LR(e)} \phi(x) = 1. \quad (5)$$

Thus,  $\Psi(LR(e)) > 1$ . This shows that  $\Psi$  is not LLRF and consequently  $\phi$  is maximal LLRF. Let  $\phi'$  be another maximal LLRF of  $G$ . Then,

$$|\phi'| = \sum_{x \in V(G)} \phi'(x). \quad (6)$$

Now, we consider three cases (i)  $\phi'(x) > (1/\beta)$  for each  $x \in V(G)$ , (ii)  $\phi'(x) \leq (1/\beta)$  for each  $x \in V(G)$ , and (iii)  $\phi'(x) > (1/\beta)$  for some  $x \in V(G)$ .

Case 1: if  $\phi'(x) > (1/\beta)$ , for each  $x \in V(G)$ . For  $LR(e) \subseteq Y$  such that  $|LR(e)| = \beta$ , we have  $\phi'(LR(e)) > 1$ . This shows  $\phi'$  is not LLRF. Thus, this case does not hold.

Case 2: let  $\phi'(x) \leq (1/\beta) \forall x \in V(G)$ . Then,

$$|\phi'| = \sum_{x \in V(G)} \phi'(x) \leq \frac{|V(G)|}{\beta} = |\phi|. \quad (7)$$

Consequently,

$$\dim_{lf}(G) = \frac{|V(G)|}{\beta}. \quad (8)$$

Case 3: assume that  $\phi'(x) > (1/\beta)$  for some  $x \in V(G)$ . Suppose that  $S = \{t \in V(G) : \phi'(t) > (1/\beta)\}$  and  $Y = \cup \{LR(e) : |LR(e)| = \beta\}$ . We note that  $S \cap Y = \emptyset$ ; otherwise, for  $|LR(e)| = \beta$ ,  $\phi'(LR(x)) > 1$  which implies that  $\phi'$  is not a LLRF. Consider

$$|\phi'| = \sum_{x \in V(G)} \phi'(x) = \sum_{x \in Y} \phi'(x) + \sum_{x \in V(G)-Y} \phi'(x). \quad (9)$$

Since  $\sum_{x \in V(G)-Y} \phi'(x) \geq \sum_{x \in V(G)-Y} \phi(x)$ , therefore,

$$\begin{aligned} |\phi'| &= \sum_{x \in V(G)} \phi'(x) = \sum_{x \in Y} \phi'(x) + \sum_{x \in V(G)-Y} \phi'(x) \geq \sum_{x \in Y} \phi(x) \\ &+ \sum_{x \in V(G)-Y} \phi(x) = \frac{|V(G)|}{\beta} = |\phi|. \end{aligned} \quad (10)$$

Consequently,

$$\dim_{lf}(G) = |\phi'| \geq |\phi| = \frac{|V(G)|}{\beta}. \quad (11)$$

Thus, from all the cases,

$$\frac{|V(G)|}{\beta} \leq \dim_{lf}(G), \text{ which completes the proof.} \quad (12)$$

Now, we present the following two corollaries as the direct consequences of the above result.

**Corollary 1.** Let  $G = (V(G), E(G))$  be a connected network,  $LR(e)$  be LRN of  $e \in E(G)$ ,  $\beta = \max\{|LR(e)| : e \in E(G)\}$ ,

$\alpha = \min\{|LR(e)|: e \in E(G)\}$ , and  $X = \cup\{LR(e): |LR(e)| = \alpha\}$ . If  $\alpha = \beta$  and  $X = V(G)$ , then

$$\dim_{lf}(G) = \frac{|V(G)|}{\beta}. \quad (13)$$

*Proof.* Since  $\alpha = \beta$  and  $X = V(G)$ , therefore, by Theorem A,  $\dim_{lf}(G) = (|V(G)|/\beta)$ . Also, by Theorem 1,  $\dim_{lf}(G) = (|V(G)|/\beta)$ . Consequently,

$$\dim_{lf}(G) = \frac{|V(G)|}{\beta}. \quad (14)$$

**Corollary 2.** Let  $G = (V(G), E(G))$  be a connected network,  $LR(e)$  be the LRN of  $e \in E(G)$ ,  $\beta = \max\{|LR(e)|: e \in E(G)\}$ ,  $\alpha = \min\{|LR(e)|: e \in E(G)\}$ , and  $X = \cup\{LR(e): |LR(e)| = \alpha\}$ . If  $\alpha = |X|$  and  $\beta = |V(G)|$ , then  $\dim_{lf}(G) = 1$ .

*Proof.* Since  $\beta = |V(G)|$ , then by Theorem 2,  $1 \leq \dim_{lf}(G)$ . Also, as  $\alpha = |X|$ , therefore, by Theorem 1,  $\dim_{lf}(G) \leq 1$ . Consequently,  $\dim_{lf}(G) = 1$ .

*Remark 1.* Corollary 2 strengthens the result proved in [18].

#### 4. LRNs of the Prism-Related Networks

In this section, the local resolving neighbourhoods of prism-related networks are classified.

**Lemma 1.** Let  $CDL_n$  with  $n \geq 4$  be a circular diagonal ladder network, where  $n \equiv 0 \pmod{2}$  and  $|V(CDL_n)| = 2n$ , where  $1 \leq i \leq n$ . We have

- (a)  $|LR(e_i)| = |LR(a_i b_i)| = 2$  and  $|\cup_{i=1}^n LR(e_i)| = 2n$ ,
- (b)  $|LR(e_i)| = |LR(b_i b_{(i+1)})|$  and  $|LR(b_i b_{(i+1)}) \cap \cup_{i=1}^n LR(e_i)| \geq |LR(e_i)|$ ,
- (c)  $|LR(e_i)| = |LR(a_i a_{(i+1)})|$  and  $|LR(a_i a_{(i+1)}) \cap \cup_{i=1}^n LR(e_i)| \geq |LR(e_i)|$ ,
- (d)  $|LR(e_i)| = |LR(a_i b_{(i+1)})|$  and  $|LR(a_i b_{(i+1)}) \cap \cup_{i=1}^n LR(e_i)| \geq |LR(e_i)|$ ,
- (e)  $|LR(e_i)| = |LR(b_i a_{(i+1)})|$  and  $|LR(b_i a_{(i+1)}) \cap \cup_{i=1}^n LR(e_i)| \geq |LR(e_i)|$ ,
- (f)  $|LR(e_i)| = |LR(a_i b_{(i-1)})|$  and  $|LR(a_i b_{(i-1)}) \cap \cup_{i=1}^n LR(e_i)| \geq |LR(e_i)|$ .

*Proof.* Assume that  $a_i$  and  $b_i$  are inner and outer vertices, respectively, for  $1 \leq i \leq n$  and  $n+1 \equiv 1 \pmod{n}$ . We have the following:

- (a) Consider  $LR(a_i b_i) = \{a_i, b_i\}$  with  $|LR(e_i)| = |LR(a_i b_i)| = 2$ . Moreover,  $|\cup_{i=1}^n LR(e_i)| = |V(CDL_n)| = 2n$ .
- (b)  $LR(b_i b_{(i+1)}) = V(CDL_n) - \{a_i, a_{(i+1)}\}$  with  $|LR(b_i b_{(i+1)})| = 2n - 2 > 2 = |LR(e_i)|$  and  $|LR(b_i b_{(i+1)}) \cap \cup_{i=1}^n LR(e_i)| = 2n - 2 > 2 = |LR(e_i)|$ .

- (c)  $LR(a_i a_{(i+1)}) = V(CDL_n) - \{b_i, b_{(i+1)}\}$  with  $|LR(a_i a_{(i+1)})| = 2n - 2 > 2 = |LR(e_i)|$  and  $|LR(a_i a_{(i+1)}) \cap \cup_{i=1}^n LR(e_i)| = 2n - 2 > 2 = |LR(e_i)|$ .
- (d)  $LR(a_i b_{(i+1)}) = V(CDL_n) - \{a_{(i+1)}, b_i\}$  with  $|LR(a_i b_{(i+1)})| = 2n - 2 > 2 = |LR(e_i)|$  and  $|LR(a_i b_{(i+1)}) \cap \cup_{i=1}^n LR(e_i)| = 2n - 2 > 2 = |LR(e_i)|$ .
- (e)  $LR(b_i a_{(i+1)}) = V(CDL_n) - \{b_{(i+1)}, a_i\}$  with  $|LR(b_i a_{(i+1)})| = 2n - 2 > 2 = |LR(e_i)|$  and  $|LR(b_i a_{(i+1)}) \cap \cup_{i=1}^n LR(e_i)| = 2n - 2 > 2 = |LR(e_i)|$ .
- (f)  $LR(b_i a_{(i-1)}) = V(CDL_n) - \{a_{(i-1)}, b_{(i+1)}\}$  with  $|LR(b_i a_{(i-1)})| = 2n - 2 > 2 = |LR(e_i)|$  and  $|LR(b_i a_{(i-1)}) \cap \cup_{i=1}^n LR(e_i)| = 2n - 2 > 2 = |LR(e_i)|$ .

**Lemma 2.** Let  $CDL_n$  with  $n \geq 5$  be a circular diagonal ladder network, where  $n \equiv 1 \pmod{2}$  and  $|V(CDL_n)| = 2n$ , where  $1 \leq i \leq n$ . We have

- (a)  $|LR(e_i)| = |LR(a_i b_i)| = 2$  and  $|\cup_{i=1}^n LR(e_i)| = 2n$ ,
- (b)  $|LR(e_i)| < |LR(b_i b_{(i+1)})|$  and  $|LR(b_i b_{(i+1)}) \cap \cup_{i=1}^n LR(e_i)| \geq |LR(e_i)|$ ,
- (c)  $|LR(e_i)| < |LR(a_i a_{(i+1)})|$  and  $|LR(a_i a_{(i+1)}) \cap \cup_{i=1}^n LR(e_i)| \geq |LR(e_i)|$ ,
- (d)  $|LR(e_i)| < |LR(a_i b_{(i+1)})|$  and  $|LR(a_i b_{(i+1)}) \cap \cup_{i=1}^n LR(e_i)| \geq |LR(e_i)|$ ,
- (e)  $|LR(e_i)| < |LR(b_i a_{(i+1)})|$  and  $|LR(b_i a_{(i+1)}) \cap \cup_{i=1}^n LR(e_i)| \geq |LR(e_i)|$ ,
- (f)  $|LR(e_i)| < |LR(a_i b_{(i-1)})|$  and  $|LR(a_i b_{(i-1)}) \cap \cup_{i=1}^n LR(e_i)| \geq |LR(e_i)|$ .

*Proof.* Assume that  $a_i$  and  $b_i$  are inner and outer vertices, respectively, for  $1 \leq i \leq n$  and  $n+1 \equiv 1 \pmod{n}$ ,  $(3n+1/2) \equiv 1 \pmod{n}$ . We have the following:

- (a) Consider  $LR(a_i b_i) = \{a_i, b_i\}$  with  $|LR(e_i)| = |LR(a_i b_i)| = 2$ . Moreover,  $|\cup_{i=1}^n LR(e_i)| = |V(CDL_n)| = 2n$ .
- (b) As  $LR(b_i b_{(i+1)}) = V(CDL_n) - \{b_{(n+2i+1/2)}, a_{(n+2i+1/2)}, a_i, a_{(i+1)}\}$  with  $|LR(b_i b_{(i+1)})| = 2n - 4 > 2 = |LR(e_i)|$  and  $|LR(b_i b_{(i+1)}) \cap \cup_{i=1}^n LR(e_i)| = 2n - 4 > 2 = |LR(e_i)|$ .
- (c) As  $LR(a_i a_{(i+1)}) = V(CDL_n) - \{a_{(n+2i+1/2)}, b_{(n+2i+1/2)}, b_i, b_{(i+1)}\}$  with  $|LR(a_i a_{(i+1)})| = 2n - 4 > 2 = |LR(e_i)|$  and  $|LR(a_i a_{(i+1)}) \cap \cup_{i=1}^n LR(e_i)| = 2n - 4 > 2 = |LR(e_i)|$ .
- (d) As  $LR(a_i b_{(i+1)}) = V(CDL_n) - \{a_{(n+2i+1/2)}, b_{(n+2i+1/2)}, a_{(i+1)}, b_i\}$  with  $|LR(a_i b_{(i+1)})| = 2n - 4 > 2 = |LR(e_i)|$  and  $|LR(a_i b_{(i+1)}) \cap \cup_{i=1}^n LR(e_i)| = 2n - 4 > 2 = |LR(e_i)|$ .
- (e) As  $LR(b_i a_{(i+1)}) = V(CDL_n) - \{a_{(i)}, b_{(i+1)}, a_{(n+2i+1/2)}, b_{(n+2i+1/2)}\}$  with  $|LR(b_i a_{(i+1)})| = 2n - 4 > 2 = |LR(e_i)|$  and  $|LR(b_i a_{(i+1)}) \cap \cup_{i=1}^n LR(e_i)| = 2n - 4 > 2 = |LR(e_i)|$ .
- (f) As  $LR(a_i b_{(i-1)}) = V(CDL_n) - \{a_{(i-1)}, b_{(i-1)}, a_{(n+2i+1/2)}, b_{(n+2i+1/2)}\}$  with  $|LR(a_i b_{(i-1)})| = 2n - 4 > 2 = |LR(e_i)|$ .

and  $|\text{LR}(b_i a_{(i+1)}) \cap \cup_{i=1}^n \text{LR}(e_i)| = 2n - 4 > 2 = |\text{LR}(e_i)|$ .

**Lemma 3.** Let  $A_n$  with  $n \geq 4$  be an antiprism network, where  $n \equiv 0 \pmod{2}$  and  $|V(A_n)| = 2n$  and  $1 \leq i \leq n$ . We have

- (a)  $|\text{LR}(e_i)| = |\text{LR}(a_i b_i)|$  and  $|\text{LR}(a_i b_{(i+1)})| = n$  and  $|\cup_{i=1}^n \text{LR}(e_i)| = 2n$ ,
- (b)  $|\text{LR}(e_i)| = |\text{LR}(b_i b_{(i+1)})|$  and  $|\text{LR}(b_i b_{(i+1)}) \cap \cup_{i=1}^n \text{LR}(e_i)| \geq |\text{LR}(e_i)|$ ,
- (c)  $|\text{LR}(e_i)| = |\text{LR}(a_i a_{(i+1)})|$  and  $|\text{LR}(a_i a_{(i+1)}) \cap \cup_{i=1}^n \text{LR}(e_i)| \geq |\text{LR}(e_i)|$ .

*Proof.* Assume that  $a_i$  and  $b_i$  are inner and outer vertices, respectively, for  $1 \leq i \leq n$ , where  $n + 1 \equiv 1 \pmod{2}$ ,  $(3n + 2/2) \equiv 1 \pmod{n}$ , and  $(3n/2) \equiv 1 \pmod{n}$ . We have

- (a)  $\text{LR}(e_i) = \text{LR}(a_i b_i) = \{b_i, b_{(n+2i+2/2)}, b_{(n+2i+2/2)+1}, b_{(n+2i+2/2)+2}, \dots, b_{(n+i-1)}, a_i, a_{(i+1)}, a_{(i+2)}, \dots, a_{(n+2i-2/2)}\}$  and  $\text{LR}(a_i b_{(i+1)}) = \{b_{(i+1)}, b_{(i+2)}, b_{(i+3)}, \dots, b_{(2i+n/2)}, a_i, a_{(n+2i+2/2)}, a_{(n+2i+2/2)+1}, a_{(n+2i+2/2)+2}, \dots, a_{(n+i-1)}\}$  with  $|\text{LR}(e_i)| = n$ . Moreover,  $|\cup_{i=1}^n \text{LR}(e_i)| = |V(A_n)| = 2n$ ,
- (b) As  $\text{LR}(b_i b_{(i+1)}) = V(A_n) - \{a_i, a_{(n+2i/2)}\}$  with  $|\text{LR}(b_i b_{(i+1)})| = 2n - 2 > n = |\text{LR}(e_i)|$  and  $|\text{LR}(b_i b_{(i+1)}) \cap \cup_{i=1}^n \text{LR}(e_i)| = 2n - 2 > n = |\text{LR}(e_i)|$ ,
- (c) As  $\text{LR}(a_i a_{(i+1)}) = V(A_n) - \{b_{(i+2)}, b_{(n+2i+2/2)}\}$  with  $|\text{LR}(a_i a_{(i+1)})| = 2n - 2 > n = |\text{LR}(e_i)|$  and  $|\text{LR}(a_i a_{(i+1)}) \cap \cup_{i=1}^n \text{LR}(e_i)| = 2n - 2 > n = |\text{LR}(e_i)|$ .

**Lemma 4.** Let  $A_n$  with  $n \geq 3$  be an antiprism network, where  $|V(A_n)| = 2n$  with  $n \equiv 1 \pmod{2}$ . For  $1 \leq i \leq n$ , we have

- (a)  $|\text{LR}(e_i)| = |\text{LR}(a_i b_i)|$  and  $|\text{LR}(a_i b_{(i+1)})| = n + 1$  and  $|\cup_{i=1}^n \text{LR}(e_i)| = 2n$ ,
- (b)  $|\text{LR}(e_i)| = |\text{LR}(b_i b_{(i+1)})|$  and  $|\text{LR}(b_i b_{(i+1)}) \cap \cup_{i=1}^n \text{LR}(e_i)| \geq |\text{LR}(e_i)|$ ,
- (c)  $|\text{LR}(e_i)| = |\text{LR}(a_i a_{(i+1)})|$  and  $|\text{LR}(a_i a_{(i+1)}) \cap \cup_{i=1}^n \text{LR}(e_i)| \geq |\text{LR}(e_i)|$ .

*Proof.* Assume that  $a_i$  and  $b_i$  are inner and outer vertices, respectively, for  $1 \leq i \leq n$ , where  $n + 1 \equiv 1 \pmod{2}$ ,  $(3n + 1/2) \equiv 1 \pmod{n}$ ,  $(3n - 1/2) \equiv 1 \pmod{n}$ , and  $2n - 1 \equiv 1 \pmod{2}$ . We have

- (a)  $\text{LR}(a_i b_i) = \{a_i, a_{(i+1)}, a_{(i+2)}, \dots, a_{(n+2i-1/2)}, b_i, b_{(n+2i+1/2)}, b_{(n+2i+3/2)}, \dots, b_{(n+i-1)}\}$  and  $\text{LR}(a_i b_{(i+1)}) = \{b_{(i+1)}, b_{(i+2)}, \dots, b_{(n+2i+1/2)}, a_i, a_{(n+2i+1/2)}, a_{(n+2i+1/2)+1}, \dots, a_{(n+i-1)}\}$  with  $|\text{LR}(e_i)| = n + 1$ . Moreover,  $|\cup_{i=1}^n \text{LR}(e_i)| = |V(A_n)| = 2n$ .

- (b)  $\text{LR}(a_i a_{(i+1)}) = V(A_n) - \{(a_{(n+2i+1/2)}, b_{(i+1)})\}$  and  $|\text{LR}(a_i a_{(i+1)})| = 2n - 2 > n + 1 = |\text{LR}(e_i)|$ .
- (c)  $\text{LR}(b_i b_{(i+1)}) = V(A_n) - \{a_i, b_{(n+2i+1/2)}\}$  and  $|\text{LR}(b_i b_{(i+1)})| = 2n - 2 > n + 1 = |\text{LR}(e_i)|$ .

**Lemma 5.** Let  $SF_n$  with  $n \geq 3$  be a sun flower network, where  $|V(SF_n)| = 2n$  and  $n \equiv 1 \pmod{2}$ . For  $1 \leq i \leq n$ , we have

- (a)  $|\text{LR}(e_i)| = |\text{LR}(a_i b_i)|$  and  $|\text{LR}(b_i a_{(i+1)})| = n + 1$  and  $|\cup_{i=1}^n \text{LR}(e_i)| = 2n$ ,
- (b)  $|\text{LR}(e_i)| = |\text{LR}(a_i a_{(i+1)})|$  and  $|\text{LR}(a_i a_{(i+1)}) \cap \cup_{i=1}^n \text{LR}(e_i)| \geq |\text{LR}(e_i)|$ .

*Proof.* Assume that  $a_i$  and  $b_i$  are inner and outer vertices, respectively, for  $1 \leq i \leq n$ , where  $n + 1 \equiv 1 \pmod{n}$ ,  $n + 2 \equiv 1 \pmod{n}$ ,  $(3n + 1/2) \equiv 1 \pmod{n}$ ,  $(3n - 1/2) \equiv 1 \pmod{n}$ , and  $2n - 1 \equiv 1 \pmod{n}$ . Now, we have

- (a)  $\text{LR}(a_i b_i) = \{a_i, a_{(n+2i+1/2)}, a_{(n+2i+1/2)+1}, \dots, a_{(n+i-1)}, b_i, b_{(n+2i+1/2)}, b_{(n+2i+1/2)+1}, \dots, b_{(n+i-1)}\}$  and  $\text{LR}(b_i a_{(i+1)}) = \{b_i, b_{(i+1)}, b_{(i+2)}, \dots, b_{((n+2i+1/2))}, a_{(i+1)}, a_{(i+2)}, a_{(i+3)}, \dots, a_{(n+i-1)}\}$  with  $|\text{LR}(e_i)| = n + 1$ . Moreover,  $|\cup_{i=1}^n \text{LR}(e_i)| = |V(SF_n)| = 2n$ .
- (b)  $\text{LR}(a_i a_{(i+1)}) = V(SF_n) - \{a_{(n+2i+1/2)}, b_i\}$  and  $|\text{LR}(a_i a_{(i+1)})| = 2n - 2$  with  $|\text{LR}(a_i a_{(i+1)})| = 2n - 2 > n + 1 = |\text{LR}(e_i)|$  and  $|\text{LR}(a_i a_{(i+1)}) \cap \cup_{i=1}^n \text{LR}(e_i)| = 2n - 2 > n + 1 = |\text{LR}(e_i)|$ .

**Lemma 6.** Let  $SF_n$  with  $n \geq 4$  be a sun flower network, where  $|V(SF_n)| = 2n$  and  $n \equiv 0 \pmod{2}$ . For  $1 \leq i \leq n$ , we have

- (a)  $|\text{LR}(e_i)| = |\text{LR}(a_i b_i)|$  and  $|\text{LR}(b_i a_{(i+1)})| = n + 1$  and  $|\cup_{i=1}^n \text{LR}(e_i)| = 2n$ ,
- (b)  $|\text{LR}(e_i)| = |\text{LR}(a_i a_{(i+1)})|$  and  $|\text{LR}(a_i a_{(i+1)}) \cap \cup_{i=1}^n \text{LR}(e_i)| \geq |\text{LR}(e_i)|$ .

*Proof.* Assume that  $a_i$  and  $b_i$  are inner and outer vertices, respectively, for  $1 \leq i \leq n$ , where  $n + 1 \equiv 1 \pmod{n}$ ,  $n + 2 \equiv 1 \pmod{n}$ ,  $(3n + 1/2) \equiv 1 \pmod{n}$ ,  $(3n/2) \equiv 1 \pmod{n}$ , and  $2n - 1 \equiv 1 \pmod{n}$ . We have

- (a)  $2n - 1 \equiv 1 \pmod{n}$  and  $\text{LR}(b_i a_{(i+1)}) = \{b_i, b_{(i+1)}, b_{(i+2)}, \dots, b_{(n+2i/2)}, a_{(i+1)}, a_{(i+2)}, a_{(i+3)}, \dots, a_{(n+2i/2)}\}$  with  $|\text{LR}(e_i)| = n + 1$ . Moreover,  $|\cup_{i=1}^n \text{LR}(e_i)| = |V(SF_n)| = 2n$ .
- (b)  $\text{LR}(a_i a_{(i+1)}) = V(SF_n) - \{b_{(n+2i/2)}, b_i\}$  and  $|\text{LR}(a_i a_{(i+1)})| = 2n - 2$  with  $|\text{LR}(a_i a_{(i+1)})| = 2n - 2 > n + 1 = |\text{LR}(e_i)|$  and  $|\text{LR}(a_i a_{(i+1)}) \cap \cup_{i=1}^n \text{LR}(e_i)| = 2n - 2 > n + 1 = |\text{LR}(e_i)|$ .

## 5. LFMD of Prism-Related Networks

The LFMD of prism-related networks is computed as follows.

**Theorem 3.** Let  $CDL_n$  with  $n \geq 4$  be a circular diagonal ladder network and  $|V(CDL_n)| = 2n$ . Then,  $\dim_{lf}(CDL_n) = n$ .

*Proof.* Case 1: For  $n = 4$ , LRNs are as follows:

$$\begin{aligned} LR_1 &= LR(b_1b_2) = V(CDL_4) - \{a_1, a_2\}, \\ LR_2 &= LR(b_2b_3) = V(CDL_4) - \{a_2, a_3\}, \\ LR_3 &= LR(b_3b_4) = V(CDL_4) - \{a_3, a_4\}, \\ LR_4 &= LR(b_4b_1) = V(CDL_4) - \{a_1, a_2\}, \\ LR_5 &= LR(a_1a_2) = V(CDL_4) - \{b_1, b_2\}, \\ LR_6 &= LR(a_2a_3) = V(CDL_4) - \{b_2, b_3\}, \\ LR_7 &= LR(a_3a_4) = V(CDL_4) - \{b_3, b_4\}, \\ LR_8 &= LR(a_4a_1) = V(CDL_4) - \{b_4, b_1\}, \\ LR_9 &= LR(a_1b_2) = V(CDL_4) - \{a_2, b_1\}, \\ LR_{10} &= LR(a_2b_3) = V(CDL_4) - \{a_3, b_2\}, \\ LR_{11} &= LR(a_3b_4) = V(CDL_4) - \{a_4, b_3\}, \\ LR_{12} &= LR(a_4b_1) = V(CDL_4) - \{a_1, b_4\}, \\ LR_{13} &= LR(a_2b_1) = V(CDL_4) - \{a_1, b_2\}, \\ LR_{14} &= LR(a_3b_2) = V(CDL_4) - \{a_2, b_3\}, \\ LR_{15} &= LR(a_4b_3) = V(CDL_4) - \{a_3, b_4\}, \\ LR_{16} &= LR(a_1b_4) = V(CDL_4) - \{a_4, b_1\}, \\ LR_{17} &= LR(b_1a_2) = V(CDL_4) - \{b_2, a_1\}, \\ LR_{18} &= LR(b_2a_3) = V(CDL_4) - \{b_3, a_2\}, \\ LR_{19} &= LR(b_3a_4) = V(CDL_4) - \{b_4, a_3\}, \\ LR_{20} &= LR(b_4a_1) = V(CDL_4) - \{b_1, a_4\}, \\ LR_{21} &= LR(a_1b_1) = \{a_1, b_1\}, \\ LR_{22} &= LR(a_2b_2) = \{a_2, b_2\}, \\ LR_{23} &= LR(a_3b_3) = \{a_3, b_3\}, \\ LR_{24} &= LR(a_4b_4) = \{a_4, b_4\}. \end{aligned}$$

As, for  $1 \leq i \leq 4$ ,  $|LR(e_i)|$  is 2 such that  $|LR(e_i)| < |LR(e_s)|$ , where  $1 \leq s \leq 20$ . Moreover,  $\cup_{i=1}^4 LR(e_i) = 8$  and  $|LR_s \cap \cup_{i=1}^4 LRe_i| = |LRe_i| = 2$ . Define  $\phi: V(CDL_4) \rightarrow [0, 1]$  as  $\phi(x) = (1/2)$  is a LRF with minimum cardinality for each  $x \in V(CDL_4)$ . Consequently, by Proposition 1,  $\dim_{lf}(CDL_4) = (|V(CDL_4)|/2) = 4$ .

Case 2: For  $n = 5$ , LRNs are as follows:

$$\begin{aligned} LR_1 &= LR(b_1b_2) = V(CDL_5) - \{b_4, a_4, a_1, a_2\}, \\ LR_2 &= LR(b_2b_3) = V(CDL_5) - \{b_5, a_5, a_2, a_3\}, \\ LR_3 &= LR(b_3b_4) = V(CDL_5) - \{b_6, a_6, a_3, a_4\}, \\ LR_4 &= LR(b_4b_5) = V(CDL_5) - \{b_2, a_2, a_4, a_5\}, \\ LR_5 &= LR(b_5b_1) = V(CDL_5) - \{b_3, a_1, a_3, a_5\}, \\ LR_6 &= LR(a_1a_2) = V(CDL_5) - \{b_4, a_4, b_1, b_2\}, \\ LR_7 &= LR(a_2a_3) = V(CDL_5) - \{b_5, a_5, b_2, b_3\}, \end{aligned}$$

$$\begin{aligned} LR_8 &= LR(a_3a_4) = V(CDL_5) - \{b_1, a_1, b_3, b_4\}, \\ LR_9 &= LR(a_4a_5) = V(CDL_5) - \{b_2, a_2, b_4, b_5\}, \\ LR_{10} &= LR(a_5a_1) = V(CDL_5) - \{b_1, a_3, b_3, b_5\}, \\ LR_{11} &= LR(a_1b_2) = V(CDL_5) - \{b_4, a_4, b_1, a_2\}, \\ LR_{12} &= LR(a_2b_3) = V(CDL_5) - \{b_5, a_5, b_2, a_3\}, \\ LR_{13} &= LR(a_3b_4) = V(CDL_5) - \{b_1, a_4, b_3, a_4\}, \\ LR_{14} &= LR(a_4b_5) = V(CDL_5) - \{b_4, a_4, b_1, a_2\}, \\ LR_{15} &= LR(a_5b_1) = V(CDL_5) - \{b_3, a_3, b_5, a_6\}, \\ LR_{16} &= LR(a_1b_5) = \{a_1, a_2, a_4, b_2, b_4, b_4\}, \\ LR_{17} &= LR(a_2b_1) = \{a_2, a_3, a_5, b_1, b_3, b_5\}, \\ LR_{18} &= LR(a_3b_2) = \{a_2, a_3, a_4, b_1, b_2, b_4\}, \\ LR_{19} &= LR(a_4b_3) = \{a_2, a_4, a_5, b_2, b_3, b_5\}, \\ LR_{20} &= LR(a_5b_4) = \{a_1, a_3, a_5, b_1, b_3, b_4\}, \\ LR_{21} &= LR(b_1a_2) = \{a_2, a_3, a_5, b_1, b_3, b_5\}, \\ LR_{22} &= LR(b_2a_3) = \{a_1, a_3, a_4, b_1, b_2, b_4\}, \\ LR_{23} &= LR(b_3a_4) = \{a_2, a_4, a_5, b_2, b_3, b_5\}, \\ LR_{24} &= LR(b_4a_5) = \{a_1, a_3, a_5, b_1, b_3, b_4\}, \\ LR_{25} &= LR(b_5a_1) = \{a_1, a_2, a_4, b_2, b_4, b_5\}, \\ LR_{26} &= LR(a_1b_1) = \{a_1, b_1\}, \\ LR_{27} &= LR(a_2b_2) = \{a_2, b_2\}, \\ LR_{28} &= LR(a_3b_3) = \{a_3, b_3\}, \\ LR_{29} &= LR(a_4b_4) = \{a_4, b_4\}, \\ LR_{30} &= LR(a_5b_5) = \{a_5, b_5\}. \end{aligned}$$

As, for  $1 \leq i \leq 5$ ,  $|LRN(e_i)| = 2$  such that  $|LR(e_i)| < |LR(e_s)|$ , where  $1 \leq s \leq 25$ . Moreover,  $\cup_{i=1}^5 LR(e_i) = V(CDL_5)$ ; this implies  $|\cup_{i=1}^5 LR(e_i)| = 10$  and  $|LR_s \cap \cup_{i=1}^5 LRe_i| \geq |LRe_i| = 2$ . Define  $\phi: V(CDL_5) \rightarrow [0, 1]$  such that  $\phi(x) = (1/2)$  is the LRF with minimum cardinality for each  $x \in V(CDL_5)$ . Consequently, by Proposition 1,  $\dim_{lf}(CDL_5) = (|V(CDL_5)|/2) = 5$ .

Case 3: For  $n \geq 6$  and  $1 \leq i \leq n$  by Lemma 1,  $|LR(e_i)| = 2 = \alpha$  and  $|R \cap \cup_{i=1}^n LR(e_i)| \geq 2$ , where  $R$  are all other LRNs. Define  $\phi: V(CDL_n) \rightarrow [0, 1]$  such that  $\phi$  is the LRF with minimum cardinality and  $|\phi| < |\phi'|$ , as  $\phi(v) = (1/2) \forall v \in V(CDL_n)$ .  $V(CDL_n) = \cup \{LR(e): |LR(e)| = 2\}$ . Consequently, by Proposition 1,  $\dim_{lf}(CDL_n) = (|V(CDL_n)|/2) = (2n/2) = n$ .

**Theorem 4.** Let  $A_n$  with  $n \geq 3$  be an antiprism network, where  $n \equiv 1 \pmod{2}$  and  $|V(A_n)| = 2n$ . Then,  $\dim_{lf}(A_n)$ ,

$$\frac{n}{n-1} \leq \dim_{lf}(A_n) \leq \frac{2n}{n+1}. \quad (15)$$

*Proof.* Case 1: For  $n = 3$ , LRNs are as follows:

$$\begin{aligned} LR_1 &= LR(a_1a_2) = \{a_1, a_2, b_1, b_3\}, \\ LR_2 &= LR(a_2a_3) = \{a_2, a_3, b_1, b_2\}, \\ LR_3 &= LR(a_3a_1) = \{a_3, a_1, b_2, b_3\}, \end{aligned}$$

$$\begin{aligned} \text{LR}_4 &= \text{LR}(a_1b_1) = \{a_1, a_2, b_1, b_3\}, \\ \text{LR}_5 &= \text{LR}(a_2b_2) = \{a_2, a_3, b_1, b_2\}, \\ \text{LR}_6 &= \text{LR}(a_3b_3) = \{a_1, a_3, b_2, b_3\}, \\ \text{LR}_7 &= \text{LR}(a_1b_2) = \{a_1, a_3, b_1, b_2\}, \\ \text{LR}_8 &= \text{LR}(a_2b_3) = \{a_1, a_2, b_1, b_3\}, \\ \text{LR}_9 &= \text{LR}(a_3b_1) = \{a_2, a_3, b_1, b_2\}. \end{aligned}$$

As, for  $1 \leq i \leq 9$ ,  $|\text{LR}(e_i)| = 4$ . Moreover,  $\cup_{i=1}^9 \text{LR}(e_i) = V(A_3) = 8$  such that  $|\cup_{i=1}^9 \text{LR}(e_i)| = 6$  and  $|\text{LRN}_s \cap \cup_{i=1}^9 \text{LR}(e_i)| > |\text{LR}(e_i)| = 4$ . Define  $\phi: V(A_3) \rightarrow [0, 1]$  as  $\phi(x) = (1/4)$  is the LRF with minimum cardinality. Consequently, by Corollary 1,  $\dim_{lf}(A_3) = (|V(A_3)|/4) = (3/2)$ .

Case 2: For  $n = 5$ , LRNs are as follows:

$$\begin{aligned} \text{LR}_1 &= \text{LR}(b_1b_2) = V(A_5) - \{a_1, b_4\}, \\ \text{LR}_2 &= \text{LR}(b_2b_3) = V(A_5) - \{a_3, b_5\}, \\ \text{LR}_3 &= \text{LR}(b_3b_4) = V(A_5) - \{a_3, b_1\}, \\ \text{LR}_4 &= \text{LR}(b_4b_5) = V(A_5) - \{a_4, b_2\}, \\ \text{LR}_5 &= \text{LR}(b_5b_1) = V(A_5) - \{a_5, b_3\}, \\ \text{LR}_6 &= \text{LR}(a_1a_2) = V(A_5) - \{a_4, b_2\}, \\ \text{LR}_7 &= \text{LR}(a_2a_3) = V(A_5) - \{a_5, b_3\}, \\ \text{LR}_8 &= \text{LR}(a_3a_4) = V(A_5) - \{a_1, b_4\}, \\ \text{LR}_9 &= \text{LR}(a_4a_5) = V(A_5) - \{a_2, b_5\}, \\ \text{LR}_{10} &= \text{LR}(a_5a_1) = V(A_5) - \{a_3, b_1\}, \\ \text{LR}_{11} &= \text{LR}(b_1a_1) = \{b_1, b_4, b_5, a_1, a_2, a_3\}, \\ \text{LR}_{12} &= \text{LR}(b_2a_2) = \{b_2, b_5, b_1, a_2, a_3, a_4\}, \\ \text{LR}_{13} &= \text{LR}(b_3a_3) = \{b_3, b_1, b_2, a_3, a_4, a_5\}, \\ \text{LR}_{14} &= \text{LR}(b_4a_4) = \{b_4, b_2, b_1, a_4, a_5, a_1\}, \\ \text{LR}_{15} &= \text{LR}(b_5a_5) = \{b_5, b_2, b_3, a_5, a_1, a_2\}, \\ \text{LR}_{16} &= \text{LR}(a_1b_2) = \{a_1, a_4, a_5, b_2, b_3, b_4\}, \\ \text{LR}_{17} &= \text{LR}(a_2b_3) = \{a_2, a_5, a_1, b_3, b_4, b_5\}, \\ \text{LR}_{18} &= \text{LR}(a_3b_4) = \{a_3, a_1, a_2, b_4, b_5, b_1\}, \\ \text{LR}_{19} &= \text{LR}(a_4b_5) = \{a_4, a_2, a_1, b_5, b_1, b_2\}, \\ \text{LR}_{20} &= \text{LR}(a_5b_1) = \{a_5, a_2, a_3, b_1, b_2, b_3\}. \end{aligned}$$

As, for  $1 \leq i \leq 10$ ,  $|\text{LR}(e_i)| = 6$  such that  $|\text{LR}(e_i)| < |\text{LR}(e_s)|$  and  $1 \leq s \leq 10$ .  $\cup_{i=1}^{10} \text{LR}(e_i) = V(A_5)$ ; this implies  $|\cup_{i=1}^{10} \text{LR}(e_i)| = 10$  and  $|\text{LRN} \cap \cup_{i=1}^{10} \text{LR}(e_i)| > |\text{LR}(e_i)| = 6$ . Define  $(\phi: V(A_5) \rightarrow [0, 1])$  as  $\phi(x) = (1/6)$  is the LRF with minimum cardinality for each  $x \in V(A_5)$ . Consequently, by Theorem 1,  $\dim_{lf}(A_5) \leq (|V(A_5)|/6) \leq (5/3)$ .

As, for  $1 \leq i \leq 10$ ,  $|\text{LR}(e_i)| = 8$ ,  $|\text{LR}(e_i)| > |\text{LR}(e_s)|$ , and  $1 \leq s \leq 10$ . Moreover,  $\cup_{i=1}^{10} \text{LR}(e_i) = V(A_5)$ . Define  $(\phi': V(A_5) \rightarrow [0, 1])$  as  $\phi'(x) = (1/8)$  is the LRF with minimum cardinality for each  $x \in V(A_5)$ . Therefore, by Theorem 2,  $\dim_{lf}(A_5) \geq (|V(A_5)|/8) \geq (5/4)$ . Consequently,

$$\frac{5}{4} \leq \dim_{lf}(A_5) \leq \frac{5}{3}. \quad (16)$$

Case 3: For  $n \geq 6$  and  $1 \leq i \leq n$  by Lemma 4,  $|\text{LR}(e_i)| = n + 1 = \alpha$  and  $|R \cap \cup_{i=1}^n \text{LR}(e_i)| \geq n + 1$ , where R are all

other LRNs. There exists an ULRF  $\phi: V(A_n) \rightarrow [0, 1]$ ,  $|\phi| < |\phi'|$  which is defined as  $\phi(v) = (1/\alpha) \forall v \in V(A_n)$ , as  $V(A_n) = \cup \{\text{LR}(e): |\text{LR}(e) = \alpha\}$ . Consequently, by Theorem 1,  $\dim_{lf}(A_n) \leq (|V(A_n)|/n + 1) \leq (2n/n + 1)$ .

Case 4: For  $|\text{LR}(b_i b_{(i+1)})| = 2n - 2 \geq |\text{LR}(e_i)|$ , moreover,  $\cup_{i=1}^{2n} \text{LR}(e_i) = V(A_n)$ . There exists a LLRF such that  $\phi': V(A_n) \rightarrow [0, 1]$  is defined as  $\phi'(x) = (1/2n - 2)$  for each  $x \in V(A_n)$ . Therefore, by Theorem 2, we have  $\dim_{lf}(A_n) \geq (n/n - 1)$ . Consequently,

$$\frac{n}{n-1} \leq \dim_{lf}(A_n) \leq \frac{2n}{n+1}. \quad (17)$$

**Theorem 5.** Let  $A_n$  with  $n \geq 4$  be an antiprism network, where  $n \equiv 0 \pmod{2}$  and  $|V(A_n)| = 2n$ . Then,

$$\frac{n}{n-1} \leq \dim_{lf}(A_4) \leq 2. \quad (18)$$

*Proof.* Case 1: For  $n = 4$ , LRNs are as follows:

$$\begin{aligned} \text{LR}_1 &= \text{LR}(b_1b_2) = V(A_4) - \{a_1, a_3\}, \\ \text{LR}_2 &= \text{LR}(b_2b_3) = V(A_4) - \{a_2, a_4\}, \\ \text{LR}_3 &= \text{LR}(b_3b_4) = V(A_4) - \{a_1, a_3\}, \\ \text{LR}_4 &= \text{LR}(b_4b_1) = V(A_4) - \{a_2, a_4\}, \\ \text{LR}_5 &= \text{LR}(a_1a_2) = V(A_4) - \{b_2, b_4\}, \\ \text{LR}_6 &= \text{LR}(a_2a_3) = V(A_4) - \{b_3, b_1\}, \\ \text{LR}_7 &= \text{LR}(a_3a_4) = V(A_4) - \{b_2, b_4\}, \\ \text{LR}_8 &= \text{LR}(a_4a_1) = V(A_4) - \{b_1, b_3\}, \\ \text{LR}_9 &= \text{LR}(b_1a_1) = \{b_1, b_4, a_1, a_2\}, \\ \text{LR}_{10} &= \text{LR}(b_2a_2) = \{b_1, b_2, a_2, a_3\}, \\ \text{LR}_{11} &= \text{LR}(b_3a_3) = \{b_2, b_3, a_3, a_4\}, \\ \text{LR}_{12} &= \text{LR}(b_4a_4) = \{b_3, b_4, a_1, a_4\}, \\ \text{LR}_{13} &= \text{LR}(b_2a_1) = \{b_2, b_3, a_1, a_4\}, \\ \text{LR}_{14} &= \text{LR}(b_3a_2) = \{b_3, b_4, a_1, a_2\}, \\ \text{LR}_{15} &= \text{LR}(b_4a_3) = \{b_1, b_4, a_2, a_3\}, \\ \text{LR}_{16} &= \text{LR}(b_1a_4) = \{b_1, b_2, a_3, a_4\}. \end{aligned}$$

As, for  $1 \leq i \leq 8$ ,  $|\text{LR}(e_i)| = 4$  such that  $|\text{LR}(e_i)| < |\text{LR}(e_s)|$ , where  $1 \leq s \leq 8$ . Moreover,  $\cup_{i=1}^8 \text{LR}(e_i) = V(A_4)$  and  $|\text{LR}_s \cap \cup_{i=1}^8 \text{LR}(e_i)| > |\text{LR}(e_i)| = 4$ . There exists an ULRF  $\phi: V(A_4) \rightarrow [0, 1]$  defined as  $\phi(x) = (1/4)$  which is the LRF with minimum cardinality  $\forall x \in V(A_4)$ . Consequently, by Theorem 1,  $\dim_{lf}(A_4) \leq (|V(A_4)|/4) \leq 2$ .

As, for  $1 \leq i \leq 8$ ,  $|\text{LR}(e_i)| = 6$  such that  $|\text{LR}(e_i)| > |\text{LR}(e_s)|$ , where  $1 \leq s \leq 8$ . Moreover,  $\cup_{i=1}^8 \text{LR}(e_i) = V(A_4)$ . There exists a LLRF  $\phi': V(A_4) \rightarrow [0, 1]$  which is defined as  $\phi'(x) = (1/6)$  for each  $x \in V(A_4)$ . Therefore, by Theorem 1, we have  $\dim_{lf}(A_4) \geq (|V(A_4)|/6) \geq (4/3)$ . Consequently,

$$\frac{4}{3} \leq \dim_{lf}(A_4) \leq 2. \quad (19)$$

TABLE 1: LFMD of networks.

Networks	LFMDs	Comment
Antiprism network $[A_n \text{ for } n \equiv 0 \pmod{2}]$	$(n/n - 1) \leq \dim_{lf}(A_n) \leq 2.$	Bounded
Antiprism network $A_n$ , where $n \equiv 1 \pmod{2}$	$(n/n - 1) \leq \dim_{lf}(A_n) \leq (2n/n + 1).$	Bounded
Sun flower network $SF_n$ .	$(n/n - 1) \leq \dim_{lf}(SF_n) \leq (2n/n + 1).$	Bounded

Case 2: For  $n \geq 5$ ,  $1 \leq i \leq n$ , by Lemma 3,  $|\text{LR}(e_i)| = n = \alpha$  and  $|\text{R} \cap \cup_{i=1}^n \text{LR}(e_i)| \geq n$ , where R are all other LRNs.

There exists an ULRF  $\phi: V(A_n) \rightarrow [0, 1]$  which is defined as  $\phi(v) = (1/\alpha) \forall v \in V(A_n)$ , as  $V(G) = \cup \{\text{LR}(e): |\text{LR}(e) = \alpha\}$ . Consequently, by Theorem 1,  $\dim_{lf}(A_n) \leq (|V(A_n)|/n) \leq (2n/n) = 2.$

Case 3: As,  $|\text{LR}(a_i a_{i+1})| = 2n - 2$ , which is greater or equal to the cardinalities of all other LRNs, moreover,  $\cup_{i=1}^{2n} \text{LR}(e_i) = V(A_n)$ . There exists a LLRF  $(\phi': V(A_n) \rightarrow [0, 1])$  which is defined as  $\phi'(x) = (1/2n - 2) \forall v \in V(A_n)$ . Therefore, by Theorem 2,  $\dim_{lf}(A_n) \geq (n/n - 1)$ . Consequently,

$$\frac{n}{n-1} \leq \dim_{lf}(A_n) \leq 2. \quad (20)$$

**Theorem 6.** Let  $SF_n$  with  $n \geq 3$  be a sun flower network and  $|V(SF_n)| = 2n$ . Then,

$$\frac{n}{n-1} \leq \dim_{lf}(SF_n) \leq \frac{2n}{n+1}. \quad (21)$$

*Proof.* Case 1: For  $n = 3$ , LRNs are as follows:

$$\begin{aligned} \text{LR}_1 &= \text{LR}(a_1 a_2) = \{a_1, a_2, b_2, b_3\}, \\ \text{LR}_2 &= \text{LR}(a_2 a_3) = \{a_2, a_3, b_3, b_1\}, \\ \text{LR}_3 &= \text{LR}(a_3 a_1) = \{a_3, a_1, b_1, b_2\}, \\ \text{LR}_4 &= \text{LR}(a_1 b_1) = \{a_1, a_3, b_1, b_3\}, \\ \text{LR}_5 &= \text{LR}(a_2 b_2) = \{a_1, a_2, b_1, b_2\}, \\ \text{LR}_6 &= \text{LR}(a_3 b_3) = \{a_2, a_3, b_2, b_3\}, \\ \text{LR}_7 &= \text{LR}(a_2 b_1) = \{b_1, b_2, a_2, a_3\}, \\ \text{LR}_8 &= \text{LR}(a_3 b_2) = \{a_1, a_3, b_2, b_3\}, \\ \text{LR}_9 &= \text{LR}(a_1 b_3) = \{a_1, a_2, b_1, b_3\}. \end{aligned}$$

As, for  $1 \leq i \leq 9$ ,  $|\text{LR}(e_i)| = 4$  and  $|\text{LRNs} \cap \cup_{i=1}^9 \text{LR}(e_i)| = |\text{LR}(e_i)| = 4$ . There exists an ULRF  $\phi: V(SF_3) \rightarrow [0, 1]$  which is defined by  $\phi(x) = (1/4)$ ,  $\forall v \in V(SF_3)$ . Consequently, by Corollary 1,  $\dim_{lf}(SF_3) = (3/2)$ .

Case 2: For  $n = 4$ , LRNs are as follows:

$$\begin{aligned} \text{LR}_1 &= \text{LR}(a_1 a_2) = \{a_1, a_2, a_3, a_4, b_2, b_4\}, \\ \text{LR}_2 &= \text{LR}(a_2 a_3) = \{a_1, a_2, a_3, a_4, b_1, b_3\}, \\ \text{LR}_3 &= \text{LR}(a_3 a_4) = \{a_1, a_2, a_3, a_4, b_2, b_4\}, \\ \text{LR}_4 &= \text{LR}(a_4 a_1) = \{a_1, a_2, a_3, a_4, b_1, b_3\}, \\ \text{LR}_5 &= \text{LR}(a_1 b_1) = \{a_1, a_4, b_1, b_2, b_4\}, \\ \text{LR}_6 &= \text{LR}(a_2 b_2) = \{a_1, a_2, b_1, b_2, b_4\}, \\ \text{LR}_7 &= \text{LR}(a_3 b_3) = \{a_2, a_3, b_1, b_2, b_3\}, \end{aligned}$$

$$\begin{aligned} \text{LR}_8 &= \text{LR}(a_4 b_4) = \{a_3, a_4, b_2, b_3, b_4\}, \\ \text{LR}_9 &= \text{LR}(a_2 b_1) = \{a_2, a_3, b_1, b_2, b_3\}, \\ \text{LR}_{10} &= \text{LR}(a_3 b_2) = \{a_3, a_4, b_2, b_3, b_4\}, \\ \text{LR}_{11} &= \text{LR}(a_4 b_3) = \{a_1, a_4, b_2, b_3, b_4\}, \\ \text{LR}_{12} &= \text{LR}(a_1 b_4) = \{a_1, a_2, b_1, b_2, b_4\}. \end{aligned}$$

As, for  $1 \leq i \leq 8$ ,  $|\text{LR}(e_i)| = 5$ , such that  $|\text{LR}(e_i)| < |\text{LR}(e_s)|$ , where  $1 \leq s \leq 4$ . Moreover,  $\cup_{i=1}^8 \text{LR}(e_i) = V(SF_4)$ . There exists  $(\phi: V(SF_4) \rightarrow [0, 1])$  defined as  $\phi(x) = (1/5)$  which is the LRF  $\forall v \in V(SF_4)$ , as  $V(SF_4) = \cup \{\text{LR}(e_i): |\text{LR}(e) = 5\}$ . Consequently, by Theorem 1,  $\dim_{lf}(SF_4) \leq (8/5)$ .

As, for  $1 \leq i \leq 4$ ,  $|\text{LR}(e_i)| = 6$  such that  $|\text{LR}(e_i)| > |\text{LR}(e_s)|$ , where  $1 \leq s \leq 8$ . There exists  $\phi': V(SF_4) \rightarrow [0, 1]$  defined as  $\phi(v) = (1/6) \forall v \in V(SF_4)$ , which is the LLRF with maximum cardinality, where  $|\phi'| < |\phi''|$ , as  $V(SF_4) = \cup \{\text{LR}(e): |\text{LR}(e) = 6\}$ . By Theorem 1,  $\dim_{lf}(SF_4) \geq (4/3)$ . Consequently,

$$\frac{4}{3} \leq \dim_{lf}(SF_4) \leq \frac{8}{5}. \quad (22)$$

Case 3: As  $n \geq 5$ ,  $1 \leq i \leq n$ ,  $|\text{LR}(e_i)| = n + 1 = \alpha$ , and  $|\text{R} \cap \cup_{i=1}^n \text{LR}(e_i)| \geq n + 1$ , where R are all other LRNs. There exists an ULRF  $\phi: V(SF_n) \rightarrow [0, 1]$  defined as  $\phi(v) = (1/\alpha) \forall v \in V(SF_n)$ , as  $V(G) = \cup \{\text{LR}(e): |\text{LR}(e) = \alpha\}$ . Consequently, by Theorem 1,  $\dim_{lf}(SF_n) \leq (|V(SF_n)|/n + 1) \leq (2n/n + 1)$ .

Case 4: As  $|\text{LR}(a_i a_{i+1})| = 2n - 2$  which is greater than the cardinalities of all other LRNs of  $SF_n$ , there exists a LLRF  $\phi': V(SF_n) \rightarrow [0, 1]$  defined by  $\phi'(v) = (1/2n - 2)$ ,  $\forall v \in V(SF_n)$ , as  $V(G) = \cup \{\text{LR}(e): |\text{LR}(e) = 2n\}$ . By Theorem 2,  $\dim_{lf}(SF_n) \geq (n/n - 1)$ . Consequently,

$$\frac{n}{n-1} \leq \dim_{lf}(SF_n) \leq \frac{2n}{n+1}. \quad (23)$$

## 6. Conclusion

In this article, we studied the various aspects of the LFMDs for the different connected networks including the existence of the exact values, lower and upper bonds and bounded- and unbounded behaviours. Mainly, the lower bond of LFMD for the arbitrary connected networks is improved from unity. As the applications of the main result, LFMDs of the prism-related networks are as follows:

- (i) The exact value LFMD of  $CDL_n$  is  $n$  and of  $A_3$  is  $(3/2)$ , where  $n \geq 4$ .

- (ii) The LFMDs of antiprism and sun flower networks are computed in bounds, see Table 1.

Moreover, we note that, for  $n \rightarrow \infty$ , the computed bounds are convergent which show their boundedness. Now, we close our discussion by proposing the following open problem: open problem. Characterize the connected networks whose LFMDs is  $(|V(G)|/a)$ , where  $a < |V(G)|$  is some integral value.

## Data Availability

The data used to support the findings of this study are included within this article. However, the reader may contact the corresponding author for more details on the data.

## Conflicts of Interest

The authors have no conflicts of interest.

## References

- [1] P. J. Slater, "Leaves of trees," *Congressus Numerantium*, vol. 14, no. 1, pp. 549–559, 1975.
- [2] F. Harary and R. Melter, "On the metric dimension of a graph," *Ars Combinatoria*, vol. 2, pp. 19–195, 1976.
- [3] J. Currie and O. R. Oellermann, "The metric dimension and metric independence of a graph," *Journal of Combinatorial Mathematics and Combinatorial Computing*, vol. 39, pp. 157–167, 2001.
- [4] Y. Shang, "Percolation in a hierarchical lattice," *Zeitschrift Natur- Forschung*, vol. 6, 2012.
- [5] S. Khuller, B. Raghavachari, and A. Rosenfeld, *Localization in Graphs*, Technical Report UMIACS-TR-94-92, University of Maryland, College Park, MD, USA, 1994.
- [6] G. Chartrand, L. Eroh, M. A. Johnson, and O. R. Oellermann, "Resolvability in graphs and the metric dimension of a graph," *Discrete Applied Mathematics*, vol. 105, no. 1-3, pp. 99–113, 2000.
- [7] M. Fehr, S. Gosselin, and O. R. Oellermann, "The metric dimension of Cayley digraphs," *Discrete Mathematics*, vol. 306, no. 1, pp. 31–41, 2006.
- [8] Y.-M. Chu, M. F. Nadeem, M. Azeem, and M. K. Siddiqui, "On sharp bounds on partition dimension of convex polytopes," *IEEE Access*, vol. 8, pp. 224781–224790, 2020.
- [9] J. B. Liu and M. F. Nadeem, "Bounds on the partition dimension of convex polytopes," *Combinatorial Chemistry and High throughout Screening*, inprint, 2020.
- [10] J.-B. Liu, M. F. Nadeem, H. M. A. Siddiqui, and W. Nazir, "Computing metric dimension of Certain families of toeplitz graphs," *IEEE Access*, vol. 7, pp. 126734–126741, 2019.
- [11] Z. S. Mufti, M. F. Nadeem, A. Ahmad, and Z. Ahmad, "Computation of edge metric dimension of barycentric subdivision of cayley graphs," *Italian Journal of Pure and Applied Mathematics*, vol. 44, pp. 714–722, 2020.
- [12] S. Arumugam and V. Mathew, "The fractional metric dimension of graphs," *Discrete Mathematics*, vol. 312, no. 9, pp. 1584–1590, 2012.
- [13] M. Feng and K. Wang, "On the metric dimension and fractional metric dimension for hierarchical product of graphs," *Applicable Analysis and Discrete Mathematics*, vol. 7, no. 2, pp. 302–313, 2013.
- [14] J. B. Liu, A. Kashif, T. Rashid, and M. Javaid, "Fractional metric dimension of generalized Jahangir graph," *Mathematics*, vol. 7, pp. 1–10, 2019.
- [15] S. Aisyah, M. Utoyo, and L. Susilowati, "On the local fractional metric dimension of corona product networks, IOP Conference," *Earth and Environmental Science Hungarica*, vol. 243, pp. 1–4, 2019.
- [16] J.-B. Liu, M. K. Aslam, and M. Javaid, "Local fractional metric dimensions of rotationally symmetric and planar networks," *IEEE Access*, vol. 8, pp. 82404–82420, 2020.
- [17] M. Javaid, S. Safdar, M. U. Farooq, and M. K. Aslam, "Computing sharp bounds for local fractional metric dimensions of cycle related graphs," *Computational Journal of Combinatorial Mathematics*, vol. 1, pp. 29–73, 2020.
- [18] M. Javaid, M. Raza, P. Kumam, and J.-B. Liu, "Sharp bounds of local fractional metric dimensions of connected networks," *IEEE Access*, vol. 8, pp. 172329–172342, 2020.
- [19] S. Yani, E. Iwan, and S. Budi, *On Some New Edge Odd Graceful Graphs*, University of Gadjah Moda, Yogyakarta, Indonesia, 2019.



## Research Article

# Multihop Neighbor Information Fusion Graph Convolutional Network for Text Classification

Fangyuan Lei <sup>1,2</sup>, Xun Liu <sup>3</sup>, Zhengming Li <sup>4</sup>, Qingyun Dai <sup>1,2</sup> and Senhong Wang <sup>5</sup>

<sup>1</sup>Guangdong Key Provincial Laboratory of Intellectual Property & Big Data, Guangdong Polytechnic Normal University, Guangzhou 510665, China

<sup>2</sup>School of Electronic and Information, Guangdong Polytechnic Normal University, Guangzhou 510665, China

<sup>3</sup>Department of Electronics, Software Engineering Institute of Guangzhou, Guangzhou 510990, China

<sup>4</sup>Industrial Training Center, Guangdong Polytechnic Normal University, Guangzhou 510665, China

<sup>5</sup>School of Information Engineering, Guangdong University of Technology, Guangzhou 510006, China

Correspondence should be addressed to Xun Liu; liuxun.stf@gmail.com

Received 27 December 2020; Revised 21 March 2021; Accepted 24 April 2021; Published 3 May 2021

Academic Editor: Andrea Semaničová-Feňovčíková

Copyright © 2021 Fangyuan Lei et al. This is an open access article distributed under the Creative Commons Attribution License, which permits unrestricted use, distribution, and reproduction in any medium, provided the original work is properly cited.

Graph convolutional network (GCN) is an efficient network for learning graph representations. However, it costs expensive to learn the high-order interaction relationships of the node neighbor. In this paper, we propose a novel graph convolutional model to learn and fuse multihop neighbor information relationships. We adopt the weight-sharing mechanism to design different order graph convolutions for avoiding the potential concerns of overfitting. Moreover, we design a new multihop neighbor information fusion (MIF) operator which mixes different neighbor features from 1-hop to  $k$ -hops. We theoretically analyse the computational complexity and the number of trainable parameters of our models. Experiment on text networks shows that the proposed models achieve state-of-the-art performance than the text GCN.

## 1. Introduction

Text classification problem is a fundamental problem in many natural language processing (NLP) applications, such as text mining, spam detection, summarization, and question-answering system [1–5]. Many deep learning approaches such as convolutional neural networks [6], recurrent neural networks (RNN) [7], and long short-term memory (LSTM) [8] are introduced to text classification.

Text could be constructed on a typical graph-structured network, and graph networks have natural advantages for processing such data. Scarselli et al. [9] proposed a graph neural network, which was widely used for text classification [10–12] and other NLP tasks [13]. Graph convolutional network (GCN) [10], which is the extension of the CNN on graph data, has shown good performance on text classification than the traditional CNN [14]. Yao et al. [15] proposed a text GCN to apply document nodes and weighted edges to construct the text network graph, and their model

outperformed the state-of-the-art text classification methods.

When the messages pass through the graph of the text network, the node's output is affected by not only the directly connected nodes but also the  $k$ -hop nodes [16]. To obtain more neighbor node information, GCN models can expand the receptive field by stacking multiple layers. However, GNN models and GCN often suffer from the oversmoothing issue [17, 18]. On the contrary, the representation ability of the shallow network structure is clearly insufficient.

To address the above issue, we propose a multihop neighbor information fusion graph convolutional network for text classification based on the GCN. In our model, we propose a novel negative minimum value fusion operator to fuse multihop neighbor information (MIF). To reduce the computational complexity, we share the trainable weight [19] among the multihop neighbor nodes. Our experimental results show that our models achieve state-of-the-art

performance in several citation text datasets with lower computational complexity.

The contributions of this paper are as follows. First, we propose a novel negative minimum value fusion operator, which fuses the feature information of multihop neighbors. Second, we propose high-efficiency graph convolutional network-based MIF to successfully capture  $k$ -hop neighbors for nodes' classification of the text dataset.

The remainder of this paper is organized as follows. In Section 2, the related works are reviewed. In Section 3, our methods are proposed. In Section 4, the experimental results are presented. Finally, we draw the concluding remarks in Section 5.

## 2. Related Work

In this section, we will describe the related work about the graph convolutional network text classification, and we also introduce the related work about the multihop neighbor information of graph convolutional networks.

**2.1. Graph Convolutional Network.** Gori et al. [20] first proposed the concept of the graph neural network (GNN), which was based on the recurrent neural network architecture. Micheli [21] developed the GNN by random walk on the graph network [18]. Morris et al. [22] proved that the graph neural network and 1D Weisfeiler-Leman had the same ability to decompose nonisomorphic graphs.

Graph convolutional networks (GCNs) were developed from convolutional neural networks [23]. However, it is difficult to apply the GCN for large-scale graphs due to the high computational burden of eigenvalue decomposition [23]. Defferrard et al. [10] proposed a localized filter using Chebyshev polynomial. Kipf and Welling [24] proposed vanilla GCN, which achieves state-of-the-art classification performance on the citation network. Niepert et al. [25] proposed PATCHY-SAN to capture the information from locally connected regions. Hamilton et al. [26] developed a set of aggregate functions by sampling nodes in the neighbor to address the limitation of transductive learning. Monti et al. [27] contributed a unified framework for generalizing convolution to non-Euclidean domains. Velickovic et al. [28] leveraged masked attention to propose a graph attention network (GAT). Ding et al. [29] developed GAT and achieved better classification performance.

Recent works have been proposed for capturing  $k$ -hop neighbor information of nodes [30–33]. Zhou and Li [33] proposed a new high-order convolution operator to capture  $k$ -hop neighbor information and developed adaptive filtering to adjust the weights of the operator. Based on the motif graph attention mechanism, Lee et al. [34] proposed motif convolutional networks to capture  $k$ -hop interactive information. Mao et al. [35] proposed a Siamese framework to capture the  $k$ -hop information in the brain network. Abu-El-Haija et al. [36–38] proposed several versions of the mix-hop convolution to mix these features of different order graph convolutions using a fully connected layer.

**2.2. Text Classification.** Recently, deep learning models are introduced into text classification, which achieve far better performance than traditional models.

With the development of deep learning techniques, increasingly deep learning models are applied for text classification. Kim [39] developed several variants of the CNN model for the text classification. Recurrent neural networks (RNNs) [2, 7] are widely applied for text classification, showing better results than traditional models.

With the development of graph network models, many researchers developed more GCN-based classification methods [26, 40–42]. Zhao et al. [42] proposed the SDGCN model to capture the interdependencies hidden in the data. Liu et al. [43] developed TensorGCN to aggregate intragraph and intergraph information of the text graph. However, Text GCN [15] has a large number of parameters and high computational complexity. We will propose a novel GCN-based model to solve the issue in the Text GCN [15].

## 3. Method

In this section, we review the definition of related graph notations and analyse the layer-wise propagation model of the GCN in detail. Then, we develop a novel information propagation method to capture and fuse the multihop neighbor information. We propose two novel frameworks to capture the rich information of the text network. Finally, we analyse the computational complexity and parameter quantities of our models.

**3.1. Notations' Definition.** We assume graph signal  $X \in R^{n \times c}$  could be characterized by the node feature matrix of the graph, where  $n$  and  $c$  represent the number of nodes and feature dimensions, respectively. Let  $A$  be the adjacency matrix representing its edge connection. We define the normalized Laplacian matrix  $L$  as  $L = I_n - D^{-1/2}AD^{-1/2}$ , where  $I_n$  and  $D$  denote the identity matrix and the degree matrix of the graph, respectively.

The popular convolutional propagation model [24] is as follows:

$$H^{(l+1)} = \text{ReLU}\left(\tilde{D}^{-1/2}\tilde{A}\tilde{D}^{-1/2}H^{(l)}\theta^{(l)}\right), \quad (1)$$

where  $\tilde{A}$  is the adjacency matrix with self-loops, namely,  $\tilde{A} = A + I_n$ . The degree matrix  $\tilde{D}$  could be written as  $\tilde{D}_{ii} = \sum_j \tilde{A}_{ij}$ , where  $H^{(l)}$  denotes the propagation matrix. If  $l=0$ , then  $H^{(0)} = X$ , which means the input signal is connected to the network. The trainable weight matrix  $\theta^{(l)}$  could be optimized by gradient descent. We repeat the application of the convolutional model to get the vanilla GCN [24] framework.

$$Y = \text{softmax}\left(\tilde{D}^{-1/2}\tilde{A}\tilde{D}^{-1/2}\text{ReLU}\left(\tilde{D}^{-1/2}\tilde{A}\tilde{D}^{-1/2}X\theta^{(0)}\right)\theta^{(1)}\right), \quad (2)$$

where  $\theta^{(0)}$  and  $\theta^{(1)}$  present different weight matrices. The classification function is softmax. The convolutional operator is essentially a linear combination of its own vertices

and one-hop neighbourhood vertices to make the same category of vertex features similar. Stacking two convolutional layers makes the vertices of the same category more closely connected and further eases the classification task. However, when more layers are applied, the vertices of different categories will be mixed and become indistinguishable, which is excessive smoothing [17, 18].

### 3.2. Multihop Neighbor Information Fusion with the Graph Convolutional Operator

*Definition 1* (multihop neighbor information fusion (MIF)).

It is assumed that matrix  $\tilde{A}$  denotes the regularized adjacency matrix of graph  $G$ , where  $\hat{A} = \tilde{D}^{-1/2} \tilde{A} \tilde{D}^{-1/2}$ .

If  $\mathbf{A} \in \mathbb{R}^{n \times n}$ , then  $\hat{A}^{(k)} \in \mathbb{R}^{n \times n}$ . The power matrix of  $\hat{A}$  is  $\hat{A}^{(k)}, \hat{A}^{(k-1)}, \dots, \hat{A}^{(1)}, \hat{A}^{(0)}$ , where  $\hat{A}^{(0)}$  denotes the identity matrix. The multihop neighbor information fusion operator is to fuse the  $k$ -hop neighbor information with the element-wise topological information which is preserved. The MIF operator is defined as follows:

$$Z^{(l)} = -\min \left( \hat{A}^{(1)} H^{(l)} W_l, \hat{A}^{(2)} H^{(l)} W_l, \dots, \hat{A}^{(k)} H^{(l)} W_l \right), \quad (3)$$

where  $\hat{A}^{(k)}$  denotes the  $k$ -hop regularized adjacency matrix and  $\hat{A}^{(k)} H^{(l)} W_l$  represents the  $k$ -hop neighbor information.

**Proposition 1.** *The multihop neighbor information fusion operator is a topological preserved operator.*

*Proof.* If  $\mathbf{A}^{(k)} \in \mathbb{R}^{n \times n}$ , then  $\mathbf{A}^{(0)}, \mathbf{A}^{(1)}, \dots, \mathbf{A}^{(k)} \in \mathbb{R}^{n \times n}$ , and the  $k$ -hop neighbor information in convolutional layer  $l$  has the same dimension,  $\hat{A}^{(1)} H^{(l)} W_l, \hat{A}^{(2)} H^{(l)} W_l, \dots, \hat{A}^{(k)} H^{(l)} W_l \in \mathbb{R}^{n \times r}$ . As defined in formula (3), the MIF operator is the element-wise operation. Therefore, the dimension of  $Z^{(l)}$  is equal to the dimension of  $\hat{A}^{(i)} H^{(l)} W_l$ . The MIF operator preserves topological information.

The MIF operator is an information aggregation layer that is used to mix  $k$ -order adjacency information. The procedure of the calculation of MIF is as follows:

- (1) Calculating the minimum value of these features from different order graph convolutions:

$$P = \min \left( \hat{A}^{(1)} H^{(l)} W_l, \hat{A}^{(2)} H^{(l)} W_l, \dots, \hat{A}^{(k)} H^{(l)} W_l \right). \quad (4)$$

We give a living example to show that the MIF operator works. It is assumed that  $k = 3$ , namely, we obtain the maximum 3-hop neighbor information. We

assume  $P_1 = \hat{A}^{(1)} H^{(l)} W_l = \begin{bmatrix} 1 & 7 \\ -1 & 0 \end{bmatrix}$ ,  $P_2 = \hat{A}^{(2)}$   
 $H^{(l)} W_l = \begin{bmatrix} -2 & 2 \\ 3 & 4 \end{bmatrix}$ , and  $P_3 = \hat{A}^{(3)} H^{(l)} W_l = \begin{bmatrix} 4 & 2 \\ -3 & -2 \end{bmatrix}$ ;  
then, the result is as follows:

$$P = \min(P_1, P_2, P_3) = \min \left[ \{P_1^{(i,j)}, P_2^{(i,j)}, P_3^{(i,j)}\} \right] = \begin{bmatrix} -2 & 2 \\ -3 & -2 \end{bmatrix}. \quad (5)$$

- (2) The output of the MIF operator is defined as negative

$$\text{for each element of } P, \text{ namely, } Z = -P = \begin{bmatrix} 2 & -2 \\ 3 & 2 \end{bmatrix}.$$

Following DIFFPOOL [44], we use the topological preserved operator MIF to improve the performance.  $\square$

**3.3. MIF Propagation Model.** To address the limitations of the Text GCN, we propose a propagation model of multihop neighbor information fusion graph convolution as follows:

$$H^{(l+1)} = \text{ReLU} \left( \text{MIF} \left( \hat{A}^{(1)} H^{(l)} W_l, \hat{A}^{(2)} H^{(l)} W_l, \dots, \hat{A}^{(k)} H^{(l)} W_l \right) \right), \quad (6)$$

where  $\text{MIF}(\cdot)$  is defined in formula (4),  $\hat{A} = \tilde{D}^{-1/2} \tilde{A} \tilde{D}^{-1/2}$ , and  $\hat{A}^{(k)}$  denotes that  $\hat{A}$  multiplies itself by  $k$  times, where  $\hat{A}^{(j)} H^{(l)} W_l$  is the  $j$ -hop graph convolution, and  $W_l$  is the weight parameter matrix. In the MixHop model [36–38], Abu-El-Haija et al. adopted different weights for different  $\hat{A}^{(k)}$ . To reduce the computational complexity, we share the weight in the same convolutional layer in the multihop convolutional operator.

In formula (6), the convolutional layers combine the multihop neighbor information from 1-hop graph convolution with  $k$ -hop graph convolution. The calculation procedure is summarized in Algorithm 1. The MIF has advantages compared to Text GCN. MIF implements feature aggregation on nodes and their  $k$ -hop neighbor nodes. Therefore, MIF contains multihop neighbor information, in which it captures more information than Text GCN. In summary, MIF merges multihop neighbor information features while avoiding the extra parameter number. Those nodes in the same category are more closely connected. Furthermore, the MIF operator suppresses excessive weighting features while retaining features with small weight values, which may prevent gradient disappearance and gradient explosion problems.

**3.4. Graph Convolutional Network Based on MIF.** In Figure 1, we propose a two-layer graph convolutional neural network using the MIF layer. The first layer is the graph convolutional layer with MIF, and the convolutional layer is represented as follows:

$$H = \sigma \left( \text{MIF} \left( \hat{A}^{(1)} XW_1, \hat{A}^{(2)} XW_1, \dots, \hat{A}^{(k)} XW_1 \right) \right), \quad (7)$$

where  $W_1$  is the weight parameter matrix between the input layer and hidden layer.

The second layer is the traditional graph convolution. We set the nonlinear activation function  $\sigma$  between the two layers as ReLU and achieve multiple classifications via softmax after the second layer. The network extends the 1-hop graph convolution to  $k$ -hop graph convolution to capture multihop neighbor interactive information. The output of our model is expressed as follows:

$$Z = \text{softmax} \left( \hat{A} \left( \text{ReLU} \left( \text{MIF} \left( \hat{A}^{(1)} XW_1, \hat{A}^{(2)} XW_1, \dots, \hat{A}^{(k)} XW_1 \right) \right) W_2 \right) \right), \quad (8)$$

where  $W_2$  represents the weight parameter matrix between the hidden layer and output layer. The trainable weight parameters  $W_1$  and  $W_2$  would be updated by gradient descent.

In the preliminary network design, we compare how many convolutional layers and hops fit to our model. The two-convolutional-layer network shows better performance than the three and more convolutional layer network. When we implement the multihop neighbor information fusion, we observe that  $k = 2$  is better for most text networks, while  $k = 3$  is better for a few networks. In further experiments, when  $k \geq 4$ , the classification results would decrease. Moreover, the larger the  $k$  value, the higher the computational cost. Therefore, we only discuss the cases of  $k = 2$  and  $k = 3$  in our models.

When  $k = 2$ , our MIF operator fuses the 1-hop graph convolutional layer and 2-hop graph convolutional layer. The 2-hop MIF graph convolutional layer (MIFGC-2) is as follows:

$$Z = \text{softmax} \left( \hat{A}^{(1)} \left( \text{ReLU} \left( \text{MIF} \left( \hat{A}^{(1)} XW_1, \hat{A}^{(2)} XW_1 \right) \right) \right) W_2 \right). \quad (9)$$

When  $k = 3$ , the 3-hop MIF graph convolutional layer (MIFGC-3) fuses from 1-hop to 3-hop convolutional layer. The NMGC-3 model is as follows:

$$Z = \text{softmax} \left( \hat{A}^{(1)} \left( \text{ReLU} \left( \text{MIF} \left( \hat{A}^{(1)} XW_1, \hat{A}^{(2)} XW_1, \hat{A}^{(3)} XW_1 \right) \right) \right) W_2 \right). \quad (10)$$

The cross-entropy loss is utilized as our model loss function:

$$\mathcal{L} = - \sum_{l \in x_L} \sum_{m=1}^M Y_{lm} \ln Z_{lm}, \quad (11)$$

where  $x_L$  denotes the nodes set with labels and  $M$  represents the number of classes.  $Y_{lm}$  denotes the real labels of tag nodes, and  $Z_{lm}$  denotes the probability value between 0 and 1 predicted by softmax.

**3.5. Computational Complexity and Parameters.** Because the actual running time is sensitive to hardware and implementations, we follow He and Sun [45] to adopt the theoretical time complexity to show the complexity rather than the actual running time. For large-scale graph networks, it is a huge challenge to directly calculate  $\hat{A}^{(k)}$ . Therefore, we calculate  $\hat{A}^{(k)} XW_1$  with right-to-left multiplication. For example, if  $k = 2$ , we calculate  $\hat{A}^{(2)} XW_1$  as  $\hat{A}(\hat{A}(XW_1))$ .  $\hat{A}$  is usually a sparse matrix with  $m$  nonzero entries. In formulas (7)–(10), our graph convolutional layers adopt the weight-sharing mechanism. Therefore, the calculation procedure is efficient.

Since different hop graph convolutions share the same weight in the same layer, the parameter quantities are consistent with the 1-hop graph convolution. It is assumed that  $\hat{A} \in R^{n \times n}$ , where  $n$  is the number of nodes;  $X \in R^{n \times r_0}$ , where  $r_0$  is the feature dimensions,  $W_1 \in R^{r_0 \times r_1}$ , where  $r_1$  represents the number of hidden neurons in the 1<sup>st</sup> layer, and  $W_2 \in R^{r_1 \times r_2}$ , where  $r_2$  represents the hidden neurons in the 2<sup>nd</sup> layer. Then, output dimension in the 1<sup>st</sup> layer as the same, namely,  $\hat{A}XW_1 \in R^{n \times r_1}$ ,  $\hat{A}^2 XW_1 \in R^{n \times r_1}$ , and  $\hat{A}^k XW_1 \in R^{n \times r_1}$ . Therefore, in the first convolutional layer of our proposed model, the computational complexity is  $O(k \times m \times r_0 \times r_1)$ , and the trainable parameters are  $O(r_0 \times r_1)$ . The whole computational complexity of our proposed model is  $O(k \times m \times r_0 \times r_1 + m \times r_1 \times r_2)$  with  $O(\sum_{i=1}^2 r_{i-1} \times r_i)$  trainable parameters. The node feature dimension is far large than the neural number, namely,  $r_0 \gg r_2$ . Therefore, the computational complexity of our network frameworks approximates  $O(k \times m \times r_0 \times r_1)$ , and trainable parameters approximate  $O(r_0 \times r_1)$ , respectively. It matches the computational complexity and parameters of vanilla GCN [24]. Similarly, Text GCN [15] takes  $O(1 \times m \times r_0 \times r_1)$  computational complexity and  $O(r_0 \times r_1)$  trainable parameters.

## 4. Experiment

We will evaluate our NMGC-2 and NMGC-3 on text networks and compare our methods with the classic method and deep learning methods, such as the embedding model, CNN-based, LSTM-based, and GCN-based. We analyse the terms of computational complexity and trainable parameters in detail. We investigate the impact of network framework parameters and training epochs on classification accuracy.

**4.1. Datasets.** We test our methods on five benchmark corpora datasets including R52 and R8 of Reuters-21578, 20-Newsgroups (20NG), Ohsumed, and Movie Review (MR). According to the preprocessing steps by Yao et al. [15], we process the text datasets and use the documents and words as nodes to build the text graph. In Table 1, the statistics characters of the datasets are described in detail.

**4.2. Baseline and Experimental Settings.** We compare with the following baseline methods as in Yao et al. [15], i.e., CNN with randomly initialized word vectors (CNN-rand) [39], CNN with pretrained word vectors (CNN-pretrain) [39],

```

input:  $\hat{A}, H^{(l)}, W$ 
output:  $H$ 
for  $i = 1; k$ 
   $T_i = \hat{A}^i H^{(l)}$ 
   $P_i = T_i W = \hat{A}^i H^{(l)} W$ 
end
 $Z^{(l)} = -\min(P_1, P_2, \dots, P_k)$ 
 $H = \text{ReLU}(Z^{(l)})$ 

```

ALGORITHM 1: MIF operation.

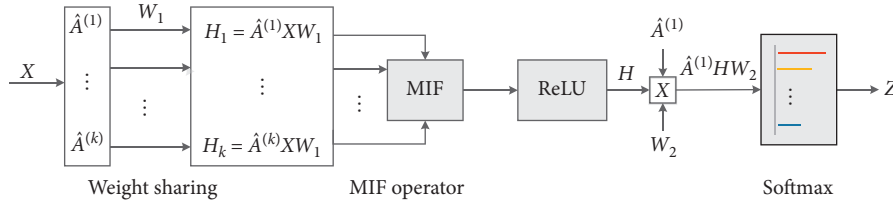


FIGURE 1: The proposed model.

predictive text embedding (PTE) [46], LSTM framework (LSTM) [2], LSTM framework with pretrained word embeddings (LSTM-pretrain) [2], fast text classifier (fastText) [47], fast text classifier with bigrams (fastText-bigrams) [47], label embedding model with attention (LEAM) [48], simple word-embedding model (SWEM) [49], graph CNN with spline filter (GCNN-S) [23], graph CNN with Fourier filter (GCNN-F) [50], and graph CNN with Chebyshev filter (GCNN-C) [10].

We tune a series of hyperparameters' (learning rate, dropout rate, hidden units, and epochs) values to determine the best hyperparameters of our model on text networks. The hyperparameters are reported in Tables 2 and 3. In our NMGC-2 and NMGC-3 models, we set  $L2$  regularization factor as 0 and use Adam [51] to optimize the learning rate, following Yao et al. [15].

**4.3. Results' Analysis.** We compare our NMGC-2 and NMGC-3 with other baseline methods in terms of test accuracy. As shown in Table 4, the proposed model NMGC-2 or NMGC-3 achieves the highest classification performance on datasets R52, R8, 20NG, and Ohsumed. Specifically, our NMGC-2 obtains the best accuracy of 94.35%, 97.31%, and 69.21% on datasets R52, R8, and Ohsumed, respectively, whereas our NMGC-3 obtains the highest accuracy of 86.68% on 20NG.

The success of NMGC-2 and NMGC-3 is mainly due to the following three aspects. (1) Our NMGC-2 and NMGC-3 models have the capability to capture the relations in terms of word-word and document-word in the datasets. (2) Our NMGC-2 and NMGC-3 make full use of the advantages of the GCN. We implement the feature information aggregation on the node and its 1-hop neighbor information (each layer) so that the node (word-word and document-word) features in the same cluster are similar, which are easy to classify. (3) Our NMGC-2 and NMGC-3 capture more and

richer feature information from 1-hop to  $k$ -hop neighbors, which may circumvent the limitations of the GCN.

On dataset MR, CNN-pretrain [39] achieves the highest classification result of 77.75%, which shows the model consecutive and short-distance semantics because CNN-pretrain [39] and LSTM-pretrain [2] model consecutive word sequences, while our NMGC-2 and NMGC-3 ignore the word orders. Another reason is that our NMGC-2 and NMGC-3 models are difficult to propagate the information among the nodes (word-word and document-word) on MR with few edges.

Compared to Text GCN [15], our NMGC-2 and NMGC-3 are better by a large margin in most cases, which demonstrates the effectiveness of our method in terms of capturing high-order interactive information.

**4.4. Hidden Units' Analyses of Our Method.** To evaluate the relationship between hidden units and the model performance, we use different hidden units to conduct experiments. We choose a representative set of hidden units as our comparative experiments in balancing computational complexity and classification performance. The results are summarized in Table 5. Specifically, our NMGC-2 uses the best hidden units of 128, 64, 128, 128, and 64 to achieve the higher accuracy on R52, R8, 20NG, Ohsumed, and MR, respectively, whereas our NMGC-3 uses the best hidden units of 128, 128, 128, 128, and 32 to achieve the better accuracy on R52, R8, 20NG, Ohsumed, and MR, respectively. We note that our NMGC-2 is always better than our NMGC-3 in many cases for different hidden units. This is most likely that our NMGC-3 suffers from oversmoothing in most cases. However, NMGC-3 outperforms NMGC-2 on short MR with few edges because NMGC-3 considers higher-order node information and propagates more label information to the entire graph network. In most cases, when the number of hidden units decreases, the accuracy of

TABLE 1: Dataset statistics.

Dataset	#training	#test	#docs	#classes	#words	#nodes	#length
R52	6532	2568	9100	52	8892	17,992	69.82
R8	5485	2189	7674	8	7688	15,362	65.72
20NG	11,314	7532	18,846	20	42,757	61,603	221.26
Ohsumed	3357	4043	7400	23	14,157	21,557	135.82
MR	7108	3554	10,662	2	18,764	29,426	20.39

TABLE 2: The hyperparameters in NMGC-2.

Dataset	Learning rate	Dropout rate	Hidden units	Epochs
R52	0.005	0.4	128	800
R8	0.01	0.4	64	200
20NG	0.005	0.5	128	330
Ohsumed	0.005	0.4	128	410
MR	0.01	0.4	64	40

TABLE 3: The hyperparameters in NMGC-3.

Dataset	Learning rate	Dropout rate	Hidden units	Epochs
R52	0.005	0.5	128	1300
R8	0.015	0.4	128	180
20NG	0.01	0.5	128	265
Ohsumed	0.01	0.6	128	210
MR	0.01	0.4	32	85

TABLE 4: Test accuracy on five text datasets. The benchmark results were reported by Yao et al. [15]. The accuracy values are the average result of 10 runs.

Method	R52	R8	20NG	Ohsumed	MR
CNN-rand [39]	85.37	94.02	76.93	43.87	74.98
CNN-pretrain [39]	87.59	95.71	82.15	58.44	77.75
PTE [46]	90.71	96.69	76.74	53.58	70.23
LSTM [2]	85.54	93.68	65.71	41.13	75.06
LSTM-pretrain [2]	90.48	96.09	75.43	51.10	77.33
fastText [47]	92.81	96.13	79.38	57.70	75.14
fastText-bigrams [47]	90.99	94.74	79.67	55.69	76.24
LEAM [48]	91.84	93.31	81.91	58.58	76.95
SWEM [49]	92.94	95.32	85.16	63.12	76.65
GCNN-S [23]	92.74	96.80	—	62.82	76.99
GCNN-F [50]	93.20	96.89	—	63.04	76.74
GCNN-C [10]	92.75	96.99	81.42	63.86	77.22
Text GCN [15]	93.56 ± 0.18	97.07 ± 0.10	86.34 ± 0.09	68.36 ± 0.56	76.74 ± 0.20
NMGC-2 (ours)	94.35 ± 0.06	97.31 ± 0.09	86.61 ± 0.06	69.21 ± 0.17	76.21 ± 0.25
NMGC-3 (ours)	93.83 ± 0.16	97.16 ± 0.10	86.68 ± 0.18	68.20 ± 0.35	76.36 ± 0.40

our method decreases, and more epochs are required to train our network.

*4.5. Computational Complexity and Trainable Weight Parameters.* We design the weight-sharing mechanism to share the weight in the proposed convolutional layer, which reduces the number of parameters. When using weight sharing, our calculations are very efficient. This naturally reduces the computational complexity. We design the weight-sharing mechanism to avoid overfitting caused by many parameters.

As shown in Table 6, we compare our method with Text GCN [15] in terms of computational complexity and the number of trainable weight parameters. The detailed derivation process of Comp. and Params. is analysed in Section 3.5. In Table 6, we observe that our NMGC-2 and NMGC-3 could match the computational complexity of Text GCN [15]. In particular, for MR, NMGC-3 is about 1 time less than Text GCN [15] in terms of computational complexity. Interestingly, our models have the least parameters on all datasets because we use the weight-sharing mechanism on these convolutions from 1-hop graph convolution to  $k$ -hop graph convolution and a smaller number of hidden units.

TABLE 5: Comparison of hidden units.

Dataset	Model	Hidden units	Epochs	Test Acc.
R52	NMGC-2 (ours)	128	800	94.35 ± 0.06
		64	1200	94.23 ± 0.20
		32	2000	94.16 ± 0.14
	NMGC-3 (ours)	128	1300	93.83 ± 0.16
		64	1100	93.29 ± 0.26
		32	2000	92.85 ± 0.37
R8	NMGC-2 (ours)	128	150	97.25 ± 0.13
		64	200	97.31 ± 0.09
		32	330	97.30 ± 0.13
	NMGC-3 (ours)	128	180	97.16 ± 0.10
		64	220	96.92 ± 0.08
		32	300	96.69 ± 0.06
20NG	NMGC-2 (ours)	128	330	86.61 ± 0.06
		64	480	86.55 ± 0.12
		32	600	86.02 ± 0.12
	NMGC-3 (ours)	128	265	86.68 ± 0.18
		64	420	86.14 ± 0.19
		32	540	85.64 ± 0.13
Ohsumed	NMGC-2 (ours)	128	410	69.21 ± 0.17
		64	495	69.07 ± 0.28
		32	795	68.46 ± 0.24
	NMGC-3 (ours)	128	210	68.20 ± 0.35
		64	305	67.50 ± 0.24
		32	415	66.25 ± 0.35
MR	NMGC-2 (ours)	128	35	76.19 ± 0.43
		64	40	76.21 ± 0.25
		32	55	76.16 ± 0.26
	NMGC-3 (ours)	128	50	76.27 ± 0.32
		64	70	76.24 ± 0.11
		32	85	76.36 ± 0.40

TABLE 6: Comparison of computational complexity and the number of trainable weight parameters. Comp. and Params. denote the computational complexity and parameters, respectively. Constant numbers 1, 2, and 3 represent the hops of the graph convolutional network, and constant numbers 200, 64, 128, and 32 denote the number of hidden units.

Method	Comp.	Params.
Text GCN [15]	$O(1 \times m \times r_0 \times 200)$	$O(r_0 \times 200)$
NMGC-2 (ours)	$O(2 \times m \times r_0 \times 64)$ (R8 and MR datasets)	$O(r_0 \times 64)$ (R8 and MR datasets)
	$O(2 \times m \times r_0 \times 128)$ (other datasets)	$O(r_0 \times 128)$ (other datasets)
NMGC-3 (ours)	$O(3 \times m \times r_0 \times 32)$ (MR dataset)	$O(r_0 \times 32)$ (MR dataset)
	$O(3 \times m \times r_0 \times 128)$ (other datasets)	$O(r_0 \times 128)$ (other datasets)

## 5. Conclusion

In this work, we propose a new multihop neighbor information fusion graph convolutional network on graph-structured data. We develop a novel MIF operator to combine the graph convolution features of multihop neighbor information from 1-hop graph convolution to  $k$ -hops. Experiments on text networks suggest that our models are capable of encoding in terms of node features and global graph topology in a way useful for graph classification. In this setting, our models achieve performance improvement compared to other methods while being computationally efficient and with less trainable parameters. In future work, we plan to study different fusion schemes and extend our model to more datasets.

## Data Availability

The data used to support the findings of this study are available from the corresponding author upon request.

## Conflicts of Interest

The authors declare that there are no conflicts of interest regarding the publication of this paper.

## Acknowledgments

This work was funded by the National Natural Science Foundation of China (U1701266, 61702117, and 61672008), the Guangdong Provincial Key Laboratory of Intellectual

Property and Big Data (2018B030322016), the Special Projects for Key Fields in Higher Education of Guangdong (2020ZDZX3077), and in part by Qingyuan Science and Technology Plan Project (Grant nos. 170809111721249 and 170802171710591).

## References

- [1] S. Lai, L. Xu, K. Liu et al., "Recurrent convolutional neural networks for text classification," in *Proceedings of the Twenty-ninth AAAI Conference on Artificial Intelligence*, Austin, TX, USA, January 2015.
- [2] P. Liu, X. Qiu, and X. Huang, "Recurrent neural network for text classification with multi-task learning," 2016, <http://arxiv.org/abs/160505101>.
- [3] H. Tao, S. Tong, H. Zhao et al., "A radical-aware attention-based model for Chinese text classification," in *Proceedings of the Thirty-Third AAAI Conference on Artificial Intelligence*, Honolulu, HI, USA, February 2019.
- [4] R. Narayan, J. K. Rout, and S. K. Jena, "Review spam detection using semi-supervised technique," *Advances in Intelligent Systems and Computing*, Springer, Berlin, Germany, pp. 281–286, 2017.
- [5] S. Reddy, D. Chen, and C. D. Manning, "Coqa: a conversational question answering challenge," *Transactions of the Association for Computational Linguistics*, vol. 7, pp. 249–266, 2019.
- [6] Y. Kim, "Convolutional neural networks for sentence classification," in *Proceedings of the 2014 Conference on Empirical Methods in Natural Language Processing (EMNLP)*, pp. 1746–1751, Doha, Qatar, October 2014.
- [7] S. Bai, J. Z. Kolter, and V. Koltun, "An empirical evaluation of generic convolutional and recurrent networks for sequence modeling," 2018, <http://arxiv.org/abs/180301271>.
- [8] D. S. Sachan, M. Zaheer, and R. Salakhutdinov, "Revisiting LSTM networks for semi-supervised text classification via mixed objective function," *Proceedings of the AAAI Conference on Artificial Intelligence*, vol. 33, pp. 6940–6948, 2019.
- [9] F. Scarselli, M. Gori, A. C. Tsoi et al., "The graph neural network model," *IEEE Transactions on Neural Networks*, vol. 20, no. 1, pp. 61–80, 2008.
- [10] M. Defferrard, X. Bresson, and P. Vandergheynst, "Convolutional neural networks on graphs with fast localized spectral filtering," *Advances in Neural Information Processing Systems*, pp. 3844–3852, Springer, Berlin, Germany, 2016.
- [11] W. Li, S. Li, S. Ma et al., "Recursive graphical neural networks for text classification," 2019, <http://arxiv.org/abs/190908166>.
- [12] L. Huang, D. Ma, S. Li et al., "Text level graph neural network for text classification," in *Proceedings of the 2019 Conference on Empirical Methods in Natural Language Processing and the 9th International Joint Conference on Natural Language Processing (EMNLP-IJCNLP)*, pp. 3444–3450, Hong Kong, China, November 2019.
- [13] K. Kowsari, K. Jafari Meimandi, M. Heidarysafa, S. Mendu, L. E. Barnes, and D. E. Brown, "Text classification algorithms: a survey," *Information*, vol. 10, no. 4, p. 150, 2019.
- [14] Z. Zhang, P. Cui, and W. Zhu, "Deep learning on graphs: a survey," *IEEE Transactions on Knowledge and Data Engineering*, 2020.
- [15] L. Yao, C. Mao, and Y. Luo, "Graph convolutional networks for text classification," *Proceedings of the AAAI Conference on Artificial Intelligence*, vol. 33, pp. 7370–7377, 2019.
- [16] Q. Zhu, B. Du, and P. Yan, "Multi-hop convolutions on weighted graphs," 2019, <http://arxiv.org/abs/191104978v1>.
- [17] Q. Li, Z. Han, and X.-M. Wu, "Deeper insights into graph convolutional networks for semi-supervised learning," in *Proceedings of the Thirty-Second AAAI Conference on Artificial Intelligence*, New Orleans, LA, USA, February 2018.
- [18] J. Zhou, G. Cui, Z. Zhang et al., "Graph neural networks: a review of methods and applications," 2018, <http://arxiv.org/abs/181208434>.
- [19] F. Lei, X. Liu, Q. Dai et al., "Hybrid low-order and higher-order graph convolutional networks," *Computational Intelligence and Neuroscience*, vol. 2020, Article ID 3283890, 9 pages, 2020.
- [20] M. Gori, G. Monfardini, and F. Scarselli, "A new model for learning in graph domains," in *Proceedings of the 2005 IEEE International Joint Conference on Neural Networks*, pp. 729–734, IEEE, Montreal, Canada, July 2005.
- [21] A. Micheli, "Neural network for graphs: a contextual constructive approach," *IEEE Transactions on Neural Networks*, vol. 20, no. 3, pp. 498–511, 2009.
- [22] C. Morris, M. Ritzert, M. Fey et al., "Weisfeiler and leman go neural: higher-order graph neural networks," *Proceedings of the AAAI Conference on Artificial Intelligence*, vol. 33, pp. 4602–4609, 2019.
- [23] J. Bruna, W. Zaremba, A. Szlam et al., "Spectral networks and locally connected networks on graphs," 2013, <http://arxiv.org/abs/13126203>.
- [24] T. N. Kipf and M. Welling, "Semi-supervised classification with graph convolutional networks," 2016, <http://arxiv.org/abs/160902907>.
- [25] M. Niepert, M. Ahmed, and K. Kutzkov, "Learning convolutional neural networks for graphs," in *Proceedings of the International Conference on Machine Learning*, pp. 2014–2023, New York, NY, USA, June 2016.
- [26] W. Hamilton, Z. Ying, and J. Leskovec, "Inductive representation learning on large graphs," in *Proceedings of the Advances in Neural Information Processing Systems*, pp. 1024–1034, Long Beach, CA, USA, July 2017.
- [27] F. Monti, D. Boscaini, J. Masci et al., "Geometric deep learning on graphs and manifolds using mixture model cnns," in *Proceedings of the IEEE Conference on Computer Vision and Pattern Recognition*, pp. 5115–5124, Honolulu, HI, USA, July 2017.
- [28] P. Veličković, G. Cucurull, A. Casanova et al., "Graph attention networks," 2017, <http://arxiv.org/abs/171010903>.
- [29] M. Ding, J. Tang, and J. Zhang, "Semi-supervised learning on graphs with generative adversarial nets," in *Proceedings of the 27th ACM International Conference on Information and Knowledge Management*, pp. 913–922, ACM, Torino Italy, October, 2018.
- [30] R. Milo, S. Shen-Orr, S. Itzkovitz et al., "Network motifs: simple building blocks of complex networks," *Science*, vol. 298, no. 5594, pp. 824–827, 2002.
- [31] R. A. Rossi, R. Zhou, and N. K. Ahmed, "Estimation of graphlet counts in massive networks," *IEEE Transactions on Neural Networks and Learning Systems*, vol. 30, no. 1, pp. 44–57, 2018.
- [32] R. A. Rossi, N. K. Ahmed, and E. Koh, "Higher-order network representation learning," in *Companion Proceedings of the Web Conference*, Lyon, France, April 2018.
- [33] Z. Zhou and X. Li, "Convolution on graph: a high-order and adaptive approach," 2017, <http://arxiv.org/abs/1706.09916>.
- [34] J. B. Lee, R. A. Rossi, X. Kong et al., "Higher-order graph convolutional networks," 2018, <http://arxiv.org/abs/180907697>.
- [35] Y. Mao, Y. Shen, G. Qin et al., "Predicting the popularity of online videos via deep neural networks," *CoRR*, p. 10718, 2017, <https://arxiv.org/abs/1711.10718>.



- [36] S. Abu-El-Haija, N. Alipourfard, H. Harutyunyan et al., “A higher-order graph convolutional layer,” in *Proceedings of the 32nd Conference on Neural Information Processing Systems (NIPS 2018)*, Montreal, Canada, December 2018.
- [37] S. Abu-El-Haija, A. Kapoor, B. Perozzi et al., “N-gcn: multi-scale graph convolution for semi-supervised node classification,” 2018, <http://arxiv.org/abs/180208888>.
- [38] S. Abu-El-Haija, B. Perozzi, A. Kapoor et al., “MixHop: higher-order graph convolutional architectures via sparsified neighborhood mixing,” in *Proceedings of the International Conference on Machine Learning*, pp. 21–29, Long Beach, CA, USA, June 2019.
- [39] Y. Kim, “Convolutional neural networks for sentence classification,” 2014, <http://arxiv.org/abs/14085882>.
- [40] H. Peng, J. Li, Y. He et al., “Large-scale hierarchical text classification with recursively regularized deep graph-cnn,” in *Proceedings of the 2018 World Wide Web Conference*, pp. 1063–1072, Lyon, France, April 2018.
- [41] A. A. Helmy, “A multilingual encoding method for text classification and dialect identification using convolutional neural network,” 2019, <http://arxiv.org/abs/190307588>.
- [42] P. Zhaoa, L. Houb, and O. Wua, “Modeling sentiment dependencies with graph convolutional networks for aspect-level sentiment classification,” 2019, <http://arxiv.org/abs/190604501>.
- [43] X. Liu, X. You, X. Zhang, J. Wu, and P. Lv, “Tensor graph convolutional networks for text classification,” *Proceedings of the AAAI Conference on Artificial Intelligence*, vol. 34, no. 5, pp. 8409–8416, 2020.
- [44] Z. Ying, J. You, C. Morris et al., “Hierarchical graph representation learning with differentiable pooling,” in *Proceedings of the Advances in Neural Information Processing Systems 31: Annual Conference on Neural Information Processing Systems*, pp. 4805–4815, Montréal, Canada, December 2018.
- [45] K. He and J. Sun, “Convolutional neural networks at constrained time cost,” in *Proceedings of the IEEE Conference on Computer Vision and Pattern Recognition*, pp. 5353–5360, Boston, MA, USA, June 2015.
- [46] J. Tang, M. Qu, and Q. Mei, “Pte: predictive text embedding through large-scale heterogeneous text networks,” in *Proceedings of the 21th ACM SIGKDD International Conference on Knowledge Discovery and Data Mining*, pp. 1165–1174, ACM, Sydney, Australia, August 2015.
- [47] A. Joulin, E. Grave, P. Bojanowski et al., “Bag of tricks for efficient text classification,” 2016, <http://arxiv.org/abs/160701759>.
- [48] G. Wang, C. Li, W. Wang et al., “Joint embedding of words and labels for text classification,” in *Proceedings of the 56th Annual Meeting of the Association for Computational Linguistics*, pp. 2321–2331, Melbourne, Australia, July 2018.
- [49] D. Shen, G. Wang, W. Wang et al., “Baseline needs more love: on simple word-embedding-based models and associated pooling mechanisms,” in *Proceedings of the 56th Annual Meeting of the Association for Computational Linguistics*, pp. 440–450, Melbourne, Australia, July 2018.
- [50] M. Henaff, J. Bruna, and Y. LeCun, “Deep convolutional networks on graph-structured data,” 2015, <http://arxiv.org/abs/150605163>.
- [51] D. P. Kingma and J. Ba, “Adam: a method for stochastic optimization,” 2014, <http://arxiv.org/abs/14126980>.

## Research Article

# Computing Exact Values for Gutman Indices of Sum Graphs under Cartesian Product

Abdulaziz Mohammed Alanazi <sup>1</sup>, Faiz Farid,<sup>2</sup> Muhammad Javaid <sup>2</sup>  
and Augustine Munagi<sup>3</sup>

<sup>1</sup>Department of Mathematics, University of Tabuk, Tabuk 71491, Saudi Arabia

<sup>2</sup>Department of Mathematics, School of Science, University of Management and Technology, Lahore 54770, Pakistan

<sup>3</sup>School of Mathematics, University of the Witwatersrand, Johannesburg, South Africa

Correspondence should be addressed to Muhammad Javaid; [javidmath@gmail.com](mailto:javidmath@gmail.com)

Received 23 February 2021; Revised 24 March 2021; Accepted 2 April 2021; Published 17 April 2021

Academic Editor: Ali Ahmad

Copyright © 2021 Abdulaziz Mohammed Alanazi et al. This is an open access article distributed under the Creative Commons Attribution License, which permits unrestricted use, distribution, and reproduction in any medium, provided the original work is properly cited.

Gutman index of a connected graph is a degree-distance-based topological index. In extremal theory of graphs, there is great interest in computing such indices because of their importance in correlating the properties of several chemical compounds. In this paper, we compute the exact formulae of the Gutman indices for the four sum graphs (S-sum, R-sum, Q-sum, and T-sum) in the terms of various indices of their factor graphs, where sum graphs are obtained under the subdivision operations and Cartesian products of graphs. We also provide specific examples of our results and draw a comparison with previously known bounds for the four sum graphs.

## 1. Introduction

Theory of topological indices (TIs) started when Wiener discovered a close correlation between boiling points of certain alkanes and sums of the distances among pairs of vertices. Later, this calculated number was named Wiener Index [1]. After 25 years, Gutman and Trinajstić discovered degree-based indices (first and second Zagreb indices) which they used to compute the total  $\pi$ -electron energy of conjugate molecules [2]. Following these discoveries, many scientists began to introduce various TIs as invariant numbers for the prediction of the certain properties of molecular structures such as boiling point, freezing point, volume, density, vaporization, and weight. Two deeper approaches, namely, quantitative structures property relationships (QSPR) and quantitative structure activity relationships (QSAR) have also been used under the subject of cheminformatics (combination of chemistry, mathematics, statistics, and information sciences) and in conjunction with TIs, to find correlation values between the physical structures and chemical properties of molecules, see [3–5].

TIs have been classified into three main classes depending upon degrees of nodes (vertices), distances among the vertices, and enumerative polynomials of the molecular graphs. Distance-based TIs are generally considered more important than the others. Some of the distance-based TIs are Wiener index [1], average distance index [6], Harary index [7, 8], degree distance index, and the Gutman index [9]. For more details, see [10–14].

In graph theory, various operations such as union, intersection, addition, and Cartesian product are used to obtain the new graphs. Yan et al. [15] defined four subdivision-related operations S, R, Q, and T. They applied these operations on a connected graph  $G$  to obtain the four new graphs  $S(G)$  (subdivided graph),  $R(G)$  (triangle parallel graph),  $Q(G)$  (line superposition graph), and  $T(G)$  (total graph), respectively. Afterwards, Das and Gutman [10] introduced the F-sum graphs using the operation of Cartesian product on the graphs  $F(G_1)$  and  $G_2$ , where  $F \in \{S, R, Q \text{ and } T\}$ . Various hexagonal chains were later derived from these F-sum graphs, which have been found isomorphic to many chemical structures. They also

determined the Wiener indices of the following S-sum  $(G_1 +_s G_2)$ , R-sum  $(G_1 +_R G_2)$ , Q-sum  $(G_1 +_Q G_2)$ , and T-sum  $(G_1 +_T G_2)$  graphs.

Recently, Liu et al. [16] computed the first general Zagreb indices of the F-sum graphs. Akhter and Imran [17] found out the sharp bounds of the general sum-connectivity index for F-sum graphs. Ahmad et al. [18] discovered the exact formulae of the general sum-connectivity index for F-sum graphs, by improving the bounds. An et al. [19] determined the upper bounds of the degree distance indices for all the F-sum graphs. Pattabiraman and Bhat [20] derived the upper bounds of the Gutman index for all the F-sum graphs. For more studies, we refer to [21–32].

In this paper, we obtain the exact values of the Gutman index for the F-sum  $(G_1 +_s G_2)$ ,  $(G_1 +_R G_2)$ ,  $(G_1 +_Q G_2)$ , and  $(G_1 +_T G_2)$  graphs. Moreover, the results are illustrated with special classes of the F-sum graphs and a comparison is drawn between the obtained exact values and the previously known bounded values.

The sections of paper are organized as follows. Section 2 comprises of preliminaries (some important definitions and statements of related lemmas). Section 3 contains the main result consisting of statements and proofs of theorems about Gutman indices of F-sum graphs. Lastly, Section 4 covers the applications of the main result to the computation of Gutman indices of particular classes of the F-sum graphs and a comparison among exact and known bounded values.

## 2. Preliminaries

We give a detailed consideration of two simple graphs  $G_1$  and  $G_2$ . The degree of a vertex  $x$  ( $\deg(x)$  or  $d(x)$ ) is equal to the number of vertices connected to it. For each  $(x, y) \in V(G_1 \times G_2)$ , degree of the vertex  $(x, y)$  is denoted by  $\deg(x, y)$ . The distance  $d(x, y)$  between two vertices  $x, y \in V(G)$  is defined as the length of the shortest path between both the vertices  $x$  and  $y$ . Further details can be found in [33, 34].

**Definition 1** (see [1]). The Wiener index  $W(G)$  of a connected graph  $G$  is defined as

$$W(G) = \frac{1}{2} \sum_{x,y \in V(G)} d(x, y). \quad (1)$$

**Definition 2** (see [11]). The degree distance index  $DD(G)$  of a connected graph  $G$  is defined as

$$DD(G) = \frac{1}{2} \sum_{x,y \in V(G)} \{d(x, y)(\deg(x) + \deg(y))\}. \quad (2)$$

**Definition 3** (see [35]). The Gutman index  $GM(G)$  of a connected graph  $G$  is defined as

$$GM(G) = \frac{1}{2} \sum_{x,y \in V(G)} \{d(x, y)(\deg(x)\deg(y))\}. \quad (3)$$

Yan et al. [15] defined four special graphs derivable from a given graph  $G$  by applying the four respective operations  $S$ ,  $R$ ,  $Q$ , and  $T$  on the graph  $G$  as follows:

- (i) Subdivided graph  $S(G)$  is formed from  $G$  if distance of one between two adjacent pair of vertices is increased by two after inserting a new vertex between them. The vertices of  $G$  are named as black vertices, while new vertices are called white vertices.
- (ii) Triangle parallel graph  $R(G)$  is formed from  $G$  if the new vertex corresponded to each edge of  $G$  is joined with the end vertices of the each respective edge. The vertices of  $G$  are named as black vertices, while new vertices are called white vertices.
- (iii) Line superposition graph  $Q(G)$  is formed when two white vertices obtained from  $S(G)$  are further joined if incident edges of these white vertices have one common end vertex in  $G$ .
- (iv) Total graph  $T(G)$  is formed from  $R(G)$  by applying the further operation  $Q$  on it.

Figure 1 illustrates the graphs obtained by the operations  $S$ ,  $R$ ,  $Q$ , and  $T$  based on the path graph  $(P_6)$ .

**Definition 4.** Let  $F \in \{S, R, Q \text{ and } T\}$ . Then,  $G_1 +_F G_2$  is called a F-sum graph with vertex set  $V(G_1 +_F G_2) = (V(G_1) \cup E(G_1)) \times V(G_2)$  and  $(u, v), (x, y) \in V(G_1 +_F G_2)$  are adjacent such that either  $u = x$  and  $(v, y) \in E(G_2)$  or  $v = y$  and  $(u, x) \in E(F(G_1))$ .

Figure 2 shows instances of S-sum  $(G_1 +_s G_2)$ , R-sum  $(G_1 +_R G_2)$ , Q-sum  $(G_1 +_Q G_2)$ , and T-sum  $(G_1 +_T G_2)$  graphs. We now state some important lemmas which are frequently used in the main results.

**Lemma 1** (see [36]). Let  $G_1$  and  $G_2$  be two simple and connected graphs.

- (a) For  $F \in \{S, R, Q, T\}$ , if both vertices  $(x, y)$  and  $(w, z)$  are black, then  $d((x, y), (w, z)|_{G_1 +_F G_2}) = d(x, w|_{F(G_1)}) + d(y, z|_{G_2})$
- (b) If one vertex  $(x, y)$  is white and second  $(w, z)$  is black with  $F \in \{S, R, Q, T\}$ , then  $d((x, y), (w, z)|_{G_1 +_F G_2}) = d(x, w|_{F(G_1)}) + d(y, z|_{G_2})$

**Lemma 2** (see [36]). Let  $G_1$  and  $G_2$  be two simple and connected graphs. If both vertices  $(x, y)$  and  $(w, z)$  are white vertices and  $F = S$  or  $R$ , then

$$d((x, y), (w, z)|_{G_1 +_F G_2}) = \begin{cases} 2 + d(y, z|_{G_2}), & \text{If } x = w, \\ d(x, w|_{F(G_1)}) + d(y, z|_{G_2}), & \text{If } x \neq w. \end{cases} \quad (4)$$

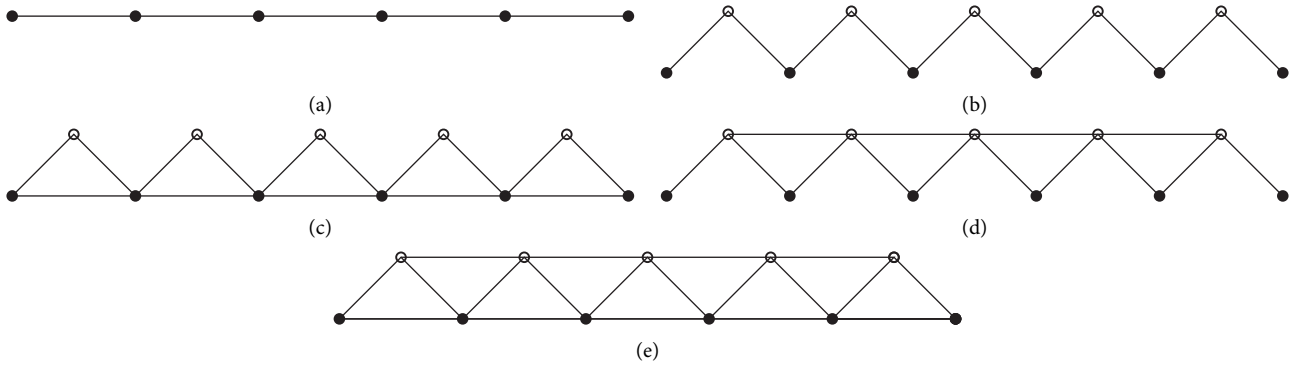


FIGURE 1: (a)  $P_6$ , (b)  $S(P_6)$ , (c)  $R(P_6)$ , (d)  $Q(P_6)$ , and (e)  $T(P_6)$ .

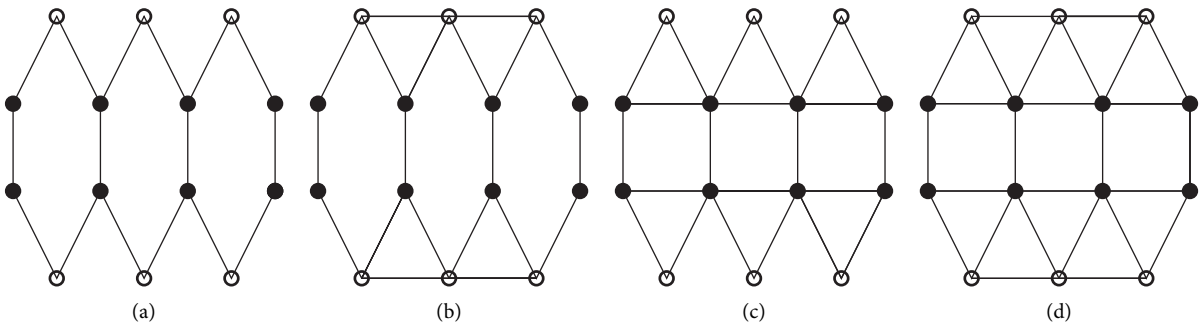


FIGURE 2: (a)  $(P_4 +_S P_2)$ . (b)  $(P_4 +_R P_2)$ . (c)  $(P_4 +_Q P_2)$ . (d)  $(P_4 +_T P_2)$ .

**Lemma 3** (see [36]). *Let  $G_1$  and  $G_2$  be two simple and connected graphs. If both vertices  $(x, y)$  and  $(w, z)$  are white vertices and  $F = Q$  or  $T$ , then*

$$d((x, y), (w, z)|G_1 +_F G_2) = \begin{cases} 2 + d(y, z|G_2), & \text{If } x = w, \\ 1 + d(x, w|F(G_1)) + d(y, z|G_2), & \text{If } x \neq w, y \neq z. \end{cases} \quad (5)$$

### 3. Main Results

This section is devoted to providing main theorems on the Gutman index of F-sum graphs  $(G_1 +_S G_2)$ ,  $(G_1 +_R G_2)$ ,  $(G_1 +_Q G_2)$ , and  $(G_1 +_T G_2)$ . Consider the set  $V(G_1) = \{u_1, u_2, u_3, \dots, u_n\}$  of black vertices with  $|E(G_1)| = k$  so that  $W = \{w_1, w_2, w_3, \dots, w_k\}$  consists of white vertices

and  $V(G_2) = \{v_1, v_2, v_3, \dots, v_m\}$  with  $|E(G_2)| = l$ . Then,  $V(G_1 +_F G_2) = \{(u_i, v_j): 1 \leq i \leq n, 1 \leq j \leq m\} \cup \{(w_i, v_j): 1 \leq i \leq k, 1 \leq j \leq m\}$ , where  $F \in \{S, R, Q, T\}$ .

**Theorem 1.** *Let  $G_1$  and  $G_2$  be connected and simple graphs. If  $(G_1 +_S G_2)$  is the S-sum graph of  $G_1$  and  $G_2$ , then*

$$\begin{aligned} GM(G_1 +_S G_2) &= m^2 GM(S(G_1)) + n^2 GM(G_2) + 4nk DD(G_2) + 16k^2 W(G_2) + 4k(m^2 - m) \\ &+ lm \sum_{i,j=1}^n \{d(u_i, u_j)|S(G_1)\} \{d(u_i) + d(u_j)\} + 2l^2 \sum_{i,j=1}^n \{d(u_i, u_j)|S(G_1)\} + 4lm \sum_{r=1}^k \sum_{i=1}^n \{d(w_r, u_i)|S(G_1)\}. \end{aligned} \quad (6)$$

*Proof.* Case 1: when both vertices are black,

for  $i, j = 1$  to  $n$  and  $p, q = 1$  to  $m$ . For S-sum  
 $\deg(u_i, v_p) = d(u_i) + d(v_p)$ ,

$$A = \frac{1}{2} \sum \left\{ d((u_i, v_p), (u_j, v_q)) (\deg(u_i, v_p) \deg(u_j, v_q)) | G_1 + {}_s G_2 \right\}, \quad (7)$$

$$\begin{aligned} A &= \frac{1}{2} \sum_{i,j=1}^n \sum_{p,q=1}^m \left\{ d(u_i, u_j) | S(G_1) + d(v_p, v_q) | (G_2) \right\} \{d(u_i) + d(v_p)\} \{d(u_j) + d(v_q)\} \\ &= \frac{1}{2} \sum_{i,j=1}^n \sum_{p,q=1}^m \left\{ d(u_i, u_j) | S(G_1) + d(v_p, v_q) | (G_2) \right\} \{d(u_i)d(u_j) + d(u_i)d(v_q) + d(v_p)d(u_j) + d(v_p)d(v_q)\} \\ &= \frac{1}{2} \sum_{i,j=1}^n \sum_{p,q=1}^m \left\{ d(u_i, u_j) | S(G_1) \right\} \{d(u_i)d(u_j) + d(u_i)d(v_q) + d(v_p)d(u_j) + d(v_p)d(v_q)\} \\ &\quad + \frac{1}{2} \sum_{i,j=1}^n \sum_{p,q=1}^m \left\{ d(v_p, v_q) | (G_2) \right\} \{d(u_i)d(u_j) + d(u_i)d(v_q) + d(v_p)d(u_j) + d(v_p)d(v_q)\} \\ &= \frac{1}{2} \sum_{i,j=1}^n \sum_{p,q=1}^m \left\{ d(u_i, u_j) | S(G_1) \right\} \{d(u_i)d(u_j)\} + \frac{1}{2} \sum_{i,j=1}^n \sum_{p,q=1}^m \left\{ d(u_i, u_j) | S(G_1) \right\} \{d(u_i)d(v_q)\} \\ &\quad + \frac{1}{2} \sum_{i,j=1}^n \sum_{p,q=1}^m \left\{ d(u_i, u_j) | S(G_1) \right\} \{d(v_p)d(u_j)\} + \frac{1}{2} \sum_{i,j=1}^n \sum_{p,q=1}^m \left\{ d(u_i, u_j) | S(G_1) \right\} \{d(v_p)d(v_q)\} \\ &\quad + \frac{1}{2} \sum_{i,j=1}^n \sum_{p,q=1}^m \left\{ d(v_p, v_q) | (G_2) \right\} \{d(u_i)d(u_j)\} + \frac{1}{2} \sum_{i,j=1}^n \sum_{p,q=1}^m \left\{ d(v_p, v_q) | (G_2) \right\} \{d(u_i)d(v_q)\} \\ &\quad + \frac{1}{2} \sum_{i,j=1}^n \sum_{p,q=1}^m \left\{ d(v_p, v_q) | (G_2) \right\} \{d(v_p)d(u_j)\} + \frac{1}{2} \sum_{i,j=1}^n \sum_{p,q=1}^m \left\{ d(v_p, v_q) | (G_2) \right\} \{d(v_p)d(v_q)\}. \end{aligned} \quad (8)$$

Substituting  $\sum_{p,q=1}^m d(v_q) = 2lm$ ,  $\sum_{i,j=1}^n d(u_j) = 2kn$ ,

$$\begin{aligned} &= \frac{m^2}{2} \sum_{i,j=1}^n \left\{ d(u_i, u_j) | S(G_1) \right\} \{d(u_i)d(u_j)\} + lm \sum_{i,j=1}^n \left\{ d(u_i, u_j) | S(G_1) \right\} d(u_i) \\ &\quad + lm \sum_{i,j=1}^n \left\{ d(u_i, u_j) | S(G_1) \right\} \{d(u_j)\} + \frac{1}{2} \sum_{i,j=1}^n \left\{ d(u_i, u_j) | S(G_1) \right\} \sum_{p,q=1}^m \{d(v_p)d(v_q)\} \\ &= \frac{m^2}{2} \sum_{i,j=1}^n \left\{ d(u_i, u_j) | S(G_1) \right\} \{d(u_i)d(u_j)\} + lm \sum_{i,j=1}^n \left\{ d(u_i, u_j) | S(G_1) \right\} d(u_i) \\ &\quad + \frac{1}{2} \sum_{p,q=1}^m \left\{ d(v_p, v_q) | (G_2) \right\} \sum_{i,j=1}^n \{d(u_i)d(u_j)\} + kn \sum_{p,q=1}^m \left\{ d(v_p, v_q) | (G_2) \right\} \{d(v_q)\} \\ &\quad + kn \sum_{p,q=1}^m \left\{ d(v_p, v_q) | (G_2) \right\} \{d(v_p)\} + n^2 GM(G_2). \end{aligned} \quad (9)$$

Substituting  $\sum_{i,j=1}^n \{d(u_i)d(u_j)\} = 4k^2$  and  $\sum_{p,q=1}^m \{d(v_p)d(v_q)\} = 4l^2$ ,

$$\begin{aligned} &= \frac{m^2}{2} \sum_{i,j=1}^n \{d(u_i, u_j)|S(G_1)\} \{d(u_i)d(u_j)\} + lm \sum_{i,j=1}^n \{d(u_i, u_j)|S(G_1)\} \{d(u_i) + d(u_j)\} \\ &+ 2l^2 \sum_{i,j=1}^n \{d(u_i, u_j)|S(G_1)\} + 4k^2W(G_2) + 2knDD(G_2) + n^2GM(G_2) \end{aligned} \quad (10)$$

Case 2: when one vertex is white and the other is black,

$$B_1 = \frac{1}{2} \sum \{d((w_r, v_p), (u_i, v_q))(\deg(w_r, v_p)\deg(u_i, v_q)|G_1 + {}_sG_2)\}. \quad (11)$$

For  $r = 1$  to  $k$ ,  $i = 1$  to  $n$ , and  $p, q = 1$  to  $m$  and  $\deg(w_r, v_p) = 2$ ,

$$\begin{aligned} B_1 &= \frac{1}{2} \sum_{r=1}^k \sum_{i=1}^n \sum_{p,q=1}^m \{d(w_r, u_i)|S(G_1) + d(v_p, v_q)|G_2\} (2)\{d(u_i) + d(v_q)\} \\ &= \sum_{r=1}^k \sum_{i=1}^n \sum_{p,q=1}^m \{d(w_r, u_i)|S(G_1)\} (du_i) + \sum_{r=1}^k \sum_{i=1}^n \sum_{p,q=1}^m \{d(w_r, u_i)|S(G_1)\} (dv_q) \\ &+ \sum_{r=1}^k \sum_{i=1}^n \sum_{p,q=1}^m \{d(v_p, v_q)|G_2\} d(u_i) + \sum_{r=1}^k \sum_{i=1}^n \sum_{p,q=1}^m \{d(v_p, v_q)|G_2\} d(v_q) \\ &= m^2 \sum_{r=1}^k \sum_{i=1}^n \{d(w_r, u_i)|S(G_1)\} (du_i) + 2lm \sum_{r=1}^k \sum_{i=1}^n \{d(w_r, u_i)|S(G_1)\} + 4k^2W(G_2) + knDD(G_2). \end{aligned} \quad (12)$$

The summation of the distances between vertices with different colours is twice the  $B_1$ , i.e.,

$$\begin{aligned} B &= 2m^2 \sum_{r=1}^k \sum_{i=1}^n \{d(w_r, u_i)|S(G_1)\} (du_i) + 4lm \sum_{r=1}^k \sum_{i=1}^n \\ &\cdot \{d(w_r, u_i)|S(G_1)\} + 8k^2W(G_2) + 2knDD(G_2). \end{aligned} \quad (13)$$

Case 3: when both vertices are white,

$$C = \frac{1}{2} \sum \{d((w_r, v_p), (w_s, v_q))(\deg(w_r, v_p)\deg(w_s, v_q)|G_1 + {}_sG_2)\}. \quad (14)$$

This summation consists of two parts  $C = C_1 + C_2$  and  $\deg(w_r, v_p) = 2$ , where

$$C_1 = \frac{1}{2} \sum \{d((w_r, v_p), (w_s, v_q))(\deg(w_r, v_p)\deg(w_s, v_q))|G_1 + {}_sG_2; r = s, p \neq q\},$$

$$C_2 = \frac{1}{2} \sum \{d((w_r, v_p), (w_s, v_q))(\deg(w_r, v_p)\deg(w_s, v_q))|G_1 + {}_sG_2; r \neq s\},$$

$$C_1 = \frac{1}{2} \sum d((w_r, v_p), (w_s, v_q))(\deg(w_r, v_p)\deg(w_s, v_q))|G_1 + {}_sG_2$$

$$= \frac{1}{2} \sum \{(2 + d(v_p, v_q))(2)(2)|G_1 + {}_sG_2\}$$

$$= 4 \sum_{r,s=1, r=s}^k \sum_{p,q=1, p \neq q}^m + 2 \sum_{r,s=1, r=s}^k \sum_{p,q=1, p \neq q}^m \{d(v_p, v_q)|G_2\}$$

$$= 4k(m^2 - m) + 4kW(G_2),$$

(15)

$$C_2 = \frac{1}{2} \sum \{d((w_r, v_p), (w_s, v_q))(\deg(w_r, v_p)\deg(w_s, v_q))|G_1 + {}_sG_2; r \neq s\}$$

$$= \frac{1}{2} \sum_{p=1}^m \sum_{q=1, q \neq p}^m \sum_{r,s=1, r \neq s}^k \{d(w_r, w_s)|S(G_1)\}\{4\} + \frac{1}{2} \sum_{p=1}^m \sum_{q=1, q \neq p}^m \sum_{r,s=1, r \neq s}^k \{d(v_p, v_q)|G_2\}\{4\}$$

$$= 2m^2 \sum_{r,s=1, r \neq s}^k \{d(w_r, w_s)|S(G_1)\} + 4(k^2 - k)W(G_2),$$

$$C = 4k(m^2 - m) + 4kW(G_2) + 2m^2 \sum_{r,s=1, r \neq s}^k \{d(w_r, w_s)|S(G_1)\} + 4(k^2 - k)W(G_2)$$

$$= 4k(m^2 - m) + 2m^2 \sum_{r,s=1, r \neq s}^k \{d(w_r, w_s)|S(G_1)\} + 4k^2W(G_2).$$

Now, Gutman index of  $G_1 +_s G_2$  is given by

$$GM(G_1 +_s G_2) = A + B + C, \text{ i.e.,}$$

$$\begin{aligned} GM(G_1 +_s G_2) &= \frac{m^2}{2} \sum_{i,j=1}^n \{d(u_i, u_j) | S(G_1)\} \{d(u_i) d(u_j)\} + lm \sum_{i,j=1}^n \{d(u_i, u_j) | S(G_1)\} \{d(u_i) + d(u_j)\} \\ &+ 2l^2 \sum_{i,j=1}^n \{d(u_i, u_j) | S(G_1)\} + 4k^2 W(G_2) + 2knDD(G_2) + n^2 GM(G_2) \\ &+ 2m^2 \sum_{r=1}^k \sum_{i=1}^n \{d(w_r, u_i) | S(G_1)\} (du_i) + 4lm \sum_{r=1}^k \sum_{i=1}^n \{d(w_r, u_i) | S(G_1)\} + 8k^2 W(G_2) \\ &+ 2knDD(G_2) + 4k(m^2 - m) + 2m^2 \sum_{r,s=1, r \neq s}^k \{d(w_r, w_s) | S(G_1)\} + 4k^2 W(G_2), \end{aligned}$$

$$\begin{aligned} GM(G_1 +_s G_2) &= m^2 \left[ \frac{1}{2} \sum_{i,j=1}^n \{d(u_i, u_j) | S(G_1)\} \{d(u_i) d(u_j)\} + \sum_{r=1}^k \sum_{i=1}^n \{d(w_r, u_i) | S(G_1)\} \{2d(u_i)\} + 2 \sum_{r,s=1, r \neq s}^k \{d(w_r, w_s) | S(G_1)\} \right] \\ &+ n^2 GM(G_2) + 4knDD(G_2) + 16k^2 W(G_2) + 4k(m^2 - m) \\ &+ lm \sum_{i,j=1}^n \{d(u_i, u_j) | S(G_1)\} \{d(u_i) + d(u_j)\} + 2l^2 \sum_{i,j=1}^n \{d(u_i, u_j) | S(G_1)\} + 4lm \sum_{r=1}^k \sum_{i=1}^n \{d(w_r, u_i) | S(G_1)\}, \\ GM(G_1 +_s G_2) &= m^2 GM(S(G_1)) + n^2 GM(G_2) + 4nkDD(G_2) + 16k^2 W(G_2) + 4k(m^2 - m) \\ &+ lm \sum_{i,j=1}^n [d(u_i, u_j) | S(G_1)] \{d(u_i) + d(u_j)\} + 2l^2 \sum_{i,j=1}^n \{d(u_i, u_j) | S(G_1)\} + 4lm \sum_{r=1}^k \sum_{i=1}^n \{d(w_r, u_i) | S(G_1)\}. \end{aligned} \tag{16}$$

**Theorem 2.** Let  $G_1$  and  $G_2$  are connected and simple graphs. If  $(G_1 +_R G_2)$  is the  $R$ -sum graph of  $G_1$  and  $G_2$ , then

$$\begin{aligned} GM(G_1 +_R G_2) &= m^2 GM(R(G_1)) + n^2 GM(G_2) + 6nkDD(G_2) + 36k^2 W(G_2) + 4k(m^2 - m) \\ &+ 2lm \sum_{i,j=1}^n \{d(u_i, u_j) | R(G_1)\} \{d(u_i) + d(u_j)\} + 2l^2 \sum_{i,j=1}^n \{d(u_i, u_j) | R(G_1)\} + 4lm \sum_{r=1}^k \sum_{i=1}^n \{d(w_r, u_i) | R(G_1)\}. \end{aligned} \tag{17}$$

*Proof.* 1) When both vertices are black,

$$A = \frac{1}{2} \sum \{d((u_i, v_p), (u_j, v_q)) (\deg(u_i, v_p) \deg(u_j, v_q)) | G_1 +_R G_2\}, \tag{18}$$



for  $i, j = 1$  to  $n$  and  $p, q = 1$  to  $m$ . For R-sum  
 $\deg(u_i, v_p) = 2d(u_i) + d(v_p)$ ,

$$\begin{aligned}
A &= \frac{1}{2} \sum_{i,j=1}^n \sum_{p,q=1}^m \{d(u_i, u_j)|R(G_1) + d(v_p, v_q)|G_2\} \{2d(u_i) + d(v_p)\} \{2d(u_j) + d(v_q)\} \\
&= \frac{1}{2} \sum_{i,j=1}^n \sum_{p,q=1}^m \{d(u_i, u_j)|R(G_1) + d(v_p, v_q)|G_2\} \{4d(u_i)d(u_j) + 2d(u_i)d(v_q) + 2d(v_p)d(u_j) + d(v_p)d(v_q)\} \\
&= \frac{1}{2} \sum_{i,j=1}^n \sum_{p,q=1}^m \{d(u_i, u_j)|R(G_1)\} \{4d(u_i)d(u_j) + 2d(u_i)d(v_q) + 2d(v_p)d(u_j) + d(v_p)d(v_q)\} \\
&\quad + \frac{1}{2} \sum_{i,j=1}^n \sum_{p,q=1}^m \{d(v_p, v_q)|G_2\} \{4d(u_i)d(u_j) + 2d(u_i)d(v_q) + 2d(v_p)d(u_j) + d(v_p)d(v_q)\} \\
&= 2 \sum_{i,j=1}^n \sum_{p,q=1}^m \{d(u_i, u_j)|R(G_1)\} \{d(u_i)d(u_j)\} + \sum_{i,j=1}^n \sum_{p,q=1}^m \{d(u_i, u_j)|R(G_1)\} \{d(u_i)d(v_q)\} \\
&\quad + \sum_{i,j=1}^n \sum_{p,q=1}^m \{d(u_i, u_j)|R(G_1)\} \{d(v_p)d(u_j)\} + \frac{1}{2} \sum_{i,j=1}^n \sum_{p,q=1}^m \{d(u_i, u_j)|R(G_1)\} \{d(v_p)d(v_q)\} \\
&\quad + 2 \sum_{i,j=1}^n \sum_{p,q=1}^m \{d(v_p, v_q)|G_2\} \{d(u_i)d(u_j)\} + \sum_{i,j=1}^n \sum_{p,q=1}^m \{d(v_p, v_q)|G_2\} \{d(u_i)d(v_q)\} \\
&\quad + \sum_{i,j=1}^n \sum_{p,q=1}^m \{d(v_p, v_q)|G_2\} \{d(v_p)d(u_j)\} + \frac{1}{2} \sum_{i,j=1}^n \sum_{p,q=1}^m \{d(v_p, v_q)|G_2\} \{d(v_p)d(v_q)\}.
\end{aligned} \tag{19}$$

Substituting  $\sum_{p,q=1}^m d(v_q) = 2lm$  and  $\sum_{i,j=1}^n d(u_j) = 2kn$ ,

$$\begin{aligned}
&= 2m^2 \sum_{i,j=1}^n \{d(u_i, u_j)|R(G_1)\} \{d(u_i)d(u_j)\} + 2lm \sum_{i,j=1}^n \{d(u_i, u_j)|R(G_1)\} d(u_i) \\
&\quad + 2lm \sum_{i,j=1}^n \{d(u_i, u_j)|R(G_1)\} d(u_i) + \frac{1}{2} \sum_{i,j=1}^n \{d(u_i, u_j)|R(G_1)\} \sum_{p,q=1}^m \{d(v_p)d(v_q)\} \\
&\quad + 2 \sum_{p,q=1}^m \{d(v_p, v_q)|G_2\} \sum_{i,j=1}^n \{d(u_i)d(u_j)\} + 2kn \sum_{p,q=1}^m \{d(v_p, v_q)|G_2\} \{d(v_q)\} \\
&\quad + 2kn \sum_{p,q=1}^m \{d(v_p, v_q)|G_2\} \{d(v_p)\} + n^2 GM(G_2).
\end{aligned} \tag{20}$$

Substituting  $\sum_{i,j=1}^n \{d(u_i)d(u_j)\} = 4k^2$  and  $\sum_{p,q=1}^m \{d(v_p)d(v_q)\} = 4l^2$ ,

$$A = 2m^2 \sum_{i,j=1}^n \{d(u_i, u_j)|R(G_1)\} \{d(u_i)d(u_j)\} + 2lm \sum_{i,j=1}^n \{d(u_i, u_j)|R(G_1)\} \{d(u_i) + d(u_j)\} + 2l^2 \sum_{i,j=1}^n \{d(u_i, u_j)|S(G_1)\} + 16k^2W(G_2) + 4knDD(G_2) + n^2GM(G_2). \quad (21)$$

Case 2: when one vertex is white and the other is black,

$$B_1 = \frac{1}{2} \sum \{d((w_r, v_p), (u_i, v_q))(\deg(w_r, v_p)\deg(u_i, v_q)|G_1 + {}_R G_2)\}. \quad (22)$$

For  $r = 1$  to  $k$ ,  $i = 1$  to  $n$ , and  $p, q = 1$  to  $m$  and  $\deg(w_r, v_p) = 2$ ,

$$\begin{aligned} B_1 &= \frac{1}{2} \sum_{r=1}^k \sum_{i=1}^n \sum_{p,q=1}^m \{d(w_r, u_i)|R(G_1) + d(v_p, v_q)|G_2\} (2) \{2d(u_i) + d(v_q)\} \\ &= 2 \sum_{r=1}^k \sum_{i=1}^n \sum_{p,q=1}^m \{d(w_r, u_i)|R(G_1)\} (du_i) + \sum_{r=1}^k \sum_{i=1}^n \sum_{p,q=1}^m \{d(w_r, u_i)|R(G_1)\} (dv_q) \\ &\quad + 2 \sum_{r=1}^k \sum_{i=1}^n \sum_{p,q=1}^m \{d(v_p, v_q)|G_2\} d(u_i) + \sum_{r=1}^k \sum_{i=1}^n \sum_{p,q=1}^m \{d(v_p, v_q)|G_2\} d(v_q) \\ &= 2m^2 \sum_{r=1}^k \sum_{i=1}^n \{d(w_r, u_i)|R(G_1)\} (du_i) + 2lm \sum_{r=1}^k \sum_{i=1}^n \{d(w_r, u_i)|R(G_1)\} + 8k^2W(G_2) + knDD(G_2). \end{aligned} \quad (23)$$

The summation of the distances between vertices with different colours is twice the  $B_1$ , i.e.,

$$B = 4m^2 \sum_{r=1}^k \sum_{i=1}^n \{d(w_r, u_i)|R(G_1)\} (du_i) + 4lm \sum_{r=1}^k \sum_{i=1}^n \{d(w_r, u_i)|R(G_1)\} + 16k^2W(G_2) + 2knDD(G_2). \quad (24)$$

Case 3: when both vertices are white, C can be cal-

culated similar to that in the previous theorem:

$$C = 4k(m^2 - m) + 2m^2 \sum_{r,s=1, r \neq s}^k \{d(w_r, w_s)|R(G_1)\} + 4k^2W(G_2). \quad (25)$$

Now, Gutman index of  $(G_1 + {}_R G_2)$  is given by

$$GM(G_1 +_R G_2) = A + B + C, \text{ i.e.,}$$

$$\begin{aligned} GM(G_1 +_R G_2) &= 2m^2 \sum_{i,j=1}^n \{d(u_i, u_j)|R(G_1)\} \{d(u_i)d(u_j)\} + 2lm \sum_{i,j=1}^n \{d(u_i, u_j)|R(G_1)\} \{d(u_i)d(u_j)\} \\ &\quad + 2l^2 \sum_{i,j=1}^n \{d(u_i, u_j)|R(G_1)\} + 16k^2W(G_2) + 4knDD(G_2) + n^2GM(G_2) \\ &\quad + 4m^2 \sum_{r=1}^k \sum_{i=1}^n \{d(w_r, u_i)|R(G_1)\} (du_i) + 4lm \sum_{r=1}^k \sum_{i=1}^n \{d(w_r, u_i)|R(G_1)\} + 16k^2W(G_2) \\ &\quad + 2knDD(G_2) + 4k(m^2 - m) + 2m^2 \sum_{r,s=1, r \neq s}^k \{d(w_r, w_s)|R(G_1)\} + 4k^2W(G_2), \\ GM(G_1 +_R G_2) &= m^2 \left[ 2 \sum_{i,j=1}^n \{d(u_i, u_j)|R(G_1)\} \{d(u_i)d(u_j)\} + \sum_{r=1}^k \sum_{i=1}^n \{d(w_r, u_i)|R(G_1)\} \{4d(u_i)\} \right. \\ &\quad \left. + 2 \sum_{r,s=1, r \neq s}^k \{d(w_r, w_s)|R(G_1)\} \right] + n^2GM(G_2) + 6knDD(G_2) + 36k^2W(G_2) + 4k(m^2 - m) \\ &\quad + 2lm \sum_{i,j=1}^n \{d(u_i, u_j)|R(G_1)\} \{d(u_i) + d(u_j)\} + 2l^2 \sum_{i,j=1}^n \{d(u_i, u_j)|R(G_1)\} + 4lm \sum_{r=1}^k \sum_{i=1}^n \{d(w_r, u_i)|R(G_1)\}, \\ GM(G_1 +_R G_2) &= m^2GM(R(G_1)) + n^2GM(G_2) + 6nkDD(G_2) + 36k^2W(G_2) + 4k(m^2 - m) \\ &\quad + 2lm \sum_{i,j=1}^n \{d(u_i, u_j)|R(G_1)\} \{d(u_i) + d(u_j)\} + 2l^2 \sum_{i,j=1}^n \{d(u_i, u_j)|R(G_1)\} + 4lm \sum_{r=1}^k \sum_{i=1}^n \{d(w_r, u_i)|R(G_1)\}, \end{aligned} \tag{26}$$

□

**Theorem 3.** Let  $G_1$  and  $G_2$  be two simple and connected graphs. If  $(G_1 +_Q G_2)$  is the  $Q$ -sum graph of  $G_1$  and  $G_2$ , then

$$\begin{aligned} GM(G_1 +_Q G_2) &= m^2GM(Q(G_1)) + n^2GM(G_2) + n(6k - t)DD(G_2) + (6k - t)^2W(G_2) \\ &\quad + \frac{1}{2}(m^2 - m)[(4k - t)^2 + 16k - 7t] + lm \sum_{i,j=1}^n \{d(u_i, u_j)|Q(G_1)\} (d(u_i) + d(u_j)) \\ &\quad + 2l^2 \sum_{i,j=1}^n \{d(u_i, u_j)|Q(G_1)\} + 2lm \sum_{r=1}^k \sum_{i=1}^n \{d(w_r, u_i)|Q(G_1)\} \deg(w_r, v_p). \end{aligned} \tag{27}$$

*Proof*

Case 1: when both vertices are black,  $A$  can be determined similar to that in Case 1 of Theorem 1:

$$\begin{aligned} A &= \frac{m^2}{2} \sum_{i,j=1}^n \{d(u_i, u_j)|Q(G_1)\} \{d(u_i)d(u_j)\} + lm \sum_{i,j=1}^n \{d(u_i, u_j)|Q(G_1)\} \{d(u_i)d(u_j)\} \\ &\quad + 2l^2 \sum_{i,j=1}^n \{d(u_i, u_j)|Q(G_1)\} + 4k^2W(G_2) + 2knDD(G_2) + n^2GM(G_2). \end{aligned} \tag{28}$$

Case 2: when one vertex is white and the other is black,

$$B_1 = \frac{1}{2} \sum \{d((w_r, v_p), (u_i, v_q))(\deg(w_r, v_p)\deg(u_i, v_q)|G_1 + QG_2)\}. \quad (29)$$

For  $r = 1$  to  $k$ ,  $i = 1$  to  $n$  and  $p, q = 1$  to  $m$ ,

$$\begin{aligned} B_1 &= \frac{1}{2} \sum_{r=1}^k \sum_{i=1}^n \sum_{p,q=1}^m \{d(w_r, u_i)|S(G_1) + d(v_p, v_q|G_2)\}(\deg(w_r, v_p)\{d(u_i) + d(v_q)\}) \\ &= \frac{1}{2} \sum_{r=1}^k \sum_{i=1}^n \sum_{p,q=1}^m \{d(w_r, u_i)|Q(G_1)\}\deg(w_r, v_p)d(u_i) + \frac{1}{2} \sum_{r=1}^k \sum_{i=1}^n \sum_{p,q=1}^m \{d(w_r, u_i)|Q(G_1)\}\deg(w_r, v_p)d(v_q) \\ &\quad + \frac{1}{2} \sum_{r=1}^k \sum_{i=1}^n \sum_{p,q=1}^m \{d(v_p, v_q|G_2)\}(\deg(w_r, v_p)d(u_i) + \frac{1}{2} \sum_{r=1}^k \sum_{i=1}^n \sum_{p,q=1}^m \{d(v_p, v_q|G_2)\}(\deg(w_r, v_p)d(v_q)) \quad (30) \\ &= \frac{m^2}{2} \sum_{r=1}^k \sum_{i=1}^n \{d(w_r, u_i)|Q(G_1)\}\deg(w_r, v_p)d(u_i) + lm \sum_{r=1}^k \sum_{i=1}^n \{d(w_r, u_i)|Q(G_1)\}\deg(w_r, v_p) \\ &\quad + 2k(4k - t)W(G_2) + \frac{1}{2}n(4k - t)DD(G_2). \end{aligned}$$

The summation of the distances between vertices with different colours is twice the  $B_1$ , i.e.,

$$\begin{aligned} B &= m^2 \sum_{r=1}^k \sum_{i=1}^n \{d(w_r, u_i)|Q(G_1)\}\deg(w_r, v_p)d(u_i) + 2lm \sum_{r=1}^k \sum_{i=1}^n \{d(w_r, u_i)|Q(G_1)\}\deg(w_r, v_p) \\ &\quad + 4k(4k - t)W(G_2) + n(4k - t)DD(G_2). \end{aligned} \quad (31)$$

Case 3: When both vertices are white,

$$C = \frac{1}{2} \sum \{d((w_r, v_p), (w_s, v_q))(\deg(w_r, v_p)\deg(w_s, v_q)|G_1 + QG_2)\}. \quad (32)$$

This summation consists of three parts  
 $C = C_1 + C_2 + C_3$ , where

$$C_1 = \frac{1}{2} \sum \{d((w_r, v_p), (w_s, v_q))(\deg(w_r, v_p)\deg(w_s, v_q)) | G_1 + Q G_2: r = s, p \neq q\},$$

$$C_2 = \frac{1}{2} \sum \{d((w_r, v_p), (w_s, v_q))(\deg(w_r, v_p)\deg(w_s, v_q)) | G_1 + Q G_2: r \neq s, p = q\},$$

$$C_3 = \frac{1}{2} \sum \{d((w_r, v_p), (w_s, v_q))(\deg(w_r, v_p)\deg(w_s, v_q)) | G_1 + Q G_2: r \neq s, p \neq q\},$$

$$C_1 = \frac{1}{2} \sum \{(2 + d(v_p, v_q))(\deg(w_r, v_p)\deg(w_s, v_q)) | G_1 + Q G_2: r = s, p \neq q\},$$

$$C_1 = \sum_{r,s=1, r \neq s}^k \sum_{p,q=1, p \neq q}^m (\deg(w_r, v_p)\deg(w_s, v_q)) + \frac{1}{2} \sum_{r,s=1}^k \sum_{p,q=1, p \neq q}^m \{d(v_p, v_q) | G_2\} (\deg(w_r, v_p)\deg(w_s, v_q)),$$

$$C_1 = (m^2 - m)[16(k - t) + 9t] + W(G_2)[16(k - t) + 9t],$$

$$C_2 = \frac{1}{2} \sum_{p,q=1, p \neq q}^m \sum_{r,s=1, r \neq s}^k \{d(w_r, w_s) | Q(G_1)\} (\deg(w_r, v_p)\deg(w_s, v_q))$$

$$= \frac{m}{2} \sum_{r,s=1, r \neq s}^k \{d(w_r, w_s) | Q(G_1)\} (\deg(w_r, v_p)\deg(w_s, v_q)),$$

$$C_3 = \frac{1}{2} \sum_{r,s=1, r \neq s}^k \sum_{p,q=1, p \neq q}^m \{1 + d(w_r, w_s) | Q(G_1) + d(v_p, v_q) | G_2\} (\deg(w_r, v_p)\deg(w_s, v_q))$$

$$= \frac{1}{2} \sum_{r,s=1, r \neq s}^k \sum_{p,q=1, p \neq q}^m (\deg(w_r, v_p)\deg(w_s, v_q)) + \frac{1}{2} \sum_{r,s=1, r \neq s}^k \sum_{p,q=1, p \neq q}^m \{d(w_r, w_s) | Q(G_1)\} (\deg(w_r, v_p)\deg(w_s, v_q))$$

$$+ \frac{1}{2} \sum_{r,s=1, r \neq s}^k \sum_{p,q=1, p \neq q}^m \{d(v_p, v_q) | G_2\} (\deg(w_r, v_p)\deg(w_s, v_q))$$

$$= \frac{1}{2} (m^2 - m)[(4k - t)^2 - (16k - 7t)] + \frac{1}{2} (m^2 - m) \sum_{r,s=1, r \neq s}^k \{d(w_r, w_s) | Q(G_1)\} (\deg(w_r, v_p)\deg(w_s, v_q))$$

$$+ [(4k - t)^2 - (16k - 7t)] W(G_2),$$

$$C = (m^2 - m)(16k - 7t) + W(G_2)(16k - 7t) + \frac{m}{2} \sum_{r,s=1, r \neq s}^k \{d(w_r, w_s) | Q(G_1)\} (\deg(w_r, v_p)\deg(w_s, v_q))$$

$$+ \frac{1}{2} (m^2 - m)[(4k - t)^2 - (16k - 7t)] + \frac{1}{2} (m^2 - m) \sum_{r,s=1, r \neq s}^k \{d(w_r, w_s) | Q(G_1)\} (\deg(w_r, v_p)\deg(w_s, v_q)),$$

$$C = \frac{1}{2} (m^2 - m)[(4k - t)^2 + 16k - 7t] + (4k - t)^2 W(G_2) + \frac{m^2}{2} \sum_{r,s=1, r \neq s}^k \{d(w_r, w_s) | Q(G_1)\} (\deg(w_r, v_p)\deg(w_s, v_q)).$$

Now, Gutman index of  $(G_1 +_Q G_2)$  is given by

$$GM(G_1 +_Q G_2) = A + B + C, \text{ i.e.,} \quad (34)$$

using values of A, B, and C from Case 1, Case 2, and Case 3, respectively,

$$\begin{aligned}
 GM(G_1 +_Q G_2) &= \frac{m^2}{2} \sum_{i,j=1}^n \{d(u_i, u_j) | Q(G_1)\} \{d(u_i) d(u_j)\} + lm \sum_{i,j=1}^n \{d(u_i, u_j) | Q(G_1)\} \{d(u_i) + d(u_j)\} \\
 &+ 2l^2 \sum_{i,j=1}^n \{d(u_i, u_j) | Q(G_1)\} + 4k^2 W(G_2) + 2kn DD(G_2) + n^2 GM(G_2) \\
 &+ m^2 \sum_{r=1}^k \sum_{i=1}^n \{d(w_r, u_i) | Q(G_1)\} \deg(w_r, v_p) d(u_i) + 2lm \sum_{r=1}^k \sum_{i=1}^n \{d(w_r, u_i) | Q(G_1)\} \deg(w_r, v_p) \\
 &+ 4k(4k - t)W(G_2) + n(4k - t)DD(G_2) + \frac{1}{2}(m^2 - m)[(4k - t)^2 + 16k - 7t] \\
 &+ (4k - t)^2 W(G_2) + \frac{m^2}{2} \sum_{r,s=1, r \neq s}^k \{d(w_r, w_s) | Q(G_1)\} (\deg(w_r, v_p) \deg(w_s, v_q)), \\
 GM(G_1 +_Q G_2) &= m^2 \left[ \frac{1}{2} \sum_{i,j=1}^n \{d(u_i, u_j) | Q(G_1)\} d(u_i) d(u_j) + \sum_{r=1}^k \sum_{i=1}^n \{d(w_r, u_i) | Q(G_1)\} \deg(w_r, v_p) d(u_i) \right. \\
 &\left. + \frac{1}{2} \sum_{r,s=1, r \neq s}^k \{d(w_r, w_s) | Q(G_1)\} (\deg(w_r, v_p) \deg(w_s, v_q)) \right] + n^2 GM(G_2) + n(6k - t)DD(G_2) \quad (35) \\
 &+ (W(G_2) [4k^2 + 4k(4k - t) + (4k - t)^2] + \frac{1}{2}(m^2 - m)[(4k - t)^2 + 16k - 7t] \\
 &+ lm \sum_{i,j=1}^n \{d(u_i, u_j) | Q(G_1)\} d(u_i) d(u_j) + 2l^2 \sum_{i,j=1}^n \{d(u_i, u_j) | Q(G_1)\} \\
 &+ 2lm \sum_{r=1}^k \sum_{i=1}^n \{d(w_r, u_i) | Q(G_1)\} \deg(w_r, v_p), \\
 GM(G_1 +_Q G_2) &= m^2 GM(Q(G_1)) + n^2 GM(G_2) + n(6k - t)DD(G_2) + (6k - t)^2 W(G_2) \\
 &+ \frac{1}{2}(m^2 - m)[(4k - t)^2 + 16k - 7t] + lm \sum_{i,j=1}^n \{d(u_i, u_j) | Q(G_1)\} (d(u_i) + d(u_j)) \\
 &+ 2l^2 \sum_{i,j=1}^n \{d(u_i, u_j) | Q(G_1)\} + 2lm \sum_{r=1}^k \sum_{i=1}^n \{d(w_r, u_i) | Q(G_1)\} \deg(w_r, v_p).
 \end{aligned}$$

**Theorem 4.** Let  $G_1$  and  $G_2$  be two simple and connected graphs. If  $(G_1 +_T G_2)$  is the T-sum graph of  $G_1$  and  $G_2$ , then

□

$$\begin{aligned}
GM(G_1 + {}_T G_2) &= m^2 GM(T(G_1)) + n^2 GM(G_2) + n(8k - t)DD(G_2) + (8k - t)^2 W(G_2) \\
&+ \frac{1}{2}(m^2 - m)[(4k - t)^2 + 16k - 7t] + 4lm \sum_{i,j=1}^n \{d(u_i, u_j)|T(G_1)\} (d(u_i)) \\
&+ 2l^2 \sum_{i,j=1}^n \{d(u_i, u_j)|T(G_1)\} + 2lm \sum_{r=1}^k \sum_{i=1}^n \{d(w_r, u_i)|T(G_1)\} \deg(w_r, v_p).
\end{aligned} \tag{36}$$

*Proof*

Case 1: when both vertices are black, A can be calculated similar to that in Case 1 of Theorem 2:

$$\begin{aligned}
A &= 2m^2 \sum_{i,j=1}^n \{d(u_i, u_j)|T(G_1)\} \{d(u_i)d(u_j)\} + 2lm \sum_{i,j=1}^n \{d(u_i, u_j)|T(G_1)\} \{d(u_i)d(u_j)\} \\
&+ 2l^2 \sum_{i,j=1}^n \{d(u_i, u_j)|T(G_1)\} + 16k^2 W(G_2) + 4knDD(G_2) + n^2 GM(G_2).
\end{aligned} \tag{37}$$

Case 2: when one vertex is white and the other is black,

$$B_1 = \frac{1}{2} \sum \{d((w_r, v_p), (u_i, v_q)) (\deg(w_r, v_p) \deg(u_i, v_q)) | G_1 + {}_T G_2\}. \tag{38}$$

For  $r = 1$  to  $k$ ,  $i = 1$  to  $n$ , and  $p, q = 1$  to  $m$ ,

$$\begin{aligned}
B_1 &= \frac{1}{2} \sum_{r=1}^k \sum_{i=1}^n \sum_{p,q=1}^m \{d(w_r, u_i)|T(G_1) + d(v_p, v_q)|(G_2)\} \deg(w_r, v_p) \{2d(u_i) + d(v_q)\} \\
&= \sum_{r=1}^k \sum_{i=1}^n \sum_{p,q=1}^m \{d(w_r, u_i)|T(G_1)\} \deg(w_r, v_p) d(u_i) + \frac{1}{2} \sum_{r=1}^k \sum_{i=1}^n \sum_{p,q=1}^m \{d(w_r, u_i)|T(G_1)\} \deg(w_r, v_p) d(v_q) \\
&+ \sum_{r=1}^k \sum_{i=1}^n \sum_{p,q=1}^m \{d(v_p, v_q)|(G_2)\} \deg(w_r, v_p) d(u_i) + \frac{1}{2} \sum_{r=1}^k \sum_{i=1}^n \sum_{p,q=1}^m \{d(v_p, v_q)|(G_2)\} \deg(w_r, v_p) d(v_q) \\
&= m^2 \sum_{r=1}^k \sum_{i=1}^n \{d(w_r, u_i)|T(G_1)\} \deg(w_r, v_p) d(u_i) + lm \sum_{r=1}^k \sum_{i=1}^n \{d(w_r, u_i)|T(G_1)\} \deg(w_r, v_p) \\
&+ 4k(4k - t)W(G_2) + \frac{1}{2} n(4k - t)DD(G_2).
\end{aligned} \tag{39}$$

The summation of the distances between vertices with different colours is twice the  $B_1$ , i.e.,

$$\begin{aligned}
B &= 2m^2 \sum_{r=1}^k \sum_{i=1}^n \{d(w_r, u_i)|T(G_1)\} \deg(w_r, v_p) d(u_i) + 2lm \sum_{r=1}^k \sum_{i=1}^n \{d(w_r, u_i)|T(G_1)\} \deg(w_r, v_p) \\
&+ 8k(4k - t)W(G_2) + n(4k - t)DD(G_2).
\end{aligned} \tag{40}$$

Case 3: when both vertices are white, C can be calculated similar to that in Case 3 of Theorem 3:

$$C = \frac{1}{2}(m^2 - m)[(4k - t)^2 + 16k - 7t] + (4k - t)^2W(G_2) + \frac{m^2}{2} \sum_{r,s=1, r \neq s}^k \{d(w_r, w_s)|Q(G_1)\} \cdot (\deg(w_r, v_p)\deg(w_s, v_q)). \tag{41}$$

Now, Gutman index of  $(G_1 +_T G_2)$  is given by

$$GM(G_1 +_T G_2) = A + B + C, \text{ i.e.,} \tag{42}$$

using values of A, B, and C from Case 1, Case 2, and Case 3, respectively,

$$\begin{aligned} GM(G_1 +_T G_2) &= 2m^2 \sum_{i,j=1}^n \{d(u_i, u_j)|T(G_1)\} \{d(u_i)d(u_j)\} + 2lm \sum_{i,j=1}^n \{d(u_i, u_j)|T(G_1)\} \{d(u_i)d(u_j)\} \\ &+ 2l^2 \sum_{i,j=1}^n \{d(u_i, u_j)|T(G_1)\} + 16k^2W(G_2) + 4knDD(G_2) + n^2GM(G_2) \\ &+ 2m^2 \sum_{r=1}^k \sum_{i=1}^n \{d(w_r, u_i)|T(G_1)\} \deg(w_r, v_p)d(u_i) + 2lm \sum_{r=1}^k \sum_{i=1}^n \{d(w_r, u_i)|T(G_1)\} \deg(w_r, v_p) \\ &+ 8k(4k - t)W(G_2) + n(4k - t)DD(G_2) + \frac{1}{2}(m^2 - m)[(4k - t)^2 + 16k - 7t] + (4k - t)^2W(G_2) \\ &+ \frac{m^2}{2} \sum_{r,s=1, r \neq s}^k \{d(w_r, w_s)|T(G_1)\} (\deg(w_r, v_p)\deg(w_s, v_q)), \end{aligned}$$

$$\begin{aligned} GM(G_1 +_T G_2) &= m^2 \left[ 2 \sum_{i,j=1}^n \{d(u_i, u_j)|T(G_1)\} (d(u_i))d(u_j) + 2 \sum_{r=1}^k \sum_{i=1}^n \{d(w_r, u_i)|T(G_1)\} \deg(w_r, v_p)du_i \right. \\ &\left. + \frac{1}{2} \sum_{r,s=1, r \neq s}^k \{d(w_r, w_s)|T(G_1)\} (\deg(w_r, v_p)\deg(w_s, v_q)) \right] + n^2GM(G_2) + n(8k - t)DD(G_2) \tag{43} \end{aligned}$$

$$\begin{aligned} &+ (W(G_2)[16k^2 + 8k(4k - t) + (4k - t)^2] + \frac{1}{2}(m^2 - m)[(4k - t)^2 + 16k - 7t] \\ &+ 4lm \sum_{i,j=1}^n \{d(u_i, u_j)|T(G_1)\} (d(u_i)) \end{aligned}$$

$$+ 2l^2 \sum_{i,j=1}^n \{d(u_i, u_j)|T(G_1)\} + 2lm \sum_{r=1}^k \sum_{i=1}^n \{d(w_r, u_i)|T(G_1)\} \deg(w_r, v_p),$$

$$\begin{aligned} GM(G_1 +_T G_2) &= m^2GM(T(G_1)) + n^2GM(G_2) + n(8k - t)DD(G_2) + (8k - t)^2W(G_2) \\ &+ \frac{1}{2}(m^2 - m)[(4k - t)^2 + 16k - 7t] + 4lm \sum_{i,j=1}^n \{d(u_i, u_j)|T(G_1)\} (d(u_i)) \\ &+ 2l^2 \sum_{i,j=1}^n \{d(u_i, u_j)|T(G_1)\} + 2lm \sum_{r=1}^k \sum_{i=1}^n \{d(w_r, u_i)|T(G_1)\} \deg(w_r, v_p). \end{aligned}$$

□



#### 4. Discussion and Conclusion

In this section, we apply the main results of Section 3 by taking  $G_1$  equal to, firstly,  $P_n$ , and secondly,  $C_n$ , while  $G_2$  is set equal to  $P_m$ . The Wiener index degree, distance index, and Gutman index of  $P_n$  are  $W(P_n) = (n(n^2 - 1)/6)$ ,

$DD(P_n) = ((n(n-1)(2n-1))/3)$ , and  $GM(P_n) = ((n-1)(2n^2 - 4n + 3)/3)$ , respectively. Now, we construct Tables 1 and 2.

Then, the following results are found by using Theorems 1-4 and Tables 3 and 4:

$$\begin{aligned}
 GM(P_n +_S P_m) &= \frac{2m^2(n-1)(8n^2 - 16n + 9)}{3} + \frac{n^2(m-1)(2m^2 - 4m + 3)}{3} \\
 &+ \frac{4n(n-1)m(m-1)(2m-1)}{3} + \frac{4mn(n-1)(m-1)(2m-1)}{3} + \frac{8(n-1)^2m(m^2-1)}{3} + 4m(n-1)(m-1) \\
 &+ \frac{4mn(m-1)(n-1)(2n-1)}{3} + \frac{8(m-1)^2n(n^2-1)}{6} + \frac{4m(m-n)(n-1)(2n-1)}{3}, \\
 GM(P_{n3} +_R P_m) &= 6m^2n(n^2-1) + \frac{n^2(m-1)(2m^2 - 4m + 3)}{3} + 2nm(n-1)(m-1)(2m-1) \\
 &+ 6(n-1)^2m(m^2-1) + 4m(n-1)(m-1) + \frac{4mn(m-1)(n-1)(2n-1)}{3} + \frac{2(m-1)^2n(n^2-1)}{3} \\
 &+ \frac{4mn(m-1)(n^2-1)}{3}, \\
 GM(P_n +_Q P_m) &= 2m^2(3n^3 - 9n^2 + 10n - 5) + \frac{n^2(m-1)(2m^2 - 4m + 3)}{3} + \frac{mn(6n-8)(m-1)(2m-1)}{3} \\
 &+ \frac{(6n-8)^2m(m^2-1)}{6} + \frac{(m^2-m)[(4n-6)^2 + 16(n-1) - 14]}{2} + \frac{2m(m-1)(2n^3 + 3n^2 - 11n + 6)}{3} \\
 &+ \frac{2(m-1)^2n(n+4)(n-1)}{3} + \frac{2m(m-1)(4n^3 - 3n^2 - n - 6)}{3}, \\
 GM(P_n +_T P_m) &= \frac{m^2(32n^3 - 96n^2 + 115n - 66)}{3} + \frac{n^2(m-1)(2m^2 - 4m + 3)}{3} + \frac{mn(8n-10)(m-1)(2m-1)}{3} \\
 &+ \frac{(8n-10)^2m(m^2-1)}{6} + \frac{(m^2-m)[(4n-6)^2 + 16(n-1) - 14]}{2} + \frac{4mn(m-1)(n-1)(2n-1)}{3} \\
 &+ \frac{2(m-1)^2n(n^2-1)}{3} + \frac{2m(m-1)(4n^3 - 3n^2 - n - 6)}{3}.
 \end{aligned}$$

(44)

TABLE 1: Wiener index, degree distance, and Gutman Index of  $F(P_n)$ .

F	$W(F(P_n))$	$DD(F(P_n))$	$GM(F(P_n))$
S	$((2n(n-1)(2n-1))/3)$	$((2(n-1)(2n-1)(4n-3))/3)$	$((2(n-1)(8n^2-16n+9))/3)$
R	$((n-1)(2n^2+2n-3))/3)$	$4(n+1)(n-1)^2$	$6n(n-1)^2$
Q	$((2n(n-1)(n+1))/3)$	$4n^3-6n^2+2n-2$	$2(3n^3-9n^2+10n-5)$
T	$((n(n-1)(4n+1))/6)$	$(2/3)(8n^3-15n^2+10n-6)$	$((32n^3-96n^2+115n-66)/3)$

TABLE 2:  $\sum_{i,j=1}^n \{d(u_i, u_j)|F(P_n)\}$ ,  $\sum_{r=1}^k \sum_{i=1}^n \{d(w_r, u_i)|F(P_n)\}$ , and  $\sum_{i,j=1}^N \{d(u_i, u_j)|F(P_n)\} (du_i + du_j)$ .

F	$\sum_{i,j=1}^n \{d(u_i, u_j) F(P_n)\}$	$\sum_{r=1}^k \sum_{i=1}^n \{d(w_r, u_i) F(P_n)\}$	$\sum_{i,j=1}^N \{d(u_i, u_j) F(P_n)\} (du_i + du_j)$
S	$((2n(n-1)(n+1))/3)$	$((n(n-1)(2n-1))/3)$	$((4n(n-1)(2n-1))/3)$
R	$((n(n^2-1))/3)$	$(n(n^2-1))/3)$	$((2n(n-1)(2n-1))/3)$
Q	$((n(n-1)(n+4))/3)$	$((n(n-1)(n+1))/3)$	$((2(2n^3+3n^2-11n+6))/3)$
T	$((n(n-1)(n+1))/3)$	$((n(n-1)(n+1))/3)$	$((2n(n-1)(2n-1))/3)$

TABLE 3: Wiener index and degree distance of  $F(C_n)$ .

F	$W(F(C_n))$	$DD(F(C_n))$	$GM(F(C_n))$
S	$n^3$	$4n^3$	$4n^3$
R	$(n(n^2+2n-1))/2)$	$n(n+2)(3n-1)$	$\begin{cases} ((n(9n^2+12n-4))/2) & \text{if } n \text{ is even} \\ ((n(9n^2+12n-5))/2) & \text{if } n \text{ is odd} \end{cases}$
Q	$(n(n^2+2n-1))/2)$	$n(n+2)(3n-1)$	$\begin{cases} ((n(9n^2+12n-4))/2) & \text{if } n \text{ is even} \\ ((n(9n^2+12n-5))/2) & \text{if } n \text{ is odd} \end{cases}$
T	$((n^2(n+1))/2)$	$4n^2(n+1)$	$8n^2(n+1)$

TABLE 4:  $\sum_{i,j=1}^n \{d(u_i, u_j)|F(P_n)\}$  and  $\sum_{r=1}^k \sum_{i=1}^n \{d(w_r, u_i)|F(P_n)\}$  of  $F(C_n)$ .

F	$\sum_{i,j=1}^n \{d(u_i, u_j) F(C_n)\}$	$\sum_{r=1}^k \sum_{i=1}^n \{d(w_r, u_i) F(C_n)\}$
S	$\begin{cases} (n^3/2) & \text{if } n \text{ is even} \\ ((n(n^2-1))/2) & \text{if } n \text{ is odd} \end{cases}$	$\begin{cases} (n^3/2) & \text{if } n \text{ is even} \\ ((n(n^2+1))/2) & \text{if } n \text{ is odd} \end{cases}$
R	$\begin{cases} (n^3/4) & \text{if } n \text{ is even} \\ ((n(n^2-1))/4) & \text{if } n \text{ is odd} \end{cases}$	$\begin{cases} ((n^2(n+2))/4) & \text{if } n \text{ is even} \\ ((n(n+1)^2)/4) & \text{if } n \text{ is odd} \end{cases}$
Q	$\begin{cases} ((n(n^2+4n-4))/4) & \text{if } n \text{ is even} \\ ((n(n^2+4n-5))/4) & \text{if } n \text{ is odd} \end{cases}$	$\begin{cases} ((n^2(n+2))/4) & \text{if } n \text{ is even} \\ ((n(n+1)^2)/4) & \text{if } n \text{ is odd} \end{cases}$
T	$\begin{cases} (n^3/4) & \text{if } n \text{ is even} \\ ((n(n^2-1))/4) & \text{if } n \text{ is odd} \end{cases}$	$\begin{cases} ((n^2(n+2))/4) & \text{if } n \text{ is even} \\ ((n(n+1)^2)/4) & \text{if } n \text{ is odd} \end{cases}$

If  $C_n$  is cycle of  $n$  vertices, then the Wiener index, degree distance index, and Gutman index of cycle are as follows:

$$W(C_n) = \begin{cases} \frac{n^3}{8}, & \text{if } n \text{ is even,} \\ \frac{n(n^2-1)}{8}, & \text{if } n \text{ is odd,} \end{cases} \tag{45}$$

$$DD(C_n) = GM(C_n) = \begin{cases} \frac{n^3}{2}, & \text{if } n \text{ is even,} \\ \frac{n(n^2-1)}{2}, & \text{if } n \text{ is odd.} \end{cases}$$

TABLE 5: Comparison between exact, computed, and bounded values.

No.	F-sum graph	Exact value	Computed value	Bounded value
1	$GM(P_3 +_S P_2)$	505	505	1024
2	$GM(P_3 +_R P_2)$	689	689	2002
3	$GM(P_3 +_Q P_2)$	619	619	1393
4	$GM(P_3 +_T P_2)$	907	907	2473
5	$GM(C_3 +_S P_2)$	921	921	2832
6	$GM(C_3 +_R P_2)$	1341	1341	3614
7	$GM(C_3 +_Q P_2)$	1617	1617	4052
8	$GM(C_3 +_T P_2)$	2373	2373	6032

It is very essential to know that, in cycle,  $du_i = 2$  and

$$\deg(w_r, v_p) = \begin{cases} 2 & \text{if } F = S \text{ or } R, \\ 4 & \text{if } F = Q \text{ or } T. \end{cases} \quad (46)$$

Then, the following results are found by using Theorems 1-4 and Tables 3 and 4:

$$GM(C_n +_S P_m) = \frac{n^2(m-1)(2m^2-4m+3)}{3} + \frac{4n^2m(m-1)(2m-1)}{3} + \frac{8n^2m(m^2-1)}{3} + 4m(n-1)(m-1) + 4m^2n^3 + (m-1) \begin{cases} n^3(5m-1), & \text{if } n \text{ is even,} \\ n^3(5m-1) - n(m-1) & \text{if } n \text{ is odd,} \end{cases}$$

$$GM(C_n +_R P_m) = \frac{n^2(m-1)(2m^2-4m+3)}{3} + 2n^2m(m-1)(2m-1) + 6n^2m(m^2-1) + 4m(n-1)(m-1) + \frac{m^2n(9n^2+12n-4)}{2} + (m-1)n^2 \left[ \frac{n(7m-1)}{2} + 2m \right] + \begin{cases} 0 & \text{if } n \text{ is even,} \\ -\frac{n(2m-1)^2}{2} & \text{if } n \text{ is odd,} \end{cases}$$

$$GM(C_n +_Q P_m) = \frac{n^2(m-1)(2m^2-4m+3)}{3} + 2n^2m(m-1)(2m-1) + 6n^2m(m^2-1) + 8n(n+1)(m^2-m) + \frac{m^2n(9n^2+12n-4)}{2} + n(m-1) \left[ \frac{n^2(7m-1)}{2} + 2n(5m-1) - 6m + 2 \right] + \begin{cases} 0 & \text{if } n \text{ is even,} \\ -\frac{n}{2} & \text{if } n \text{ is odd,} \end{cases}$$

$$GM(C_n +_T P_m) = \frac{n^2(m-1)(2m^2-4m+3)}{3} + \frac{8n^2m(m-1)(2m-1)}{3} + \frac{32n^2m(m^2-1)}{3} + 8n(n+1)(m^2-m) + 8m^2n^2(n+1) + n(m-1) \left[ \frac{n^2(9m-1)}{2} + 4mn \right] + \begin{cases} 0 & \text{if } n \text{ is even,} \\ -\frac{n(m-1)^2}{2} & \text{if } n \text{ is odd.} \end{cases} \quad (47)$$

After deriving formulae, a comparison among the exact values, computed values, and bounded values is also drawn in Table 5.

Now, we close our discussion with the comments that the upper bounds for the Gutman indices on the F-sum (S-sum, R-sum, Q-sum, and T-sum) graphs are obtained in

[20]. In this paper, we considered for the improvement of the already existing bounds and determined the exact values of the Gutman indices for the F-sum graphs. However, the problem is still open to find the exact values of other distance-based TIs for these sum graphs.

## Data Availability

All data used to support the findings of the study are included within the article and can be obtained from the corresponding author upon request.

## Conflicts of Interest

The authors have no conflicts of interest.

## Acknowledgments

This research was partially supported by the research grant S-1440-0145, Deanship of Scientific Research, University of Tabuk, Tabuk-71491, Saudi Arabia.

## References

- [1] H. Wiener, "Structural determination of paraffin boiling points," *Journal of the American Chemical Society*, vol. 69, no. 1, pp. 17–20, 1947.
- [2] I. Gutman and N. Trinajstić, "Graph theory and molecular orbitals. total  $\phi$ -electron energy of alternant hydrocarbons  $\pi$ -electron energy of alternant hydrocarbons," *Chemical Physics Letters*, vol. 17, no. 4, pp. 535–538, 1972.
- [3] J. Devillers and A. T. Balaban, *Topological Indices and Related Descriptors in QSAR and QSPR*, Gordon and Breach, Amsterdam, The Netherlands, 1999.
- [4] M. V. Diudea, *QSPR/QSAR Studies by Molecular Descriptors*, NOVA, New York, NY, USA, 2001.
- [5] F. Yan, Q. Shang, S. Xia, Q. Wang, and P. Ma, "Application of topological index in predicting ionic liquids densities by the quantitative structure property relationship method," *Journal of Chemical & Engineering Data*, vol. 60, no. 3, pp. 734–739, 2015.
- [6] F. R. K. Chung, "The average distance and the independence number," *Journal of Graph Theory*, vol. 12, no. 2, pp. 229–235, 1988.
- [7] O. Ivanciuc, T.-S. Balaban, and A. T. Balaban, "Design of topological indices. part 4. reciprocal distance matrix, related local vertex invariants and topological indices," *Journal of Mathematical Chemistry*, vol. 12, no. 1, pp. 309–318, 1993.
- [8] D. Plaviscic, S. Nikolic, N. Trinajstic, and Z. Mihalic, "On the Hirary index for characterization of chemical graph," *Journal of Mathematical Chemistry*, vol. 12, pp. 235–250, 1993.
- [9] A. A. Dobrynin, R. Entringer, and I. Gutman, "Wiener index of trees, theory and applications," *Acta Applicandae Mathematicae*, vol. 66, no. 3, pp. 211–249, 2001.
- [10] K. C. Das and I. Gutman, "On Wiener and multiplicative Wiener indices of graphs," *Discrete Applied Mathematics*, vol. 206, pp. 9–14, 2016.
- [11] K. C. Das, I. Gutman, and M. J. Nadjafi-Arani, "Relations between distance-based and degree-based topological indices," *Applied Mathematics and Computation*, vol. 270, pp. 142–147, 2015.
- [12] A. A. Dobrynin and A. A. Kochetova, "Degree distance of a graph: a degree analog of the wiener index," *Journal of Chemical Information and Computer Sciences*, vol. 34, no. 5, pp. 1082–1086, 1994.
- [13] R. C. Entringer, "Distance in graph: tree," *Journal of Combinatorial Mathematics and in Computer Chemistry*, vol. 26, pp. 2465–2484, 1997.
- [14] E. Flapan, *When Topology Meets Chemistry*, Cambridge University Press and the Mathematical Association of America, Cambridge, UK, 2000.
- [15] W. Yan, B.-Y. Yang, and Y.-N. Yeh, "The behavior of Wiener indices and polynomials of graphs under five graph decorations," *Applied Mathematics Letters*, vol. 20, no. 3, pp. 290–295, 2007.
- [16] J.-B. Liu, S. Javed, M. Javaid, and K. Shabbir, "Computing first general zagreb index of operations on graphs," *IEEE Access*, vol. 7, pp. 47494–47502, 2019.
- [17] S. Akhter and M. Imran, "The sharp bounds on general sum-connectivity index of four operations on graphs," *Journal of Inequalities and Applications*, vol. 241, pp. 1–10, 2016.
- [18] M. Ahmad, M. Saeed, M. Javaid, and M. Hussain, "Exact formula and improved bounds for general sum-connectivity index of graph-operations," *IEEE Access*, vol. 7, pp. 167290–167299, 2019.
- [19] M. An, L. Xiong, and K. Das, "Two upper bounds for the degree distances of four sums of graphs," *Filomat*, vol. 28, no. 3, pp. 579–590, 2014.
- [20] K. Pattabiraman and M. A. Bhat, "Upper bounds on product degree distance of F-sum of graphs," *Discrete Mathematics, Algorithms and Applications*, vol. 11, no. 04, pp. 1950045–1950059, 2019.
- [21] A. Ahmad and A. N. Koam, "Computing the topological descriptors of line graph of the complete m-ary trees," *Journal of Intelligent and Fuzzy Systems*, vol. 1, no. 39, pp. 1081–1088, 2020.
- [22] H. M. Awais, M. Javaid, and M. Jamal, "Forgotten Index of generalized F-sum graphs," *Journal of Prime Research in Mathematics*, vol. 15, pp. 115–128, 2019.
- [23] H. M. Awais, M. Javaid, and A. Raheem, "Hyper-Zagreb index of graph based on generalized subdivision-related operations," *Punjab University Journal of Mathematics*, vol. 52, no. 5, pp. 89–103, 2020.
- [24] H. M. Awais, M. Javaid, and A. Akbar, "First general zagreb index of generalized F-sum graphs," *Discrete Dynamics in Nature and Society*, vol. 2020, Article ID 2954975, 16 pages, 2020.
- [25] M. Javaid, S. Javed, A. M. Alanazi, and M. R. Alotaibi, "Computing analysis of zagreb indices for generalized sum graphs under strong product," *Journal of Chemistry*, vol. 2021, Article ID 6663624, 20 pages, 2021.
- [26] M. Javaid, U. Ali, and J.-B. Liu, "Computing analysis for first zagreb connection index and coindex of resultant graphs," *Mathematical Problems in Engineering*, vol. 2021, Article ID 6019517, 19 pages, 2021.
- [27] W. Gao, Z. Iqbal, M. Ishaq, A. Aslam, M. Aamir, and M. A. Binayamin, "Bound on topological descriptors of the corona product of F-sum of connected graphs," *IEEE Access*, vol. 10, p. 1109, 2017.
- [28] J.-B. Liu, M. Javaid, and H. M. Awais, "Computing zagreb indices of the subdivision-related generalized operations of graphs," *IEEE Access*, vol. 7, pp. 105479–105488, 2019.
- [29] J.-B. Liu, S. Akram, M. Javaid, A. Raheem, and R. Hasni, "Bounds of degree-based molecular descriptors for generalized F-sum graphs," *Discrete Dynamics in Nature and Society*, vol. 2021, Article ID 8821020, 17 pages, 2021.

- [30] U. Ahmad and S. Hameed, "Study of topological indices in a class of benzenoid graphs," *Computational Journal of Combinatorial Mathematics*, vol. 1, pp. 19–30, 2020.
- [31] Z.-B. Peng, S. Javed, M. Javaid, and J.-B. Liu, "Computing FGZ index of sum graphs under strong product," *Journal of Mathematics*, vol. 2021, Article ID 6654228, 16 pages, 2021.
- [32] Z. Zhang, Z. S. Mufti, M. F. Nadeem, Z. Ahmad, M. K. Siddiqui, and M. R. Farahani, "Computing topological indices for para-line graphs of anthracene," *Open Chemistry*, vol. 1, no. 17, pp. 955–962, 2019.
- [33] R. Diestel, *Graph Theory*, Springer-Verlag, New York, NY, USA, 2000.
- [34] D. B. West, *Introduction to Graph Theory*, Prentice Hall, Inc., Hoboken, NJ, USA, 1996.
- [35] I. Gutman, "Selected properties of the Schultz molecular topological index," *Journal of Chemical Information and Computer Sciences*, vol. 34, no. 5, pp. 1087–1089, 1994.
- [36] M. Eliasi and B. Taeri, "Four new sums of graphs and their Wiener indices," *Discrete Applied Mathematics*, vol. 157, no. 4, pp. 794–803, 2009.

## Research Article

# Dominating Topological Analysis and Comparison of the Cellular Neural Network

**Farukh Ejaz** <sup>1</sup>, **Muhammad Hussain** <sup>1</sup>, **Hamad Almohamedh** <sup>2</sup>,  
**Khalid M. Alhamed** <sup>3</sup>, **Rana Alabdan** <sup>4</sup>, and **Sultan Almotairi** <sup>5</sup>

<sup>1</sup>Department of Mathematics, COMSATS University Islamabad (CUI), Lahore, Pakistan

<sup>2</sup>Faculty of King Abdulaziz City for Science and Technology (KACST), Riyadh, Saudi Arabia

<sup>3</sup>IT Programs Center, Faculty of IT Department, Institute of Public Administration, Riyadh 11141, Saudi Arabia

<sup>4</sup>Department of Information Systems, Faculty of Computer and Information Sciences College, Majmaah University, Majmaah 11952, Saudi Arabia

<sup>5</sup>Department of Natural and Applied Sciences, Faculty of Community College, Majmaah University, Majmaah 11952, Saudi Arabia

Correspondence should be addressed to Hamad Almohamedh; [halmohamedh@kacst.edu.sa](mailto:halmohamedh@kacst.edu.sa) and Sultan Almotairi; [almotairi@mu.edu.sa](mailto:almotairi@mu.edu.sa)

Received 28 December 2020; Revised 20 January 2021; Accepted 29 March 2021; Published 17 April 2021

Academic Editor: Ali Ahmad

Copyright © 2021 Farukh Ejaz et al. This is an open access article distributed under the Creative Commons Attribution License, which permits unrestricted use, distribution, and reproduction in any medium, provided the original work is properly cited.

Graph theory is a discrete branch of mathematics for designing and predicting a network. Some topological invariants are mathematical tools for the analysis of connection properties of a particular network. The Cellular Neural Network (CNN) is a computer paradigm in the field of machine learning and computer science. In this article we have given a close expression to dominating invariants computed by the dominating degree for a cellular neural network. Moreover, we have also presented a 3D comparison between dominating invariants and classical degree-based indices to show that, in some cases, dominating invariants give a better correlation on the cellular neural network as compared to classical indices.

## 1. Introduction

In advance technology, computer science networking, electrical networks, and some biological networks have the maximum ability to send and transfer useful data and information in a very small amount of time with accuracy. With a rapid growth of networking science, many advanced and connected complex interconnection networks have been developed. Social networking, World Wide Web (WWW), ecological networking, genetic interconnection networks, and metabolic networks are such examples of complex advanced networks. In information technology, these fantastic and high-limit frameworks have become a need of time.

World Wide Web (WWW) is a framework between PC systems and the internal network that employs convection suites and known as Internet Protocol (IP). It is a planned to assimilate business, government, and social structure of

neighbourhood extension. They are correlated and connected by electronic and optical systems of remote organization. The Internet passes a large amount of information among different people through social media, newspaper, electronic mail, and many applications such as skype and Google meet [1, 2].

Graph theory has a large number of applications in many areas of science such as engineering, computer science, computer networking, software engineering, and electrical and hardware engineering. An interconnection framework or network with a finite number of nodes (computer systems) and the links (connections) between them can be presented as a finite simple connected graph with a finite number of vertices and edges. Inspired by the topological descriptor's ability to modify a chemical structure, many researchers have decided to apply it to the networking sciences [3].

Theoretical approaches of graph theory to the field of cheminformatics for describing topological properties of the oxide and silicate network are given in [4–7]. A naturally existing network of germanium phosphide and its topologies is discussed in [8]. A hexagon star network is comparatively described via valency-based topological descriptors in [9]. Ahmad et al. derived some degree-based polynomials for swapped networks in [10]. An embedded form of benzene ring in a p-type surface is topologically explained in [11].

## 2. Cellular Neural Network

A Cellular Neural Network or Cellular Nonlinear Network (CNN) is a computing paradigm in computer science and machine learning. It is very important in communication between neighbouring units. Solving Partial Differential Equations (PDEs), image processing, analyzing 3D surfaces, and reducing problems in geodesic maps and sensory-motor organs are some applications of the CNN. CNN processors are the systems of finite fixed topology, locally connected fixed location, and multiple inputs with a single output of nonlinear processing units. In the CNN processor, each cell (processor) has one output due to which it is communicated by other cells. The CNN processor was introduced by Leon Chua and Lin Yang in 1988. In the original Chua Yang CNN processor (CY-CNN), cells are weighted sum of different inputs whereas the output was a piecewise linear function [12].

Topologically, cells can be arranged on an infinite plane of a toroidal space. Some architecture topologies of the CNN are the Multiple-Neighbourhood-Size CNN (MNS-CNN), Multilayer CNN (ML-CNN), and single-Layer CNN (SL-CNN). Mathematically, the relationship between cells and its neighbours in the area of influence can be modeled by Dominating Invariants (DIs). A CNN network can be presented as an array of  $p \times q$  matrix in which each cell  $a_{ij}$  has feed-forward synapses  $e_{uv} f_{uv}$  which is the input and has feed-back synapses  $g_{uv} h_{uv}$  which is the output of the neighbourhood cell. Mathematically,

$$a_{ij} = -a_{ij} + \sum_{uv \in S_{ij}(\tau)} e_{uv} f_{uv} + \sum_{uv \in S_{ij}(\tau)} g_{uv} h_{uv} + z_{ij}, \quad (1)$$

where  $w_{ij}$ : = input,  $z_{ij}$ : = threshold,  $a_{ij}$ : = cellstate,  $y_{ij}$ : = output,  $i = 1, 2, \dots, p$ ,  $j = 1, 2, \dots, q$ ,  $1 \leq u \leq p$ ,  $1 \leq v \leq q$ , and  $S_{ij}$  is the sphere of influence to neighbourhood cells.

$$S_{ij} = \{a_{ij} : \max(|u - i|, |v - j|) \leq \tau, \quad 1 \leq u \leq p, 1 \leq v \leq q\}, \quad (2)$$

In the following, we are presenting a  $3 \times 3$  CNN in which a cell  $a_{ij}$  is locally coupled to  $a_{uv}$ , where

$$(u, v) = (i + 1, j + 1), (i + 1, j), (i + 1, j - 1), (i, j + 1), (i, j - 1), (i - 1, j + 1), (i - 1, j), (i - 1, j - 1). \quad (3)$$

Here, each of these is the first-degree neighbour of  $a_{ij}$  [13, 14]. A depiction of the cellular neural network is shown in Figure 1, and its presentation as a simple connected graph on  $6 \times 6$  cells is given in Figure 2.

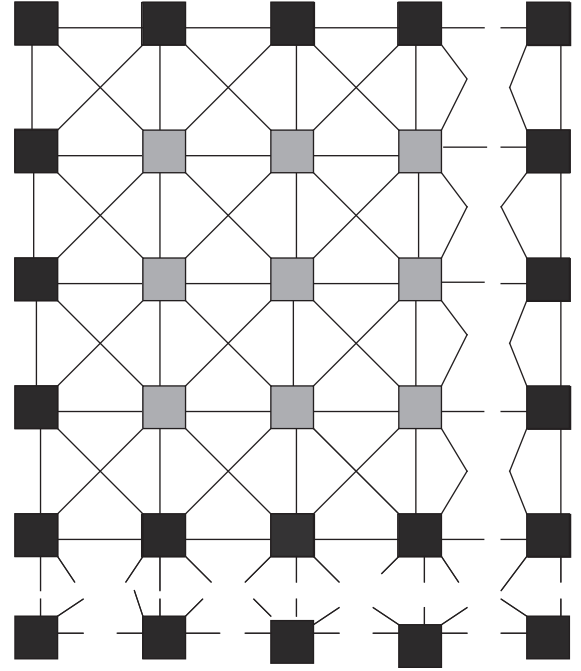


FIGURE 1: A depiction of the cellular neural network.

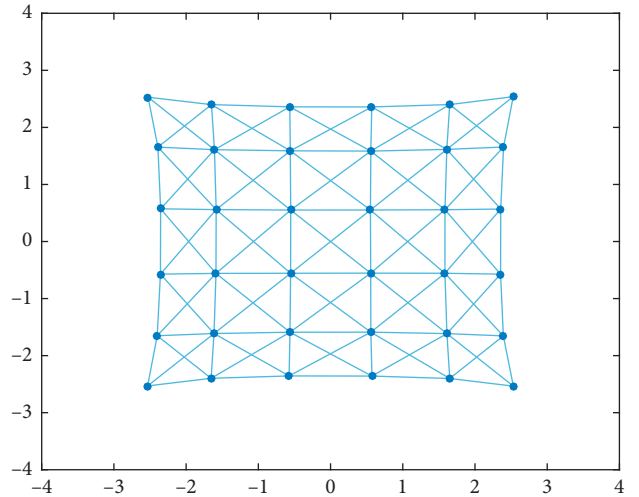


FIGURE 2: Cellular neural network CNN (6, 6).

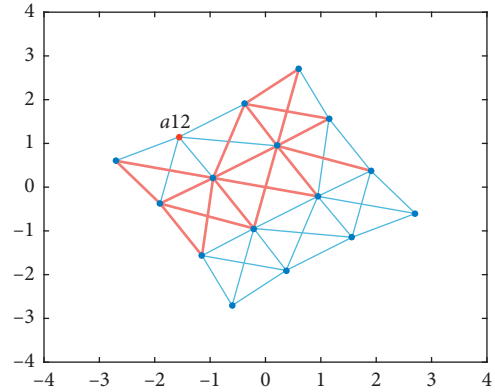
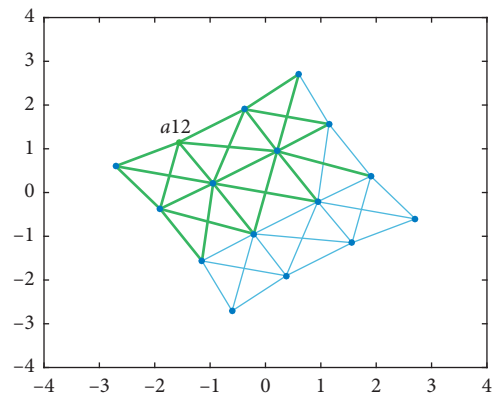
## 3. Dominating Degree and the Cellular Neural Network

A CNN can easily be depicted as a simple connected graph with a finite number of cells and links between them with no multiple edges. In a graph, the number of connections to a cell is called its degree. In context of graphs, all the vertices connected to its adjacent edges are called neighbourhood vertices. Excluding a vertex and considering its neighbourhood vertices gives open neighbourhood of the vertex while on including the vertex and counting all the edges adjacent to all vertices in neighbourhood gives us a closed neighbourhood of the vertex. Graphically, a vertex dominates all the edges in its close neighbourhood. So, here, we

define the count of all such edges dominated by a vertex in its closed neighbourhood as the dominating degree ( $\zeta_p$ ) of the vertex ( $p$ ). In other words, the total number of different edges in the close neighbourhood of a vertex is its dominating degree. In the previous section, for the CNN,  $S_{ij}$  represents the open neighbourhood and all  $(u, v) = (i + 1, j + 1), (i + 1, j), (i + 1, j - 1), (i, j + 1), (i, j - 1)$  are its neighbouring cells for a cell  $a_{ij}$ . In the following, we show a  $4 \times 4$  CNN highlighting particularly  $a_{12}$  with its open neighbourhood with all red-colored edges in Figure 3 and closed neighbourhood with all green edges in Figure 4.

On counting the number of connections in the closed neighbourhood of  $a_{12}$ , we will state it as a dominating degree. Similarly, working on the same way on finding the dominating degree of each cell and generalizing the cellular neural network as a simple connected graph, we concluded that it has total  $pq$  cells and total  $4pq - 3p - 3q + 2$  connections in a CNN( $p \times q$ ) graph. On calculating the dominating degree for each cell in a  $p \times q$  network with  $p$  cells in an  $i$ -th row and  $q$  cells in  $j$ -th column, we finalize a partition of dominating degrees of any two directly connected cells. So, with  $p, q > 4$ , we concluded that there are total 14 different types of connections based on dominating degrees of two directly connected cells. Here, we will describe the number of these connections differentiated on the basis of dominating degrees of two directly connected end cells. Say two cells  $p$  and  $q$  are directly connected in a CNN( $p \times q$ ) with  $p, q > 4$ ; then, their dominating degrees will be  $\zeta_p$  and  $\zeta_q$ , respectively. We will express two directly connected cells  $p$  and  $q$  as  $p \sim q$  with dominating degrees as  $\zeta_p$  and  $\zeta_q$ . Therefore, we have

$$\begin{aligned}
 |p \sim q| &= \left| \{(\zeta_p, \zeta_q) | \zeta_p = 52, \zeta_q = 52\} \right| = 4pq - 19(p + q) + 90, \\
 |p \sim q| &= \left| \{(\zeta_p, \zeta_q) | \zeta_p = 52, \zeta_q = 43\} \right| = 6(p + q) - 56, \\
 |p \sim q| &= \left| \{(\zeta_p, \zeta_q) | \zeta_p = 43, \zeta_q = 43\} \right| = 2p + 2q - 16, \\
 |p \sim q| &= \left| \{(\zeta_p, \zeta_q) | \zeta_p = 52, \zeta_q = 35\} \right| = 4, \\
 |p \sim q| &= \left| \{(\zeta_p, \zeta_q) | \zeta_p = 43, \zeta_q = 35\} \right| = 8, \\
 |p \sim q| &= \left| \{(\zeta_p, \zeta_q) | \zeta_p = 43, \zeta_q = 28\} \right| = 6p + 6q - 56, \\
 |p \sim q| &= \left| \{(\zeta_p, \zeta_q) | \zeta_p = 35, \zeta_q = 28\} \right| = 8, \\
 |p \sim q| &= \left| \{(\zeta_p, \zeta_q) | \zeta_p = 28, \zeta_q = 28\} \right| = 2p + 2q - 2, \\
 |p \sim q| &= \left| \{(\zeta_p, \zeta_q) | \zeta_p = 43, \zeta_q = 23\} \right| = 8, \\
 |p \sim q| &= \left| \{(\zeta_p, \zeta_q) | \zeta_p = 35, \zeta_q = 23\} \right| = 8, \\
 |p \sim q| &= \left| \{(\zeta_p, \zeta_q) | \zeta_p = 28, \zeta_q = 23\} \right| = 8, \\
 |p \sim q| &= \left| \{(\zeta_p, \zeta_q) | \zeta_p = 23, \zeta_q = 23\} \right| = 4, \\
 |p \sim q| &= \left| \{(\zeta_p, \zeta_q) | \zeta_p = 35, \zeta_q = 15\} \right| = 4, \\
 |p \sim q| &= \left| \{(\zeta_p, \zeta_q) | \zeta_p = 23, \zeta_q = 15\} \right| = 8.
 \end{aligned}
 \tag{4}$$


 FIGURE 3: Open neighbourhood of  $a_{12}$ .

 FIGURE 4: Closed neighbourhood of  $a_{12}$ .

## 4. Dominating Invariants

Reti et al. referred neighbourhood-based topological invariants for first Zagreb and second Zagreb naming as neighbourhood first Zagreb index  $NM_1$  and neighbourhood second Zagreb index  $NM_2$ , respectively [15]. On the same lines, on relying definition of the dominating degree of a vertex, we have defined some Dominating Topological Invariants (DTIs). These invariants are computed on the basis of the dominating degree of the node associated to a network.

**4.1. Dominating Randić Invariant.** Taking any real number  $\alpha$ , dominating Randić invariant is computed as follows:

$$R_\alpha^d = \sum_{p \sim q} (\zeta_p \cdot \zeta_q)^\alpha. \tag{5}$$

**4.2. Dominating Geometric Invariant.** In a simple connected network, the dominating geometric invariant is computed as follows [16]:

$$G^d = \sum_{p \sim q} \frac{2\sqrt{\zeta_p \cdot \zeta_q}}{\zeta_p + \zeta_q}. \tag{6}$$



4.3. *Dominating Atomic Bond Connectivity Invariant.* In a simple connected network, the dominating atomic bond connectivity invariant is computed as follows [17]:

$$ABC^d = \sum_{p \sim q} \sqrt{\frac{\zeta_p + \zeta_q - 2}{\zeta_p \cdot \zeta_q}}. \quad (7)$$

## 5. Main Results

This section includes our main results for the CNN ( $p \times q$ ) network on dominating invariants. In [18], Imran et al. explained some topological properties for Cellular Neural

Networks based on classical degree-based invariants. They have derived some close results on Randić index, geometric index, and atomic bond connectivity index for the CNN. In this article, we have discussed some dominating invariants computed on dominating degrees in the cellular neural network and a 3D comparison between classical degree indices and dominating invariants.

5.1. *Theorem.* Consider Cellular Neural Network CNN ( $p \times q$ ) with  $p, q \geq 5$  as a simple connected graph, then its dominating Randić invariant for real values of  $\alpha = 1, -1, (1/2), (-1/2)$  is closely expressed as

$$\begin{aligned} R_1^d &= 10816pq - 25470(p + q) + 59096, \\ R_{-1}^d &= \frac{676}{pq} + \frac{1046775}{244985104} + \frac{19535052347}{1619964000200}, \\ R_{(1/2)}^d(\text{CNN}(p \times q)) &= 208pq + (-846 + 12\sqrt{301} + 12\sqrt{559})(p + q) + (3524 \\ &\quad + 112\sqrt{5} + 20\sqrt{21} + 16\sqrt{161} - 112\sqrt{301} + 8\sqrt{345} + 8\sqrt{455} \\ &\quad - 112\sqrt{559} + 8\sqrt{805} + 8\sqrt{989} + 8\sqrt{1505}), \quad (8) \\ R_{(-1/2)}^d(\text{CNN}(p \times q)) &= \frac{pq}{13} + \left( \frac{3}{\sqrt{301}} + \frac{3}{\sqrt{559}} - \frac{3873}{15652} \right) (p + q) + \frac{147293}{179998} - \frac{4\sqrt{301}}{43} \\ &\quad + \frac{4}{7\sqrt{5}} + \frac{4}{5\sqrt{21}} + \frac{4}{\sqrt{161}} + \frac{8}{\sqrt{345}} + \frac{2}{\sqrt{455}} - \frac{28}{\sqrt{559}} + \frac{8}{\sqrt{805}} + \frac{8}{\sqrt{989}} \\ &\quad + \frac{8}{\sqrt{1505}}. \end{aligned}$$

*Proof.* By using the dominating degrees of directly connected cells  $p \sim q$  and the computing definition of dominating Randić invariant for  $\alpha = 1$ , we have

$$\begin{aligned} R_1^d &= (52 \times 52)(4 \times p \times q - 19(p + q) + 90) + (52 \times 43)(6(p + q) - 56) \\ &\quad + (43 \times 43)(2(p + q) - 8) + 4 \times (52 \times 35) + 8 \times (43 \times 35) \\ &\quad + (43 \times 28)(6(p + q) - 56) + 8 \times (35 \times 28) + (28 \times 28)(2(p + q \\ &\quad - 10)) + 8 \times (23 \times 43) + 8 \times (23 \times 35) + 8 \times (23 \times 28) + 4 \\ &\quad \times (23 \times 23) + 4 \times (35 \times 15) + 8 \times (23 \times 15). \quad (9) \end{aligned}$$

On computing, we have

$$\begin{aligned}
 R_1^d &= 10816pq - 25470(p + q) + 59096, \\
 R_{-1}^d &= \left(\frac{1}{52 \times 52}\right)(4 \times p \times q - 19(p + q) + 90) + \left(\frac{1}{52 \times 43}\right)(6(p + q) - 56) \\
 &\quad + \left(\frac{1}{43 \times 43}\right)(2(p + q - 8)) + 4 \times \left(\frac{1}{52 \times 35}\right) + 8 \times \left(\frac{1}{43 \times 35}\right) + \left(\frac{1}{43 \times 28}\right)(6(p + q) - 56) \\
 &\quad + 8 \times \left(\frac{1}{35 \times 28}\right) + \left(\frac{1}{28 \times 28}\right)(2(p + q - 10)) + 8 \times \left(\frac{1}{23 \times 43}\right) + 8 \times \left(\frac{1}{23 \times 35}\right) \\
 &\quad + 8 \times \left(\frac{1}{23 \times 28}\right) + 4 \times \left(\frac{1}{23 \times 23}\right) + 4 \times \left(\frac{1}{35 \times 15}\right) + 8 \times \left(\frac{1}{23 \times 15}\right).
 \end{aligned} \tag{10}$$

On computing, we have

$$\begin{aligned}
 R_{-1}^d &= \frac{676}{pq} + \frac{1046775}{244985104} + \frac{19535052347}{1619964000200}, \\
 R_{(1/2)}^d &= (\sqrt{52 \times 52})(4 \times pq - 19(p + q) + 90) + (\sqrt{52 \times 43})(6(p + q) - 56) \\
 &\quad + (\sqrt{43 \times 43})(2(p + q - 8)) + 4(\sqrt{52 \times 35}) + 8 \times (\sqrt{43 \times 35}) \\
 &\quad + (\sqrt{43 \times 28})(6(p + q) - 56) + 8 \times (\sqrt{35 \times 28}) \\
 &\quad + (\sqrt{28 \times 28})(2(p + q - 10)) + 8 \times (\sqrt{23 \times 43}) + 8 \times (\sqrt{23 \times 35}) \\
 &\quad + 8 \times (\sqrt{23 \times 28}) + 4 \times (\sqrt{23 \times 23}) + 4 \times (\sqrt{35 \times 15}) + 8 \\
 &\quad \times (\sqrt{23 \times 15}).
 \end{aligned} \tag{11}$$

On computing, we have

$$\begin{aligned}
 R_{(1/2)}^d (\text{CNN}(p \times q)) &= 208pq + (-846 + 12\sqrt{301} + 12\sqrt{559})(p + q) + (3524 \\
 &\quad + 112\sqrt{5} + 20\sqrt{21} + 16\sqrt{161} - 112\sqrt{301} + 8\sqrt{345} + 8\sqrt{455} \\
 &\quad - 112\sqrt{559} + 8\sqrt{805} + 8\sqrt{989} + 8\sqrt{1505}), \\
 R_{(-1/2)}^d &= \left(\frac{1}{\sqrt{52 \times 52}}\right)(4 \times p \times q - 19(p + q) + 90) + \left(\frac{1}{\sqrt{52 \times 43}}\right)(6(p + q) - 56) + \left(\frac{1}{\sqrt{43 \times 43}}\right) \\
 &\quad (2(p + q - 8)) + 4 \left(\frac{1}{\sqrt{52 \times 35}}\right) + 8 \left(\frac{1}{\sqrt{43 \times 35}}\right) + \left(\frac{1}{\sqrt{43 \times 28}}\right)(6(p + q) - 56) + 8 \left(\frac{1}{\sqrt{35 \times 28}}\right) \\
 &\quad + \left(\frac{1}{\sqrt{28 \times 28}}\right)(2(p + q - 10)) + 8 \left(\frac{1}{\sqrt{23 \times 43}}\right) + 8 \left(\frac{1}{\sqrt{23 \times 35}}\right) + 8 \left(\frac{1}{\sqrt{23 \times 28}}\right) + 4 \left(\frac{1}{\sqrt{23 \times 23}}\right) \\
 &\quad + 4 \left(\frac{1}{\sqrt{35 \times 15}}\right) + 8 \left(\frac{1}{\sqrt{23 \times 15}}\right).
 \end{aligned} \tag{12}$$

On computing, we have

$$R_{(-1/2)}^d(\text{CNN}(p \times q)) = \frac{pq}{13} + \left( \frac{3}{\sqrt{301}} + \frac{3}{\sqrt{559}} - \frac{3873}{15652} \right) (p+q) + \frac{147293}{179998} - \frac{4\sqrt{301}}{43} \\ + \frac{4}{7\sqrt{5}} + \frac{4}{5\sqrt{21}} + \frac{4}{\sqrt{161}} + \frac{8}{\sqrt{345}} + \frac{2}{\sqrt{455}} - \frac{28}{\sqrt{559}} + \frac{8}{\sqrt{805}} + \frac{8}{\sqrt{989}} + \frac{8}{\sqrt{1505}}. \quad (13)$$

5.2. *Corollary.* In dominating Randić invariant,  $\alpha = 1, -1$  are also known as dominating second Zagreb and dominating modified second Zagreb invariants, respectively.

5.3. *Theorem.* Consider Cellular Neural Network CNN ( $p \times q$ ) with  $p, q \geq 5$  as a simple connected graph, then its dominating geometric invariant is closely expressed as

$$GA^d(\text{CNN}(p \times q)) \\ = 4pq + \left( \frac{24\sqrt{301}}{71} + \frac{24\sqrt{559}}{95} - 15 \right) (p+q) + \frac{32\sqrt{5}}{9} + \frac{4\sqrt{21}}{5} \\ + \frac{32\sqrt{161}}{51} - \frac{224\sqrt{301}}{71} + \frac{8\sqrt{345}}{19} + \frac{16\sqrt{455}}{87} - \frac{224\sqrt{559}}{95} + \frac{8\sqrt{805}}{29} \\ + \frac{8\sqrt{989}}{33} + \frac{8\sqrt{1505}}{39} + 58. \quad (14)$$

*Proof.* By using dominating degrees of CNN ( $p \times q$ ) for two directly connected cells  $p \sim q$  and substituting the computed formula for  $GA^d$ , we get the desired result.  $\square$

5.4. *Theorem.* Consider Cellular Neural Network CNN ( $p \times q$ ) with  $p, q \geq 5$  as a simple connected graph, then its dominating atomic bond connectivity invariant is closely expressed as

$$ABC^d(\text{CNN}(p \times q)) = \frac{\sqrt{102}}{13} pq + \left( 3\sqrt{\frac{93}{559}} + 3\sqrt{\frac{69}{301}} + \frac{3\sqrt{6}}{14} + \frac{4\sqrt{21}}{43} - \frac{19\sqrt{102}}{52} \right) (p+q) \\ + \left( 16\sqrt{\frac{19}{1505}} + 16\sqrt{\frac{2}{115}} + 16\sqrt{\frac{3}{115}} - 28\sqrt{\frac{93}{559}} + 2\sqrt{\frac{17}{91}} + 4\sqrt{\frac{7}{23}} - \frac{15\sqrt{6}}{7} + \frac{16\sqrt{7}}{35} \right) \\ + \left( \frac{8\sqrt{11}}{23} - 4\sqrt{\frac{483}{43}} + \frac{4\sqrt{305}}{35} - \frac{32\sqrt{21}}{43} + \frac{45\sqrt{102}}{26} + \frac{64}{\sqrt{989}} \right). \quad (15)$$

*Proof.* By using dominating degrees of CNN ( $p \times q$ ) for two directly connected cells  $p \sim q$  and substituting the computed formula for  $ABC^d$ , we get the desired result.

In light of all the abovementioned theorems, we state the following proposition basing on the fact that the dominating degree in a graph is closely related to closed neighbourhood of a vertex.  $\square$

5.5. *Proposition.* Let  $G$  be a simply connected graph with finite order and size; if  $G$  is free from  $C_3$  as its subgraph, then any network or structure isomorphic to  $G$  will give equal

topological results regarding neighbourhood indices and dominating invariants.

## 6. Graphical Comparison

In this section, we will provide a 3D graphical comparison between dominating invariants and classical degree-based indices.

Graphical comparison shows that, for  $\alpha = 1, (1/2)$  (Figures 5 and 6), dominating Randić invariant is faster than classical degree-based Randić index and has better

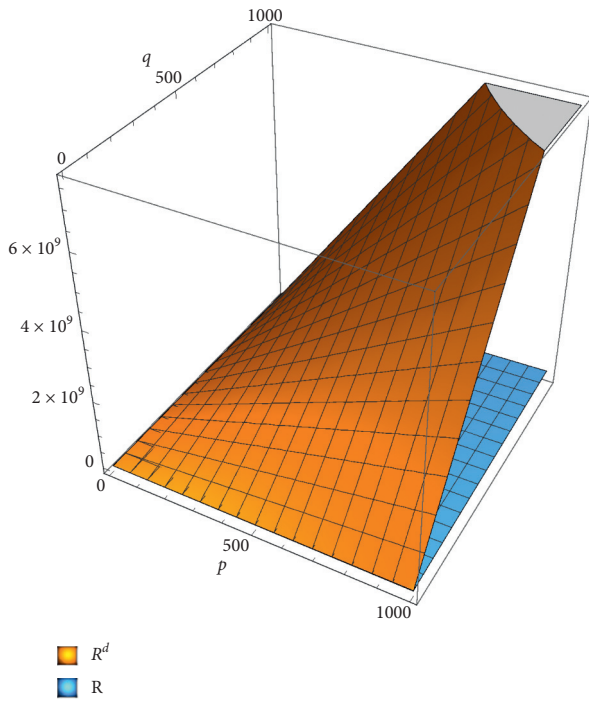


FIGURE 5: Comparison between dominating Randić invariant and classical Randić index for  $\alpha = 1$ .

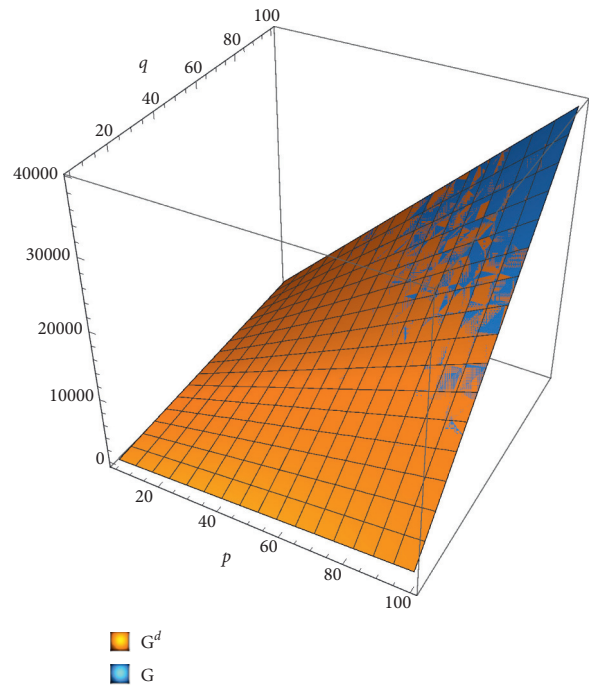


FIGURE 7: Comparison between the dominating geometric invariant and classical geometric index.

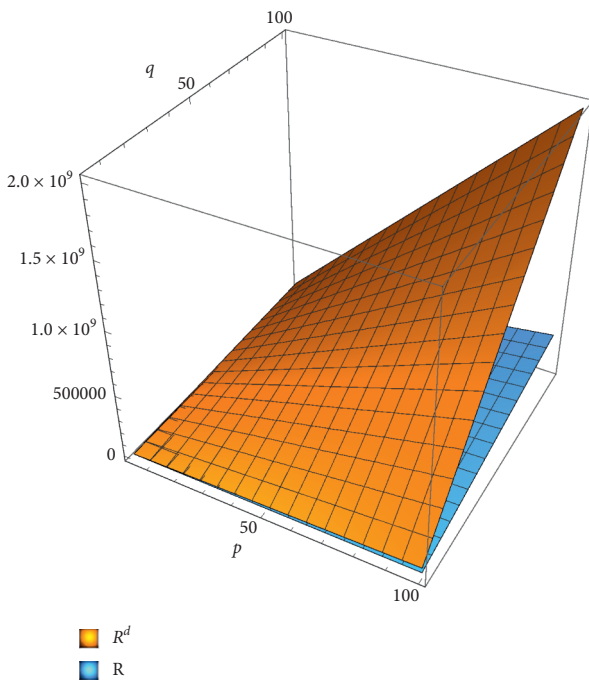


FIGURE 6: Comparison between dominating Randić invariant and classical Randić index for  $\alpha = (1/2)$ .

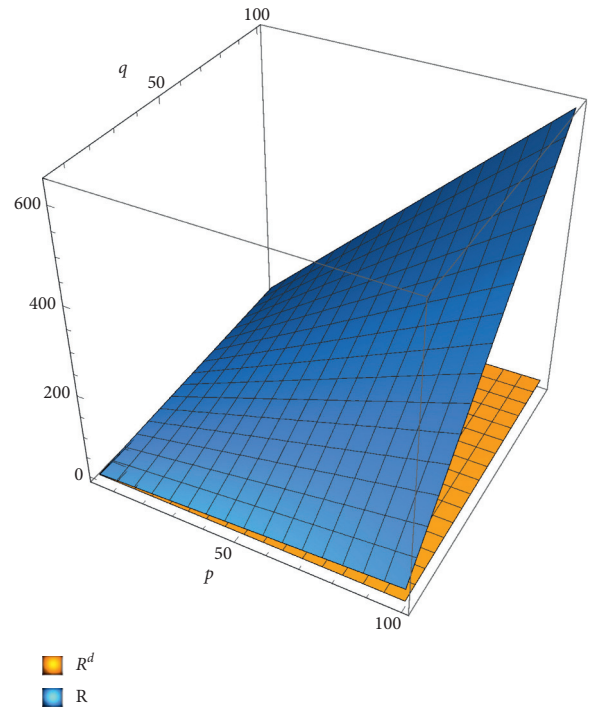


FIGURE 8: Comparison between dominating Randić invariant and classical Randić index for  $\alpha = -1$ .

topological properties over the cellular neural networks as dominating invariants are computed on the dominating degree of a cell over its neighbouring cells. Similarly, the dominating geometric invariant is faster

than the classical degree-based geometric index as shown in Figure 7. In Figures 8–10, Randić invariant for  $\alpha = -1, (-1/2)$  and the atomic bond connectivity invariant are compared, respectively.

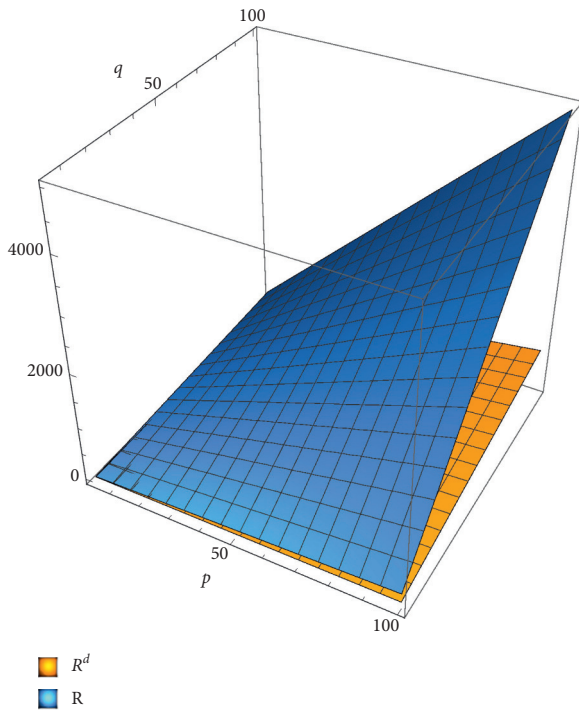


FIGURE 9: Comparison between dominating Randi's invariant and classical Randi's index for  $\alpha = (-1/2)$ .

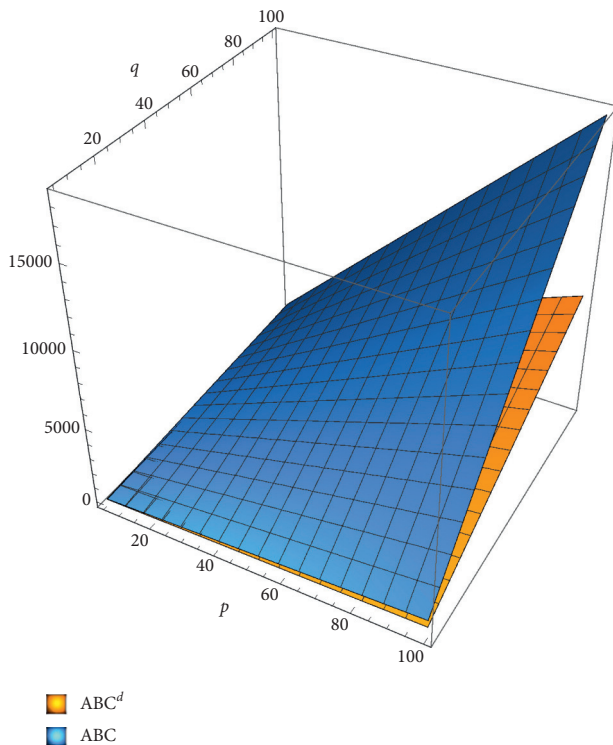


FIGURE 10: Comparison between the dominating ABC invariant and classical ABC index.

## 7. Conclusions

According to the mathematical analysis and comparison carried out by graphical analysis, we concluded that the

dominating-degree-based invariants have better predicting ability. Our results show that dominating-degree-based invariants show faster and more predicting ability for the cellular neural network. This may lead to help far better analysis to predict topological properties of the cellular neural network in the future.

## Data Availability

No data were used to support the study.

## Conflicts of Interest

The authors declare that they have no conflicts of interest.

## Acknowledgments

The authors extend their appreciation to the Deanship of Scientific Research at Majmaah University for funding this work under project number no. R-2021-120.

## References

- [1] L. O. Chua and L. Yang, "Cellular neural networks: applications," *IEEE Transactions on Circuits and Systems*, vol. 35, no. 10, pp. 1273–1290, 1988.
- [2] L. O. Chua and L. Yang, "Cellular neural networks: theory," *IEEE Transactions on Circuits and Systems*, vol. 35, no. 10, pp. 1257–1272, 1988.
- [3] H. Dekker and B. D. Colbert, "Network robustness and graph topology," *Proceedings of the 27th Australasian Conference on Computer Science*, vol. 26, pp. 359–368, 2004.
- [4] H. Ali, H. M. A. Siddiqui, and M. K. Shafiq, "On degree-based topological descriptors of oxide and silicate molecular structures," *MAGNT Research Report's*, vol. 4, no. 4, pp. 135–142, 2016.
- [5] M. Paul and I. Rajasingh, "Topological properties of silicate networks," in *Proceedings of the 2009 5th IEEE GCC Conference and Exhibition*, pp. 1–5, Kuwait City, Kuwait, March 2009.
- [6] B. Rajan, A. William, C. Grigorious, and S. Stephen, "On certain topological indices of silicate, honeycomb and hexagonal networks," *Journal of Computer and Mathematical Sciences*, vol. 3, no. 5, pp. 498–556, 2012.
- [7] F. Simonraj and A. George, "Topological properties of few poly oxide, poly silicate, DOX and DSL networks," *International Journal of Future Computer and Communication*, vol. 2, no. 2, p. 90, 2013.
- [8] F. Ejaz, M. Hussain, and R. Hasni, "On topological aspects of bilayer Germanium Phosphide," *Journal of Mathematics and Computer Science*, vol. 22, no. 4, pp. 347–362, 2021.
- [9] A. N. A. Koam, A. Ahmad, and M. F. Nadeem, "Comparative study of valency-based topological descriptor for hexagon star network," *Computer Systems Science and Engineering*, vol. 36, no. 2, pp. 293–306, 2021.
- [10] A. Ahmad, R. Hasni, K. Elahi, and M. A. Asim, "Polynomials of degree-based indices for swapped networks modeled by optical transpose interconnection system," *IEEE Access*, vol. 8, pp. 214293–214299, 2020.
- [11] A. Ahmad, "On the degree based topological indices of benzene ring embedded in  $P$ -type-surface in 2D network," *Hacettepe Journal of Mathematics and Statistics*, vol. 47, no. 1, 2018.

- [12] F. Corinto and M. Gilli, "Comparison between the dynamic behaviour of Chua-Yang and full-range cellular neural networks," *International Journal of Circuit Theory and Applications*, vol. 31, no. 5, pp. 423–441, 2003.
- [13] T. Roska and L. O. Chua, "The CNN universal machine: an analogic array computer," *IEEE Transactions on Circuits and Systems II: Analog and Digital Signal Processing*, vol. 40, no. 3, pp. 163–173, 1993.
- [14] Q. A. A. Ruhimat and G. W. Fajariyanto, "Firmansyah and slam, "Optimal computer network based on graph topology model," in *Journal of Physics: Conference Series*, vol. 1211, no. 1, Article ID 012007, 2019.
- [15] T. Réti, A. Ali, P. Varga, and E. Bitay, "Some properties of the neighborhood first Zagreb index," *Discrete Mathematics Letters*, vol. 2, pp. 10–17, 2019.
- [16] D. Vukičević and B. Furtula, "Topological index based on the ratios of geometrical and arithmetical means of end-vertex degrees of edges," *Journal of Mathematical Chemistry*, vol. 46, no. 4, pp. 1369–1376, 2009.
- [17] B. Zhou and N. Trinajstić, "On a novel connectivity index," *Journal of Mathematical Chemistry*, vol. 46, no. 4, pp. 1252–1270, 2009.
- [18] M. Imran, M. K. Siddiqui, A. Q. Baig, W. Khalid, and H. Shaker, "Topological properties of cellular neural networks," *Journal of Intelligent & Fuzzy Systems*, vol. 37, no. 3, pp. 3605–3614, 2019.

## Research Article

# On Cyclic-Vertex Connectivity of $(n, k)$ -Star Graphs

Yalan Li <sup>1</sup>, Shumin Zhang <sup>2</sup>, and Chengfu Ye<sup>2</sup>

<sup>1</sup>School of Computer, Qinghai Normal University, Xining 810001, China

<sup>2</sup>School of Mathematics and Statistics, Qinghai Normal University, Xining 810001, China

Correspondence should be addressed to Shumin Zhang; zhangshumin@qhnu.edu.cn

Received 28 January 2021; Revised 31 March 2021; Accepted 3 April 2021; Published 13 April 2021

Academic Editor: Roslan Hasni

Copyright © 2021 Yalan Li et al. This is an open access article distributed under the Creative Commons Attribution License, which permits unrestricted use, distribution, and reproduction in any medium, provided the original work is properly cited.

A vertex subset  $F \subseteq V(G)$  is a cyclic vertex-cut of a connected graph  $G$  if  $G - F$  is disconnected and at least two of its components contain cycles. The cyclic vertex-connectivity  $\kappa_c(G)$  is denoted as the cardinality of a minimum cyclic vertex-cut. In this paper, we show that the cyclic vertex-connectivity of the  $(n, k)$ -star network  $S_{n,k}$  is  $\kappa_c(S_{n,k}) = n + 2k - 5$  for any integer  $n \geq 4$  and  $k \geq 2$ .

## 1. Introduction

Let  $G = (V, E)$  be a simple connected graph, where  $V$  and  $E$  are the vertex set and the edge set, respectively.  $G[H]$  is an induced subgraph by  $H \subseteq V$ , whose vertex set is  $H$  and whose edge set consists of all the edges of  $G$  with both ends in  $H$ . For any vertex  $v$ , define the neighborhood  $N_G(v) = \{u \in V \mid (u, v) \in E\}$ . Let  $S \subseteq V(G)$  and the set  $\cup_{v \in S} N_G(v) \setminus S$  is denoted by  $N_G(S)$ . We use  $N(v)$  to replace  $N_G(v)$ ,  $N(S)$  to replace  $N_G(S)$ , and  $N[S]$  to replace  $N_G[S]$ . A graph  $G$  is said to be  $k$ -regular if  $d(v) = k$  for any vertex  $v \in V$ . For any subset  $F \subseteq V(G)$ ,  $G \setminus F$  or  $G - F$  denotes the graph obtained by removing all vertices in  $F$  from  $G$ . If there exists a nonempty subset  $F \subseteq G$  such that  $G \setminus F$  is disconnected, then  $F$  is called a vertex-cut of  $G$ . The connectivity  $\kappa(G)$  is the minimum number of vertices whose removal results in a disconnected graph or only one vertex left. Let  $\delta(G)$  and  $g(G)$  denote the minimum degree and the girth of  $G$ , respectively. As usual, we use  $K_n$  and  $C_n$  to denote the complete graph and the cycle of order  $n$ , respectively.

In this work, we study a kind of restricted vertex-connectivity known as the cyclic vertex-connectivity. A vertex subset  $F \subseteq V$  is a cyclic vertex-cut of  $G$  if  $G - F$  has at least two components containing cycles. Not all connected graphs have a cyclic vertex-cut. The cyclic vertex-connectivity  $\kappa_c(G)$  of a graph  $G$  is the cardinality of the minimum cyclic vertex-cut of  $G$ . When  $G$  has no cyclic vertex-cut, the definition of  $\kappa_c(G)$  can be found in [1] using Betti number. A graph  $G$  is

said to be  $\kappa_c$ -connected if  $G$  has a cyclic vertex-cut. Similarly, changing “edge” to “vertex,” the cyclic edge-connectivity  $\lambda_c(G)$  of graph  $G$  can be defined.

The definition of the cyclic vertex- (edge-) connectivity dates to Tait in attacking four color conjecture [2] and the graph colouring [2, 3]. It is used in many classic fields, such as integer flow conjectures [4] and  $n$ -extendable graphs [5, 6]. In many works, the cyclic vertex-connectivity has been studied. Cheng et al. [7] studied the cyclic vertex-connectivity of Cayley graphs generated by transposition trees. Yu et al. [8] obtained the cyclic vertex-connectivity of star graphs. For more research studies on the cyclic vertex-connectivity, see [7, 9–11] for references.

This paper focuses on the cyclic vertex-connectivity of the  $(n, k)$ -star network  $S_{n,k}$ . We will show that  $\kappa_c(S_{n,k}) = n + 2k - 5$  for any integer  $n \geq 4, k \geq 2$  and find out the minimum circle vertex-cut structure of the  $(n, k)$ -star network  $S_{n,k}$ .

## 2. Some Preliminaries

We provide the definition of the  $(n, k)$ -star graph  $S_{n,k}$  and its structural properties, which are useful for the following discussion.

For convenience, let  $\langle n \rangle = \{1, 2, \dots, n\}$  and  $V(n, k) = \{q_1 q_2 \dots q_k : q_i \in \langle n \rangle, q_i \neq q_j, 1 \leq i \neq j \leq k\}$  for any integers  $n$  and  $k$  with  $1 \leq k \leq n$ . Clearly,  $|V(n, k)| = n! / (n, k)!$ .

**Definition 1** (see [12]). The  $(n, k)$ -star graph, denoted by  $S_{n,k}$  (see Figure 1), is a graph with the vertex-set  $V(n, k)$  and the edge set defined as follows:

- (1) A vertex  $q_1q_2 \cdots q_i \cdots q_k$  is adjacent to the vertex  $q_iq_2 \cdots q_1 \cdots q_k$  through an edge of dimension  $i$ , where  $2 \leq i \leq k$  (i.e., exchange  $q_1$  with  $q_i$ )
- (2) A vertex  $q_1q_2 \cdots q_i \cdots q_k$  is adjacent to the vertex  $yq_2 \cdots q_i \cdots q_k$  through an edge of dimension 1, where  $y \in \langle n \rangle \setminus \{q_1, q_2, \dots, q_k\}$  (i.e., replace  $q_1$  by  $y$ )

The edges of type (1) are referred to as  $i$ -edges, and the corresponding neighboring vertices are called  $i$ -neighbors. The edges of type (2) are referred to as 1-edges, and the corresponding neighboring vertices are called 1-neighbors. Let  $S_{n,k}^i$  be induced by all the vertices having the symbol  $i$  in one of the rightmost  $k - 1$  positions of  $S_{n,k}$ . Clearly,  $S_{n,k}$  can

be decomposed into  $n$  subgraphs  $S_{n,k}^i$  and  $S_{n,k}^i \cong S_{n-1,k-1}$ , where  $1 \leq i \leq n$  and  $2 \leq k \leq n$ .

**Lemma 1** (see [13]). The  $(n, k)$ -star graph  $S_{n,k}$  has the following properties:

- (1)  $S_{n,k}$  is a graph of degree  $n - 1$  with  $n!/(n - k)!$  vertices and  $(n - 1)n!/2(n - k)!$  edges.
- (2)  $S_{n,1} \cong K_n$ ,  $S_{n,n-1} \cong S_n$ , and  $S_{n,n-2} \cong AN_n$ , where  $K_n$  is a complete graph,  $S_n$  is a  $n$ -dimensional star graph, and  $AN_n$  is a  $n$ -dimensional alternating group network.
- (3)  $E(i, j)$  is the set of all cross edges between any two subgraphs  $S_{n,k}^i$  and  $S_{n,k}^j$  ( $i \neq j \in \langle n \rangle$ ), and  $|E(i, j)| = ((n - 2)!/(n - k)!)$ .
- (4) For any two vertices  $u$  and  $v$  in  $S_{n,k}$ ,

$$|N(u) \cap N(v)| = \begin{cases} n - k - 1, & \text{if } (u, v) \in E(S_{n,k}) \text{ is 1-edge,} \\ 1, & \text{if } (u, v) \notin E(S_{n,k}) \text{ and } N(u) \cap N(v) \neq \emptyset, \\ 0, & \text{otherwise.} \end{cases} \quad (1)$$

**Lemma 2** (see [13]).  $S_{n,k}$  is a  $(n - 1)$ -regular  $(n - 1)$ -connected graph.

**Theorem 1** (see [14]). Let  $F$  be a faulty vertex set of  $S_{n,k}$  ( $n \geq 5, k \geq 3, n - k \geq 2$ ) with  $|F| \leq n + 2k - 6$ . Then, the survival graph  $S_{n,k} \setminus F$  satisfies one of the following conditions:

- (1)  $S_{n,k} \setminus F$  is connected
- (2)  $S_{n,k} \setminus F$  has two components, one of which has exactly one vertex or two vertices with one 1-edge
- (3)  $S_{n,k} \setminus F$  has three components, two of which are singletons

**Lemma 3** (see [13]). If a cycle has a length at least 6 in an  $S_{n,k}$ , then it contains one  $i$ -edge,  $2 \leq i \leq k$ .

**Theorem 2** (see [8]). For any integer  $n \geq 4$ ,  $\kappa_c(S_n) = 6(n - 3)$ .

### 3. Main Result

By Lemma 1 and Theorem 2, we know  $S_{n,n-1} \cong S_n$  if  $k = n - 1$  and  $\kappa_c(S_n) = 6(n - 3)$ . Thus, we determine the value of  $\kappa_c(S_{n,k})$  with  $n - k \geq 2$  for  $n \geq 4, k \geq 2$ .

**Lemma 4.** For  $n \geq 4$ , the girth of  $S_{n,2}$  is 3 and the edges of every 3-cycle are 1-edges.

*Proof.* Choose any vertex  $u_1$  from  $S_{n,2}$  and make it as  $u_1 = q_1q_2$ . Since  $n \geq 4$ , there exist  $q_i, q_j \in \langle n \rangle \setminus \{q_1, q_2\}$  and  $q_i \neq q_j$ . From the definition of  $S_{n,2}$ , we have two vertices  $u_2 = q_iq_2$  and  $u_3 = q_jq_2$  in  $V(S_{n,2})$  and  $\{u_1u_2, u_2u_3,$

$u_3u_1\} \in E(S_{n,2})$ . Clearly,  $u_1u_2u_3u_1$  is one 3-cycle, and all the edges of it are 1-edges. Hence, the lemma holds.  $\square$

**Lemma 5.** Let  $C$  be any cycle of length 3 in  $S_{n,2}$  ( $n \geq 4$ ). Then,  $|N_{S_{n,2}}(C)| = n - 1$ .

*Proof.* From Lemma 4, we can suppose  $C = (q_1q_2)(q_3q_2)(q_4q_2)(q_1q_2)$ . Let  $S = \{q_5q_2, q_6q_2, \dots, q_nq_2\} \subseteq V(S_{n,2})$ , then  $|S| = n - 4$ . By the definition of  $S_{n,2}$ , we have

$$\begin{aligned} N_{S_{n,2}}(q_1q_2) \setminus \{q_3q_2, q_4q_2\} &= S \cup \{q_2q_1\}, \\ N_{S_{n,2}}(q_3q_2) \setminus \{q_1q_2, q_4q_2\} &= S \cup \{q_2q_3\}, \\ N_{S_{n,2}}(q_4q_2) \setminus \{q_1q_2, q_3q_2\} &= S \cup \{q_2q_4\}. \end{aligned} \quad (2)$$

So,

$$|N_{S_{n,2}}(C)| = |S \cup \{q_2q_1, q_2q_3, q_2q_4\}| = n - 4 + 3 = n - 1. \quad (3) \quad \square$$

**Lemma 6.** Let  $C$  be a 3-cycle of  $S_{n,2}$  ( $n \geq 4$ ). Then,  $N_{S_{n,2}}(C)$  is a cyclic vertex-cut of  $S_{n,2}$ .

*Proof.* Clearly,  $S_{n,2} - N_{S_{n,2}}(C)$  is disconnected and contains  $C$  as a connected component. In order to prove the lemma, it suffices to show that the subgraph  $H = S_{n,2} - N_{S_{n,2}}[C]$  has a cycle. In fact, we can prove a stronger property  $\delta(H) \geq 2$  as follows.

Suppose  $C = (q_1q_2)(q_3q_2)(q_4q_2)(q_1q_2)$ . By Lemma 5,  $N_{S_{n,2}}(C) = S \cup \{q_2q_1, q_2q_3, q_2q_4\}$  and  $S = \{q_5q_2, q_6q_2, \dots, q_nq_2\}$ . If  $\delta(H) \leq 1$ , and then there exists a vertex



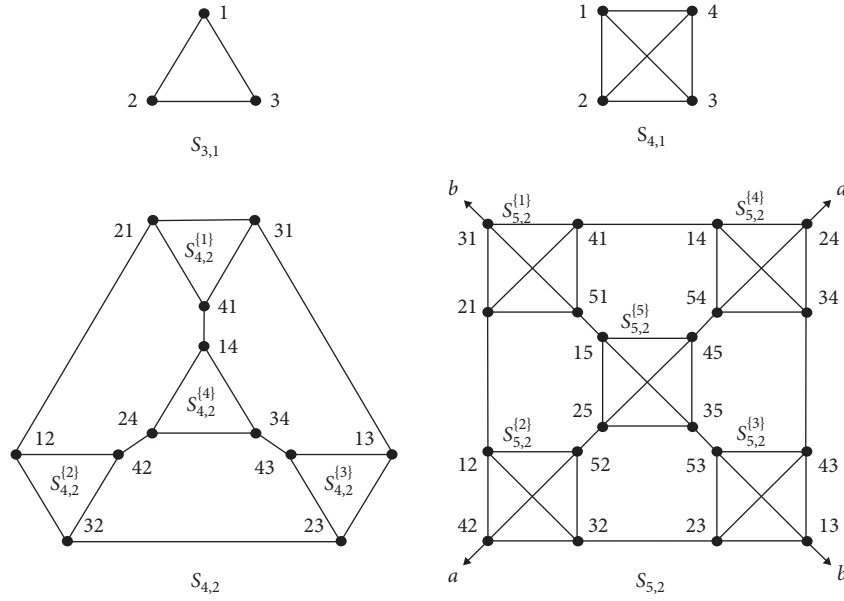


FIGURE 1: Some examples of the  $(n, k)$ -star graph  $S_{3,1}$ ,  $S_{4,1}$ ,  $S_{4,2}$ , and  $S_{5,2}$

$v \in V(H)$  satisfying  $N_H(v) = 1$  and  $v \notin S \cup \{q_2q_1, q_2q_3, q_2q_4\}$ . Since  $S_{n,2}$  is  $n - 1$ -regular,  $v \in V(H)$  has at least  $n - 2$  ( $\geq 2$ ) neighbors in  $N_{S_{n,2}}(C)$ . Let  $v_1$  and  $v_2$  be two distinct vertices in  $N_{S_{n,2}}(v) \cap N_{S_{n,2}}(C) \subseteq S \cup \{q_2q_1, q_2q_3, q_2q_4\}$ .

If  $v_1, v_2 \in S$ , without loss of generality, let  $v_1 = q_iq_2$ ,  $v_2 = q_jq_2$ , where  $q_i, q_j \in \{q_5, q_6, \dots, q_n\}$  and  $q_i \neq q_j$ . By Definition 1, all the edges in  $S_{n,2}$  are  $i$ -edges or 1-edges. Since  $vv_1, vv_2 \in E(S_{n,2})$ ,  $v = q_sq_2$ , and  $q_s \in \{q_5, q_6, \dots, q_n\} \setminus \{q_i, q_j\}$ . It means  $v \in S$ , contradicting  $v \notin S \cup \{q_2q_1, q_2q_3, q_2q_4\}$ .

If  $v_1 \in S$  and  $v_2 \in \{q_2q_1, q_2q_3, q_2q_4\}$ , without loss of generality, then let  $v_1 = q_iq_2$  and  $v_2 = q_2q_j$ , where  $q_i \in \{q_5, q_6, \dots, q_n\}$  and  $q_j \in \{q_1, q_3, q_4\}$ . Since  $vv_1, vv_2 \in E(S_{n,2})$ ,  $v = q_jq_2$ , and  $q_j \in \{q_1, q_3, q_4\}$ , it means  $v \in C$ , contradicting  $v \in H = S_{n,2} - N_{S_{n,2}}[C]$ .

If  $v_1, v_2 \in \{q_2q_1, q_2q_3, q_2q_4\}$ , clearly, if  $vv_1 \in E(S_{n,2})$ , then  $vv_2 \notin E(S_{n,2})$ . If  $vv_2 \in E(S_{n,2})$ , then  $vv_1 \notin E(S_{n,2})$ , similarly, contradicting  $vv_1, vv_2 \in E(S_{n,2})$ .

From the above discussion, we know that  $\delta(H) \geq 2$ . Furthermore,  $N_{S_{n,2}}(C)$  is a cyclic vertex-cut of  $S_{n,2}$ .

Combining Lemma 5 and 6, we have the following theorem.  $\square$

**Theorem 3.** For any integer  $n \geq 4$ ,  $\kappa_c(S_{n,2}) = n - 1$ .

*Proof.* Let  $C$  be a 3-cycle in  $S_{n,2}$  and  $F = N_{S_{n,2}}(C)$ . By Lemmas 5 and 6,  $F$  is a cyclic vertex-cut of  $S_{n,2}$ . Hence,  $\kappa_c(S_{n,2}) \leq |F| = n - 1$ . By Lemma 2,  $\kappa(S_{n,2}) = n - 1$ . We have  $\kappa_c(S_{n,2}) \geq \kappa(S_{n,2}) = n - 1$ , and then  $\kappa_c(S_{n,2}) = n - 1$ .  $\square$

**Theorem 4.** For any integer  $n \geq 5, k \geq 3, n - k \geq 2$ , and  $\kappa_c(S_{n,k}) = n + 2k - 5$ .

*Proof.* Let  $F$  be a faulty vertex set of  $S_{n,k}$  with  $|F| \leq n + 2k - 6$ . By Theorem 1,  $S_{n,k} - F$  is connected or  $S_{n,k} - F$  is disconnected, and at most one of its component contains cycles.

Hence,  $\kappa_c(S_{n,k}) \geq n + 2k - 5$ . To prove the converse, we need to find a cyclic vertex-cut  $F$  of  $S_{n,k}$  with  $|F| = n + 2k - 5$ .

Suppose  $v = q_1q_2 \cdots q_k \in V(S_{n,k})$ , we have two vertices  $u, w$  such that  $vu$  and  $vw$  are 1-edges by  $n - k \geq 2$ . Without loss of generality, we can assume  $u = q_{k+1}q_2 \cdots q_k$  and  $w = q_{k+2}q_2 \cdots q_k$ . From the definition of  $S_{n,k}$ , we have  $uw \in E(S_{n,k})$ . Hence,  $C_3 = uvwu$  in  $S_{n,k}$ . Let  $A = \{q_jq_2 \cdots q_k \mid j = k + 3, k + 4, \dots, n\}$ , then  $A = N_{S_{n,k}}(u) \cap N_{S_{n,k}}(v) \cap N_{S_{n,k}}(w)$  and  $|A| = n - k - 2$ . Since  $u, v, w$  have another  $k - 1$   $i$ -neighbors in  $S_{n,k} \setminus A$ , respectively,  $|N_{S_{n,k}}(C_3)| = |A| + 3(k - 1) = n - k - 2 + 3(k - 1) = n + 2k - 5$ . Clearly,  $S_{n,k} - N_{S_{n,k}}(C_3)$  is disconnected and contains  $C_3$  as a connected component. In order to find a cyclic vertex-cut, it suffices to show that  $S_{n,k} - N_{S_{n,k}}[C_3]$  has a cycle. In fact, we can prove  $\delta(S_{n,k} - N_{S_{n,k}}[C_3]) \geq 2$ . Suppose that there exists one vertex  $x$  of  $S_{n,k} - N_{S_{n,k}}[C_3]$  with  $d_{S_{n,k} - N_{S_{n,k}}[C_3]}(x) = 1$ . Since  $S_{n,k}$  is  $n - 1$ -regular ( $n - 1 \geq 4$ ),  $|N_{S_{n,k}}(x) \cap N_{S_{n,k}}(C_3)| \geq 3$ .

If  $x$  is adjacent to one neighbor vertex of  $u, v$ , and  $w$ , respectively, it means there are three vertices  $u', v'$ , and  $w'$  such that  $u' \in N_{S_{n,k} - C_3}(u), v' \in N_{S_{n,k} - C_3}(v), w' \in N_{S_{n,k} - C_3}(w)$ , and  $\{u', v', w'\} \subseteq N_{S_{n,k}}(x) \cap N_{S_{n,k}}(C_3)$ . Then, all of  $uu', vv',$  and  $ww'$  are  $i$ -edges. Let  $u' = q_sq_2 \cdots q_{k+1} \cdots q_k, v' = q_tq_2 \cdots q_1 \cdots q_k, w' = q_mq_2 \cdots q_{k+2} \cdots q_k$  and  $s, t, m \in \{2, 3, \dots, k\}$ . By the definition of  $S_{n,k}$ , we know  $x$  is adjacent to at most one of  $u', v'$ , and  $w'$ , a contradiction.

If  $x$  is adjacent to two neighbor vertices of  $u$  and one neighbor vertex of  $v$ , it means there are three vertices  $u_1, u_2$ , and  $v_1$  such that  $u_1, u_2 \in N_{S_{n,k} - C_3}(u), v_1 \in N_{S_{n,k} - C_3}(v)$ , and  $\{u_1, u_2, v_1\} \subseteq N_{S_{n,k}}(x) \cap N_{S_{n,k}}(C_3)$ . From the definition of  $S_{n,k}$ , both  $uu_1$  and  $uu_2$  are 1-edges and  $x = q_tq_2 \cdots q_{k+1} \cdots q_k, t \in \{k + 3, k + 4, \dots, n\}$ . Furthermore,  $x \in N(C_3)$ , a contradiction with  $x \in S_{n,k} - N_{S_{n,k}}[C_3]$ .

If  $x$  is adjacent to three neighbor vertices of  $u$ , it means there are three vertices  $u_1, u_2$ , and  $u_3$  such that  $u_1, u_2, u_3 \in N_{S_{n,k} - C_3}(u)$  and  $\{u_1, u_2, u_3\} \subseteq N_{S_{n,k}}(x) \cap N_{S_{n,k}}(C_3)$ .

From the definition of  $S_{n,k}$ , all of  $uu_1, uu_2$ , and  $uu_3$  are 1-edges and  $x = q_t q_2 \cdots q_{k+1} \cdots q_k$  and  $t \in \{k+3, k+4, \dots, n\}$ . Furthermore,  $x \in N(C_3)$ , a contradiction with  $x \in S_{n,k} - N_{S_{n,k}}[C_3]$ .

From the above discussion, we know that  $\delta(S_{n,k} - N_{S_{n,k}}[C_3]) \geq 2$ . Then,  $S_{n,k} - N_{S_{n,k}}[C_3]$  contains a cycle, and  $N_{S_{n,k}}(C_3)$  is a cyclic vertex-cut of  $S_{n,k}$  with  $|N_{S_{n,k}}(C_3)| = n + 2k - 5$ . Hence,  $\kappa_c(S_{n,k}) \geq n + 2k - 5$ . The theorem holds.

Combining Theorems 3 and 4, we have the following theorem.  $\square$

**Theorem 5.** For any integer  $n \geq 4, k \geq 2$ , and  $\kappa_c(S_{n,k}) = n + 2k - 5$ .

## 4. Conclusion

In this paper, we determine the cyclic vertex-connectivity of the  $(n, k)$ -star network  $S_{n,k}$ . We can consider the cyclic vertex-connectivity of other graphs and the cyclic edge-connectivity of the  $(n, k)$ -star network  $S_{n,k}$  in our future research.

## Data Availability

No data were used in this study.

## Conflicts of Interest

The authors declare that they have no conflicts of interest.

## Acknowledgments

This work was supported by the Natural Science Foundation of Qinghai Province, China (nos. 2021-ZJ-703 and 2019-ZJ-7012).

## References

- [1] N. Robertson, "Minimal cyclic-4-connected graphs," *Transactions of the American Mathematical Society*, vol. 284, no. 2, p. 665, 1984.
- [2] P. Tait, "On the colouring of maps," *Proceedings of the Royal Society of Edinburgh*, vol. 10, pp. 501–503, 1880.
- [3] G. D. Birkhoff, "The reducibility of maps," *Bulletin of The American Mathematical Society*, vol. 35, no. 2, p. 1913.
- [4] C. Q. Zhang, "Integer flows and cycle covers of graphs," *Biotechniques*, vol. 4, no. 4, pp. 206–207, 1997.
- [5] D. A. Holton, D. Lou, and M. D. Plummer, "On the 2-extendability of planar graphs," *Discrete Mathematics*, vol. 96, no. 2, pp. 81–99, 1991.
- [6] D. Lou and D. A. Holton, "Lower bound of cyclic edge connectivity for n-extendability of regular graphs," *Discrete Mathematics*, vol. 112, no. 1–3, pp. 139–150, 1993.
- [7] E. Cheng, L. Lipták, K. Qiu, and Z. Shen, "Cyclic vertex-connectivity of cayley graphs generated by transposition trees," *Graphs and Combinatorics*, vol. 29, no. 4, pp. 835–841, 2013.
- [8] Z. Yu, Q. Liu, and Z. Zhang, "Cyclic vertex connectivity of star graphs," in *Proceedings of the International Conference on Combinatorial Optimization and Applications*, vol. 3, pp. 433–442, Zhangjiajie, China, August 2011.
- [9] Da Huang and Z. Zhang, *On Cyclic Vertex-Connectivity of Cartesian Product Digraphs*, Springer-Verlag New York, Inc., New York, NY, USA, 2012.
- [10] D. Lou, L. Teng, and X. Wu, "A polynomial algorithm for cyclic edge connectivity of cubic graphs," *Australas.j.combin*, vol. 24, no. 24, pp. 247–259, 2014.
- [11] D. Qin, Y. Tian, L. Chen, and J. Meng, "Cyclic vertex-connectivity of cartesian product graphs," *Parallel Algorithms and Applications*, vol. 34, no. 4, 2017.
- [12] Y. Lv and Y. Xiang, "Conditional fault-tolerant routing of  $(n, k)$ -star graphs," *International Journal of Computer Mathematics*, vol. 93, no. 10, 2015.
- [13] C. Wei-Kuo and C. Rong-Jaye, "The  $(n, k)$ -star graph: a generalized star graph," *Information Processing Letters*, vol. 56, no. 5, pp. 259–264, 1995.
- [14] S. Zhou, "The conditional fault diagnosability of  $(n, k)$ -star graphs," *Applied Mathematics and Computation*, vol. 218, no. 19, pp. 9742–9749, 2012.

## Research Article

# On the Edge Metric Dimension of Different Families of Möbius Networks

Bo Deng,<sup>1,2</sup> Muhammad Faisal Nadeem ,<sup>3</sup> and Muhammad Azeem ,<sup>3,4</sup>

<sup>1</sup>School of Mathematics and Statistics, Qinghai Normal University, Xining, China

<sup>2</sup>Academy of Plateau Science and Sustainability, Xining, Qinghai 810008, China

<sup>3</sup>Department of Mathematics, COMSATS, University Islamabad Lahore Campus, Lahore, Pakistan

<sup>4</sup>Department of Aerospace Engineering, Faculty of Engineering, Universiti Putra Malaysia, Seri Kembangan, Malaysia

Correspondence should be addressed to Muhammad Faisal Nadeem; [mfaisalnadeem@gmail.com](mailto:mfaisalnadeem@gmail.com)

Received 20 December 2020; Revised 27 February 2021; Accepted 1 March 2021; Published 25 March 2021

Academic Editor: Ali Ahmad

Copyright © 2021 Bo Deng et al. This is an open access article distributed under the Creative Commons Attribution License, which permits unrestricted use, distribution, and reproduction in any medium, provided the original work is properly cited.

For an ordered subset  $Q_e$  of vertices in a simple connected graph  $G$ , a vertex  $x \in V$  distinguishes two edges  $e_1, e_2 \in E$ , if  $d(x, e_1) \neq d(x, e_2)$ . A subset  $Q_e$  having minimum vertices is called an edge metric generator for  $G$ , if every two distinct edges of  $G$  are distinguished by some vertex of  $Q_e$ . The minimum cardinality of an edge metric generator for  $G$  is called the edge metric dimension, and it is denoted by  $\dim_e(G)$ . In this paper, we study the edge resolvability parameter for different families of Möbius ladder networks and we find the exact edge metric dimension of triangular, square, and hexagonal Möbius ladder networks.

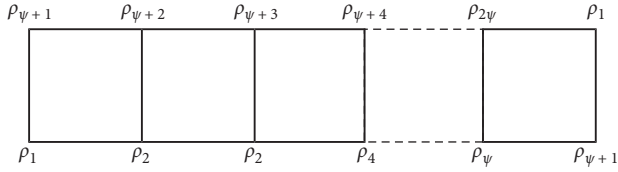
## 1. Introduction

A simple connected graph  $G = (V, E)$  with vertex set and edge set  $V$  and  $E$ , respectively. For two vertices  $a_1, a_2 \in V$ , the distance  $d(a_1, a_2)$  between vertices  $a_1$  and  $a_2$  is the count of edges between them. A vertex  $v \in V$  is said to distinguish two vertices  $a_1$  and  $a_2$ , if  $d(v, a_1) \neq d(v, a_2)$ . A set  $Q \subset V$  is called a resolving set of  $G$ , if any pair of distinct vertices of  $G$  is distinguished by some element of  $Q$ . A resolving set of minimum cardinality is named as metric basis, and its cardinality is the metric dimension of  $G$ , denoted by  $\dim(G)$ . A vertex  $v \in V$  and an edge  $e = a_1a_2 \in E$ , and the distance between  $v$  and  $e$  is defined as  $d(v, e) = \min\{d(v, a_1), d(v, a_2)\}$ . A vertex  $x \in V$  distinguishes two edges  $e_1, e_2 \in E$ , if  $d(x, e_1) \neq d(x, e_2)$ . A subset  $Q_e$  having minimum vertices from a connected graph  $G$  is an edge resolving set for  $G$ , if every two distinct edges of  $G$  are distinguished by some vertex of  $Q_e$ . The minimum cardinality of an edge resolving set for  $G$  is called the edge metric dimension and is denoted by  $\dim_e(G)$ .

In 1975, the idea of metric dimension was delivered by Slater [1], he named the metric generators as locating sets which relates to the problem of uniquely recognizing the

position of intruders in networks. On the same idea, in 1976 the concept of metric dimension of a graph was independently introduced by Harary and Melter in [2], and these time metric generators were named as resolving sets. One can think that instead of distinguishing two distinct vertices of graph according to chosen subset of vertices, two edges can be distinct with the same subset of vertices. For this concept, Kelenc et al. [3] introduced a new parameter named as the edge metric dimension. In this, they used graph metric to identify each pair of edges by the distance of graph to a chosen subset of vertices.

As far as the idea of metric dimension is extensively studied and used in different fields of science as applications, Chartrand et al. in [4] relate the metric dimension of graph with the drug discovery and pharmacological activity, Khuller et al. in [5] try to put thinking that a robot can be shifted from Euclidean space to graph structure and left his thought as an application of metric dimension in robot navigation, and the metric dimension of Hamming graphs leads Chvátal to the analysis of mastermind games and opens the doors for researchers to view application of metric dimension in complex digital games [6], and in [7, 8], Erdős and Lindström assume that the metric dimension can be

FIGURE 1: Möbius ladder network  $ML_\psi$ .

used in various coin-weighting problems. Resolving sets have served as inspiration for many theoretical studies of graphs.

The edge metric dimension is the natural generalization of resolving set, and readers are directed towards the interesting literature containing the metric dimension of different classes of graphs for example, Ali et al. [9, 10] studied the metric dimension of Möbius networks and some other cycle-related graphs, Kuziak et al. [11] discussed the strong metric dimension of graphs, Liu et al. [12, 13] discussed the metric dimension of cocktail party, Toeplitz, and jellyfish graphs, and some cycle-related graphs were studied with the concept of metric dimension by Ahmad et al. [14]. Recently, the edge metric dimension becomes a very common topic in resolvability and a lot of families of graphs are studied. Koam and Ahmad [15] studied edge metric dimension of barycentric subdivision of Cayley graph. The convex polytope graph was discussed by Zhang and Gao in [16] and Ahsan et al. in [17]. Yang et al. discussed some chemical structures related to wheel graphs in [18]. Raza and Bataineh did comparative analysis between metric and edge metric dimension in [19]. Moreover, some interesting study of edge metric dimension can be found in [20, 21], where Okamoto et al. studied the local metric dimension and Yero briefly discussed the definition of metric and its related concepts. Mixed metric dimension is another type of dimension which satisfies the conditions of metric and edge metric dimensions simultaneously. Mixed metric dimension of different families of graphs is studied and gives their exact values, such as Raza et al. studied the mixed metric dimension different rotationally symmetric graphs and gave

their exact values [22], Raza and Ji computed the mixed metric dimension of the generalize Petersen graph  $P(n, 2)$  [23], and results on mixed metric dimension of some path-related graphs are discussed by Raza et al. in [24].

In general, the edge metric dimension of a graph is NP-hard [3]. There is no general relation between metric and edge metric dimension of graphs but, in [3], Kelenc et al. inquired about the families of graphs which have  $\dim(G) = \dim_e(G)$ ,  $\dim(G) < \dim_e(G)$ , and  $\dim(G) > \dim_e(G)$ . In this paper, we find the edge metric dimension of different families of Möbius ladder networks and give a comparison between the metric and edge metric dimension of these families, in the response of this question.

*Definition 1.* The minimum number of edges  $h$  between two vertices  $a_1, a_2$  of a cycle (sub) graph is called as  $h$ -size gap between  $a_1, a_2$ .

## 2. Edge Metric Dimension of Möbius Ladder Network

Möbius ladder  $ML_\psi$  is built by a grid of  $\psi \times 1$ , and this grid is twisted at  $180^\circ$ ; now, paste the extreme most left and right paths of vertices as seen in Figure 1. It contains  $\psi$ -horizontal cycles of order four. The metric dimension of  $ML_\psi$  is three [9], and in our first result, we prove that the edge metric dimension of  $ML_\psi$  is four.

**Theorem 1.** Let  $ML_\psi$  be a Möbius ladder network with  $\psi \geq 3$ . Then,

$$\dim_e(ML_\psi) = 4. \quad (1)$$

*Proof.* Consider the edge resolving set  $Q_e = \{\rho_1, \rho_2, \rho_{\lfloor (\psi+3)/2 \rfloor}, \rho_{\psi+1}\}$ , to prove that the  $\dim_e(ML_\psi) = 4$ , first of all, we show that  $\dim_e(ML_\psi) \leq 4$ , and for this claim, following are the distances of all edges with respect to edge resolving set:

$$d(\rho_\omega \rho_{\psi+\omega}, \rho_1) = \begin{cases} \omega - 1, & \text{if } \omega = 1, 2, \dots, \lfloor \frac{\psi+2}{2} \rfloor, \\ \lfloor \frac{\psi+3}{2} \rfloor - \omega + \lfloor \frac{\psi-1}{2} \rfloor, & \text{if } \omega = \lfloor \frac{\psi+3}{2} \rfloor, \dots, \psi, \end{cases}$$

$$d(\rho_\omega \rho_{\omega+1}, \rho_1) = \begin{cases} \omega - 1, & \text{if } \omega = 1, 2, \dots, \lfloor \frac{\psi+2}{2} \rfloor; \\ \lfloor \frac{\psi+4}{2} \rfloor - \omega + \lfloor \frac{\psi-1}{2} \rfloor, & \text{if } \omega = \lfloor \frac{\psi+4}{2} \rfloor, \dots, \psi. \end{cases}$$

$$d(\rho_{\psi+\omega} \rho_{\psi+\omega+1}, \rho_1) = \begin{cases} \omega, & \text{if } \omega = 1, 2, \dots, \lfloor \frac{\psi}{2} \rfloor; \\ \lfloor \frac{\psi-1}{2} \rfloor - \omega + \lfloor \frac{\psi+2}{2} \rfloor, & \text{if } \omega = \lfloor \frac{\psi+2}{2} \rfloor, \dots, \psi - 1. \end{cases}$$

$$\begin{aligned}
 d(\rho_{2\psi}\rho_1, \rho_1) &= 0, \\
 d(\rho_{2\psi}\rho_1, \rho_2) &= 2, \\
 d(\rho_{2\psi}\rho_1, \rho_{\lfloor(\psi+3/2)\rfloor}) &= \left\lfloor \frac{\psi}{2} \right\rfloor, \\
 d(\rho_\omega\rho_{\psi+\omega}, \rho_2) &= \begin{cases} 1, & \text{if } \omega = 1; \\ \omega - 2, & \text{if } \omega = 2, 3, \dots, \left\lfloor \frac{\psi+5}{2} \right\rfloor; \\ \left\lfloor \frac{\psi}{2} \right\rfloor - \omega + \left\lfloor \frac{\psi+7}{2} \right\rfloor, & \text{if } \omega = \left\lfloor \frac{\psi+7}{2} \right\rfloor, \dots, \psi. \end{cases} \\
 d(\rho_\omega\rho_{\omega+1}, \rho_2) &= \begin{cases} 0, & \text{if } \omega = 1; \\ \omega - 2, & \text{if } \omega = 2, 3, \dots, \left\lfloor \frac{\psi+4}{2} \right\rfloor; \\ \left\lfloor \frac{\psi+6}{2} \right\rfloor - \omega + \left\lfloor \frac{\psi-1}{2} \right\rfloor, & \text{if } \omega = \left\lfloor \frac{\psi+6}{2} \right\rfloor, \dots, \psi. \end{cases} \\
 d(\rho_{\psi+\omega}\rho_{\psi+\omega+1}, \rho_2) &= \begin{cases} 1, & \text{if } \omega = 1; \\ \omega - 1, & \text{if } \omega = 2, 3, \dots, \left\lfloor \frac{\psi+3}{2} \right\rfloor; \\ \left\lfloor \frac{\psi+5}{2} \right\rfloor - \omega + \left\lfloor \frac{\psi-1}{2} \right\rfloor, & \text{if } \omega = \left\lfloor \frac{\psi+5}{2} \right\rfloor, \dots, \psi - 1. \end{cases} \\
 d(\rho_\omega\rho_{\psi+\omega}, \rho_{\lfloor\psi+3/2\rfloor}) &= \begin{cases} \left\lfloor \frac{\psi}{2} \right\rfloor, & \text{if } \omega = 1; \\ \left\lfloor \frac{\psi-1}{2} \right\rfloor - \omega + 2, & \text{if } \omega = 2, 3, \dots, \left\lfloor \frac{\psi+3}{2} \right\rfloor; \\ \omega - \left\lfloor \frac{\psi+5}{2} \right\rfloor + 1, & \text{if } \omega = \left\lfloor \frac{\psi+5}{2} \right\rfloor, \dots, \psi. \end{cases} \\
 d(\rho_\omega\rho_{\omega+1}, \rho_{\lfloor\psi+3/2\rfloor}) &= \begin{cases} \left\lfloor \frac{\psi-1}{2} \right\rfloor - \omega + 1, & \text{if } \omega = 1, 2, \dots, \left\lfloor \frac{\psi+1}{2} \right\rfloor; \\ \omega - \left\lfloor \frac{\psi+3}{2} \right\rfloor, & \text{if } \omega = \left\lfloor \frac{\psi+3}{2} \right\rfloor, \dots, \psi, \end{cases} \\
 d(\rho_{\psi+\omega}\rho_{\psi+\omega+1}, \rho_{\lfloor\psi+3/2\rfloor}) &= \begin{cases} \left\lfloor \frac{\psi+1}{2} \right\rfloor - \omega + 1, & \text{if } \omega = 1, 2, \dots, \left\lfloor \frac{\psi+1}{2} \right\rfloor; \\ \omega - \left\lfloor \frac{\psi+3}{2} \right\rfloor + 1, & \text{if } \omega = \left\lfloor \frac{\psi+3}{2} \right\rfloor, \dots, \psi - 1, \end{cases} \\
 d(\rho_\omega\rho_{\psi+\omega}, \rho_{\psi+1}) &= \begin{cases} \omega - 1, & \text{if } \omega = 1, 2, \dots, \left\lfloor \frac{\psi+2}{2} \right\rfloor; \\ \left\lfloor \frac{\psi+4}{2} \right\rfloor - \omega + \left\lfloor \frac{\psi-1}{2} \right\rfloor, & \text{if } \omega = \left\lfloor \frac{\psi+4}{2} \right\rfloor, \dots, \psi, \end{cases} \\
 d(\rho_\omega\rho_{\omega+1}, \rho_{\psi+1}) &= \begin{cases} \omega, & \text{if } \omega = 1, 2, \dots, \left\lfloor \frac{\psi}{2} \right\rfloor; \\ \left\lfloor \frac{\psi-1}{2} \right\rfloor - \omega + \left\lfloor \frac{\psi+2}{2} \right\rfloor, & \text{if } \omega = \left\lfloor \frac{\psi+2}{2} \right\rfloor, \dots, \psi, \end{cases} \\
 d(\rho_{\psi+\omega}\rho_{\psi+\omega+1}, \rho_{\psi+1}) &= \begin{cases} \omega - 1, & \text{if } \omega = 1, 2, \dots, \left\lfloor \frac{\psi+2}{2} \right\rfloor; \\ \left\lfloor \frac{\psi-1}{2} \right\rfloor - \omega + \left\lfloor \frac{\psi+4}{2} \right\rfloor, & \text{if } \omega = \left\lfloor \frac{\psi+4}{2} \right\rfloor, \dots, \psi - 1, \end{cases} \\
 d(\rho_{2\psi}\rho_1, \rho_{\psi+1}) &= 1.
 \end{aligned} \tag{2}$$

From the above given representation of all edges with respect to edge resolving set  $Q_e$ , no two edges have the same representation, and it proved that  $\dim_e(\text{ML}_\psi) \leq 4$ .

Now, on contrary,  $\dim_e(\text{ML}_\psi) = 3$  implies that the cardinality of edge metric generator  $Q'_e$  is three, following is some discussion for this contradiction:

Case 1: if the first two vertices with zero-size gap and last two vertices with any arbitrary size of gap are selected in the edge metric generator  $Q'_e = \{\rho_1, \rho_2, \rho_\omega\}$  with  $3 \leq \omega \leq \psi$ , then it implies the same representations in the edges  $d(\rho_1\rho_{\psi+1}|Q'_e) = d(\rho_1\rho_{2\psi}|Q'_e)$ , and it is concluded that we cannot take these types of vertices in the edge metric generator with cardinality three.

Case 2: if all three vertices with any arbitrary size of gap are selected and  $Q'_e = \{\rho_\omega, \rho_j, \rho_k\}$  with  $1 \leq \omega, j, k \leq \psi$ , then it implies the same representations in the edges which are  $d(\rho_1\rho_{\psi+1}|Q'_e) = d(\rho_1\rho_{2\psi}|Q'_e)$ , and it is also concluded that we cannot take these types of vertices in the edge metric generator with cardinality three.

Case 3: now, the vertices with index  $\psi + 2 \leq \omega, j, k \leq 2\psi$  with any of the gap-size are chosen and  $Q'_e = \{\rho_\omega, \rho_j, \rho_k\}$ , then it implies the same representations in the edges which are  $d(\rho_1\rho_2|Q'_e) = d(\rho_1\rho_{\psi+1}|Q'_e)$ , and again, we conclude that we cannot take these types of vertices in the edge metric generator with cardinality three.

Case 4: now, the vertices  $\rho_\omega, \rho_j, \rho_k \in V(\text{ML}_\psi)$  are chosen with any of the size of gap, then there exist an edge from lower horizontal edges and another edge from upper horizontal edges having the same representations to each other with respect to the selected edge metric generator, i.e.,  $d(\rho_p\rho_{p+1}|Q'_e) = d(\rho_{\psi+p}\rho_{\psi+p+1}|Q'_e)$  where  $1 \leq p \leq \psi - 1$ , and finally, we concluded that with any gap-size in the edge metric generator with cardinality three is not

possible, which implies the contradiction that  $\dim_e(\text{ML}_\psi) \neq 3$ . Moreover, this proves the double inequality which is

$$\dim_e(\text{ML}_\psi) = 4. \quad (3)$$

### 3. Edge Metric Dimension of Hexagonal Möbius Ladder Network

Hexagonal Möbius ladder  $\text{HML}_\psi$  is built in [25], it can be constructed by dividing each horizontal edge of a square grid by inserting a new vertex, it becomes a grid of  $\psi \times 1$  with each cycle having order six, and now, twist this grid at  $180^\circ$  and paste the extreme most left and right paths of vertices as shown in Figure 2. This graph contains  $\psi$ -horizontal cycles of order six. The metric dimension of the hexagonal Möbius ladder network is three [25]. In this section, we proved that edge metric dimension is also three for the hexagonal Möbius ladder network.

**Theorem 2.** Let  $\text{HML}_\psi$  be a hexagonal Möbius ladder network with  $\psi \geq 2$ . Then,

$$\dim_e(\text{HML}_\psi) = 3. \quad (4)$$

*Proof.* Consider the edge resolving set  $Q_e = \{\rho_1, \rho_2, \rho_{2\psi}\}$  when  $\psi = 2, 3$ ,  $Q_e = \{\rho_1, \rho_{\psi+1}, \rho_{2\psi}\}$  when  $\psi \geq 4$  (even), and  $Q_e = \{\rho_1, \rho_\psi, \rho_{2\psi}\}$  when  $\psi \geq 5$  (odd). To show that the  $\dim_e(\text{HML}_\psi) = 3$ , we will use the method of double inequality. For  $\dim_e(\text{HML}_\psi) \leq 3$ , following are the distances of all edges with respect to edge resolving set.

Distances of all vertices with respect to  $\rho_2$  are as follows:

$$d(\rho_\omega\rho_{\psi+\omega}, \rho_2) = \begin{cases} 1, & \text{if } \omega = 1, \text{ and } \psi = 2; \\ \omega - 2, & \text{if } \omega = 3, \text{ and } \psi = 2; \\ 1, & \text{if } \omega = 1, \text{ and } \psi = 3; \\ \omega - 2, & \text{if } \omega = 3, 5, \text{ and } \psi = 3, \end{cases}$$

$$d(\rho_\omega\rho_{\omega+1}, \rho_2) = \begin{cases} 0, & \text{if } \omega = 1; \\ \omega - 2, & \text{if } \omega = 2, 3, \dots, \psi + 2; \\ 2\psi + 2 - \omega, & \text{if } \omega = \psi + 3, \psi + 4, \dots, 2\psi, \end{cases}$$

$$d(\rho_{2\psi+\omega}\rho_{2\psi+\omega+1}, \rho_2) = \begin{cases} 2, & \text{if } \omega = 1, 2; \\ \omega - 1, & \text{if } \omega = 3, 4, \dots, \psi + 1; \\ 2\psi + 2 - \omega, & \text{if } \omega = \psi + 2, \psi + 3, \dots, 2\psi - 1. \end{cases}$$

$$d(\rho_{4\psi}\rho_1, \rho_2) = 2,$$

$$d(\rho_{4\psi}\rho_1, \rho_1) = 0,$$

$$d(\rho_\omega\rho_{\psi+\omega}, \rho_{2\psi}) = \begin{cases} 1, & \text{if } \omega = 1, 3 \text{ and } \psi = 2; \\ 1, & \text{if } \omega = 1, 5 \text{ and } \psi = 3; \\ 3, & \text{if } \omega = \psi = 3. \end{cases}$$

$$\begin{aligned}
 d(\rho_\omega \rho_{\psi+\omega}, \rho_1) &= \begin{cases} \omega - 1, & \text{if } \omega = 1, 3, \dots, \psi + 1, \text{ and } \psi \text{ even;} \\ 2\psi + 1 - \omega, & \text{if } \omega = \psi + 3, \psi + 5, \dots, 2\psi - 1, \text{ and } \psi \text{ even;} \\ \omega - 1, & \text{if } \omega = 1, 3, \dots, \psi, \text{ and } \psi \text{ odd;} \\ 2\psi + 1 - \omega, & \text{if } \omega = \psi + 2, \psi + 4, \dots, 2\psi - 1, \text{ and } \psi \text{ odd,} \end{cases} \\
 d(\rho_\omega \rho_{\omega+1}, \rho_1) &= \begin{cases} \omega - 1, & \text{if } \omega = 1, 2, \dots, \psi + 1; \\ 2\psi + 1 - \omega, & \text{if } \omega = \psi + 2, \psi + 3, \dots, 2\psi. \end{cases} \\
 d(\rho_{2\psi+\omega} \rho_{2\psi+\omega+1}, \rho_1) &= \begin{cases} \omega, & \text{if } \omega = 1, 2, \dots, \psi; \\ 2\psi - \omega, & \text{if } \omega = \psi + 1, \dots, 2\psi - 1. \end{cases} \\
 d(\rho_\omega \rho_{\psi+\omega}, \rho_\psi) &= |\psi - \omega|, \quad \omega = 1, 3, \dots, 2\psi - 1, \\
 d(\rho_\omega \rho_{\omega+1}, \rho_\psi) &= \begin{cases} \psi - \omega - 1, & \text{if } \omega = 1, 2, \dots, \psi - 1; \\ \omega - \psi, & \text{if } \omega = \psi, \psi + 1, \dots, 2\psi. \end{cases} \\
 d(\rho_{2\psi+\omega} \rho_{2\psi+\omega+1}, \rho_\psi) &= \begin{cases} \psi - \omega, & \text{if } \omega = 1, 2, \dots, \psi - 1; \\ \omega - \psi + 1, & \text{if } \omega = \psi, \psi + 1, \dots, 2\psi - 1, \end{cases} \\
 d(\rho_{4\psi} \rho_1, \rho_\psi) &= d(\rho_{4\psi} \rho_1, \rho_{\psi+1}) = \psi, \\
 d(\rho_{4\psi} \rho_1, \rho_{2\psi}) &= 2, \\
 d(\rho_\omega \rho_{\psi+\omega}, \rho_{\psi+1}) &= \begin{cases} \psi - \omega + 1, & \text{if } \omega = 1, 3, \dots, \psi + 1; \\ \omega - \psi - 1, & \text{if } \omega = \psi + 3, \psi + 5, \dots, 2\psi - 1, \end{cases} \tag{5} \\
 d(\rho_\omega \rho_{\omega+1}, \rho_{\psi+1}) &= \begin{cases} \psi - \omega, & \text{if } \omega = 1, 2, \dots, \psi; \\ \omega - \psi - 1, & \text{if } \omega = \psi + 1, \dots, 2\psi. \end{cases} \\
 d(\rho_{2\psi+\omega} \rho_{2\psi+\omega+1}, \rho_{\psi+1}) &= \begin{cases} \psi - \omega + 1, & \text{if } \omega = 1, 2, \dots, \psi; \\ \omega - \psi, & \text{if } \omega = \psi + 1, \psi + 2, \dots, 2\psi - 1, \end{cases} \\
 d(\rho_\omega \rho_{\psi+\omega}, \rho_{2\psi}) &= \begin{cases} 1, & \text{if } \omega = 1; \\ \omega + 1, & \text{if } \omega = 3, 5, \dots, \psi - 1, \text{ and } \psi \geq 4 \text{ (even);} \\ 2\psi - \omega, & \text{if } \omega = \psi + 1, \psi + 3, \dots, 2\psi - 1, \text{ and } \psi \geq 4 \text{ (even);} \\ \omega + 1, & \text{if } \omega = 3, 5, \dots, \psi - 2, \text{ and } \psi \geq 5 \text{ (odd);} \\ 2\psi - \omega, & \text{if } \omega = \psi, \psi + 2, \dots, 2\psi - 1, \text{ and } \psi \geq 5 \text{ (odd),} \end{cases} \\
 d(\rho_\omega \rho_{\omega+1}, \rho_{2\psi}) &= \begin{cases} \omega + 1, & \text{if } \omega = 1, 2, \dots, \psi - 1; \\ 2\psi - 1 - \omega, & \text{if } \omega = \psi, \psi + 1, \dots, 2\psi - 1; \\ 0, & \text{if } \omega = 2\psi, \end{cases} \\
 d(\rho_{2\psi+\omega} \rho_{2\psi+\omega+1}, \rho_{2\psi}) &= \begin{cases} \omega + 1, & \text{if } \omega = 1, 2, \dots, \psi - 1; \\ 2\psi - \omega, & \text{if } \omega = \psi, \psi + 1, \dots, 2\psi - 2; \\ 2, & \text{if } \omega = 2\psi - 1. \end{cases}
 \end{aligned}$$

It is clear to see that the representations of all edges with respect to edge resolving set  $Q_e$  are distinct, and it is proved that  $\dim_e(\text{HML}_\psi) \leq 3$ .

Now, for  $\dim_e(\text{HML}_\psi) \geq 3$ , the contradiction method implies that  $\dim_e(\text{HML}_\psi) = 2$ .

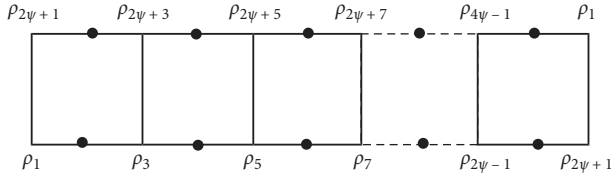
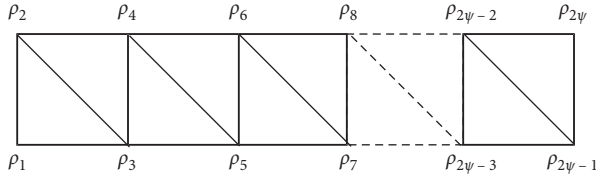
If two vertices are chosen with any arbitrary size of gap and  $Q'_e = \{\rho_\omega, \rho_j\}$  with  $1 \leq \omega, j \leq 4\psi$ , then it implies the same representations in the edges which are either  $d(\rho_p \rho_{\psi+p} | Q'_e) = d(\rho_{2\psi+q} \rho_{2\psi+q+1} | Q'_e)$  where  $1 \leq p, q \leq 2\psi - 1$  and  $p = \text{odd}$  or  $d(\rho_p \rho_{p+1} | Q'_e) = d(\rho_{2\psi+p} \rho_{2\psi+p+1} | Q'_e)$  where  $1 \leq p \leq 2\psi - 1$ , and it is also concluded that we cannot take vertices in edge metric generator with cardinality two. So, it is not possible that  $\dim_e(\text{HML}_\psi) = 2$ , which implies that  $\dim_e(\text{HML}_\psi) = 3$ .  $\square$

#### 4. Edge Metric Dimension of Triangular Ladder Network

The ladder network can be built by the cross product of two path graphs  $L_\psi = P_\psi \times P_2$ . Triangular ladder  $TL_\psi$  is built by inserting new edges of  $L_\psi$  vertices  $\rho_\omega \rho_{\omega+1}$  where  $\omega$  is even indices. This graph contains  $2\psi - 2$ -cycles of order three shown in Figure 3. Following is the edge metric generator of this network.

**Theorem 3.** Let  $TL_\psi$  be a triangular ladder network with  $\psi \geq 3$ . Then,

$$\dim_e(TL_\psi) = 4. \tag{6}$$

FIGURE 2: Hexagonal Möbius ladder network  $HML_\psi$ .FIGURE 3: Triangular ladder network  $TL_\psi$ .

*Proof.* Let  $Q_e = \{\rho_1, \rho_2, \rho_{2\psi-2}, \rho_{2\psi-1}\}$  be the edge resolving set. To show that the  $\dim_e(TL_\psi) = 4$ , we will prove first for  $\dim_e(TL_\psi) \leq 4$ , following are the representations of all edges with respect to edge resolving set:

$$d(\rho_\omega \rho_{\omega+1}, \rho_1) = \begin{cases} \frac{\omega-1}{2}, & \text{if } \omega = 1, 3, \dots, 2\psi-3; \\ \frac{\omega+2}{2}, & \text{if } \omega = 2, 4, \dots, 2\psi-4, \end{cases}$$

$$d(\rho_\omega \rho_{\omega+2}, \rho_1) = \begin{cases} \frac{\omega-1}{2}, & \text{if } \omega = 1, 3, \dots, 2\psi-3; \\ \frac{\omega+2}{2}, & \text{if } \omega = 2, 4, \dots, 2\psi-4, \end{cases}$$

$$d(\rho_\omega \rho_{\omega+1}, \rho_2) = \begin{cases} \frac{\omega-1}{2}, & \text{if } \omega = 1, 3, \dots, 2\psi-1; \\ \frac{\omega-2}{2}, & \text{if } \omega = 2, 4, \dots, 2\psi-2, \end{cases}$$

$$d(\rho_\omega \rho_{\omega+2}, \rho_2) = \begin{cases} 1, & \text{if } \omega = 1; \\ \frac{\omega-1}{2}, & \text{if } \omega = 3, 5, \dots, 2\psi-3; \\ \frac{\omega-2}{2}, & \text{if } \omega = 2, 4, \dots, 2\psi-2, \end{cases}$$

$$d(\rho_\omega \rho_{\omega+1}, \rho_{2\psi-2}) = \begin{cases} \left| \psi - 2 - \frac{\omega-1}{2} \right|, & \text{if } \omega = 1, 3, \dots, 2\psi-1; \\ \frac{2\psi-\omega-2}{2}, & \text{if } \omega = 2, 4, \dots, 2\psi-2; \end{cases}$$

$$d(\rho_\omega \rho_{\omega+2}, \rho_{2\psi-2}) = \begin{cases} \frac{2\psi-\omega-3}{2}, & \text{if } \omega = 1, 3, \dots, 2\psi-5; \\ 1, & \text{if } \omega = 2\psi-3; \\ 0, & \text{if } \omega = 2; \\ \frac{\omega-4}{2}, & \text{if } \omega = 4, 6, \dots, 2\psi-2, \end{cases}$$

$$d(\rho_\omega \rho_{\omega+1}, \rho_{2\psi-1}) = \begin{cases} \frac{2\psi-\omega-1}{2} & \text{if } \omega = 1, 3, \dots, 2\psi-1; \\ \frac{2\psi-\omega-2}{2} & \text{if } \omega = 2, 4, \dots, 2\psi-2; \end{cases}$$

$$d(\rho_\omega \rho_{\omega+2}, \rho_{2\psi-1}) = \begin{cases} \frac{2\psi-\omega-1}{2}, & \text{if } \omega = 1, 3, \dots, 2\psi-3; \\ \frac{2\psi-\omega}{2}, & \text{if } \omega = 2, 4, \dots, 2\psi-2. \end{cases} \quad (7)$$

Above given representations of all edges with respect to edge resolving set  $Q_e$  are unique, and it is proved that  $\dim_e(TL_\psi) \leq 4$ . Now, for  $\dim_e(TL_\psi) \geq 4$ , choose on contrary which implies that  $\dim_e(TL_\psi) = 3$ . Analogously, the cardinality of edge metric generator  $Q'_e$  is three, following is some discussion for this contradiction:

Case 1: if all vertices with any arbitrary size of gap are selected and  $Q'_e = \{\rho_1, \rho_\omega, \rho_j\}$  with  $3 \leq \omega, j(\text{odd}) \leq 2\psi-1$ , then it implies the same representations in the edges which are  $d(\rho_2 \rho_3 | Q'_e) = d(\rho_3 \rho_4 | Q'_e)$ , and it is concluded that we cannot take vertices like this in the edge metric generator with cardinality three.

Case 2: if all vertices with any arbitrary size of gap are selected and  $Q'_e = \{\rho_\omega, \rho_j, \rho_k\}$  with  $1 \leq \omega, j, k(\text{odd}) \leq 2\psi-1$ , then it implies the same representations in the edges which are either  $d(\rho_1 \rho_3 | Q'_e) = d(\rho_2 \rho_3 | Q'_e)$  or  $d(\rho_p \rho_{p+1} | Q'_e) = d(\rho_q \rho_{q+2} | Q'_e)$  where  $2 \leq p, q(\text{even}) \leq 2\psi$ , and it is also concluded that we cannot take vertices in the edge metric generator with cardinality three.

Case 3: if all vertices with any arbitrary size of gap are selected and  $Q'_e = \{\rho_\omega, \rho_j, \rho_k\}$  with  $2 \leq \omega, j, k(\text{even}) \leq 2\psi$ , then it implies the same representations in the edges which are  $d(\rho_1 \rho_2 | Q'_e) = d(\rho_2 \rho_3 | Q'_e)$ , and it is also concluded that we cannot take vertices in the edge metric generator with cardinality three.

Case 4: now, the vertices  $\rho_\omega, \rho_j, \rho_k \in V(TL_\psi)$  without choosing the size of gap, then there exist an edge from joining edges and another one edge from upper horizontal edges having the same representation to each other with respect to the decided edge metric generator, i.e.,  $d(\rho_p \rho_{p+1} | Q'_e) = d(\rho_q \rho_{q+2} | Q'_e)$  where  $2 \leq p, q(\text{even}) \leq 2\psi$ , and finally, we concluded that we cannot take any type of vertices with any gap-size in the edge metric generator with cardinality three, which implies the contradiction that  $\dim_e(TL_\psi) \neq 3$ . Moreover, this proves the double inequality which is

$$\dim_e(TL_\psi) = 4. \quad (8)$$

□



### 5. Edge Metric Dimension of Triangular Möbius Ladder Network

Figure 3 shows a triangular ladder network; now, twist this network at  $180^\circ$  and paste the extreme most left and right paths of vertices, and it will come up to a new type of graph named as triangular Möbius ladder graph  $TML_\psi$ . This graph contains  $2\psi - 2$ -horizontal cycles of order three, which can be seen in Figure 4. Following results are the edge metric dimension of the triangular Möbius ladder network.

**Theorem 4.** Let  $TML_\psi$  be a triangular Möbius ladder network with  $\psi \geq 5$ . Then,

$$\dim_e(TML_\psi) = 4. \tag{9}$$

*Proof.* Consider the edge resolving set  $Q_e = \{\rho_4, \rho_5, \rho_6, \rho_7\}$ , when  $\psi = 5$ ,  $Q_e = \{\rho_1, \rho_4, \rho_{\psi+2}, \rho_{\psi+3}\}$ , when  $\psi \geq 6$  (even), and  $Q_e = \{\rho_3, \rho_{\psi-1}, \rho_{\psi+2}, \rho_{2\psi-2}\}$ , and when  $\psi \geq 7$  (odd). To show that the  $\dim_e(TML_\psi) = 4$ , we will use the method of double inequality, for  $\dim_e(TML_\psi) \leq 4$ , following are the representations of all edges with respect to the edge resolving set.

When  $\psi = 5$ ,

$$d(\rho_\omega \rho_{\omega+1}, \rho_4) = \begin{cases} 1, & \text{if } \omega = 1, 2, \\ \frac{\omega - 3}{2}, & \text{if } \omega = 3, 5, 7, \\ \frac{\omega - 4}{2}, & \text{if } \omega = 4, 6, 8, \end{cases}$$

$$d(\rho_{2\psi-2}\rho_2, \rho_4) = d(\rho_{2\psi-3}\rho_2, \rho_4) = d(\rho_{2\psi-1}\rho_1, \rho_4) = 2,$$

$$d(\rho_\omega \rho_{\omega+2}, \rho_4) = \begin{cases} 2 - \omega, & \text{if } \omega = 1, 2, \\ \frac{\omega - 1}{2}, & \text{if } \omega = 3, 5, \\ \frac{\omega - 4}{2}, & \text{if } \omega = 4, 6, 8, \end{cases}$$

$$d(e_1, \rho_5) = \begin{cases} \left\lfloor \frac{5 - \omega}{2} \right\rfloor & \text{if } \omega = 1, 3, 5, 7, \\ \frac{4 - \omega}{2} & \text{if } \omega = 2, 4, 6, \end{cases}$$

$$d(\rho_{2\psi-2}\rho_2, \rho_5) = d(\rho_{2\psi-1}\rho_1, \rho_5) = 2, d(\rho_{2\psi-3}\rho_2, \rho_5) = 1,$$

$$d(\rho_\omega \rho_{\omega+2}, \rho_5) = \begin{cases} \omega; & \text{if } \omega = 1, 2, \\ 0; & \text{if } \omega = 3, 5, \\ 1; & \text{if } \omega = 4, 6, \end{cases}$$

$$d(\rho_\omega \rho_{\omega+1}, \rho_6) = \begin{cases} \left\lfloor \frac{5 - \omega}{2} \right\rfloor & \text{if } \omega = 1, 3, 5, 7, \\ \left\lfloor \frac{6 - \omega}{2} \right\rfloor, & \text{if } \omega = 2, 4, 6, \end{cases}$$

$$d(\rho_{2\psi-2}\rho_2, \rho_6) = d(\rho_{2\psi-1}\rho_1, \rho_6) = 1,$$

$$d(\rho_{2\psi-3}\rho_2, \rho_6) = 2,$$

$$d(\rho_\omega \rho_{\omega+2}, \rho_6) = \begin{cases} \frac{2}{\omega}; & \omega = 1, 2, \\ 1; & \omega = 3, 5, \\ 0; & \text{if } \omega = 4, 6, \end{cases}$$

$$d(\rho_\omega \rho_{\omega+1}, \rho_7) = \begin{cases} 1; & \text{if } \omega = 1, \\ \frac{7 - \omega}{2}; & \text{if } \omega = 3, 5, 7, \\ \frac{6 - \omega}{2}; & \text{if } \omega = 2, 4, 6, \end{cases}$$

$$d(\rho_{2\psi-2}\rho_2, \rho_7) = d(\rho_{2\psi-1}\rho_1, \rho_7) = 1,$$

$$d(\rho_{2\psi-3}\rho_2, \rho_6) = 0,$$

$$d(\rho_\omega \rho_{\omega+2}, \rho_6) = \begin{cases} \frac{5 - \omega}{2}; & \text{if } \omega = 1, 3, 5, \\ 2; & \text{if } \omega = 2, 4 \\ 1; & \text{if } \omega = 6. \end{cases} \tag{10}$$

When  $\psi \geq 6$  (even),

$$d(\rho_\omega \rho_{\omega+1}, \rho_1) = \begin{cases} \frac{\omega - 2}{2}; & \text{if } \omega = 1, 3, \dots, \psi - 1, \\ \frac{2\psi - \omega - 3}{2}; & \text{if } \omega = \psi + 1, \psi + 3, \dots, 2\psi - 3, \\ \frac{\omega}{2}; & \text{if } \omega = 2, 4, \dots, \psi, \\ \frac{2\psi - \omega}{2}; & \text{if } \omega = \psi + 2, \psi + 4, \dots, 2\psi - 4, \end{cases}$$

$$d(\rho_{2\psi-2}\rho_2, \rho_1) = d(\rho_{2\psi-3}\rho_2, \rho_1) = 1,$$

$$d(\rho_{2\psi-1}\rho_1, \rho_1) = 0,$$

$$d(\rho_\omega \rho_{\omega+2}, \rho_1) = \begin{cases} \frac{\omega - 2}{2}; & \text{if } \omega = 1, 3, \dots, \psi - 1, \\ \frac{2\psi - \omega - 1}{2}; & \text{if } \omega = \psi + 1, \psi + 3, \dots, 2\psi - 5, \\ \frac{\omega}{2}; & \text{if } \omega = 2, 4, \dots, \psi - 2, \\ \frac{2\psi - \omega - 2}{2}; & \text{if } \omega = \psi, \psi + 2, \dots, 2\psi - 4, \end{cases}$$

$$d(\rho_\omega \rho_{\omega+1}, \rho_4) = \begin{cases} 1; & \text{if } \omega = 1, 2, \\ \frac{\omega-3}{2}; & \text{if } \omega = 3, 5, \dots, \psi+3, \\ \frac{2\psi-\omega+3}{2}; & \text{if } \omega = \psi+5, \psi+7, \dots, 2\psi-3 \\ \frac{\omega-4}{2}; & \text{if } \omega = 4, 6, \dots, \psi+2, \\ \frac{2\psi-\omega+2}{2}; & \text{if } \omega = \psi+4, \psi+6, \dots, 2\psi-4. \end{cases}$$

$$d(\rho_{2\psi-2}\rho_2, \rho_4) = d(\rho_{2\psi-3}\rho_2, \rho_4) = d(\rho_{2\psi-1}\rho_1, \rho_4) = 2. \quad (11)$$

When  $\psi \geq 7$  (odd),

$$d(\rho_\omega \rho_{\omega+2}, \rho_4) = \begin{cases} 2-\omega; & \text{if } \omega = 1, 2, \\ \frac{\omega-1}{2}; & \text{if } \omega = 3, 5, \dots, \psi+1, \\ \frac{2\psi-\omega+1}{2}; & \text{if } \omega = \psi+3, \psi+5, \dots, 2\psi-5, \\ \frac{\omega-4}{2}; & \text{if } \omega = 4, 6, \dots, \psi+2, \\ \frac{2\psi-\omega+2}{2}; & \text{if } \omega = \psi+4, \psi+6, \dots, 2\psi-4, \end{cases}$$

$$d(\rho_\omega \rho_{\omega+1}, \rho_{\psi+2}) = \begin{cases} \frac{\psi-2}{2}; & \text{if } \omega = 1, \\ \left\lfloor \frac{\psi-\omega+1}{2} \right\rfloor; & \text{if } \omega = 3, 5, \dots, 2\psi-3, \\ \left\lfloor \frac{\psi-\omega-2}{2} \right\rfloor; & \text{if } \omega = 2, 4, \dots, 2\psi-4, \end{cases}$$

$$d(\rho_{2\psi-2}\rho_2, \rho_{\psi+2}) = d(\rho_{2\psi-3}\rho_2, \rho_{\psi+2}) = d(\rho_{2\psi-1}\rho_1, \rho_{\psi+2}) = \frac{\psi-4}{2},$$

$$d(\rho_\omega \rho_{\omega+2}, \rho_{\psi+2}) = \begin{cases} \frac{\psi-\omega+1}{2}; & \text{if } \omega = 1, 3, \dots, \psi-1, \\ \frac{\psi-\omega+3}{2}; & \text{if } \omega = \psi+1, \psi+3, \dots, 2\psi-5, \\ \frac{\psi-\omega}{2}; & \text{if } \omega = 2, 4, \dots, \psi, \\ \frac{\omega-\psi-2}{2}; & \text{if } \omega = \psi+2, \psi+4, \dots, 2\psi-4, \end{cases}$$

$$d(\rho_\omega \rho_{\omega+1}, \rho_{\psi+3}) = \begin{cases} \frac{\psi-4}{2}; & \text{if } \omega = 1, \\ \left\lfloor \frac{\psi-\omega+3}{2} \right\rfloor; & \text{if } \omega = 3, 5, \dots, 2\psi-3, \\ \frac{\psi-2}{2}; & \text{if } \omega = 2, \\ \left\lfloor \frac{\psi-\omega+4}{2} \right\rfloor; & \text{if } \omega = 4, 6, \dots, 2\psi-4, \end{cases}$$

$$d(\rho_{2\psi-2}\rho_2, \rho_{\psi+3}) = d(\rho_{2\psi-1}\rho_1, \rho_{\psi+3}) = \frac{\psi-4}{2},$$

$$d(\rho_{2\psi-3}\rho_2, \rho_{\psi+3}) = \frac{\psi-6}{2},$$

$$d(\rho_\omega \rho_{\omega+2}, \rho_{\psi+3}) = \begin{cases} \frac{\psi-2}{2}; & \text{if } \omega = 1, 2, \\ \left\lfloor \frac{\psi-\omega+1}{2} \right\rfloor; & \text{if } \omega = 3, 5, \dots, 2\psi-5, \\ \frac{\psi-\omega+2}{2}; & \text{if } \omega = 4, 6, \dots, \psi, \\ 1; & \text{if } \omega = \psi+2, \\ \frac{\omega-\psi-2}{2}; & \text{if } \omega = \psi+4, \psi+6, \dots, 2\psi-4. \end{cases} \quad (12)$$

It is clear to see the distinct representations of all edges with respect to edge resolving set  $Q_e$ , and it is proved that  $\dim_e(\text{TML}_\psi) \leq 4$ .

Now, for  $\dim_e(\text{TML}_\psi) \geq 4$ , choose the contradiction method, and it implies that  $\dim_e(\text{TML}_\psi) = 3$ . Now, the cardinality of edge metric generator  $Q'_e$  is three, following is some discussion for this contradiction:

Case 1: if three vertices with any arbitrary size of gap are selected and  $Q'_e = \{\rho_\omega, \rho_j, \rho_k\}$  with  $1 \leq \omega, j, k (\text{odd}) \leq 2\psi-3$ , then it implies the same distances in the edges which are either  $d(\rho_1\rho_2|Q'_e) = d(\rho_1\rho_{2\psi-1}|Q'_e)$ , and it is also concluded that we cannot take vertices in the edge metric generator with cardinality three.

Case 2: if all vertices with any arbitrary size of gap can choose such as  $Q'_e = \{\rho_\omega, \rho_j, \rho_k\}$  with  $2 \leq \omega, j, k (\text{even}) \leq 2\psi-2$ , then it implies the same distances in the edges which are  $d(\rho_1\rho_2|Q'_e) = d(\rho_2\rho_3|Q'_e)$ , and it is also concluded that we cannot take vertices in the edge metric generator with cardinality three.

Case 3: now, the vertices  $\rho_\omega, \rho_j, \rho_k \in V(\text{TML}_\psi)$  without choosing the size of gap, then there exist an edge from joining edges and another one edge from upper horizontal edges having the same distances to each other with respect to the decided edge metric generator, i.e.,  $d(\rho_p\rho_{p+1}|Q'_e) = d(\rho_p\rho_{p+2}|Q'_e)$  where  $2 \leq p (\text{even}) \leq 2\psi-4$  or  $d(\rho_p\rho_{p+2}|Q'_e) = d(\rho_q\rho_{q+1}|Q'_e)$  where  $1 \leq p (\text{odd}) \leq 2\psi-5$ , and finally, we concluded that we cannot take any type of vertices with any gap-size in the edge metric generator with cardinality three, which implies the contradiction that  $\dim_e(\text{TML}_\psi) \neq 3$ . Moreover, this proves the double inequality which is

$$\dim_e(\text{TML}_\psi) = 4. \quad (13) \quad \square$$

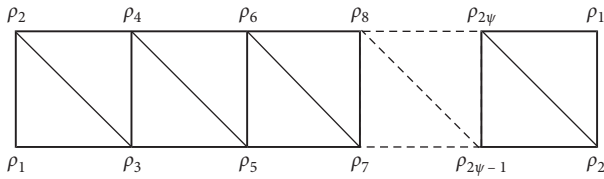


FIGURE 4: Triangular Möbius ladder network  $TM\mathcal{L}_\psi$ .

### 6. Conclusion

In the response of the question proposed by Kelenc et al. [3], in this article, we discussed some networks which have  $\dim(G) = \dim_e(G)$ . Hexagonal Möbius ladder has three metric and edge metric dimensions. Triangular ladder, triangular Möbius ladder, and Möbius ladder fall in the category which have  $\dim(G) < \dim_e(G)$ . Moreover, there is no change in the metric dimension and edge metric dimension of triangular ladder graph after making it triangular Möbius ladder and have  $\dim_e(G) = \dim(G) + 1 = 4$ .

### Data Availability

The data used to support the findings of this study are included within the manuscript.

### Conflicts of Interest

The authors declare that they have no conflicts of interest to report regarding the present study.

### Acknowledgments

This study was supported by the NSFQH 11(no. 2018-ZJ-925Q).

### References

- [1] P. J. Slater, "Leaves of trees, proceeding of the 6th southeastern conference on combinatorics, graph theory, and computing," *Congressus Numerantium*, vol. 14, pp. 549–559, 1975.
- [2] F. Harary and R. A. Melter, "On the metric dimension of a graph," *Ars Combinatoria*, vol. 2, pp. 191–195, 1976.
- [3] A. Kelenc, N. Tratnik, and I. G. Yero, "Uniquely identifying the edges of a graph: the edge metric dimension," *Discrete Applied Mathematics*, vol. 251, pp. 204–220, 2018.
- [4] G. Chartrand, L. Eroh, M. A. Johnson, and O. R. Oellermann, "Resolvability in graphs and the metric dimension of a graph," *Discrete Applied Mathematics*, vol. 105, no. 1–3, pp. 99–113, 2000.
- [5] S. Khuller, B. Raghavachari, and A. Rosenfeld, "Landmarks in graphs," *Discrete Applied Mathematics*, vol. 70, no. 3, pp. 217–229, 1996.
- [6] V. Chvátal, "Mastermind," *Combinatorica*, vol. 3, no. 3–4, pp. 325–329, 1983.
- [7] P. Erdős and P. R. Alfréd, "On two problems of information theory," *Matematikai Kutato Intezetenek Kozlomenyei. Magyar Tudomanyos Akademia*.vol. 8, pp. 229–243, 1963.
- [8] B. Lindström, "On a combinatory detection problem," *Matematikai Kutato Intezetenek Kozlomenyei. Magyar Tudomanyos Akademia*.vol. 9, pp. 195–207, 1964.

- [9] M. Ali, G. Ali, M. Imran, A. Q. Baig, and M. K. Shafiq, "On the metric dimension of Möbius ladders," *Ars Combinatoria*, vol. 105, pp. 403–410, 2012.
- [10] M. Ali, G. Ali, U. Ali, and M. T. Rahim, "On cycle related graphs with constant metric dimension," *Open Journal of Discrete Mathematics*, vol. 2, no. 1, pp. 21–23, 2012.
- [11] D. Kuziak, J. A. Rodríguez-Velázquez, and I. G. Yero, "On the strong metric dimension of product graphs," *Electronic Notes in Discrete Mathematics*, vol. 46, pp. 169–176, 2014.
- [12] J.-B. Liu, M. F. Nadeem, H. M. A. Siddiqui, and W. Nazir, "Computing metric dimension of certain families of Toeplitz graphs," *IEEE Access*, vol. 7, pp. 126734–126741, 2019.
- [13] J.-B. Liu, A. Zafari, and H. Zarei, "Metric dimension, minimal doubly resolving sets, and the strong metric dimension for jellyfish graph and cocktail party graph," *Complexity*, vol. 2020, Article ID 9407456, 7 pages, 2020.
- [14] A. Ahmad, M. Baća, and S. Sultan, "Computing the metric dimension of kayak paddles graph and cycles with chord," *Proyecciones (Antofagasta)*, vol. 39, no. 2, pp. 287–300, 2020.
- [15] A. N. A. Koam and A. Ahmad, "Barycentric subdivision of Cayley graphs with constant edge metric dimension," *IEEE Access*, vol. 8, pp. 80624–80628, 2020.
- [16] Y. Zhang and S. Gao, "On the edge metric dimension of convex polytopes and its related graphs," *Journal of Combinatorial Optimization*, Springer, vol. 39, no. 2, pp. 334–350, 2020.
- [17] M. Ahsan, Z. Zahid, S. Zafar, A. Rafiq, M. Sarwar Sindhu, and M. Umar, "Computing the edge metric dimension of convex polytopes related graphs," *Journal of Mathematics and Computer Science*, vol. 22, no. 2, pp. 174–188, 2020.
- [18] B. Yang, M. Rafiullah, H. M. A. Siddiqui, and S. Ahmad, "On resolvability parameters of some wheel-related graphs," *Journal of Chemistry*, vol. 2019, Article ID 9259032, 9 pages, 2019.
- [19] Z. Raza and M. S. Bataineh, "The comparative analysis of metric and edge metric dimension of some subdivisions of the wheel graph," *Asian-European Journal of Mathematics*, vol. 14, no. 4, p. 2150062, 2020.
- [20] F. Okamoto, B. Phinezy, and P. Zhang, "The local metric dimension of a graph," *Mathematica Bohemica*, vol. 135, no. 3, pp. 239–255, 2010.
- [21] I. G. Yero, "Vertices, edges, distances and metric dimension in graphs," *Electronic Notes in Discrete Mathematics*, vol. 55, pp. 191–194, 2016.
- [22] H. Raza, J.-B. Liu, and S. Qu, "On mixed metric dimension of rotationally symmetric graphs," *IEEE Access*, vol. 8, pp. 11560–11569, 2020.
- [23] H. Raza and Y. Ji, "Computing the mixed metric dimension of a generalized Petersen graph  $P(n, 2)$ ," *Frontiers in Physics*, vol. 8, p. 211, 2020.
- [24] H. Raza, Y. Ji, and S. Qu, "On mixed metric dimension of some path related graphs," *IEEE Access*, vol. 8, pp. 188146–188153, 2020.
- [25] M. F. Nadeem, M. Azeem, and A. Khalil, "The locating number of hexagonal Möbius ladder network," *Journal of Applied Mathematics and Computing*, 2020.

## Research Article

# Computing Edge Weights of Symmetric Classes of Networks

Hafiz Usman Afzal,<sup>1</sup> Muhammad Javaid ,<sup>1</sup> Abdulaziz Mohammed Alanazi,<sup>2</sup> and Maryam Gharamah Alshehri<sup>2</sup>

<sup>1</sup>Department of Mathematics, School of Science, University of Management and Technology, Lahore 54770, Pakistan

<sup>2</sup>Department of Mathematics, University of Tabuk, Tabuk, Saudi Arabia

Correspondence should be addressed to Muhammad Javaid; javaidmath@gmail.com

Received 22 January 2021; Revised 17 February 2021; Accepted 1 March 2021; Published 20 March 2021

Academic Editor: Ali Ahmad

Copyright © 2021 Hafiz Usman Afzal et al. This is an open access article distributed under the Creative Commons Attribution License, which permits unrestricted use, distribution, and reproduction in any medium, provided the original work is properly cited.

Accessibility, robustness, and connectivity are the salient structural properties of networks. The labelling of networks with numeric numbers using the parameters of edge or vertex weights plays an eminent role in the study of the aforesaid properties. The systems interlinked in a network are transformed into a graphical network, and specific numeric labels assigned to the converted network under certain rules assist us in the regulation of data traffic, bandwidth, and coding/decoding of signals. Two major classes of such network labellings are magic and antimagic. The notion of super  $(a, 0)$  edge-antimagic labelling on networks was identified in the late nineties. The present article addresses super  $(a, 0)$  edge-antimagicness of union of the networks' star  $S_n$ , the path  $P_n$ , and copies of paths and the rooted product of cycle  $C_n$  with  $K_{2,m}$ . We also provide super  $(a, 0)$  edge-antimagic labelling of the rooted product of cycle  $C_n$  and planar pancyclic networks. Further, we design a super  $(a, 0)$  edge-antimagic labelling on a pancyclic network containing chains of  $C_6$  and three different symmetrically designed lattices. Moreover, our findings have also been recapitulated in the shape of 3-D plots and tables.

## 1. Introduction

In this section, we shall define our problem and explain the objective of this study in Section 1.1, followed by Section 1.2, consisting of the definitions and results which we will use in our findings. Some previously performed work in this area will also be discussed in this section. Moreover, Section 1.3 concerns with applications of antimagic and magic labelling in various branches of networking, engineering, and computer science.

*1.1. Problem Definition and Objective of the Study.* In the fields of networking and computer science, the magic and antimagic labelling on networks are designed due to their extensive applications. Numerous results have been obtained on numeric labelling of several operations on networks such as Cartesian, lexicographical, corona, and modular products of various kinds of connected networks

(see [1,2] for instance). The present article addresses super  $(a, 0)$  edge-antimagic labelling of the rooted product of  $K_{2,m}$  and  $C_n$  taking its disjoint union with the star, path, and copies of paths. We shall also design super  $(a, 0)$  edge-antimagic labelling on rooted product of specifically designed planar pancyclic networks with cycle  $C_n$ . Moreover, we shall design super  $(a, 0)$  edge-antimagic labelling on planar pancyclic networks containing chains of  $C_6$  and three different symmetric lattice networks (notated as  $\mathbb{L}_n^1$ ,  $\mathbb{L}_n^2$ , and  $\mathbb{L}_n^3$ ). Except lattice networks, interestingly, all networks discussed in this note are planar. The overlapping probability of various networking elements minimizes in the course of planar networks. In organizations, this issue of entities' overlapping is one of the major reasons of inefficiency. The test ready antimagic labellings obtained in this note on particular networks can be utilized in various projects of computer science and engineering admitting suitable and equivalently designed schemes of networking.

*1.2. Definitions and Preliminaries.* Some useful definitions and preliminary results in the context of this note shall be discussed in this section. We will also mention some relevant studies previously done in this field.

An ordered 2-tuple comprising two sets, i.e., set of nodes termed as vertex set  $V(\mathbb{G})$  and connection between these vertices termed as edge set  $E(\mathbb{G})$ , is called a network  $\mathbb{G}$ , where  $E(\mathbb{G})$  is contained in  $V(\mathbb{G}) \times V(\mathbb{G})$ . A network  $\mathbb{G}$  can either be connected or consists of connected components. We will consider nonempty and simple networks throughout, having  $V(\mathbb{G})$  as its vertex set and  $E(\mathbb{G})$  as its edge set with order  $|V(\mathbb{G})| = p$  and size  $|E(\mathbb{G})| = q$ . The network  $\mathbb{G}$  in this case is termed as a  $(p, q)$ -network. Reference [3] is referred to for further discernment into the network terminologies.

A labelling is a function that maps +ive integers (non-zero) onto the component(s) of a network under specified constraints. If the components include vertices and edges both, then this labelling is termed as total. The labellings are referred to as vertex or edge labellings if they cover, respectively,  $V(\mathbb{G})$  or  $E(\mathbb{G})$  alone in the domain. Magic and antimagic labelling are two main classes of labelling. Precisely, equal or unequal vertex/edge weights refer to magic or antimagic labellings, respectively.

*Definition 1.* For a  $(p, q)$ -network  $\mathbb{G} = (V(\mathbb{G}), E(\mathbb{G}))$ , the bijective function  $\delta$  form  $V(\mathbb{G}) \cup E(\mathbb{G})$  onto  $\{1, 2, \dots, p + q\}$  is termed as  $(a, d)$  edge-antimagic total labelling with the constraint that the edge weights  $\delta(x) + \delta(xy) + \delta(y)$ , for each  $xy \in E(\mathbb{G})$ , constitute a sequence of consecutive positive integers, where  $a$  is the minimum edge weight and common difference is  $d$ .  $\mathbb{G}$  is referred to be an  $(a, d)$  edge-antimagic total network, if such a labelling exists.

*Definition 2.* A super  $(a, d)$  edge-antimagic total labelling is in fact an  $(a, d)$  edge-antimagic total labelling in which minimum labels  $1, 2, \dots, p$  are assigned to vertices of the  $(p, q)$ -network  $\mathbb{G}$ .  $\mathbb{G}$  is termed to be a super  $(a, d)$  edge-antimagic total network in this case.

In Definitions 1 and 2, the minimum edge weight  $a$  becomes constant  $c$  at  $d = 0$ , for all edges  $xy \in E(\mathbb{G})$ , which is referred to as magic sum or magic constant for the network  $\mathbb{G}$ .

*Definition 3.* A network  $\mathbb{G}$  is termed as a pancyclic network if it contains cycle of every order from 3 to  $|V(\mathbb{G})|$ .

*Definition 4.* Let  $\mathbb{G}_1$  and  $\mathbb{G}_2$  be two simple networks. The network obtained by taking  $|V(\mathbb{G}_1)|$  copies of  $\mathbb{G}_2$  and then for each point (vertex)  $v_j$  in  $V$  (called the root vertex)  $(\mathbb{G}_1)$ ,  $v_j$  is being replaced with the  $j$ th copy of  $\mathbb{G}_2$ , termed as the rooted product of the networks  $\mathbb{G}_1$  and  $\mathbb{G}_2$ . It is notated as  $\mathbb{G}_1 \circ \mathbb{G}_2$ .

Further in the article, the abbreviations are being used as given in Table 1.

We further provide some specific definitions within the corresponding section of our main results' section.

The idea of magic labelling on networks was identified by Sadláček in 1963 [4]. The notion of antimagic labelling, for vertex sums of networks, was presented by Ringel and

TABLE 1: Notations and their abbreviations used in the article.

Terminology	Abbreviation
$(a, d)$ edge-antimagic	$(a, d)$ -EAM
Super $(a, d)$ edge-antimagic	S- $(a, d)$ -EAM

Hartsfield [5] later. Kotzig and Rosa brought into the light the concept of magic valuations of networks in [6] which was in fact the  $(a, 0)$ -EAM total labelling on networks (studied by Ringel and Llado [7] in 1996). The notion of S- $(a, 0)$ -EAM total labelling of networks was defined by Enomoto et al. [8] with the terminology super edge-magic labelling. Simanjantuk et al. highlighted  $(a, d)$ -EAM total labelling of networks in [9] in year 2000.

The literature of  $(a, 0)$ -EAM total labelling of networks includes the following interesting and useful conjectures.

**Conjecture 1.** All trees admit  $(a, 0)$ -EAM total labelling [6].

**Conjecture 2.** All trees admit S- $(a, 0)$ -EAM total labelling [8].

Graph theorists, in the support of Conjecture 2, have been rectifying several particular classes of trees. Using an encryption of a computer programme, this conjecture has been verified for the trees having at most 17 vertices by Lee and Shah [10]. Specifically, the derivations can be seen for stars, subdivided stars [11, 12, 13, 14, 15],  $w$ -trees [16, 17, 18], banana trees [19], caterpillars [20], subdivided caterpillars [21], and the union of books and stars [22]. Further relevant works can be found in [23–25]. However, this conjecture is still open for working. Enomoto et al. proved that if a simple  $(p, q)$ -network  $\mathbb{G}$  is S- $(a, 0)$ -EAM total, then  $2p - 3$  is at least  $q$  [8]. They further derived that the network  $K_{m,n}$  is S- $(a, 0)$ -EAM total  $\Leftrightarrow m$  or  $n$  is 1. Figueroa-Centeno et al. derived that the union of networks  $K_{1,m} \cup K_{1,n}$  is S- $(a, 0)$ -EAM total if either  $m = \eta_1(n + 1)$  or  $n = \eta_2(n + 1)$  [26]. The network  $C_n$  is also proved to be S- $(a, 0)$ -EAM total only if  $n \equiv 1 \pmod{2}$  in [8]. In [27],  $C_3 \cup C_n$  has been proven to be S- $(a, 0)$ -EAM total only when  $6 \leq n \equiv 0 \pmod{2}$ . The generalized prism  $D_{m,n}$  is proven to be S- $(a, 0)$ -EAM total for all odd values of  $m$  in [28]. Baig et al. classified a class of planar pancyclic networks in [29] and exhibited its S- $(a, 0)$ -EAM total labelling for all possible values of the parameters involved. An immensely advantageous lemma on S- $(a, 0)$ -EAM total networks is as follows. Liu et al. studied the bounds of the minimum and maximum edge weights for super  $(a, d)$ -EAM total labelling on a generalized class of subdivided caterpillars in [30] for various values of  $d$ . In [31], Ahmad et al. studied the super  $(a, 0)$ -EAM total labelling of certain Toeplitz graphs combined with isolated vertices  $nK_1$ , for various values of  $n$  (also known as super edge-magic deficiency of networks). The properties and existence of super  $(a, d)$  vertex-antimagic labelling of regular graphs have been discussed in [32]. In [33], Ahmad et al. constructed the  $\alpha$ -labelling, a special case of graceful labelling (labelling in which distinct edge weights are considered with respect to the difference of vertices' labels) on trees, and transformed this labelling to edge-antimagic vertex labelling

of trees. In [34],  $S$ -( $a, 0$ )-EAM total labelling on the graphs  $G \cup nK_1$  has been studied, where  $G$  represents the unicyclic graph, whereas  $S$ -( $a, 0$ )-EAM total labelling of networks like zig-zag triangle and disjoint union of combs and stars has been studied in [35].

**Lemma 1** (see [28]). *A  $(\wp, \mathfrak{F})$ -network  $\mathbb{G}$  is  $S$ -( $a, 0$ )-EAM total if and only if there is a bijection  $\delta: V(\mathbb{G}) \rightarrow \{1, 2, \dots, \wp\}$  such that the set  $S = \{\delta(x) + \delta(y) | xy \in E(\mathbb{G})\}$  consists of  $\mathfrak{F}$  consecutive integers. In such a case,  $\delta$  extends to an  $S$ -( $a, 0$ )-EAM total labelling of  $\mathbb{G}$  with magic constant  $\mathfrak{R} = \wp + \mathfrak{F} + s$ , where  $s = \min(S)$  and  $S = \{\mathfrak{R} - (\wp + 1), \mathfrak{R} - (\wp + 2), \dots, \mathfrak{R} - (\wp + \mathfrak{F})\}$ .*

In Lemma 1, the sum  $\delta(x) + \delta(y)$  is called as edge sum for each edge  $xy \in E(\mathbb{G})$ . This lemma will be used frequently in our derivations, as it keeps this sufficient to label the vertices of a network only to make the network  $S$ -( $a, 0$ )-EAM total, if the edge sums are positive consecutive integers. The following result is also very pertinent as far as  $S$ -( $a, 0$ )-EAM total networks are concerned.

**Theorem 1.** *A simple network  $G$  admits an  $S$ -( $a, 0$ )-EAM total labelling  $\Leftrightarrow G$  admits an  $S$ -( $a - |E(G)| + 1, 2$ )-EAM total labelling [36].*

*1.3. Applications in Networking, Computer Science, and Engineering.* In software engineering, network labelling keeps on attaining an improved role in the security codes' encryption in order to encounter the attacks of trojans onto the precious data designed by hackers and also in designing of algorithm that helps the transmission of data to various networks and similar devices. The configurations of software in the encryption of their updated version is being improved by the use of reference labels and test ready labels nowadays. For connected components of networks in binary graphics, the mechanism which is predominantly nurturing the creation of clearer graphics involves labelling [37]. The study of magic labelling has been appearing to be more useful gradually in the data mining. The task of collection of data for the derivation of latest information gets more uncomplicated by designating equal weightage data as a single element. Resultantly, in organizations, the data mining task is becoming facile and more simplistic with far less consumption of time and effort due to the usage of magic labelling.

*1.3.1. Networking.* The primary hallmarks in networking are the functioning and optimization of the networks that demand management, construction, and concrete planning of networks at its base. Wireless and wired networking are two fundamental types of networking. The importance and large-scale usage of wired networking cannot be denied in the present era as well. The application of robust tools like network labelling is getting attention due to an escalation in the usage of wireless networking, in order to attain more precision in this field (see [38]). The modern era is of network communication whose part and parcel is radio transmission. The

interference, making the job of channel assignment more complicated, is one of the major concerns in radio transmission. The transmission of concurrent networks that are constraint-free, admitting same instance surfacing, is the central reason of this unwanted interruption [39,40]. The magic labelling assists in the allotment of constant weights to the networks that are concurrent. Such interferences are eliminated by using this procedure. The radio labelling on networks is playing a tremendous part in the reduction of interference issue in wireless networking from the last decade or so. For the automatic routing in networks, the ( $a, 0$ )-antimagic labelling is particularly very useful. In this regard, a suitable constant edge-weight function is designed on a particular network, which helps routing for automatic detection of the succeeding node in the network (see [41]).

*1.3.2. Telecommunication.* In modern era, telecommunication involves most successful application of network labelling commercially [42]. In network telecommunication, a utility coverage region is split into a polygonal area described as a cell. Such a cell serves as a separate station. Using its radio transceiver, the base cell is designed to be a hub with the capacity to interface with other mobile stations. The defiance task here for the base cell is to facilitate with the ability to re-use utmost channels, avoiding any violation of the constraints. This challenge is being tackled by assigning a label to each user, while the communication loop of this user acquires a distinct label. Resultantly, any pair of communication terminals identifies the link label of connection path automatically by simple use of graceful antimagic or magic labelling. The label of the path specifies uniquely the two users which it interlinks conversely (see [43]).

*1.3.3. Urban Planning.* Consider the wheel  $W_6$ , the helm  $H_6$ , and prism  $D_5$  in Figure 1 as a specific example. The edges of the networks  $W_6$  and  $H_6$  are labelled with consecutive labels ranging from 1 up to the size of the network such that the label appearing on all the vertices is distinct, i.e., we are provided here with the vertex antimagic labelling of the networks, whereas with edge weight 29 (constant), edge-magic labelling on  $D_5$  is given [44,45]. As an example, the chambers are identified by point (vertices) and admissible pathways to approach these chambers are identified by edges, in a surveillance design of highly secured building. A total disturbance in the labelling will occur if a person attempts to breach a single legal pathway. The magic constant, in the scenario of design like  $D_5$ , gets disordered promptly in case of violation in the pathway. This disorder, through programming software, will abruptly alert to the security concerned that the legitimate pathway has been breached. Once such magic or antimagic labellings are designed on a network, they can be used for surveillance of all the networks having the same hubs and connections. Antimagic and magic labelling both are equally valuable in this regard. In urban planning, this is one of the large-scale

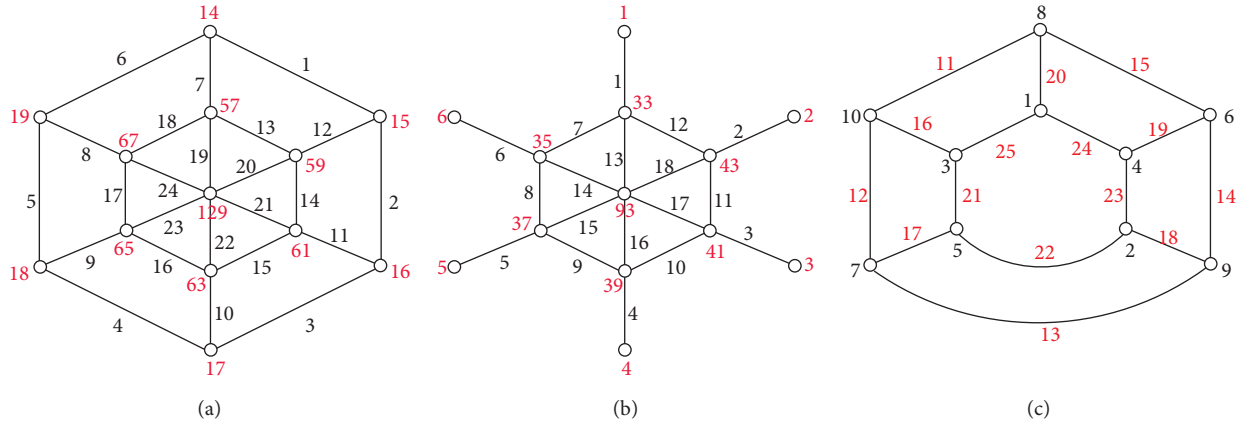


FIGURE 1: Vertex-antimagic total labelling of the wheel  $W_6$  and helm  $H_6$  and edge-magic labelling total of the prism  $D_5$  [44,45].

usages of the concept of labelling. That is, as a model for surveillance of the extensively secure areas, these labellings perform their distinct role [46].

**1.3.4. Robotics.** The routing and functioning of inducted robots at places like restaurants and factories in the form of production lines and machine units derive assistance by making use of any such suitable labelling function. In order to keep robotic components kinetic or make them stationary, these labelling functions assist to opt which operation to be skipped at which instant and vice versa. The antimagic labelling and distance-based dimensions alike tools help to minimize the time and maximize the accuracy of robots in their routing [47]. In the industry, these tools are causing a massive reduction in the cost.

## 2. Main Results

This section contains our main findings. It is divided into four subsections further. In Section 2.1, the S- $(a, 0)$ -EAM total labelling on the union of  $K_{2,m} \circ C_n$  with copies of paths, the star, and the path shall be designed, whereas in Section 2.2, we derive an S- $(a, 0)$ -EAM total labelling on the rooted product of network  $C_n$  and pancyclic networks  $H_1$  and  $H_2$  (planar also). Further, S- $(a, 0)$ -EAM total

labelling of planar pancyclic network  $\Gamma_n$  and symmetric lattice networks  $\mathbb{L}_n^1$ ,  $\mathbb{L}_n^2$ , and  $\mathbb{L}_n^3$  shall be exhibited in Sections 2.3 and 2.4, respectively.

**2.1. S- $(a, 0)$ -EAM Total Labelling of the Disjoint Union of  $C_n \circ K_{2,m}$  and  $P_n$ ,  $S_n$  and  $mP_2$ .** Our main motivation to explore the findings in this section is the following open problem of Ngurah et al. [48].

*Open Problem.* For  $n \geq 2$  and  $m \geq 3$ , is there any S- $(a, 0)$ -EAM total labelling of  $nK_{2,m}$ ?

In fact, the rooted product  $C_n \circ K_{2,m}$  contains  $n$  copies of the complete bipartite network  $K_{2,m}$ . A cycle  $C_n$  is a 2-regular network of order  $n$ , whereas the complete bipartite network  $K_{2,m}$  is class-wise regular in which one partitioned class of vertices is 2-regular and other is  $m$ -regular, where  $|V(K_{2,m})| = m + 2$ .

**Theorem 2.** For  $2 \leq m \equiv 0 \pmod{2}$  and  $3 \leq n \equiv 1 \pmod{2}$ , the network  $(C_n \circ K_{2,m}) \cup K_{1,n} \cup (n-1/2)K_1$  admits an S- $(a, 0)$ -EAM total labelling having  $a = 3mn + 8n + 2$ .

*Proof.* Consider the network  $G_1 \cong (C_n \circ K_{2,m}) \cup K_{1,n} \cup (n-1/2)K_1$  with connection scheme as below:

$$\begin{aligned}
 V(G_1) &= \{x_j^i : 1 \leq i \leq n, 1 \leq j \leq m\} \cup \{y_i, z_i : 1 \leq i \leq n\} \\
 &\quad \cup \{p_i : 1 \leq i \leq n\} \cup \{c_i : 1 \leq i \leq (n-1/2)\} \cup \{c\}, \\
 E(G_1) &= \{y_i x_j^i : 1 \leq i \leq n, 1 \leq j \leq m\} \\
 &\quad \cup \{z_i x_j^i : 1 \leq i \leq n, 1 \leq j \leq m\} \cup \{c p_i : 1 \leq i \leq n\} \\
 &\quad \cup \{y_i y_{i+1} : 1 \leq i \leq n-1\} \cup \{y_1 y_n\}.
 \end{aligned} \tag{1}$$

Here,  $|V(G_1)| = (7n + 2mn + 1/2)$  and  $|E(G_1)| = 2n(m + 1)$ . Define a labelling  $f_1: V(G_1) \rightarrow \{1, 2, \dots, (7n + 2mn + 1/2)\}$  as

(i) For  $m = 2$ :

$$f_1(x_j^i) = \begin{cases} \frac{5n+i}{2}, & j = 1, i \equiv 1 \pmod{2}, 1 \leq i \leq n, \\ \frac{4n+i}{2}, & j = 1, i \equiv 0 \pmod{2}, 2 \leq i \leq n-1, \\ n(m+2) - (i-1), & j = 2, 1 \leq i \leq n. \end{cases} \quad (2)$$

(ii) For  $m > 2$ :

$$f_1(x_j^i) = \begin{cases} \frac{5n+i}{2}, & j = \frac{m}{2}, i \equiv 1 \pmod{2}, 1 \leq i \leq n, \\ \frac{4n+i}{2}, & j = \frac{m}{2}, i \equiv 0 \pmod{2}, 2 \leq i \leq n-1, \\ n(m+2) - (i-1), & j = \frac{m}{2} + 1, 1 \leq i \leq n, \\ n(j+3) - (i-1), & 1 \leq i \leq n, 1 \leq j \leq \frac{m}{2} - 1. \\ nj - (i-1) + n: & 1 \leq i \leq n, \frac{m}{2} + 2 \leq j \leq m. \end{cases} \quad (3)$$

(iii) The remaining labels for  $m \geq 2$  are as follows:

$$f_1(y_i) = \begin{cases} \frac{i+2n+1}{2}, & i \equiv 1 \pmod{2}, 1 \leq i \leq n, \\ \frac{i+3n+1}{2}, & i \equiv 0 \pmod{2}, 2 \leq i \leq n-1, \end{cases}$$

$$f_1(z_i) = \begin{cases} n(m+1) + \frac{i+2n+1}{2}, & i \equiv 1 \pmod{2}, 1 \leq i \leq n, \\ n(m+1) + \frac{i+3n+1}{2}, & i \equiv 0 \pmod{2}, 2 \leq i \leq n-1. \end{cases} \quad (4)$$

$$f_1(p_i) = i, \quad 1 \leq i \leq n,$$

$$f_1(c) = \frac{7n+2mn+1}{2},$$

$$f_1(c_i) = mn + 3n + i, \quad 1 \leq i \leq \frac{n-1}{2}.$$



All edge sums generated by the labelling scheme  $f_1$  constitute a sequence of consecutive integer  $(5n + 3/2), (5n + 5/2), (5n + 7/2), \dots, (4mn + 9n + 1/2)$ . So, by Lemma 1,  $f_1$  extends to an  $S$ - $(a, 0)$ -EAM total labelling of the network  $G_1$  having magic constant  $a = 3mn + 8n + 2$ .

**Theorem 3.** For  $3 \leq m \equiv 1 \pmod{2}$  and  $3 \leq n \equiv 1 \pmod{2}$ , the network  $(C_n \circ K_{2,m}) \cup K_{1,n} \cup (n - 1/2)K_1$  admits an  $S$ - $(a, 0)$ -EAM total labelling with  $a = 3mn + 8n + 2$ .

*Proof.* Consider  $G_2 \cong (C_n \circ K_{2,m}) \cup K_{1,n} \cup (n - 1/2)K_1$ , a network with odd  $m$  as follows:

$$\begin{aligned} V(G_2) &= \{x_j^i: 1 \leq i \leq n, 1 \leq j \leq m\} \cup \{y_i, z_i: 1 \leq i \leq n\} \\ &\quad \cup \{p_i: 1 \leq i \leq n\} \cup \{c_i: 1 \leq i \leq (n - 1/2)\} \cup \{c\}, \\ E(G_2) &= \{y_i x_j^i: 1 \leq i \leq n, 1 \leq j \leq m\} \cup \{z_i x_j^i: 1 \leq i \leq n, 1 \leq j \leq m\} \cup \{c p_i: 1 \leq i \leq n\} \\ &\quad \cup \{y_i y_{i+1}: 1 \leq i \leq n - 1\} \cup \{y_1 y_n\}. \end{aligned} \tag{5}$$

Here,  $|V(G_2)| = (7n + 2mn + 1/2)$  and  $|E(G_2)| = 2n(m + 1)$ . We define a labelling  $f_2: V(G_2) \rightarrow \{1, 2, \dots, (7n + 2mn + 1/2)\}$  as follows:

(i) For  $m = 3$ :

$$f_2(x_j^i) = \begin{cases} \frac{5n+i}{2}, & j = 2, i \equiv 1 \pmod{2}, 1 \leq i \leq n, \\ \frac{4n+i}{2}, & j = 2, i \equiv 0 \pmod{2}, 2 \leq i \leq n - 1, \\ n(m+2) - (i-1), & j = 3, 1 \leq i \leq n, \\ 4n - (i-1), & j = 1, 1 \leq i \leq n. \end{cases} \tag{6}$$

(ii) For  $m > 3$ :

$$f_2(x_j^i) = \begin{cases} \frac{5n+i}{2}, & j = \frac{m+1}{2}, i \equiv 1 \pmod{2}, 1 \leq i \leq n, \\ \frac{4n+i}{2}, & j = \frac{m+1}{2}, i \equiv 0 \pmod{2}, 2 \leq i \leq n - 1, \\ n(m+2) - (i-1), & j = \frac{m+3}{2}, 1 \leq i \leq n, \\ n(j+3) - (i-1), & 1 \leq i \leq n, 1 \leq j \leq \frac{m-1}{2}. \\ nj - (i-1) + n, & 1 \leq i \leq n, \frac{m+5}{2} \leq j \leq m. \end{cases} \tag{7}$$

(iii) The remaining labels for  $m \geq 3$  are as follows:

$$\begin{aligned}
 f_2(y_i) &= \begin{cases} \frac{i+2n+1}{2}, & i \equiv 1 \pmod{2}, 1 \leq i \leq n, \\ \frac{i+3n+1}{2}, & i \equiv 0 \pmod{2}, 2 \leq i \leq n-1, \end{cases} \\
 f_2(z_i) &= \begin{cases} n(m+1) + \frac{i+2n+1}{2}, & i \equiv 1 \pmod{2}, 1 \leq i \leq n, \\ n(m+1) + \frac{i+3n+1}{2}, & i \equiv 0 \pmod{2}, 2 \leq i \leq n-1, \end{cases} \\
 f_2(p_i) &= i, \quad 1 \leq i \leq n, \\
 f_2(c) &= \frac{7n+2mn+1}{2}, \\
 f_2(c_i) &= mn+3n+i, \quad 1 \leq i \leq \frac{n-1}{2}.
 \end{aligned} \tag{8}$$

All edge sums generated by the above labelling scheme  $f_2$  constitute a sequence of consecutive integer  $(5n+3/2), (5n+5/2), (5n+7/2), \dots, (4mn+9n+1/2)$ . By Lemma 1,  $f_2$  extends to an  $S-(a, 0)$ -EAM total labelling of the network  $G_2$  having  $a = 3mn + 8n + 2$ .

**Theorem 4.** For  $2 \leq m \equiv 0 \pmod{2}$  and  $3 \leq n \equiv 1 \pmod{2}$ , the network  $(C_n \circ K_{2,m}) \cup nP_2$  admits an  $S-(a, 0)$ -EAM total labelling with  $a = (6mn + 17n + 3/2)$ .

*Proof.* Let  $G_3 \cong (C_n \circ K_{2,m}) \cup nP_2$  be a network for  $mn \equiv 1 \pmod{2}$  with vertices:

$$\begin{aligned}
 V(G_3) &= \{x_j^i: 1 \leq i \leq n, 1 \leq j \leq m\} \cup \{y_i, z_i: 1 \leq i \leq n\} \\
 &\quad \cup \{p_i, q_i: 1 \leq i \leq n\}, \\
 E(G_3) &= \{y_i x_j^i: 1 \leq i \leq n, 1 \leq j \leq m\} \cup \{z_i x_j^i: 1 \leq i \leq n, 1 \leq j \leq m\} \\
 &\quad \cup \{p_i q_i: 1 \leq i \leq n\} \\
 &\quad \cup \{y_i y_{i+1}: 1 \leq i \leq n-1\} \cup \{y_1 y_n\}.
 \end{aligned} \tag{9}$$

Here,  $|V(G_3)| = n(m+4)$  and  $|E(G_3)| = 2n(m+1)$ . A labelling function  $f_3: V(G_3) \rightarrow \{1, 2, \dots, n(m+4)\}$  is defined as follows:

(i) For  $m = 2$ :

$$f_3(x_j^i) = \begin{cases} \frac{1}{2}(5n+i), & j = 1, 1 \leq i \leq n, i \equiv 1 \pmod{2}, \\ \frac{1}{2}(4n+i), & j = 1, i \equiv 0 \pmod{2}, 2 \leq i \leq n-1, \\ n(m+2) - (i-1), & j = 2, 1 \leq i \leq n. \end{cases} \tag{10}$$

(ii) For  $m > 2$ :

$$f_3(x_j^i) = \begin{cases} \frac{1}{2}(5n+i), & j = \frac{m}{2}, i \equiv 1 \pmod{2}, 1 \leq i \leq n, \\ \frac{1}{2}(4n+i), & j = \frac{m}{2}, i \equiv 0 \pmod{2}, 2 \leq i \leq n-1, \\ n(m+2) - (i-1), & j = \frac{m}{2} + 1, 1 \leq i \leq n, \\ n(j+3) - (i-1), & 1 \leq i \leq n, 1 \leq j \leq \frac{m}{2} - 1. \\ nj - (i-1) + n: & 1 \leq i \leq n, \frac{m}{2} + 2 \leq j \leq m. \end{cases} \tag{11}$$

(iii) The remaining labels for  $m \geq 2$  are as follows:

$$f_3(y_i) = \begin{cases} \frac{i+2n+1}{2}, & i \equiv 1 \pmod{2}, 1 \leq i \leq n, \\ \frac{i+3n+1}{2}, & i \equiv 0 \pmod{2}, 2 \leq i \leq n-1, \end{cases}$$

$$f_3(z_i) = \begin{cases} n(m+1) + \frac{i+2n+1}{2}, & i \equiv 1 \pmod{2}, 1 \leq i \leq n, \\ n(m+1) + \frac{i+3n+1}{2}, & i \equiv 0 \pmod{2}, 2 \leq i \leq n-1. \end{cases}$$

$$f_3(q_i) = \begin{cases} n(m+1) + \frac{5n-i+2}{2}: & i \equiv 1 \pmod{2}, 1 \leq i \leq n, \\ n(m+1) + \frac{6n-i+2}{2}: & i \equiv 0 \pmod{2}, 2 \leq i \leq n-1, \end{cases}$$

$$f_3(p_i) = i, \quad 1 \leq i \leq n. \quad (12)$$

All edge sums generated by the above labelling scheme  $f_3$  constitute a sequence of consecutive integer  $(5n+3/2), (5n+5/2), (5n+7/2), \dots, (4mn+9n+1/2)$ . So, by Lemma 1,  $f_3$

extends to an  $S-(a, 0)$ -EAM total labelling of the network  $G_3$  admitting magic constant  $a = (6mn + 17n + 3/2)$ .

**Theorem 5.** For  $3 \leq m \equiv 1 \pmod{2}$  and  $3 \leq n \equiv 1 \pmod{2}$ , the network  $(C_n \circ K_{2,m}) \cup nP_2$  admits an  $S-(a, 0)$ -EAM total labelling with  $a = (6mn + 17n + 3/2)$ .

*Proof.* Consider the network  $G_4 \cong (C_n \circ K_{2,m}) \cup nP_2$ , for odd  $m$  with the construction:

$$V(G_4) = \{x_j^i: 1 \leq i \leq n, 1 \leq j \leq m\} \cup \{y_i, z_i: 1 \leq i \leq n\} \\ \cup \{p_i, q_i: 1 \leq i \leq n\},$$

$$E(G_4) = \{y_i x_j^i: 1 \leq i \leq n, 1 \leq j \leq m\} \\ \cup \{z_i x_j^i: 1 \leq i \leq n, 1 \leq j \leq m\} \cup \{p_i q_i: 1 \leq i \leq n\} \\ \cup \{y_i y_{i+1}: 1 \leq i \leq n-1\} \cup \{y_1 y_n\}. \quad (13)$$

Here,  $|V(G_4)| = n(m+4)$  and  $|E(G_4)| = 2n(m+1)$ . Define a function  $f_4: V(G_4) \rightarrow \{1, 2, \dots, n(m+4)\}$  as follows:

(i) For  $m = 3$ :

$$f_4(x_j^i) = \begin{cases} \frac{1}{2}(5n+i), & j = 2, i \equiv 1 \pmod{2}, 1 \leq i \leq n, \\ \frac{1}{2}(4n+i), & j = 2, i \equiv 0 \pmod{2}, 2 \leq i \leq n-1, \\ n(m+2) - (i-1), & j = 3, 1 \leq i \leq n, \\ 4n - (i-1), & j = 1, 1 \leq i \leq n. \end{cases} \quad (14)$$

(ii) For  $m > 3$ :

$$f_4(x_j^i) = \begin{cases} \frac{1}{2}(5n+i), & j = \frac{m+1}{2}, i \equiv 1 \pmod{2}, 1 \leq i \leq n, \\ \frac{1}{2}(4n+i), & j = \frac{m+1}{2}, i \equiv 0 \pmod{2}, 2 \leq i \leq n-1, \\ n(m+2) - (i-1), & j = \frac{m+3}{2}, 1 \leq i \leq n, \\ n(j+3) - (i-1), & 1 \leq i \leq n, 1 \leq j \leq \frac{m-1}{2}. \\ nj - (i-1) + n: & 1 \leq i \leq n, \frac{m+5}{2} \leq j \leq m. \end{cases} \quad (15)$$

(iii) The remaining labels for  $m \geq 3$  are as follows:

$$f_4(y_i) = \begin{cases} \frac{i+2n+1}{2}, & i \equiv 1 \pmod{2}, 1 \leq i \leq n, \\ \frac{i+3n+1}{2}, & i \equiv 0 \pmod{2}, 2 \leq i \leq n-1, \end{cases}$$

$$f_4(z_i) = \begin{cases} n(m+1) + \frac{i+2n+1}{2}, & i \equiv 1 \pmod{2}, 1 \leq i \leq n, \\ n(m+1) + \frac{i+3n+1}{2}, & i \equiv 0 \pmod{2}, 2 \leq i \leq n-1, \end{cases}$$

$$f_4(q_i) = \begin{cases} n(m+1) + \frac{5n-i+2}{2}, & i \equiv 1 \pmod{2}, 1 \leq i \leq n, \\ n(m+1) + \frac{6n-i+2}{2}, & i \equiv 0 \pmod{2}, 2 \leq i \leq n-1, \end{cases}$$

$$f_4(p_i) = i, \quad 1 \leq i \leq n. \tag{16}$$

All edge sums generated by the above labelling scheme  $f_4$  constitute a sequence of consecutive integer  $(5n+3/2), (5n+5/2), (5n+7/2), \dots, (4mn+9n+1/2)$ . So,

by Lemma 1,  $f_4$  extends to an S- $(a, 0)$ -EAM total labelling of the network  $G_4$  admitting  $a = (6mn+17n+3/2)$ .

**Theorem 6.** For  $2 \leq m \equiv 0 \pmod{2}$  and  $3 \leq n \equiv 1 \pmod{2}$ , the network  $(C_n \circ K_{2,m}) \cup P_{n+1}$  admits an S- $(a, 0)$ -EAM total labelling with  $a = (6mn+17n+3/2)$ .

*Proof.* Consider the network  $G_5 \cong (C_n \circ K_{2,m}) \cup P_{n+1}$ , for  $n \geq 3$  odd, with connections:

$$V(G_5) = \{x_j^i: 1 \leq i \leq n, 1 \leq j \leq m\} \cup \{y_i, z_i: 1 \leq i \leq n\} \cup \{p_i: 1 \leq i \leq n+1\},$$

$$E(G_5) = \{y_i x_j^i: 1 \leq i \leq n, 1 \leq j \leq m\} \cup \{z_i x_j^i: 1 \leq i \leq n, 1 \leq j \leq m\} \cup \{y_1 y_n\} \cup \{p_i p_{i+1}: 1 \leq i \leq n\} \cup \{y_i y_{i+1}: 1 \leq i \leq n-1\}. \tag{17}$$

Here,  $|V(G_5)| = 3n+mn+1$  and  $|E(G_5)| = 2n(m+1)$ . A labelling  $f_5: V(G_5) \rightarrow \{1, 2, \dots, mn+3n+1\}$  is defined as follows:

(i) For  $m = 2$ :

$$f_5(x_j^i) = \begin{cases} \frac{1}{2}(4n+i+1), & j=1, i \equiv 1 \pmod{2}, 1 \leq i \leq n, \\ \frac{1}{2}(3n+i+1), & j=1, i \equiv 0 \pmod{2}, 2 \leq i \leq n-1, \\ \frac{1}{2}(2mn+3n-2i+3), & j=2, 1 \leq i \leq n. \end{cases} \tag{18}$$

(ii) For  $m > 2$ :

$$f_5(x_j^i) = \begin{cases} \frac{1}{2}(4n+i+1), & j = \frac{m}{2}, i \equiv 1 \pmod{2}, 1 \leq i \leq n, \\ \frac{1}{2}(3n+i+1), & j = \frac{m}{2}, i \equiv 0 \pmod{2}, 2 \leq i \leq n-1, \\ \frac{1}{2}(2mn+3n-2i+3), & j = \frac{m}{2} + 1, 1 \leq i \leq n, \\ \frac{1}{2}(2nj+5n-2i+3), & 1 \leq i \leq n, 1 \leq j \leq \frac{m}{2} - 1, \\ \frac{1}{2}(2nj+n-2i+3): & 1 \leq i \leq n, \frac{m}{2} + 2 \leq j \leq m. \end{cases} \tag{19}$$

(iii) The remaining labels for  $m \geq 2$  are as follows:

$$f_5(y_i) = \begin{cases} \frac{n+i+2}{2}, & i \equiv 1 \pmod{2}, 1 \leq i \leq n, \\ \frac{2n+i+2}{2}, & i \equiv 0 \pmod{2}, 2 \leq i \leq n-1, \end{cases}$$

$$f_5(z_i) = \begin{cases} n(m+1) + \frac{n+i+2}{2}, & i \equiv 1 \pmod{2}, 1 \leq i \leq n, \\ n(m+1) + \frac{2n+i+2}{2}, & i \equiv 0 \pmod{2}, 2 \leq i \leq n-1, \end{cases}$$

$$f_5(p_i) = \begin{cases} \frac{i+1}{2}, & i \equiv 1 \pmod{2}, 1 \leq i \leq n, \\ \frac{1}{2}(2mn+5n+i+1), & i \equiv 0 \pmod{2}, 2 \leq i \leq n+1. \end{cases} \tag{20}$$

All edge sums generated by the above labelling scheme  $f_5$  constitute a sequence of consecutive integer  $(3n+5/2), (3n+7/2), (3n+9/2), \dots, (4mn+7n+3/2)$ . Therefore, by Lemma 1,  $f_5$  extends to an S- $(a, 0)$ -EAM total labelling of

the network  $G_5$  admitting magic constant  $a = (6mn + 13n + 7/2)$ .

**Theorem 7.** For  $3 \leq m \equiv 1 \pmod{2}$  and  $3 \leq n \equiv 1 \pmod{2}$ , the network  $(C_n \circ K_{2,m}) \cup P_{n+1}$  admits an S- $(a, 0)$ -EAM total labelling with  $a = (6mn + 13n + 7/2)$ .

*Proof.* Consider the network  $G_6 \cong (C_n \circ K_{2,m}) \cup P_{n+1}$ , for both  $m$  and  $n \geq 3$ , as follows:

$$V(G_6) = \{x_j^i: 1 \leq i \leq n, 1 \leq j \leq m\} \cup \{y_i, z_i: 1 \leq i \leq n\} \cup \{p_i: 1 \leq i \leq n+1\},$$

$$E(G_6) = \{y_i x_j^i: 1 \leq i \leq n, 1 \leq j \leq m\} \tag{21}$$

$$\cup \{z_i x_j^i: 1 \leq i \leq n, 1 \leq j \leq m\} \cup \{y_1 y_n\}$$

$$\cup \{p_i p_{i+1}: 1 \leq i \leq n\} \cup \{y_i y_{i+1}: 1 \leq i \leq n-1\}.$$

Here,  $|V(G_6)| = 3n + mn + 1$  and  $|E(G_6)| = 2n(m+1)$ . A labelling  $f_6: V(G_6) \rightarrow \{1, 2, \dots, 3n + mn + 1\}$  is designed as follows:

(i) For  $m = 3$ :

$$f_6(x_j^i) = \begin{cases} \frac{1}{2}(4n+i+1), & j = 2, i \equiv 1 \pmod{2}, 1 \leq i \leq n, \\ \frac{1}{2}(3n+i+1), & j = 2, i \equiv 0 \pmod{2}, 2 \leq i \leq n-1, \\ \frac{1}{2}(2mn+3n-2i+3), & j = 3, 1 \leq i \leq n, \\ \frac{1}{2}(7n-2i+3), & j = 1, 1 \leq i \leq n. \end{cases} \tag{22}$$

(ii) For  $m > 3$ :

$$f_6(x_j^i) = \begin{cases} \frac{1}{2}(4n+i+1), & j = \frac{m+1}{2}, i \equiv 1 \pmod{2}, 1 \leq i \leq n, \\ \frac{1}{2}(3n+i+1), & j = \frac{m+1}{2}, i \equiv 0 \pmod{2}, 2 \leq i \leq n-1, \\ \frac{1}{2}(2mn+3n-2i+3), & j = \frac{m+3}{2}, 1 \leq i \leq n, \\ \frac{1}{2}(2nj+5n-2i+3), & 1 \leq i \leq n, 1 \leq j \leq \frac{m-1}{2}, \\ \frac{1}{2}(2nj+n-2i+3), & 1 \leq i \leq n, \frac{m+5}{2} \leq j \leq m. \end{cases} \tag{23}$$

(iii) The remaining labels for  $m \geq 3$  are as follows:

$$\begin{aligned}
 f_6(y_i) &= \begin{cases} \frac{n+i+2}{2}, & i \equiv 1 \pmod{2}, 1 \leq i \leq n, \\ \frac{2n+i+2}{2}, & i \equiv 0 \pmod{2}, 2 \leq i \leq n-1, \end{cases} \\
 f_6(z_i) &= \begin{cases} n(m+1) + \frac{n+i+2}{2}, & i \equiv 1 \pmod{2}, 1 \leq i \leq n, \\ n(m+1) + \frac{2n+i+2}{2}, & i \equiv 0 \pmod{2}, 2 \leq i \leq n-1, \end{cases} \\
 f_6(p_i) &= \begin{cases} \frac{i+1}{2}, & i \equiv 1 \pmod{2}, 1 \leq i \leq n, \\ \frac{1}{2}(2mn+5n+i+1), & i \equiv 0 \pmod{2}, 2 \leq i \leq n+1. \end{cases}
 \end{aligned} \tag{24}$$

The edge sums generated by the above labelling scheme  $f_6$  constitute a sequence of consecutive integer  $(3n+5/2), (3n+7/2), (3n+9/2), \dots, (4mn+7n+3/2)$ . By Lemma 1,  $f_6$  extends to an  $S-(a,0)$ -EAM total labelling of the network  $G_6$  having magic constant  $a = (6mn+13n+7/2)$ .

*Observations.* The network  $C_n$  is  $S-(a,0)$ -EAM total for  $n \equiv 1 \pmod{2}$  only [8], pointing out that  $C_4$  is not  $S-(a,0)$ -EAM total. The networks in Theorems 2, 4, and 6 contain interesting substructures. Keeping  $m = 2$  fixed for these results,  $S-(a,0)$ -EAM total families of networks involving  $n$  copies of  $C_4$  can be obtained. For instance,  $S-(a,0)$ -EAM total labelling (again by using Lemma 1) of  $(C_5 \circ C_4) \cup K_{1,5} \cup 2K_1, (C_5 \circ C_4) \cup 5P_2$ , and  $(C_5 \circ C_4) \cup P_6$  is presented in Figure 2.

The following results from Theorems 2–7 are direct consequences of Theorem 1.

**Theorem 8.**  $\forall m \geq 2$  and  $3 \leq n \equiv 1 \pmod{2}$ ,  $(C_n \circ K_{2,m}) \cup K_{1,n} \cup (n-1/2)K_1$  admits an  $S-(mn+6n+3,2)$ -EAM total labelling.

**Theorem 9.**  $\forall m \geq 2$  and  $3 \leq n \equiv 1 \pmod{2}$ ,  $(C_n \circ K_{2,m}) \cup nP_2$  admits an  $S-((2mn+13n+5/2),2)$ -EAM total labelling.

**Theorem 10.**  $\forall m \geq 2$  and  $3 \leq n \equiv 1 \pmod{2}$ ,  $(C_n \circ K_{2,m}) \cup P_{n+1}$  admits an  $S-((2mn+9n+9/2),2)$ -EAM total labelling.

**2.2.  $S-(a,0)$ -EAM Total Labelling of Rooted Product of Pancyclic Networks with  $C_n$ .** The present section deals with

$S-(a,0)$ -EAM total labelling of the rooted product of two specific planar non-isomorphic pancyclic networks and the cycle  $C_n$ .

A specific pancyclic network  $H_1$  is defined as follows.

*Definition 5.*  $H_1$  is a pancyclic network having the following construction.

$$\begin{aligned}
 V(H_1) &= \{y, x_1, x_2, x_3, x_4, x_5, x_6, z\}, \\
 E(H_1) &= \{x_1x_3, x_3x_5, x_2x_4, x_4x_6, x_1x_2, \\
 &\quad \cdot x_3x_4, x_5x_6, x_2x_3, x_4x_5\} \cup \{yx_1, yx_2, zx_5, zx_6\}.
 \end{aligned} \tag{25}$$

**Theorem 11.** For  $n \equiv 1 \pmod{2}$ , the rooted product  $C_n \circ H_1$  admits an  $S-(a,0)$ -EAM total labelling having magic constant  $a = (45n+3/2)$ .

*Proof*

(i) For  $n = 1$ ,  $C_1 \circ H_1 \cong H_1$ . The vertex labelling  $\{y, x_1, x_2, x_3, x_4, x_5, x_6, y, z: 2, 1, 4, 3, 6, 5, 8, 7\}$  extends to an  $S-(24,0)$ -EAM total labelling of  $C_n \circ H_1$ , by Lemma 1.

(ii) For  $n \geq 3$ .

Consider the network  $C_n \circ H_1$  with  $|V(C_n \circ H_1)| = 8n$  and  $|E(C_n \circ H_1)| = 14n$  connected as per the following scheme:

$$\begin{aligned}
 V(C_n \circ H_1) &= \{x_i, v_i: 1 \leq i \leq n\} \cup \{y_i, z_i, w_i: 1 \leq i \leq 2n\}, \\
 E(C_n \circ H_1) &= \{y_i y_{i+1}, w_i w_{i+1}, z_i z_{i+1}: 1 \leq i \leq 2n-1, i \equiv 1 \pmod{2}\} \\
 &\quad \cup \{y_i z_i, z_i w_i: 1 \leq i \leq 2n\} \cup \{x_i x_{i+1}: 1 \leq i \leq n-1\} \\
 &\quad \cup \{x_1 x_n\} \cup \{z_i y_{i+1}, w_i z_{i+1}: 1 \leq i \leq 2n-1, i \equiv 1 \pmod{2}\} \\
 &\quad \cup \{x_i y_{2i-1}, x_i y_{2i}, v_i w_{2i-1}, v_i w_{2i}: 1 \leq i \leq n\}.
 \end{aligned} \tag{26}$$

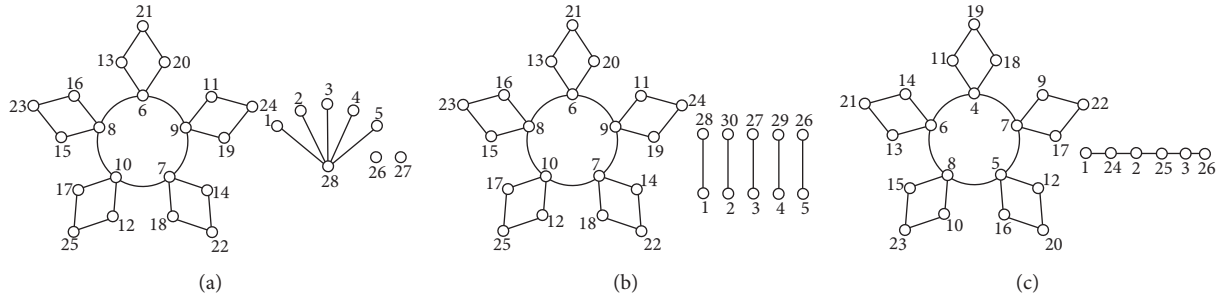


FIGURE 2: An  $S$ -( $a, 0$ )-EAM total labelling (using Lemma 1) of the cyclic networks (a)  $(C_5 \circ C_4) \cup K_{1,5} \cup 2K_1$ , (b)  $(C_5 \circ C_4) \cup 5P_2$ , and (c)  $(C_5 \circ C_4) \cup P_6$ .

Consider a labelling  $\psi_1: V(C_n \circ H_1) \longrightarrow \{1, 2, \dots, |V(C_n \circ H_1)| = 8n\}$  defined as

$$\begin{aligned}
 \psi_1(x_i) &= \begin{cases} \frac{i+1}{2}, & i \equiv 1 \pmod{2}, 1 \leq i \leq n, \\ \frac{i+n+1}{2}, & i \equiv 0 \pmod{2}, 2 \leq i \leq n-1, \end{cases} \\
 \psi_1(y_i) &= \begin{cases} \frac{6n-i+2}{2}, & i \equiv 0 \pmod{2}, 2 \leq i \leq 2n, \\ \frac{6n+i+1}{4}, & i \equiv 1 \pmod{4}, 1 \leq i \leq 2n-1, \\ \frac{4n+i+1}{4}, & i \equiv 3 \pmod{4}, 3 \leq i \leq 2n-3, \end{cases} \\
 \psi_1(z_i) &= \begin{cases} \frac{16n+i}{4}, & i \equiv 0 \pmod{4}, 4 \leq i \leq 2n-2, \\ \frac{12n+i+3}{4}, & i \equiv 1 \pmod{4}, 1 \leq i \leq 2n-1, \\ \frac{18n+i}{4}, & i \equiv 2 \pmod{4}, 2 \leq i \leq 2n, \\ \frac{14n+i+3}{4}, & i \equiv 3 \pmod{4}, 3 \leq i \leq 2n-3, \end{cases} \\
 \psi_1(w_i) &= \begin{cases} \frac{12n-i+1}{2}, & i \equiv 1 \pmod{2}, 1 \leq i \leq 2n-1, \\ \frac{26n+i+2}{4}, & i \equiv 0 \pmod{4}, 4 \leq i \leq 2n-2, \\ \frac{24n+i+2}{4}, & i \equiv 2 \pmod{4}, 2 \leq i \leq 2n, \end{cases} \\
 \psi_1(v_i) &= \begin{cases} \frac{15n+i}{2}, & i \equiv 1 \pmod{2}, 1 \leq i \leq n, \\ \frac{14n+i}{2}, & i \equiv 0 \pmod{2}, 2 \leq i \leq n-1. \end{cases}
 \end{aligned} \tag{27}$$

All edge sums generated by the above labelling scheme  $\psi_1$  form a sequence of consecutive integer  $(n + 3/2), (n + 5/2), (n + 7/2), \dots, (29n + 1/2)$ . Therefore, by Lemma 1,  $\psi_1$  extends to an S- $(a, 0)$ -EAM total labelling of the network  $C_n \circ H_1$  having magic constant  $(45n + 3/2)$ .

*Definition 6.* We define a pancyclic network  $H_2 \neq H_1$  having vertex set:

$$\begin{aligned} V(H_2) &= \{y, x_1, x_2, x_3, x_4, x_5, x_6, z\}, \\ E(H_2) &= \{x_1x_3, x_3x_5, x_2x_4, x_4x_6, x_1x_2, x_5x_6, x_2x_3, x_4x_5\} \cup \{yx_1, yx_2, zx_5, zx_6, yz\}. \end{aligned} \tag{28}$$

**Theorem 12.** For  $n \equiv 1 \pmod{2}$ , the rooted product  $C_n \circ H_2$  admits an S- $(a, 0)$ -EAM total labelling with magic constant  $a = (45n + 3/2)$ .

*Proof*

- (i) For  $n = 1$ ,  $C_1 \circ H_2 \cong H_2$ .
- (ii) For  $n \geq 3$ .

Consider  $C_n \circ H_2$  with  $|V(C_n \circ H_2)| = 8n$  and  $|E(C_n \circ H_2)| = 14n$  with the following connection:

$$\begin{aligned} V(C_n \circ H_2) &= \{x_i, v_i: 1 \leq i \leq n\} \cup \{w_i, y_i, z_i: 1 \leq i \leq 2n\}, \\ E(P_n \circ H_2) &= \{y_i y_{i+1}, w_i w_{i+1}: 1 \leq i \leq 2n - 1, i \equiv 1 \pmod{2}\} \\ &\cup \{y_i z_i, z_i w_i: 1 \leq i \leq 2n\} \cup \{x_i x_{i+1}: 1 \leq i \leq n - 1\} \cup \{x_1 x_n\} \\ &\cup \{z_i y_{i+1}, w_i z_{i+1}: 1 \leq i \leq 2n - 1, i \equiv 1 \pmod{2}\} \\ &\cup \{x_i y_{2i-1}, x_i y_{2i}, v_i w_{2i-1}, v_i w_{2i}, x_i v_i: 1 \leq i \leq n\}. \end{aligned} \tag{29}$$

The labelling scheme for  $n = 1$  and  $n \geq 3$  is the same as  $\psi_1$  designed in Theorem 11.

A direct derivation from Theorem 1 is given as follows.

**Theorem 13.** For  $n \equiv 1 \pmod{2}$ ,  $C_n \circ H_1$  and  $C_n \circ H_2$  are S- $((17n + 5/2), 2)$ -EAM total.

2.3. S- $(a, 0)$ -EAM Total Labelling of a Pancyclic Class of Networks: Extension of a Result Appearing in [29]. In [29], Baig et al. provided a result regarding S- $(a, 0)$ -EAM total labelling of a pancyclic class of networks involving chains of cycle  $C_4$ . Here, we shall introduce a pancyclic family of networks involving chains of cycle  $C_6$ , while our point of convergence is the S- $(a, 0)$ -EAM total labelling of this class. Thus, we further extend the results of Baig et al. [29].

*Definition 7.* The pancyclic network  $\Gamma_n$  is a network with order  $|V(\Gamma_n)| = 6n$  and  $|E(\Gamma_n)| = 12n - 3$ , with structure as follows:

$$\begin{aligned} V(\Gamma_n) &= \{z_i, x_i, y_i: 1 \leq i \leq 2n\}, \\ E(\Gamma_n) &= \{y_i y_{i+1}, x_i x_{i+1}, z_i z_{i+1}: 1 \leq i \leq 2n - 1\} \cup \{x_i y_i, x_i z_i, y_i z_i: 1 \leq i \leq 2n\}. \end{aligned} \tag{30}$$

Figure 3 reveals general formation of  $\Gamma_n$ .

In Figure 4, we have shown the network  $\Gamma_2$  and its contained cycles of orders 3, 4, ..., 12.

In the upcoming result, we show that the pancyclic network  $\Gamma_n$  is S- $(a, 0)$ -EAM total.

**Theorem 14.** For all positive integers  $n$ , the pancyclic network  $\Gamma_n$  is S- $(a, 0)$ -EAM total having magic constant  $18n$ .

*Proof*

- (i) For  $n=1$ , the labelling  $\{z_1, z_2, x_1, x_2, y_1, y_2: 3, 5, 2, 4, 1, 6\}$  extends to an S- $(18, 0)$ -EAM total labelling of  $\Gamma_1$  by Lemma 1.
- (ii) For  $n \geq 3$ .

Define here a labelling  $g: V(\Gamma_n) \rightarrow \{1, 2, \dots, 6n\}$  as

$$\begin{aligned} g(x_i) &= \begin{cases} 3i: i \equiv 1 \pmod{2}, & 1 \leq i \leq 2n - 1, \\ 3i - 1: i \equiv 0 \pmod{2}, & 2 \leq i \leq 2n, \end{cases} \\ g(y_i) &= \begin{cases} 3i - 2: i \equiv 1 \pmod{2}, & 1 \leq i \leq 2n - 1, \\ 3i: i \equiv 0 \pmod{2}, & 2 \leq i \leq 2n, \end{cases} \\ g(z_i) &= \begin{cases} 3i - 1: i \equiv 1 \pmod{2}, & 1 \leq i \leq 2n - 1, \\ 3i - 2: i \equiv 0 \pmod{2}, & 2 \leq i \leq 2n. \end{cases} \end{aligned} \tag{31}$$

All edge sums generated by the above labelling scheme constitute a sequence of consecutive integers  $3, 4, \dots, 12n - 1$ . Therefore, by Lemma 1,  $g$  extends to an S- $(a, 0)$ -EAM total labelling of  $\Gamma_n$  having magic constant  $a = 18n$ .

Again from Theorem 1, we have a direct consequence as follows.

**Theorem 15.** For all positive integers  $n$ , the pancyclic network  $\Gamma_n$  admits an S- $(6n + 4, 2)$ -EAM total labelling.



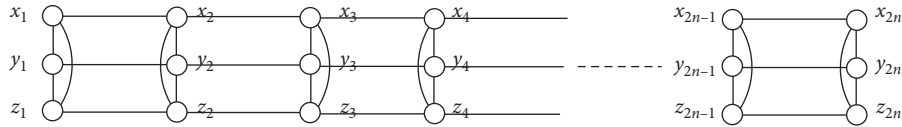


FIGURE 3: The general formation of the pancyclic network  $\Gamma_n$ .

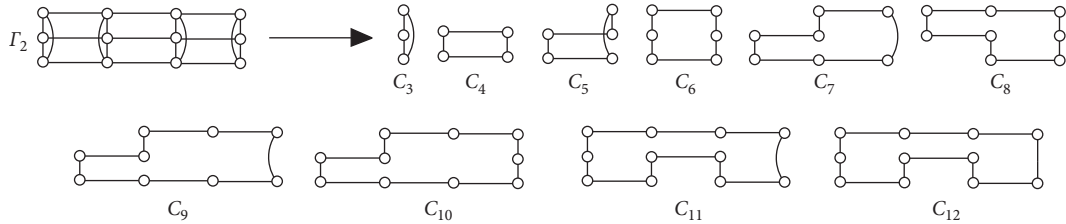


FIGURE 4: The network  $\Gamma_2$  having order 12 and its contained cycles  $C_3, C_4, \dots, C_{12}$ .

2.4. S-(a,0)-EAM Total Labelling of Symmetric Lattice Networks

Definition 8. Consider a tripartite network  $\mathbb{T}$  having vertex-edge connections as follows:

$$\begin{aligned} V(\mathbb{T}) &= \{x, y, z, u, v, w\}, \\ E(\mathbb{T}) &= \{uv, vw, xy, yz, uy, wy, xv, zv, vy\}. \end{aligned} \tag{32}$$

In this section, we study the S-(a,0)-EAM total labelling of symmetric lattice networks  $\mathbb{L}_n^1, \mathbb{L}_n^2$ , and  $\mathbb{L}_n^3$ . These symmetric lattices contain  $n$  copies of the tripartite network  $\mathbb{T}$ .

Definition 9

- (i) For  $n = 1, \mathbb{L}_1^1 \cong \mathbb{T}$ .
- (ii) For  $n \geq 2$ .

The lattice network  $\mathbb{L}_n^1$  is a network with order  $6n$  and size  $12n - 3$  defined as follows:

$$\begin{aligned} V(\mathbb{L}_n^1) &= \{x_i, y_i, c_i: 1 \leq i \leq 2n\}. \\ E(\mathbb{L}_n^1) &= \{c_i y_{i+1}, c_i x_{i+1}, c_i y_i, c_i x_i: 1 \leq i \leq 2n - 1, i \equiv 1 \pmod{2}\} \\ &\cup \{c_i c_{i+1}: 2 \leq i \leq 2n - 1\} \cup \{x_i x_{i+1}, y_i y_{i+1}: i \equiv 0 \pmod{2}, 2 \leq i \leq 2(n - 1)\}, \\ &\cup \{c_i y_{i-1}, c_i x_{i-1}, c_i y_i, c_i x_i: i \equiv 0 \pmod{2}, 2 \leq i \leq 2n\}. \end{aligned} \tag{33}$$

Figure 5 illustrates the general formation of the lattice network  $\mathbb{L}_n^1, \forall n \in \mathbb{N}$ .

Theorem 16. For all positive integers  $n$ , the lattice network  $\mathbb{L}_n^1$  is S-(a,0)-EAM total having magic constant  $18n$ .

Proof

- (i) For  $n = 1$ : the vertex labelling  $\{x_1, c_1, y_1, x_2, c_2, y_2: 3, 1, 2, 5, 6, 4\}$  extends to an S-(18,0)-EAM total labelling of  $\mathbb{L}_1^1$ , by Lemma 1.
- (ii) For  $n > 1$ .

We are defining a labelling  $\varphi_1: V(\mathbb{L}_n^1) \longrightarrow \{1, 2, \dots, 6n\}$  as follows:

$$\begin{aligned} \varphi_1(x_i) &= \begin{cases} 3i: i \equiv 1 \pmod{2}, & 1 \leq i \leq 2n - 1, \\ 3i - 1: i \equiv 0 \pmod{2}, & 2 \leq i \leq 2n, \end{cases} \\ \varphi_1(y_i) &= \begin{cases} 3i - 1: i \equiv 1 \pmod{2}, & 1 \leq i \leq 2n - 1, \\ 3i - 2: i \equiv 0 \pmod{2}, & 2 \leq i \leq 2n, \end{cases} \\ \varphi_1(c_i) &= \begin{cases} 3i - 2: i \equiv 1 \pmod{2}, & 1 \leq i \leq 2n - 1, \\ 3i: i \equiv 0 \pmod{2}, & 2 \leq i \leq 2n. \end{cases} \end{aligned} \tag{34}$$

All edge sums generated by the above labelling scheme constitute a sequence of consecutive integers  $3, 4, \dots, 12n - 3$ . So, by Lemma 1,  $\varphi_1$  extends to an S-(a,0)-EAM total labelling of  $\mathbb{L}_n^1$  admitting magic constant  $18n$ .

Definition 10

- (i) For  $n = 1, \mathbb{L}_1^2 \cong \mathbb{T}$ .
- (ii) For  $n \geq 2$ .

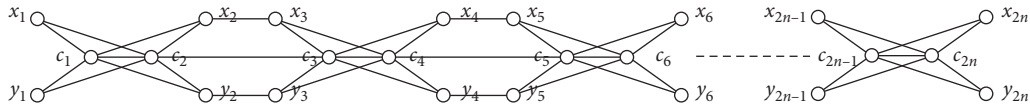


FIGURE 5: The general formation of the lattice network  $\mathbb{L}_n^1, \forall n \in \mathbb{N}$ .

The lattice network  $\mathbb{L}_n^2$  having order  $10n - 4$  and size  $20n - 11$  is defined as follows:

$$\begin{aligned}
 V(\mathbb{L}_n^2) &= \{x_i, y_i: 1 \leq i \leq 2n\} \cup \{c_i: 1 \leq i \leq 2(2n - 1)\} \cup \{u_i, v_i: 1 \leq i \leq n - 1\}. \\
 E(\mathbb{L}_n^2) &= \{c_i y_{i+2/2}, c_i x_{i+2/2}, c_i y_{i/2}, c_i x_{i/2}: 2 \leq i \leq 2(2n - 1), i \equiv 2 \pmod{4}\} \\
 &\cup \{c_i y_{i+2/2}, c_i y_{i+3/2}, c_i x_{i+2/2}, c_i x_{i+3/2}: i \equiv 1 \pmod{4}, 1 \leq i \leq 4n - 3\} \\
 &\cup \{c_i c_{i+1}: 1 \leq i \leq 4n - 3, i \equiv 1 \pmod{4}\} \cup \{u_i v_i: 1 \leq i \leq n - 1\} \\
 &\cup \{x_i u_{i/2}, y_i v_{i/2}: 2 \leq i \leq 2(n - 1), i \equiv 0 \pmod{2}\} \\
 &\cup \{u_i x_{2i+1}, v_i y_{2i+1}, u_i c_{4i-1}, v_i c_{4i-1}, u_i c_{4i}, v_i c_{4i}: 1 \leq i \leq n - 1\} \\
 &\cup \{c_i c_{i+1}: i \equiv 0 \pmod{2}, 2 \leq i \leq 4(n - 1)\}.
 \end{aligned} \tag{35}$$

In Figure 6, we have presented the general formation of the lattice network  $\mathbb{L}_n^2, \forall n \in \mathbb{N}$ .

**Theorem 17.** For all positive integers  $n$ , the lattice network  $\mathbb{L}_n^2$  is  $S-(a, 0)$ -EAM total with magic constant  $30n - 12$ .

*Proof*

- (i) For  $n = 1$ : the vertex labelling  $\{x_1, c_1, y_1, x_2, c_2, y_2: 3, 1, 2, 5, 6, 4\}$  extends to an  $S-(18, 0)$ -EAM total labelling of  $\mathbb{L}_1^2$ , by Lemma 1.
- (ii) For  $n > 1$ .

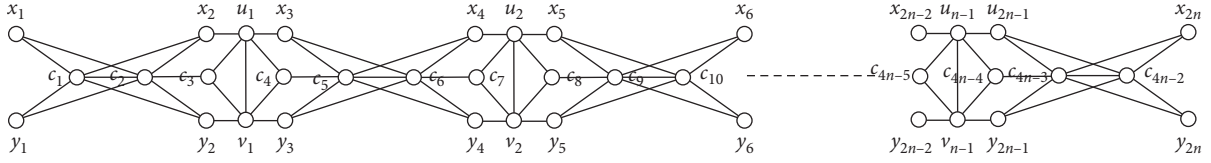
A labelling  $\varphi_2: V(\mathbb{L}_n^2) \rightarrow \{1, 2, \dots, 10n - 4\}$  is defined as follows:

$$\begin{aligned}
 \varphi_2(x_i) &= \begin{cases} 5i - 2: i \equiv 1 \pmod{2}, & 1 \leq i \leq 2n - 1, \\ 5i - 5: i \equiv 0 \pmod{2}, & 2 \leq i \leq 2n, \end{cases} \\
 \varphi_2(y_i) &= \begin{cases} 5i - 3: i \equiv 1 \pmod{2}, & 1 \leq i \leq 2n - 1, \\ 5i - 6: i \equiv 0 \pmod{2}, & 2 \leq i \leq 2n, \end{cases} \\
 \varphi_2(c_i) &= \begin{cases} \frac{1}{2}(5i - 3): 1 \leq i \leq 4n - 3, & i \equiv 1 \pmod{4}, \\ \frac{1}{2}(5i + 2): 2 \leq i \leq 4n - 2, & i \equiv 2 \pmod{4}, \\ \frac{1}{2}(5i - 1): 3 \leq i \leq 4n - 5, & i \equiv 3 \pmod{4}, \\ \frac{1}{2}(5i): 4 \leq i \leq 4(n - 1), & i \equiv 0 \pmod{4}, \end{cases} \\
 \varphi_2(u_i) &= 10i - 1, \quad 1 \leq i \leq n - 1, \\
 \varphi_2(v_i) &= 10i - 2, \quad 1 \leq i \leq n - 1.
 \end{aligned} \tag{36}$$

All edge sums generated by the above labelling scheme constitute a sequence of consecutive integers  $3, 4, \dots, 20n - 9$ . So, by Lemma 1,  $\varphi_2$  extends to an  $S-(a, 0)$ -EAM total labelling of  $\mathbb{L}_n^2$  having magic constant  $30n - 12$ .

*Definition 11*

- (i) For  $n = 1, \mathbb{L}_1^3 \cong \mathbb{T}$ .
- (ii) For  $n \geq 2$ .

FIGURE 6: The general formation of the lattice network  $\mathbb{L}_n^2, \forall n \in \mathbb{N}$ .

The lattice network  $\mathbb{L}_n^3$  having order  $10n - 4$  and size  $20n - 11$  is defined as follows:

$$\begin{aligned}
 V(\mathbb{L}_n^3) &= \{x_i, y_i: 1 \leq i \leq 2n\} \cup \{c_i: 1 \leq i \leq 2(2n - 1)\} \cup \{u_i, v_i: 1 \leq i \leq n - 1\}, \\
 E(\mathbb{L}_n^3) &= \{c_i y_{i+2/2}, c_i x_{i+2/2}, c_i y_{i/2}, c_i x_{i/2}: 2 \leq i \leq 2(2n - 1), i \equiv 2 \pmod{4}\} \\
 &\cup \{c_i y_{i+2/2}, c_i y_{i+3/2}, c_i x_{i+1/2}, c_i x_{i+3/2}: 1 \leq i \leq 4n - 3, i \equiv 1 \pmod{4}\} \\
 &\cup \{x_i u_{i/2}, y_i v_{i/2}: i \equiv 0 \pmod{2}, 2 \leq i \leq 2(n - 1)\} \cup \{c_i c_{i+1}: 1 \leq i \leq 4n - 3\} \\
 &\cup \{u_i x_{2i+1}, v_i y_{2i+1}, u_i c_{4i-1}, v_i c_{4i-1}, u_i c_{4i}, v_i c_{4i}: 1 \leq i \leq n - 1\}.
 \end{aligned} \tag{37}$$

Figure 7 illustrates the general form of the lattice network  $\mathbb{L}_n^3, \forall n \in \mathbb{N}$ .

**Theorem 18.** For all positive integers  $n$ , the lattice network  $\mathbb{L}_n^3$  is  $S$ -( $a, 0$ )-EAM total with magic constant  $30n - 12$ .

*Proof.* For  $\mathbb{L}_n^3$ , the labelling design is similar as in Theorem 17.

### 3. Illustration through Examples and Proposed Open Problems

**3.1. Examples.** The  $S$ -(132, 0)-EAM total labelling of  $(C_5 \circ K_{2,6}) \cup K_{1,5} \cup 2K_1$  and  $S$ -(163, 0)-EAM total labelling of  $(C_7 \circ K_{2,5}) \cup K_{1,7} \cup 3K_1$  are presented, respectively, in Figures 8(a) and 8(b). In Figure 8(a), the parameters are  $\{n = 5, m = 6\}$  and  $a = 132$ , while in Figure 8(b), the parameters are  $\{n = 7, m = 5\}$  and  $a = 163$ . These are perfect according to our depiction of the magic constants in the proofs of Theorems 2 and 3.

Similarly, Figures 9 and 10 illustrate Theorems 4 and 5 and Theorems 6 and 7, respectively, for the values of the parameters given in each. The values of  $a$  here are perfectly similar as depicted in our main findings.

Figures 11(a) and 11(b) illustrate Theorems 11 and 12, respectively, for  $n = 5$ .

Figure 12 reveals an example of Theorem 15 corresponding to parameter  $n = 3$ .

Figures 13–15 refer to the illustration of  $S$ -( $a, 0$ )-EAM total labelling of lattice networks  $\mathbb{L}_5^1, \mathbb{L}_4^2$ , and  $\mathbb{L}_4^3$  (Theorems 16–18).

Due to facilitation of Lemma 1, edge labels are not needed to be provided in all of the above illustrative figures. As the edge sums constitute a sequence of +ve consecutive integers, assigning the remaining labels  $\{q, q - 1, \dots, p + 2, p + 1\}$  to the edges in ascending or descending order will generate  $S$ -( $a', 2$ ) or  $(a, 0)$ -EAM total labelling on that network, respectively, where  $a$

(magic constant) and  $a'$  (minimum edge weight) attain some suitable values accordingly. More precisely, according to Lemma 1, this vertex labelling, consisting of consecutive integers, extends to an  $S$ -( $a, 0$ )-EAM total labelling of the networks.

**3.2. Open Problems.** The open problems relevant to the findings (Theorems 2–7) of Section 2 are proposed as follows:

- (i) For  $2 \leq n \equiv 0 \pmod{2}$ , obtain any  $S$ -( $a, 0$ )-EAM total labelling of the  $(C_n \circ K_{2,m}) \cup K_{1,n} \cup (n - 1/2)K_1$ .
- (ii) For  $2 \leq n \equiv 0 \pmod{2}$ , obtain any  $S$ -( $a, 0$ )-EAM total labelling of  $(C_n \circ K_{2,m}) \cup nP_2$ .
- (iii) For  $2 \leq n \equiv 0 \pmod{2}$ , obtain any  $S$ -( $a, 0$ )-EAM total labelling of  $(C_n \circ K_{2,m}) \cup P_{n+1}$ .
- (iv) For  $2 \leq n \equiv 0 \pmod{2}$ , determine  $S$ -( $a, 0$ )-EAM total labelling of  $G_1, G_2, G_3, G_4, G_5$ , and  $G_6$  for any other magic constants (i.e., for any other value of  $a$ ) than computed here.
- (v) For  $l, m$  and  $n$  positive integers, determine any  $S$ -( $a, 0$ )-EAM total labelling for the following networks:
  - (1)  $(C_n \circ K_{2,m}) \cup K_{1,\ell}$
  - (2)  $(C_n \circ K_{2,m}) \cup lP_2$
  - (3)  $(C_n \circ K_{2,m}) \cup P_l$

Open problems related to Theorems 11 and 12 are given as follows:

- (i) For  $2 \leq n \equiv 0 \pmod{2}$ , find any  $S$ -( $a, 0$ )-EAM total labelling of  $C_n \circ H_1$ .
- (ii) For  $2 \leq n \equiv 0 \pmod{2}$ , find any  $S$ -( $a, 0$ )-EAM total labelling of  $C_n \circ H_2$ .
- (iii) For  $3 \leq n \equiv 1 \pmod{2}$ , determine some  $S$ -( $a, 0$ )-EAM total labelling of  $C_n \circ H_1$  and  $C_n \circ H_2$  with a different magic constant than obtained here, i.e., for any other value of  $a$ .

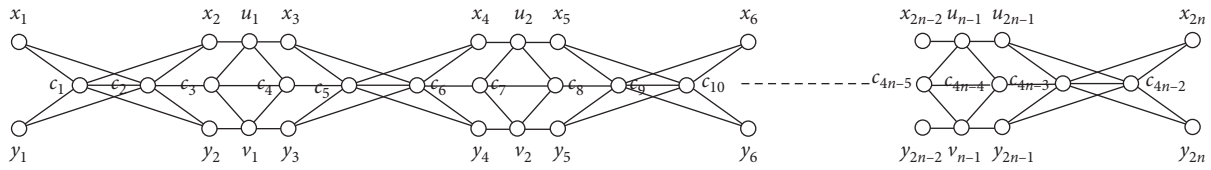


FIGURE 7: The general formation of the lattice network  $\mathbb{L}_n^3, \forall n \in \mathbb{N}$ .

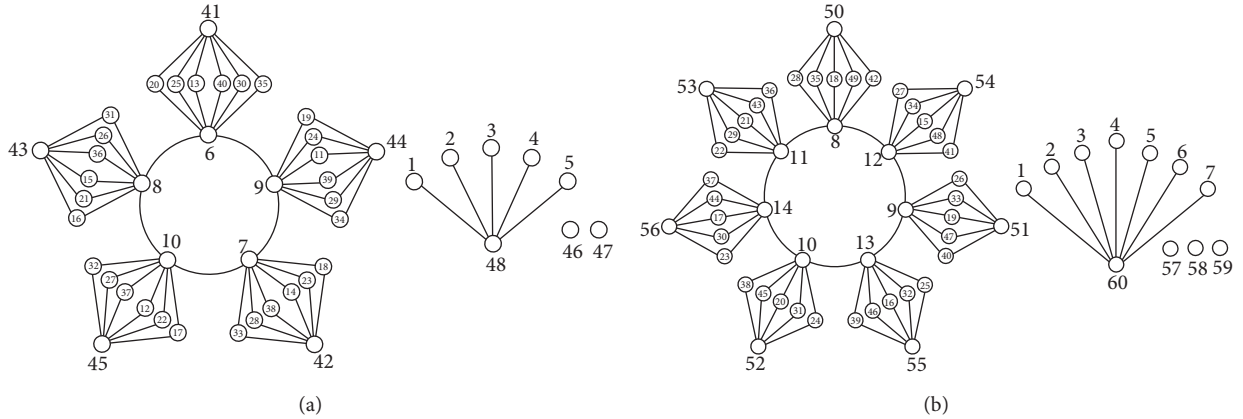


FIGURE 8: An S- (132, 0)-EAM total labelling of  $(C_5 \circ K_{2,6}) \cup K_{1,5} \cup 2K_1$  ( $\leftarrow A$ ) and an S- (163, 0)-EAM total labelling of  $(C_7 \circ K_{2,5}) \cup K_{1,7} \cup 3K_1$  ( $\leftarrow B$ ).

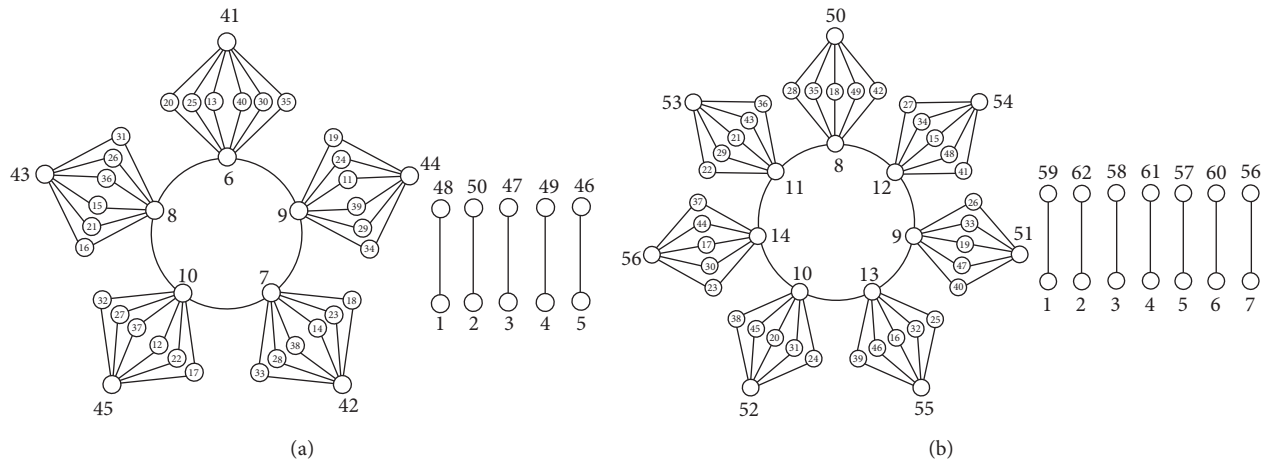


FIGURE 9: An S- (134, 0)-EAM total labelling of  $(C_5 \circ K_{2,6}) \cup 5P_2$  ( $\longrightarrow A$ ) and an S- (165, 0)-EAM total labelling of  $(C_7 \circ K_{2,5}) \cup 5P_2$  ( $\longrightarrow B$ ).

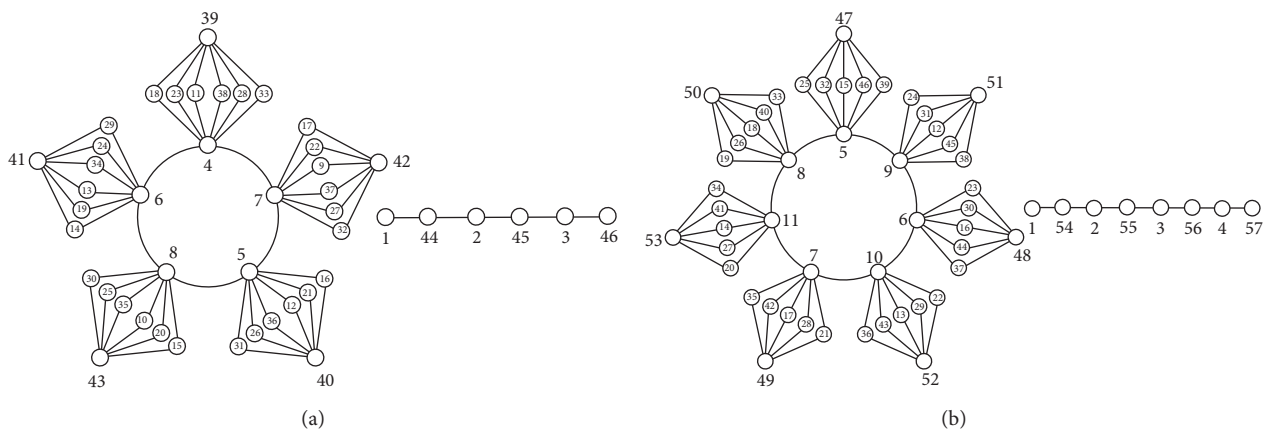


FIGURE 10: An S- (126, 0)-EAM total labelling of  $(C_5 \circ K_{2,6}) \cup P_6$  ( $\longrightarrow A$ ) and an S- (154, 0)-EAM total labelling of  $(C_7 \circ K_{2,5}) \cup P_8$  ( $\longrightarrow B$ ).

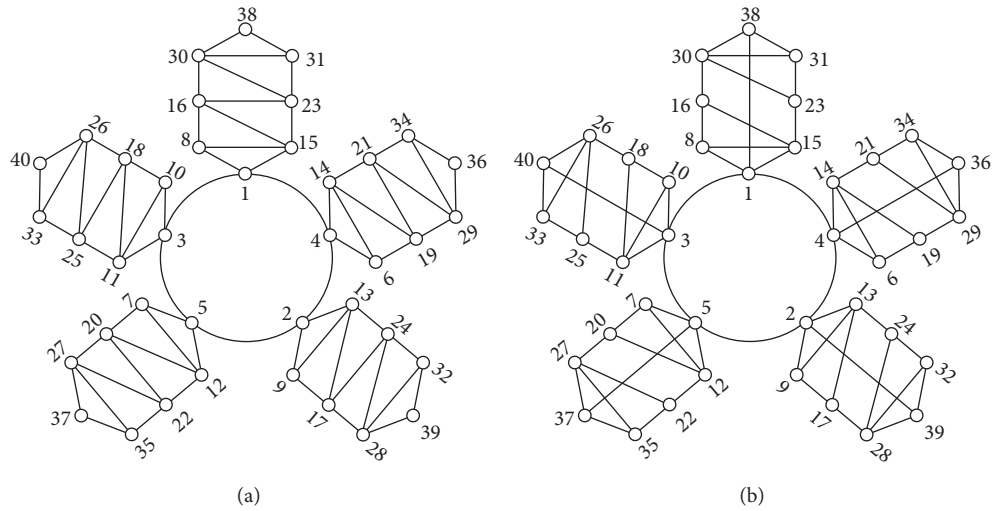


FIGURE 11: An S-(114, 0)-EAM total labelling of  $C_5 \circ H_1$  ( $\rightarrow A$ ) and  $C_5 \circ H_2$  ( $\rightarrow B$ ).

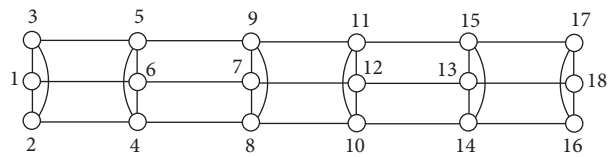


FIGURE 12: An S-(54, 0)-EAM total labelling of  $\Gamma_3$ .

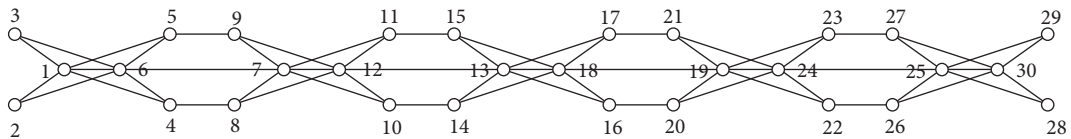


FIGURE 13: An S-(90, 0)-EAM total labelling of the lattice network  $\mathbb{L}_5^1$ .

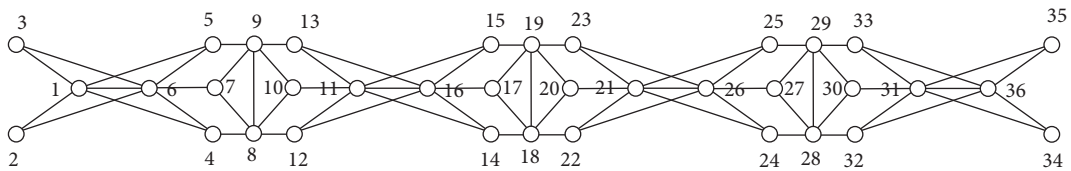


FIGURE 14: An S-(108, 0)-EAM total labelling of the lattice network  $\mathbb{L}_4^2$ .

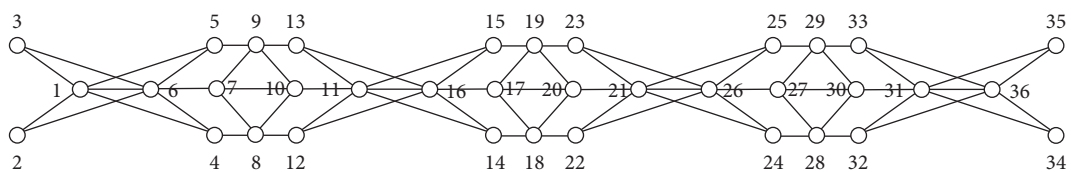


FIGURE 15: An S-(108, 0)-EAM total labelling of the lattice network  $\mathbb{L}_4^3$ .

TABLE 2: Synopsis of main theorems.

Network	Parameters	$a$ ( $d=0$ )	$a'$ ( $d=2$ )	Planar V nonplanar
$(C_n \circ K_{2,m}) \cup K_{1,n} \cup (n-1/2)K_1$	$m \geq 2, \text{ odd } n \geq 3$	$8n + 3mn + 2$	$6n + mn + 3$	Planar
$(C_n \circ K_{2,m}) \cup nP_2$	$m \geq 2, \text{ odd } n \geq 3$	$(1/2)(17n + 6mn + 3)$	$(1/2)(13n + 2mn + 5)$	Planar
$(C_n \circ K_{2,m}) \cup P_{n+1}$	$m \geq 2, \text{ odd } n \geq 3$	$(1/2)(13n + 6mn + 7)$	$(1/2)(9n + 2mn + 9)$	Planar
$C_n \circ H_1$ and $C_n \circ H_2$	$n$ is odd	$(1/2)(45n + 3)$	$(1/2)(17n + 5)$	Planar
$\Gamma_n$	$\forall n \in \mathbb{N}$	$18n$	$6n + 4$	Planar
$\mathbb{L}_n^1$	$\forall n \in \mathbb{N}$	$18n$	$6n + 4$	Nonplanar
$\mathbb{L}_n^2$ and $\mathbb{L}_n^3$	$\forall n \in \mathbb{N}$	$30n - 12$	$10n$	Nonplanar

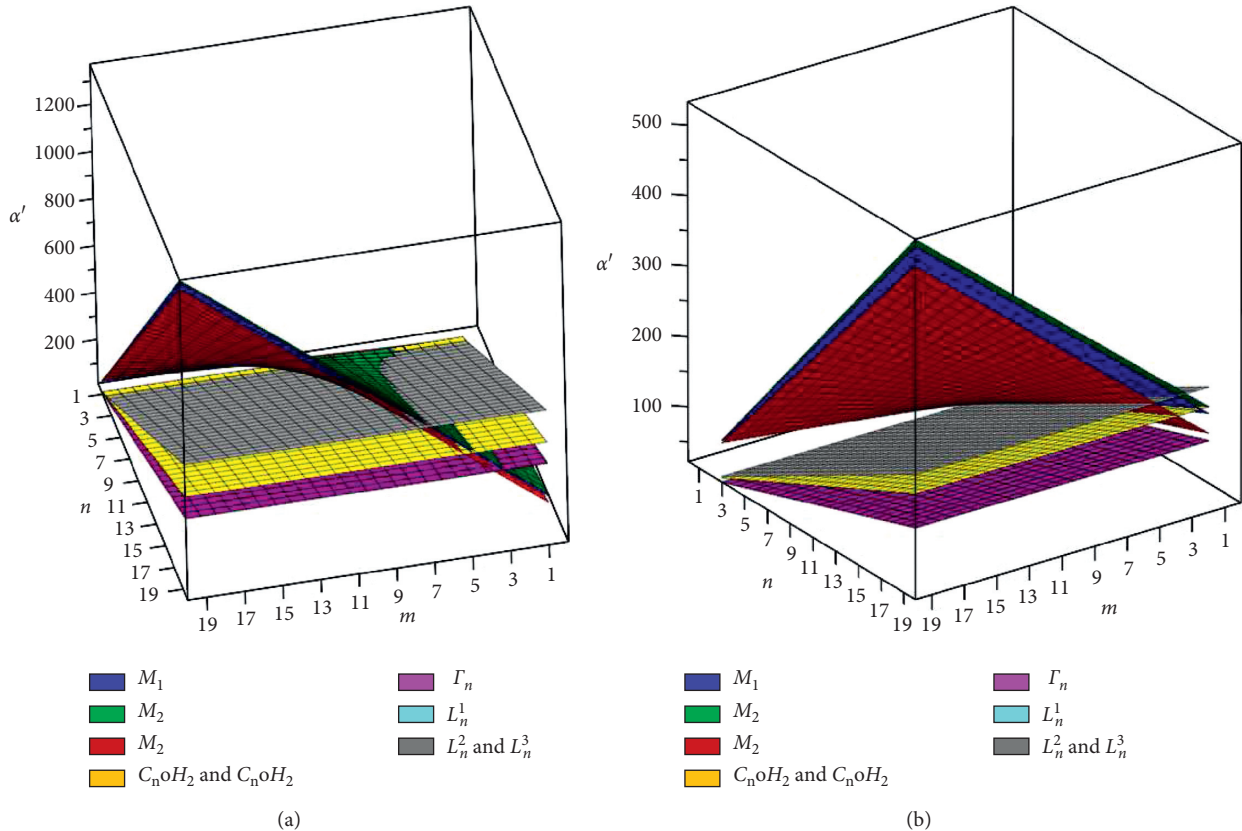


FIGURE 16: Comparison of the magic constants ( $\rightarrow A$ ) and the minimum edge weights ( $\rightarrow B$ ) of  $M_1, M_2, M_3, C_n \circ H_1, C_n \circ H_2, \Gamma_n, \mathbb{L}_n^1, \mathbb{L}_n^2$ , and  $\mathbb{L}_n^3$ , for  $m \geq 2$  and  $3 \leq n \equiv 1 \pmod{2}$ .

### 4. Synopsis and 3-D Comparison of the Magic Constants and Minimum Edge Weights

This section consists of the synopsis (Section 4.1) and 3-D graphical plots and comparison of the magic constants ( $a$ ) and minimum edge weights ( $a'$ ) of our findings (Section 4.2).

4.1. *Synopsis.* Table 2 exhibits the computational results of our findings. The possible parameters for which we have determined S- $(a, 0)$  and S- $(a', 2)$ -EAM total labellings are indicated through parameters column head.

4.2. *Graphical Behavior of the Magic Constants and Minimum Edge Weights.* Figure 16 shows the graphical comparison of the magic constants ( $\rightarrow A$ ) and minimum edge weights ( $\rightarrow B$ ), in 3-D, of the networks  $M_1 \cong (C_n \circ K_{2,m}) \cup K_{1,n} \cup (n-1/2)K_1, M_2 \cong (C_n \circ K_{2,m}) \cup nP_2, M_3 \cong (C_n \circ K_{2,m}) \cup P_{n+1}, C_n \circ H_1, C_n \circ H_2, \Gamma_n, \mathbb{L}_n^1, \mathbb{L}_n^2$ , and  $\mathbb{L}_n^3$ , respectively. Moreover, Figure 16(a) shows that the most dominant layer is the one with green color. It interprets that among the magic constants of the networks discussed in this note,  $(C_n \circ K_{2,m}) \cup nP_2$  attains highest values with the increase of the values of the parameters.

Figure 17 illustrates the relative 3-D comparison of the magic constants and minimum edge weights (corresponding to  $d = 2$ ) of the networks  $(C_n \circ K_{2,m}) \cup K_{1,n} \cup (n-1/2)K_1,$

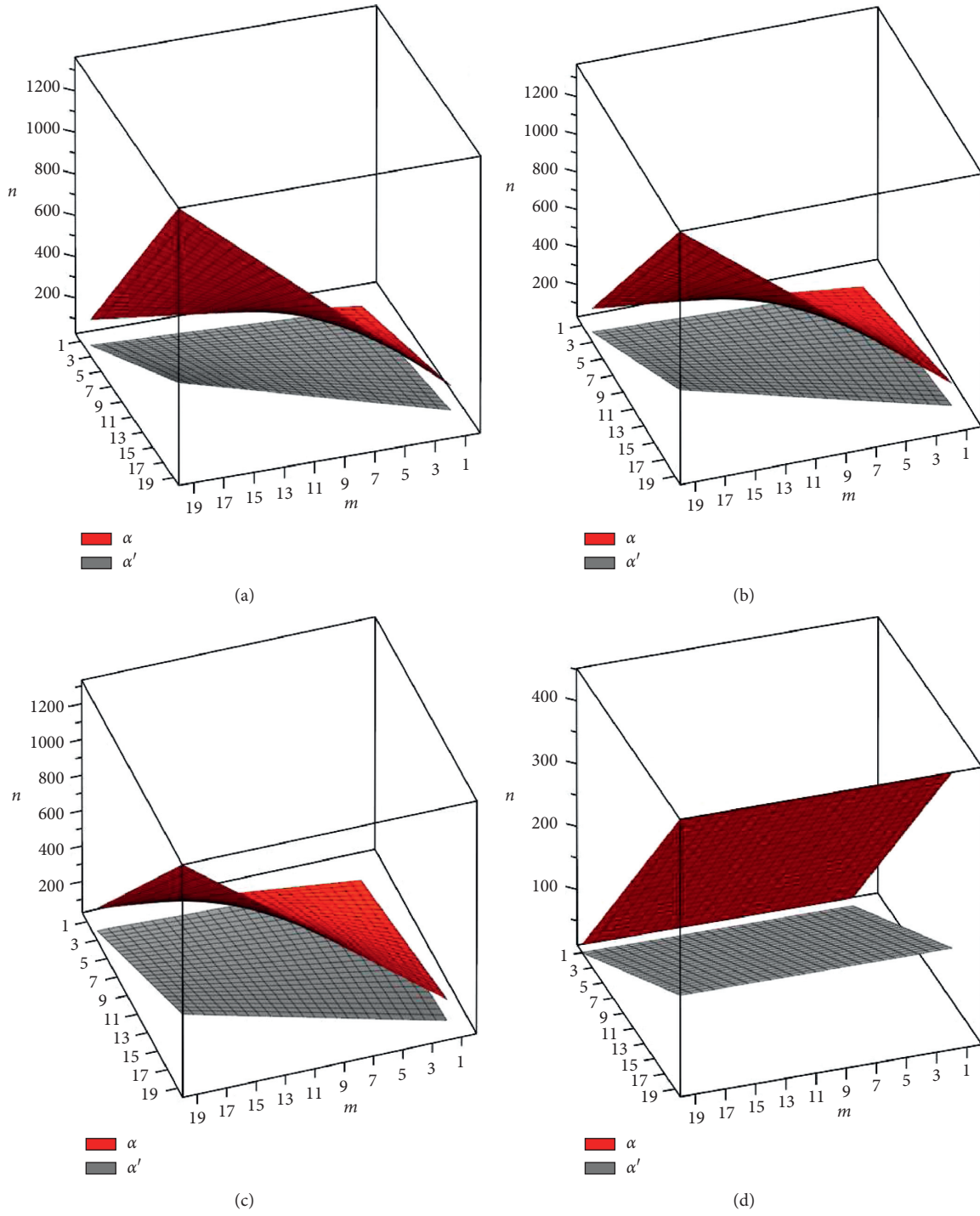


FIGURE 17: Continued.

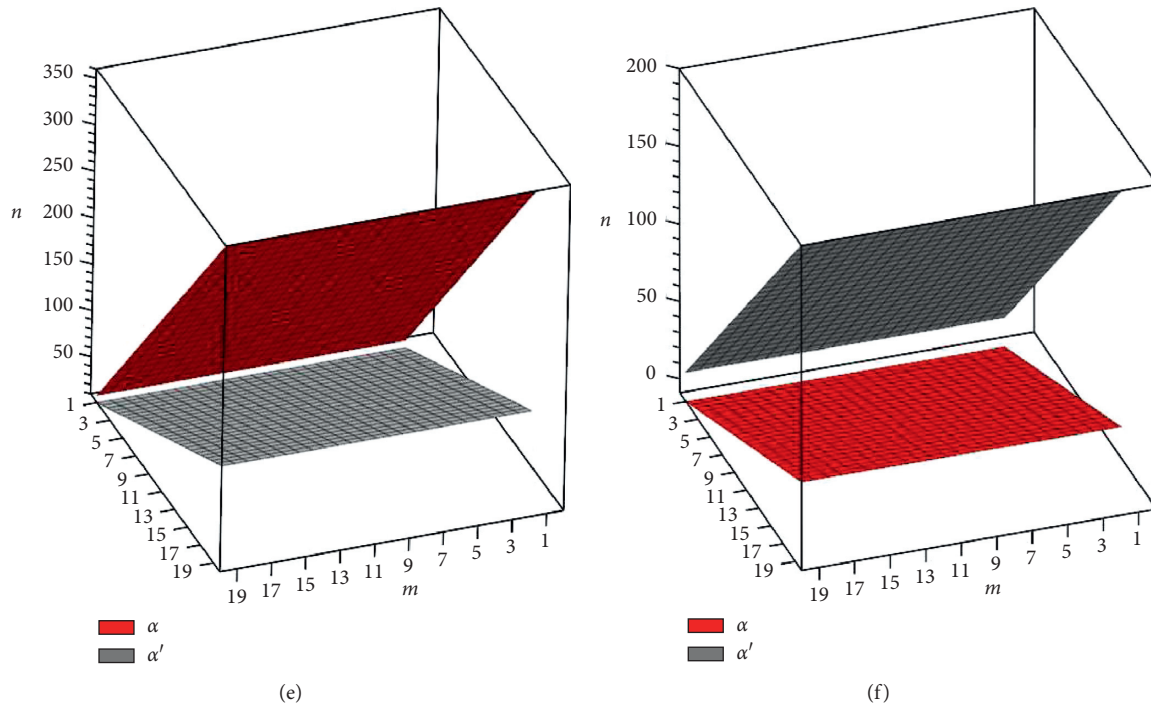


FIGURE 17: Simultaneous relative comparison of the magic constants and the minimum edge weights of  $M_1$  ( $\rightarrow A$ ),  $M_2$  ( $\rightarrow B$ ),  $M_3$  ( $\rightarrow C$ ),  $\{C_n \circ H_1, C_n \circ H_2\}$  ( $\rightarrow D$ ),  $\Gamma_n$  ( $\rightarrow E$ ),  $\{\mathbb{L}_n^1, \mathbb{L}_n^2, \mathbb{L}_n^3\}$  ( $\rightarrow F$ ), for  $m \geq 2$  &  $3 \leq n \equiv 1 \pmod{2}$

$(C_n \circ K_{2,m}) \cup nP_2$ ,  $(C_n \circ K_{2,m}) \cup P_{n+1}$ ,  $C_n \circ H_1$ ,  $C_n \circ H_2$ ,  $\Gamma_n$ ,  $\mathbb{L}_n^1$ ,  $\mathbb{L}_n^2$  and  $\mathbb{L}_n^3$ , for different values of the parameters.

### 5. Conclusion

In the present article,

- (i) We have designed S- $(a, 0)$ -EAM total labelling of the rooted product of cycle  $C_n$  and complete bipartite network  $K_{2,m}$  taking its disjoint union with paths and stars. The findings are related to the open problem on  $nK_{2,m}$  provided by Ngurah et al. in [48].
- (ii) We have provided S- $(a, 0)$ -EAM total labelling of rooted product of  $C_n$  and pancyclic networks  $H_1$  and  $H_2$ .
- (iii) We have extended the result provided in [29] by Baig et al. through exhibiting S- $(a, 0)$ -EAM total labelling of pancyclic network  $\Gamma_n$  involving chains of  $C_6$ .
- (iv) We have exhibited S- $(a, 0)$ -EAM total labelling of symmetrically designed lattice networks  $\mathbb{L}_n^1$ ,  $\mathbb{L}_n^2$ , and  $\mathbb{L}_n^3$ .
- (v) We have illustrated our findings through 3-D graphical comparison.
- (vi) For further working in this field, several research problems have also been opened.
- (vii) The obtained schemes are now all set to serve as test ready labellings for programmers, networking professionals, and engineers to avail them where they find these appropriate.

### Data Availability

The data used to support the findings of this study are included within this article. However, the reader may contact the corresponding author for more details on the data.

### Conflicts of Interest

The authors declare that they have no conflicts of interest.

### References

- [1] Z. Shao, "L (2,1)-labeling of the strong product of paths and cycles," *The Scientific World Journal*, vol. 2014, Article ID 741932, 2014.
- [2] T.-M. Wang and C.-C. Hsiao, "On anti-magic labeling for graph products," *Discrete Mathematics*, vol. 308, no. 16, pp. 3624–3633, 2008.
- [3] D. B. West, *Introduction to Graph Theory*, Prentice-Hall, Upper Saddle River, NJ, USA, 2001.
- [4] J. Sedl, "Problem 27 in the theory of graphs and its applications," in *Proceedings of the Symposium*, pp. 163–167, Smolenice, Slovakia, 1963.
- [5] N. Hartsfield and G. Ringel, *Pearls in Graph Theory*, Academia Press, New York, NY, USA, 1990.
- [6] A. Kotzig and A. Rosa, "Magic valuations of finite graphs," *Canadian Mathematical Bulletin*, vol. 13, no. 4, pp. 451–461, 1970.
- [7] G. Ringel and A. S. Llado, "Another tree conjecture," *Bull ICA*, vol. 18, pp. 83–85, 1996.
- [8] H. Enomoto, A. Llado, T. Nakamigawa, and G. Ringel, "Super edge-magic graphs," *SUT Journal of Mathematics*, vol. 34, pp. 105–109, 1998.



- [9] R. Simanjuntak, F. Bertault, and M. Miller, "Two new (a,d)- EAT graph labelings," in *Proceedings of the Eleventh Australian Workshop of Combinatorial Algorithm*, pp. 179–189, Ballarat, Australia, 2000.
- [10] S. M. Lee and Q. X. Shan, *All Trees with at Most 17 Vertices Are Super Edge-Magic*, University Southern Illinois., Carbondale, Australia, 2002.
- [11] M. Javaid, A. A. Bhatti, and M. K. Aslam, "Super (a,d)-edge antimagic total labeling of a subclass of trees," *AKCE International Journal of Graphs and Combinatorics*, vol. 14, no. 2, pp. 158–164, 2017.
- [12] M. Javaid, "On super edge-antimagic total labeling of subdivided stars," *Discussiones Mathematicae Graph Theory*, vol. 34, no. 4, pp. 691–705, 2014.
- [13] M. Javaid and A. A. Bhatti, "On super edge- antimagic total labeling of subdivided stars," *Ars Combinatoria*, vol. 105, pp. 503–512, 2012.
- [14] A. Raheem, A. Q. Baig, and M. Javaid, "On (a, d) -EAT labeling of subdivision of  $K_1, r$ ," *Journal of Information and Optimization Sciences*, vol. 39, no. 3, pp. 643–650, 2018.
- [15] A. N. M. Salman, A. A. G. Ngurah, and N. Izzati, "On super edge- magic total labeling of a subdivision of a star," *Utilitas Mathematica*, vol. 81, pp. 275–284, 2010.
- [16] M. Javaid and A. A. Bhatti, "On super edge- antimagic total labeling of generalized extended -trees," *AKCE International Journal of Graphs and Combinatorics*, vol. 11, pp. 115–126, 2014.
- [17] M. Javaid, A. A. Bhatti, and M. Hussain, "On edge- antimagic total labeling of extended -trees," *Utilitas Math*, vol. 87, pp. 293–303, 2012.
- [18] M. Javaid, M. Hussain, K. Ali, and K. H. Dar, "Super edge-magic total labeling on -trees," *Utilitas Math*, vol. 86, pp. 183–191, 2011.
- [19] M. Hussain and E. T. Boskoro, "Slamin, on super edge magic total labeling of banana trees," *Utilitas Mathematica*, vol. 79, pp. 243–251, 2009.
- [20] K. A. Sugeng, M. Miller, and M. Baa, "edge- antimagic total labelings of caterpillars," *Lecture Notes in Computer Science*, vol. 3330, Article ID 169aAS180, 2005.
- [21] M. Javaid, A. A. Bhatti, and M. Hussain, "On super edge-antimagic total labeling of subdivided caterpillar," *Utilitas Math*, vol. 98, pp. 227–241, 2015.
- [22] R. M. Figueroa-Centeno, R. Ichishima, and F. A. Muntaner-Batle, "On super edge- magic graph," *Ars Combinatoria*, vol. 64, pp. 81–95, 2002.
- [23] A. A. Bhatti, A. Nisar, and M. Kanwal, "Radio number of wheel like graphs," *International Journal on Applications of Graph Theory In Wireless Ad Hoc Networks And Sensor Networks*, vol. 3, no. 4, pp. 39–57, 2011.
- [24] J. A. Gallian, "A dynamic survey of graph labeling," *The Electronic Journal of Combinatorics*, 2019.
- [25] R. Khennoufa and O. Togni, "The radio antipodal and radio numbers of the hypercube," *Ars Combinatoria*, vol. 102, pp. 447–461, 2011.
- [26] R. Figueroa-Centeno, R. Ichishima, and F. Muntaner-Batle, "On edge-magic labelings of certain disjoint unions of graphs," *Australas. J. Combin.* vol. 32, pp. 225–242, 2005.
- [27] R. M. Figueroa-Centeno, R. Ichishima, F. A. Muntaner-Batle, and A. Oshima, "A magical approach to some labeling conjectures," *Discussiones Mathematicae Graph Theory*, vol. 31, no. 1, pp. 79–113, 2011.
- [28] R. M. Figueroa-Centeno, R. Ichishima, and F. A. Muntaner-Batle, "The place of super edge-magic labelings among other classes of labelings," *Discrete Mathematics*, vol. 231, no. 1-3, pp. 153–168, 2001.
- [29] A. Q. Baig, H. U. Afzal, M. Imran, and I. Javaid, "Super edge-magic labeling of volvox and pancyclic graphs," *Util. Math.* vol. 93, pp. 49–56, 2014.
- [30] J.-B. Liu, M. K. Aslam, M. Javaid, and A. Raheem, "Computing edge-weight bounds of antimagic labeling on a class of trees," *IEEE Access*, vol. 7, pp. 93375–93386, 2019.
- [31] A. Ahmad, M. F. Nadeem, and A. Gupta, "On super edge- magic deficiency of certain Toeplitz graphs," *Hacettepe Journal of Mathematics and Statistics*, vol. 47, no. 3, pp. 1–7, 2018.
- [32] A. Ahmad, K. Ali, M. Bača, P. Kovář, and A. Semaničová-Feňovčíková, "Vertex-antimagic labelings of regular graphs," *Acta Mathematica Sinica, English Series*, vol. 28, no. 9, pp. 1865–1874, 2012.
- [33] M. Bača and M. K. Siddiqui, "Construction of tree from smaller graceful trees," *Utilitas Mathematica*, vol. 99, no. 1, pp. 175–186, 2016.
- [34] A. Ahmad and F. A. Muntaner-Batle, "On super edge magic deficiency of unicyclic graphs," *Utilitas Math*, vol. 98, pp. 379–386, 2015.
- [35] A. Ahmad, A. Q. Baig, and M. Imran, "On super edge-magicness of graphs," *Utilitas Math*, vol. 89, pp. 373–380, 2012.
- [36] P. R. L. Pushpam and A. Saibulla, "Super edge- antimagic total labeling of some classes of graphs," *SUT Journal of Mathematics*, vol. 48, no. 1, pp. 1–12, 2012.
- [37] N. L. Prasanna, K. Sravanthi, and N. Sudhakar, "Applications of graph labeling in major areas of computer science," *International Journal of Research in Computer and Communication Technology*, vol. 3, pp. 819–823, 2014.
- [38] N. L. Prasanna, "Applications of graph labeling in communication networks," *Oriental Journal of Computer Science and Technology*, vol. 7, pp. 893–897, 2014.
- [39] M. Andreas, *Wireless Communications*, Wiley-IEEE, New York, NY, USA, 2005.
- [40] R. Wakefield, *Radio Broadcasting*, W2UC, Union College, Schenectady, NY, USA, 1959.
- [41] Z. Zhou, S. Das, and H. Gupta, "Connected K-coverage problem in sensor networks," in *Proceedings. 13th International Conference on Computer Communications and Networks*, pp. 373–378, IEEE Cat. No.04EX969), Chicago, IL, USA, 2004.
- [42] M. S. Vinutha and P. Arathi, "Applications of graph coloring and labeling in computer science," *International Journal on Future Revolution in Computer Science and Communication Engineering*, vol. 3, pp. 14–15, 2017.
- [43] I. Katzela and M. Naghshineh, "Channel assignment schemes for cellular mobile telecommunication systems: a comprehensive survey," *IEEE Personal Communications*, vol. 3, no. 3, pp. 10–31, 1996.
- [44] A. Krishnaa, "On antimagic labellings of some cycle related graphs," *Journal of Discrete Mathematical Sciences and Cryptography*, vol. 15, pp. 225–235, 2012.
- [45] A. Krishnaa, "Formulas and algorithms of antimagic labelings of Some helm related graphs," *Journal of Discrete Mathematical Sciences and Cryptography*, vol. 19, no. 2, pp. 435–445, 2016.
- [46] A. Krishnaa, "Some applications of labelled graphs," *International Journal of Mathematics Trends and Technology*, vol. 37, no. 3, pp. 19–23, 2016.
- [47] J. P. Desai, "A graph theoretic approach for modeling mobile robot team formations," *Journal of Robotic Systems*, vol. 19, no. 11, pp. 511–525, 2002.
- [48] A. A. G. Ngurah, E. T. Baskoro, R. Simanjuntak, and S. Uttunggadewa, "On the super edge-magic strength and deficiency of graphs," *Kyoto CCGT*, vol. 4535, pp. 144–154, 2008.

## Research Article

# Near-Coincidence Point Results in Norm Interval Spaces via Simulation Functions

Misbah Ullah,<sup>1</sup> Muhammad Sarwar <sup>1</sup>, Hassen Aydi ,<sup>2,3,4</sup> and Yaé Ulrich Gaba <sup>3,5,6</sup>

<sup>1</sup>Department of Mathematics, University of Malakand, Chakdara Dir (L), Pakistan

<sup>2</sup>Université De Sousse, Institut Supérieur D'Informatique et des Techniques de Communication, H. Sousse 4000, Tunisia

<sup>3</sup>Department of Mathematics and Applied Mathematics, Sefako Makgatho Health Sciences University, Ga-Rankuwa, South Africa

<sup>4</sup>China Medical University Hospital, China Medical University, Taichung 40402, Taiwan

<sup>5</sup>Quantum Leap Africa (QLA), AIMS Rwanda Centre, Remera Sector KN 3, Kigali, Rwanda

<sup>6</sup>Institut de Mathématiques et de Sciences Physiques (IMSP/UAC), Laboratoire de Topologie Fondamentale, Computationnelle et leurs Applications (Lab-ToFoCApp), BP 613, Porto-Novo, Benin

Correspondence should be addressed to Muhammad Sarwar; sarwarwati@gmail.com, Hassen Aydi; hassen.aydi@isima.rnu.tn, and Yaé Ulrich Gaba; yaeulrich.gaba@gmail.com

Received 23 December 2020; Revised 6 February 2021; Accepted 9 February 2021; Published 15 March 2021

Academic Editor: Ali Ahmad

Copyright © 2021 Misbah Ullah et al. This is an open access article distributed under the Creative Commons Attribution License, which permits unrestricted use, distribution, and reproduction in any medium, provided the original work is properly cited.

Recently, Wu in 2018 established interesting results in the framework of interval spaces. He initiated the idea of near-fixed points and proved some related basic results in metric interval, norm interval, and hyperspaces. In 2015, Khojasteh et al. gave the concept of simulation functions and studied some fixed-point results in metric spaces. Motivated by this work, we give some near-coincidence point results in norm interval spaces using the concept given by Khojasteh et al. Examples are also provided for the validation of the results.

## 1. Introduction

Many researchers are still showing high interest in the field of metric fixed-point theory. They are working in different directions and generalizing the remarkable results in this area [1–4]. The first one who took interest in this area was Poincaré. Later, Brouwer established a (topological) fixed-point theorem. The metric fixed-point theory attracts researchers due to its applications in both applied and pure mathematics. There are many applications of metric fixed-point theory in the existence of solutions for nonlinear systems. In 1922, Banach [5] established a remarkable result, known as the Banach contraction principle (BCP).

This BCP was modified and generalized in different forms and structures. Among them, there are dislocated quasi metric spaces [6], cone metric spaces [7], generalized metric spaces [8], controlled metric spaces [9], orthogonal partial  $b$ -metric spaces [10], etc.

Khojasteh et al. [11] modified the contractive condition by introducing the concept of a simulation function

$S: [0, \infty) \times [0, \infty) \rightarrow \mathbb{R}$ . Later, Roldan Lopez de Hierro et al. [12, 13] extended the stated concept and investigated some coincidence point results in metric spaces. With the help of a simulation-type function, Argoubi et al. [14] gave interesting results in partial ordered metric spaces. Alharbi et al. [15] made a generalization by combining the concept of simulation and admissible functions in the related literature. Alsubaie et al. [16] proved some common fixed-point results for two mappings in the setting of metric spaces by using the concept of a simulation function. Alqahtani et al. [17] proved fixed-point results by introducing the concept of a bilateral contraction which is a combination of Ćirić- and Caristi-type contractions. In [18], the authors studied the existence and uniqueness of a common fixed point in the setting of  $b$ -metric spaces, by using the concept of extended  $Z$ -contractions associated with an  $\psi$ -simulation function. In [19], the authors established results on the existence of best proximity points of certain mappings using simulation functions in complete metric spaces. Later, Karapinar [20] presented some fixed-point results by defining a new

contractive condition via admissible mappings imbedded in a simulation function.

Recently, Wu [21] initiated the concept of interval spaces. These spaces contain all closed bounded intervals over the set  $\mathbb{R}$ . Over the interval spaces, he defined a metric, as well as a norm using the equivalence relation  $\Omega$ . These spaces are called metric intervals and norm interval spaces, respectively. He studied near-fixed-point results in metric intervals, as well as in norm interval spaces. After this, he gave the concept of a hyperspace, which is a space containing all possible subsets of a vector space. He defined null sets, as well as the equivalence relation  $\Omega$  in a hyperspace and defined a norm over this type of spaces. He also presented near-fixed-point results in hyperspaces. For more details, see [22–24].

Inspired by the work done in [11, 21, 22], we established some near-coincidence point results in metric interval and hyperspaces [25] via a simulation function. We also presented some near-coincidence point results in norm interval spaces via a simulation function. For validation of results and definitions, some examples are provided.

## 2. Preliminaries

In this section, some basic definitions and results are stated related to the existing literature.

**2.1. Interval Spaces.** Let  $I$  be the set containing all close bounded intervals of the form  $[\sigma, v]$ , where  $\sigma, v \in \mathbb{R}$  and  $\sigma \leq v$ . Also,  $\sigma \in \mathbb{R}$  is considered as an element  $[\sigma, \sigma] \in I$  [21].

The binary operation of addition and scaler multiplication is stated as follows:

$$\begin{aligned} [\sigma, v] \oplus [\sigma', v'] &= [\sigma + \sigma', v + v'], \\ k[\sigma, v] &= \begin{cases} [k\sigma, kv], & k \geq 0, \\ [kv, k\sigma], & k < 0. \end{cases} \end{aligned} \quad (1)$$

Due to the inverse property, the above space does not fulfill the condition of a conventional vector space. For  $[\sigma, v] \in I$ , the subtraction

$$[\sigma, v] \ominus [\sigma, v] = [\sigma, v] \oplus [-v, -\sigma] = [\sigma - v, v - \sigma] \quad (2)$$

does not give the zero element  $[0, 0]$ . So the inverse of  $[\sigma, v]$  does not exist. For the above deficiency, the null set was defined by Wu [21] as follows.

**2.2. Null Set.** The null set contains all the elements of the type  $[-\sigma, \sigma]$ , and so it is defined as follows:

$$\Omega = \{[\sigma, v] \ominus [\sigma, v]; [\sigma, v] \text{ is an element of } I\}, \quad (3)$$

or

$$\Omega = \{-\alpha, \alpha; \alpha \geq 0\}. \quad (4)$$

**2.3. Binary Relation  $\Omega$ .** We write  $[\sigma, v] \Omega [\sigma', v']$  iff there exist  $\omega_1, \omega_2 \in \Omega$  such that

$$[\sigma, v] \oplus \omega_1 = [\sigma', v'] \oplus \omega_2. \quad (5)$$

Clearly, we can have  $[\sigma, v] = [\sigma', v'] \Rightarrow [\sigma, v] \Omega [\sigma', v']$  by taking  $\omega_1 = \omega_2 = [0, 0]$ . However, the converse is not true in general.

**Proposition 1** (see [21]).  $\Omega$  is an equivalence relation.

According to the equivalence relation  $\Omega$ , the equivalence class of almost identical intervals is defined as  $\langle [\sigma, v] \rangle = \{[\mathfrak{p}, \mathfrak{q}] \in I: [\sigma, v] \Omega [\mathfrak{p}, \mathfrak{q}]\}$  for any  $[\sigma, v] \in I$ .

**2.4. Norm Interval Space.** The pair  $(I, \|\cdot\|)$  fulfilling the following axioms is called a norm interval space [21]:

- (i)  $\|[\sigma, v]\| = 0$  implies  $[\sigma, v] \in \Omega$
- (ii)  $\|\alpha[\sigma, v]\| = |\alpha| \|[\sigma, v]\|$
- (iii)  $\|[\sigma, v] \oplus [\sigma', v']\| \leq \|[\sigma, v]\| + \|[\sigma', v']\|$  for all  $[\sigma, v], [\sigma', v'] \in I$ , where  $I$  contains all close bounded intervals over  $\mathbb{R}$  with the null set  $\Omega$  and  $\|\cdot\|$  is a real-valued mapping on  $I$

We say that the null condition is satisfied by  $\|\cdot\|$  if the condition (iii) is replaced by

$$\|[\sigma, v]\| = 0 \quad \text{if and only if } [\sigma, v] \in \Omega. \quad (6)$$

$\|\cdot\|$  is said to satisfy the null equalities if for all  $\omega_1, \omega_2 \in \Omega$  and  $[\sigma, v], [\sigma', v'] \in I$ , the following equalities hold:

- (1)  $\|([\sigma, v] \oplus \omega_1) \ominus ([\sigma', v'] \oplus \omega_2)\| = \|[\sigma, v] \ominus [\sigma', v']\|$
- (2)  $\|([\sigma, v] \oplus \omega_1) \ominus ([\sigma', v'])\| = \|[\sigma, v] \ominus [\sigma', v']\|$
- (3)  $\|([\sigma, v]) \ominus ([\sigma', v'] \oplus \omega_2)\| = \|[\sigma, v] \ominus [\sigma', v']\|$

**Definition 1.** If  $(I, \|\cdot\|)$  is a norm interval space, then

- (i) The mapping  $\|\cdot\|$  is said to satisfy the null super-inequality if

$$\|[\sigma, v] \oplus \omega\| \geq \|[\sigma, v]\|, \quad \text{for any } [\sigma, v] \in I \text{ and } \omega \in \Omega. \quad (7)$$

- (ii) The mapping  $\|\cdot\|$  is said to satisfy the null sub-inequality if

$$\|[\sigma, v] \oplus \omega\| \leq \|[\sigma, v]\|, \quad \text{for any } [\sigma, v] \in I \text{ and } \omega \in \Omega. \quad (8)$$

- (iii) The mapping  $\|\cdot\|$  is said to satisfy the null equality if

$$\|[\sigma, v] \oplus \omega\| = \|[\sigma, v]\|, \quad \text{for any } [\sigma, v] \in I \text{ and } \omega \in \Omega. \quad (9)$$

**Example 1.** Let  $\|\cdot\|$  be a nonnegative real-valued function defined on  $I$  by

$$\|[\sigma, v]\| = |\sigma + v|. \quad (10)$$

Then,  $(I, \|\cdot\|)$  forms a norm interval space such that  $\|\cdot\|$  satisfies the null equality.

**Proposition 2** (see [21]). Let  $(I, \|\cdot\|)$  be a norm interval space such that  $\|\cdot\|$  satisfies the null super-inequality. Then, for any  $[\sigma, v], [\sigma', v'], [\sigma_1, v_1], [\sigma_2, v_2], \dots, [\sigma_m, v_m]$ , we have

$$\begin{aligned} \|\llbracket \sigma, v \rrbracket \ominus \llbracket \sigma', v' \rrbracket\| \leq & \|\llbracket \sigma, v \rrbracket \ominus \llbracket \sigma_1, v_1 \rrbracket\| + \|\llbracket \sigma_1, v_1 \rrbracket \ominus \llbracket \sigma_2, v_2 \rrbracket\| \\ & + \dots + \|\llbracket \sigma_m, v_m \rrbracket \ominus \llbracket v, v' \rrbracket\|. \end{aligned} \quad (11)$$

**Proposition 3.** Let  $(I, \|\cdot\|)$  be a norm interval space; then, the following hold:

(i) If  $\|\cdot\|$  satisfies the null equality, then for all  $[\sigma, v], [\sigma', v'] \in I$ ,

$$[\sigma, v] \underline{\Omega}[\sigma', v'] \text{ implies } \|\llbracket \sigma, v \rrbracket\| = \|\llbracket \sigma', v' \rrbracket\|. \quad (12)$$

(ii) For any  $[\sigma, v], [\sigma', v'] \in I$ ,

$$\|\llbracket \sigma, v \rrbracket \ominus \llbracket \sigma', v' \rrbracket\| = 0, \quad \text{implies } [\sigma, v] \underline{\Omega}[\sigma', v']. \quad (13)$$

(iii) If  $\|\cdot\|$  satisfies the null super-inequality and null condition, then for any  $[\sigma, v], [\sigma', v'] \in I$ ,

$$[\sigma, v] \underline{\Omega}[\sigma', v'], \quad \text{implies } \|\llbracket \sigma, v \rrbracket \ominus \llbracket \sigma', v' \rrbracket\| = 0. \quad (14)$$

For proof of the above propositions, see [21].

**Definition 2.** Let  $(I, \|\cdot\|)$  be a norm interval space. A sequence  $\{[\sigma_n, v_n]\}_{n=1}^{+\infty}$  is said to converge to a limit  $[\sigma, v]$  if and only if

$$\lim_{n \rightarrow \infty} \|\llbracket \sigma_n, v_n \rrbracket \ominus \llbracket \sigma, v \rrbracket\| = 0. \quad (15)$$

**Proposition 4.** Consider a norm interval space  $(I, \|\cdot\|)$  with the null set  $\Omega$ .

(i) If the null super-inequality holds for  $\|\cdot\|$ , then the convergence of the sequence  $\{[\sigma_n, v_n]\}_{n=1}^{+\infty}$  to  $[\sigma, v]$  and  $[\sigma', v']$  simultaneously implies  $\langle \llbracket \sigma, v \rrbracket \rangle = \langle \llbracket \sigma', v' \rrbracket \rangle$

(ii) If the null equality holds for  $\|\cdot\|$  and the sequence  $\{[\sigma_n, v_n]\}_{n=1}^{+\infty}$  converges to  $[\sigma, v]$ , then for any  $[\sigma', v'] \in \langle \llbracket \sigma, v \rrbracket \rangle$ , the given sequence will also converge to  $[\sigma', v']$

**Definition 3.** Consider the norm interval space  $(I, \|\cdot\|)$  with the null set  $\Omega$ , where  $\|\cdot\|$  satisfies the null equality. If  $[\sigma, v] \in I$  is the limit of the sequence  $\{[\sigma_n, v_n]\}_{n=1}^{+\infty}$ , then  $\langle \llbracket \sigma, v \rrbracket \rangle$  is called the class limit. We can also write

$$\lim_{n \rightarrow \infty} [\sigma_n, v_n] = \langle \llbracket \sigma, v \rrbracket \rangle. \quad (16)$$

**Proposition 5** (see [21]). In the norm interval space  $(I, \|\cdot\|)$  if the null super-inequality holds for  $\|\cdot\|$ , the class limit is unique.

**Definition 4.** A sequence  $\{[\sigma_n, v_n]\}_{n=1}^{+\infty}$  in a norm interval space  $(I, \|\cdot\|)$  is called a Cauchy sequence if and only if for any  $\varepsilon > 0$ , there exists  $K \in \mathbb{N}$  such that

$$\|\llbracket \sigma_n, v_n \rrbracket \ominus \llbracket \sigma_m, v_m \rrbracket\| < \varepsilon, \quad (17)$$

for  $m, n > K$  with  $m \neq n$ . If every Cauchy sequence is convergent in  $I$ , then  $I$  is complete.

**Definition 5.** A complete norm interval space  $(I, \|\cdot\|)$  is called a Banach interval space.

**Example 2.** Let  $\|\cdot\|$  be a nonnegative real-valued function defined on  $I$  by

$$\|\llbracket \sigma, v \rrbracket\| = |\sigma + v|. \quad (18)$$

Then,  $(I, \|\cdot\|)$  forms a Banach interval space such that  $\|\cdot\|$  satisfies the null equality.

**Definition 6.** Let  $F$  be a self-mapping on  $I$ . Then, the point  $[\sigma_o, v_o] \in I$  is called a near-fixed point of  $F$  if and only if  $F[\sigma_o, v_o] \underline{\Omega}[\sigma_o, v_o]$ .

**Definition 7** (see [11, 12]). A function  $S: [0, \infty) \times [0, \infty) \rightarrow \mathbb{R}$  is called a simulation function if the following conditions hold:

$$S_1. S(0, 0) = 0$$

$$S_2. S(\alpha, \beta) < \beta - \alpha \text{ for all } \alpha, \beta > 0$$

$S_3.$  If  $\{\alpha_n\}, \{\beta_n\}$  are two sequences in  $(0, \infty)$  such that  $\lim_{n \rightarrow \infty} \alpha_n = \lim_{n \rightarrow \infty} \beta_n > 0$  and  $\alpha_n < \beta_n$  for all  $n \in \mathbb{N}$ , then

$$\lim_{n \rightarrow \infty} \sup S(\alpha_n, \beta_n) < 0. \quad (19)$$

By  $(S_2)$ , we must have

$$S(\alpha, \alpha) < 0. \quad (20)$$

The following are some interesting examples of simulation functions:

(i)  $S(\alpha, \beta) = \chi(\beta) - \Upsilon(\alpha)$  for all  $\alpha, \beta \in [0, \infty)$  where  $\chi$  and  $\Upsilon$  are continuous on  $[0, \infty)$  such that  $\gamma(\alpha) = \chi(\alpha)$  if and only if  $\alpha = 0$  and  $\gamma(\alpha) < \alpha \leq \chi(\alpha)$  for all  $\alpha > 0$ . If we take  $\gamma(\beta) = \lambda\beta$  and  $\chi(\alpha) = \alpha$ , then  $S(\alpha, \beta) = \lambda\beta - \alpha$ .

(ii)  $S(\alpha, \beta) = \beta - \chi(\beta) - \alpha$  for all  $\alpha, \beta \in [0, \infty)$  where  $\chi$  is continuous on  $[0, \infty)$  such that  $\chi(\alpha) = 0$  if and only if  $\alpha = 0$  (see Example 2.2 in [11]).

(iii)  $S(\alpha, \beta) = \beta\chi(\beta) - \alpha$  for all  $\alpha, \beta \in [0, \infty)$  where  $\chi$  is a mapping such that  $\lim_{\alpha \rightarrow r^+} \chi(t) < 1$  for all  $r > 0$  [12].

(iv)  $S(\alpha, \beta) = \eta(\beta) - \alpha$  for all  $\alpha, \beta \in [0, \infty)$ , where  $\eta$  is an upper semicontinuous function so that  $\eta(\alpha) < \alpha$  for all  $\alpha > 0$  and  $\eta(0) = 0$  [12].

### 3. Results and Discussion

**Proposition 6.** In an interval space  $I$  with the null set  $\Omega$ ,  $[\sigma, v] \underline{\Omega} [\sigma', v']$  iff  $\sigma' - \sigma = v - v'$ .

*Proof.* Let us suppose that  $[\sigma, v] \underline{\Omega} [\sigma', v']$ ; then, by definition, there exist  $[-k, k]$  and  $[-h, h]$  in  $\Omega$  such that

$$[\sigma, v] \oplus [-k, k] = [\sigma', v'] \oplus [-h, h], \quad (21)$$

that is,

$$[\sigma - k, v + k] = [\sigma' - h, v' + h]. \quad (22)$$

This implies that

$$\begin{aligned} \sigma - k &= \sigma' - h, \\ v + k &= v' + h, \\ \sigma - \sigma' &= k - h, \\ v - v' &= -k + h, \\ \sigma - \sigma' &= k - h, \\ v - v' &= -(k - h). \end{aligned} \quad (23)$$

Putting the values of  $k - h$  from the 1st equality in the second equality, we have

$$v - v' = -(\sigma - \sigma'), \quad \text{implies } \sigma' - \sigma = v - v'. \quad (24)$$

Conversely, now, let us suppose that  $\sigma' - \sigma = v - v'$ ; then, we have to show that

$$[\sigma, v] \underline{\Omega} [\sigma', v']. \quad (25)$$

Hence,

$$\begin{aligned} \sigma' - \sigma &= v - v' = k, \\ \sigma' - \sigma &= k, \\ v - v' &= k, \\ \sigma &= \sigma' - k, \\ v &= v' + k, \end{aligned} \quad (26)$$

which implies

$$\begin{aligned} [\sigma, v] &= [\sigma' - k, v' + k], \\ [\sigma, v] &= [\sigma', v'] \oplus [-k, k], \end{aligned} \quad (27)$$

and so from the last equality, we have

$$[\sigma, v] \underline{\Omega} [\sigma', v']. \quad (28)$$

□

*Example 3.* Taking the intervals  $[3, 7]$  and  $[4, 6]$ , we have  $4 - 3 = 7 - 6 = 1$  and hence by the above function, we have  $[3, 7] \underline{\Omega} [4, 6]$ . For verification, take  $\omega_1 = [0, 0]$  and  $\omega_2 = [-1, 1]$ . Then,

$$[3, 7] \oplus [0, 0] = [4, 6] \oplus [-1, 1]. \quad (29)$$

*Definition 8.* For a point  $[\sigma, v] \in I$ , if  $F[\sigma, v] \underline{\Omega} g[\sigma, v]$ , then the point  $[\sigma, v]$  is called a near-coincidence point of  $F$  and  $g$ .

*Example 4.* Taking the function  $F[x, y] = [x^2 - 1, 2y^2 + 1]$  and  $g[x, y] = [x^2, 2y^2]$ , then we can verify that  $[3, 5]$  is the near-coincidence point for the functions defined above.

*Definition 9.* If  $F$  and  $g$  are two self-mappings over  $(I, \|\cdot\|)$  such that

$$\lim_{n \rightarrow \infty} \|Fg[\sigma_n, v_n] \ominus gF[\sigma_n, v_n]\| = 0, \quad (30)$$

then the mappings are called compatible.

*Definition 10.* If  $Fg[\sigma, v] \underline{\Omega} gF[\sigma, v]$  for all  $[\sigma, v] \in (I, d)$ , then  $F$  and  $g$  are called commuting mappings.

*Definition 11.*  $F$  is a  $(Z_{\|\cdot\|}, g)$ -contraction in  $(I, \|\cdot\|)$  corresponding to a simulation function  $S \in Z$  if

$$S(\|F[\sigma, v] \ominus F[\sigma', v']\|, \|g[\sigma, v] \ominus g[\sigma', v']\|) \geq 0, \quad (31)$$

for all  $[\sigma, v], [\sigma', v'] \in I$  such that  $g[\sigma, v] \underline{\Omega} g[\sigma', v']$ .

*Example 5.* Define the mappings  $F$  and  $g$  as  $F[x, y] = [x^2 - 1, 2y^2 + 1]$  and  $g[x, y] = [x^2, 2y^2]$ ; then,  $F$  satisfies the criteria of  $(Z_{\|\cdot\|}, g)$ -contraction in  $(I, \|\cdot\|)$  according to the simulation function  $S(s, t) = \lambda t - s$ , where  $\lambda \geq 1$ .

*Definition 12.* For a sequence  $\{[\sigma_n, v_n]\}$  in the Banach interval space  $(I, \|\cdot\|)$ , if

$$g([\sigma_{n+1}, v_{n+1}]) \underline{\Omega} F([\sigma_n, v_n]), \quad \text{for all } n \geq 0, \quad (32)$$

then the sequence is known as a Picard  $(F, g)$  sequence at the point  $[\sigma_o, v_o]$ .

**Theorem 1.** Let  $F[\sigma, v] = [f_1(\sigma), f_2(v)]$  and  $G[\sigma, v] = [g_1(\sigma), g_2(v)]$  be two self-mappings over the interval space  $I$ , where  $f_1(\sigma) \leq f_2(v)$  and  $g_1(\sigma) \leq g_2(v)$  for all  $\sigma \leq v$ . If  $\sigma$  is a coincidence point for  $f_1$  and  $g_1$  and  $v$  is a coincidence point for  $f_2$  and  $g_2$ , then  $[\sigma, v]$  is a near-coincidence point for  $F$  and  $G$ .

*Proof.* As  $\sigma$  and  $v$  are coincidence points for  $f_1, g_1$  and  $f_2, g_2$ , respectively, we have

$$\begin{aligned} f_1(\sigma) &= g_1(\sigma), \\ f_2(v) &= g_2(v). \end{aligned} \quad (33)$$

This implies that

$$\begin{aligned} [f_1(\sigma), f_2(v)] &= [g_1(\sigma), g_2(v)], \\ [f_1(\sigma), f_2(v)] &\underline{\Omega} [g_1(\sigma), g_2(v)], \end{aligned} \quad (34)$$

$$F[\sigma, v] \underline{\Omega} G[\sigma, v].$$

Hence, a near-coincidence point for the mappings  $F$  and  $G$  is  $[\sigma, \nu]$  over the interval space  $I$ . The converse of the above statement is not true in general, because  $[f_1(\sigma), f_2(\nu)] \Omega [g_1(\sigma), g_2(\nu)]$  does not imply  $f_1(\sigma) = g_1(\sigma)$  and  $f_2(\nu) = g_2(\nu)$ .  $\square$

*Example 6.* Taking the function  $F[x, y] = [x^2, |y| + 1]$  and  $G[x, y] = [|x|, y^2 + 1]$ , then clearly  $-1$  is a coincidence point for  $x^2$  and  $|x|$  and  $1$  is a coincidence point for  $|y| + 1$  and  $y^2 + 1$ . So,  $[-1, 1]$  is a near-coincidence point for  $F$  and  $G$  since  $F[-1, 1] = [1, 2] = G[1, 2]$ . For justifying the converse of the above statement, we can verify that  $[-(1/2), (1/2)]$  is a near-coincidence point for  $F$  and  $G$ , but  $-(1/2)$  and  $(1/2)$  are not coincidence points for  $x^2$  and  $|x|$  and  $|y| + 1$  and  $y^2 + 1$ , respectively. As  $F[-(1/2), (1/2)] = [(1/4), (3/2)]$  and  $G[-(1/2), (1/2)] = [(1/2), (5/4)]$ , to prove that  $[-(1/2), (1/2)]$  is a near-coincidence point; we have to show  $[(1/4), (3/2)] \Omega [(1/2), (5/4)]$ . Taking  $\omega_1 = [0, 0]$  and  $\omega_2 = [-(1/4), (1/4)]$ , we have

$$\left[\frac{1}{4}, \frac{3}{2}\right] \oplus [0, 0] = \left[\frac{1}{2}, \frac{5}{4}\right] \oplus \left[-\frac{1}{4}, \frac{1}{4}\right]. \quad (35)$$

**Lemma 1.** Let  $F[\sigma, \nu] = [f_1(\sigma), f_2(\nu)]$  and  $G[\sigma, \nu] = [g_1(\sigma), g_2(\nu)]$  be two self-mappings over the interval space  $I$ , where  $f_1(\sigma) \leq f_2(\nu)$  and  $g_1(\sigma) \leq g_2(\nu)$  for all  $\sigma \leq \nu$ . If  $g_1(\sigma) - f_1(\sigma) = f_2(\nu) - g_2(\nu)$  for some  $[\sigma, \nu] \in I$ , then  $[\sigma, \nu]$  is a near-coincidence point for  $F$  and  $G$ .

*Proof.* Using Proposition 6,  $g_1(\sigma) - f_1(\sigma) = f_2(\nu) - g_2(\nu)$  implies that  $[f_1(\sigma), f_2(\nu)] \Omega [g_1(\sigma), g_2(\nu)]$ , i.e.,

$$F[\sigma, \nu] \Omega G[\sigma, \nu]. \quad (36)$$

Hence, it is proved that  $[\sigma, \nu]$  is a near-coincidence point for  $F$  and  $G$ .  $\square$

**Lemma 2.** Consider a Banach interval space  $I$  with a  $(Z_{\|\cdot\|}, g)$ -contraction  $F$ . If  $[\sigma, \nu]$  and  $[\sigma', \nu']$  both are the near-coincidence points for  $F$  and  $g$ , then

$$F[\sigma, \nu] \Omega g[\sigma, \nu] \Omega g[\sigma', \nu'] \Omega F[\sigma', \nu']. \quad (37)$$

Furthermore, the equivalence class of a near-coincidence point is unique if  $F$  or  $g$  is injective.

*Proof.* Let  $[\sigma, \nu]$  and  $[\sigma', \nu']$  be two near-coincidence points of  $F$  and  $g$ . Then, we have

$$\begin{aligned} F[\sigma, \nu] \Omega g[\sigma, \nu], \\ F[\sigma', \nu'] \Omega g[\sigma', \nu']. \end{aligned} \quad (38)$$

In the above requirement, the two equalities are clear. We only need to show that  $g[\sigma, \nu] \Omega g[\sigma', \nu']$ . On the contrary, let us suppose that  $g[\sigma, \nu] \Omega \bar{g}[\sigma', \nu']$ ; so we have

$$\|g[\sigma, \nu] \ominus g[\sigma', \nu']\| \geq 0. \quad (39)$$

As the mapping  $F$  is a  $(Z_{\|\cdot\|}, g)$ -contraction, by definition, we have

$$\begin{aligned} 0 \leq S(\|F[\sigma, \nu] \ominus F[\sigma', \nu']\|, \|g[\sigma, \nu] \ominus g[\sigma', \nu']\|) \\ = S(\|g[\sigma, \nu] \ominus g[\sigma', \nu']\|, \|g[\sigma, \nu] \ominus g[\sigma', \nu']\|). \end{aligned} \quad (40)$$

The last inequality is a contradiction to (20) in the definition of the simulation function, i.e.,  $S(r, r) < 0$ , where  $r > 0$ . So our supposition is wrong and we accept that  $g[\sigma, \nu] \Omega g[\sigma', \nu']$ .

Hence, we prove that

$$F[\sigma, \nu] \Omega g[\sigma, \nu] \Omega g[\sigma', \nu'] \Omega F[\sigma', \nu']. \quad (41)$$

Furthermore, let  $F$  be injective; then, the equivalence class of a near-coincidence point is unique. By the above work, we have

$$F[\sigma, \nu] \Omega g[\sigma, \nu] \Omega g[\sigma', \nu'] \Omega F[\sigma', \nu']. \quad (42)$$

It implies that

$$F[\sigma, \nu] \Omega F[\sigma', \nu']. \quad (43)$$

As  $F$  is injective,  $[\sigma, \nu] \Omega [\sigma', \nu']$ . It further implies that  $\langle [\sigma, \nu] \rangle = \langle [\sigma', \nu'] \rangle$ .  $\square$

**Theorem 2.** Consider a  $(z_{\|\cdot\|}, g)$ -contraction  $F$  in the Banach interval space  $(I, \|\cdot\|)$  where  $\|\cdot\|$  satisfies the null equality and  $F$  and  $g$  are continuous and compatible mappings. Assume that the space is satisfying the  $CLR_{(F,g)}$  property. Then, a near-coincidence point exists for  $F$  and  $g$ .

*Proof.* As the space  $(I, \|\cdot\|)$  satisfies the  $CLR_{(F,g)}$  property, i.e., there exists a Picard sequence  $\{[\sigma_n, \nu_n]\}$ , such that

$$g[\sigma_{n+1}, \nu_{n+1}] \Omega F[\sigma_n, \nu_n], \quad \text{for all } n \geq 0. \quad (44)$$

There are two possibilities: either the sequence  $\{[\sigma_n, \nu_n]\}$  contains a near-coincidence point, or it converges to the near-coincidence point. We will take the case that the sequence does not contain a near-coincidence point. Hence,

$$g[\sigma_n, \nu_n] \Omega F[\sigma_n, \nu_n] \Omega g[\sigma_{n+1}, \nu_{n+1}], \quad \text{for all } n \geq 0. \quad (45)$$

The result will be proved in the following steps.

First of all, we will show that

$$\lim_{n \rightarrow \infty} \|g[\sigma_n, \nu_n] \ominus g[\sigma_{n+1}, \nu_{n+1}]\| = 0. \quad (46)$$

As  $F$  is a  $(z_{\|\cdot\|}, g)$ -contraction, by  $CLR_{(F,g)}$  property and condition (ii) of a simulation function, we have

$$\begin{aligned} 0 \leq S(\|F[\sigma_n, \nu_n] \ominus F[\sigma_{n+1}, \nu_{n+1}]\|, \|g[\sigma_n, \nu_n] \ominus g[\sigma_{n+1}, \nu_{n+1}]\|) \\ = S(\|g[\sigma_{n+1}, \nu_{n+1}] \ominus g[\sigma_{n+2}, \nu_{n+2}]\|, \|g[\sigma_n, \nu_n] \ominus g[\sigma_{n+1}, \nu_{n+1}]\|) \\ < \|g[\sigma_n, \nu_n] \ominus g[\sigma_{n+1}, \nu_{n+1}]\| - \|g[\sigma_{n+1}, \nu_{n+1}] \ominus g[\sigma_{n+2}, \nu_{n+2}]\|. \end{aligned} \quad (47)$$

This implies that

$$0 < \|g[\sigma_{n+1}, \nu_{n+1}] \ominus g[\sigma_{n+2}, \nu_{n+2}]\| < \|g[\sigma_n, \nu_n] \ominus g[\sigma_{n+1}, \nu_{n+1}]\|. \quad (48)$$

The sequence  $\{\|g[\sigma_n, \nu_n] \ominus g[\sigma_{n+1}, \nu_{n+1}]\|\}$  is nonnegative and decreasing, so it converges to a limit, say  $\mathbb{L}$ , i.e.,

$$\lim_{n \rightarrow \infty} \|g[\sigma_n, \nu_n] \ominus g[\sigma_{n+1}, \nu_{n+1}]\| = \mathbb{L}. \quad (49)$$

We have to show that  $\mathbb{L} = 0$ . On the contrary, let us suppose that  $\mathbb{L} > 0$ . Consider the sequences with the same limit  $r_n = \{\|g[\sigma_{n+1}, \nu_{n+1}] \ominus g[\sigma_{n+2}, \nu_{n+2}]\|\}$  and  $s_n = \{\|g[\sigma_n, \nu_n] \ominus g[\sigma_{n+1}, \nu_{n+1}]\|\}$  such that  $r_n < s_n$  for all  $n \in \mathbb{N}$ .

Now, by condition (iii) of the simulation function, we have

$$\begin{aligned} 0 &> \limsup_{n \rightarrow \infty} (S(r_n, s_n)) \\ &= \limsup_{n \rightarrow \infty} (S(\|g[\sigma_{n+1}, \nu_{n+1}] \ominus g[\sigma_{n+2}, \nu_{n+2}]\|, \\ &\quad \|g[\sigma_n, \nu_n] \ominus g[\sigma_{n+1}, \nu_{n+1}]\|)). \end{aligned} \quad (50)$$

It is a contradiction because

$$S(\|g[\sigma_{n+1}, \nu_{n+1}] \ominus g[\sigma_{n+2}, \nu_{n+2}]\|, \|g[\sigma_n, \nu_n] \ominus g[\sigma_{n+1}, \nu_{n+1}]\|) > 0. \quad (51)$$

Thus,  $\mathbb{L} = 0$ . That is,

$$\lim_{n \rightarrow \infty} \|g[\sigma_n, \nu_n] \ominus g[\sigma_{n+1}, \nu_{n+1}]\| = 0. \quad (52)$$

Next, we will show that the sequence  $\{g[\sigma_n, \nu_n]\}$  is a Cauchy sequence. Let us suppose, on the contrary, that  $\{g[\sigma_n, \nu_n]\}$  is not Cauchy. So there will exist  $\varepsilon_o > 0$  such that for all  $N \in \mathbb{N}$ , there exist positive integers  $m, n$  such that

$$\|g[\sigma_n, \nu_n] \ominus g[\sigma_m, \nu_m]\| > \varepsilon_o. \quad (53)$$

We can construct two partial subsequences  $\{g[\sigma_{n_k}, \nu_{n_k}]\}$  and  $\{g[\sigma_{m_k}, \nu_{m_k}]\}$  such that  $n_o \leq n_k \leq m_k$  and

$$\|g[\sigma_{n_k}, \nu_{n_k}] \ominus g[\sigma_{m_k}, \nu_{m_k}]\| > \varepsilon_o, \quad \text{for all } k \in \mathbb{N}. \quad (54)$$

Let  $m_k$  be the smallest positive integer in  $\{n_k, n_k + 1, n_k + 2, \dots\}$ . Then,

$$\|g[\sigma_{m_k-1}, \nu_{m_k-1}] \ominus g[\sigma_{n_k}, \nu_{n_k}]\| \leq \varepsilon_o, \quad \text{for all } k \in \mathbb{N}. \quad (55)$$

Also,  $m_k > n_k$  from (54), so  $m_k \geq n_k + 1$  for all  $k \in \mathbb{N}$ . But  $m_k = n_k + 1$  is not possible taking into account (52) and (54) simultaneously. So, we have  $m_k \geq n_k + 2$  for any  $k \in \mathbb{N}$ . It follows that  $n_{k+1} < m_k < m_{k+1}$  for all  $k \in \mathbb{N}$ . From (54) and (55), we have

$$\begin{aligned} \varepsilon_o &< \|g[\sigma_{m_k}, \nu_{m_k}] \ominus g[\sigma_{n_k}, \nu_{n_k}]\| \\ &\leq \|g[\sigma_{m_k}, \nu_{m_k}] \ominus g[\sigma_{m_k-1}, \nu_{m_k-1}]\| + \|g[\sigma_{m_k-1}, \nu_{m_k-1}] \ominus g[\sigma_{n_k}, \nu_{n_k}]\| \\ &\leq \|g[\sigma_{m_k}, \nu_{m_k}] \ominus g[\sigma_{m_k-1}, \nu_{m_k-1}]\| + \varepsilon_o, \quad \text{for all } k \in \mathbb{N}. \end{aligned} \quad (56)$$

Therefore,

$$\lim_{k \rightarrow \infty} \|g[\sigma_{m_k}, \nu_{m_k}] \ominus g[\sigma_{n_k}, \nu_{n_k}]\| = \varepsilon_o. \quad (57)$$

Also,

$$\lim_{k \rightarrow \infty} \|g[\sigma_{m_{k+1}}, \nu_{m_{k+1}}] \ominus g[\sigma_{n_{k+1}}, \nu_{n_{k+1}}]\| = \varepsilon_o. \quad (58)$$

As  $F$  is a  $(Z_d, g)$ -contraction associated with  $S$ ,

$$\begin{aligned} 0 &\leq S(\|F[\sigma_{m_k}, \nu_{m_k}] \ominus F[\sigma_{n_k}, \nu_{n_k}]\|, \|g[\sigma_{m_k}, \nu_{m_k}] \ominus g[\sigma_{n_k}, \nu_{n_k}]\|) \\ &= S(\|g[\sigma_{m_{k+1}}, \nu_{m_{k+1}}] \ominus g[\sigma_{n_{k+1}}, \nu_{n_{k+1}}]\|, \|g[\sigma_{m_k}, \nu_{m_k}] \ominus g[\sigma_{n_k}, \nu_{n_k}]\|) \\ &< \|g[\sigma_{m_k}, \nu_{m_k}] \ominus g[\sigma_{n_k}, \nu_{n_k}]\| - \|g[\sigma_{m_{k+1}}, \nu_{m_{k+1}}] \ominus g[\sigma_{n_{k+1}}, \nu_{n_{k+1}}]\|. \end{aligned} \quad (59)$$

Thus,

$$0 < \|g[\sigma_{m_{k+1}}, \nu_{m_{k+1}}] \ominus g[\sigma_{n_{k+1}}, \nu_{n_{k+1}}]\| < \|g[\sigma_{m_k}, \nu_{m_k}] \ominus g[\sigma_{n_k}, \nu_{n_k}]\|. \quad (60)$$

Let

$$\begin{aligned} r_n &= \|g[\sigma_{m_{k+1}}, \nu_{m_{k+1}}] \ominus g[\sigma_{n_{k+1}}, \nu_{n_{k+1}}]\|, \\ s_n &= \|g[\sigma_{m_k}, \nu_{m_k}] \ominus g[\sigma_{n_k}, \nu_{n_k}]\|. \end{aligned} \quad (61)$$

Clearly,  $r_n, s_n > 0$ ,  $\lim_{n \rightarrow \infty} r_n = \lim_{n \rightarrow \infty} s_n = \varepsilon_o$ , and  $r_n < s_n$ .

So by  $S_3$ ,

$$\begin{aligned} 0 &\leq \limsup_{k \rightarrow \infty} S(\|g[\sigma_{m_{k+1}}, \nu_{m_{k+1}}] \ominus g[\sigma_{n_{k+1}}, \nu_{n_{k+1}}]\|, \\ &\quad \|g[\sigma_{m_k}, \nu_{m_k}] \ominus g[\sigma_{n_k}, \nu_{n_k}]\|) < 0, \end{aligned} \quad (62)$$

which is a contradiction. Thus,  $\{g[\sigma_n, \nu_n]\}$  is a Cauchy sequence in  $(I, d)$ .

That is,  $\{g[\sigma_n, \nu_n]\}$  is a Cauchy sequence. Now, as the space is complete, the sequence  $\{g[\sigma_n, \nu_n]\}$  will converge to a limit  $[\sigma, \nu]$ . Since the mappings  $F$  and  $g$  are continuous, one writes

$$\begin{aligned} g[\sigma_n, \nu_n] &\longrightarrow [\sigma, \nu], \quad \text{implies } gg[\sigma_n, \nu_n] \longrightarrow g[\sigma, \nu], \\ g[\sigma_n, \nu_n] &\longrightarrow [\sigma, \nu], \quad \text{implies } Fg[\sigma_n, \nu_n] \longrightarrow F[\sigma, \nu]. \end{aligned} \quad (63)$$

The compatibility of the mappings yields that

$$\lim_{n \rightarrow \infty} \|Fg[\sigma_n, \nu_n] \ominus gF[\sigma_n, \nu_n]\| = 0. \quad (64)$$

Consider

$$\begin{aligned} \|F[\sigma, \nu] \ominus g[\sigma, \nu]\| &= \lim_{n \rightarrow \infty} \|Fg[\sigma_n, \nu_n] \ominus gg[\sigma_{n+1}, \nu_{n+1}]\| \\ &= \lim_{n \rightarrow \infty} \|Fg[\sigma_n, \nu_n] \ominus gF[\sigma_n, \nu_n]\|, \\ \|F[\sigma, \nu] \ominus g[\sigma, \nu]\| &= 0. \end{aligned} \quad (65)$$

From the above function, we have  $F[\sigma, \nu] \Omega g[\sigma, \nu]$ ; i.e.,  $[\sigma, \nu]$  is a near-coincidence point of  $F$  and  $g$ .  $\square$

*Example 7.* Consider the two continuous self-mappings  $F$  and  $g$  in the Banach interval space  $(I, \|\cdot\|)$  defined by

$$\begin{aligned} F[\sigma, v] &= [2\sigma - 4, 2v + 4]. \\ g[\sigma, v] &= [\sigma - 2, v + 2]. \end{aligned} \tag{66}$$

The function  $F$  is a  $(z_{\|\cdot\|}, g)$ -contraction according to the simulation function  $S(s, t) = \lambda t - s$ , where  $\lambda \geq 2$ . Also, the functions  $F$  and  $g$  are compatible. The sequence  $\{(-1/n), (1/n)\}$  is a Picard sequence, i.e.,

$$\begin{aligned} g([\sigma_{n+1}, v_{n+1}]) &\underset{=}{\Omega} F([\sigma_n, v_n]), \quad \text{for all } n \geq 2, \\ g\left(\left[\frac{-1}{n+1}, \frac{1}{n+1}\right]\right) &\underset{=}{\Omega} F\left(\left[\frac{-1}{n}, \frac{1}{n}\right]\right), \\ \left[\frac{-1}{n+1} - 2, \frac{1}{n+1} + 2\right] &\underset{=}{\Omega} \left[\frac{-2}{n} - 4, \frac{2}{n} + 4\right]. \end{aligned} \tag{67}$$

We can easily show that  $g([\sigma_{n+1}, v_{n+1}]) \underset{=}{\Omega} F([\sigma_n, v_n])$ , for all  $n \geq 0$ , by taking  $\omega_1 = [(-((2n^2 + 3n + 2)/n(n+1))), ((2n^2 + 3n + 2)/n(n+1))]$  and  $\omega_2 = [0, 0]$ . Then,

$$\begin{aligned} \left[\frac{-1}{n+1} - 2, \frac{1}{n+1} + 2\right] &\oplus \left[\frac{2n^2 + 3n + 2}{n(n+1)}, \frac{2n^2 + 3n + 2}{n(n+1)}\right] \\ &= \left[\frac{-2}{n} - 4, \frac{2}{n} + 4\right] \oplus [0, 0]. \end{aligned} \tag{68}$$

If we replace the compatibility of mappings by commuting mappings, then the following corollary can be stated.

**Corollary 1.** Consider the continuous and commuting mappings  $F$  and  $g$  in the Banach interval space  $(I, \|\cdot\|)$  such that the criteria of  $Z$ -contraction is satisfied by  $F$ . Assume that  $CLR(F, g)$  property holds in  $I$ ; then, a near-coincidence point exists for  $F$  and  $g$ .

**Corollary 2.** Consider a Banach interval space  $(I, \|\cdot\|)$  with two self-mappings  $F$  and  $g$ . Then, a near-coincidence point exists for  $F$  and  $g$  if

$$\|F[\sigma, v] \ominus F[\sigma', v']\| \leq \lambda \|g[\sigma, v] \ominus g[\sigma', v']\|, \tag{69}$$

for all  $[\sigma, v], [\sigma', v'] \in I$ , where  $g[\sigma, v] \underset{\neq}{\Omega} g[\sigma', v']$  and  $\lambda \in [0, 1)$ .

*Proof.* Taking the simulation function  $S(\sigma, v) = \lambda v - \sigma$  for all  $\sigma, v \in [0, \infty)$  and  $\lambda \in [0, 1)$ , according to the above condition, we have

$$\begin{aligned} \|F[\sigma, v] \ominus F[\sigma', v']\| &\leq \lambda \|g[\sigma, v] \ominus g[\sigma', v']\|, \\ &\text{for all } [\sigma, v], [\sigma', v'] \in I. \end{aligned} \tag{70}$$

It implies that

$$\begin{aligned} 0 &\leq \lambda \|g[\sigma, v] \ominus g[\sigma', v']\| - \|F[\sigma, v] \ominus F[\sigma', v']\| \\ &\leq S(\|F[\sigma, v] \ominus F[\sigma', v']\|, \|g[\sigma, v] \ominus g[\sigma', v']\|). \end{aligned} \tag{71}$$

The last inequality allows to say that  $F$  is a  $Z_{\|\cdot\|}$ -contraction, and hence, by Theorem 2, there will be a near-coincidence point for  $F$  and  $g$ .  $\square$

**Corollary 3.** Consider a Banach interval space  $(I, \|\cdot\|)$  with self-mappings  $F$  and  $g$  such that

$$\begin{aligned} \|F[\sigma, v] \ominus F[\sigma', v']\| &\leq \|g[\sigma, v] \ominus g[\sigma', v']\| \\ &- \Phi(\|g[\sigma, v] \ominus g[\sigma', v']\|) \end{aligned} \tag{72}$$

$$\forall [\sigma, v], [\sigma', v'] \in I,$$

where  $\Phi$  is a lower semicontinuous function defined on  $[0, \infty)$  so that  $\Phi^{-1}(0) = 0$ ; then,  $F$  and  $g$  have a near-coincidence point in  $I$ .

*Proof.* It suffices to take the simulation function  $S(\sigma, v) = v - \Phi(v) - \sigma$  for all  $\sigma, v \in [0, \infty)$ . Then, we can easily prove that  $F$  is a  $z$ -contraction. So by Theorem 2, there exists a near-coincidence point for  $F$  and  $g$ .  $\square$

### Data Availability

No data were used to support this study.

### Conflicts of Interest

The authors declare that they have no conflicts of interest.

### Acknowledgments

The third and fourth authors thank Sefako Makgatho Health Sciences University for its support. The fourth author would like to acknowledge that his contribution to this work was carried out with the aid of a grant from the Carnegie Corporation provided through the African Institute for Mathematical Sciences.

### References

- [1] M. A. Khasmi and W. A. Kirk, "An introduction to metric spaces and fixed point theory," *Nonlinear Functional Analysis and Applications*, pp. 20–24, 2002.
- [2] R. Kannan, "Some results on fixed points," *Bulletin of the Calcutta Mathematical Society*, vol. 60, pp. 71–78, 1968.
- [3] S. K. Chatterjee, "Fixed-point theorems," *Comptes Rendus de l'Académie Bulgare des Sciences*, vol. 25, pp. 727–730, 1972.
- [4] C. T. Aage and J. N. Salunke, "Fixed points for weak contractions in G-metric spaces," *Applied Mathematics. E-Notes*, vol. 12, pp. 23–28, 2012.
- [5] S. Banach, "Sur les opérations dans les ensembles abstraits et leur applications aux equations intégrales," *Fundamenta Mathematicae*, vol. 3, pp. 133–181, 1922.
- [6] M. Kohli, R. Shrivastava, and M. Sharma, "Some results on fixed points theorem in dislocated quasi metric spaces," *International Journal of Theoretical and Applied Sciences*, vol. 2, no. 1, pp. 27–28, 2010.
- [7] H. L. Guang and Z. Xian, "Cone metric spaces and fixed point theorems of contractive mappings," *Journal of Mathematical*



- Analysis and Applications*, vol. 332, no. 2, pp. 1468–1476, 2007.
- [8] E. Karapinar, S. Czerwik, and H. Aydi, “ $(\alpha, \psi)$ -Meir-Keeler contraction mappings in generalized b-metric spaces,” *Journal of Function Spaces*, vol. 2018, Article ID 3264620, 4 pages, 2018.
- [9] N. Aydi, H. Aydi, N. Souayah, and T. Abdeljawad, “Controlled metric type spaces and the related contraction principle,” *Mathematics*, vol. 6, no. 10, p. 194, 2018.
- [10] K. Javed, H. Aydi, F. Uddin, and M. Arshad, “On orthogonal partial b-metric spaces with an application,” *Journal of Mathematics*, vol. 2021, Article ID 6692063, 7 pages, 2021.
- [11] F. Khojasteh, S. Shukla, and S. Radenović, “A new approach to the study of fixed point theorems via simulation functions,” *Filomat*, vol. 29, no. 6, pp. 1189–1194, 2015.
- [12] A.-F. Roldán-López-de-Hierro, E. Karapinar, C. Roldán-López-de-Hierro, and J. Martínez-Moreno, “Coincidence point theorems on metric spaces via simulation functions,” *Journal of Computational and Applied Mathematics*, vol. 275, pp. 345–355, 2015.
- [13] A. F. Roldan Lopez de Hierro, E. Karapinar, and D. O’Regan, “Coincidence point theorem on quasi metric spaces via simulation functions and application to G-metric spaces,” *Journal of Fixed Point Theory and Applications*, vol. 20, no. 3, p. 112, 2018.
- [14] H. Argoubi, B. Samet, and C. Vetro, “Nonlinear contractions involving simulation functions in a metric space with a partial order,” *Journal of Nonlinear Sciences and Applications*, vol. 8, pp. 1082–1094, 2015.
- [15] A. S. S. Alharbi, H. H. Alsulami, and E. Karapinar, “On the power of simulation and admissible functions in metric fixed point theory,” *Journal of Function Spaces*, vol. 2017, Article ID 2068163, 7 pages, 2017.
- [16] R. Alsubaie, B. Alqahtani, E. Karapinar, and A. F. Roldán López de Hierro, “Extended simulation function via rational expressions,” *Mathematics*, vol. 8, no. 5, p. 710, 2020.
- [17] O. Alqahtani and E. Karapinar, “A bilateral contraction via simulation function,” *Filomat*, vol. 33, no. 15, pp. 4837–4843, 2019.
- [18] M. A. Alghamdi, S. G. Ozyurt, and E. Karapinar, “A note on extended Z-contraction,” *Mathematics*, vol. 8, p. 195, 2020.
- [19] E. Karapinar and F. Khojasteh, “An approach to best proximity points results via simulation functions,” *Journal of Fixed Point Theory and Applications*, vol. 19, no. 3, pp. 1983–1995, 2017.
- [20] E. Karapinar, “Fixed points results via simulation functions,” *Filomat*, vol. 30, no. 8, pp. 2343–2350, 2016.
- [21] H. C. Wu, “A new concept of fixed point in metric and normed interval spaces,” *Mathematics*, vol. 6, no. 11, p. 219, 2018.
- [22] H. C. Wu, “Near fixed point theorem in hyperspaces,” *Mathematics*, vol. 6, no. 6, p. 90, 2018.
- [23] R. E. Moore, *Interval Analysis*, Prentice-Hall, Englewood Cliffs, NJ, USA, 1966.
- [24] H. C. Wu, “Hahn-Banach theorems in nonstandard normed interval spaces,” *Nonlinear Analysis*, vol. 72, pp. 469–477, 2010.
- [25] M. Ullah, M. Sarwar, H. Khan, T. Abdeljawad, and A. Khan, “Near-coincidence point results in metric interval and hyperspace via simulation functions,” *Advances in Difference Equations*, vol. 2020291 pages, 2020.

## Research Article

# Graphs Associated with the Ideals of a Numerical Semigroup Having Metric Dimension 2

Ying Wang,<sup>1,2</sup> Muhammad Ahsan Binyamin ,<sup>3</sup> Wajid Ali,<sup>3</sup> Adnan Aslam ,<sup>4</sup>  
and Yongsheng Rao <sup>2</sup>

<sup>1</sup>Department of Network Technology, South China Institute of Software Engineering, Guangzhou, China

<sup>2</sup>Institute of Computing Science and Technology, Guangzhou University, Guangzhou 510006, China

<sup>3</sup>Department of Mathematics, GC University, Faisalabad, Pakistan

<sup>4</sup>Department of Natural Sciences and Humanities, University of Engineering and Technology, Lahore (RCET), Pakistan

Correspondence should be addressed to Muhammad Ahsan Binyamin; ahsanbinyamin@gmail.com

Received 18 December 2020; Revised 7 January 2021; Accepted 23 January 2021; Published 9 February 2021

Academic Editor: Ali Ahmad

Copyright © 2021 Ying Wang et al. This is an open access article distributed under the Creative Commons Attribution License, which permits unrestricted use, distribution, and reproduction in any medium, provided the original work is properly cited.

Let  $\Lambda$  be a numerical semigroup and  $I \subset \Lambda$  be an irreducible ideal of  $\Lambda$ . The graph  $G_I(\Lambda)$  assigned to an ideal  $I$  of  $\Lambda$  is a graph with elements of  $(\Lambda \setminus I)^*$  as vertices, and any two vertices  $x$  and  $y$  are adjacent if and only if  $x + y \in I$ . In this work, we give a complete characterization (up to isomorphism) of the graph  $G_I(\Lambda)$  having metric dimension 2.

## 1. Introduction

In algebraic combinatorics, the study of graphs associated with algebraic objects is one of the most important and fascinating fields of research. During the last couple of decades, a lot of research is carried out in this field. There are many papers on assigning graphs to rings, groups, and semigroups [1–6]. Several authors [7–13] studied different properties of these graphs including diameter, girth, domination, metric dimension, central sets, and planarity.

We start by defining some basic concept related to graph theory. A graph  $G = (V(G), E(G))$  has a vertex set  $V(G)$  and the edge set  $E(G)$ . The cardinality of the vertex set and edge set is called the order and size of  $G$ , respectively. A path in  $G$  is a sequence of edges  $u_1u_2, u_2u_3, \dots, u_{k-1}u_k$ . A graph  $G$  is connected if every pair of vertices  $x, y \in V(G)$  is connected by a path. The distance between two vertices  $x, y \in V(G)$  is denoted by  $d(x, y)$  and is the length of the shortest path between them. The diameter of  $G$  is denoted by  $d(G)$  and is defined as the largest distance between the vertices of  $G$ . Let  $U = \{u_1, u_2, \dots, u_r\}$  be an ordered subset of  $V(G)$ . Then, the  $r$ -tuple  $(d(u, u_1), d(u, u_2), \dots, d(u, u_r))$  is the representation  $u$  with respect to  $U$ . The vertex  $u$  is said to be resolved by  $U$  if  $(d(u, u_1), d(u, u_2), \dots, d(u, u_r)) \neq (d(v, u_1), d(v, u_2), \dots,$

$d(v, u_r))$  for any vertex  $v \in V(G)$ . The set  $U$  is called resolving set of  $G$  if distinct vertices of  $G$  have distinct representations with respect to  $U$ , and it is called basis of  $G$  if it is a resolving set with minimal cardinality. The metric dimension of  $G$ , denoted by  $\mu(G)$ , is the cardinality of basis. The concept of metric dimension was introduced by Slater [14] and later studied by Harary and Melter [15]. It has many applications, for example, robot navigation [16], pharmaceutical chemistry [17, 18], sonar and coast guard long range navigation [14], and combinatorial optimization [19].

Let  $\mathbb{N}$  be set of nonnegative integers. A subset  $\Lambda \subset \mathbb{N}$  is said to be numerical semigroup if the following holds:

- (1)  $0 \in \Lambda$
- (2)  $x + y \in \Lambda$  for all  $x, y \in \Lambda$
- (3)  $\mathbb{N} \setminus \Lambda$  is finite

It is easy to observe that the numerical semigroup is a commutative monoid. Thus, the set of numerical semigroups classifies the set of all submonoids of  $(\mathbb{N}, +)$ . The elements of the set  $\mathbb{N} \setminus \Lambda$  are called gaps of  $\Lambda$ , and the largest element of this set is known as Frobenius number. Note that every numerical semigroup is finitely generated; that is, there exist a set  $A = \{a_1, a_2, \dots, a_t\}$  such that  $\Lambda = \langle A \rangle = \{n_1a_1 + \dots,$

$n_t a_t; n_1, \dots, n_t \in \mathbb{N}$ ). Moreover, every numerical semigroup has a unique minimal system of generators. The cardinality of the minimal system of generators is called embedding dimension of  $\Lambda$ . It is denoted by  $e_\Lambda$ . A subset  $I$  of numerical semigroup  $\Lambda$  is ideal (integral ideal) of  $\Lambda$  if for all  $x \in I$  and  $s \in \Lambda$  and the element  $x + s \in I$ . An ideal  $I$  is called irreducibly ideal if it cannot be written as intersections of two or more than two ideals which contained it properly. For more details on theory of numerical semigroup, the interested readers can refer to [20].

Recently, several authors studied the metric dimension of the graphs associated with the algebraic objects. Solymaniyarniab et al. [21] gave some metric dimension formula for annihilator graphs. Bailey et al. [22] studied the constructions of resolving sets of Kneseer and Johnson graphs and provided bounds on their metric dimension. Faisal et al. [23] studied the metric dimension of the commuting graph of a dihedral group. The metric dimension of a zero-divisor graph of a commutative ring was studied in [13], while the metric dimension of a total graph of a finite commutative ring was studied in [24]. For more results on the metric dimension, we refer the readers to [25–30].

## 2. Notation and Preliminaries

Let  $\Lambda = \langle \mathcal{A} \rangle$  be a numerical semigroup, where  $\mathcal{A} = \{a_1, a_2, \dots, a_n\}$  is the minimal system of generators of  $\Lambda$ . Then, every  $x \in \Lambda$  has a representation of the form  $u_1 a_1 + u_2 a_2 + \dots + u_n a_n$ , where  $u_1, u_2, \dots, u_n$  are nonnegative integers. Let  $1 \leq p \leq n$  be a fixed integer. We say that an element  $x \in \Lambda$  has a  $p$ -representation if there exist  $a_{i_1}, a_{i_2}, \dots, a_{i_p} \in \mathcal{A}$  and  $u_{i_1}, u_{i_2}, \dots, u_{i_p}$  positive integers such that  $x = u_{i_1} a_{i_1} + u_{i_2} a_{i_2} + \dots + u_{i_p} a_{i_p}$ ; that is,  $x$  can be written as linear combination of exactly  $p$  generator of  $\Lambda$ . Let  $\Lambda_p$  denote the set containing all the elements  $x \in \Lambda$ , which have a  $p$  representation. It is easy to see that

$$\Lambda = \bigcup_{p=1}^n \Lambda_p. \quad (1)$$

Note that an element  $x \in \Lambda$  may have more than one  $p$  representations. For an element  $x \in \Lambda_p$ , we use the notation  $\Sigma_p$  if it has a unique  $p$  representation and  $\Sigma_{p,1}, \Sigma_{p,2}, \dots, \Sigma_{p,r}$  if it has  $r$  number of  $p$  representations. Let  $\Sigma_p \in \Lambda_p$ , then there exist two  $p$ -tuples, the coefficients  $p$  tuple  $(u_{i_1}, u_{i_2}, \dots, u_{i_p}) \in \mathbb{Z}_{>0}^p$ , and the generators  $p$ -tuple  $(a_{i_1}, a_{i_2}, \dots, a_{i_p}) \in \mathbb{Z}_{>0}^p$  such that  $\Sigma_p = u_{i_1} a_{i_1} + u_{i_2} a_{i_2} + \dots + u_{i_p} a_{i_p}$ . We denote the coefficient and generators  $p$  tuple of an element  $\Sigma_p$  by  $c(\Sigma_p)$  and  $g(\Sigma_p)$ , respectively. Also, the  $j$ -th component of  $c(\Sigma_p)$  and  $g(\Sigma_p)$  is denoted by  $c_j(\Sigma_p)$  and  $g_j(\Sigma_p)$ , respectively. By using the above notations, for any  $x \in \Lambda$ , we define

$$\begin{aligned} \Lambda_p(x) &= \{\Sigma_p: \Sigma_p = x\}, \\ \Lambda(x) &= \bigcup_{p=1}^n \Lambda_p(x). \end{aligned} \quad (2)$$

For a  $p$ -representation  $\Sigma_p = u_{i_1} a_{i_1} + u_{i_2} a_{i_2} + \dots + u_{i_p} a_{i_p}$ , we set

$$\mathcal{B}(\Sigma_p) = \left\{ v_{i_1} a_{i_1} + v_{i_2} a_{i_2} + \dots + v_{i_p} a_{i_p}; 0 \leq v_{i_j} \leq u_{i_j}, 1 \leq j \leq p \right\}. \quad (3)$$

**Lemma 1.** *With the notations defined above, we have*

$$\mathcal{B}(x) = \bigcup_{\Sigma_p \in \Lambda(x)} \mathcal{B}(\Sigma_p). \quad (4)$$

*Proof.* The proof of this lemma follows from the definition of  $\mathcal{B}(x)$ .

Let  $\Lambda$  be a numerical semigroup and  $I \subset \Lambda$  be irreducible ideal of  $\Lambda$ . Binyamin et al. [31] assigned a graph to numerical semigroup  $\Lambda$  and studied its properties. Peng Xu et al. [32] assign a graph  $G_I(\Lambda)$  to the ideal  $I$  of numerical semigroup  $\Lambda$  with vertex set  $V(G_I(\Lambda)) = (\Lambda \setminus I)^*$  and two vertices  $x, y$  are adjacent if and only if  $x + y \in I$ . Barucci [33] showed that every irreducible ideal  $I$  of numerical semigroup  $\Lambda$  can be expressed in the form  $\Lambda \setminus B(x)$ , where  $B(x) = \{y \in \Lambda: x - y \in \Lambda\}$ , for some  $x \in \Lambda$ . Hence, the vertex set of the graph  $G_I(\Lambda)$  is the set  $\{v_i: i \in B^*(x)\}$  for some  $x \in \Lambda$ . Peng Xu et al. [32] proved that the graph  $G_I(\Lambda)$  is always connected and diameter 2. The aim of this paper is to find all the graphs  $G_I(\Lambda)$  having metric dimension 2. The following result by Chartrand et al. [18] gives bound on the order of graph with given metric dimension  $k$  and diameter  $d$ .  $\square$

**Theorem 1.** *Let  $G$  be a graph with metric dimension  $k$  and  $|V(G)| = n$ . Let  $d$  be the diameter of  $G$ . Then,  $|V(G)| \leq d^k + k$ .*

Hence, to find graphs  $G_I(\Lambda)$  with metric dimension 2, it is enough to classify all graphs  $G_I(\Lambda)$  of order less than or equal to 6. In the next section, we give bounds for the graphs  $G_I(\Lambda)$  of orders 4 and 5.

### 2.1. Bounds for the Graphs $G_I(\Lambda)$ of Orders 4 and 5

**Lemma 2.** *Let  $\Lambda = \langle \mathcal{A} \rangle$  be a numerical semigroup of embedding dimension  $n \geq 2$ . Then,  $|G_I(\Lambda)| \neq 4$ , if one of the following holds:*

- (1)  $\Lambda_p(x) \neq \emptyset$  for some  $p \geq 3$ .
- (2)  $|\Lambda_1(x)| \geq 3$ .
- (3)  $|\Lambda_2(x)| \geq 2$ .
- (4)  $\Lambda_1(x) = \emptyset$  and  $|\Lambda_2(x)| = 1$ .
- (5)  $|\Lambda_1(x)| = 2$  and  $|\Lambda_2(x)| = 1$ .

*Proof*

- (1) If  $\Lambda_p(x) \neq \emptyset$  for some  $p \geq 3$ , then there is a  $p$ -representation  $\Sigma_p$  of  $x$  in  $\Lambda_p(x)$ . This gives  $g_1(\Sigma_p), g_2(\Sigma_p), g_3(\Sigma_p), g_1(\Sigma_p) + g_2(\Sigma_p), g_1(\Sigma_p) + g_3(\Sigma_p), g_2(\Sigma_p) + g_3(\Sigma_p), x \in \mathcal{B}^*(\Sigma_p) \subseteq \mathcal{B}^*(x)$ . This implies  $|G_I(\Lambda)| \neq 4$ .

- (2) If  $|\Lambda_1(x)| \geq 3$ , then there are  $\Sigma_{1,1}, \Sigma_{1,2}, \dots, \Sigma_{1,r} \in \Lambda_1(x)$  with  $r \geq 3$ . We assume that  $g(\Sigma_{1,1}) < g(\Sigma_{1,2}) < \dots < g(\Sigma_{1,r})$  and then  $c(\Sigma_{1,1}) \geq 5$ . This gives  $g(\Sigma_{1,1}), 2g(\Sigma_{1,1}), 3g(\Sigma_{1,1}), 4g(\Sigma_{1,1}), 5g(\Sigma_{1,1}) \in \mathcal{B}^*(\Sigma_{1,1})$ , and therefore,  $|G_I(\Lambda)| \neq 4$ .
- (3) If  $|\Lambda_2(x)| \geq 2$ , then we have  $\Sigma_{2,1}, \Sigma_{2,2}, \dots, \Sigma_{2,s} \in \Lambda_2(x)$  with  $s \geq 2$ . One can easily see that  $\mathcal{B}^*(\Sigma_{2,1}) \cup \mathcal{B}^*(\Sigma_{2,2}) \cup \dots \cup \mathcal{B}^*(\Sigma_{2,s})$  must contain  $g_1(\Sigma_{2,1}), g_2(\Sigma_{2,1}), g_1(\Sigma_{2,2}), g_2(\Sigma_{2,2}), g_1(\Sigma_{2,1}) + g_2(\Sigma_{2,1})$  and  $g_1(\Sigma_{2,2}) + g_2(\Sigma_{2,2})$ . Therefore,  $|G_I(\Lambda)| \neq 4$ .
- (4) Lemma 1: If  $\Lambda_1(x) = \emptyset$  and  $|\Lambda_2(x)| = 1$  then there is the unique 2-representation  $\Sigma_2$  of  $x$ . Now if  $\Lambda_p(x) \neq \emptyset$  for some  $p \geq 3$  then from (1), it follows that  $|G_I(\Lambda)| \neq 4$ , and if  $\Lambda_p(x) = \emptyset$  for all  $p \geq 3$ , then gives  $\mathcal{B}^*(x) = \mathcal{B}^*(\Sigma_2)$ . So if  $c(\Sigma_2) = (1, 1)$ , then  $|G_I(\Lambda)| = 3$ ; otherwise,  $|G_I(\Lambda)| > 4$ . Consequently,  $|G_I(\Lambda)| \neq 4$ .
- (5) If  $|\Lambda_1(x)| = 2$  and  $|\Lambda_2(x)| = 1$ , then we can assume  $\Sigma_{1,1}, \Sigma_{1,2} \in \Lambda_1(x)$  and  $\Sigma_2 \in \Lambda_2(x)$ . This gives  $g(\Sigma_{1,1}), g(\Sigma_{1,2}), g_1(\Sigma_2), g_2(\Sigma_2), g_1(\Sigma_2) + g_2(\Sigma_2)$  are in  $\mathcal{B}^*(x)$ , and therefore,  $|G_I(\Lambda)| \neq 4$ .  $\square$

**Lemma 3.** Let  $\Lambda = \langle \mathcal{A} \rangle$  be a numerical semigroup of embedding dimension  $n \geq 2$ . Then,  $|G_I(\Lambda)| \neq 5$ , if one of the following holds:

- (1)  $\Lambda_p(x) \neq \emptyset$  for some  $p \geq 3$ .
- (2)  $|\Lambda_1(x)| \geq 2$ .
- (3)  $|\Lambda_2(x)| \geq 3$ .
- (4)  $|\Lambda_1(x)| = 1$  and  $|\Lambda_2(x)| = 2$ .

$$\begin{aligned} \mathcal{B}^*(x) &= \mathcal{B}^*(\Sigma_{1,1}) \cup \mathcal{B}^*(\Sigma_{1,2}) = \{g(\Sigma_{1,1}), 2g(\Sigma_{1,1}), \dots, c(\Sigma_{1,1}) \cdot g(\Sigma_{1,1})\} \cup \{g(\Sigma_{1,2}), 2g(\Sigma_{1,2}), \dots, c(\Sigma_{1,2}) \cdot g(\Sigma_{1,2})\} \\ &= \{g(\Sigma_{1,1}), 2g(\Sigma_{1,1}), \dots, c(\Sigma_{1,1}) \cdot g(\Sigma_{1,1}), g(\Sigma_{1,2}), 2g(\Sigma_{1,2}), \dots, c(\Sigma_{1,2}) \cdot g(\Sigma_{1,2})\}. \end{aligned} \quad (5)$$

We show that  $\{\mathcal{B}^*(\Sigma_{1,1}) \cap \mathcal{B}^*(\Sigma_{1,2})\} \setminus \{c(\Sigma_{1,2}) \cdot g(\Sigma_{1,2})\} = \emptyset$ . Let  $p \cdot g(\Sigma_{1,1}) = q \cdot g(\Sigma_{1,2})$  for some  $q < p < c(\Sigma_{1,1})$  with  $q = 2, 3, \dots, c(\Sigma_{1,2}) - 1$ . Then,  $p \cdot g(\Sigma_{1,1}) + (c(\Sigma_{1,1}) - p) \cdot g(\Sigma_{1,1}) = c(\Sigma_{1,1}) \cdot g(\Sigma_{1,1})$ , and we get  $q \cdot g(\Sigma_{1,2}) + (c(\Sigma_{1,1}) - p) \cdot g(\Sigma_{1,1}) = x$ . This gives  $\Lambda_2(x) \neq \emptyset$ , a contradiction. Therefore, we have  $|\mathcal{B}^*(x)| = c(\Sigma_{1,1}) + c(\Sigma_{1,2}) - 1$ . As  $|G_I(\Lambda)| = 4$ ,  $c(\Sigma_{1,1}) = 3$  and  $g(\Sigma_{1,2}) = 2$  is the only possibility. This gives case (2).

Let  $|\Lambda_1(x)| = 1 = |\Lambda_2(x)|$  and  $\Lambda_p(x) = \emptyset, \forall p \geq 3$ . Then, we can assume  $\Sigma_1 \in \Lambda_1(x)$  and  $\Sigma_2 \in \Lambda_2(x)$  are the only possible 1-representation and 2-representation of  $x$ , respectively. By (2) in Lemma 2, we have  $c(\Sigma_2) = (1, 1)$ . In this case, it is easy to see that  $\mathcal{B}^*(x) = \{g(\Sigma_1), 2g(\Sigma_1), \dots, c(\Sigma_1) \cdot g(\Sigma_1), g_1(\Sigma_2), g_2(\Sigma_2)\}$ . Then,  $|\mathcal{B}^*(x)| = 4$  gives  $c(\Sigma_1) = 2$  and we get case (3).  $\square$

*Proof.* This lemma can be proved in a similar way as we proved Lemma 2.  $\square$

## 2.2. Computation of Irreducible Ideals for the Graphs $G_I(\Lambda)$ of Orders 4 and 5

**Lemma 4.** Let  $\Lambda = \langle \mathcal{A} \rangle$  be a numerical semigroup of embedding dimension  $n \geq 2$ . If  $|G_I(\Lambda)| = 4$ , then  $x$  is one of the following:

- (1)  $x = 4g(\Sigma_1)$ .
- (2)  $x = 3g(\Sigma_{1,1})$  and  $x = 2g(\Sigma_{1,2})$ .
- (3)  $x = 2g(\Sigma_1)$  and  $x = g_1(\Sigma_2) + g_2(\Sigma_2)$ .

*Proof.* If  $|G_I(\Lambda)| = 4$ , then from Lemma 2, it follows that  $x \in \Lambda$  satisfies one of the following conditions:

- $|\Lambda_1(x)| \leq 2$  and  $\Lambda_p(x) = \emptyset, \forall p \geq 2$ .
- $|\Lambda_1(x)| = 1, |\Lambda_2(x)| = 1$  and  $\Lambda_p(x) = \emptyset, \forall p \geq 3$ .

If  $|\Lambda_1(x)| = 1$  and  $\Lambda_p(x) = \emptyset, \forall p \geq 2$ , then  $x$  has a unique 1-representation  $\Sigma_1$ . By Lemma 1, we get  $\mathcal{B}^*(x) = \mathcal{B}^*(\Sigma_1) = \{g(\Sigma_1), 2g(\Sigma_1), \dots, c(\Sigma_1) \cdot g(\Sigma_1)\}$ . As  $|G_I(\Lambda)| = 4$ , it follows that  $c(\Sigma_1) = 4$ . This gives case (1).

Now if  $|\Lambda_1(x)| = 2$  and  $\Lambda_p(x) = \emptyset, \forall p \geq 2$ , then there are exactly two 1-representations, say  $\Sigma_{1,1}$  and  $\Sigma_{1,2}$  of  $x$ . Assume that  $g(\Sigma_{1,1}) < g(\Sigma_{1,2})$ , then  $c(\Sigma_{1,2}) < c(\Sigma_{1,1})$  and  $c(\Sigma_{1,1})$  is not a multiple of  $c(\Sigma_{1,2})$ . Then, it follows from Lemma 1 that

**Lemma 5.** Let  $\Lambda = \langle \mathcal{A} \rangle$  be a numerical semigroup of embedding dimension  $n \geq 2$ . If  $|G_I(\Lambda)| = 5$ , then  $x$  is one of the following:

- (1)  $x = 5g(\Sigma_1)$ .
- (2)  $x = 2g_1(\Sigma_2) + g_2(\Sigma_2)$ .
- (3)  $x = g_1(\Sigma_{2,1}) + g_2(\Sigma_{2,1})$  and  $x = g_1(\Sigma_{2,2}) + g_2(\Sigma_{2,2})$ .
- (4)  $x = 3g(\Sigma_1)$  and  $x = g_1(\Sigma_2) + g_2(\Sigma_2)$ .

*Proof.* Given that  $|G_I(\Lambda)| = 5$ , then from Lemma 5, it follows that  $x \in \Lambda$  satisfies one of the following conditions:

- $|\Lambda_1(x)| = 1$  and  $\Lambda_p(x) = \emptyset, \forall p \geq 2$ .
- $|\Lambda_2(x)| \leq 2$  and  $\Lambda_p(x) = \emptyset, \forall p \neq 2$ .
- $|\Lambda_1(x)| = 1, |\Lambda_2(x)| = 1$  and  $\Lambda_p(x) = \emptyset, \forall p \geq 3$ .

These possibilities can be checked in a similar way as we did in Lemma 4 to get the required result.  $\square$

### 3. Graphs $G_I(\Lambda)$ with Metric Dimension 2

**Theorem 2.** *There are exactly 5 nonisomorphic graphs  $G_I(\Lambda)$  with metric dimension 2.*

We prove Theorem 2 in a sequence of following lemmas.

**Lemma 6.** *There are exactly 2 nonisomorphic graphs  $G_I(\Lambda)$  with 4 or less vertices and metric dimension 2.*

*Proof.* It is trivial to note that no such graph exists for  $|G_I(\Lambda)| = 2, 3$ .

Now if  $|G_I(\Lambda)| = 4$ , then from Lemma 4, we have the following possibilities:

- (1)  $x = 4g(\Sigma_1)$  with  $\Lambda_p(x) = \emptyset, \forall p \geq 2$ .
- (2)  $x = 3g(\Sigma_{1,1}) = 2g(\Sigma_{1,2})$  with  $\Lambda_p(x) = \emptyset, \forall p \geq 2$ .
- (3)  $x = 2g(\Sigma_1) = g_1(\Sigma_2) + g_2(\Sigma_2)$  with  $\Lambda_p(x) = \emptyset, \forall p \geq 3$ .

If (1) holds, then  $I = \Lambda \setminus \mathcal{B}^*(4g(\Sigma_1))$ , and therefore,  $G_I(\Lambda)$  is isomorphic to the graph given in Figure 1. So metric dimension of  $G_I(\Lambda)$  is 2.

Now if (2) or (3) holds, then either  $I = \Lambda \setminus \mathcal{B}^*(3g(\Sigma_{1,1}))$  or  $I = \Lambda \setminus \mathcal{B}^*(2g(\Sigma_1))$ . In both cases,  $G_I(\Lambda)$  is isomorphic to the graph given in Figure 2, and therefore, metric dimension of  $G_I(\Lambda)$  is 2.  $\square$

**Lemma 7.** *There are exactly 3 nonisomorphic graphs  $G_I(\Lambda)$  with 5 vertices and metric dimension 2.*

*Proof.* If  $|G_I(\Lambda)| = 5$ , then from Lemma 5, we have the following possibilities:

- (1)  $x = 5g(\Sigma_1)$  with  $\Lambda_p(x) = \emptyset, \forall p \geq 2$ .
- (2)  $x = 2g_1(\Sigma_2) + g_2(\Sigma_2)$  with  $\Lambda_p(x) = \emptyset, \forall p \neq 2$ .
- (3)  $x = g_1(\Sigma_{2,1}) + g_2(\Sigma_{2,1}) = g_1(\Sigma_{2,2}) + g_2(\Sigma_{2,2})$  with  $\Lambda_p(x) = \emptyset, \forall p \neq 2$ .
- (4)  $x = 3g(\Sigma_1)$  and  $x = g_1(\Sigma_2) + g_2(\Sigma_2)$  with  $\Lambda_p(x) = \emptyset, \forall p \geq 3$ .

If (1) holds, then  $I = \Lambda \setminus \mathcal{B}^*(5g(\Sigma_1))$ , and therefore,  $G_I(\Lambda)$  is isomorphic to the graph given in Figure 3.

Now, if (2) holds, then  $I = \Lambda \setminus \mathcal{B}^*(2g_1(\Sigma_2) + g_2(\Sigma_2))$ , and therefore,  $G_I(\Lambda)$  is isomorphic to the graph given in Figure 4.

If (3) or (4) holds, then  $I = \Lambda \setminus \mathcal{B}^*(g_1(\Sigma_{2,1}) + g_2(\Sigma_{2,1}))$  or  $I = \Lambda \setminus \mathcal{B}^*(3g(\Sigma_1))$ . In both cases,  $G_I(\Lambda)$  is isomorphic to the graph given in Figure 5.

For all these 3 cases, one can easily show that metric dimension of  $G_I(\Lambda)$  is 2.

Finally, it is required to check all the graphs  $G_I(\Lambda)$  of order six having metric dimension 2. Binyamin et al. [34] proved that if  $|G_I(\Lambda)| = 6$ , then  $G_I(\Lambda)$  is isomorphic to one of the graphs given in Table 1. Now, it is easy to see that all the graphs given in Table 1 have metric dimension 3.  $\square$

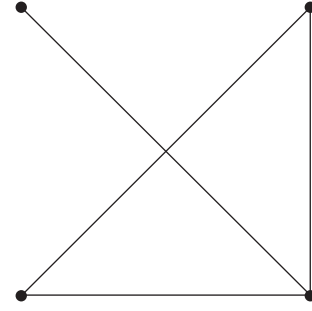


FIGURE 1: Graphs  $G_I(\Lambda)$  When  $x = 4g(\Sigma_1)$  with  $\Lambda_p(x) = \emptyset, \forall p \geq 2$ .

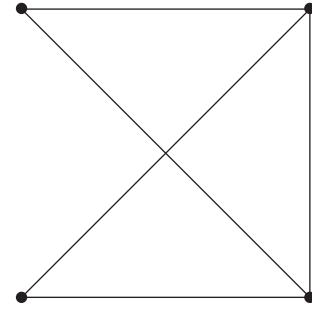


FIGURE 2: Graph  $G_I(\Lambda)$  for the remaining two cases.

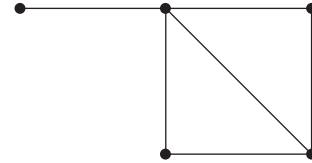


FIGURE 3: Graphs  $G_I(\Lambda)$  When  $x = 5g(\Sigma_1)$  with  $\Lambda_p(x) = \emptyset, \forall p \neq 2$ .

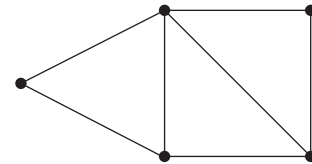


FIGURE 4: Graphs  $G_I(\Lambda)$  When  $x = 2g(\Sigma_2)$  with  $\Lambda_p(x) = \emptyset, \forall p \neq 2$ .

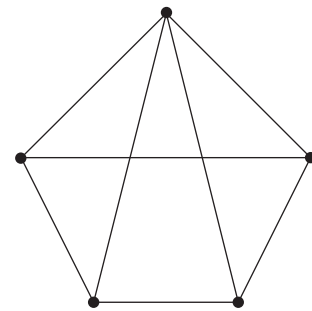


FIGURE 5: Graph  $G_I(\Lambda)$  for the remaining two cases.

TABLE 1: Graph  $G_I(\Lambda)$  of order 6 up to isomorphism.

Type	Degree sequence	Graph
1	(1, 2, 3, 3, 4, 5)	
2	(2, 3, 3, 4, 5, 5)	
3	(2, 3, 4, 4, 4, 5)	
4	(3, 3, 4, 4, 4, 5)	
5	(3, 4, 4, 4, 4, 5)	

TABLE 1: Continued.

Type	Degree sequence	Graph
6	(4, 4, 4, 4, 5, 5)	

**Data Availability**

No data are required for the study.

**Conflicts of Interest**

The authors declare that they have no conflicts of interest.

**Acknowledgments**

This work was supported by the National Key R and D Program of China (no. 2018YFB1005100), Innovation Projects in Universities of Guangdong Province (no. 2020KTSCX21), and Development Project of Young Scientific and Technological Talents in Higher Education of Guizhou Province (no. QianJiaoHe KY[2021]250).

**References**

- [1] M. Afkhami and K. Khashyarmansh, "The intersection graph of ideals of a lattice," *Note di Matematica*, vol. 34, no. 2, pp. 135–143, 2014.
- [2] D. F. Anderson and P. S. Livingston, "The zero-divisor graph of a commutative ring," *Journal of Algebra*, vol. 217, no. 2, pp. 434–447, 1999.
- [3] D. F. Anderson and A. Badawi, "The total graph of a commutative ring," *Journal of Algebra*, vol. 320, no. 7, pp. 2706–2719, 2008.
- [4] A. Badawi, "On the annihilator graph of a commutative ring," *Communications in Algebra*, vol. 42, no. 1, pp. 108–121, 2014.
- [5] M. Behboodi and Z. Rakeei, "The annihilating-ideal graph of commutative rings I," *Journal of Algebra and Its Applications*, vol. 10, no. 4, pp. 727–739, 2011.
- [6] H. R. Maimani, M. Salimi, A. Sattari, and S. Yassemi, "Comaximal graph of commutative rings," *Journal of Algebra*, vol. 319, no. 4, pp. 1801–1808, 2008.
- [7] D. F. Anderson and S. B. Mulay, "On the diameter and girth of a zero-divisor graph," *Journal of Pure and Applied Algebra*, vol. 210, no. 2, pp. 543–550, 2007.
- [8] T. Tamizh Chelvam and K. Selvakumar, "Central sets in annihilating-ideal graph of a commutative ring," *Journal of*

- Combinatorial Mathematics and Combinatorial Computer*, vol. 88, pp. 277–288, 2014.
- [9] T. Tamizh Chelvam and K. Selvakumar, “Domination in the directed zero-divisor graph of ring of matrices,” *Journal of Combinatorial Mathematics and Combinatorial Computer*, vol. 91, pp. 155–163, 2014.
- [10] S. Akbari, H. R. Maimani, and S. Yassemi, “When a zero-divisor graph is planar or a complete  $r$ -partite graph,” *Journal of Algebra*, vol. 270, no. 1, pp. 169–180, 2003.
- [11] I. Beck, “Coloring of commutative rings,” *Journal of Algebra*, vol. 116, pp. 208–226, 1998.
- [12] R. F. Bailey and P. J. Cameron, “Base size, metric dimension and other invariants of groups and graphs,” *Bulletin of the London Mathematical Society*, vol. 43, no. 2, pp. 209–242, 2011.
- [13] S. Pirzada and R. Raja, “On the metric dimension of a zero-divisor graph,” *Communications in Algebra*, vol. 45, no. 4, pp. 1399–1408, 2017.
- [14] P. J. Slater, “Leaves of trees,” *Congressus Numerantium*, vol. 14, pp. 549–559, 1975.
- [15] F. Harary and R. A. Melter, “On the metric dimension of a graph,” *Ars Combinatoria*, vol. 2, pp. 191–195, 1976.
- [16] S. Khuller, B. Raghavachari, and A. Rosenfeld, “Localization in graphs,” Technical report CS-TR- 3326, University of Maryland at College Park, College Park, MD, USA, 1994.
- [17] P. J. Cameron and J. H. Van Lint, “Designs, graphs, codes and their links,” in *London Mathematical Society Student Texts*-Cambridge University Press, Cambridge, UK, 1991.
- [18] G. Chartrand, L. Eroh, M. A. Johnson, and O. R. Oellermann, “Resolvability in graphs and the metric dimension of a graph,” *Discrete Applied Mathematics*, vol. 105, no. 1–3, pp. 99–113, 2000.
- [19] A. Sebo and E. Tannier, “On metric generators of graphs,” *Mathematics of Operations Research*, vol. 29, pp. 383–393, 2004.
- [20] J. C. Rosales and P. A. Garcia-Sanchez, “Numerical semigroups,” *Note di Matematica*, vol. 34, pp. 135–143, 2014.
- [21] V. Soleymanivarniab, A. Tehrani, and R. Nikandish, “The metric dimension of annihilator graphs of commutative rings,” *Journal of Algebra and Its Applications*, vol. 19, no. 5, 2020.
- [22] R. F. Bailey, J. Cáceres, D. Garijo et al., “Resolving sets for Johnson and kneser graphs,” *European Journal of Combinatorics*, vol. 34, no. 4, pp. 736–751, 2013.
- [23] F. Ali, M. Salman, and S. Huang, “On the commuting graph of dihedral group,” *Communications in Algebra*, vol. 44, no. 6, pp. 2389–2401, 2016.
- [24] D. Dolzan, “The metric dimension of the total graph of a finite commutative ring,” *Canadian Mathematical Bulletin*, vol. 59, no. 4, pp. 748–759, 2016.
- [25] A. N. A. Koam and A. Ahmad, “Barycentric subdivision of cayley graphs with constant edge metric dimension,” *IEEE Access*, vol. 8, no. 1, pp. 80624–80628, 2020.
- [26] M. B. Ali Ahmad, “Saba sultan, on metric dimension and minimal doubly resolving sets of harary graph,” *AMUC*, vol. 89, no. 1, pp. 123–129, 2020.
- [27] A. N. A. Koam, A. Ahmad, and A. Haider, “Radio number associated with zero divisor graph,” *Mathematics*, vol. 8, no. 12, p. 2187, 2020.
- [28] Z. Shao, S. M. Sheikholeslami, P. Wu, and J.-B. Liu, “The metric dimension of some generalized Petersen graphs,” *Discrete Dynamics in Nature and Society*, vol. 2018, Article ID 4531958, 10 pages, 2018.
- [29] Z. Shao, P. Wu, E. Zhu, and L. Chen, “On metric dimension in some hex derived networks,” *Sensors*, vol. 19, no. 1, p. 94, 2019.
- [30] E. Zhu, A. Taranenko, Z. Shao, and J. Xu, “On graphs with the maximum edge metric dimension,” *Discrete Applied Mathematics*, vol. 257, pp. 317–324, 2019.
- [31] M. A. Binyamin, H. M. A. Siddiqui, N. M. Khan, A. Aslam, and Y. Rao, “Characterization of graphs associated with numerical semigroups,” *Mathematics*, vol. 7, no. 6, p. 557, 2019.
- [32] P. Xu, M. A. Binyamin, A. Aslam, W. Ali, H. Mahmood, and H. Zhou, “Characterization of graphs associated to the ideal of the numerical semigroups,” *Journal of Mathematics*, vol. 14, 2020.
- [33] V. Barucci, “Decompositions of ideals into irreducible ideals in numerical semigroups,” *Journal of Commutative Algebra*, vol. 2, no. 3, pp. 281–294, 2010.
- [34] M. Ahsan Binyamin, W. Ali, A. Aslam, and H. Mahmood, “Classification of planar graphs associated to the ideal of the numerical semigroup,” 2012, <https://arxiv.org/abs/2012.10434>.

## Research Article

# Connectivity and Wiener Index of Fuzzy Incidence Graphs

Juanyan Fang,<sup>1</sup> Irfan Nazeer,<sup>2</sup> Tabasam Rashid ,<sup>2</sup> and Jia-Bao Liu <sup>3</sup>

<sup>1</sup>Institute of Information Technology & Engineering Management, Tongling College, Tongling 244000, China

<sup>2</sup>University of Management and Technology (UMT), Lahore, Pakistan

<sup>3</sup>School of Mathematics and Physics, Anhui Jianzhu University, Hefei 230601, China

Correspondence should be addressed to Jia-Bao Liu; liujiabaoad@163.com

Received 9 December 2020; Revised 7 January 2021; Accepted 25 January 2021; Published 4 February 2021

Academic Editor: Ali Ahmad

Copyright © 2021 Juanyan Fang et al. This is an open access article distributed under the Creative Commons Attribution License, which permits unrestricted use, distribution, and reproduction in any medium, provided the original work is properly cited.

Connectivity is a key theory in fuzzy incidence graphs (FIGs). In this paper, we introduced connectivity index (CI), average connectivity index (ACI), and Wiener index (WI) of FIGs. Three types of nodes including fuzzy incidence connectivity enhancing node (FICEN), fuzzy incidence connectivity reducing node (FICRN), and fuzzy incidence connectivity neutral node (FICNN) are also discussed in this paper. A correspondence between WI and CI of a FIG is also computed.

## 1. Introduction and Preliminaries

Zadeh [1] presented the theory of fuzzy set (FS) to resolve complications in tackling with precariousness. Since then, the FS theory becomes a rich area in multiple disciplines, including mathematics, computer science, and signal processing. The theory of graphs has been considered to play a vital role in dealing with real-life situations. A graph is an easy way of expressing information, including the relationship between different objects. The objects are shown by nodes, and relations are represented by edges. In this paper, all graphs are finite, simple, without loops, and undirected. When there is a lack of certainty in the illustration of the objects and their association, we need to draw a fuzzy graph (FG) model. Zadeh's FS provided a productive ground for the theory of FGs which has been proposed by Rosenfeld [2]. In a graph, the strength of connectedness (SC) between any two vertices is either 0 or 1, whereas in FG, it is a real number  $\in [0, 1]$ . The study of FGs leads many scientists to contribute in this field, such as Yeh and Bang [3] studied the concept of FGs independently and discussed its applications in clustering analysis. Bhattacharya and Suraweera [4] discussed an algorithm to compute the max-min powers and property of FGs. Bhutani [5] worked on automorphism of FGs. Mordeson [6] introduced fuzzy line graphs. Bhutani and Rosenfeld [7, 8] studied strong arcs as well as fuzzy end

nodes in FGs. Sunitha and Vijayakumar [9, 10] defined fuzzy trees and fuzzy blocks in FGs. Samanta et al. [11] inaugurated completeness and regularity of generalized FGs. Samanta and Pal [12] studied fuzzy planner graphs. Mathew and Sunitha [13] classified the edges of a FG as an  $\alpha$ -strong,  $\beta$ -strong, and  $\delta$ -edge. Mathew and Sunitha [14, 15] presented vertex, edge connectivity, and cycle connectivity in FGs. Mathew et al. [16] initiated saturation in FGs, and Binu et al. [17] explored CI and its application in FGs. Binu et al. [18] investigated CI of FG and its application to human trafficking. For some other significant works on graphs and FGs, one may refer to [19–25].

Wiener [26] was the first who investigated WI when he was studying about the boiling point of paraffin. After the landmark work of Harold Wiener about WI, in the middle of 1970s, new results related to WI were described. In graphs, WI has been studied in different fields such as Chemistry, Mathematics, and Physics. Binu et al. [27] discussed WI of FG and its application to illegal immigration networks.

FGs are unable to provide any information on the effect of a vertex on edges of the graph. Therefore, this disadvantage opens a way to introduce FIGs. FIGs talk about the effect of a vertex on an edge. Dinesh [28] presented the idea of FIGs. For example, if vertices show different residence societies and edges show roads joining these residence societies, we can have a FG expressing the extent of traffic from



one society to another. The society has the maximum number of residents and will have maximum ramps in society. So, if  $c$  and  $d$  are two societies and  $cd$  is a road joining them, then  $(c, cd)$  could express the ramp system from the road  $cd$  to the society  $c$ . In the case of an unweighted graph,  $c$  and  $d$  both will have an influence of 1 on  $cd$ . In a directed graph, the influence of  $c$  on  $cd$  represented by  $(c, cd)$  is 1, whereas  $(d, cd)$  is 0. This idea can be generalized by FIGs. Mordeson [29] studied numerous connectivity perceptions in FIGs. Malik et al. [30] explained different uses of FIGs. Mordeson et al. [31] proposed a fuzzy incidence (HTML translation failed) blocks along with their applications. Mordeson and Mathew [32] discussed different connectivity ideas in FIGs.

The motivation of our work is that CI, ACI, and WI of FGs exists in literature, but these indices are unknown for FIGs. These indices will make a way to study different properties of FIGs at length. This is why we propose these concepts for FIGs. Our work will open the new doors for many researchers to study FIGs in detail. The outline of this paper is as follows. In Section 1, we provide elementary definitions, results, and expressions of FIGs, which are required for the development of the content. In Section 2, we discuss CI of FIGs. Section 3 describes certain boundaries for CI of FIGs. CI of vertex and edge deleted fuzzy incidence subgraph (FIS) is illustrated in Section 4. Section 5 explains ACI and its characteristics. In Section 6, we discuss WI of FIG and a relationship between connectivity and WI. Below, we present some preliminary definitions from [17, 19, 32].

Let  $G$  be a simple graph with vertex set  $V(G)$  and edge set  $E(G)$ . Then, an incidence graph (IG) is given by  $G = (V, E, I)$ , where  $I \subseteq V \times E$ . An IG is shown in Figure 1, and if  $(u, uv)$  is in IG, then  $(u, uv)$  is said to be an incidence pair or pair. Assume an IG  $G = (V, E, I)$ . A sequence  $v_0, (v_0, v_0v_1), v_0v_1, (v_1, v_0v_1), v_1, \dots, v_{n-1}, (v_{n-1}, v_{n-1}v_n), v_{n-1}v_n, (v_n, v_{n-1}v_n), v_n$  is said to be a walk. It is closed if  $v_0 = v_n$ . A walk is called a path if it has all distinct vertices. An IG is said to be connected if all pair of vertices are joined by a path. An edge  $ab$  is said to be a fuzzy bridge (FB) if the deletion of  $ab \in \theta^*$  lessens the SC between some pair of vertices in  $G$ .

In this paper, minimum is represented by  $\wedge$  and maximum is expressed by  $\vee$ .

**Definition 1.** Consider a graph  $G = (V, E)$ , and  $\eta$  and  $\theta$  are fuzzy subsets of  $V$  and  $E$ , respectively. Assume  $V \times E$  has a fuzzy subset  $\psi$ . If  $\psi(v^*, e^*) \leq \eta(v^*) \wedge \theta(e^*)$  for every  $v^* \in V$  and  $e^* \in E$ , then  $\psi$  is called a FI of  $G$ .

**Definition 2.** Assume a graph  $G = (V, E)$  and  $(\eta, \theta)$  be a fuzzy subgraph of  $G$ , if  $\psi$  is a FI of  $G$ , then  $G = (\eta, \theta, \psi)$  is called a FIG of  $G$ .

**Definition 3.** Consider a FIG  $G = (\eta, \theta, \psi)$ . Then,  $H = (\kappa, \phi, \Omega)$  is a FIS of  $G$  if  $\kappa \subseteq \eta, \phi \subseteq \theta$  and  $\Omega \subseteq \psi$ .

**Definition 4.** Assume  $G = (\eta, \theta, \psi)$  is a FIG. A FI path  $\lambda$  from  $g$  to  $h, g, gh \in \eta^* \cup \theta^*$ , is defined as a sequence of elements  $\eta^*, \theta^*$ , and  $\psi^*$  beginning with  $g$  and closing with  $h$ . The

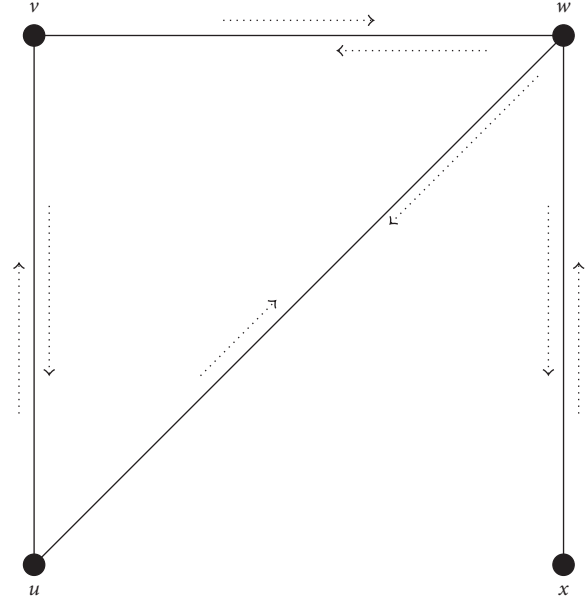


FIGURE 1: Incidence graph.

minimum value of  $\psi(x, xg)$  is called incidence strength (IS), where  $(x, xg) \in \lambda$ .

In FIG, the incidence paths (IPs) can take distinct forms.  $u_0 = (u_0, u_0u_1), u_0u_1$  is an IP of length one.  $u_0 = (u_0, u_0u_1), u_0u_1, (u_1, u_0u_1)u_1$  is an IP of length two.

**Definition 5.** Consider  $G$  be a FIG. An incidence pair  $(a, ab)$  is strong if  $\psi(a, ab) \geq \text{ICONN}_{G-(a,ab)}(a, ab)$  where  $\text{ICONN}_{G-(a,ab)}(a, ab)$  shows the highest IS of  $a - ab$ . If  $\psi(a, ab) > \text{ICONN}_{G-(a,ab)}(a, ab)$ , then the pair is called  $\alpha$ -strong. If  $\psi(a, ab) = \text{ICONN}_{G-(a,ab)}(a, ab)$ , then this type of pair is  $\beta$ -strong. If an incidence pair is  $\alpha$ -strong or  $\beta$ -strong, then this kind of pair is a strong pair. If HTML translation failed, then this type of pair is called  $\delta$ -incidence pair.

**Definition 6.** Assume  $G$  be a FIG. If all pairs of  $\lambda$  are strong, then an IP  $\lambda$  in  $G$  is called strong IP.

**Definition 7.** Consider  $G = (\eta, \theta, \psi)$  be a FIG.  $H = (\kappa, \phi, \Omega)$  is called a subgraph of  $G$  if  $\kappa(a) = \eta(a)$  for all  $a \in \kappa^*$ ,  $\phi(ab) = \theta(ab)$  for all  $ab \in \phi^*$ , and  $\Omega(a, ab) = \psi(a, ab)$  for all pair  $(a, ab) \in \Omega^*$ .

**Proposition 1.** If  $H$  is a FIS of  $G$ , then  $\text{ICONN}_{H(a,ab)} \leq \text{ICONN}_{G(a,ab)}$ .

**Definition 8.** A FIG of  $G$  is said to be complete if  $\psi(a, ab) = \eta(a) \wedge \theta(ab)$  for every  $(a, ab) \in \psi^*$ .

**Definition 9** (see [19]). The distance  $d(u, v)$  between two vertices  $u, v \in V(G)$  is the minimum number of edges in a path between  $u$  and  $v$  in  $G$ .

**Definition 10.** In a graph  $G$ , a path of shortest length is called geodesic.

**Definition 11.** (see [19]). WI of a graph  $G$  is the sum of distances between all pairs of vertices of  $G$ . Then, the WI of a graph  $G$  is given by  $W(G) = \sum_{u,v \in V(G)} d(u, v)$ .

## 2. Connectivity Index of Fuzzy Incidence Graph

Connectivity is a common parameter associated with a network. This section includes the introduction and formula to calculate CI of FIG. For easiness, in the coming sections, we will take  $\eta(a) = 1$  for every  $a \in \eta^*$ .

**Definition 12.** Let  $G = (\eta, \theta, \psi)$  be a FIG. The CI of  $G$  is given by

$$CI(G) = \sum_{a,b \in \eta^*} \eta(a)\eta(b)ICONN_G(a, b), \quad (1)$$

$ICONN_G(a, b)$  is the maximum value of ISs for all the possible IPs between  $a$  and  $b$ .

**Example 1.** Assume  $G$  is a FIG given in Figure 2 having  $\eta^* = \{i, j, k, l\}$ ;  $\theta(ij) = 0.8, \theta(ik) = 0.4, \theta(jk) = 0.7, \theta(kl) = 0.9$ ;  $\psi(i, ij) = 0.7, \psi(j, ji) = 0.5, \psi(i, ik) = 0.3, \psi(k, ki) = 0.2, \psi(j, jk) = 0.3, \psi(k, kj) = 0.7, \psi(k, kl) = 0.7$ , and  $\psi(l, lk) = 0.3$  with  $CI(G) = 2.0$ .

The connectivity indices of subgraphs of FIGs can never be surpassed that of the FIGs. Therefore, a subgraph  $H$  of FIG  $G$  will have to be less than or equal to CI than the  $CI(G)$ . This is shown in the coming proposition.

**Proposition 2.** If  $H = (\kappa, \phi, \Omega)$  is a FIS of  $G = (\eta, \theta, \psi)$ , then  $CI(H) \leq CI(G)$ .

*Proof.* Let  $a, b \in \kappa^*$ . As  $H = (\kappa, \phi, \Omega)$  is a FIS of  $G = (\eta, \theta, \psi)$ ,  $\kappa(a) \leq \eta(a)$ . Also, if  $H$  is a FIS of  $G$ , then  $ICONN_H(a, b) \leq ICONN_G(a, b)$  for any two  $a, b \in \kappa^*$ . This implies  $\sum_{a,b \in \kappa^*} \kappa(a)\kappa(b) ICONN_H(a, b) \leq \sum_{a,b \in \eta^*} \eta(a)\eta(b) ICONN_G(a, b)$  which implies  $CI(H) \leq CI(G)$ .  $\square$

**Example 2.** Consider  $G$  be a FIG provided in Figure 3 having  $\eta^* = \{i, j, k\}$ ,  $\theta(ij) = 0.8, \theta(ik) = 0.4, \theta(jk) = 0.7$ ;  $\psi(i, ij) = 0.7, \psi(j, ji) = 0.5, \psi(i, ik) = 0.3, \psi(k, ki) = 0.2, \psi(j, jk) = 0.3, \psi(k, kj) = 0.7$ . It is a subgraph of a FIG given in Example 1 (Figure 2) with  $CI$  1.1.

## 3. Bounds for Connectivity Index of Fuzzy Incidence Graph

This section discusses some bounds for the CI of FIGs. Every FIG has a different CI. Therefore, all FIGs have different bounds for the CI. From all FIGs, the complete FIGs will have the highest CI. It is shown in the next theorem.

**Theorem 1.** Consider a FIG,  $G$  having  $|\eta^*| = n$ , then  $0 \leq CI(G) \leq CI(G'')$ , where  $G''$  indicates a complete FIG.

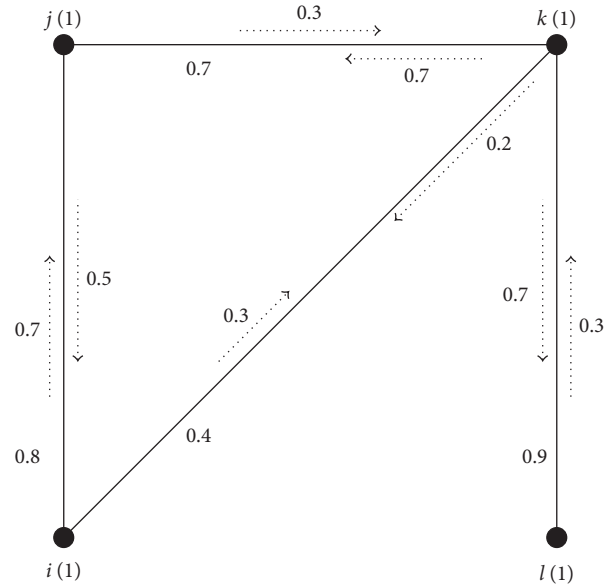


FIGURE 2: A fuzzy incidence graph with  $CI = 2.0$ .

*Proof.* Assume  $G$  is a FIG. If  $|\theta^*| = 0$ , then  $CI$  of  $G = 0$ . Let  $G''$  be the complete FIG having  $|\eta^*| = n$  and  $\eta''(a) = \eta(a)$ . Then,  $\theta(a, b) \leq \theta''(a, b)$ . Also,  $ICONN_G(a, b) \leq ICONN_{G''}(a, b)$ . This implies  $0 \leq CI(G) \leq CI(G'')$ .  $\square$

**Example 3.** Assume  $G''$  is a complete FIG given in Figure 4 having  $\eta^* = \{i, j, k\}$ ,  $\theta(ij) = 0.8, \theta(ik) = 0.4, \theta(jk) = 0.7$ ,  $\psi(i, ij) = 0.8, \psi(j, ji) = 0.8, \psi(i, ik) = 0.4, \psi(k, ki) = 0.4, \psi(j, jk) = 0.7$  and  $\psi(k, kj) = 0.7$ . We get  $CI(G'') = 2.2$ .

## 4. Vertex-Deleted and Edge-Deleted Fuzzy Incidence Subgraphs with Connectivity Indices

This section talks about the deletion of some edge or vertex of any FIG will become a cause of reducing a CI of FIG. An edge deleted and vertex deleted subgraph of a FIG will have small values of CI. The CI of FISs relies upon the nature of vertex or edge deleted.

**Example 4.** Let  $G = (\eta, \theta, \psi)$  be the FIG given in Figure 5 with  $\eta^* = \{p, q, r, s, t\}$ ,  $\theta(pq) = 0.7, \theta(pr) = 0.5, \theta(qr) = 0.9, \theta(rs) = 0.3, \theta(rt) = 0.5, \theta(st) = 0.6$ ;  $\psi(p, pq) = 0.6, \psi(q, qp) = 0.7, \psi(p, pr) = 0.4, \psi(r, rp) = 0.2, \psi(q, qr) = 0.8, \psi(r, rq) = 0.6, \psi(r, rs) = 0.2, \psi(s, sr) = 0.3, \psi(r, rt) = 0.5, \psi(t, tr) = 0.4, \psi(s, st) = 0.6$ , and  $\psi(t, ts) = 0.4$ . After calculation, we get  $CI(G) = 4.6$ , whereas  $CI(G - qr) = 3.0$  and  $CI(G - rt) = 3.4$ . Here, we conclude that deletion of some of the incidence pair reduces  $CI(G)$ . This motivation leads us to the following result.

**Theorem 2.** Let  $G = (\eta, \theta, \psi)$  be a FIG and  $G^* = (\eta^*, \theta^*, \psi^*)$  be the FIS of  $G$  by deleting an incidence pair  $(a, ab) \in \psi^*$ . Then,  $CI(G^*) < CI(G)$  iff  $(a, ab)$  is a FB.

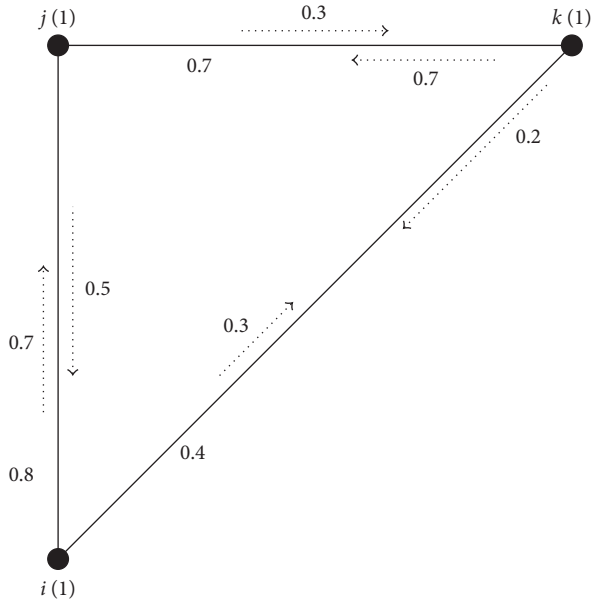


FIGURE 3: Subgraph of the fuzzy incidence graph in Figure 2.

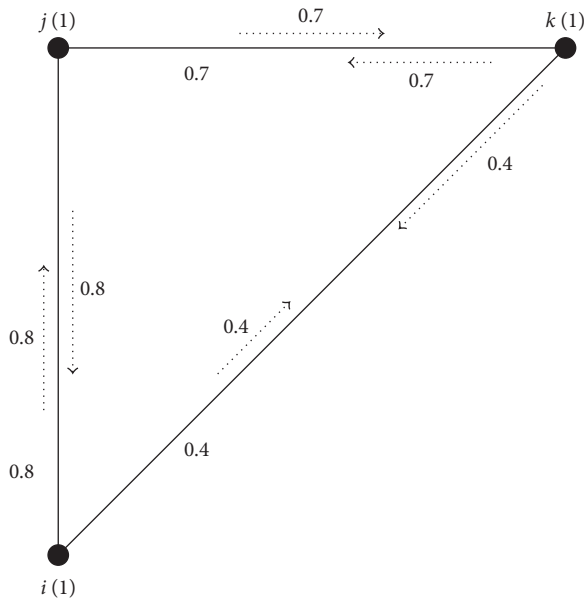


FIGURE 4: A complete fuzzy incidence graph.

*Proof.* Consider a pair  $(a, ab)$  be a FB. Then, according to definition of FB,  $\text{ICONN}_{G-(a,ab)}(a, b) < \text{ICONN}_G(a, b)$ , which shows that  $\text{CI}(G^*) < \text{CI}(G)$ . Conversely, assume that  $\text{CI}(G^*) < \text{CI}(G)$ . Now, consider three different cases:

Case 1: consider a  $\delta$ -pair,  $\psi(a, ab)$ , and then  $\psi(a, ab) < \text{ICONN}_{G-(a,ab)}(a, b)$  which implies  $\text{ICONN}_{G-(a,ab)}(a, b) < \text{ICONN}_G(a, b)$ . This implies  $\text{CI}(G^*) < \text{CI}(G)$ .

Case 2: consider a  $\beta$ -strong incidence pair  $\psi(a, ab)$ . Then,  $\psi(a, ab) = \text{ICONN}_{G-(a,ab)}(a, b)$  which means that there is an another strongest path  $a, (a, ab), ab, (b, ab), b$  different from the edge  $\psi(a, ab)$ . The IS

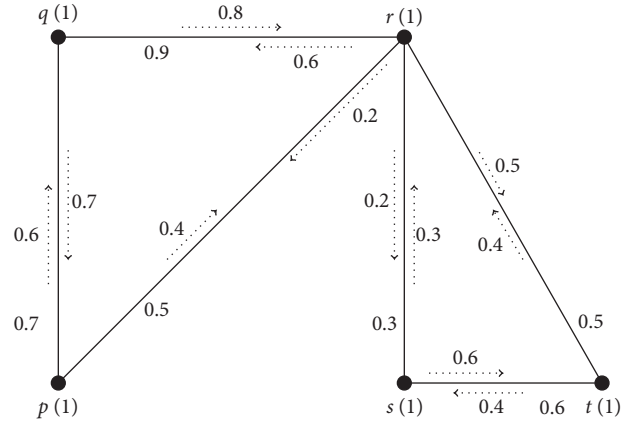


FIGURE 5: Fuzzy incidence graph with CI 4.6.

does not affect when we delete  $\psi(a, ab)$ . This means  $\text{CI}(G^*) = \text{CI}(G)$ .

Case 3: consider an  $\alpha$ -strong incidence pair  $\psi(a, ab)$ . Then,  $\psi(a, ab) > \text{ICONN}_{G-(a,ab)}(a, b)$ . This means an edge  $ab$  is the only strongest path whose strength is equal to  $\psi(a, ab)$ . From this, it is obvious that  $\text{CI}(G^*) < \text{CI}(G)$ . As by definition  $\alpha$ , strong arcs are FBs. This means if  $\text{CI}(G^*) < \text{CI}(G)$ , then  $ab$  is a FB. This shows that  $\text{CI}(G^*) < \text{CI}(G)$  iff  $uv$  is a FB.  $\square$

## 5. ACI of FIG

We measure the average flow in the network to check how much flow is stable in the network. Therefore, in this section, we are going to introduce a new parameter named ACI of FIG. Assume the FIG given in Example 1.

*Example 5.* Assume  $G$  is a FIG given in Example 1 (Figure 2) having  $\eta^* = \{i, j, k, l\}$ ,  $\theta(ij) = 0.8, \theta(ik) = 0.4, \theta(jk) = 0.7, \theta(kl) = 0.9; \psi(i, ij) = 0.7, \psi(j, ji) = 0.5, \psi(i, ik) = 0.3, \psi(k, ki) = 0.2, \psi(j, jk) = 0.3, \psi(k, kj) = 0.7, \psi(k, kl) = 0.7$  and  $\psi(l, lk) = 0.3$  with  $\text{CI}(G) = 2.0$ .  $G$  contains  $4!/((4-2)!) = 6$  pairs of nodes with  $\text{ACI}(G) = \text{CI}(G)/6 = 2/6 = 0.33$ .

*Definition 13.* Consider a FIG. The ACI of FIG is given by

$$\text{ACI}(G) = \frac{1}{\binom{n}{2}} \sum_{a,b \in \eta^*} \eta(a)\eta(b)\text{ICONN}_G(a, b). \quad (2)$$

*Definition 14.* Assume a FIG and  $z \in \eta^*$ .  $z$  will be FICRN of  $G$  if  $\text{ACI}(G-z) < \text{ACI}(G)$ . We call  $z$  a FICEN if  $\text{ACI}(G-z) > \text{ACI}(G)$ .  $z$  will be FICNN if  $\text{ACI}(G-z) = \text{ACI}(G)$ .

*Example 6.* Let  $G$  be a FIG given in Figure 6 with (HTML translation failed),  $\theta(ij) = 0.3, \theta(ik) = 0.8, \theta(jk) = 0.7, \theta(jn) = 0.5, \theta(kl) = 0.9, \theta(lm) = 0.8; \psi(i, ij) = 0.3, \psi(j, ji) = 0.2, \psi(i, ik) = 0.4, \psi(k, ki) = 0.6, \psi(j, jk) = 0.6, \psi(k, kj) = 0.7, \psi(j, jn) = 0.5, \psi(n, nj) = 0.4, \psi(k, kl) = 0.8, \psi(l, lk) = 0.2, \psi(l, lm) = 0.3$ , and  $\psi(m, ml) = 0.7$ .  $\text{ACI}(G) = 0.3, \text{ACI}(G-i) = 0.29, \text{ACI}(G-j) = 0.25, \text{ACI}(G-k) =$

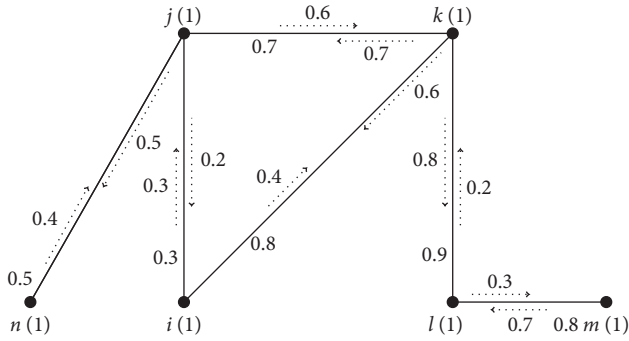


FIGURE 6: Fuzzy incidence graph with FICRN and FICENs.

0.11,  $ACI(G - l) = 0.36$ ,  $ACI(G - m) = 0.34$ ,  $ACI(G - n) = 0.29$ . Therefore,  $i, j, k$ , and  $n$  are FICRN;  $l$  and  $m$  are FICENs.

In the following proposition with the help of CI, we classify these nodes:

**Proposition 3.** Consider a FIG. Let  $z \in \eta^*$  having  $n = |\eta^*| \geq 3$ . Assume  $q = CI(G)/CI(G - z)$ .  $z$  is a FICEN iff  $q < n/(n - 2)$ .  $z$  is a FICRN iff  $q > n/(n - 2)$ .  $z$  is a FICNN iff  $q = n/(n - 2)$ .

*Proof.* Let  $z$  be FICNN of FIG. Then,  $ACI(G) = ACI(G - z)$ , that is,  $CI(G)/\binom{n}{2} = CI(G - z)/\binom{n-1}{2}$  and  $CI(G)/CI(G - z) = \binom{n}{2}/\binom{n-1}{2}$ , which implies  $CI(G)/CI(G - z) = n/(n - 2)$ . By reversing the argument, the sufficient part can easily be proved. In similar manners, the other two cases can be solved.  $\square$

**Definition 15.** Let  $G$  be a FIG.  $G$  will be FI connectivity enhancing graph if  $G$  contains minimum one FICEN. If  $G$  contains no FICEN and has minimum one FICRN, then we call it FI connectivity reducing graph. We call  $G$  a FI connectivity neutral graph if all nodes of  $G$  are neutral.

### 6. Wiener Index of FIG

In this section, we establish the concept of WI. WI is a topological index used in different fields like medicine, communication, and cryptology. A proper definition to calculate WI of FIG is given next.

**Definition 16.** Let  $G$  be a FIG. WI of  $G$  can be calculated as

$$WI(G) = \sum_{a,b \in \eta^*} \eta(a)\eta(b)d_s(a,b), \quad (3)$$

where  $d_s(a,b)$  represents weights of those strong geodesics from  $a - b$  whose sum is minimum.

**Example 7.** Consider  $G$  be a FIG given in Figure 7 with  $\eta^* = \{i, j, k\}$ ,  $\theta(ij) = 0.7, \theta(ik) = 0.8, \theta(jk) = 0.7; \psi(i, ij) = 0.6, \psi(j, ji) = 0.6, \psi(i, ik) = 0.8, \psi(k, ki) = 0.8, \psi(j, jk) =$

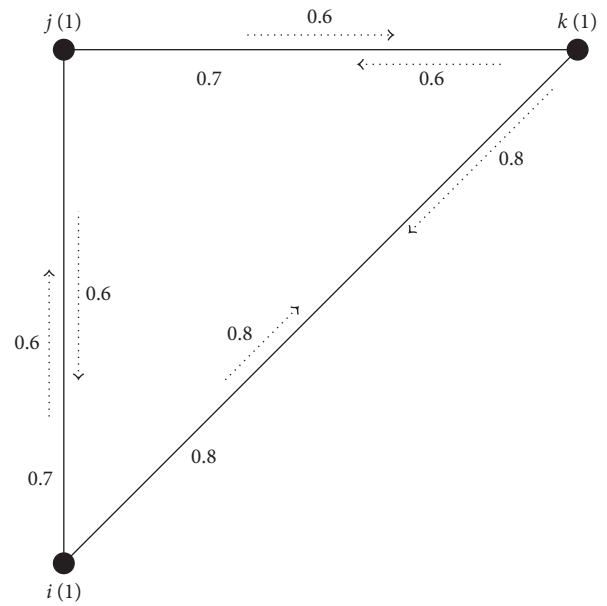


FIGURE 7: Fuzzy incidence graph with  $WI(G) = 4$ .

$0.6, \psi(k, k j) = 0.6$ . Here, each incidence pair is a strong pair. Because  $i - j$  is a geodesic, it is a strongest path from  $i - j$ . Similarly,  $i - k$  and  $j - k$  are all strongest paths. Thus,  $WI(G) = 4$ .

Assume a FIG. Let  $H$  be the FIS of  $G$ . Then, it is not necessary that  $WI(H) \leq WI(G)$ . It can be seen in the next example

**Example 8.** Let  $H = (\kappa, \phi, \Omega)$  is a FIS (see Figure 8) of  $G = (\eta, \theta, \psi)$  (in Figure 7) such that  $\phi(ik) = 0$  and  $\phi(ij) = 0.7, \phi(jk) = 0.7, \Omega(i, ij) = 0.6, \Omega(j, ij) = 0.6, \Omega(j, jk) = 0.6, \Omega(k, jk) = 0.6$ . Geodesic from  $i$  to  $k$  is  $i, j, k$ .  $d_s(i, j) = \psi(i, ij) + \psi(j, j j) = 1.2$  Similarly,  $d_s(i, k) = 2.4, d_s(j, k) = 1.2$ . Then,  $WI(H) = 4.8$  and  $WI(G) = 4 < WI(H) = 4.8$ .

#### Link between WI and CI of a FIG

In FIGs, it could be noted that CI will be less than WI.

**Example 9.** Consider a FIG given in Figure 9 with  $\eta^* = \{i, j, k, l\}$ ,  $\theta(ij) = 0.8, \theta(ik) = 0.4, \theta(jk) = 0.7, \theta(kl) = 0.9; \psi(i, ij) = 0.5, \psi(j, ji) = 0.7, \psi(i, ik) = 0.3, \psi(k, ki) = 0.2, \psi(j, jk) = 0.3, \psi(k, k j) = 0.7, \psi(k, kl) = 0.7$ , and  $\psi(l, lk) = 0.3$ . This FIG contains each pair strong except  $\psi(i, ki) = 0.2$  because  $ICONN_{G-(i,ki)} = 0.3$ . For  $(i, k) \in \eta^* \times \eta^* \setminus \psi(i, ki)$ . Now,  $CI(G) = 0.5 + 0.3 + 0.3 + 0.3 + 0.3 + 0.3 = 2$  and  $WI(G) = 1.2 + 2.2 + 3.2 + 1 + 2 + 1 = 10.6$  Thus,  $CI(G) < WI(G)$ .

**Theorem 3.** Assume a FIG having  $|\eta^*| \geq 3$ . Then,  $WI(G) > CI(G)$ .

*Proof.* Consider a FIG with  $|\eta^*| \geq 3$ . For every  $a, b \in \eta^*$ , the sum of membership values of every strong incidence pairs connecting  $a$  and  $b$  is  $d_s(a,b)$ , whereas the minimum membership value of all strong incidence pairs is

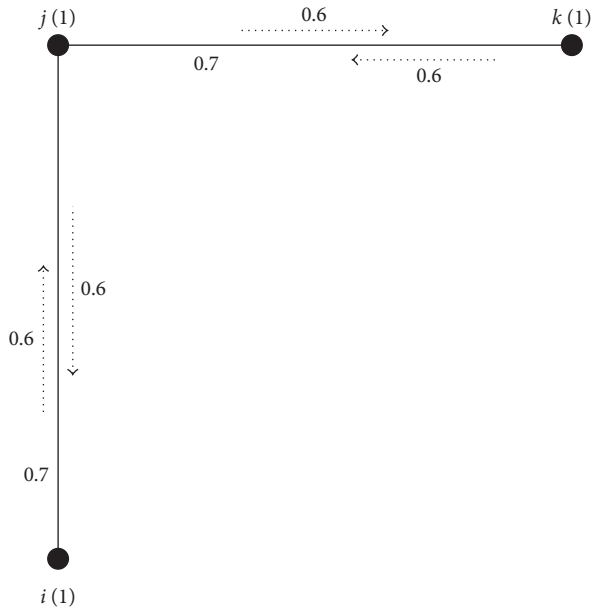


FIGURE 8: Fuzzy incidence subgraph of Figure 7.

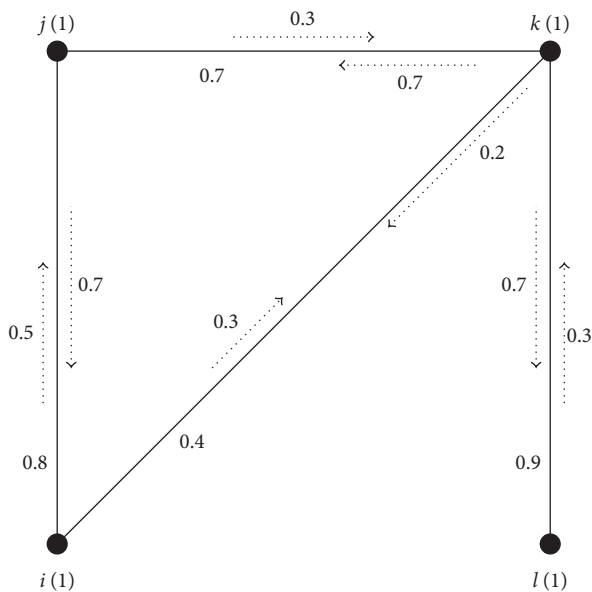


FIGURE 9: Fuzzy incidence graph with  $CI < WI$ .

$ICONN_G(a, b)$ , which means  $ICOON_G(a, b) < d_s(a, b)$ . This implies  $\sum_{a,b \in \eta^*} \eta(a)\eta(b)ICONN_G(a, b) < \sum_{a,b \in \eta^*} \eta(a)\eta(b)d_s(a, b)$ . Hence,  $CI(G) < WI(G)$ .  $\square$

**Theorem 4.** Assume a complete FIG,  $G$  with  $|\eta^*| = 2$ , and  $(a) = (b) = 1$ . Then,  $2CI(G) = WI(G)$ .

*Proof.* Consider  $G$  be a complete FIG with  $|\eta^*| = 2$  and  $(a) = (b) = 1$ .  $\exists$  There exist a strong path  $P''$  which is the strongest path in complete FIG,  $G$ . For any two nodes  $a, b \in \eta^*$ , the sum of membership values of incidence pair in the only strongest path  $P''$  connecting  $a$  with  $b$  is  $d_s(a, b)$ , whereas the minimum membership value of incidence pair

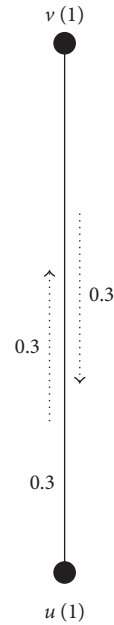


FIGURE 10: Complete fuzzy incidence graph with  $2CI(G) = WI(G)$ .

of  $P$  is  $ICONN_G(a, b)$ . This implies  $2ICONN_G(a, b) = d_s(a, b)$ . Thus,  $2\sum_{a,b \in \eta^*} \eta(a)\eta(b)ICONN_G(a, b) = \sum_{a,b \in \eta^*} \eta(a)\eta(b)d_s(a, b)$ . Hence,  $2CI(G) = WI(G)$ .  $\square$

*Example 10.* Let  $G$  be the complete FIG, as shown in Figure 10. Here,  $u, v \in \eta^*$  and  $\theta(uv) = 0.3, \psi(u, uv) = 0.3, \psi(v, uv) = 0.3$ . Clearly,  $CI(G) = 0.3$  and  $WI(G) = 0.6$ .

### 7. Conclusion

Connectivity is an essential parameter attached to a network. The idea of connectivity is inseparable from the theory of FIGs. In this paper, we have come up with different results about WI and CI of FIGs. Relevant examples related to WI and CI of FIGs are too obtained. In this article, CI, ACI, and WI of FIGs linked with networks are expressed. Nodes of FIGs are classified as FICRN, FICEN, and FICNN by using these incidences. Various types of FIGs are also obtained. A crucial relationship between CI and WI of FIG is derived too. Our objective is to enlarge our research work to soft FIGs, bipolar FIGs, threshold FIGs, competition FIGs, regular FIGs, and  $q$ -rung FIGs. More similar results and applications will be reported in upcoming papers.

### Data Availability

No data were used to support this study.

### Conflicts of Interest

The authors declare that there are no conflicts of interest regarding the publication of this paper.

## Acknowledgments

This paper was supported by the Anhui Natural Science Research Project (2017) under Grant no. KJ2017A469 and Top-Notch Talents Cultivation Project (gxgnfx2020099) of Anhui Higher Education.

## References

- [1] L. A. Zadeh, "Fuzzy sets," *Information and Control*, vol. 8, no. 3, pp. 338–353, 1965.
- [2] A. Rosenfeld, "Fuzzy graphs," in *Fuzzy Sets and Their Applications*, L. A. Zadeh, K. S. Fu, and M. Shimura, Eds., pp. 77–95, Academic Press, New York, NY, USA, 1975.
- [3] R. T. Yeh and S. Y. Bang, "Fuzzy relations, fuzzy graphs and their applications to clustering analysis," in *Fuzzy Sets and Their Applications*, L. A. Zadeh, K. S. Fu, and M. Shimura, Eds., pp. 125–149, Academic Press, Cambridge, MA, USA, 1975.
- [4] P. Bhattacharya and F. Suraweera, "An algorithm to compute the supremum of max-min powers and a property of fuzzy graphs," *Pattern Recognition Letters*, vol. 12, no. 7, pp. 413–420, 1991.
- [5] K. R. Bhutani, "On automorphisms of fuzzy graphs," *Pattern Recognition Letters*, vol. 9, no. 3, pp. 159–162, 1989.
- [6] J. N. Mordeson, "Fuzzy line graphs," *Pattern Recognition Letters*, vol. 14, no. 5, pp. 381–384, 1993.
- [7] K. R. Bhutani and A. Rosenfeld, "Fuzzy end nodes in fuzzy graphs," *Information Sciences*, vol. 152, pp. 323–326, 2003.
- [8] K. R. Bhutani and A. Rosenfeld, "Strong arcs in fuzzy graphs," *Information Sciences*, vol. 152, pp. 319–322, 2003.
- [9] M. S. Sunitha and A. Vijayakumar, "A characterization of fuzzy trees," *Information Sciences*, vol. 113, no. 3–4, pp. 293–300, 1999.
- [10] M. S. Sunitha and A. Vijayakumar, "Blocks in fuzzy graphs," *The Journal of Fuzzy Mathematics*, vol. 13, no. 1, pp. 13–23, 2005.
- [11] S. Samanta, B. Sarkar, D. Shin, and M. Pal, "Completeness and regularity of generalized fuzzy graphs," *Springer Plus*, vol. 5, no. 1, p. 1979, 2016.
- [12] S. Samanta and M. Pal, "Fuzzy planar graphs," *IEEE Transactions on Fuzzy Systems*, vol. 23, no. 6, pp. 1936–1942, 2015.
- [13] S. Mathew and M. S. Sunitha, "Types of arcs in a fuzzy graph," *Information Sciences*, vol. 179, no. 11, pp. 1760–1768, 2009.
- [14] S. Mathew and M. S. Sunitha, "Node connectivity and arc connectivity of a fuzzy graph," *Information Sciences*, vol. 180, no. 4, pp. 519–531, 2010.
- [15] S. Mathew and M. S. Sunitha, "Cycle connectivity in fuzzy graphs," *Journal of Intelligent & Fuzzy Systems*, vol. 24, no. 3, pp. 549–554, 2013.
- [16] S. Mathew, H. L. Yang, and J. K. Mathew, "Saturation in fuzzy graphs," *New Mathematics and Natural Computation*, vol. 14, no. 01, pp. 113–128, 2018.
- [17] M. Binu, S. Mathew, and J. N. Mordeson, "Connectivity index of a fuzzy graph and its application to human trafficking," *Fuzzy Sets and Systems*, vol. 360, pp. 117–136, 2019.
- [18] M. Binu, S. Mathew, and J. N. Mordeson, "Connectivity index of a fuzzy graph and its application to human trafficking," *Fuzzy Sets Systems*, vol. 360, pp. 117–136, 2019.
- [19] N. Jicy and S. Mathew, "Some new connectivity parameters for weighted graphs," *Journal of Uncertainty in Mathematics Science*, vol. 2014, pp. 1–9, 2014.
- [20] S. Mathew and M. S. Sunitha, "Some connectivity concepts in weighted graphs," *Advances and Applications in Discrete Mathematics*, vol. 6, no. 1, pp. 45–54, 2010.
- [21] S. Mathew, J. N. Mordeson, and D. Malik, *Fuzzy Graph Theory*, Springer, Berlin, Germany, 2018.
- [22] J. N. Mordeson, S. Mathew, and D. Malik, *Fuzzy Graph Theory with Applications to Human Trafficking*, Springer, Berlin, Germany, 2018.
- [23] J. N. Mordeson and S. Mathew, "Human trafficking: source, transit, destination designations," *New Mathematics and Natural Computation*, vol. 13, no. 3, pp. 209–218, 2017.
- [24] J. N. Mordeson, S. Mathew, and R. A. Borzooei, "Vulnerability and government response to human trafficking: vague graphs," *New Mathematics and Natural Computation*, vol. 14, no. 2, pp. 202–219, 2018.
- [25] S. Samanta, M. Pal, H. Rashmanlou, and R. A. Borzooei, "Vague graphs and strengths," *Journal of Intelligent & Fuzzy Systems*, vol. 30, no. 6, pp. 3675–3680, 2016.
- [26] H. Wiener, "Structural determination of paraffin boiling points," *Journal of the American Chemical Society*, vol. 69, no. 1, pp. 17–20, 1947.
- [27] M. Binu, S. Mathew, and J. N. Mordeson, "Wiener index of a fuzzy graph and application to illegal immigration networks," *Fuzzy Sets and Systems*, vol. 384, pp. 132–147, 2019.
- [28] T. Dinesh, "Fuzzy incidence graph—an introduction," *Advances in Fuzzy Sets and Systems*, vol. 21, no. 1, pp. 33–48, 2016.
- [29] J. N. Mordeson, "Fuzzy incidence graphs," *Advances in Fuzzy Sets and Systems*, vol. 21, no. 2, pp. 121–133, 2016.
- [30] D. Malik, J. N. Mordeson, and S. Mathew, "Fuzzy incidence graphs: applications to human trafficking," *Information Sciences*, vol. 447, pp. 244–255, 2018.
- [31] J. N. Mordeson and S. Mathew, "Fuzzy incidence blocks and their applications in illegal migration problems," *New Mathematics and Natural Computation*, vol. 13, pp. 245–260, 2017.
- [32] S. Mathew and J. N. Mordeson, "Connectivity concepts in fuzzy incidence graphs," *Information Sciences*, vol. 382–383, pp. 326–333, 2017.